Lecture Notes in Mechanical Engineering

B. B. V. L. Deepak
M. V. A. Raju Bahubalendruni
D. R. K. Parhi
B. B. Biswal *Editors*

Recent Advancements in Product Design and Manufacturing Systems

Select Proceedings of IPDIMS 2023

Springer

Lecture Notes in Mechanical Engineering

Series Editors

Fakher Chaari, National School of Engineers, University of Sfax, Sfax, Tunisia

Francesco Gherardini, Dipartimento di Ingegneria “Enzo Ferrari”, Università di Modena e Reggio Emilia, Modena, Italy

Vitalii Ivanov, Department of Manufacturing Engineering, Machines and Tools, Sumy State University, Sumy, Ukraine

Mohamed Haddar, National School of Engineers of Sfax (ENIS), Sfax, Tunisia

Editorial Board

Francisco Cavas-Martínez, Departamento de Estructuras, Construcción y Expresión Gráfica Universidad Politécnica de Cartagena, Cartagena, Spain

Francesca di Mare, Institute of Energy Technology, Ruhr-Universität Bochum, Bochum, Germany

Young W. Kwon, Department of Manufacturing Engineering and Aerospace Engineering, Graduate School of Engineering and Applied Science, Monterey, USA

Tullio A. M. Tolio, Department of Mechanical Engineering, Politecnico di Milano, Milano, Italy

Justyna Trojanowska, Poznan University of Technology, Poznan, Poland

Robert Schmitt, RWTH Aachen University, Aachen, Germany

Jinyang Xu, School of Mechanical Engineering, Shanghai Jiao Tong University, Shanghai, China

Lecture Notes in Mechanical Engineering (LNME) publishes the latest developments in Mechanical Engineering—quickly, informally and with high quality. Original research or contributions reported in proceedings and post-proceedings represents the core of LNME. Volumes published in LNME embrace all aspects, subfields and new challenges of mechanical engineering.

To submit a proposal or request further information, please contact the Springer Editor of your location:

Europe, USA, Africa: Leontina Di Cecco at Leontina.dicecco@springer.com
China: Ella Zhang at ella.zhang@cn.springernature.com
India, Rest of Asia, Australia, New Zealand: Swati Meherishi at swati.meherishi@springer.com

Topics in the series include:

- Engineering Design
- Machinery and Machine Elements
- Mechanical Structures and Stress Analysis
- Automotive Engineering
- Engine Technology
- Aerospace Technology and Astronautics
- Nanotechnology and Microengineering
- Control, Robotics, Mechatronics
- MEMS
- Theoretical and Applied Mechanics
- Dynamical Systems, Control
- Fluid Mechanics
- Engineering Thermodynamics, Heat and Mass Transfer
- Manufacturing Engineering and Smart Manufacturing
- Precision Engineering, Instrumentation, Measurement
- Materials Engineering
- Tribology and Surface Technology

Indexed by SCOPUS, EI Compendex, and INSPEC.

All books published in the series are evaluated by Web of Science for the Conference Proceedings Citation Index (CPCI).

To submit a proposal for a monograph, please check our Springer Tracts in Mechanical Engineering at https://link.springer.com/bookseries/11693.

B. B. V. L. Deepak ·
M. V. A. Raju Bahubalendruni · D. R. K. Parhi ·
B. B. Biswal
Editors

Recent Advancements in Product Design and Manufacturing Systems

Select Proceedings of IPDIMS 2023

Springer

Editors
B. B. V. L. Deepak
Department of Industrial Design
National Institute of Technology Rourkela
Rourkela, Odisha, India

D. R. K. Parhi
Department of Mechanical Engineering
National Institute of Technology Rourkela
Rourkela, Odisha, India

M. V. A. Raju Bahubalendruni
Department of Mechanical Engineering
National Institute of Technology
Puducherry
Karaikal, Pondicherry, India

B. B. Biswal
Odisha University of Technology
and Research
Bhubaneswar, Odisha, India

ISSN 2195-4356 ISSN 2195-4364 (electronic)
Lecture Notes in Mechanical Engineering
ISBN 978-981-97-6731-1 ISBN 978-981-97-6732-8 (eBook)
https://doi.org/10.1007/978-981-97-6732-8

© The Editor(s) (if applicable) and The Author(s), under exclusive license to Springer Nature Singapore Pte Ltd. 2025

This work is subject to copyright. All rights are solely and exclusively licensed by the Publisher, whether the whole or part of the material is concerned, specifically the rights of translation, reprinting, reuse of illustrations, recitation, broadcasting, reproduction on microfilms or in any other physical way, and transmission or information storage and retrieval, electronic adaptation, computer software, or by similar or dissimilar methodology now known or hereafter developed.
The use of general descriptive names, registered names, trademarks, service marks, etc. in this publication does not imply, even in the absence of a specific statement, that such names are exempt from the relevant protective laws and regulations and therefore free for general use.
The publisher, the authors and the editors are safe to assume that the advice and information in this book are believed to be true and accurate at the date of publication. Neither the publisher nor the authors or the editors give a warranty, expressed or implied, with respect to the material contained herein or for any errors or omissions that may have been made. The publisher remains neutral with regard to jurisdictional claims in published maps and institutional affiliations.

This Springer imprint is published by the registered company Springer Nature Singapore Pte Ltd.
The registered company address is: 152 Beach Road, #21-01/04 Gateway East, Singapore 189721, Singapore

If disposing of this product, please recycle the paper.

Preface

This book comprises the proceedings of the Fifth International Conference on Innovative Product Design and Intelligent Manufacturing Systems (ICIPDIMS'23) held at National Institute of Technology, Rourkela, India, during 6–7 December 2023. The present ICIPDIMS is the fifth in a series of annual conferences held at National Institute of Technology, Rourkela. This conference is aimed at expanding the program by including all aspects related to product innovation and its manufacturing with the aid of computers technology. The aim of the conference is to provide a forum for delegates from the industry and academia to exchange ideas and presenting their research works. In addition, it is an ideal venue for interactions and for them to establish the all-important contacts with each other.

The national and international advisory boards of IPDIMS peer-reviewed the 205 submitted research articles and shortlisted 120 papers for oral presentation. ICIPDIMS'23 has two keynote speakers and thirteen technical sessions. The chapters in this book cover the research areas—product innovation, UX/UI, HCI, CAD/CAM and Robotics.

On behalf of the Organizing Committee, we thank all the authors, delegates, institutions and organizations that participated in the conference. We also thank the members of the National and International Programme Committee for their support during the peer-reviewing process which is highly essential to maintain the quality of the conference.

We also thank the dedicated group of student volunteers of NIT Rourkela for assisting to organize the conference. Finally, we thank to editorial support team of LNME, Springer Nature for their continuous assistance toward the proceedings publication.

Rourkela, India
May 2024

Prof. B. B. V. L. Deepak, (Convener, IPDIMS)
Prof. D. R. K. Parhi, (Chairman, IPDIMS)

Contents

Advances in Manufacturing Technology

Optimizing Quadcopter Structural Design: A Numerical Analysis on Strength and Stability 3
S. Shivani and Kamlesh Kumar

Multi-Objective Optimization of Brake Force Distribution for Enhanced Thermal Management in Hydraulic Brake Systems using PESA 2 Algorithm 21
Indranil Banik and Arup Kumar Nandi

Development of an Intuitive Autonomous Ground Robot for Indoor Delivery Applications 33
Jerin Peter, Mervin Joe Thomas, S. Gokulkrishna, Kiran Cholappally, and Santhakumar Mohan

Development of a Computer-Assisted Vision-Based Inspection Monitoring System for Quality Assurance 45
Prajwal S. Bhide and P. V. Manivannan

Analysis of Challenges of IoT Adoption for Smart City Application 55
Rashmi Prava Das, Debendra Muduli, and Ashish Kumar Luhach

Finite Element Modelling and Comparative Assessment of Single-Level Cervical Disc Replacement with Fusion Surgery 67
Akshansh Sharma and Sandeep Kumar Parashar

A Statistical Method-Based Auto-Fitted Genetic Algorithm for Damage Diagnosis 79
Sasmita Sahu, Monalisa Das, Shakti P. Jena, Rita Kumari Sahu, Bijaya Bijeta Nayak, and Dayal R. Parhi

Emovere Agnitio by Textual Tweets Using Machine Learning 87
B. Prasanna Kumar, Venkata Kishore Kumar Rejeti, T. Bhavani Shanvitha, S. Jyothi Sri, Y. Prathyusha, S. Keerthana, and D. Anand

Government Bidding Security Management System Using Blockchain 97
Venkata Kishore Kumar Rejeti, G. Rajesh Chandra, T. Venkata Sai Vardhan, T. Manoj Sai, S. Srihas, S. K. Karimulla Saleem, and D. Anand

Resource Forecasting of Geographical Area Using Big Data Analytics 111
Venkata Kishore Kumar Rejeti, G. Rajesh Chandra, V. Mounika, S. K. Thasleema Thanveer, V. Jyothika, Y. Harika, and D. Anand

Design Optimization and Aerothermodynamic Analysis Over a Supersonic Vehicle 123
Divij Arora, R. Balaji, and Amit Kumar Thakur

Evaluation of Weldability and Optimization of TIG Welding Process Parameters for Maximized Yield Strength 135
Guambo Mondo, Bikash Ranjan Moharana, Shoeb Ahmed Syed, and Kamalakanta Muduli

Terahertz-Frequency Propagation for Autonomous Transport Infrastructure 147
Aezeden Mohamed and Janne Heilala

Energy-Efficient Coffee Pulper 155
Andy Ray and Aezeden Mohamed

Community Perception on Groundwater Quality Versus Analytical Quality in the Coastal Areas of Visakhapatnam, India—Opinion Versus Actuality 165
Sirisha Korrai, Nallamilli Satish Reddy, Madhavi Earle, Hemanshu Mediboyana, and Bharani Meruva

Simulation Modeling and Analysis for Supply Chain Disruptions: A Case Study from a Process Industry in Kerala 175
Veedhi Shyam Nishanth, B. Abhiram, Madineni Bhavana, Vani Amrutha Mutyala, Arun Thomas, T. Rathnakaran, and Vinay V. Panicker

Integrating Hand Gesture Tracking with Physical and Digital Twins of Robotic Arm 185
Ojas Jain and Krishnaiah Jallu

Performance Enhancement of Pump Parameters Through Innovative Spring Design of Mechanical Seal for a Heat Exchanger 195
I. Ramu, G. Suresh Bau, N. V. V. Manikanta, and M. Venu

Materials Processing for Product Design

Enhancing Biocompatibility and Performance of Multi-directionally Expanding Materials for Dental Applications: Design and Analysis 207
M. B. Kumbhar and T. Jagadeesha

Synthesis of Hybrid Nanofluids, Properties, and Its Applications—A Comprehensive Review 221
Sudhakara Rao Bammidi, Vijay Miditana, and Ravibabu Sajja

Application of Hybrid Decision-Making Method in Ranking Polymer Biomaterials for Interim Dental Crowns 233
Akula Siva Bhaskar and Akhtar Khan

Analysis on Mechanical Properties of Aluminium MMC with Graphite and Boron Nitride Powder 247
Neelapu Madhu Latha and I. N. Niranjan Kumar

Development of Battery Case Design Using Banana Fibre 263
G. Manikandan, M. Boopathi, S. Narasimmabharathi, S. Vimal, M. K. Rithik, and T. S. Sanjay

Data Simulation: Creep Behavior in Ti–6Al–4V Alloy 277
Jones Woya, Malachi Mai, and Aezeden Mohamed

Influence of Stability Improvement Methods Over the Thermal Conductivity of Al_2O_3-DI Nanofluids 287
Ravi Kiran Mudidana, Vijay Miditana, and V. Rambabu

Development of High-performance Welding Consumables and Filler Materials: A Review 299
Anish K. Raj, Bikash Ranjan Moharana, Sunita Routray, and Kalinga Simant Bal

Frictional and Wear Behavior of Polyol Ester—Commercial Motorbike Engine Oil Blend under Boundary Lubrication Conditions 313
B. Koteswara Rao, V. Srinivas, S. Jai Kumar, L. S. Pradeep, and M. S. Srikar

Investigation of Turning Parameters on AL7075 Alloy Reinforcement with Silicon Carbide for a Surface Roughness of Composite Material 325
S. Padmanabhan, Ch. Siva Ramakrishna, A. Lalitha Saravanan, Ramesh Bokde, S. Venugopal, V. Manikkavasakan, and Krishna Kant Pandey

Design and Analysis of Gudgeon Pin to Minimize Stress Concentration by Selecting Different Material Through FEA 339
J. Kumaraswamy, Ch. Siva Ramakrishna, S. Ramasubramanian, Rahul Mishra, D. T. Sakhare, K. Karthik, S. Baskar, and Krishna Kant Pandey

Identifying the Influence of the WEDM Process Variable on Performance Indicators: MRR During the Machining of Inconel X-750 353
Smita Padhan, Sudhansu Ranjan Das, and Pankaj Charan Jena

Experimental Investigation of Corrosion Effect of Automotive Fuel Tank for Biofuels 365
T. Vinod Kumar, M. Chandrasekaran, R. Pugazhenthi, Abhishek Sharma, Anil Singh Yadav, Rahul Kumar, and Gopal Kaliyaperumal

Dynamic Instability of a Sandwich Revolving Beam Non-uniform Along Width and Depth Under Pulsating Load 379
Nabakishor Dang, Madhusmita Pradhan, Madhumita Mohanty, Prasanta Kumar Pradhan, and Pusparaj Dash

Application of AI/ML

Low Birth Weight Prediction Using Machine Learning 393
G. Harika, T. Venkata Lakshmi, P. Santhosh Prudhvi Raj, U. D. Prasan, and M. Jayanthi Rao

Complaint Management System for State Government Authority 403
A. Siva Sankar, Venkata Kishore Kumar Rejeti, Shaik Thanda Moddinsha, S. Rakesh, V. Himanish, M. Vinod, and D. Anand

Implementing a Support Vector Machine Algorithm on Social Media Flat Forms to Detect and Restrict Cyberbullying Conversations 415
M. Jayanthi Rao, P. Prasanthi, B. Ramakrishna, K. G. Durga Prasad, and M. Ramanaiah

Multi-objective Optimal Power Flow Using Krill Herd Algorithm 429
Bondalapati Devasahayam and B. Venkateswara Rao

Optimal Reactive Power Dispatch Using Improved Grey Wolf Algorithm 445
K. Bhaskara Sandhya, S. N. V. S. K. Chaitanya, B. Venkateswara Rao, and R. Ashok Bakkiyaraj

Construction of Cascaded Deep Neural Network with Optimization-Based Feature Selection in CT Images for Detecting Laryngeal Cancer 459
P. Naga Padmavathi, M. Sree Devi, V. V. R. Maheswara Rao, and Amara S. A. L. G. Gopala Gupta

Smart Voting System Using Deep Learning 473
P. Prasanthi, K. Aneesha, P. Sujith, S. Deepika, S. Sai Vamsi, and M. Jayanthi Rao

Mechanism of Data Sharing Using Secured Keyword Search in Cloud Computing 483
Umamaheswararao Mogili, Aezeden Mohamed, and Collettah Kasup

Prediction of Covid-19 Recovery Chances Using Supervised Machine Learning Classification 495
R. Dhanalakshmi, A. Nivashini, and N. Vijayaraghavan

Considerations in Product Design and Development

Reviving Sawantwadi's Colorful Legacy: Exploring Artisan Perspectives on Traditional Wood Crafts 507
Omkar Sadashiv Rane and Suyash Khaneja

Unfolding a Hidden Risk of Direct 3D Software Usage for Animation Character Design 521
Ananda Karmakar and Anirban Chowdhury

Creating a Compatible Design Solution Through Sari Drapes for Visually Challenged Women of India 531
Shagun Swaroop and Anirban Chowdhury

An Experimental Educational Tool for Financial Literacy in Children of 3–10 Years 545
Debashis Majumder, Ipsita Dasgupta, and Mugdha Tambe

Challenges of Sustainable Urban Planning in Odisha (India): Using the OCRA Method 555
Kallol Bera and Suchismita Satapathy

Design and Development of an IoT-Enabled Ergonomic Material Handling Equipment for Effective Inventory Management 565
M. Rajesh, Arpitha, Kruthi, Sanskruti, and Trisha Nair

Journeying with Peace of Mind: Reinventing Luggage Safety for Land Explorers 575
Prasanna Prakash Halbe and Nitin Hadap

Design Challenges and Solutions to Create Toys with Reference to Sawantwadi Wooden Toy Manufacturing 589
Omkar Sadashiv Rane, Sudeep Ray, and Suyash Khaneja

Leveraging Technology to Enhance Hiker Safety: A Design Intervention 603
Naureen Khan, Pranita Ranade, and Indresh Kumar Verma

Textile Defect Classification Using Deep Convolutional Neural Networks (DCNN) 619
Sri Sashank Potluru, Tarun Karnati, Ramesh Mande, Hruthi sri Gudavalli, and Sai Manikanta Miriyala

Creative Explorations with Bias in Design Thinking Process 637
Deepshikha and Nisheeth Yadav

Textile Crafts of Bharat 655
Deepshikha and Avinav Krishna

Cost-Effective and Sustainable Design: A Review of the Variables that Contribute to Exorbitant Rental Rates in PNG 683
Collettah Kasup and Aezeden Mohamed

Presence of Gestalt Traits in a Brand Logo and Its Impact in Evoking the Intended Meaning 691
Ruchi Srivastav and Anirban Chowdhury

Skill Development and Assessment Through Game-Based Learning: A Review 707
Venkateswara Rao Tadiboyina, B. B. V. L. Deepak, and Dhananjay Singh Bisht

About the Editors

Dr. B. B. V. L. Deepak is currently working at National Institute of Technology, Rourkela in the Department of Industrial Design. He received his Master's and Ph.D. degrees from the National Institute of Technology-Rourkela in 2010 and 2015 respectively. He has 11 years of research and teaching experience in Manufacturing and Product Design fields. He produced 4-Ph.D. theses and is supervising 4-Ph.D. scholars. He published more than 100 papers in various peer-reviewed journals and conferences along with 1-patent. He has successfully completed three sponsored research projects and currently handling two sponsored research projects in the field of robotics and automation. He received several national and international awards such as Ganesh Mishra Memorial Award-2019, IEI Young Engineer Award-2018 (Mechanical Engineering field), Early Career Research Award-2017, etc.

Dr. M. V. A. Raju Bahubalendruni is currently working as Assistant Professor in the Department of Mechanical Engineering at NIT-Puducherry, India. He has completed his masters in Machine Design at Andhra University College of Engineering and joined at HCL technologies Bengaluru. He worked on several aircraft programmes like c27J, Bombardier, Honda Jet, Bell-407. He completed his Ph.D. degree from National Institute of Technology Rourkela. He is currently an active researcher in the manufacturing and automation domain (Assembly, Disassembly, Industrial Robotics, Human-robot collaboration, Additive manufacturing, Topology Optimization, Advanced cellular structures, Augmented reality/Virtual Reality). He is one of the potential research professionals with more than 11 years of total Academic, Industrial and R&D experience. He has received multiple research grants form (Science and Engineering Research Board (SERB), Department of Science and Technology (DST). He has published close to 80 articles in reputed national and international journals and well cited. He has received many BEST-Paper awards and Best reviewer awards by several publishers. He has been awarded with Gold Medal "BRUNDA-BANSAHU MEMORIAL AWARD" by Institute of Engineers India (IEI-Odisha) in 2016 for his research contribution, received National level (Indian) Young Engineer award-2017 in the mechanical stream by IEI.

Prof. D. R. K. Parhi is working in NIT Rourkela as a Professor (HAG). He is currently heading the Department of Mechanical Engineering. He has received his Ph.D. in Mobile Robotics field from Cardiff School of Engineering, UK. He has 26 years of research and teaching experience in Robotics and Artificial Intelligence fields. He has guided more than 20 Ph.D. Theses and published more than 300 papers in various journals and conferences along with 3-patents. He has also completed and currently handling several sponsored research projects in the field of robotics.

Prof. B. B. Biswal is currently acting as vice-chancellor of the Odisha University of Technology and Research. He also served as Director of National Institute of Technology, Meghalaya during 2017 to 2022. He is also a Professor (HAG) in the Department of Industrial Design of NIT Rourkela. He has 37 years of research and teaching experience in FMS, CAD/CAM, Robotics fields. He has guided more than 15 Ph.D. Theses and published more than 200 papers in various journals and conferences along with 3-patents/copyrights. He has international collaboration with Loughborough University and Slovak University of Technology in Bratislava. He has also completed and currently handling several sponsored research projects in his research field.

Advances in Manufacturing Technology

Optimizing Quadcopter Structural Design: A Numerical Analysis on Strength and Stability



S. Shivani and Kamlesh Kumar

Abstract A rotorcraft UAV, adaptable for diverse applications, faces design challenges in tailoring quadcopters for purposes ranging from surveillance to heavy-lift operations. The quadcopter, characterized by its four-rotor configuration, offers simplicity, stability, and agility. The structural design of its body frame is crucial, serving as the foundation for integrity, resilience, weight distribution, and stability. This study employs Fusion 360 and ANSYS Workbench for comprehensive design and finite element analysis of seven quadcopter frame configurations, all utilizing Aluminum 6061. Rigorous assessments, including static, dynamic, and modal analyses, inform the selection of the optimal frame design in terms of structural integrity and efficiency.

Keywords Quadcopter · ANSYS · Structural analysis · Explicit dynamics · Modal analysis · Multirotor · UAV

1 Introduction

A quadcopter, also known as a quadrotor, is a UAV characterized by its four-rotor configuration, allowing precise control of position and orientation in three-dimensional space, including vertical take-off and agile maneuvering. This symmetrical design, constructed from lightweight materials like carbon fiber or aluminum, incorporates four brushless electric motors and propellers—two clockwise and two

S. Shivani
Centre of Excellence in Avionics and Navigation, Mechanical and Manufacturing Engineering, Manipal Institute of Technology, Manipal Academy of Higher Education, Manipal, India
e-mail: shivani.s1@learner.manipal.edu

K. Kumar (✉)
Centre of Excellence in Avionics and Navigation, Department of Aeronautical and Automobile Engineering, Manipal Institute of Technology, Manipal Academy of Higher Education, Manipal, India
e-mail: kamlesh.kumar@manipal.edu

© The Author(s), under exclusive license to Springer Nature Singapore Pte Ltd. 2025

B. B. V. L. Deepak et al. (eds.), *Recent Advancements in Product Design and Manufacturing Systems*, Lecture Notes in Mechanical Engineering,
https://doi.org/10.1007/978-981-97-6732-8_1

counterclockwise. Electronic Speed Controllers (ESCs) regulate motor speed under the command of a flight controller equipped with accelerometers, gyroscopes, and magnetometer, ensuring stability, and executing flight instructions. Additionally, a rechargeable lithium-polymer or lithium-ion battery provides power, while optional components like GPS modules, onboard computers, cameras with gimbals, sensors for collision avoidance and telemetry, and telecommand systems enhance capabilities for diverse applications. Quadcopters offer versatility, energy efficiency, and cost-effectiveness across industries, though limitations include limited flight times, payload constraints, sensitivity to adverse weather, and regulatory compliance, necessitating thoughtful deployment strategies. Their evolution spans decades, with breakthroughs in stability, control algorithms, and miniaturization during the 1990s, followed by widespread consumer adoption in the 2010s and ongoing advancements in the 2020s, promising increased efficiency and autonomy in various industrial applications.

The quadcopter's unique four-propeller configuration offers several advantages over traditional helicopters [1]. This design not only provides superior payload capacity but also allows for finer control precision. By reducing mechanical complexities, it enhances maneuverability and increases overall efficiency, enabling precise navigation and the transportation of heavier payloads. Consequently, it has become the preferred choice in a wide range of aerial applications.

The quadcopter's design has garnered popularity across diverse applications owing to its inherent characteristics of simplicity, stability, and agility. The research challenges and objective of the problem were the understanding of a quadcopter for designing for purpose, from low-lift applications such as spydrones and barrel-launch drones to heavy-lift applications such as armed drones, shell-dropping drones, and sprayers. Understanding its structure, strength requirements, and CFD analysis, current research presented to highlight structure design with single or hybrid material selection which is mainly focused on optimizing its stability by analyzing the strength requirements, arm deflection effects, joint load, vibration, etc.

For several basic reasons, the structural design of a quadcopter's body frame is extremely important. First, it takes on the function of the structural base, guaranteeing the UAV's durability and integrity to withstand the rigors of flight, including probable strains and unanticipated collisions. Second, the weight distribution greatly influenced by the design of the frame, which directly affects the quadcopter's stability and maneuverability. Therefore, achieving a balanced center of gravity becomes necessary to guarantee both the effectiveness and safety of flight operations as well as the safe deployment or execution of payloads.

To optimize structural integrity, minimize weight, and enhance the overall performance of quadcopters, finite element analysis (FEA) plays a pivotal role through virtual simulations. Specifically, FEA is crucial in the process of topology optimization [2]. The FEA methodology was majorly implemented through ANYSY for structural, modal, acoustic, and harmonic analysis to optimize the designs [3–8]. The performance of quadcopter body frames made of various materials, including aluminum, acrylic butadiene styrene (ABS), polylactic acid (PLA), carbon fiber-reinforced plastic (CFRP), and sandwich structures made of aluminum, copper alloys,

and stainless steel, could also be investigated using FEA-based analysis [9–13]. It was revealed that using a sandwiched structure or a combination of materials in the body frame could significantly increase the flight time [12, 14]. In addition to structural considerations, the choice of propellers, motor speed, and Electronic Speed Controllers (ESCs) is critical. These components must be carefully selected and configured to ensure optimal performance, stability, and lift capacity of the quadcopter [15, 16]. A substantial portion of quadcopter research has focused on propeller analysis and optimization. This is because propeller design and characteristics have a profound impact on a quadcopter's overall effectiveness, safety, and suitability for specific applications. Consequently, it remains a key area of investigation for researchers and engineers [1, 17–19]. Propeller-based body frame analyses indicated that four-blade propeller designs outperform two-blade designs due to lower stress levels, reduced deformation, and improved manufacturing potential [20]. Moreover, research in this field extends to micro to large quadcopters and 3D-printed drones, which can be rigorously simulated and tested before proceeding with manufacturing [2, 11, 21, 22]. Current efforts in this area concentrate on utilizing flight data to further optimize quadcopter design. It is worth noting that the stability of quadcopters is significantly influenced by vibrations, as evidenced by flight data analysis, and other structural anomalies are also under scrutiny [23, 24]. Generative design methodologies hold promise in structural design, effectively optimizing structures for performance, reducing weight, and eliminating potential points of failure [25]. Additionally, the mathematical modeling of control systems for fault detection, inspection, and monitoring has yielded significant success [26–31]. The dynamics governing angular acceleration, Newton's second law, and the Coriolis effect are thoroughly explored and incorporated into a comprehensive model [32]. Modeling quadcopters in MATLAB offers the advantage of designing and testing several types of controllers, further contributing to advancements in this field [33].

It can be concluded that the multifaceted nature of quadcopter research encompasses structural analysis, materials optimization, propeller design, stability enhancement, and control system development, all of which collectively advance the field of quadcopter technology. Notably, it is evident that within the realm of structural analysis, a predominant focus has been directed toward either the propeller system or the body frame base as primary areas of investigation. However, it is imperative to underscore the pivotal role played by the design of quadcopter arms within the body frame. These components hold paramount importance in ensuring both the structural integrity and stability of quadcopters during their flight operations. Quadcopter arms serve as critical elements in the equitable distribution of weight, the provision of support for various payloads, and the mitigation of undesirable vibrations—all of which are fundamental prerequisites for achieving optimal efficiency and safety in quadcopter operations.

Furthermore, the meticulous tailoring of quadcopter arm designs to align with specific mission requirements exerts a profound influence on various facets, including aerodynamics, crash resistance, and overall performance. However, despite its pivotal significance, it is evident that there exists a dearth of comprehensive studies in the domain of quadcopter arm analysis and optimization. In this research, seven

different designs of quadcopter arms are considered for comprehensive assessments encompassing structural, modal, and dynamics studies to discern the most optimal configuration. This concerted effort represents a critical stride toward advancing the understanding and refinement of quadcopter arm design, thereby contributing to the overarching body of knowledge in the realm of quadcopter technology.

This study uses Fusion 360, finite element analysis (FEA), and the ANSYS Workbench Environment to present a thorough design and modeling of seven different quadcopter's body frame configurations.

2 Theory

2.1 Quadcopter

Quadcopter design draws upon a multifaceted array of scientific theories and engineering principles. Fundamentally rooted in Newton's Laws of Motion, these aerial vehicles leverage aerodynamics, fluid dynamics, and materials science to optimize airframe and propeller design. Control theory plays a pivotal role, underpinning the creation of sophisticated control systems that stabilize quadcopters, control their movements, and enable complex flight maneuvers. Electronics, circuits, sensors, and robotics principles facilitate autonomous navigation and data processing, while computer science and mathematical modeling support the development of control algorithms. Considerations encompass battery technology, structural engineering, thermodynamics, and energy efficiency to enhance performance and safety. Compliance with safety regulations and communication theory also guides their integration into airspace. This interdisciplinary amalgamation culminates in the creation of efficient, capable, and reliable quadcopters for various applications.

2.2 FEA Analysis

Finite element analysis (FEA) is a numerical method used for structural analysis of a quadcopter frame, involving processes like modeling, meshing, applying boundary conditions, analysis, and verification [6, 19]. The analysis includes calculating stresses, strains, and deformations to verify strength, stability, and optimize the frame's design for performance and safety specifications. Critical calculations involve determining maximum bending moment, shear force, bending stress, shear stress, and critical load for buckling to ensure the frame can withstand required loads and stresses [3]. Dimensions for the frame are determined based on the calculated maximum bending moment, which causes the frame to bend and resisted by the cross-sectional shape and material properties of the frame [13]. The maximum shear force, resisted by the cross-sectional area of the frame, is half of the total weight of

the quadcopter. Shear stress then calculated using the shear force and cross section dimensions. Bending stress is determined by calculating the moment of inertia and distance from the neutral axis to the outermost point of the cross section, compared to the material's yield stress to prevent plastic deformation. Euler buckling analysis performed to determine the critical load at which the frame will buckle and fail, based on the modulus of elasticity and moment of inertia of the material [7, 9, 11].

3 Modeling

3.1 Modeling a Quadcopter

Modeling a quadcopter involves creating a mathematical or computational representation of its dynamics and behavior, a complex task considering various physical and environmental factors affecting its flight. Engineers and researchers often make assumptions to simplify the mathematical representation for tractable models used in control system design. The gyroscopic effect in a quadcopter significantly influences yaw stability and motion in response to roll and pitch commands, necessitating careful management for stable flight [34]. Both the rigid body and the four rotors, with some cases neglecting rotor gyroscopic effects [35], induce gyroscopic moments. Ground effect, occurring when a quadcopter flies close to the ground, is another assumption that impacts design considerations. Managing ground effect involves prioritizing thrust-to-weight ratio, adaptable altitude and yaw control systems, sensor enhancements, simulations, testing, and pilot training adjustments for flight stability [36, 37]. Quadrotor modeling must consider the drag and lift force of propeller rotation, generating thrust for flight and control forces for stability and maneuvering. Propeller thrust force is directly proportional to the square of rotation speed, while drag force's relationship is complex and influenced by factors like propeller design and airflow conditions [38–40]. Clockwise and anticlockwise propeller rotation with opposite pitch balances the torque generated during rotations.

3.2 Structural Body Frame of Quadcopter and Stability

The quadcopter's structural frame, made of materials like carbon fiber or aluminum alloy, is designed for lightweight durability. It typically consists of four arms extending from a central hub to support motors and propellers, with considerations for weight distribution, vibration dampening, and optional features like foldability or propeller guards for stability and functionality [41]. The inertia tensor, crucial for modeling and controlling rotational dynamics, is placed with respect to the center of mass, where Ixx resists roll, Iyy resists pitch, and Izz resists yaw [41]. Friction forces and moments, originating from components like motor bearings, propeller

shafts, and air resistance, impact performance and efficiency, necessitating careful design and maintenance [42]. While often neglected due to their relatively small magnitude, frictional forces and moments require attention to ensure optimal aerodynamics, weight, power efficiency, and stability [26, 31]. In quadcopter design, the Center of Mass (CoM) is the concentrated mass point impacting balance and stability, while the Coordinate System Origin (CSO) serves as the reference point for spatial measurements and control algorithms, typically coinciding with the CoM for simplified modeling and control [43]. Precise placement of these points is fundamental for stable flight and effective control. Some research explores intentional differences in CoM and CSO positions to study their effects on flight dynamics, control strategies, and performance under specific scenarios. Blade flapping effects, common in rotorcraft, may be negligible in quadcopters due to their small propeller sizes [22, 44]. Modeling adjustments for scenarios like sloped terrains, obstacles during take-off and landing, and wind conditions are crucial for safe and precise flight operations [45, 46].

3.3 Development of Software Model

The model was developed on Fusion 360 for a total mass of 1 kg. The quadcopter arms were modified and considered for seven different cases as shown in Fig. 1a–g. The models were considered for a two-layered rib structure, a one-layered rib structure, and a solidified structure. Another set was considered based on cross sections, i.e., circular and rectangular cross sections. Further two more cases were considered to reduce the mass constraint of the rectangular cross section one. The considered cases were a web structure as well as an internal layered structure.

3.4 Finite Element Analysis

Finite element analyses were conducted on ANSYS to understand the stability and rigidity of the structure. The material considered for the frames was Aluminum 6061 T6. Aluminum 6061 is a widely used aerospace material with a density of 2700 kg/m^3 (Table 1).

The tetrahedral meshing of 2 mm mesh size was used for every model. Tetrahedral meshing is favored for its flexibility in handling complex geometries, adaptivity for localized refinement, and suitability for 3D modeling in engineering and scientific simulations. Its ability to conform to irregular boundaries and versatility in representing intricate shapes make it valuable in various applications, but the choice of mesh type should align with specific simulation requirements.

The rigidity of the quadcopter body frame was analyzed considering the equality between the vertical thrust produced by each motor and the weight of the quadcopter during the flight time. To determine the thrust required for a small, lightweight

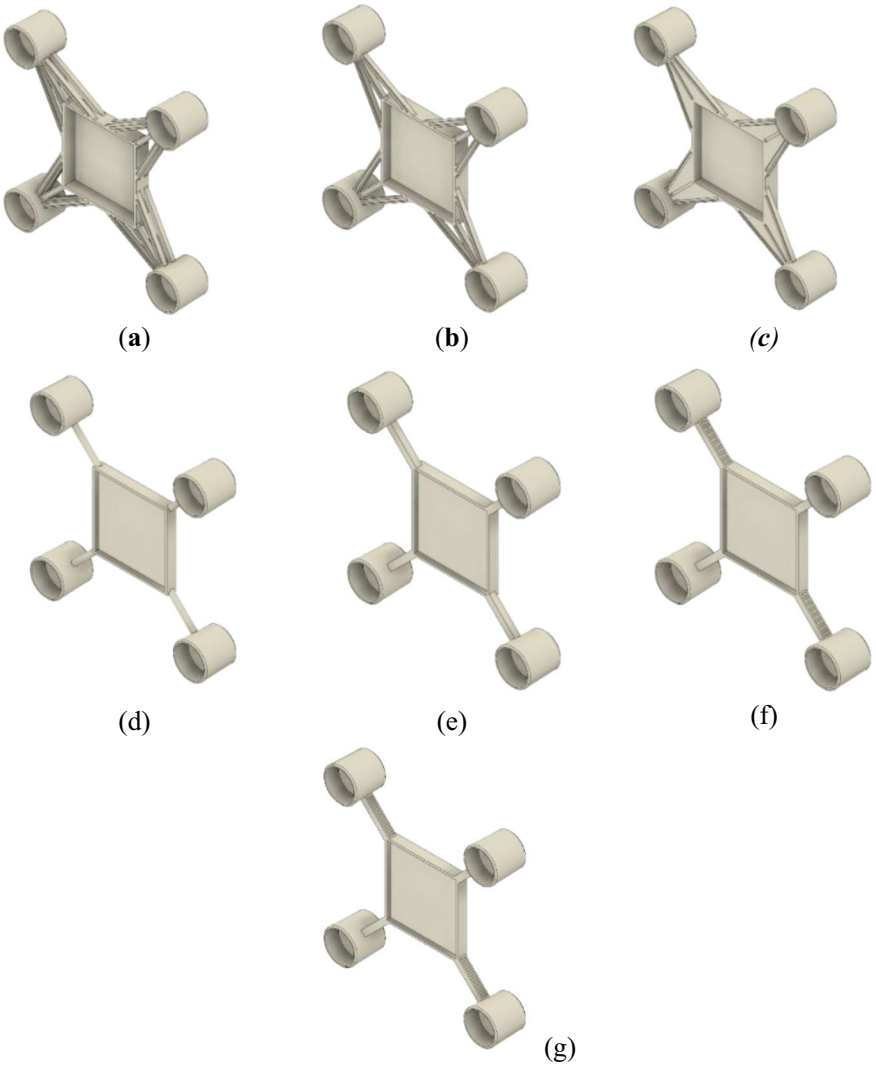


Fig. 1 Quadcopter arms with seven different cases: **a** case1-two-layered rib structure; **b** case2-one-layered rib structure; **c** case3-solidified structure; **d** case4-circular cross section; **e** case5-rectangular cross section; **f** case6-rectangular cross section with grid; **g** case7-rectangular cross section with parallel grids

drone, several factors must be considered, including the weight of the drone, all flight accessories, desired flight time, and flying style (i.e., hovering, forward flight, or acrobatics).

The following formula can be used to calculate the required thrust:

Table 1 Material properties of aluminum 6061 T6

Property	Units	Magnitude
Density	kg/m^3	2700
Ultimate tensile strength	MPa	310
Tensile yield strength	MPa	276
Modulus of elasticity	GPa	68.9
Notched tensile strength	MPa	324
Ultimate bearing strength	MPa	607
Bearing yield strength	MPa	386

$$\text{Thrust}(N) = \text{Weight}(N) \times \text{Thrust - to - Weight Ratio} \tag{1}$$

The Thrust-to-Weight Ratio (TWR) is the ratio of the maximum thrust that a motor can produce to the weight of the drone. A typical TWR for a quadcopter is around 2:1, indicating that the motor can produce twice the weight of the drone in thrust [3, 5, 8].

The considered drone weighs 1 kg (9.81 N), and we want to achieve a TWR of 2:1.

$$\text{Total thrust} = 1 \text{ kg} \times 2 \tag{2}$$

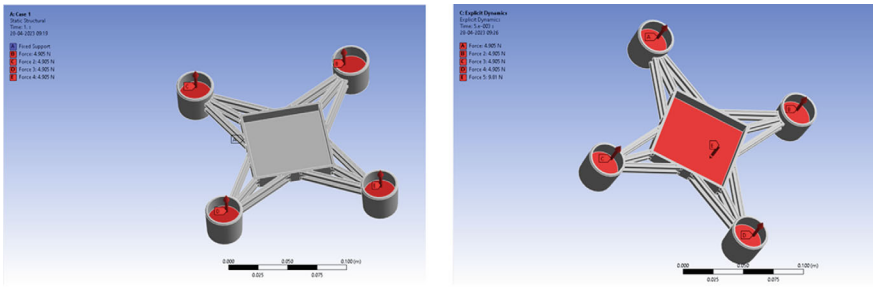
$$\text{Thrust} = 9.81 \text{ N} \times 2 = 19.62 \text{ N} \tag{3}$$

Next, we need to divide the total thrust required by four to get the thrust required for each motor since a quadcopter has four motors.

$$\text{Thrust per motor} = \text{Total thrust}/4; \tag{4}$$

$$\text{Thrust per motor} = 19.62 \text{ N}/4 \Rightarrow \text{Thrust per motor} = 4.905 \text{ N} \tag{5}$$

Therefore, each of the four motors in a 1 kg quadcopter must be capable of producing at least 4.905 N of thrust to achieve a TWR of 2:1. The boundary conditions calculated were provided to the simulation as shown in Fig. 2.



(**a**) (**b**)

Fig. 2 Boundary conditions of **a** static structural analysis, **b** dynamic analysis

4 Result and Discussions

4.1 Static Structural Analysis

The ANSYS static structural analysis was carried out on a quadcopter frame to assess its strength and stability. Finite element analysis (FEA) was performed to model the response of the quadcopter frame to various loads and ascertain its maximum stress, deformation, and safety factor. The deformations obtained from static structural analyses are shown in Fig. 3.

The analyses revealed that the quadcopter frames could withstand the loads for which they were designed without exceeding their yield strength or safety factor. The maximum stress and deformation values were well below the permissible limits, indicating that the quadcopter frame was structurally sound and capable of supporting the other quadcopter components. The stress contours obtained from the analyses

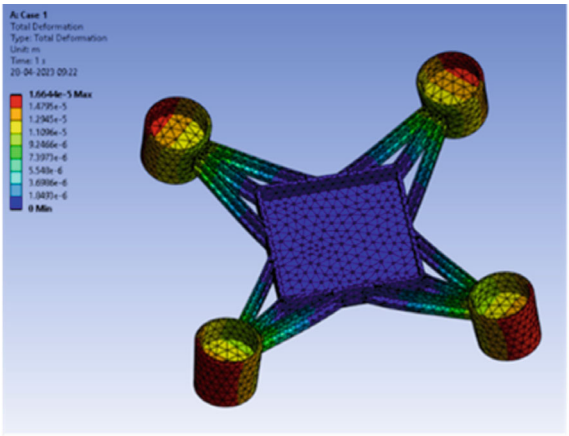


Fig. 3 Total deformation results based on static structural analysis of case 1

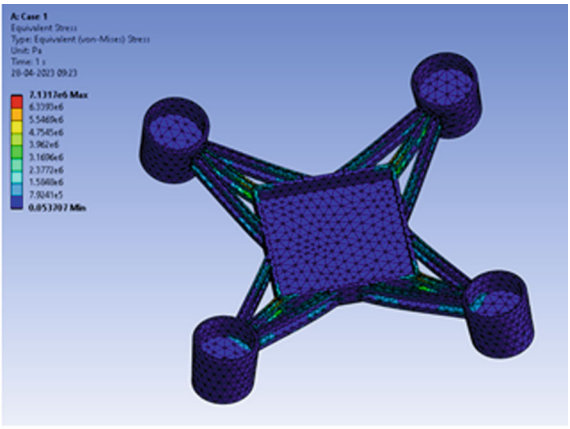


Fig. 4 Von Mises stress results based on static structural analysis of case 1

Table 2 Results of static structural analyses

Cases	Maximum deformation (m)	Maximum stress
Case 1	0.000016644	7.1317 e6 Pa
Case 2	0.0002345	35.513 e6 Pa
Case 3	0.000075664	7.8823 e6 Pa
Case 4	0.00013172	21.067 e6 Pa
Case 5	0.000074202	8.7438 e6 Pa
Case 6	0.00011729	19.945 e6 Pa
Case 7	0.000040787	7.6094 e6 Pa

are shown in Fig. 4. The results of both total deformation and von Mises stress are provided in Table 2.

Furthermore, the findings of the analysis identified areas where the quadcopter frame could be further optimized to enhance its strength and stability. For instance, optimizing the design of the motor mounts or adding extra supports to distribute the load more evenly could alleviate stress concentrations around these areas.

4.2 Dynamic Structural Analysis

A dynamic structural analysis using ANSYS Explicit Dynamics on a quadcopter frame to assess its ability to withstand high-impact loads and collisions during flight. By simulating various high-impact scenarios, we evaluated the stress, deformation, and damage to the quadcopter frame. The results of the analysis showed that the quadcopter frame can withstand high-impact loads without considerable damage or deformation. The simulations showed that the quadcopter frame has a high tolerance for impact loads due to its lightweight design and the use of strong, durable materials.

The total deformation contours and the von Mises stress results from dynamic analyses are shown in Figs. 5 and 6, respectively. The results of both total deformation and von Mises stress from dynamic analyses are provided in Table 3.

However, our analysis also revealed areas where the quadcopter frame could be further optimized to improve its resistance to high-impact loads. We found that the motor mounts and arms were susceptible to failure under extreme loading conditions, and thus, these areas could be reinforced or redesigned to increase their strength and durability. Additionally, our simulations demonstrated that the location and orientation of the components on the quadcopter frame significantly affected its resistance to high-impact loads. By adjusting the placement and orientation of the components, the quadcopter frame could be further optimized to improve its strength and durability under extreme loading conditions.

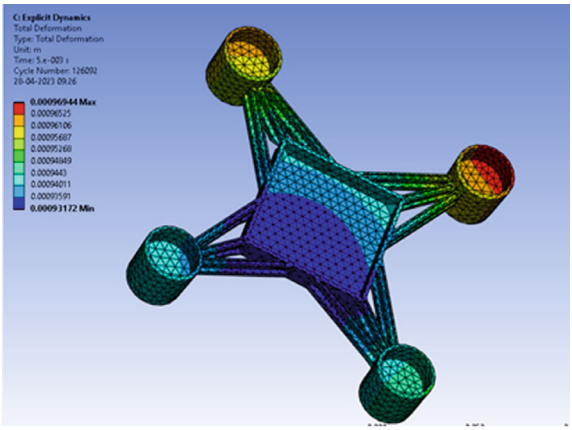


Fig. 5 Total deformation results based on dynamic structural analysis of case 1

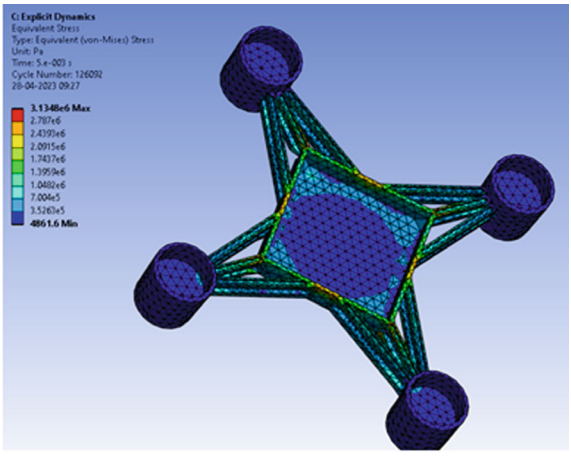


Fig. 6 Von Mises stress results based on dynamic structural analysis of case 1

Table 3 Results of dynamic structural analyses

Cases	Maximum deformation (m)	Maximum stress
Case 1	0.00096944	3.1348 e6 Pa
Case 2	0.00090454	12.788 e6 Pa
Case 3	0.00074806	0.62157 e6 Pa
Case 4	0.000019739	6.4024 e6 Pa
Case 5	0.0009047	1.159 e6 Pa
Case 6	0.0009117	0.4433 e6 Pa
Case 7	0.000045363	6.6708 e6 Pa

4.3 Modal Analysis

A modal analysis of a quadcopter frame was performed using ANSYS to assess its vibration characteristics and natural frequencies. Further, evaluated the mode shapes and natural frequencies of the quadcopter frame by simulating various vibration scenarios. The results are shown in Figs. 7 and 8. The first-mode frequency or the natural frequency of all the cases is provided in Table 4. This frequency represents the rate at which the system oscillates when subjected to external forces or disturbances, and it is a fundamental parameter in structural and mechanical engineering analysis. The specific value of the first-mode frequency depends on the characteristics of the system, including its mass distribution, stiffness, and boundary conditions.

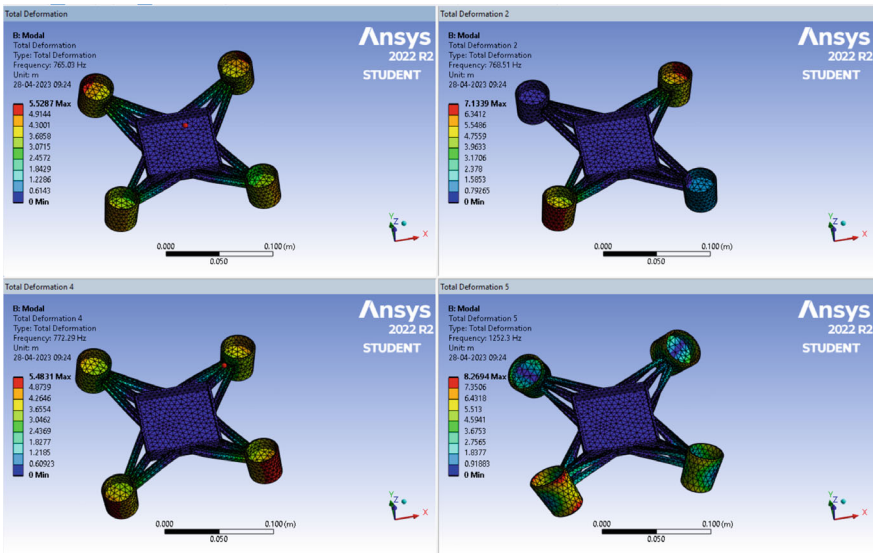


Fig. 7 Total deformation results of first 4 modes of case 1 based on modal analyses

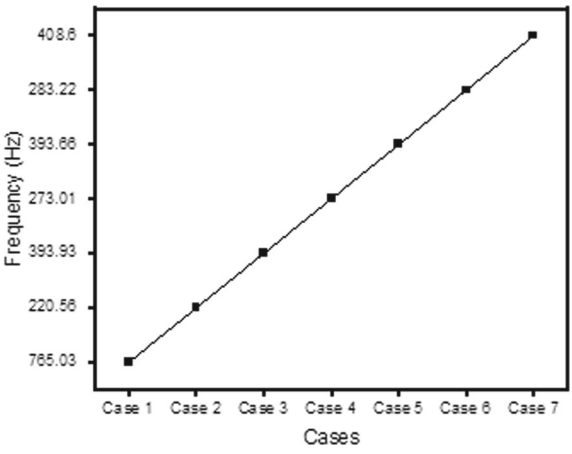


Fig. 8 First mode frequency of all cases

Table 4 First mode frequency based on modal analyses results

Cases	First mode frequency (Hz)
Case 1	765.03
Case 2	220.56
Case 3	393.93
Case 4	273.01
Case 5	393.66
Case 6	283.22
Case 7	408.6

The analysis showed that the quadcopter frame had multiple natural frequencies that fell within the expected range of flight vibrations. The mode shapes indicated that vibrations were focused on the motor mounts and arms, indicating that these areas are potential sources of failure.

Based on the results of the static structural analysis, it was found that case 2—the model with a single-layered rib structure—exhibited the highest stress concentration and deformation, while the double-layered rib structure experienced the least. Additionally, the rectangular cross section showed less stress concentration and deformation compared to the circular cross section. Similar conclusions can be made based on the results of the dynamic analyses. The introduction of web structure or layers in lieu of solid material reduced the likelihood of failure. The results of the modal analyses showed that the double-layered rib structure exhibited the highest first-mode frequency. A higher first-mode frequency suggests that the body has a strong resistance to deformation or vibration in the mode associated with this frequency. Furthermore, the rectangular cross section demonstrated better stability than the circular cross section, and the addition of layers and webs improved stability.

5 Result and Discussions

This study conducted a comprehensive examination of the influence of structural factors on quadcopter stability and strength, offering valuable insights into the design and analysis of quadcopter structures to enhance their stability and safety. A succinct review of current quadcopter design methodologies and analytical techniques was performed, followed by a meticulous numerical simulation analysis of how quadcopter arm geometry affects stability and strength. The research's findings indicate that quadcopter frames typically exhibit adequate load-bearing capabilities within their design parameters, without surpassing their yield strength or safety margins. However, areas such as motor mounts and arms may benefit from reinforcement or redesign to bolster their strength and overall durability. Notably, the location and orientation of components on the quadcopter frame were revealed to exert a significant impact on its resistance to high-impact loads. Adjusting these factors presents an opportunity to enhance the frame's strength and durability, especially under extreme loading conditions.

In terms of structural design, static and dynamic analyses were performed on a drone model, uncovering key insights. Specifically, a double-layered rib structure emerged as the optimal choice, as it exhibited minimal stress concentration and deformation. Furthermore, the adoption of a rectangular cross section, in lieu of a circular one, displayed reduced stress concentration and deformation, thereby contributing to improved stability. Introducing web structures or additional layers proved effective in mitigating the risk of structural failure. These findings collectively shed light on the critical considerations for quadcopter structural design, emphasizing the importance of tailoring geometric elements and reinforcement strategies to enhance both stability and resilience.

6 Conflicts of Interest

The authors declare no conflict of interest with the Centre of Excellence in Avionics and Navigation, Manipal Academy of Higher Education project work funded by the Government of India.

Acknowledgements The project was completed with the full support of the "Centre of Excellence in Avionics and Navigation. Manipal Academy of Higher Education (MAHE), Manipal. Software license utilized from the Department of Mechanical Engineering, MIT Manipal.

References

1. Ahmad F, Kumar P, Khan Y, Patil PP (2020) Flow and structural analysis of a quadcopter UAV. Int J Adv Res Eng Technol 11(8):880–888

2. Nvss S, Esakki B, Yang LJ, Udayagiri C, Vepa KS (2022) Design and development of unibody quadcopter structure using optimization and additive manufacturing techniques. Designs 6(1):10008. https://doi.org/10.3390/designs6010008
3. Javir AV, Pawar K, Dhudum S, Patale N, Patil S (2015) Design, analysis and fabrication of quadcopter. J Adv Res Mech Civil Eng 2(3):16–27
4. Md-Ahmed F, Zafar MN, Mohanta JC (2020) Modeling and analysis of quadcopter F450 FRAME. In: Proceedings of the 2020 international conference on contemporary computing and applications, IC3A 2020. Institute of Electrical and Electronics Engineers Inc., pp 196–201. https://doi.org/10.1109/IC3A48958.2020.233296
5. Singh R, Kumar R, Mishra A, Agarwal A (2020) Structural analysis of quadcopter frame. Mater Today Proceed 22:3320–3329. https://doi.org/10.1016/j.matpr.2020.03.295
6. Wei P, Yang Z, Wang Q (2015) The design of quadcopter frame based on finite element analysis. In: Proceedings of the 3rd international conference on mechatronics, robotics and automation (ICMRA 2015), vol 15. https://doi.org/10.2991/icmra-15.2015.260
7. Fruncillo F, Federico L, Cicala M, Citarella R (2022) Development and validation of an Aero-propulsive and Aeroacoustic simulation model of a quadcopter drone. Drones 6(6):143. https://doi.org/10.3390/drones6060143
8. Kuantama E, Craciun D, Tarca R (2016) Quadcopter body frame model and analysis. Annals of the Oradea University. Fascicle of Management and Technological Engineering. https://doi.org/10.15660/AUOFMTE.2016-1.3205
9. Kumar R, Kumar G, Zunaid M, Ansari NA (2020) Numerical analysis of quadcopter in different weather conditions of regions in India. In: Materials today: proceedings. Elsevier, pp 378–382. https://doi.org/10.1016/j.matpr.2020.11.681
10. Ahmad F, Kumar P, Patil PP (2021) Vibration characteristics-based pre-stress analysis of a quadcopter's body frame. In: Materials today: proceedings. Elsevier, pp 10329–10333. https://doi.org/10.1016/j.matpr.2020.12.458
11. Shelare SD, Aglawe KR, Khope PB (2021) Computer aided modeling and finite element analysis of 3-D printed drone. In: Materials today: proceedings. Elsevier, pp 3375–3379. https://doi.org/10.1016/j.matpr.2021.07.162
12. Zhang Q, Chen J, Yang L, Dong W, Sheng X, Zhu X (2015) Structure optimization and implementation of a lightweight sandwiched quadcopter. In: Lecture notes in computer science (including subseries lecture notes in artificial intelligence and lecture notes in bioinformatics). Springer, pp 220–229. https://doi.org/10.1007/978-3-319-22873-0_20
13. Ahmad F, Kumar P, Bhandari A, Patil P (2018) Finite element analysis based material optimization of a quadcopter body frame. Int J Mech Product 8(7):1342–1347
14. Bahuguna R, Sharma R, Biswas S, Nandakumar P (2020) Design and analysis of solar quadcopter. Recent trends in automation and automobile engineering. HBRP publication
15. Parihar P, Bhawsar P, Hargod P (2016) Design and development analysis of quadcopter. Int J Adv Comput Technol 5(6):2128–2133
16. Tatale O, Anekar N, Phatak S, Sarkale S (2019) Quadcopter: design, construction and testing. Int J Res Eng Appl Manag 4:1386
17. Ahmad F, Kumar P, Patil PP, Kumar V (2021) Design and modal analysis of a quadcopter propeller through finite element analysis. In: Materials today: proceedings. Elsevier, pp 10322–10328. https://doi.org/10.1016/j.matpr.2020.12.457
18. Ahmad F, Bhandari A, Kumar P, Patil PP (2019) Modeling and mechanical vibration characteristics analysis of a quadcopter propeller using FEA. In: IOP conference series: materials science and engineering. IOP Publishing Ltd. https://doi.org/10.1088/1757-899X/577/1/012022
19. Ahmad F, Kmar P, Patil PP (2020) Structural analysis of a quadcopter propeller using finite element method. In: Proceedings of the 2020 international conference on advances in computing, communication and materials (ICACCM). IEEE, pp 59–64. https://doi.org/10.1109/ICACCM50413.2020.9212874
20. Ahmad F, Kumar P, Patil PP, Dobriyal R, Avikal S (2023) Comparative analysis of two and four blades quadcopter propellers based on finite element method. Mater Today Proc 32:50

21. Bouabdallah S, Murrieri P, Siegwart R (2004) Design and control of an indoor micro quadrotor. www.aerovironment.com
22. Pounds P, Mahony R, Corke P (2010) Modelling and control of a large quadrotor robot. Control Eng Pract 18(7):691–699. https://doi.org/10.1016/j.conengprac.2010.02.008
23. Lakshmanan D, Saravanan P, Vadivelu P, Nivitha D, Yaswanth MS (2020) Performance analysis of medium altitude low-cost autonomous quadcopter. In: IOP conference series: materials science and engineering. Institute of Physics Publishing. https://doi.org/10.1088/1757-899X/764/1/012037
24. Jeon S, Kang J, Kim J, Cha H (2022) Detecting structural anomalies of quadcopter UAVs based on LSTM autoencoder. Pervasive Mob Comput 88:1736. https://doi.org/10.1016/j.pmcj.2022.101736
25. Bright J, Suryaprakash R, Akash S, Giridharan A (2021) Optimization of quadcopter frame using generative design and comparison with DJI F450 drone frame. IOP Conf Ser Mater Sci Eng 1012(1):012019. https://doi.org/10.1088/1757-899x/1012/1/012019
26. Freddi A, Monteriù A, Longhi S (2009) A model-based fault diagnosis system for a mini-quadrotor. In: Proceedings of the 7th workshop on advanced control and diagnosis (ACD)
27. Bertin S, Stéphan P, Ammann J (2022) Assessment of RTK quadcopter and structure-from-motion photogrammetry for fine-scale monitoring of coastal topographic complexity. Remote Sens 14(7):1679. https://doi.org/10.3390/rs14071679
28. Ostojić G, Stankovski S, Tejić B, Đukić N, Tegeltija S (2015) Design, control and application of quadcopter. Int J Ind Eng Manag 6(1):43–48
29. Katiar A, Rashdi R, Ali Z, Baig U (2018) Control and stability analysis of quadcopter. In: Proceedings of the 2018 international conference on computing, mathematics and engineering technologies (iCoMET). IEEE, pp 1–6. https://doi.org/10.1109/ICOMET.2018.8346419
30. Wang P, Man Z, Cao Z, Zheng J, Zhao Y (2016) Dynamics modelling and linear control of quadcopter. In: Proceedings of the 2016 international conference on advanced mechatronic systems (ICAMechS). IEEE, pp 498–503. https://doi.org/10.1109/ICAMechS.2016.7813499
31. Mian AA, Wang DB (2008) Dynamic modeling and nonlinear control strategy for an under-actuated quad rotor rotorcraft. J Zhejiang Univ Sci A 9(4):539–545. https://doi.org/10.1631/jzus.A071434
32. Ali MZ, Ahmed A, Afridi HK (2020) Control system analysis and design of quadcopter in the presence of unmodelled dynamics and disturbances. IFAC-Papers On Line 53(2):8840–8846. https://doi.org/10.1016/j.ifacol.2020.12.1397
33. Ahmed AH, Ouda AN, Kamel AM, Elhalwagy YZ (2015) Design and analysis of quadcopter classical controller. In: Proceedings of the 16th international conference on aerospace sciences and aviation technology, ASAT-16—May 26–28
34. Bouabdallah S, Siegwart R (2005) Backstepping and sliding-mode techniques applied to an indoor micro quadrotor. In: Proceedings of the 2005 IEEE international conference on robotics and automation. IEEE, pp 2247–2252. https://doi.org/10.1109/ROBOT.2005.1570447
35. Das A, Lewis F, Subbarao K (2009) Backstepping approach for controlling a quadrotor using Lagrange form dynamics. J Intell Robot Syst Theory Appl 56(1–2):127–151. https://doi.org/10.1007/s10846-009-9331-0
36. Bouabdallah S, Siegwart R (2007) Design and control of a miniature quadrotor. In: Advances in unmanned aerial vehicles. Springer, Dordrecht, pp 171–210. https://doi.org/10.1007/978-1-4020-6114-1_6
37. Guenard N, Hamel T, Eck L (2006) Control laws for the tele operation of an unmanned aerial vehicle known as an X4-flyer. In: Proceedings of the 2006 IEEE/RSJ international conference on intelligent robots and systems. IEEE, pp 3249–3254. https://doi.org/10.1109/IROS.2006.282432
38. Pounds P, Mahony R, Gresham J, Corke P, Roberts J (2004) Towards dynamically-favourable quad-rotor aerial robots. In: Barnes N, Austin D (eds) Proceedings of the 2004 Australasian conference on robotics and automation. Australian Robotics and Automation Association (ARAA), Australia, p 110

39. Bouadi H, Simoes Cunha S, Drouin A, Mora-Camino F (2011) Adaptive sliding mode control for quadrotor attitude stabilization and altitude tracking. In: Proceedings of the 2011 IEEE 12th international symposium on computational intelligence and informatics (CINTI). IEEE, pp 449–455. https://doi.org/10.1109/CINTI.2011.6108547
40. Dikmen IC, Arisoy A, Temeltas H (2009) Attitude control of a quadrotor. In: Proceedings of the 2009 4th international conference on recent advances in space technologies. IEEE, pp 722–727. https://doi.org/10.1109/RAST.2009.5158286
41. Güçlü A (2012) Attitude and altitude control of an outdoor quadrotor a thesis submitted to the graduate school of natural and applied sciences of Atilim University
42. Wierema M (2008) Design, implementation and flight test of indoor navigation and control system for a quadrotor UAV. TU Delft
43. Mokhtari A, Benallegue A (2004) Dynamic feedback controller of Euler angles and wind parameters estimation for a quadrotor unmanned aerial vehicle. In: Proceedings of the IEEE international conference on robotics and automation, 2004. Proceedings. ICRA '04. 2004. IEEE, pp 2359–2366. https://doi.org/10.1109/ROBOT.2004.1307414
44. Hoffmann G, Huang H, Waslander S, Tomlin C (2007) Quadrotor helicopter flight dynamics and control: theory and experiment. In: AIAA guidance, navigation and control conference and exhibit. American Institute of Aeronautics and Astronautics, Reston. https://doi.org/10.2514/6.2007-6461
45. Cabecinhas D, Naldi R, Marconi L, Silvestre C, Cunha R (2010) Robust take-off and landing for a quadrotor vehicle. In: Proceedings of the 2010 IEEE international conference on robotics and automation. IEEE, pp. 1630–1635. https://doi.org/10.1109/ROBOT.2010.5509430
46. Ghazbi SN, Aghli Y, Alimohammadi M, Akbari AA (2016) Quadrotors unmanned aerial vehicles: a review. Int J Smart Sens Intell Syst 9(1):309–333

Multi-Objective Optimization of Brake Force Distribution for Enhanced Thermal Management in Hydraulic Brake Systems using PESA 2 Algorithm



Indranil Banik and Arup Kumar Nandi

Abstract Brake force distribution is a pivotal aspect of vehicular safety and performance, profoundly impacting the heat generation and dissipation within drum brake systems. This research investigates the intricate relationship between brake force distribution ratio (β) and the heat flux experienced by drum brakes during variable braking events. The present research is motivated to find an appropriate β and thereby employs computational modeling to elucidate the multifaceted effects of force distribution on the thermal behavior of hydraulic drum brakes. Respective design parameters are chosen to optimize the hydraulic brake design components using multi-objective evolutionary algorithm (MOEA). An optimal β of 0.686 is determined, which splits the brake forces appropriately between the front and rear axles to obtain a balanced heat flux of 1.98 W/mm^2. Such insights are invaluable for designing safer and more efficient braking systems, with inferences on the vehicle braking performance, longevity, and overall road safety.

Keywords Drum brakes · Brake force distribution · Brake performance · Heat flux · Multi-objective evolutionary algorithm · Optimization

1 Introduction

When a vehicle's brakes are used, the brake shoes press against the inner surface of the brake drum, creating friction that slows down the vehicle. The distribution of brake force plays a crucial role in determining the uniformity of contact between the brake shoes and the brake drum. If the force distribution is uneven, it causes uneven wear on the brake lining and patchy heat distribution. This can lead to hotspots,

I. Banik (✉)
Academy of Scientific and Innovative Research (AcSIR), Ghaziabad, Uttar Pradesh, India
e-mail: indranil.cmeri20a@acsir.res.in

I. Banik · A. K. Nandi
CSIR-Central Mechanical Engineering Research Institute, Durgapur, West Bengal, India
e-mail: nandi@cmeri.res.in

© The Author(s), under exclusive license to Springer Nature Singapore Pte Ltd. 2025

B. B. V. L. Deepak et al. (eds.), *Recent Advancements in Product Design and Manufacturing Systems*, Lecture Notes in Mechanical Engineering,
https://doi.org/10.1007/978-981-97-6732-8_2

where certain areas of the brake drum experience elevated temperatures (localized overheating) and subsequently reducing braking efficiency.

Ahmed et al. [1] investigated the impact of modifying the drum brake lining morphology on braking performance, focusing on the effects of baseline temperature and brake oil pressure, since elevated temperatures especially during fade and recovery cycles can cause increased wear and shortened lifespan of the brake lining. Wai et al. [2] studied the design of wheel cylinder for delineating the brake torque generation and temperature rise of the rear drum brakes of the hydraulic braking system. It may be inferred that there is an increase in friction factor (10–19%) at high contact pressure, and this effect can be ascribed to the thermo-mechanical loading [3]. The uneven distribution of heat also contributes to the warping of the brake drum, resulting in brake pedal pulsation and reduced braking performance, as well as brake fade where the friction material becomes less effective at stopping the vehicle.

Improved *brake force distribution* (BFD) enhances brake performance, leading to better directional stability, reduced braking distance and time, and ultimately improving vehicle safety [4, 5] without causing uneven wear or excessive heat build-up [6]. The utilization of fuzzy inference and reinforcement learning techniques, with input parameters of brake pedal opening and change rate, enhances the control performance and functionality of hydraulic brake systems [7, 8].

In the realm of material or friction study, a systematic analysis of the brake momentary temperature fields entails the establishment of a model-based design approach, coupled with numerical analyses under different topography characteristics and vehicle duty cycles [9] to enhance comprehension of the brake drum's temperature traits with changes in brake cylinder pressure. Nevertheless, it is crucial to acknowledge that this method exclusively concentrates on the mechanical aspect, thereby restricting the study's scope. To ensure safe and effective braking under varying road conditions, it is essential to consider several factors like adhesion coefficient, wheel camber angle, etc. and their relationship with brake temperature, applied force, and vehicle speed. At high temperatures, the reduction in lining friction coefficient can lead to critical situations. In this instance, the braking force is drastically reduced. By automatically adopting brake cylinder pressure, machine learning methods are utilized to develop deceleration feedback-based braking system to optimize braking time, temperature and addresses oscillations resulting from fluctuations in the friction coefficient during braking [10, 11]. Another strategy is to alter the brake configuration throughout the braking process in accordance with fluctuations in the coefficient of lining friction to maintain the proper BFD due to the high sensitivity of the produced brake force to such variations [12, 13]. But in practical case, this is not viable as it renders complications in brake design and manufacturing. To alleviate the issue of low precision and meager robustness, advanced algorithms for estimating master cylinder pressure was devised taking into account the changes in friction coefficient of brake lining of electro-hydraulic brake system and vehicle inertia under specific conditions, such as road slope variations and temperature fluctuations [14, 15].

Hence, the primary aim of this paper is to formulate a well-balanced BFD that takes into consideration the longevity of brake components by appropriate heat dissipation and improve performance of the overall hydraulic braking system. This is achieved by

parametric optimization of the drum brake components to ensure maximum efficacy under variable vehicle initial speed and braking conditions using Pareto envelope-based selection algorithm (PESA 2) [16]. It is a sophisticated optimization technique that is extensively used to tackle multi-objective optimization problems (MOOPs) like B-spline curve approximation [17], renewable energy based multi-generation systems [18], etc. The remainder of the paper is organized as follows: Sect. 2 outlines the design analysis and problem formulation, along with the optimization algorithm employed in this study. Section 3 provides a concise overview of the results and discussions. The paper concludes with Sect. 4.

2 Design Analysis and Problem Formulation

Twin leading shoe-type drum brake installed at the rear wheels is considered for optimization to improve the brake design for better thermal management. Light duty passenger vehicle is taken into account for the said purpose.

2.1 Objective Functions

Temperature Increment Function. During braking, vehicle momentum is mainly converted to thermal energy through friction between brake shoe and drum. Increment in temperature rise at the rear axle can be calculated in accordance with the percentage of brake force deployed at respective axles and it is defined by Eq. (1) [19].

$$\text{Minimization} \quad f_T = \frac{1}{2} \frac{m_a v_a^2}{(m_d c_d + m_h c_h) \times 10^{-9}} (1 - \beta) \tag{1}$$

where m_a represents the overall vehicle mass (Kg); m_d denotes the individual combined drum brake mass (Kg); m_h signifies the collective mass of the heating metal composites connecting friction plate to the brake drum (Kg); c_d and c_h are their respective specific heat capacity (J/Kg K); v_a is the initial vehicle velocity (m/s).

$$m_d = 2\rho_d e \cdot (2\pi R) b_2 \tag{2}$$

$$m_h = 2\rho_h j \cdot (2\theta R) b_1 \tag{3}$$

j is the thickness of the brake shoe, b_1 and b_2 define the friction plate width and brake drum width correspondingly; whereas e denotes the thickness of the brake drum, θ is the arc length of contact between the friction material and the rotor, R defines the brake effective action radius, d is the brake piston/cylinder diameter; the substantial

material concentration of the brake drum and brake shoes is denoted by ρ_d and ρ_h, respectively. Considering, η as the braking efficiency, β can be expressed as [20]:

$$\beta = \frac{R_f \eta_f d_f^2}{R_f \eta_f d_f^2 + R_r \eta_r d_r^2} \tag{4}$$

Subscript (f) and (r) in Eq. (4) defines configuration at front and rear axles, respectively. Therefore, β is a function of the following specified design variables as demarcated in Eq. (5).

$$\beta = f\left(R_f, R_r, d_f, d_r\right) \tag{5}$$

Brake Stability Function. When the road friction coefficient matches the vehicle's braking rate, the adhesion conditions are important for effective deceleration [21]. If the adhesion coefficient is significantly lower, issues such as skidding or loss of control can occur. The ideal scenario would be comparable utilization of the braking rate and adhesion coefficient, resulting in a more appropriate distribution of braking torque. The corresponding objective function with fixed β can be defined as follows [22]:

$$\text{Minimization} \quad f_S = \sqrt{\left(\phi_f - z\right)^2 + \left(\phi_r - z\right)^2} \tag{6}$$

where φ_f and φ_r are road adhesion utilization coefficients during deceleration at front and rear wheels, respectively, and are expressed as follows:

$$\phi_f = \frac{L\beta z}{n + z \cdot h_g} \tag{7}$$

$$\phi_r = \frac{L(1-\beta)z}{m - z \cdot h_g} \tag{8}$$

In this context, m and n denote the distance of the vehicle's center of gravity (C.G.) from front and rear axles, respectively (m), L is the wheelbase (m), h_g is the height of vehicle C.G. from the road surface (m) and z denotes the brake strength.

2.2 Constraint Functions

Wheel Lock Sequence Constraint. Once the rear wheels lock and the vehicle's angular deviation surpasses a specific threshold, regaining control becomes unattainable even with full release of the brakes. Therefore, wheel lock sequence is very much important in designing the braking system. The locking of the front wheels should

precede that of the rear wheels, ensuring that the loss of steering control is mitigated through a partial release of the brakes when the front wheels are locked. According to *Economic Commission of Europe* (ECE), for brake strength varying in the range $0.1 \leq z \leq 0.78$, the constraint in relation to order of wheel lock can be articulated as follows:

$$\phi_f \geq \phi_r \Rightarrow \beta \geq \frac{n + z \cdot h_g}{L} \tag{9}$$

Heat Flux Constraint on Friction Liners. Wear, scuffing, and material deterioration are all significantly influenced by the surface temperature that is produced in the contact regions during braking [23]. This induces degradation of the drum brake friction lining with heat dissipation to the surroundings. Considering, wheel slip = 4%, with maximum brake strength, $z = 0.75$ and brake line pressure (p) varying in range (6.0–7.5) MPa; decelerating from $v_a = 100$ km/h without brake self-lockup and percentage heat distribution onto rotor = 0.90, the allowable heat flux or the maximum energy dissipating rate of the brake drum = 2.35 W/mm^2 [24]. Hence, the following constraint function illustrates the specific rate at which energy is dissipated by the frictional liners:

$$\frac{m_a v_a^2}{8t\theta \cdot R \cdot b_1} \leq 2.35 \tag{10}$$

where t = Braking time (s) = v_a/z;

2.3 Domain of the Design Variables

Main factors effecting the heat flux and brake force distribution of the friction braking system are θ, R, d, e, $b_{1,}$ and b_2. Therefore, the specified brake system parameters are chosen as design variables to solve the optimization problem. The domain of the design variables is stated as follows:

$$\begin{aligned} &90^\circ \leq \theta \leq 120^\circ && 5 \text{ mm} \leq e \leq 16 \text{ mm} \\ &36 \text{ mm} \leq b_1 \leq 75 \text{ mm} && 90 \text{ mm} \leq b_2 \leq 120 \text{ mm} \\ &90 \text{ mm} \leq R_f \leq 160 \text{ mm} && 70 \text{ mm} \leq R_r \leq 150 \text{ mm} \\ &40 \text{ mm} \leq d_f \leq 60 \text{ mm} && 30 \text{ mm} \leq d_r \leq 50 \text{ mm} \end{aligned}$$

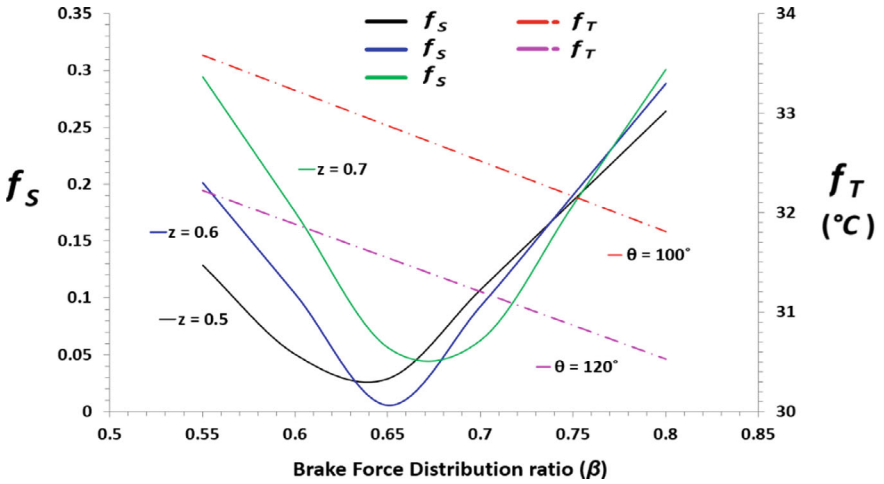


Fig. 1 Plot of f_T and f_S with respect to brake force distribution ratio (β)

2.4 Analysis of the Objective Functions with respect to BFD

The common variable between f_T and f_S is β. Other variables affecting f_T are (θ, e, b_1, b_2) and that for f_S are (z, m, n, h_g). Keeping other design specifications persistent, the variations of f_T and f_S corresponding to β are shown in Fig. 1.

Though with increase in brake line pressure at the respective axles, temperature of the brake lining should upsurge, but in current scope f_T decreases with a linear slope of 0.3463° per 0.05 unit increase in β since brake surface area increases correspondingly. From Fig. 1, it can be observed that the value of f_T attains minimum at 30.5 °C for $\theta = 120°$.

Conversely, while f_S serves as minimization function, a decrease in β leads to insufficient brake torque generation by the front wheels, resulting in limited adhesion utilization and potential rear wheel lockup. Whereas with augmentation in β, more braking forces are exerted onto front wheels enhancing dynamic stability of the vehicle during braking. Consequently, the variation of f_T and f_S with respect to β is contradictory corresponding to other design parameters and hence serves the basis of optimization.

2.5 Optimization Algorithm

PESA 2 is intended to construct a convex hull known as the Pareto envelope around these non-dominated solutions in the objective space. During selection, solutions lying on this envelope are prioritized for their representativeness and diversity, ensuring a comprehensive coverage of the trade-offs among conflicting objectives.

PESA 2 is more efficient than other evolutionary algorithms because it combines the Pareto dominance concept with cluster analysis to effectively select features in multi-label datasets [25] by using Pareto ellipsoids to represent and visualize parametric uncertainty, thereby enhancing sample diversity and algorithm exploration [26] to find global optimal results specifically in relation to optimal driving strategy [27].

The basic working principle of PESA 2 is illustrated in Fig. 2. The PESA 2 algorithm initiates by generating a randomly composed internal population (IP) alongside an empty archive population (AP). Non-dominated solutions within the IP are first integrated into the AP, and subsequent genetic operators are applied to produce offspring. Notably, candidate solution selection for the mating pool relies on a squeeze factor rather than the domination criteria employed by NSGA 2 [28]. The archive undergoes continual updates as each offspring is incorporated one by one. If the size of the updated archive population (TAP) surpasses a predefined limit, surplus solutions with the maximum squeeze factor are randomly eliminated to uphold a consistent size for the AP. The settings of PESA 2 parameters used in solving the MOOP are defined in Table 1.

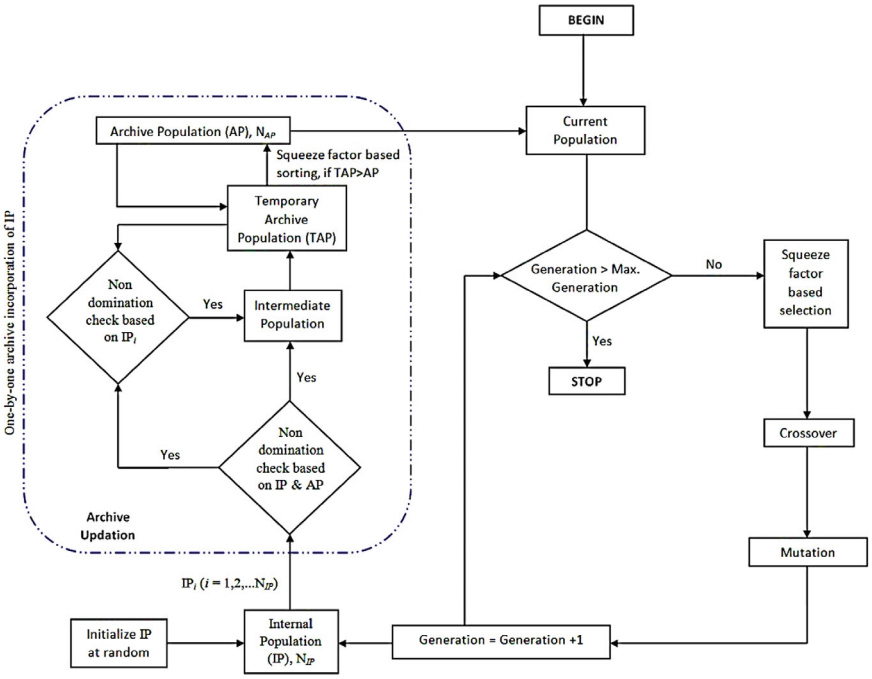


Fig. 2 Working principle of PESA 2

Table 1 Values of different EA-parameters

Attributes	Values	Attributes	Values
Number of generations	150	Random seed	0.4
Population size	100	Archive population	200
Chromosome length	160	Grid size	12
Crossover probability	0.97	Mutation probability	0.01

3 Results and Discussion

Determining the optimal design parameters for the hydraulic braking system under a fixed BFD requires considering the values of diverse vehicle model parameters outlined in Table 2. ε denotes the abrasion factor existing between the friction plate and brake drum. Considering, $\eta = \eta_f = \eta_r$, the required objectives are analyzed initially for viability of multi-objective optimization and then solved using PESA 2.

Table 3 enlists the Pareto optimal solutions acquired from solving the MOOP using PESA 2 which are statistically evaluated on the basis of mean and standard deviation. It can be observed that when decelerating from higher initial velocity, temperature increment of the drum brakes is comparatively higher for the same brake strength.

Figures 3 and 4 represent the Pareto fronts at varying deceleration range for different initial velocity v_a, respectively. Minimization of f_S is inversely proportionate to the operating brake temperature rise (also seen in Fig. 1) since with higher brake strength, the brake friction lining is rubbed more generating high heat energy. But

Table 2 Model parameters [5]

Attributes	Values	Attributes	Values
m_a	1950 kg	j	10 mm
p	6.82 MPa	m	1.30 m
ε	0.35	n	1.45 m
c_d, c_h	482 J/Kg K	hg	0.575 m
ρ_d, ρ_h	7570 kg/m^3	η	0.8

Table 3 Performance analysis of PESA 2

Objective functions		$v_a = 50$ km/h		$v_a = 80$ km/h	
		Wet road ($\mu = 0.4$)	Dry road ($\mu = 0.8$)	Wet road ($\mu = 0.4$)	Dry road ($\mu = 0.8$)
		$z = (0.20–0.35)$	$z = (0.40–0.75)$	$z = (0.20–0.35)$	$z = (0.40–0.75)$
f_T	Mean	22.816	27.526	26.377	34.814
	Std. Dev	1.072	5.137	2.717	3.751
f_S	Mean	0.047	0.046	0.087	0.112
	Std. Dev	0.038	0.032	0.045	0.079

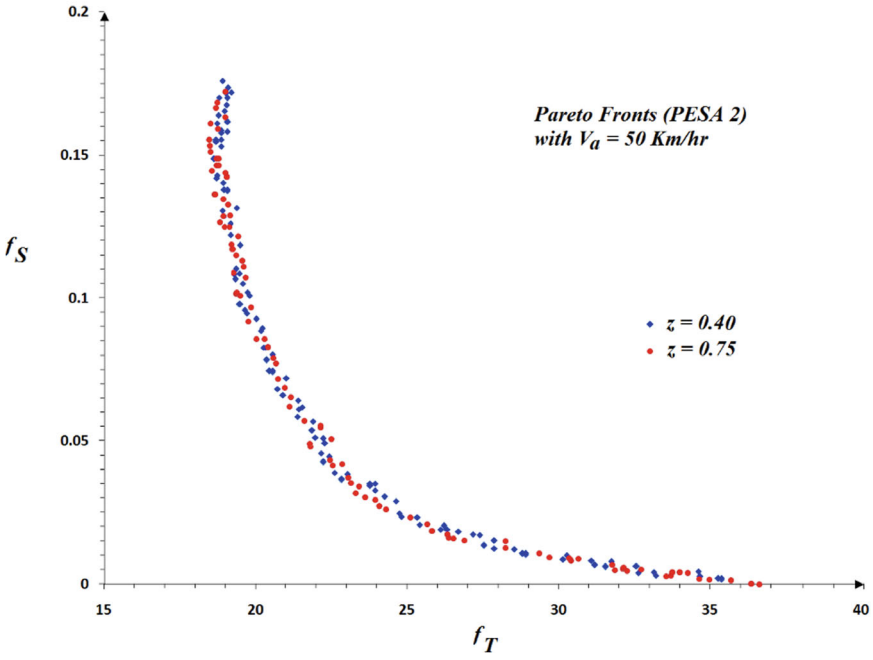


Fig. 3 PESA 2 Pareto fronts at different brake strength (z) for $v_a = 50$ km/h

since both f_T and f_S are minimization function, they are having confrontational behavior of the Pareto fronts as observed in Figs. 3 and 4. It is observed that, for 2° rise in f_T, the average percentage change in f_S is approximately 23.54%. Maximum temperature observed while decelerating from $v_a = 80$ km/h, with higher brake strength is 43.5 °C.

Gaining insight into the scope of each objective and the configuration of the Pareto optimal frontier offers valuable guidance for decision-making. However, the critical step lies in identifying and selecting a singular preferred Pareto optimal solution for integration into the design strategy. In this present problem, reference point-based multi-criteria decision-making (MCDM) technique is adopted after the optimization process [29] to identify a single preferred solution.

Optimal brake design parameters obtained by MCDM are enlisted in Table 4. Suitable fixed β obtained using Eq. (4) is 0.686 with even distribution among left and right wheels. This helps in a balanced heat distribution with maximum heat flux of 1.98 W/mm^2 which is in allowable range according to Eq. (10). This reduces the wear of friction lining at higher deceleration rates. Using optimized design variables in Table 4, maximum increment in temperature rise during braking operation is in range of (24.8–27.3) °C which is in accordance with specifications guidance for substituting brake linings and drum brake linings in motorized vehicles and trailers [30].

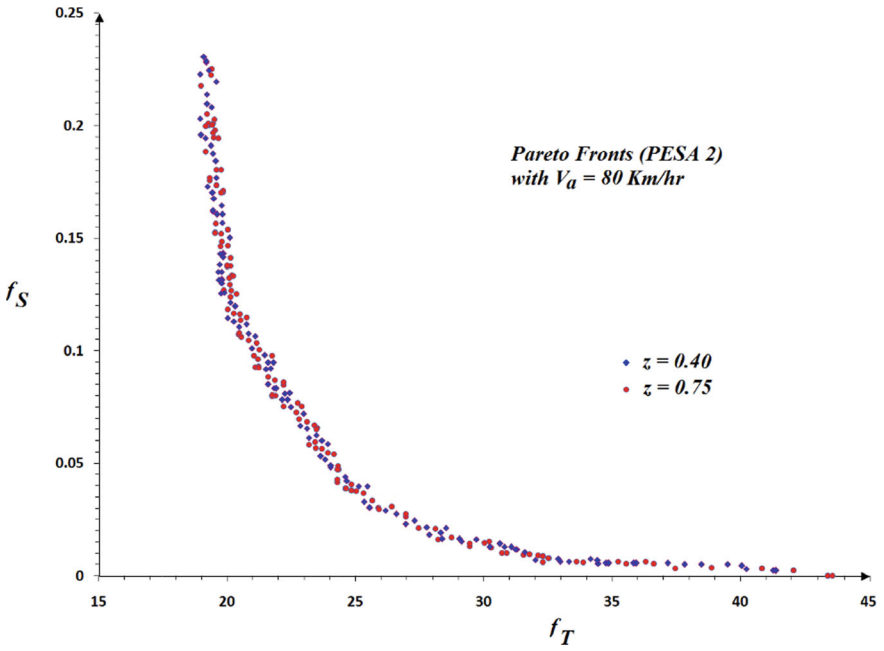


Fig. 4 PESA 2 Pareto fronts at different brake strength (z) for $v_a = 80$ km/h

Table 4 Optimized decision variables after MCDM for brake strength varying in the range $0.2 \leq z \leq 0.75$

Design variables	θ (°)	e (mm)	R_f (mm)	R_r (mm)	d_f (mm)	d_r (mm)	b_1 (mm)	b_2 (mm)
Optimal value	115.83	12.69	133.44	106.17	40.034	30.32	74.67	92.91
Std. Dev	2.622	2.968	11.260	7.295	2.875	1.476	1.270	9.28

4 Conclusion

In this paper, an attempt is made to find optimal design parameters of a hydraulic drum brake system that will help in proper heat dissipation maintaining suitable temperature field on the brake drum. The optimization yields a trade-off between the objectives among the Pareto optimal solutions and thereby optimum results are obtained using reference point-based MCDM technique. Correspondingly, a balanced β is found out that will help in maximizing the road adhesion utilization while maintaining the dynamic stability of the vehicle restricting wheel lock.

Upon examining the outcomes and juxtaposing them with ECE regulations, it is evident that the optimization model employed is suitable for designing hydraulic

brake systems, particularly in attaining balanced heat flux levels during higher deceleration rates. The research enhances our understanding of the complex relationship between brake force distribution and heat flux in drum brakes, which can be used to design more efficient brake systems that dissipate heat effectively and provide consistent and reliable braking performance even under diverse operating conditions.

Acknowledgements The first author is thankful to Council of Scientific and Industrial Research (CSIR), New Delhi, India, for supporting this research under the CSIR-JRF (GATE) fellowship program.

Conflict of Interest The authors have no conflict of interest.

References

1. Ahmed I, Sofan H, Abdelwahed K, Fatouh Y, Allam EM (2019) Effect of changing drum brakes lining form on the brake performance. Int Res J Eng Technol 06(02):798
2. Wai KK, San NA, Tun HM (2014) Design of wheel cylinder and average temperature rise of brake drum for rear drum brake of hydraulic brake system. Int J Sci Eng Technol Res 3(11):2563–2569
3. Shahid E, Wang X, Fan Z, Gui L (2018) Numerical simulation of the stress, temperature and wear behaviours of the drum brake. IOP Confer Ser Mater Sci Eng 398(1):11. https://doi.org/10.1088/1757-899X/398/1/012018
4. Her H, Cho W, Yi K (2011) Vehicle stability control using individual brake force based on tire force information. In: Proceedings of the 14th international IEEE conference on intelligent transportation systems, Washington, DC, pp 1205–1210
5. Bryant D, Day A (2022) Braking of road vehicles, 2nd edn. Butterworth-Heinemann
6. Yan M, Xu J (2018) Prediction model for brake-drum temperature of large trucks on consecutive mountain downgrade routes based on energy conservation law. Math Probl Eng 2018:1–10. https://doi.org/10.1155/2018/4587673
7. Wyrwał D, Lindner T, Nowak P, Białek M (2020) Control strategy of hydraulic cylinder based on deep reinforcement learning. In: Proceedings of the 2020 international conference mechatronic systems and materials (MSM), Bialystok, Poland, pp 1–5. https://doi.org/10.1109/MSM49833.2020.9202351
8. Chen P, He Z, Chen C, Xu J (2018) Control strategy of speed servo systems based on deep reinforcement learning. Algorithms 11(5):65. https://doi.org/10.3390/a11050065
9. Patekar M, Patil J, Palanivelu S, Bhat B (2017) Transient 1D mathematical model for drum brake system to predict the temperature variation with realistic boundary conditions. In: SAE technical paper 2017-26-0299. https://doi.org/10.4271/2017-26-0299
10. Wang Y, Wen X, Meng H, Zhang X, Li R, Serra R (2023) Accuracy improvement of braking force via deceleration feedback functions applied to braking systems. Sensors 23(13):5975. https://doi.org/10.3390/s23135975
11. Nakazawa S (2021) Accuracy improvement of braking distance by deceleration feedback function applying to brake system. Quart Rep RTRI 62(3):167–172. https://doi.org/10.2219/rtriqr.62.3_167
12. Mahmoud K (2005) Theoretical and experimental investigations on a new adaptive duo servo drum brake with high and constant brake shoe factor. Thesis. https://www.researchgate.net/publication/315759957
13. Cao L, Downey A, Laflamme S, Taylor D, Ricles J (2015) Variable friction device for structural control based on duo-servo vehicle brake: modeling and experimental validation. J Sound Vibr 348:41–56. https://doi.org/10.1016/j.jsv.2015.03.011

14. Seo M, Yoo C, Park S-S, Nam K (2018) Development of wheel pressure control algorithm for electronic stability control (ESC) system of commercial trucks. Sensors 18(7):2317. https://doi.org/10.3390/s18072317
15. Shi B, Xiong L, Yu Z (2021) Pressure estimation based on vehicle dynamics considering the evolution of the brake linings' coefficient of friction. Actuators 10(4):76. https://doi.org/10.3390/act10040076
16. Corne D, Jerram N, Knowles J, Oates M (2001) PESA-II: region-based selection in evolutionary multi objective optimization. In: Proceedings of the 6th international conference on parallel probably solving from nature PPSN-VI
17. Ülker E (2013) B-Spline curve approximation using Pareto envelope-based selection algorithm-PESA. Int J Comput Commun Eng 2(1):60
18. Cao Y, Rad HN, Jamali DH, Hashemian N, Ghasemi A (2020) "A novel multi-objective spiral optimization algorithm for an innovative solar/biomass-based multi-generation energy system": 3E analyses, and optimization algorithms comparison. Energy Conver Manag 219:112961
19. Zhang Y, Zhang H, Lu C (2012) Study on parameter optimization design of drum brake based on hybrid cellular multi-objective genetic algorithm. Math Probl Eng 2012:734193. https://doi.org/10.1155/2012/734193
20. Banik I, Nandi AK, Mondal B (2023) Finding a generic fixed brake force distribution through optimizing hydraulic brake system parameters to prevent wheel lock. World J Eng 31:106. https://doi.org/10.1108/WJE-04-2023-0106
21. Li YF, Zhou LL (2012) Optimization design of EV electro-hydraulic composite braking system control algorithm with multi-boundary conditions. Chin J Mech Eng 23(21):2635–2640
22. Fengjiao Z, Minxiang W (2015) Multi-objective optimization of the control strategy of electric vehicle electro-hydraulic composite braking system with genetic algorithm. Adv Mech Eng 7(3):8491. https://doi.org/10.1177/1687814014568491
23. Dinberu B, Yoseph B (2019) Investigation of mechanical and thermal properties of drum brake for light duty vehicle application. IJISET Int J Innov Sci Eng Technol 6:6
24. Limpert R (2011) Brake design and safety, 2nd edn. SAE International
25. Gu Q, Chen S, Jiang S, Xiong N (2021) Improved strength Pareto evolutionary algorithm based on reference direction and coordinated selection strategy. Int J Intell Syst 36(9):4693–4722. https://doi.org/10.1002/int.22476
26. Nondy J, Gogoi TK (2021) Performance comparison of multi-objective evolutionary algorithms for exergetic and exergoenvironomic optimization of a benchmark combined heat and power system. Energy 12:1135. https://doi.org/10.1016/J.ENERGY.2021.121135
27. Khanra M, Nandi A (2020) Optimal driving-based trip planning of electric vehicles using evolutionary algorithms: a driving assistance system. Appl Soft Comput 93:106361. https://doi.org/10.1016/j.asoc.2020.106361
28. Deb K, Pratap A, Agarwal S, Meyarivan T (2002) A fast and elitist multi-objective genetic algorithm: NSGA-II. Trans Evol Comp 6(2):182–197. https://doi.org/10.1109/4235.996017
29. Song W, Zhu J (2021) A goal-reference-point decision-making method based on normal cloud model and its application in distribution network planning evaluation. Inform Sci 577:883–898. https://doi.org/10.1016/j.ins.2021.08.064
30. The Automotive Research Association of India (2009) Guideline specifications for replacement brake lining assemblies and drum brake linings for power-driven vehicles and their trailers. Ministry Of Shipping, Road Transport and Highways

Development of an Intuitive Autonomous Ground Robot for Indoor Delivery Applications



Jerin Peter, Mervin Joe Thomas, S. Gokulkrishna, Kiran Cholappally, and Santhakumar Mohan

Abstract Efficient and reliable parcel delivery services are always desired in different sectors such as hospitals, offices, industries and households. One promising solution to meet, this need is the application of Autonomous Mobile Robots (AMRs) capable of navigating complex indoor environments to deliver packages and goods. Generally, AMRs are used for the last-mile delivery of parcels. The end users of such robots have different skill sets, and the robot must have a simple user interface to ensure easy usability. This paper presents an AMR with an intuitive Graphic User Interface (GUI) and aesthetic design. It is enough for the end user to define the goal locations on the resulting map shown on the robot screen. The AMR will autonomously navigate to the given goal location. Besides, the effectiveness of sensor fusion and a comparative study of various combinations of sensor fusion are also described in this paper. In addition, the application of LiDAR odometry and its performance is also analyzed in this paper. The primary objective of this study is to identify an approach that improves the AMR's tracking accuracy and makes it suitable for dynamic work environments. This paper describes the development of an AMR for last-mile delivery purposes, and its proof of concept is evaluated on the fabricated prototype.

Keywords Autonomous robot · SLAM · ROS · Path planning · Graphic user interface (GUI)

J. Peter
IIT Palakkad Technology IHub Foundation, Palakkad, India

M. J. Thomas
Robotics Laboratory, Department of Mechanical Engineering, NIT Karnataka, Surathkal, India

S. Gokulkrishna · K. Cholappally
Rajagiri School of Engineering and Technology, Kakkanad, India

S. Mohan (✉)
Department of Mechanical Engineering, IIT Palakkad, Palakkad, India
e-mail: santhakumar@iitpkd.ac.in

© The Author(s), under exclusive license to Springer Nature Singapore Pte Ltd. 2025

B. B. V. L. Deepak et al. (eds.), *Recent Advancements in Product Design and Manufacturing Systems*, Lecture Notes in Mechanical Engineering,
https://doi.org/10.1007/978-981-97-6732-8_3

1 Introduction

The rise of e-commerce, online marketplaces, and various on-demand services has spurred the need for innovative solutions to optimize the delivery process. Automating delivery procedures significantly improve the quality time required for skilled tasks. The future is directed toward unconventional delivery modes ranging from ground to aerial. Nowadays, the application of autonomous robots is seen in hospitals [1], nuclear power plants [2], material handling [3], postal service [4] and even for household applications as companion or hospitality robots [5]. Autonomous robots are getting popular as they improve efficiency, safety, security and cost-effectiveness. Besides, such robots can navigate complex environments without human intervention. With advancements in sensors, GPS, onboard processors and Artificial Intelligence (AI), autonomous delivery robots are revolutionizing how goods are delivered.

Choosing the appropriate material handling system and the level of automation is quite challenging, depending on the environment in which the robot has to operate. Even though the application of Automated Guided Vehicles (AGVs) is a cost-effective solution for material handling, they cannot bypass obstacles along the path. Also, constant changes in floor plan layouts, vulnerability to light and occurrence of surface stains complicate the usage of AGVs [6]. To overcome such drawbacks with AGVs, Automated Mobile Robots (AMRs) are becoming popular among researchers. AMRs, with the help of sensors and onboard processors, can map the operating environment and navigate from the start to the goal point without needing predefined reference points. Through the Simultaneous Localization and Mapping (SLAM) technique, by processing the sensor data, the AMR creates a map of the operating environment and correspondingly determines its instantaneous position [7]. The other established indoor navigation methods include magnetic navigation [8], Wi-Fi and Radio Frequency Identification (RFID) positioning. Like AGVs, the magnetic navigation technique cannot make an autonomous detour when an obstacle comes along its path. On the other hand, Wi-Fi and RFID positioning techniques are expensive and tend to have poor positional accuracy [9]. Moreover, these methods are less reliable when power failure or out-of-orbit accident occurs. Under such situations, the robot cannot localize itself and should be manually resumed by the user. Sun et al. [10] suggest that a low-cost solution to improve the precision and reliability of AMRs is through a multisensory information integration technique. The Robot Operating System (ROS) navigation stack is an open-source platform for autonomous robot navigation in virtual and real environments [11]. The SLAM algorithm can be implemented using the GMapping tool that combines the odometry data with LiDAR readings to create a two-dimensional map of the operating environment. Oliveira et al. [12] proposed a multimodal ROS framework for multisensory fusion. They established a conversion model enabling interconnection between multiple sensors and interactive positioning and labeling of data sensors to facilitate the calibration procedure. Similarly, Florea and Buiu [13] showcased the advantage of sensor fusion for autonomous drone waypoint navigation.

Another major challenge with the application of autonomous robots is that, in most cases, the end users may not be skilled robotists. Therefore, the communication between the robot and the end user must be straightforward, similar to a mobile phone interface. This very reason motivates the primary objective of this paper to integrate the robot with an intuitive Graphical User Interface (GUI) for its easy set-up and functioning. This research attempts to navigate the AMR through the GUI and study its performance to avoid dynamic obstacles to reach the goal point under different scenarios. The AMR is designed for autonomous delivery using Jetson Nano as the primary processor and integrating LiDAR technology for mapping and navigation. Feedback data from LiDAR and accelerometers are used to modify the settings of the temporal elastic band (TEB) algorithm to ensure positional accuracy.

This paper is organized as follows: Sect. 2 describes the AMR's architecture and construction. Section 3 describes the methodology of AMR navigation and its integration with the Graphical User Interface (GUI). Section 4 presents the various results and discussion. Finally, a summary of the work and the scope for future work is presented in Sect. 5.

2 Robot Architecture and Hardware

The purpose of the proposed AMR is for last-mile parcel delivery within indoor environments. The AMR is intended for use in offices, hospitals and households. Therefore, the robot should maneuver through dynamic operating environments. In addition, the robot should be aesthetically appealing and user-friendly. Figure 1a shows the rendered image of the proposed AMR and Fig. 1b shows its corresponding fabricated model for proof of concept. The body of the AMR has been 3D printed using the PLA + material. The strength of the plastic joints is enhanced by fusing them through heating. The body was painted with a glossy white paint scheme. The AMR body rests entirely on a 3 mm mild steel sheet metal chassis frame, as shown in Fig. 1c. Figure 1c also depicts the motors attached to the wheels of the AMR.

Four RMCS-220X high torque DC motors with a 0.2° resolution quadrature optical encoder actuate the wheels. Each motor is connected to Teensy 3.6 using I2C communication. I2C communication is established by connecting the SDA and SCL pins of the Teensy 3.6 to the corresponding pins on the motor. Power and ground connections are established between the Teensy 3.6, motor, and power supply. A 24,000 mAh LIFEPO4 Rechargeable Battery with a nominal voltage of 12 V is mounted at the center of the frame to distribute the weight equally to all motors. The AMR is designed with specific weight limits and is currently limited to 8 kg. The circuit connections are kept on the top plate of the robot. Four spacers were provided between the top and bottom plates for an effective pathway for the LiDAR rays. The Jetson Nano is fitted onto a 3D-printed case with a cooling fan for efficient heat dissipation and mounted on top of the battery. The Jetson Nano used in the subsystem runs on Ubuntu 20.04 with ROS noetic installed. All the control algorithms are run inside the Jetson Nano. The Nano and the remote computer are connected to the same



(a) (b) (c)

Fig. 1 **a** Rendered CAD model of the proposed AMR; **b** Fabricated prototype of the AMR; **c** Sheet metal base support for the AMR

network. The ROS core is run on the Nano, thus enabling access to ROS nodes across the network and controlling the robot via Wi-Fi. The Teensy 3.6 microcontroller is more robust than the conventional Arduino boards. Besides, the SparkFun 9DoF Razor is a nine-axis Inertial Measurement Unit (IMU) that combines a SAMD21 microprocessor with an MPU-9250 that gives the position and orientation of the robot. In this work, the data from the encoder and IMU are fused using an extended Kalman filter to achieve better tracking accuracy and reliability. A 7-inch QLED touch display is also provided to establish an interface with the user. Figure 2 shows the block diagram of the robot architecture explained in this paper.

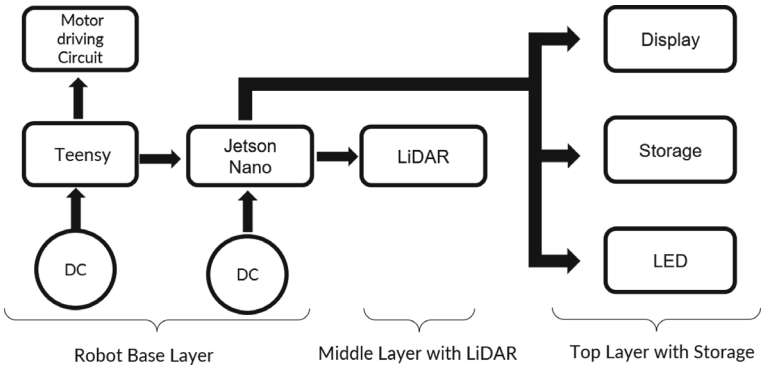


Fig. 2 Proposed AMR architecture

3 Methodology

3.1 Mapping and Navigation

The two major tasks of the AMR are mapping and navigation operations. This work utilizes the Hector Simultaneous Localization and Mapping (SLAM) algorithm to enable the robot to determine its position and simultaneously generate the map of the operating environment. The application of the Hector SLAM package is proven to improve the mapping and navigation accuracy of the robot [14]. It projects the laser scan data onto a grid map and extracts feature points like edges and corners. These feature points are instrumental in constructing an environment map, as they allow for calculating the robot's position relative to these points. To enhance the accuracy of the estimated robot position, Hector SLAM utilizes scan-matching techniques. This involves comparing the current laser scan data with the previous scan data to calculate the robot's motion and update its position accordingly. Localization accuracy is improved by continuously refining the position estimate through scan matching.

Figure 3 displays the flowchart of the AMR path planning strategy. The move_base node in ROS receives data from sensors and encoders, acting as an interface for the robot's navigation. In conjunction with Hector SLAM, a map server stores the map on the Jetson Nano microprocessor. This map encompasses the robot's region, including static obstacles. During navigation, the robot must handle obstacle detection while simultaneously mapping the environment and accounting for new obstacles that may arise in real time, such as dynamic or moving obstacles. This is addressed by employing local and global path planners for the AMR. Considering the global map information, the global planner generates a trajectory for the robot. The local planner ensures that the robot can maneuver through the environment along the global path while dynamically adapting to obstacle configuration changes. The local planner converts the plan generated by the global planner into suitable waypoints, considering the presence of new obstacles in the environment.

This paper uses the Adaptive Monte Carlo Localization (AMCL) approach to track the robot's pose relative to a known map. AMCL is a probabilistic localization system for robots moving in a 2D plane. Figure 4 shows the various nodes of navigation used for the AMR. The move_base node plays a crucial role in the navigation process. It receives inputs from various sensors, including LiDAR and wheel encoders, as well as information from the saved map and the user's goal location input. The move_base node generates a cmd_vel command, representing the desired linear and angular velocities for the robot to move according to the dynamic environment. The cmd_vel command is then fed back to the base controller, which is connected to the motors. The base controller translates the linear and angular velocities into motor PWM values, controlling the robot's movement. Additionally, the base controller reads motor encoder data and publishes it to the Jetson Nano via Rosserial.

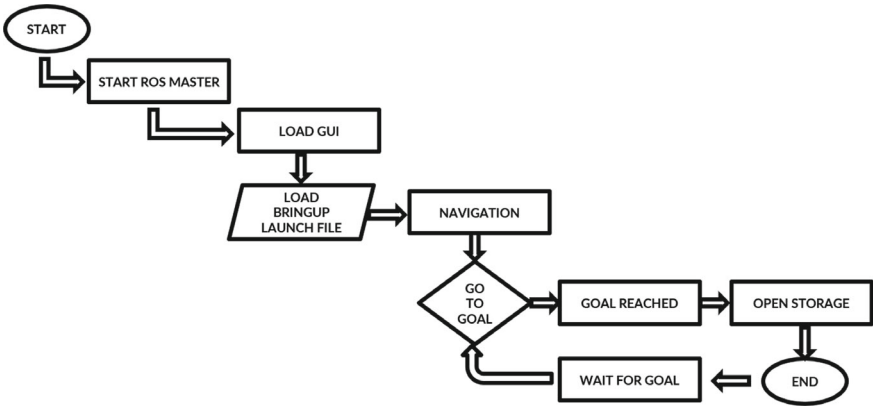


Fig. 3 AMR path planning flowchart

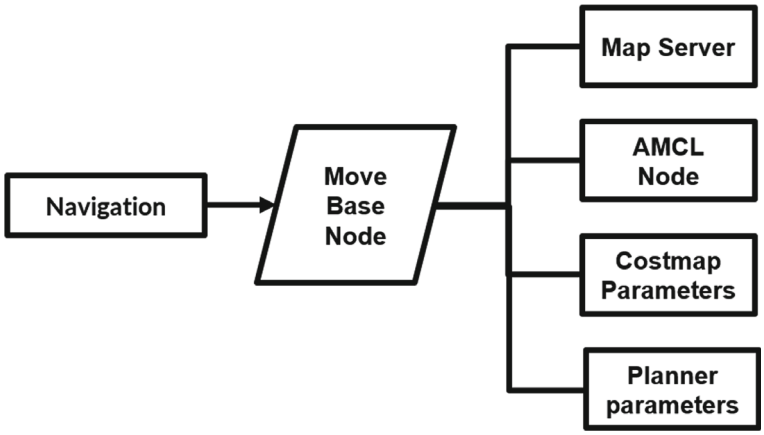


Fig. 4 Navigation nodes used for the AMR

3.2 Graphical User Interface (GUI)

The GUI has been designed to control and monitor the functioning of the AMR easily. It provides an intuitive interface for various functionalities, including robot control, component information, navigation, and system status. In this work, the GUI is built using ROS, PyQt5, rviz_python library, and Actionlib. Figure 5 shows the homepage of the GUI created for the proposed AMR. The NOVA-Bot GUI has a clean and user-friendly interface designed using PyQt5.

It features a main window with various pages accessible through a stacked widget. The interface includes buttons, labels, progress bars, and other interactive elements for seamless navigation and interaction. The home page serves as the central hub of the GUI. It provides quick access to various features and functionalities, including

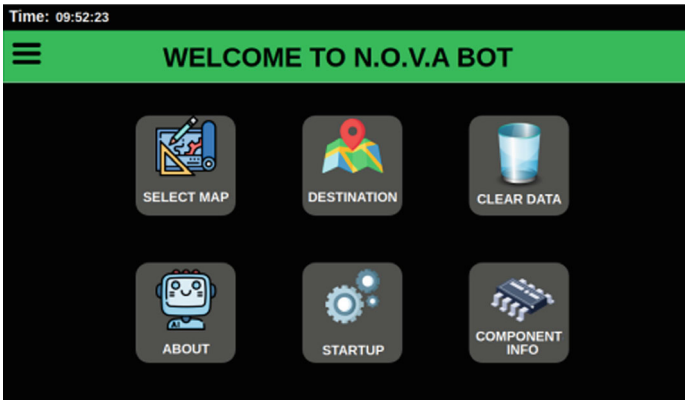


Fig. 5 Homepage of the GUI for the proposed AMR

robot control, information pages, component tests, and system status. The destination page allows users to select predefined destinations for the robot to navigate. The goal points are represented by buttons and correspond to specific locations of interest on the map. The startup robo feature initializes the robot's systems and prepares it for operation. It includes checks for hardware connectivity, sensor calibration and system readiness. All the launch files required to start the robot can be launched from the GUI using a button click, which initializes a subprocess (launch file). After the startup, the robot can be visualized using the inbuilt RVIZ in the GUI, as shown in Fig. 6. The initial robot position can be defined through this interface. Then, the goal position can be given using a predefined button or as a custom goal location on the map. The GUI uses move_base to navigate the robot to the goal location. When the goal is reached, the user can open the robot storage space and take the parcel. This interface uses RVIZ Python to enable visualization of the robot map and the path it develops from the sensor data. Moreover, this interface can establish unique, non-predefined goals for the robot. It also can move the robot to a particular goal point when a button is pressed. The AMR has a screen share feature that helps users view the robot's status en route.

4 Results and Discussion

The performance of the AMR is first analyzed in a virtual environment made in Gazebo. LiDAR is integrated into the virtual robot to enable navigation within the simulation environment. The Time Elastic Band (TEB) planner algorithm made autonomous navigation in a simulation environment possible, and the robot could recognize obstacles and effectively complete its goal. The TEB planner generates an initial path from the robot's current position to its goal position and then iteratively optimizes it while considering its dynamic constraints (such as maximum velocity,

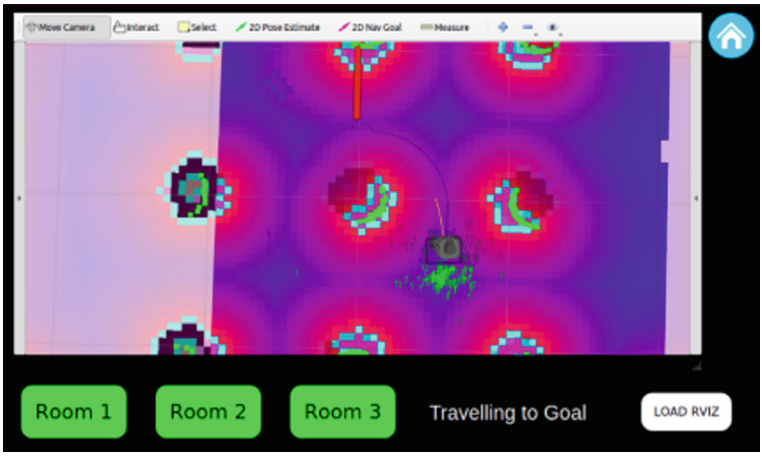


Fig. 6 GUI displaying the instantaneous position of AMR using RVIZ

acceleration and turning radius). Figure 7 shows the tracking of the robot in the virtual environment.

The next phase involves the performance evaluation of the fabricated prototype of the proposed AMR. The user can give the goal commands after the GUI has been fully loaded. The move base node is responsible for planning the path according to the path planning algorithms. To study the effectiveness of sensor fusion, this paper presents an error analysis of the robot under three conditions: (1) using only wheel odometry and (2) combining wheel odometry with IMU data along with magnetometer turned off, (3) combining wheel odometry with IMU data along with magnetometer turned

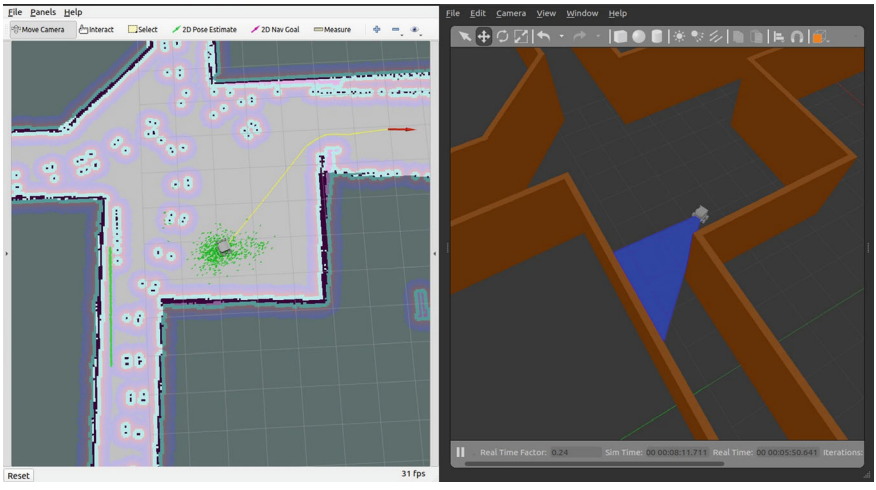


Fig. 7 Autonomous navigation of robot in a simulation environment using TEB algorithm

Table 1 Position error of robot with and without IMU

Trial	Wheel odometry (m)	Wheel odometry + IMU (magnetometer off) (m)	Wheel odometry + IMU (magnetometer on) (m)	LiDAR-based odometry (m)
1	0.20	0.04	0.03	0.02
2	0.22	0.03	0.03	0.02
3	0.20	0.03	0.03	0.015
1	0.20	0.04	0.03	0.02
2	0.22	0.03	0.03	0.02

on and (4) LiDAR-based odometry. The measurements were taken with respect to the center of the robot's base and the ground truth of the navigation goal point. Sensor fusion was performed using an extended Kalman filter-based node in ROS, which combines data from the IMU and wheel encoders. This fusion helps mitigate errors caused by wheel slip or drift, improving positioning accuracy. The results in Table 1 demonstrate that combining the encoder data with IMU data significantly enhances the robot's pose estimation accuracy, improving it by over 85% with the magnetometer turned on compared to using wheel odometry alone. On the other hand, the LiDAR odometry method showed even more better results. This better performance with LiDAR odometry is due to its independence from wheel slip. LiDAR sensors can provide highly accurate distance measurements, typically with sub-centimeter precision. Wheel odometry relies on wheel encoders, which may introduce errors due to wheel slippage and variations in wheel size. While LiDAR-based odometry offers many advantages, it is important to note that it may come with higher costs than wheel odometry or simple wheel + IMU fusion solutions. Besides, the GUI is a user-friendly interface, allowing operators or observers to monitor the robot's progress and quickly ascertain when it reaches its intended goal. Its real-time robot visualization ensures accurate and up-to-date information is readily available.

5 Conclusion and Scope for Future Work

This paper focuses on developing an intuitive robot to help with autonomous delivery within dynamic environments. A fully custom GUI has been developed in which the user can give the goal commands. When a navigation goal button is pressed and the position of the goal location is given, the robot moves to the goal location by planning a path considering the obstacles that came into the picture while mapping. The storage bay on the robot helps users to place the parcel that is to be delivered.

The future scope for autonomous delivery robots encompasses advancements in navigation, AI/ML, swarm robotics, charging and maintenance capabilities, human–robot interaction, environmental adaptability and regulatory considerations. Continued research and development in these areas will unlock the full potential

of autonomous delivery robots, revolutionizing the way goods and services are transported and delivered.

Acknowledgements The authors sincerely thank the Rajagiri School of Engineering and Technology, Kakkanad, India, for providing the necessary technical support and space to conduct experimental tests and performance evaluation of the robot. The authors also thank Asimov Robotics, Kerala, India, for their valuable guidance and support in the designing and manufacturing process. Further, the authors thank IIT Palakkad Technology IHub Foundation, Kerala, India, for financially supporting the first and second authors' research.

References

1. Fragapane G, Hvolby H, Sgarbossa F, Strandhagen JO (2020) Autonomous mobile robots in hospital logistics. In: IFIP advances in information and communication technology, pp 1–9. https://doi.org/10.1007/978-3-030-57993-7_76
2. Tokatli O et al (2021) Robot-assisted glovebox teleoperation for nuclear industry. Robotics 10(3):85. https://doi.org/10.3390/robotics10030085
3. Vashist A et al (2020) Indoor wireless localization using consumer-grade 60 GHz equipment with machine learning for intelligent material handling. In: Digest of technical papers—IEEE international conference on consumer electronics, pp 1–6. https://doi.org/10.1109/ICCE46568.2020.9043072
4. Lee D, Kang G, Kim B, Shim DH (2021) Assistive delivery robot application for real-world postal services. IEEE Access 9:141981–141998. https://doi.org/10.1109/ACCESS.2021.3120618
5. Thomas MJ, Lal V, Baby AK, Rabeeh M, James A, Raj AK (2021) Can technological advancements help to alleviate COVID-19 pandemic? A review. J Biomed Inform 117:1–22
6. De Ryck M, Versteyhe M, Debrouwere F (2020) Automated guided vehicle systems, state-of-the-art control algorithms and techniques. J Manufact Syst 54:152–173. https://doi.org/10.1016/j.jmsy.2019.12.002
7. Xu X et al (2022) A review of multisensor fusion SLAM systems based on 3D LIDAR. Remote Sens 14(12):1–27. https://doi.org/10.3390/rs14122835
8. Takebayashi T, Miyagusuku R, Ozaki K (2021) Development of magnetic-based navigation by constructing maps using machine learning for autonomous mobile robots in real environments. Sensors 21(12):3972. https://doi.org/10.3390/s21123972
9. Zhao S (2021) The cloudlet MEC enabling ISAR based indoor localization and navigation system using passive UHF RFID. In: Proceedings of the 3rd international academic exchange conference on science and technology innovation, pp 331–336. https://doi.org/10.1109/IAECST54258.2021.9695729
10. Sun Y, Guan L, Chang Z, Li C, Gao Y (2019) Design of a low-cost indoor navigation system for food delivery robot based on multisensor information fusion. Sensors 19(22):980. https://doi.org/10.3390/s19224980
11. Peter J, Thomas MJ (2022) Development of a low-cost multipurpose autonomous navigation robot. In: IEEE world conference on applied intelligence and computing, pp 451–454. https://doi.org/10.1109/aic55036.2022.9848857
12. Oliveira M, Castro A, Madeira T, Pedrosa E, Dias P, Santos V (2020) A ROS framework for the extrinsic calibration of intelligent vehicles: a multisensor, multimodal approach. Robot Autonom Syst 131:1–27. https://doi.org/10.1016/j.robot.2020.103558
13. Florea AG, Buiu C (2019) Sensor fusion for autonomous drone waypoint navigation using ros and numerical p systems: a critical analysis of its advantages and limitations. In: Proceedings of

22nd international conference on control systems and computer science, pp 112–117. https://doi.org/10.1109/CSCS.2019.00027
14. Nagla S (2020) 2D hector SLAM of indoor mobile robot using 2D lidar. In: IEEE 2nd international conference on power, energy, control and transmission systems, proceedings, pp 1–4. https://doi.org/10.1109/ICPECTS49113.2020.9336995

Development of a Computer-Assisted Vision-Based Inspection Monitoring System for Quality Assurance



Prajwal S. Bhide and P. V. Manivannan

Abstract In a product-based manufacturing layout, the operator must inspect multiple similar products, making the process monotonous and strenuous. The quality control stage is mandatory in any manufacturing industry before the final product is dispatched. Of many quality inspection procedures, visual inspection is the most widely used. However, the visual inspection process becomes repetitive due to the vast number of products to be inspected daily. Hence, the operator carrying the inspection process is prone to human limitations like fatigue, which results in error, i.e. missing some of the inspection points. To mitigate this problem, a Computer-Assisted Visual Inspection System (CAVIS) has been proposed in this work, which monitors and ensures inspection carried out by the operator. In CAVIS, a hand-tracking model detects and tracks the operator's hand motion, i.e. the pointing finger used to touch the inspection markings to be checked. The present work is divided mainly into two parts: developing the inspection system algorithm to determine the coordinates of inspection marks in the image captured by a vision camera and subsequently tracking and ensuring the operator touches all the inspection markings using the pointing finger in real time, i.e. validating the developed system through experimental investigation.

Keywords Manual inspection · Computer-assisted inspection · MediaPipe hands · Industry 4.0 · Machine vision

Presented at the 5th International Conference on Innovative Product Design and Intelligent Manufacturing Systems (IPDIMS 2023), NIT Rourkela on 6 December, 2023.

P. S. Bhide (✉) · P. V. Manivannan
Department of Mechanical Engineering, Indian Institute of Technology Madras, Chennai 600036, India
e-mail: me22s013@smail.iitm.ac.in

P. V. Manivannan
e-mail: pvm@iitm.ac.in

© The Author(s), under exclusive license to Springer Nature Singapore Pte Ltd. 2025

B. B. V. L. Deepak et al. (eds.), *Recent Advancements in Product Design and Manufacturing Systems*, Lecture Notes in Mechanical Engineering,
https://doi.org/10.1007/978-981-97-6732-8_4

1 Introduction

Industry 4.0 is a manufacturing philosophy emphasizing cutting-edge automated systems, adaptable and efficient data exchanges, innovation in product design, and more individualized and agile manufacturing processes. Incorporating machine vision technology into the various manufacturing phases is one of the many elements of the Industry 4.0 culture [1].

Machine vision represents an important approach in Industry 4.0 culture. It finds application in automated visual inspection, offering robust solutions to various business challenges. Gradually replacing human quality assessments, this technology provides clear advantages regarding accuracy and resilience in object recognition. Including machine vision in manufacturing industries improves productivity and reduces lead time, thus providing efficient operation [2]. The transition of Industrial inspection in Industry 4.0 through leveraging machine vision technologies such as image processing and Human–Machine interactions has been discussed in detail in [3]. Taking an example of the automotive industry, a comprehensive analysis of the past five years has been done, which showed that machine vision-related technology finds more applications in quality-related objectives [4]. To ensure quality, many non-contact inspection systems have been developed over the years. The authors studied the various non-contact inspection methods, which include: visual inspection, thermal imaging, X-ray inspection, ultrasound inspection, and acoustic emission testing for defect identification in flip chip solder joints. Each method has different advantages, which have been discussed in [5].

A vision-based inspection system proves to be advantageous over others due to its high speed and throughput. Vision-based systems can be programmed and configured to inspect a wide range of products and easily integrated into automated manufacturing processes. By effectively integrating computer vision techniques with the inspection in assembly lines, the inspection process times can be reduced.

In this research work, a novel method that aids the operator in ensuring the correctness of inspection markings is discussed. The developed algorithm can be extended to a wide variety of applications; since it uses a hand-tracking model instead of working with very specific features.

2 Relevant Work

In the past few years, image-processing techniques, along with deep learning, have extensively been used in industries for various inspection procedures. A three-stage method is proposed to identify the defective product: image pre-processing, ROI extraction and image identification. The image pre-processing and ROI extraction have been done by leveraging the Gaussian filter and Hough transform, whereas a deep learning model is used for image identification. By combining these three, the computational time has been reduced [6]. The study presents an image-processing

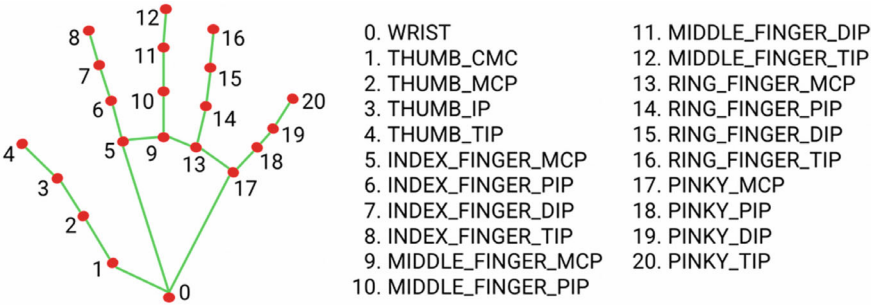


Fig. 1 21 key point landmarks on the detected hand. Image obtained from [13]

technique to inspect numerous flaws in hardwood flooring products. To effectively identify the surface flaws, surface patterns and colour were removed using the well-known object detection method YOLO [7]. A visual inspection pipeline leveraging ML models is proposed, which reduces the labelling of a dataset and visual inspection workload. One of the visual tasks required to ensure the correctness of the company-printed logo for which the pipeline was implemented [8].

With rapid technological developments, human–computer interaction has emerged as a bridge to the transition from Industry 4.0 to Industry 5.0 [9]. The authors in [10] have developed a human–computer interaction system that uses hand gestures detected and identified with MediaPipe. More details about the MediaPipe open-source framework can be seen in [11]. MediaPipe offers an end-to-end hand-tracking solution that achieves real-time performance on numerous platforms without using any specialized hardware like depth cameras. The model has been trained on 30 k real-world images, giving an average precision of 95.7% in detecting and tracking complex hand gestures [12]. Considering its accuracy in detecting palm and hand landmarks (shown in Fig. 1), it can be used in our use case where the hand motions are simple.

3 Methodology

Instead of developing a neural network that caters to solving a specific purpose, the proposed method adopts the state-of-the-art hand-tracking model developed by MediaPipe. Since the focus is on detecting hand movements, the proposed work serves for general use rather than specific use. The complete application is mainly divided into two parts. First, determining the pixel values of markings on the image plane is described in detail. The second part deals with the working of the visual inspection process. The code for both of these parts was developed in Python programming language. The Python Integrated Development Environment used was PyCharm Community Edition. The hardware required for implementing this idea includes

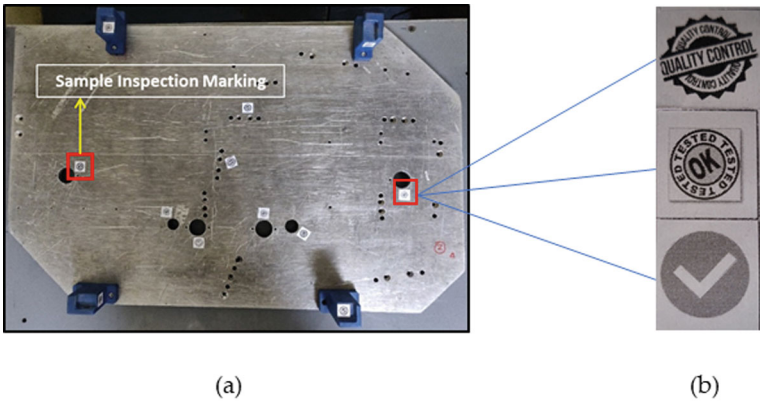


Fig. 2 **a** Component to be visually inspected, **b** Inspection stickers used for experimentation

any USB camera, a computer system supporting the camera and Python interpreters and setup to mount the camera.

In manufacturing industries, usually, the part is placed on fixtures in the respective assembly/inspection stations; hence, the orientation of every individual component is always the same. Generally, to maintain uniformity, the location of inspection markings on a component is fixed so the inspection marking coordinates (pixel positions) will remain constant in the image plane, and every component placed on the fixture will have inspection markings in the exact location. This chalks out the need to detect the different inspection markings through object detection or other techniques.

For our use case, 12 printed inspection stickers (as shown in Fig. 2) in place of inspection markings have been pasted on the component for validation.

3.1 Determining Pixel Values of Markings

An algorithm has been developed to obtain the pixel values of the inspection markings. The algorithm stores the pixel values of these markings when the operator touches the marker on the component with their pointing finger for 2 s. Following that, a white circle will appear on the monitor in the exact location of the inspection point, indicating that the pixel values for the selected spot have been captured, as shown in Fig. 3. The relevant pixel values will also be displayed in the output window. This process completes when the inspection markings' pixel values have been identified. Pixel values determined for a single component can be used for all similar parts thereafter; hence, the process needs to be performed only once.

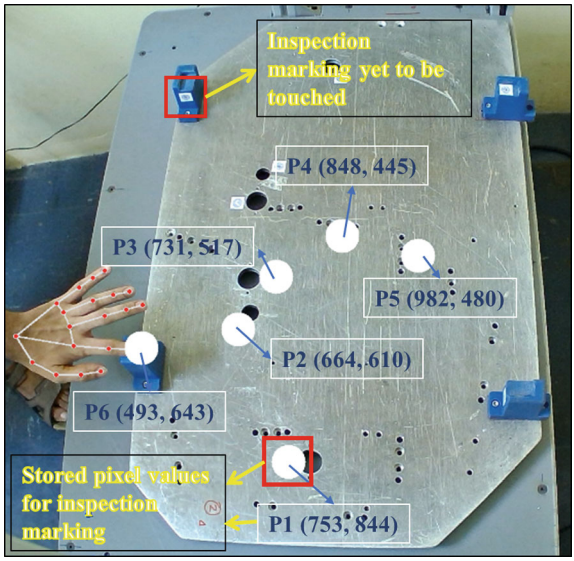


Fig. 3 Determining the pixel values/coordinates (x, y) of inspection points

3.2 Inspection Process

Once the pixel values of all the required inspection markings are known, the inspection process can be started. In the proposed computer-aided visual inspection process, points of interest are initially highlighted with a blue circle before commencement, as shown in Fig. 4a. When the operator contacts an inspection point/marking with their index finger and maintains contact for a duration exceeding 0.2 s (per the operational parameters), it signifies the completion of the visual inspection for that specific point. Then, the colour of the inspected point transitions to a distinctive black, accompanied by the display of an "OK" indicator within the corresponding circle on the monitor interface, as shown in Fig. 4b.

The 0.2-s threshold was carefully determined to minimize accidental inspections by unintended hand gestures while promoting operator efficiency. Even if the markings are absent on a component, resulting in an error by the operator, the algorithm will consider the process incomplete because the operator would not have touched the required coordinates of the missing marking. The application indicates an incomplete examination if an operator interrupts the inspection (e.g. with a keyboard interrupt). Only after the operator touches all the coordinates of the inspection markings does the application signify successful inspection.

Notepad files (.txt files) have been used to store the output of the inspection process. A content of "1" indicates explicitly that the visual inspection was successfully completed, while "0" denotes the opposite. Separate notepad files for each point have been generated and managed to precisely track the status of visual inspections for each location. This framework makes it easier to quickly identify missing inspection markings, enabling immediate corrective action.

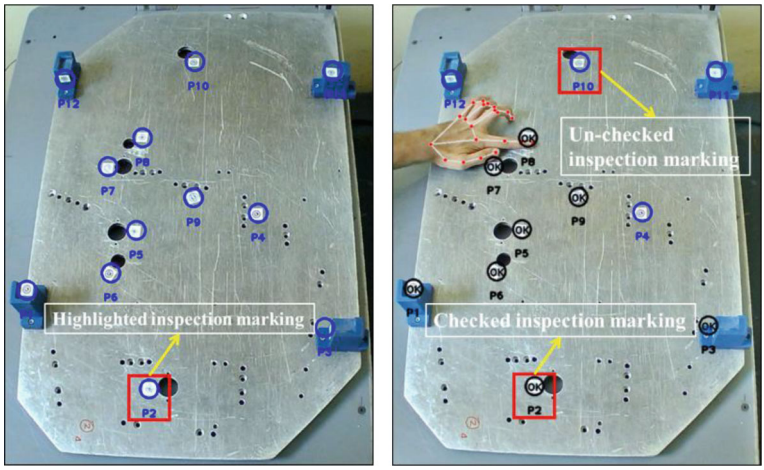


Fig. 4 **a** Picture depicting the component before the start of the inspection process, **b** Picture depicting the component in the middle of the inspection process

4 Results and Discussion

To prove that the proposed method (Manual-Computer vision method) is faster than manually putting a mark (Manual-manual method) on the inspection stickers (inspection markings), experiments were conducted. A defined number of inspection stickers were checked by manually marking with a pen and then with our proposed method for ten repetitions. The sequence of checking and the sticker/stickers to be inspected were kept the same, and the time taken to complete the process was calculated. The checking process, both manual-manual and manual-computer vision, was conducted as fast as humanly possible to reduce the uncertainties. The data collected from these experiments is given in Tables 1 and 2.

Table 1 Time taken (in seconds) for manually putting a mark on the inspection stickers

No. of stickers	Trial 1	Trial 2	Trial 3	Trial 4	Trial 5	Trial 6	Trial 7	Trial 8	Trial 9	Trial 10
2	1.81	1.75	1.42	1.33	1.54	1.28	1.37	1.94	1.45	1.72
4	2.35	2.6	2.67	2.74	2.58	2.7	2.45	2.26	2.89	2.6
6	3.14	3.42	3.36	3.52	3.7	3.26	3.3	3.4	3.59	3.45
8	5.2	5.33	5.22	5.09	4.97	4.88	5.18	5.07	4.66	4.54
10	6.1	6.24	5.9	6.04	5.98	5.83	5.77	5.97	5.75	5.81
12	7.7	7.68	7.54	7.87	7.54	7.49	7.21	7.11	7.01	7.02

Table 2 Time taken (in seconds) in using the index finger as a way to ensure the rightness of the inspection stickers

No. of stickers	Trial 1	Trial 2	Trial 3	Trial 4	Trial 5	Trial 6	Trial 7	Trial 8	Trial 9	Trial 10
2	1.1	0.87	1.12	1.03	1.6	1.47	1.53	1.26	1.31	1.2
4	2.12	2.05	2.21	1.97	2.02	2.43	2.25	2.25	2.13	2.38
6	2.8	2.98	2.82	2.64	2.46	2.73	2.54	2.66	2.79	2.72
8	4.08	3.85	4.23	4.11	3.86	3.93	4.11	4.09	3.8	3.75
10	5.07	5.01	5.32	4.93	4.78	5.39	5.09	5.03	5.12	5.22
12	7.15	6.37	6.56	6.58	6.13	6.45	6.56	6.74	6.29	6.3

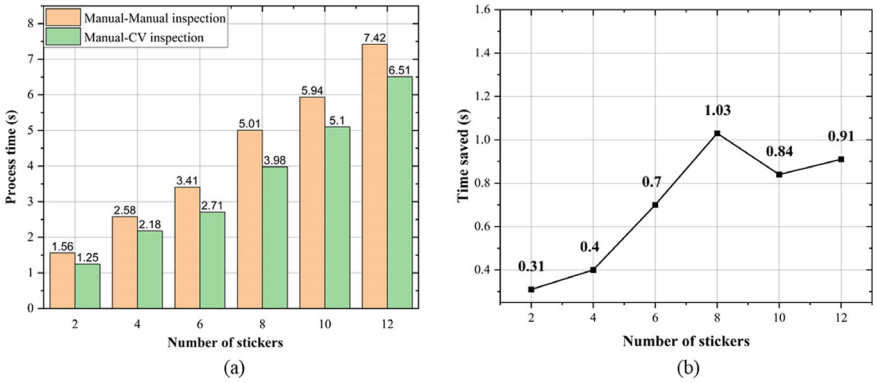


Fig. 5 **a** Average computational time (in seconds for ten repetitions) for the manual-manual method and manual-computer vision (CV) method, **b** average time saved versus the number of stickers

In Fig. 5a, it can be seen that the proposed method is less time-consuming than the manual-manual inspection method and would not compromise the overall process time.

As the time taken to complete the checking process depends on the number of stickers and their location on the component, it cannot be concluded that the time taken will increase linearly as the number of stickers increases. From Fig. 5a and b, it can be seen that the time saved goes from 0.31 s for two stickers to 0.91 s for twelve stickers, peaking at 1.03 s for eight stickers. Even though the relationship is not linear, the time saved increases with increased stickers. More time is saved when the number of inspection markings is more significant, and based on the number of products dispatched, the time saved will increase. Even though the proposed method is slightly faster, the main advantage of this method is that even if the markings are absent on a component, resulting in an error by the operator, the algorithm will consider the process incomplete because the operator would not have touched the required coordinates of the missing marking. Hence, the component would be

regarded as uninspected and not allowed to move to the next station in the assembly line.

To prove that the proposed method works better than existing vision-based techniques for general-purpose applications, the same process (i.e. inspection of sheet metal with holes) has been performed with template matching, widely used in several existing vision-based inspection solutions. The goal of template matching is to identify occurrences of a template image in the target image. In this work, a normalized cross-correlation template matching algorithm has been used, which has detected eleven inspection stickers (as one of the stickers was not completely visible in the image frame) in 3.6 s. To compare the computational times, all algorithms were executed on the same system (12th Gen Intel(R) Core (TM) i7-12,700 2.10 GHz; 16 GB installed RAM), and the positioning and resolution (1920 $\times$ 1080 pixels) of the USB3 camera were also kept the same. After executing the algorithm for ten iterations, the following limitations are observed. Firstly, the inspection stickers need to be very clearly visible in the image frame; furthermore, the position and orientation of the stickers need to be fixed, and the appearance of the stickers should be the same as that provided in the template image for accurate and precise detection. This method's outcome was also influenced by varying lighting conditions. Due to this, the template matching works for specific purposes under properly illuminated conditions. However, the method developed in this research works well in most conditions and can be used for inspecting a variety of objects (i.e. as a general-purpose inspection algorithm).

5 Conclusion

Visual inspection markings are significant for the dealer and necessary for the customer to ensure the delivered component meets all the operational and safety requirements. To check the correctness of inspection markings, since our proposed method uses hand tracking instead of detecting a specific product/object, it can be applied to a very generic use case. The teaching process is straightforward and can be implemented to determine the pixel values in a live video feed. Given the fixed orientation of components, the inspection markings do not have to lie on a single plane or be totally visible in order to be verified using the suggested method. To implement this method, the assembly line should already be equipped with basic monitor interfaces, and the algorithm may then be fed to a microcontroller or a computer, if available. As the proposed method assumes that the location of the inspection markings is similar, it will not give the desired results in cases where the inspection markings are put randomly on a component. Future work will extend the currently developed algorithm for components with variable orientations and having inspection markings placed randomly. The current algorithm is suitable for operation with a single hand; in future, the work shall be extended to accommodate operation with multiple hands/operators to further the inspection process speed.

References

1. Oztemel E, Gursev S (2020) Literature review of Industry 4.0 and related technologies. J Intell Manufact 31:127–182
2. Javaid M, Haleem A, Singh RP, Rab S, Suman R (2022) Exploring impact and features of machine vision for progressive industry 4.0 culture. Sens Int 3:100132. Author F, Author S, Author T (1999) Book title, 2nd edn. Publisher, Location
3. Zouhal Z, Benfriha K, El-Helou M, El-Zant C, Charrier Q, El-Assal O, Najmi G (2021) Approach for industrial inspection in the context of industry 4.0. In: Proceedings of the 2021 international conference on electrical, computer, communications and mechatronics engineering (ICECCME). IEEE, pp 1–5
4. Konstantinidis FK, Mouroutsos SG, Gasteratos A (2021) The role of machine vision in industry 4.0: an automotive manufacturing perspective. In: Proceedings of the 2021 IEEE international conference on imaging systems and techniques (IST). IEEE, pp 1–6
5. Su L, Yu X, Li K, Pecht M (2020) Defect inspection of flip chip solder joints based on non-destructive methods: a review. Microelectr Reliabil 110:113657
6. Wang J, Fu P, Gao RX (2019) Machine vision intelligence for product defect inspection based on deep learning and Hough transform. J Manufact Syst 51:52–60
7. Xia J, Jeong Y, Yoon J (2023) An automatic machine vision-based algorithm for inspection of hardwood flooring defects during manufacturing. Eng Appl Artif Intell 123:106268
8. Rožanec JM, Zajec P, Trajkova E, Šircelj B, Brecelj B, Novalija I, Dam P, Fortuna B, Mladenić D (2022) Towards a comprehensive visual quality inspection for industry 4.0. IFAC-PapersOnLine 55(10):690–695
9. Zalozhnev AY, Ginz VN (2023) Industry 4.0: underlying technologies. In: Industry 5.0: human-computer interaction as a tech bridge from industry 4.0 to Industry 5.0. Proceedings of the 2023 9th international conference on web research (ICWR). IEEE, pp 232–236
10. Boruah BJ, Talukdar AK, Sarma KK (2021) Development of a learning-aid tool using hand gesture based human computer interaction system. In: Proceedings of the 2021 advanced communication technologies and signal processing (ACTS). IEEE, pp 1–5
11. Lugaresi C, Tang J, Nash H, McClanahan C, Uboweja E, Hays M, Zhang F, Chang CL, Yong MG, Lee J, Chang WT (2019) Mediapipe: a framework for building perception pipelines. arXiv preprint arXiv:1906.08172
12. Zhang F, Bazarevsky V, Vakunov A, Tkachenka A, Sung G, Chang CL, Grundmann M (2020) Mediapipe hands: on-device real-time hand tracking. arXiv preprint arXiv:2006.10214
13. Google Developers (n.d.) Hand landmark model. Retrieved September 19, 2023, from https://developers.google.com/mediapipe/solutions/vision/hand_landmarker

Analysis of Challenges of IoT Adoption for Smart City Application



Rashmi Prava Das, Debendra Muduli, and Ashish Kumar Luhach

Abstract The Internet of Things (IoT) is an architecture for a network that processes and analyzes sensitive data in order to deliver a variety of services to a large number of users. IoT devices are capable of delivering a wide variety of value-added services in a variety of smart city applications. Nevertheless, there have been a lot of worries voiced concerning data privacy, confidentiality, and security in relation to the IoT, as well as consumer resistance to adopting such innovative technology. This article examines difficulties linked to the expansion of the IoTs and their adoption by users in smart city applications using Step-wise Weight Assessment Ratio Analysis (SWARA) technique. A total of 30 factors that inhibit IoT adoption were analyzed and categorized under 5 major factors. It revealed that, functional and technological barriers offer more resistance to IoT adoption for smart city application in India.

Keywords IoT · SWARA · Smart city · Optimization

1 Introduction

The Internet of Things (IoT) is a network of networked devices that convey potentially sensitive data to many users. These devices serve as part of the IoT. The IoT has altered people's perspectives on life in every sphere in which they are active [1]. Every day, more and more devices are becoming connected to the Internet, which is transforming once-simple things into ones that are smart, intelligent, and can work together to make decisions. Since 2010, the number of IoT-connected devices has exceeded the human population. These devices have substantial uses in the household, smart

R. P. Das (✉) · D. Muduli
Department of Computer Science and Engineering, C V Raman Global University, Bhubaneswar 752054, India
e-mail: rashmidas3@gmail.com

A. K. Luhach
School of Electrical and Communication Engineering, Papua New Guinea University of Technology, Lae 411, Papua New Guinea

© The Author(s), under exclusive license to Springer Nature Singapore Pte Ltd. 2025

B. B. V. L. Deepak et al. (eds.), *Recent Advancements in Product Design and Manufacturing Systems*, Lecture Notes in Mechanical Engineering,
https://doi.org/10.1007/978-981-97-6732-8_5

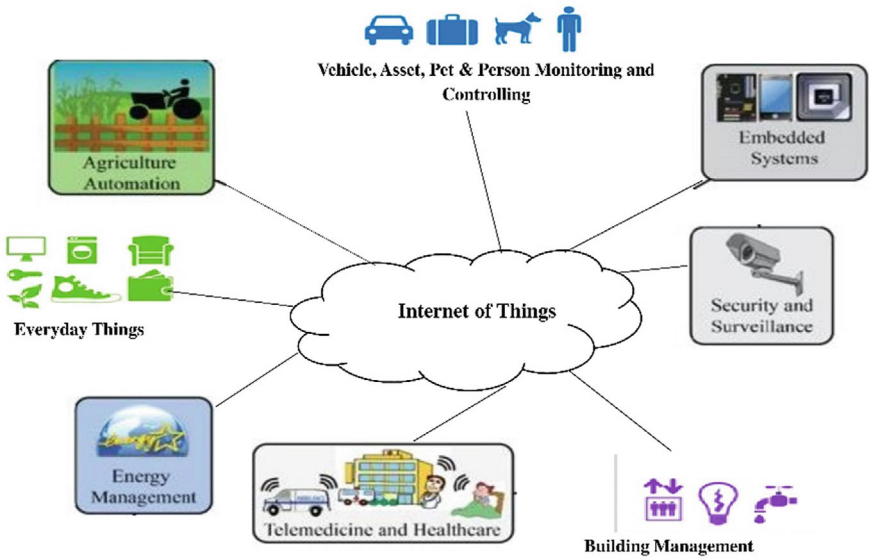


Fig. 1 Smart city applications of IoT

city applications and the market, which makes them extremely essential [2, 3]. A smart city is an urban environment that employs information and communication technology (ICT) and other closely connected technologies to improve the efficacy of everyday urban activities and the quality of service (QoS) delivered to urban people [4]. Applications of IoT have been utilized in smart cities, including those in the fields of agriculture, meteorology, smart grids, and waste management. Figure 1 highlights some of the smart city applications of IoT.

At the same time, it is important to be concerned about the security threats that create roadblocks for the services that it delivers [4]. Some people are worried about using these smart devices because IoT devices and networks can be dangerous. IoT security management is important because the communication networks are vulnerable to many security risks [1] and IoT devices are connected through the Internet, which is by definition an unsecure environment. Certain industries, such as the medical industry, for instance, are susceptible to security risks that could potentially endanger people's lives [4, 5]. Hence, there is wide concern and dilemma among decision makers regarding use of IoT in smart city applications. The major contribution of the paper is developing a framework to analyze the obstacles that stand in the way of the continued development of IoT applications for smart city operations and their inhibiting strength using a multi-criteria decision making (MCDM) tool SWARA. The following is a list of the objectives that this research aims to accomplish:

- Explore the impediments for adoption of IoT for smart city operations in India.
- Examine the degree of inhibiting impact of these impediments on adoption of IoT

The paper is organized in the following manner. Relevant previous literature is provided in Sect. 2, and Sect. 3 discusses the SWARA methodology used in this research. Analysis of the results are presented in Sect. 4. Section 5 reports implications of this research followed by Sect. 6 that reports the conclusion. Finally, limitations of this study and directions of future research are reported in Sect. 7.

2 Relevant Literature

Since marketing and management researchers have been focusing their attention on how consumers react to innovative concepts, products, and services for a number of years, they have come to the conclusion that, in terms of innovation, consumer responses can be broken down into two primary paradigms: innovation adoption and innovation resistance. Mani and Chouk [6] conducted an in-depth study of models developed to examine the customer's reaction to innovation. They chose to adopt one of these theoretical models and then modify it by adding additional obstacles defined by the IoT technology. According to the findings of the study, the adoption of IoT services among users is influenced by a number of different aspects. Skepticism in general regarding IoT devices, incomplete human interactions, and a lack of skills and training to take advantage of those services were some of the problems that were emphasized [7]. Managing security risks is an essential component of IoT applications, despite the fact that this study only tested hypotheses about the effect of recognizing security risks on the acceptance of the IoT innovations for consumers [8, 9]. Although security risk was listed as one of the barriers in this study, the study only tested hypotheses about the effect of recognizing security risks on the acceptance of the IoT innovations. It is very crucial, in order to be able to advertise the new product or service, to have an understanding of the elements that could cause the customer population to accept and adopt the innovation. In addition, it is essential to have a solid understanding of the reasons why customers are resistant to new products and services. There have been two substantial research projects done, both of which highlight the factors that consumers consider to be barriers to accepting innovative items. According to Mani and Chouk [6], there are three barriers associated with the digital character of IoTs: a barrier relating to technology vulnerability; an ideology barrier; and an individual barrier. In this particular piece of research, we make use of both of these models.

3 The SWARA Method

The SWARA technique, developed by Keruliene et al. [10], has been suggested for application in the real-world problems as a specialized tool for supporting decision making in order to carry out legislative activities and evaluate dispute perseverance from a social, economic, and environmental point of view. The Analytic Hierarchy

Process (AHP) and the Analytic Network Process (ANP) are widely recognized multi-criteria decision making (MCDM) methodologies that rely on the use of pair-wise comparisons. The aforementioned approaches rely on the calculation of criteria weights from other methods, but SWARA is a policy-based approach that assigns weights to criteria based on their priority. Due to the fact that SWARA analysis comprises two essential processes, the first of which is the expert prioritizing of the measures and the subsequent of which is the computation of comparative weights, it has been recommended as a reliable decision support tool by several researchers [11–13]. The steps of SWARA technique employed in this research are summarized below and also shown in Fig. 2.

Step 1: Identification of the variables those have an influence on the system.

The task that the experts carry out in this step is to rank the defined barriers according to their relevance. Based on expert opinion, the most significant variable is put first, while the variable that is considered to be the least significant is put last.

Step 2: Determination of comparative importance of average values (l_k).

During this stage of the process, beginning with the second ordered measure, the importance values are calculated. These values indicate the degree to which one criterion (N_k) is more significant than the previous one N_{k+1}

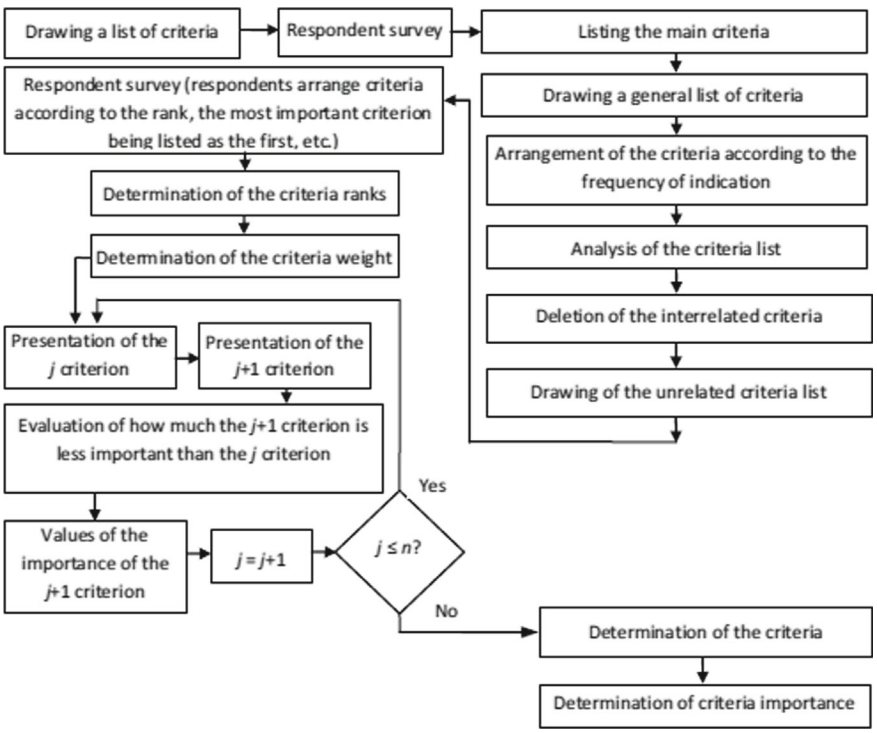


Fig. 2 SWARA approach for evaluation of IoT adoption impediments (Kersuliene et al. [10])

Step 3: Evaluation of the coefficients (M_k).

$$M_k = \begin{cases} 1, & k = 1 \\ l_k + 1, & k > 1 \end{cases} \tag{1}$$

Step 4: Computation of recalculated weights (Qj).

$$p_k = \begin{cases} 1, & k = 1 \\ \frac{p_{k-1}}{M_k}, & k > 1 \end{cases} \tag{2}$$

Step 5: Computation of the relative weights (W_j) *of the variables considered in the study.*

$$R_k = \frac{p_k}{\sum_{t=1}^{n} p_t} \tag{3}$$

where n denotes the number of the barriers.

4 Result Analysis

Based on a scan of relevant literature, thirty elements were identified that were assumed to have a negative influence on the adoption of IoT in the operational activities of smart cities in India. These elements were further classified into a total of five different categories: functional barriers, psychological barriers, technical vulnerabilities, ideological barriers, and individual barriers. The results of applying SWARA's calculations to the weights of barriers and sub-barriers are presented in Tables 1, 2, 3, 4, 5, and 6. The barriers and sub-barriers have been organized in a manner that is consistent with the priorities that were established by the specialists. A comparison of the value and relevance of barriers and sub-barriers (S_j) was also carried out by experts using the questionnaire. This was done in order to determine which was more important. The weights of the barriers were used as a basis for determining the final weights of the sub-barriers. The grading system consisted of steps that were equal to 5%. That is to say, the experts recommended comparing and valuing differences on the basis of percentage increments of 5: 5, 10, 15%, and so on. The final statistics in this section were determined by taking the suggestions made by various experts and averaging them.

After completing all of the necessary calculations using the SWARA approach, Table 7 provides a summary of the weights of the criterion and sub-criteria, as well as the corresponding ranking of both barriers and sub-barriers based on the final weights acquired.

Table 1 Final weights of barriers

Barriers	l_k	M_k	$p_k = \frac{p_{k-1}}{M_k}$	$R_k = \frac{p_k}{\sum_{t=1}^{n} p_t}$
B1		1	1	0.259
B3	0.17	1.17	0.854	0.221
B4	0.14	1.14	0.749	0.194
B2	0.13	1.13	0.663	0.171
B5	0.12	1.12	0.591	0.153

Table 2 Final weights of sub-barriers under B1

Sub-barriers	l_k	M_k	$p_k = \frac{p_{k-1}}{M_k}$	$R_k = \frac{p_k}{\sum_{t=1}^{n} p_t}$	Final weights
B1–1		1	1	0.218	0.056
B1–2	0.19	1.19	0.840	0.183	0.047
B1–7	0.18	1.18	0.712	0.155	0.040
B1–4	0.17	1.17	0.608	0.132	0.034
B1–3	0.15	1.15	0.529	0.115	0.029
B1–5	0.13	1.13	0.468	0.102	0.026
B1–6	0.11	1.11	0.422	0.092	0.023

Table 3 Final weights of sub-barriers under B2

Sub-barriers	l_k	M_k	$p_k = \frac{p_{k-1}}{M_k}$	$R_k = \frac{p_k}{\sum_{t=1}^{n} p_t}$	Final weights
B2–3		1	1	0.266	0.045
B2–2	0.18	1.18	0.847	0.225	0.038
B2–1	0.16	1.16	0.730	0.194	0.033
B2–4	0.17	1.17	0.624	0.166	0.028
B2–5	0.13	1.13	0.552	0.147	0.025

Table 4 Final weights of sub-barriers under B3

Sub-barriers	l_k	M_k	$p_k = \frac{p_{k-1}}{M_k}$	$R_k = \frac{p_k}{\sum_{t=1}^{n} p_t}$	Final weights
B3–1		1	1	0.218	0.048
B3–2	0.19	1.19	0.840	0.183	0.040
B3–3	0.18	1.18	0.712	0.155	0.034
B3–4	0.17	1.17	0.608	0.132	0.029
B3–6	0.13	1.13	0.538	0.117	0.026
B3–5	0.15	1.15	0.468	0.102	0.022
B3–7	0.12	1.12	0.418	0.091	0.020

Table 5 Final weights of sub-barriers under B4

Sub-barriers	l_k	M_k	$p_k = \frac{p_{k-1}}{M_k}$	$R_k = \frac{p_k}{\sum_{t=1}^{n} p_t}$	Final weights
B4–1		1	1	0.237	0.046
B4–2	0.18	1.18	0.847	0.201	0.039
B4–3	0.17	1.17	0.724	0.171	0.033
B4–4	0.15	1.15	0.629	0.149	0.029
B4–5	0.16	1.16	0.543	0.128	0.024
B4–6	0.14	1.14	0.476	0.112	0.021

Table 6 Final weights of sub-barriers under B5

Sub-barriers	l_k	M_k	$p_k = \frac{p_{k-1}}{M_k}$	$R_k = \frac{p_k}{\sum_{t=1}^{n} p_t}$	Final weights
B5–2		1	1	0.264	0.040
B5–1	0.18	1.18	0.847	0.224	0.034
B5–4	0.16	1.16	0.730	0.193	0.029
B5–3	0.15	1.15	0.635	0.168	0.025
B5–5	0.12	1.12	0.567	0.150	0.023

5 Discussions and Implications of This Study

There is no question that the IoT and the digital technologies that support it have piqued the attention of practitioners as well as researchers in a wide variety of industries, and it is projected that this interest will continue to grow [13, 14]. There is also no question that this interest will continue to increase. In recent years, a large number of academics from a variety of fields have conducted a vast number of studies on the difficulties associated with the implementation of IoT in a variety of municipal activities. However, there are not many studies in the available literature that concentrate on the difficulties associated with the adoption of IoT, particularly in the context of emerging economies. This study, identified the roadblocks to IoT application in smart cities from studies by Rejeb et al. [15]; Razmjoo et al. [16]; Bellini et al. [17]; Rajyalakshmi and Lakshmanna [18] and Asha et al. [19] which are reported in Table 7 but also their interdependence. This will help decision makers who are interested in IoT integration in smart city applications by providing them with a comprehensive understanding of the challenges they might encounter during the process of integrating IoT. In this regard, the study will help decision makers who are interested in IoT integration in smart city applications by providing them with an understanding of the interdependence of the roadblocks. The following is a list of additional implications that can be drawn from this research in addition to this one:

Table 7 Weights of barriers and sub-barriers of the model

Symbols	Barriers and sub-barriers	Final weights	Prioritization of barriers based on final weights	Ranking of sub-barriers based on final weights
B1	*Functional barriers*	*0.259*	*1*	
B1–1	Connectivity	0.056		1
B1–2	Network	0.047		3
B1–3	Value	0.029		11
B1–4	Usage	0.034		9
B1–5	Risk	0.026		13
B1–6	Vendor sustainability concern	0.023		16
B1–7	Data portability	0.040		6
B2	*Psychological barriers*	*0.171*	*4*	
B2–1	Reputation	0.033		10
B2–2	Perception	0.038		8
B2–3	Resistance to change	0.045		5
B2–4	Emotional state	0.028		12
B2–5	State of health	0.025		14
B3	*Technological vulnerabilities barriers*	*0.221*	*2*	
B3–1	Business model	0.048		2
B3–2	Security threats	0.040		6
B3–3	Vulnerabilities	0.034		9
B3–4	Big data	0.029		11
B3–5	Interoperability	0.022		17
B3–6	Technical issues	0.026		13
B3–7	Managing all together	0.020		19
B4	*Ideological barriers*	*0.194*	*3*	
B4–1	Price concern	0.046		4
B4–2	Privacy concern	0.039		7
B4–3	Unclear return on investment	0.033		10
B4–4	Complexity perception	0.029		11
B4–5	Legal barrier and uncertainty	0.024		15
B4–6	Fear of punishment if something goes wrong	0.021		18
B5	*Individual barriers*	*0.153*	*5*	
B5–1	Skills and experience	0.034		9
B5–2	Awareness	0.040		6

(continued)

Table 7 (continued)

Symbols	Barriers and sub-barriers	Final weights	Prioritization of barriers based on final weights	Ranking of sub-barriers based on final weights
B5–3	Language barrier	0.025		14
B5–4	Lack of interest	0.029		11
B5–5	Personally identifiable information (PII) concern	0.023		16

Final weights of sub-barriers, B2–4 = 0.166 × 0.171 = 0.028 and B4–3 = 0.171 × 0.194 = 0.033

- A hierarchical framework of the IoT barriers was constructed for the purpose of this study using SWARA. This framework might make it easier for decision makers to devise a strategy that will lessen the effect that these obstacles have on the overall process [20, 21].
- It has been found that organizational resistance is the most important issue that has the most significant impact on preventing the implementation of IoT. The outcomes of the research indicate that this component is also responsible for influencing each of the other obstacles. As a consequence of this, individuals who are responsible for making decisions should organize awareness workshops to educate staff members about the advantages of using IoT. This will assist in lowering the amount of resistance that is now present.
- According to the conclusions of this study, another key hurdle is the lack of knowledge regarding the cost of implementation and the return on investment. Despite the fact that cities in undeveloped nations often have little financial resources, these towns could nevertheless study the possibility of potential government funding schemes that are made available by the governments of a range of countries [22, 23]. They also have the choice to investigate the funding opportunities provided by public–private partnerships (PPP), which is another option available to them.
- According to the findings of the study, utilizing SWARA for both the analysis of the interaction that already exists between the barriers to the widespread implementation of IoT and the computation of the degree to which these components have an influence on the system is recommended. Both academic scholars and professionals in the field could benefit from employing this methodology in order to acquire a more in-depth comprehension of other difficulties that are analogous. Cities in poor nations often have limited funds and access to a limited number of professionals due to the nation's overall level of poverty. Therefore, rather than building their very unique processes and operational strategies, they frequently seek to duplicate the ways used by a few other adjacent cities [24, 25]. This is because they believe that this will be more efficient. This tactic has been found to have catastrophic flaws in a variety of different places around the country.
- The findings of this research could be helpful for decision makers in formulating appropriate policies to reduce the influence of hurdles and having a better grasp of the variables that are impacting IoT integration in their operational practices.

6 Conclusions

Continued urbanization and population growth are driving the need for new ways to urban management that have a low impact on public life, governance, and the environment. Integration of intelligent urbanization has been made simpler as a result of the incorporation of information and communications technology (ICT) into the operations of municipal governments. Thanks to the IoT, which made it possible for traditional networks to achieve this capability, traditional networks can now connect millions of connected devices. The IoT, which is vital for the creation of smart cities, has made it a great deal easier than it ever has been previously to connect real time and everyday deliverables across networks that already exist. Nevertheless, the adoption of IoT for smart city operational tasks is being hampered by a variety of problems. According to this research, there are thirty such variables that have a detrimental impact on the adoption of IoT. Using SWARA, we determined the degree to which each individual element contributed to the adoption of IoT negatively. The findings of the study could be put to use by those responsible for making decisions in order to identify crucial factors and devise ways for minimizing the negative impact such factors have.

7 Limitations and Scope of Future Work

A literature review was carried out with the purpose of determining the challenges that prevent undeveloped countries from making use of the Internet of Things in smart city applications. To validate these challenges, statistical validation was never used at any time in the process. In further study, a statistical analysis will be carried out in order to produce a validated collection of issues related to the usage of IoT in the operational procedures of smart cities. This collection will be developed in order to improve smart cities. It is conceivable that in the future, more exhaustive empirical investigations will be carried out in order to determine the influence that these issues will have on the adoption of IoT in municipal operations in order to make them smarter [22–25]. It is likely that in the future, more in-depth empirical research will be carried out in the United States. It is feasible to use fuzzy logic-based analysis as a means for dealing with the fuzziness that is intrinsically linked with human judgment when doing surveys that are based on questionnaires. This can be done as a method of conducting surveys that are based on questionnaires.

References

1. Peter O, Swain S, Muduli K, Ramasamy A (2022) IoT in combating COVID-19 pandemics: lessons for developing countries. In: Assessing COVID-19 and other pandemics and epidemics using computational modelling and data analysis, pp 113–131

2. Bouzguenda I, Alalouch C, Fava N (2019) Towards smart sustainable cities: a review of the role digital citizen participation could play in advancing social sustainability. Sustain Cit Soc 50:101627
3. Rana AK, Das RP, Rosak-Szyrocka J, Wolniak R, Islam SMN, Muduli K, Sharma V, Bhushan B, Dewan R (2023) Comprehensive analysis of services towards enhancing security in IoT-based advanced smart home. Smart Cit
4. Swain S, Oyekola PO, Muduli K (2022) Intelligent technologies for excellency in sustainable operational performance in the healthcare sector. Int J Soc Ecol Sustain Develop 13(5):1–16
5. Swain S, Muduli K, Kommula VP, Sahoo KK (2022) Innovations in internet of medical things, artificial intelligence, and readiness of the healthcare sector towards health 4.0 adoption. Int J Soc Ecol Sustain Develop 13(1):1–14
6. Mani Z, Chouk I (2018) Consumer resistance to innovation in services: challenges and barriers in the internet of things era. J Product Innov Manag 35(5):780–807
7. Braghin C, Lilli M, Riccobene E (2023) A model-based approach for vulnerability analysis of IoT security protocols: the Z-wave case study. Comput Sec 127:103037
8. Qin Y, Li X, Wu J, Yu K (2022) A management method of chronic diseases in the elderly based on IoT security environment. Comput Electr Eng 102:108188
9. Mehmood Y, Ahmad F, Yaqoob I, Adnane A, Imran M, Guizani S (2017) Internet-of-things-based smart cities: recent advances and challenges. IEEE Commun Mag 55(9):16–24
10. Keršuliene V, Zavadskas EK, Turskis Z (2010) Selection of rational dispute resolution method by applying new step-wise weight assessment ratio analysis (SWARA). J Bus Econ Manag 11(2):243–258
11. Mishra D, Muduli K, Sevcik L, Jana SK, Ray M (2023) Combating of associated issues for sustainable agri-food sectors. Sustainability 15(13):10096
12. Hashemkhani-Zolfani S, Bahrami M (2014) Investment prioritizing in high tech industries based on SWARA-COPRAS approach. Technol Econ Develop Econ 20(3):534–553
13. Alimardani M, Hashemkhani-Zolfani S, Aghdaie MH, Tamošaitienė J (2013) A novel hybrid SWARA and VIKOR methodology for supplier selection in an agile environment. Technol Econ Develop Econ 19(3):533–548
14. Joshi S, Sharma M, Das RP, Rosak-Szyrocka J, Żywiołek J, Muduli K, Prasad M (2022) Modeling conceptual framework for implementing barriers of AI in public healthcare for improving operational excellence: experiences from developing countries. Sustainability 14(18):11698
15. Rejeb A, Rejeb K, Simske S, Treiblmaier H, Zailani S (2022) The big picture on the internet of things and the smart city: a review of what we know and what we need to know. Internet Things 19:100565
16. Razmjoo A, Gandomi A, Mahlooji M, Astiaso Garcia D, Mirjalili S, Rezvani A et al (2022) An investigation of the policies and crucial sectors of smart cities based on IoT application. Appl Sci 12(5):2672
17. Bellini P, Nesi P, Pantaleo G (2022) IoT-enabled smart cities: a review of concepts, frameworks and key technologies. Appl Sci 12(3):1607
18. Rajyalakshmi V, Lakshmanna K (2022) A review on smart city-IoT and deep learning algorithms, challenges. Int J Eng Syst Model Simul 13(1):3–26
19. Asha A, Arunachalam R, Poonguzhali I, Urooj S, Alelyani S (2023) Optimized RNN-based performance prediction of IoT and WSN-oriented smart city application using improved honey badger algorithm. Measurement 210:112505
20. Muduli K, Barve A (2015) Analysis of critical activities for GSCM implementation in mining supply chains in India using fuzzy analytical hierarchy process. Int J Bus Excel 8(6):767–797
21. Muduli K, Barve A (2013) Developing a framework for study of GSCM criteria in Indian mining industries. APCBEE Proced 5:22–26
22. Muduli K, Barve A, Tripathy S, Biswal JN (2016) Green practices adopted by the mining supply chains in India: a case study. Int J Environ Sustain Develop 15(2):159–182
23. Biswal JN, Muduli K, Satapathy S, Yadav DK (2019) A TISM based study of SSCM enablers: an Indian coal-fired thermal power plant perspective. Int J Syst Assur Eng Manag 10:126–141

24. Muduli K, Kusi-Sarpong S, Yadav DK, Gupta H, Jabbour CJC (2021) An original assessment of the influence of soft dimensions on implementation of sustainability practices: implications for the thermal energy sector in fast growing economies. Operat Manag Res 14:337–358
25. Dash M, Shadangi PY, Muduli K, Luhach AK, Mohamed A (2021) Predicting the motivators of telemedicine acceptance in COVID-19 pandemic using multiple regression and ANN approach. J Stat Manag Syst 24(2):319–339

Finite Element Modelling and Comparative Assessment of Single-Level Cervical Disc Replacement with Fusion Surgery



Akshansh Sharma and Sandeep Kumar Parashar

Abstract Total Disc Replacement (TDR) can be considered as an alternative solution to overcome the drawbacks of fusion surgery since it holds the potential to reduce the contingency of adjacent segment loading. Biomechanical performances of commercial cervical Artificial disc (representing TDR surgery) have been examined and compared with INT (C3–C4–C5 intact spine) and C-cage (conventional cage) through FEA using Hypermesh (v.13) under the physiological loadings (lateral bending, axial rotation, extension, flexion). When both the virtually implanted models were compared with INT model, minimum von Mises stresses in intervertebral disc (IVD at C3–C4 level) and adequate proportional ROM were found in the Artificial disc model, while the maximum IVD stresses and constrained ROM were found in the model with C-cage. Artificial disc conceived to reduce the adjacent IVD stresses and it is capable to maintain adequate ROM, it allows appropriate mobility in comparison to the C-cage. Thus, TDR may be considered as an alternative solution for the fusion surgery.

Keywords TDR · ACDF · Artificial disc · Cage · Cervical biomechanics · MRI · IVD · Artificial disc · ROM

1 Introduction

Anterior cervical discectomy and fusion (ACDF) treatment with fusion cage has a high acceptance rate for curing the problem of degenerative disc diseases in the cervical spine due to its high success rate (up to 95%) after surgery [1, 2]. While, the results obtained from the clinical shreds of evidence showed that ACDF surgery

A. Sharma (✉) · S. K. Parashar
Department of Mechanical Engineering, Rajasthan Technical University, Kota, Rajasthan, India
e-mail: akshansh2694@gmail.com

S. K. Parashar
e-mail: skparashar@rtu.ac.in

© The Author(s), under exclusive license to Springer Nature Singapore Pte Ltd. 2025

B. B. V. L. Deepak et al. (eds.), *Recent Advancements in Product Design and Manufacturing Systems*, Lecture Notes in Mechanical Engineering,
https://doi.org/10.1007/978-981-97-6732-8_6

may accelerate the chances of adjacent segment loading [3, 4]. The main cause of increment in adjacent segment loading was a reduction in the segment mobility which led to increase the pressure in the adjacent Intervertebral disc (IVD).

Jacob et al. [5] concluded in his in vitro study that chances of disc degeneration may increase in the adjacent disc to the ACDF site due to an increase in intradiscal pressure. Gore et al. [6] provided in his clinical study that 16% of those patients cured through ACDF surgeries required reoperations due to severe adjacent-level degeneration after the fusion surgery. Dmitriev et al. found in his biomechanical study that fusion surgery may lead to an increase in ROM at the neighbouring segment, reduced ROM at the fusion site and increase in pressure in adjacent IVD. In another investigation utilizing simulation-based finite element method (FEM), Dmitriev et al. [7] observed that the Z brace fusion cage demonstrated superior efficacy compared to the conventional cage implant in anterior cervical discectomy and fusion (ACDF).

A fusion cage or spine cage is a type of prosthesis that is used in the treatment of IVD diseases so that the height of vertebrae could be maintained and functions of the diseased disc could be accomplished by these fusion cages. These cages provide structural stability to spine vertebrates as well as act as load-bearing devices. The type, design, and material of these fusion cages depend on their location of implant and type of problem occurring in the spinal vertebrae. Recently, three types of materials are used for the manufacturing of commercial cage Polyetheretherketone (PEEK), composite, and titanium alloy. The most commonly used material for cage manufacturing is PEEK, because of its high biocompatibility, nontoxicity, and non-resorbable polymer. PEEK material also resembles closer to the cortical bone in terms of material properties in comparison to other cage material (titanium alloy).

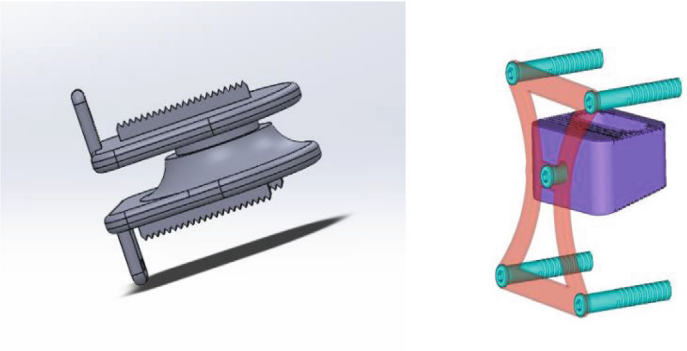
Artificial disc replacement which is also known as total disc replacement is a type of arthroplasty in which degenerated IVD is removed from the patient and restored through artificial devices in order to relieve the patient from the pain that occurred due to a degenerative disc problem [8, 9]. It can be considered as an alternative operation to the ACDF process, in which the main target is to relieve the patient from the pain and to provide normal spine motion. This option can be treated as a far better option to overcome the disadvantages of the ACDF process, mainly it helps to overcome the breakage of adjacent vertebrae due to adjacent vertebrae loading. The TDR devices are structured in such a way as to optimize the extent of movement within the context of natural disc mobility and allow for the greatest range of mobility. The present simulation-based finite element work provides a comparison between TDR surgery and ACDF surgery in a biomechanical perspective by comparing the biomechanical effects (intradiscal pressure and ROM) on the adjacent IVD for both Artificial disc (representing TDR surgery) and C-cage (representing ACDF surgery) designs.

2 Material and Methodology

Fusion cage used in the current study has fairly similar design features as that of a commercial product, Conventional Fusion Cage (C-Cage) Mid-range tapered STALIFTM C (C147561-2T). It is considered to be made from PEEK material (Polyetheretherketone) as shown in Fig. 1. The block-like structure of C-cage helps to maintain the foraminal height and decompression of spine vertebral bodies. The cage design was provided with the teeth on both surfaces that help to maintain the better friction and biological fixation into the endplates of vertebral bodies. A cavity was also provided in the C-cage structure for filling the bone-graft material so as to facilitate bone formation and enhance the fusion rate. To show the importance of maintaining the stability of cage in fusion surgery, a cervical supporting plate with screws had also been developed in the current study though it was kept suppressed during the analysis due to some limitations. The other model used in the present study was an Artificial disc that is used in TDR surgery as it consists of a ball-socket joint that helps to allow all the possible movement of the human cervical spine like flexion, extension, lateral bending, and axial rotation. Toothed surfaces were developed on the artificial disc implant that helps in better biological fixation in the endplates of the vertebrae. All the 3D CAD models used in the current study have been developed using SOLIDWORKS'14 as shown in Fig. 1.

Figure 2 exhibits the magnetic resonance imaging (MRI) scans of a 32-year-old male patient. These scans were utilized to construct a three-dimensional (3D) representation of the C3–C4–C5 cervical spine segment. By modifying the threshold bone density range within the 3D slicer software, the raw model was developed in Standard Tessellation Language (STL) format.

The inability to achieve relative motion and describe distinct material properties within the rigid and hollow raw 3D model of the C3–C4–C5 cervical spine necessitated the creation of a new 3D model using surface modelling in a CAD software



(a) (b)

Fig. 1 3D CAD models of **a** Artificial disc **b** C-cage

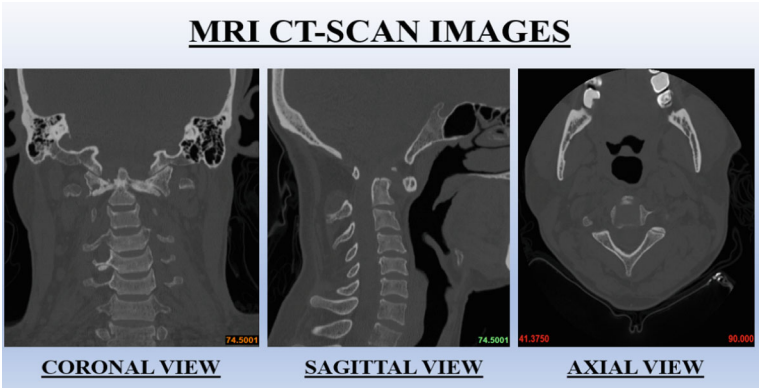


Fig. 2 MRI CT scan images of a male patient

(CREO). Thus, a new CAD model based on the "STL" file of the original model was developed, for the attainment of relative motion and the definition of desired material properties. Tetrahedron meshing was done using Hypermesh (v.13) for all the solid parts while ligaments were developed using linear truss elements as shown in Fig. 3. The material properties assigned based on previous literature review [10, 11] to the finite element models are summarized in Table 1.

0.5 coefficient of friction was assumed to the surface interface of the implant and vertebral body endplates [5]. The thickness of the cortical shell was 0.5 mm in the bone structure of C3–C4–C5 model [12], while the IVD was developed of 7 mm thickness and 4 cm diameter [11, 13].

A total of three models were developed for the present study work which consists of one intact (INT) model and two virtually implanted models. These two implanted

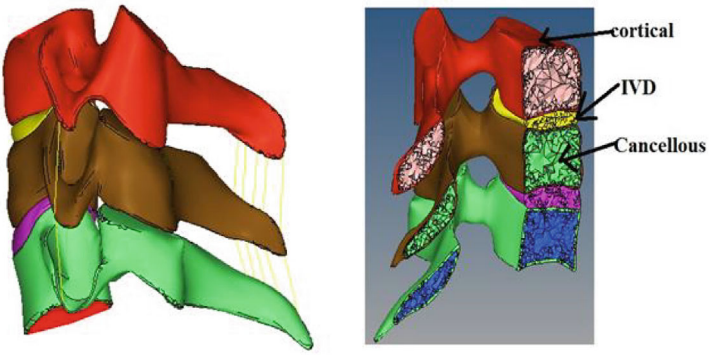


Fig. 3 Hypermesh intact (INT) model with tetrahedron elements and cross-sectional view [11]

Table 1 Material characteristics of developed C3–C4–C5 CAD model [10, 11]

Material	Young's modulus (E) (MPa)	Poisson's ratio (μ)	Density (ρ) (Kg/mm^3)
Bone (cortical)	10,000	0.29	1.83×10^{-6}
Cancellous bone	100	0.29	10^{-6}
Cartilaginous endplates	500	0.4	1.83×10^{-6}
IVD (nucleus pulposus)	1	0.49	1.36×10^{-6}
IVD (annular matrix)	4.2	0.45	–
IVD (annulus fibrosus)	450	0.4	1.2×10^{-6}
Anterior longitudinal ligaments	54.5	–	–
Posterior longitudinal ligaments	20	–	–
Implant material PEEK	3500	0.3	1320 kg/m^3

models were generated by virtual insertion of C-cage and Artificial disc into the C4–C5 vertebral space at the centre-centre location after removal of IVD disc as shown in Fig. 4.

The models were examined under the physiological environment of extension, flexion, axial rotation and lateral bending. An axial load of 73.6 N with 1 Nm bending moment was employed at the superior endplate of the C3 while the inferior endplate C5 was kept fixed [9, 10]. The range of motion (ROM) was determined by the ultimate position and angular movement of the C3 vertebral body, using the displacement control approach for spinal movement simulation. The total number of elements developed in meshing using Hypermesh was 695,937, 27,163, 195,080, and 417,056 with elements size 0.50, 0.40, 0.25 and 0.20 mm for C3–C4–C5 cervical model, IVD, C-cage, and Artificial disc, respectively. For comparing the biomechanical efficiency of the fusion surgery and TDR surgery, effects of C-cage and Artificial disc designs on the adjacent segment C3–C4 IVD loads and proportion-segmental ROMs were compared across all three models.

3 Analysis Results

3.1 Von Mises Stresses at C3–C4 IVD

After the analysis, stresses developed in IVD at C3–C4 level in both the ACDF and TDR model were compared with the stress values of INT model. The highest values of von Mises stresses were observed in the case of the C-cage model under all the given physiological loading conditions (Flexion: 5.824 MPa; Extension: 5.388 MPa;

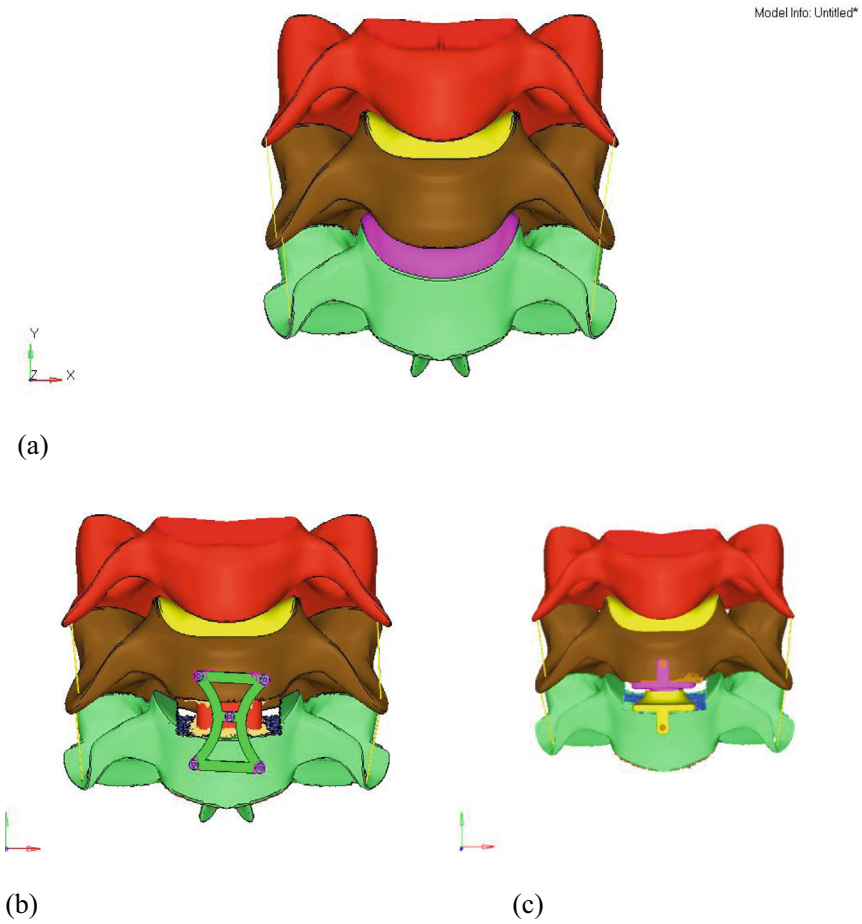


Fig. 4 Models virtually assembled at centre-centre location of C4–C5 vertebrae. **a** INT model [11], **b** C-cage model, **c** artificial disc model

Lateral bending: 5.331 MPa; Axial rotation: 10.612 MPa). In the INT model, the reported von Mises stresses were flexion (3.012 MPa); extension (3.332 MPa); lateral bending (3.56 MPa); axial rotation (4.16 MPa). The lowest von Mises stresses were observed in the case of the Artificial disc model among all the models (Flexion: 2.380 MPa; Extension: 2.102 MPa; Lateral bending: 1.728 MPa; Axial rotation: 3.849 MPa). The observed stress values are minimum in the case of Artificial disc because no friction coefficient was assigned in surface contact of the ball-socket joint of Artificial disc and it is capable to support six-degree of freedom motion under the given physiological loading conditions. Distribution of stresses and its magnitudes over the IVD of the C3–C4 vertebral segment due applied physiological loading is shown in Fig. 5.

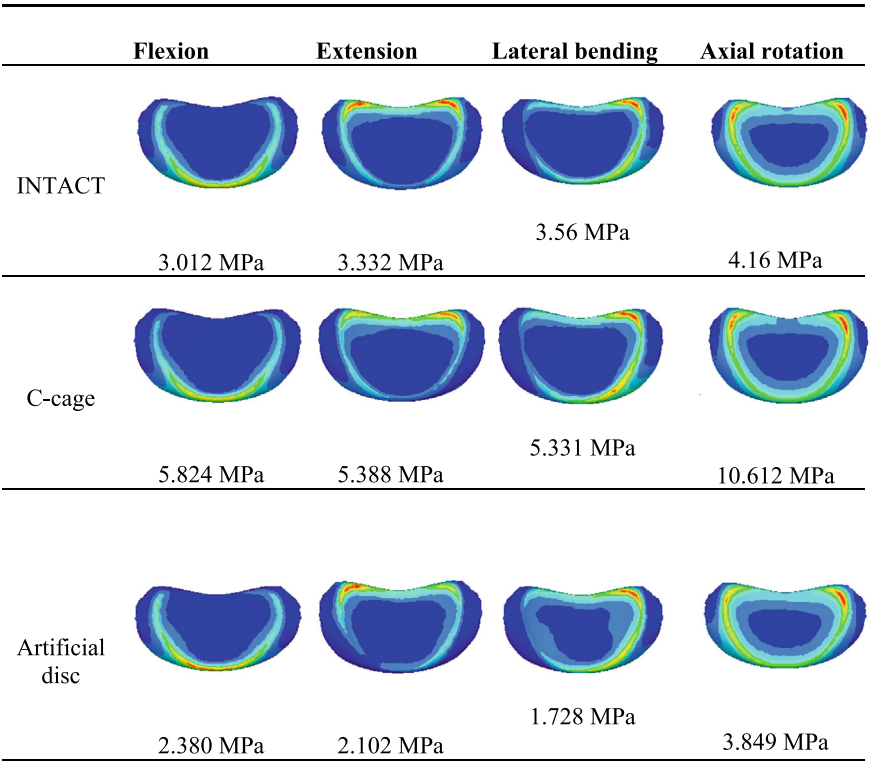


Fig. 5 Von Mises stresses at C3–C4 IVD in all the simulated models (INT, C-cage, Artificial disc)

3.2 Proportion of Segmental ROMs

When the models were subjected to the loading circumstances during the analysis, they deviated from their mean positions. The C3–C4 segment had a different deflection than the C4–C5 section because the inferior endplate of the C5 vertebrae was fixed. The proportional range of motion observed under flexion, extension, lateral bending, and axial rotation were different due to different moment direction.

A balanced proportion was observed in complete structural ROM of INT model (without any implant). The observed ROM in INT model is follows: (Flexion: C3–C4 = 55%, C4–C5 = 45%; Extension: C3–C4 = 51%, C4–C5 = 49%; Lateral bending: C3–C4 = 55%, C4–C5 = 45%; Axial rotation: C3–C4 = 53%, C4–C5 = 47%). Both implant-inserted models provided highly influenced results. Increase in proportional ROM was found in case of C-cage model in all physiological loading conditions (Flexion: C3–C4 = 67%, C4–C5 = 33%; Extension: C3–C4 = 63%, C4–C5 = 37%; Lateral bending: C3–4 = 67%, C4–C5 = 33%; Axial rotation: C3–C4 = 73%, C4–C5 = 27%). For the Artificial disc model, output values observed opposite to the C-cage model but fairly similar to INT model was found (Flexion: C3–C4 = 49%,

C4–C5 = 51%; Extension: C3–C4 = 49%, C4–C5 = 51%; Lateral bending: C3–C4 = 39%, C4–C5 = 61%; Axial rotation: C3–C4 = 42%, C4–C5 = 58%). Figure 6 provides the better visualization of the proportional ROM in the form of bar-graph.

3.3 Other Mechanical Parameters

The current study provides general biomechanical performances of the cervical implants used in both fusion and TDR surgery. Other mechanical parameters such as force–deflection and moment deflection are not provided directly in this present work because of the use of the displacement control method instead of moment control one.

The disc stresses observed during analysis show low-stress values due to the structure receiving a lesser load (i.e. the needed moment for reaching specific ROMs). As a result, the higher moment is required to produce extension, lateral bending, flexion, and axial rotation in case of C-cage model which confirms the stiffness order of present as follows: C-cage model > INT model > Artificial disc model.

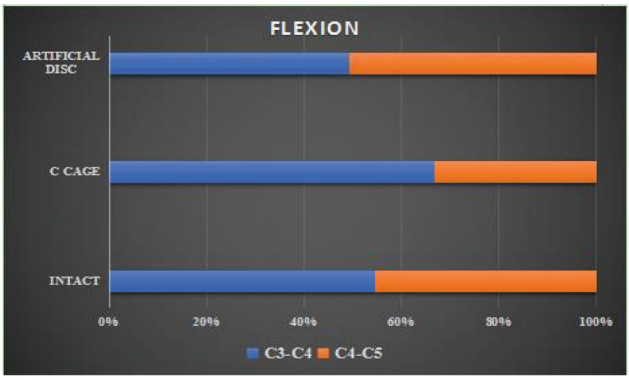
4 Discussion

In the current work, biomechanical effects of a cervical fusion cage and artificial disc were evaluated and compared with the base INT cervical model using finite element analyses of Hypermesh. Results obtained through all the simulated C3–C4–C5 models provide significant data for identifying whether an Artificial disc is effective and beneficial or not over the conventional fusion cage (C-cage). In the C-cage cervical spine model, a higher extent of ROM was transferred to C3-C4 IVD as that of the INT model under all the physiological loading conditions. The increased ROM at IVD causes the over-compression to the disc structure, which is the major cause that intensifies the intradiscal pressure of IVD. The functionality of the Artificial disc design can be regarded as encompassing shock absorption, motion transmission, and potentially preventing adjacent segment loading subsequent to TDR surgery. Hence, the contingency of adjacent-level disc degeneration may hopefully be reduced with TDR surgery in comparison with ACDF surgery.

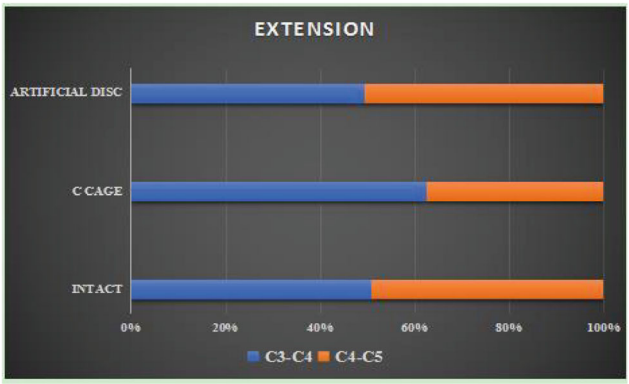
Assumptions of Work

Some assumptions that have been taken into consideration while performing the current finite element study are as follows:

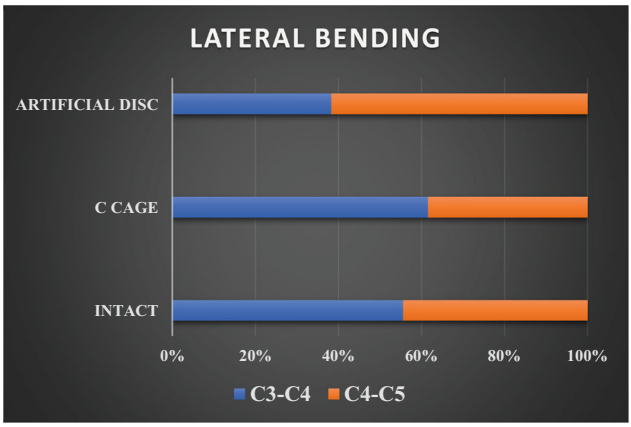
- Material properties that have been assigned to various components in the present finite element study are considered to be isotropic, homogeneous, and linear elastic. The main goal of the present work is based on different designs of cervical



(a)

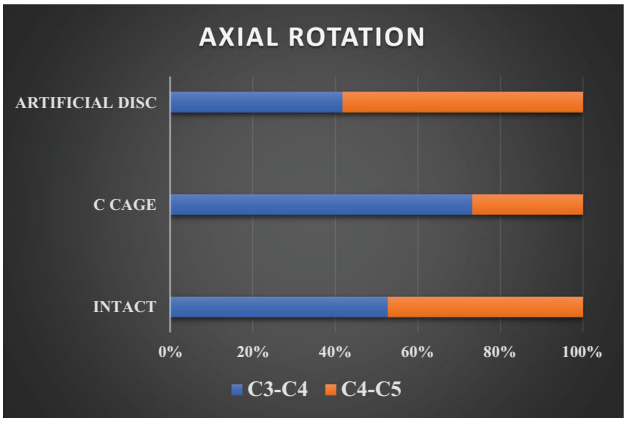


(b)



(c)

Fig. 6 Proportional ROM **a** flexion, **b** extension, **c** lateral bending, and **d** axial rotation



(d)

Fig. 6 (continued)

spine implants. The effects of a bony structure's simplified material properties on the results obtained through simulation can be considered as relatively smaller.

- The current work doesn't take a degenerative intervertebral disc model because of its high complications of material assignment and surface irregularity.
- The friction coefficient is assigned in between the interface contact of implant and bone structure so that proper surface contact can be established during the finite element study.
- Limited ligaments support is provided at posterior tubercle and side facet joints. As there may be a large number of ligaments can be seen on both the anterior and posterior side of the human spine.
- The cervical implant's position is determined by the type of degeneration in the IVD disc, which can have a distinct effect on cervical spine mobility. In the present study, the implants are virtually implanted in the intervertebral space in the centre-centre position.
- Due to the high complexity of MRI cervical images, the raw radiographic model has a high number of faces which can't be analysed in normal analytical software easily. Hence, only the model from C3–C4–C5 has been recreated for analysis purpose and results are evaluated at only single superior adjacent C3–C4 before/after implantation at the C4–C5 level.

5 Conclusion

The supreme aim behind ACDF and TDR surgery is to regain the segmental stability at damaged IVD site employing either fusion cage or by an artificial disc in order to provide significant strength in axial support. But from the present static analysis

under all physiological conditions, C-cage (conventional fusion cage) was found to be risky as it may accelerate the chances of adjacent-level disc degeneration. The notion of TDR surgery, the Artificial disc implant, for the cervical spine can be considered as an alternative solution to ACDF surgery as it protects the neighbouring IVD from overstress and excessive mobility in the early stages after the surgery. FEM has become a potent tool in orthopaedics, providing surgeon with enhanced knowledge and understanding of bone biomechanics for treating both intact and odd cervical conditions. It is undeniable that FEM has the potential to make a significant impact on spine research and holds great promise for future applications. Detailed examination of clinical trials will be required to identify the effectiveness and efficiency of the TDR surgery over the gold standard conventional fusion surgery.

6 Future Scope

The future study can be performed over the complete human spine model with high range analytical software, in which multiple implantations can be achieved at various intervertebral spaces to identify their effects on spine mobility and adjacent loading at both superior and inferior locations.

Funding No financial support was provided to the author(s) for the current research and article publication.

References

1. Zdeblick TA, Phillips FM (2003) Interbody cage devices. Spine 28:S2–S7
2. Brodke DS, Zdeblick TA (1992) Modified Smith-Robinson procedure for anterior cervical discectomy and fusion. Spine 17:S427–S430
3. Maiman DJ, Kumaresan S, Yoganandan N (1999) Biomechanical effect of anterior cervical spine fusion on adjacent segments. Biomed Mater Eng 9:27–38
4. Sugawara T, Itoh Y, Hirano Y (2009) Long-term outcome and adjacent disc degeneration after anterior cervical discectomy and fusion with titanium cylindrical cages. Acta Neurochir 151:303–309
5. Jacobs B, Krueger EG, Leivy DM (1970) Cervical spondylosis with radiculopathy: results of anterior diskectomy and interbody fusion. JAMA 211:2135–2139
6. Gore DR, Gardner GM, Sepic SB (1986) Roentgenographic findings following anterior cervical fusion. Skeletal Radiol 15:556–559
7. Dmitriev AE, Cunningham BW, Hu N (2005) Adjacent level intradiscal pressure and segmental kinematics following a cervical total disc arthroplasty: an in vitro human cadaveric model. Spine 30:1165–1172
8. Liu F, Cheng J, Komistek S (2007) In vivo evaluation of dynamic characteristics of the normal, fused, and disc replacement cervical spines. Spine 32(23):2578–2584
9. Chen JW, Chen WC, Lai YS (2015) Effect of a novel compressible artificial disk on biomechanical performance of cervical spine: a finite element study. Adv Mech Eng 7:1–5
10. Ng HW, Teo EC, Lee KK (2003) Finite element analysis of cervical spinal instability under physiologic loading. J Spinal Disord Tech 16:55–65

11. Sharma A, Parashar SK (2023) Investigative study of anterior cervical discectomy and fusion surgery using finite element method. Lecture notes in mechanical engineering. Springer, Singapore, pp 333–340
12. Edwards WT, Zheng YG, Ferrara LA (2006) Structural features and thickness of the vertebral cortex in the thoracolumbar spine. Spine 26:218–225
13. Raj PP (2008) Intervertebral disc: anatomy physiology pathophysiology treatment. Pain Pract 8(1):18–44

A Statistical Method-Based Auto-Fitted Genetic Algorithm for Damage Diagnosis



Sasmita Sahu, Monalisa Das, Shakti P. Jena, Rita Kumari Sahu, Bijaya Bijeta Nayak, and Dayal R. Parhi

Abstract From the last two decades, lots of research have been done on the non-destructive testing (NDT) and structural health monitoring (SHM) techniques. Though the conventional NDT methods are effective, the complete reliability on them is not possible due to the countable time period. For all the catastrophic failure, time plays an important role. If appropriate time of structural and mechanical failure will not be estimated, it will be disastrous. So, in this paper, method describing on online technique has been proposed. An evolutionary algorithm has been used to generate an online method to identify and detect the damage. In the application of any evolutionary algorithm, large numbers of data are required. It has been observed that during the collection of data, error is accumulated. Error needs to be reduced. So, to minimize the error amount during the data collection, the relation between dependent variables and independent variables has been figured out. In this work, the result from the genetic algorithm (GA) and the auto-fitted GA has been compared. From the comparison, it can be clearly noticed that the results from the auto-fitted GA are more convergent and the percentage of error is less. The novelty of this study is the application of hierarchical GA with the statistical bootstrap method for damage detection and its severity measurement.

Keywords Damage · Natural frequencies · Genetic algorithm · Bootstrap method

S. Sahu · M. Das (✉) · R. K. Sahu · B. B. Nayak
School of Mechanical Engineering, Kalinga Institute of Industrial Technology, Deemed to Be University, Bhubaneswar, Odisha 751024, India
e-mail: monali123_das@yahoo.com

S. P. Jena
Nalanda Institute of Technology, Bhubaneswar, Odisha 754005, India
e-mail: sasmita.sahufme@kiit.ac.in

D. R. Parhi
Department of Mechanical Engineering, National Institute of Technology, Rourkela, Odisha 769008, India

© The Author(s), under exclusive license to Springer Nature Singapore Pte Ltd. 2025

B. B. V. L. Deepak et al. (eds.), *Recent Advancements in Product Design and Manufacturing Systems*, Lecture Notes in Mechanical Engineering,
https://doi.org/10.1007/978-981-97-6732-8_7

1 Introduction

This work depicts about the beam structural damage diagnosis. The dynamic characteristics are the significant features which are taken into consideration for the damage detection. It is the most important work of the system designer is to make sure that the system natural frequencies should not coincide with the excitation frequency due to different types of loading [1, 2]. The shift in the natural frequencies can be used to modify the structural design. Also the dynamic features are source of information about the health condition of the structural element [3]. The measured natural frequencies can be used for the diagnosis of damages or faults.

The typical approach of application of evolutionary algorithm problems of system vibrations is carrying out a series of numerical and analytical model to obtain required Eigen frequencies. The application of evolutionary algorithm for damage detection can be used as the inverse engineering problem. The inverse engineering problem refers to the problem where the desired reaction (like the Eigen frequencies) of the system is known or decided but the physical systems is unknown. These problems are difficult to solve because a unique solution is rarely possible. All methods of the inverse problem solution are based on the single or multiple analysis of the direct problem. In this paper, for damage identification is considered using Finite Element (FE). Various studies have addressed the direct-sensitivity based methods for FE models [4–6]. This research work explains about novel vibration based damage diagnosis method using meta heuristic algorithm coupled with FE method [7].

Meta heuristic optimization methods used for fault diagnosis methods can generally be divided into; gradient based methods and computational intelligence (Artificial Intelligence) methods such as different evolutionary algorithms [8, 9]. Most of these methods are inspired from nature and nature influenced theories. For instance, the superiority of Genetic Algorithm (GA) based method is proved significant in comparison with gradient based damage detection methods [10]. In this paper Genetic Algorithm is used for it's ability to find global solution in the complex search domain with different local minimum points without using many constraints. Further the robustness of the algorithm lies on the multiple points which can be used to find the best solution easily with less computational effort as compared to gradient based methods.

Genetic Algorithms are the natural selection based Artificial Intelligence (AI) technique. This has been extensively used in many engineering fields successfully after its introduction by John Holland in 1975. It has been found from the literature that these algorithms give much significant global optimization than the traditional gradient based algorithms. Comparing with the traditional algorithms, the Genetic Algorithms used to calculate the solution by using objective function without the gradient information [11]. Besides, the parallel solution in searching process make it strong enough not to fall in local minima. Due to the above mentioned advantages, the Genetic Algorithm act more efficiently and effectively [12]. But, it has also been observed that the use of small population may involve uncertainty in the variables. So, to account the problem involved, Boot-Strapping can be used. Boot- Strapping

can be used to account the uncertainty of the variables [13]. Boot-Strapping can be used to account the uncertainty of the variables used in a soft computing algorithm or model. This is basically done by resampling (repetition of the process many times on the different samples generated with replacements) for estimation, instead of using complete data to estimate them once [14, 15].

2 Application of Finite Element Method for Getting Dynamic Responses from the Cracked and Uncracked Beams

It is known to all the researchers that all the damage diagnosis problems are non-linear problems and are damped excited vibration paradigm which needs more computational effort. So, to simplify the problem and to lessen the computational burden, the vibrational behavior of the structural system with a non-propagating transverse crack has been considered. For modeling the problem, a 2D model of the cracked beam is employed. The type of crack considered in this case is an open-type crack which makes the cracked problem a linear type. The region around the crack is discretized into a number of elements. The material of the beam is assumed to be homogeneous, elastic, and linear. The crack surface is assumed to be plane and smooth.

For the finite element method frame work, the governing equations of motion for the dynamic behavior of the beam are given below:

$$m\ddot{u} + c\dot{u} + Ku = F_{\text{ext}} \tag{1}$$

m—mass of the beam
$\ddot{u}$—acceleration
$\dot{u}$—velocity
u—displacement
F_{ext}—external excitation

The presence of the crack divides the crack into two parts. Due to the crack formation and propagation, internal energy is dissipated in the form of potential energy. In this case, the form of energy is strain energy. So, the strain energy for the uncracked structure is given below:

$$U_0 = \frac{1}{2}\int_0^l \frac{M^2}{\text{EI}}\text{d}x \tag{2}$$

M—bending moment of the beam.

Neglecting the effect of axial force, the additional strain energy can be given as follows:

$$U_{\text{ad}} = b \int_0^a \left\{ \left[\left(k_{lm} + k_{lp} \right)^2 + k_{IIp}^2 \right] / E' \right\} \, \mathrm{d}a \tag{3}$$

From the definition of the compliance, the flexibility coefficient for an element without crack is obtained as follows:

$$C_{ij} = \frac{\partial^2 U_0}{\partial T_1 \partial T_2} \tag{4}$$

T_1—shear force

T_2—bending moment

The additional flexibility due to crack is given as follows:

$$C_{ij'} = \frac{\partial^2 U_1}{\partial T_1 \partial T_2} \tag{5}$$

From the flexibility coefficient, the stiffness matrix can be derived. Applying these stiffness matrices, the modal parameters for the cracked and uncracked beam are obtained.

3 Application of Statistical Method in Genetic Algorithm for Damage Diagnosis

Genetic algorithm (GA) is a computer simulation of natural genetics and evolution. These simulations are basically used to solve optimization problems. In this investigation work, the genetic algorithm is mainly used to be applied for reverse engineering. So, first a population of possible solutions are created using finite element analysis (which is a direct method to get the natural frequencies for given crack depth and crack location). In every iterations, the population evolves toward the convergent optimized solution for the damage detection. The evolutionary algorithm evolves through the following steps:

1. Genetic selection
2. Genetic crossbreeding
3. Genetic mutation
4. Termination

In general, in the damage diagnostic problems, a set of chromosomes with the genes are created. Here, each chromosome contains five numbers of genes. Each gene is encoded using binary encoding method. Here, each gene is encoded using three binary numbers.

Chromosome ↔ Gene 1, Gene 2, Gene 3, Gene 4, Gene 5

Gene 1, Gene 2, Gene 3 ↔ First three natural frequencies
Gene 4, Gene 5 ↔ Crack Depth, Crack Location

Algorithm of Genetic Algorithm for Damage Diagnosis

The steps of genetic algorithm are as follows:

1. Initial population is created with ten numbers of possible solutions (chromosomes).
2. Then, the individuals pass through natural selection process for the evaluation of the individuals. For this step, an objective function has been designed.
3. After finding the best two individuals, they are considered for reproduction using the crossover method. Here a two-point crossover used for crossover.
4. From the crossover reproduction two off-springs are generated. These off-springs are with other ten numbers of chromosomes. They are evaluated again. Then, the best ten numbers of chromosomes are again added to the population. In this way, the population remains constant.
5. The above process is repeated for number of iterations, till the solution remains the same for at least two numbers of iterations.
6. If the above condition prevails, then mutation is opted.
7. For mutation, only 0.1% of mutation rate is used. In this case, flip type of mutation is used. In this type of mutation, the binary numbers used for coding the gene or chromosome are flipped.
8. Finally, the algorithm is terminated after twenty numbers of generations or one minute of time period.

4 Bootstrapping

Resampling is a method of frequently drawing samples from the training dataset. These samples are from the training dataset. These samples are then used for auto-adjust for retrieving more specific information about the data model. This is required in a data analysis method used in different algorithms to improve the accuracy and estimate the uncertainty level in finding out the best global solution.

There many statistical method for executing resampling. Resampling is a method to generate new data points in the data set by arbitrarily choosing data from the existing data sample. The significance lies in the estimation of the properties of a data set which is unknown or difficult to approximate particularly when the sample size is small. Particularly, in the work, the sample or data size is kept small for the smooth running of the genetic algorithm. If the data numbers will increase, the algorithm may stalk in the local solutions.

The most common methods for resampling are the following:

1. Cross-validation

2. Bootstrapping

In this paper, bootstrapping has been used for the resampling of data. Bootstrapping is a type of method used to determine the robustness of the model by selecting random numbers of subsets from original dataset. In this method, for each run, some of the data are not considered while some of the data are not considered while some of them are repeated, once or more times. By using the replacement technique, it is able to create a new hypothetical sample that can help in the training the estimated values.

The most important steps that are involved in bootstrapping method are given below.

1. The sample size is arbitrarily chosen.
2. Choose an observation from the training data set in random order.
3. Add these observations with sample picked.

The main advantage of bootstrapping is to find out the uncertainty in the data collection, when the sample size is small. This can be used to perform hypothesis tests and compare the distributions. It is widely used in many fields.

5 Results and Discussions

First of all the data samples are created using the direct methods where crack depth and crack location are given and natural frequencies are generated. These data are used to form a sample space. The data are then normalized by comparing the input and output variables of uncracked and cracked beams. The dataset contains twenty number of data sets. As the sample size is small, so to lessen the uncertainty, a statistical method named bootstrapping has been used. The results extracted from the standalone genetic algorithm and with the auto-fitted genetic algorithm (with the use of bootstrapping method) have been compared, and the results are given Tables 1 and 2. The errors have been calculated using the following equations.

$$\text{Percentage of error} = ((\text{data of FEA} - \text{data from the given technique}) / (\text{data of FEA})) \times 100 \quad (6)$$

6 Conclusion

Many load-carrying systems and structure may experience same local damage during their service period. It is inevitable that cracks are the main cause of the structural failure. In order to keep away from sudden failure due to the presence of the crack, it

Table 1 Results from genetic algorithm compared with FEA

Sl. No.	nfnf	nsnf	ntnf	ncd	ncl	rcd using the GA analysis	rcl using the GA analysis	Percentage error ncd	Percentage error ncl
1	0.9933	0.9914	0.9968	0.324	0.2184	0.311	0.2099	3.87	3.85
2	0.9929	0.9928	0.9981	0.3	0.203	0.288	0.1953	3.78	3.78
3	0.9944	0.9944	0.9975	0.2874	0.233	0.2763	0.224	3.83	3.82
4	0.9962	0.99769	0.9991	0.124	0.2185	0.1192	0.2101	3.81	3.81
5	0.9976	0.9972	0.9967	0.274	0.3623	0.2635	0.3484	3.81	3.82

Table 2 Results from auto-fitted genetic algorithm compared with FEA

Sl. No.	nfnf	nsnf	ntnf	ncd	ncl	rcd using auto-fitted GA analysis	rcl using auto-fitted GA analysis	Percentage error ncd	Percentage error ncl
1	0.9933	0.9914	0.9968	0.324	0.2184	0.315	0.212	2.47	2.48
2	0.9929	0.9928	0.9981	0.3	0.203	0.2924	0.1979	2.52	2.49
3	0.9944	0.9944	0.9975	0.2874	0.233	0.28	0.2271	2.51	2.52
4	0.9962	0.99769	0.9991	0.124	0.2185	0.12	0.213	2.51	2.51
5	0.9976	0.9972	0.9967	0.274	0.3623	0.267	0.353	2.5	2.5

is desirable to detect cracks before they cause more serious consequences and eventual system failure. There are numerous research works on model-based methods for damage detection in structures during recent years. Among the works, the use of vibration-based methods provides the most desirable alternatives to actually disassembling the structures. In recent years, the study of non-linear mapping of various soft computing methods has been conducted. Among these soft computing methods, genetic algorithm attracts attention because it is not necessary to have much data in advance which can be noticed from the results.

Many of the soft computing evolutionary algorithms require the prior knowledge on both modal frequencies and mode shapes. As the genetic algorithm doesn't require any prior knowledge, this is one of the reasons for getting better results from the genetic algorithm. But genetic algorithm has some short comings in using of data sample. It has been observed that many times when the sample size remains small, due to uncertainty, the efficacy of the running algorithm decreases. So, to counter this problem, bootstrapping method has been used before the training of the data in genetic algorithm. Due to the resampling techniques applied by bootstrapping method, the genetic algorithm models can be auto-fitted to give better results as compared to the standalone genetic algorithm. The results from genetic algorithm compared with FEA are given in Table 1, and the result is having 3.8% but the error

drastically decreases with the use of bootstrapping (given in Table 2) to 2.5% as compared to FEA.

References

1. Waghulde KB, Kumar B (2014) Vibration analysis of cracked cantilever beam with suitable boundary conditions. Int J Innov Sci Eng Technol 1(10):20–24
2. Jae SA, Seung HY, Kwang SW (2014) Free vibration analysis of patch repaired plates with a through crack by *p*-convergent layer wise element. Sci World J 12:1–8
3. Majumdar A, Nanda B, Maiti DK, Maity D (2014) Structural damage detection based on modal parameters using continuous ant colony optimization. Adv Civil Eng 2014:174185
4. Lu K, Liang ZW, Guo ZY, Sheng CY, Chao W (2014) Crack analysis of multi-plate intersection welded structure in port machinery using finite element stress calculation and acoustic emission testing. Int J Hybrid Inform Technol 7(5):323–340
5. Musmar MA, Rjoub MI, Hadi MAA (2014) Nonlinear finite element analysis of shallow reinforced concrete beams using Solid65 element. ARPN J Eng Appl Sci 9(2):85–89
6. Pal MK, Rajagopal A (2014) Sensitivity analysis of linear elastic cracked structures using generalized finite element method. Int J Comput Methods Eng Sci Mech 32:422–437
7. Miao B, Wang M, Yang S, Luo Y, Yang C (2020) An optimized damage identification method of beam using wavelet and neural network. Engineering 12(10):748–765
8. Bhuyar LB, Kshirsagar SV (2011) Crack detection in machine-structure by evolutionary algorithm. J Anu Books 4:19–27
9. Haryanto I, Setiawan JD, Budiyono A (2009) Structural damage detection using randomized trained neural networks. Intelligent unmanned systems: theory and applications. Springer, Berlin, pp 245–255
10. Jiang S, Zhang W (2023) A hybrid approach of modified bootstrap and physics-based methods for probabilistic fatigue life prediction considering overload effects. Probabil Eng Mech 70:103343. https://doi.org/10.1016/j.probengmech.2022.103343
11. Niezrecki C (2015) Structural health monitoring and damage detection, vol 7
12. Golnaz SS, Nigro MB, Pakzad SN, Pan Y (2014) Structural damage detection and localisation using multivariate regression models and two-sample control statistics. Struct Infrastruct Eng 32:1–17
13. Worden DNK, Cross EJ (2015) On robust regression analysis as a means of exploring environmental and operational conditions for SHM data. J Sound Vibr 347:279–296
14. Husnain MNM, Akramin MRM, Chuan ZL, Shaari MS, Takahashi A, Akmal MH (2022) Probabilistic stress intensity factor prediction of surface crack using bootstrap sampling method. Int J Integr Eng 14(8):118–125
15. Jin S, Wang D, Jiang D (2023) Seismic fragility analysis of containment structure subjected to near fault ground motions. Prog Nucl Energy 161:104734. https://doi.org/10.1016/j.pnucene.2023.104734

Emovere Agnitio by Textual Tweets Using Machine Learning



B. Prasanna Kumar, Venkata Kishore Kumar Rejeti, T. Bhavani Shanvitha, S. Jyothi Sri, Y. Prathyusha, S. Keerthana, and D. Anand

Abstract Millions of people are connected to one another in the modern digital world through social media and the internet. The entire globe is embracing innovation. Each year brings new breakthroughs due to technical advancements. Twitter and Emotion Recognition are a couple of these developments. Twitter is used to get opinions about trends, goods, etc. On the social networking site, Twitter, individuals may utilize text messages and GIFs to share their thoughts and opinions about actual events. Written texts are the most popular means for individuals to interact with one another and share their ideas. In this research, we offer a sentiment analysis system that uses an ensemble of classifiers to automatically recognize emotions in text. Text is one of the most popular means of human expression of feelings and ideas, especially on social networking sites. Deep Learning and AI are used in previous methodologies. We are putting out a methodology that uses machine learning to identify the emotion based on user opinions. Opinion mining and sentiment analysis in machine learning are useful tools for analyzing people's feelings, attitudes, and views about various topics without requiring human tweet reading. The emotions may be predicted using the vote classifier algorithm. All feelings are divided into three categories: "Positive," "Negative," and "Neutral" We are giving a comment in addition to the degree of emotion.

Keywords Machine learning · Voting classifier · Sentiment analysis · Emotion analysis · Opinion mining · Classification · Feature extraction · Tweets · Social media · Ensemble classifier · Twitter

B. P. Kumar · V. K. K. Rejeti (✉) · T. B. Shanvitha · S. Jyothi Sri · Y. Prathyusha · S. Keerthana
Department of CSE, KKR and KSR Institute of Technology and Sciences, Guntur, Andhra Pradesh, India
e-mail: mail2rvkk@gmail.com

D. Anand
Department of CSE, Koneru Lakshmaiah Education Foundation, Vaddeswaram, Andhra Pradesh, India

© The Author(s), under exclusive license to Springer Nature Singapore Pte Ltd. 2025

B. B. V. L. Deepak et al. (eds.), *Recent Advancements in Product Design and Manufacturing Systems*, Lecture Notes in Mechanical Engineering,
https://doi.org/10.1007/978-981-97-6732-8_8

1 Introduction

The internet is currently the primary medium used by individuals to convey their thoughts, sentiments, and emotions. On social media, millions of individuals share, discuss, publish, and remark on every global event, piece of news, or action. Every one of us encounters many events in our everyday lives, and the result is the formation of feelings around them. Emotion is a powerful emotion pertaining to a person's circumstances or relationships. It influences consumer choices significantly in a variety of industries, including e-commerce, dining establishments, film, and contentment with goods or services.

Human emotions may be conveyed through a variety of mediums, including textual information, voice, gestures, and facial expressions. Written language is the primary form of communication in social media and is the most widely used method of communication between humans and computer systems. Social media has drastically transformed human communication in recent years by offering new ways to instantly link individuals worldwide with information, news, and events. Many articles, news stories, and text messages are uploaded on a daily basis on a variety of websites, blogs, news portals, e-commerce platforms, social media platforms, etc.

Language is a well-known instrument for information transmission, communication, and emotion transmission. The current situation helps satisfy essential demands for social contact by integrating individual blogs and allowing emotional identification in our everyday lives. Many social media platforms have been available for communication, with well-known social networks like Twitter facilitating global user opinion sharing. The most crucial factor in the social media ecosystem is the ability to identify emotions from a variety of angles.

Twitter is a widely used social networking site with a lot of demand globally. Users can create free Twitter accounts, which have the capacity to reach a large number of people. With the help of social media sites like Twitter, citizens, lawmakers, news organizations, and other stakeholders now have more ways to directly reach a wide audience with their voices. It is impossible for one individual to read every tweet and have a comprehensive understanding of the world at large because of their sheer volume. Furthermore, people may cooperatively share their thoughts with their online peers. Effective procedures and strategies are needed to automatically extract different types of information from social media.

Social media monitoring may be used to measure attitudes about current affairs (a practice known as sentiment analysis) or to identify emotions in material that has been created. Sentiment analysis, when used in an automated manner, refers to the technique of recognizing and classifying text according to the views expressed in it. The approach primarily focuses on analyzing the mindset of the individual who submitted the writing.

Sentiment Analysis

Sentiment analysis is a machine learning technique that looks for positive or negative polarity in texts. Machine learning algorithms are trained with textual examples of

emotions so that they can identify sentiment without the need for human input. In other words, computers may acquire new abilities without having to be deliberately taught to do so thanks to machine learning. Sentiment analysis models may be trained to identify context, sarcasm, and improper word use in addition to additional meanings. As an example: Superb user interface. I see now. An engineering degree would be useful. When taken out of context, the terms "very user-friendly" and "helpful" may be seen favorably, yet this is unquestionably a critical comment. With sentiment analysis, computers can automatically interpret and understand text input in a similar way to a human.

Twitter was founded in March 2006 by Jack Dorsey, Noah Glass, Biz Stone, and Evan Williams, and it was released in July of the same year. And as of right now, Elon Musk owns Twitter. Right now, one of the most widely used and effective social networking sites is Twitter. People converse about their daily lives as well as a range of social, political, and international issues. Users have the ability to like, comment on, and retweet posts. Users on Twitter can friend or follow each other. Twitter allows one connection, in contrast to all other social networking sites. This means that one user can add another user without the other user replying. These encounters create a network of communication.

Twitter is a social networking service that gained a lot of popularity due to its frequent posting schedule and lack of limitations. Twitter posts are referred to as tweets, and they can only be 280 characters long. Given the character restriction and the widespread usage of Twitter by users of all ages to voice opinions on many topics, Twitter data is a popular option for text analysis jobs.

2 Related Work

Instead of using deep learning and classification, Deshpande and Paswan [1] presented a hybrid approach model for emotion recognition that combines keyword-based and learning-based models. They used the Twitter API to gather tweets for the suggested methodology. They used Twitter4J, an open-source Java framework, to view the most recent tweets. The pre-processing of the raw Twitter data included tokenization, stemming, and stop-word removal. SentiWordNet dictionary was used for sentiment analysis. Tweets were categorized as favorable, negative, or neutral based on scores. Using *n*-gram, repetitive tweet content that results from retweets was eliminated. POS tagging and topic modeling are two NLP approaches that were utilized to train the model. To classify emotions, two classification models were developed. The Unison model, the conventional approach of classifying emotions, was one of them. Random forest was the second model that was suggested. By comparing the random forest model's performance with the current unison model, metrics like accuracy, precision, recall, and F1-score were examined. The results demonstrated that the random forest model outperformed the unison model. In the end, they divided tweets into 12 emotional categories.

Deepika and Prasad [2] conducted more study on the topic of emotional identification in textual tweets using voting classifiers. As a vote classifier, this work proposed a novel mix of LR and SGD to classify tweets as happy or sad. Here, the authors applied the TF-IDF method. It is clear that the recommended voting classifier outperforms all other classifiers in terms of accuracy, recall, and F1-score. In order to improve performance, future research will assess additional feature engineering techniques and look at other ensemble model combinations. Research will also be done on new approaches to dealing with caustic remarks. Ileri and Karagoz [3] used a collective classification algorithm to detect user emotions in a different study. The tweets that were gathered were written in Turkish. The network topology, which has Twitter users as nodes and their relationships as edges, served as the input for the collective categorization framework. The performance of the suggested approaches had been examined using five distinct models. It was demonstrated that the suggested models' accuracy was almost as accurate as the best models already in use.

Maheshkar and Sarin [4] gave a Review and Analysis of Emotion Detection from Tweets using Twitter Datasets. They studied recognizing multiple emotions from slang unstructured tweets data as there are existing methods for detecting emotion from structured textual tweets. The hybrid method was presented for the classification of multiple emotions and to observe these classification models two techniques such as binary validity and pattern recognition were used. Sentiment analysis approaches include Naive Bayes, support vector machine classifier, and K-nearest neighbor. Along with other datasets, they worked on AIT-2018. Twitter data is gathered using the Twitter API, and dictionary-based technique was employed. Six emotions were used to mark each tweet and reply. Since adjectives, verbs, and adverbs are crucial for identifying emotions in sentences, only these types of words were taken into consideration. Their research revealed that WordNet is inferior than EmoSenticNet lexicon. Agarwal and Gupta [5] created a hybrid deep learning classification system utilizing hybrid convolutional neural networks and recurrent neural networks. They mentioned that sometimes not only internal features but also external features were responsible for actual sentiment detection and proposed a system for emotion detection from both internal and external features. This research found that the proposed H-CNN produces 2.5% accuracy than conventional deep learning classifiers. Object identification from image and video input with a high crowd would affect the accuracy of the system. The system didn't seem to eliminate noise, which might impact the accuracy.

Krommyda et al. [6] used a rule-based approach for emotion recognition considering text along with available emoji in the text. Twitter streaming API and Tweepy library were used to collect data from Twitter with Python. From the Hashtags, words were extracted, if it contains only one word then it would be searched across the nltk dictionary. If it was in camel case style, then capital letters were used to split the hashtag. In case the words were not found in the dictionary, then the hashtag would be discarded. Tweet pre-processor Python library was used to remove mentions and URLs. Except the valid words, others were eliminated. Emojis were classified into nine categories where eight of them existed in plutchik's wheel. About 4000 emojis were examined, and only 6% of them concluded under these eight categories. The

remaining emojis were under the ninth category. If the available emoji belonged to the ninth category, then it would be replaced with corresponding text. Two datasets were developed with the proposed system and datasets were used in EU-funded RESIST project.

Perikos and Hatzilygeroudis [7] worked on emotion recognition using ensemble of classifiers. The three classifiers used were Naïve Bayes, maximum entropy, and a knowledge-based tool. The dataset contained 750 sentences from different sources such as Twitter posts, news articles, and news headlines. It was shown that Naïve Bayes performed better than other two classifiers with the entire dataset. MaxEnt performed better on article and headline sentences, whereas knowledge-based tool performed better on only need headlines.

3 System Architecture

The below Fig. 1 shows the overall flow of the data at each and every stage of processing and finally result will be shown.

Figure 1 talks about how the data is collected from the twitter. And the collected data is stored in the data set, and next, we will preprocess the data set and split the data set into two groups and evaluate the results.

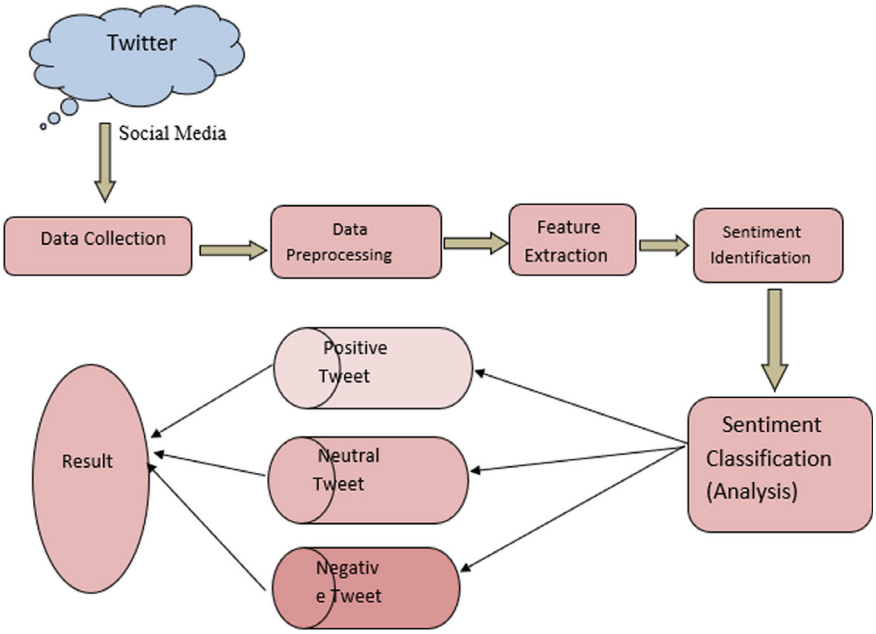


Fig. 1 Block diagram

Figure 2 explains about how the voting classifier algorithm can be worked for the given data.

A vast amount of textual data are in the form of tweets, posts, comments, and messages. This data is used to analyze and understand human emotions expressed in text. Social media platforms like Twitter serve as valuable sources of diverse and real-time textual data.

Emotions can be expressed through various forms of media, including text, images, videos, and audio. In textual data, emotions are often conveyed through words, phrases, and tone. For example, positive emotions might be expressed through words like "happy," "excited," or exclamation marks, while negative emotions could be conveyed through words like "sad," "angry," or negative language. Machine

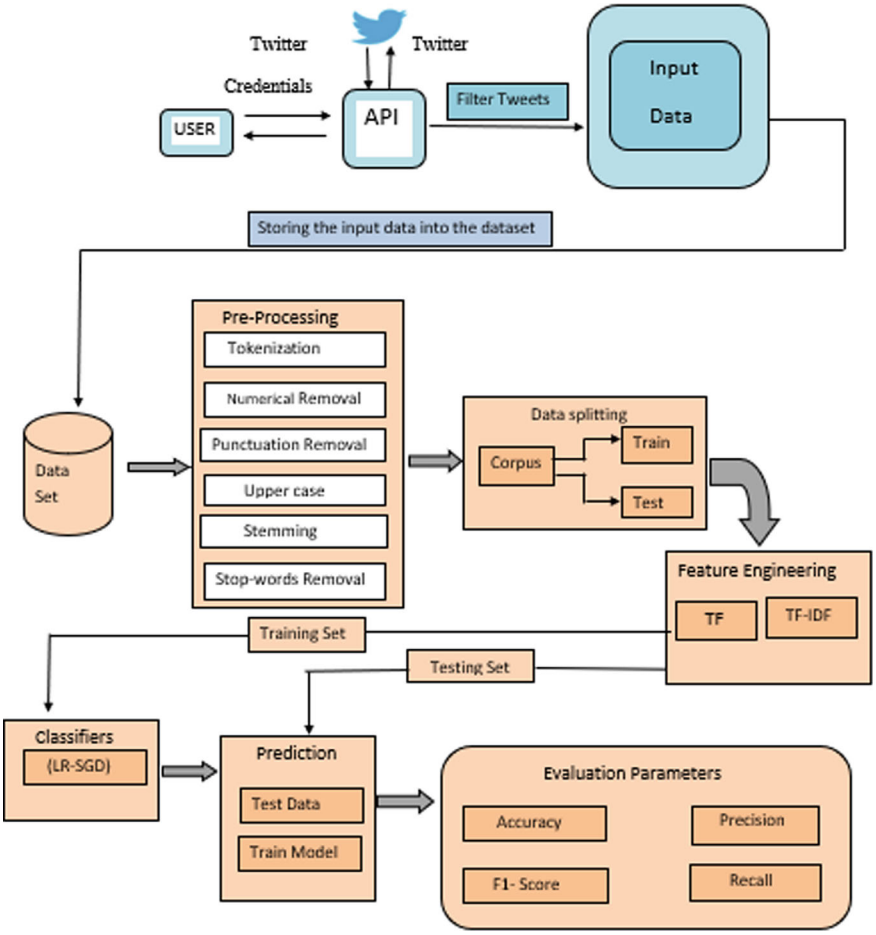


Fig. 2 System architecture diagram

learning models can effectively analyze textual data from social media, enabling the detection and understanding of emotions expressed by users.

Twitter is the social networking site that's being used here. Machine learning models are essential tools for analyzing emotions expressed in textual tweets on this platform because they can handle many languages, process large volumes of data quickly, understand context, and filter out noise.

Opinion mining, or sentiment analysis, is a natural language processing (NLP) approach that is used to identify the sentiment or emotional tone that is communicated in a textual material, like a review, comment, or tweet. Determining whether the text expresses a good, negative, or neutral sentiment is the aim of sentiment analysis. Sentiment analysis is made possible by machine learning technology, which offers the methods and algorithms required to evaluate and comprehend textual input. This makes it possible for applications such as emotion detection in tweets to effectively classify the conveyed sentiments or emotions.

In March 2006, Jack Dorsey, Biz Stone, and Evan Williams founded Twitter, which went live in July of the same year. Character limits, microblogging, followers, hashtags, retweets and likes, real-time nature, and open API are some of the features that set it apart from other social networking sites and make it an effective tool for public conversation, communication, and information sharing.

The ability to gain immediate insights, respond effectively to changing conditions, and make data-driven decisions that can have a significant impact on various aspects of business, research, and crisis management. Using Twitter API's you can collect real-time and historical data from Twitter for various applications such as sentiment analysis, trend analysis, and social media monitoring.

The steps involved in data pre-processing are data cleaning, data transformation, data integration, data reduction, data splitting, and data formatting. It is essential for clean, well-organized data enhances accuracy, reduces overfitting, speeds up training, and provides a better understanding of the underlying patterns in the data, leading to more reliable and interpretable machine learning models.

Naïve Bayes, SVM, logistic regression, decision Tree, random forest, SGD are the ML models used here. Voting classifier leverages the strengths of multiple models to provide a more accurate and reliable prediction, especially in cases where individual models may have limitations.

4 Implementation

Step 1: Data Collection

By using the Twitter API to create an app, one may receive real-time access to Twitter posts. To access the real-time tweets, we utilize the free and open-source Java tool Twitter4J. A user can accomplish the following with Twitter4J: In addition to posting tweets, he may view the user timeline, send and receive messages, and read the most recent tweets in real time. The confidentiality and privacy of the user are guaranteed

by the Twitter4J library. The dataset contains the tweets that have been gathered. Whenever analysis is needed, the most recent data is used thanks to the benefit of utilizing real-time data.

Step 2: Pre-Processing

The dataset includes raw, superfluous data. It may be partially or fully organized. Such superfluous input lengthens the model's training period and may cause performance degradation. Thus, it is removable. Pre-processing is essential for increasing the models' effectiveness and conserving computer power. Pre-processing of the text can improve the model's prediction accuracy. Tokenization, numerical removal, punctuation removal, upper case (case conversion), and stop-word removal are among the pre-processing stages that can be carried out.

Step 3: Data Splitting

After the pre-processing, the data can be split into two sets: training set and testing set.

Step 4: Feature Engineering

For the supervised machine learning classifiers to be trained, the textual data must be in vector form. Thus, vector characteristics are created from textual features.

5 Result

This section provides the overall result of the system. From the table, we can draw a graph comparing the seven algorithms SVM, decision tree, Naïve Bayes, random forest, gradient boosting model, voting classifier (logistic regression and Stochastic Gradient Descent) against performance measures precision, F1-score, accuracy, recall as shown below (Fig. 3, Table 1).

The results of the accuracy 77, 75, 77, 76, 75, 75, 80% are shown, respectively. It is clearly depicting that the accuracy from our proposed model is much higher than the accuracy of the existing models. Unlike other models, we proposed a system which uses an ensemble of models as voting classifiers which increases the accuracy of the system.

6 Conclusion

Our project classifies the Tweets into positive, negative, or neutral. For classifying them, we used combination of two models logistic regression and Stochastic Gradient Descent. We conclude that involving ensemble of models increases the efficiency. We applied sentiment analysis only on the Twitter dataset and what if the dataset is a combination of data from other sources but not only Twitter. One algorithm may

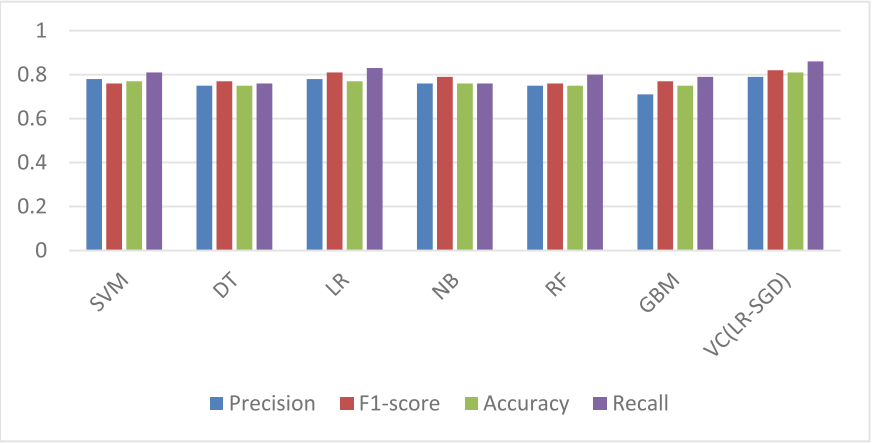


Fig. 3 Comparing the classification result of all machine learning models using TF-IDF characteristics

Table 1 ML classifiers with TF-IDF

ML models	Precision (%)	F1-score (%)	Accuracy (%)	Recall (%)
SVM	78	76	77	81
DT	75	77	75	76
LR	78	81	77	83
NB	76	79	76	76
RF	75	76	75	80
GBM	71	77	75	79
VC (LR-SGD)	79	82	80	85

work efficiently on a particular type of data. So, in this case, multiple models are needed for better performance. And we suggest our model works better in this case with much better accuracy and precision values.

References

1. Deshpande A, Paswan R (2020) Real-time emotion recognition of twitter posts using a hybrid approach. ICTACT J Soft Comput 10(04):302
2. Deepika G, Prasad GNR (2022) Emotion recognition by textual tweets classification using voting classifier (LR-SGD). Int J Adv Res Comput Commun Eng 9:6286–6295
3. Ileri I, Karagoz P (2016) Detecting user emotions in twitter through collective classification, detecting user emotions in Twitter through collective classification. In: Proceedings of the 8th international joint conference on knowledge discovery, knowledge engineering and knowledge management (IC3K 2016). KDIR, pp 205–212. https://doi.org/10.5220/0006037502050212

4. Maheshkar V, Sarin SK (2022) Review and analysis of emotion detection from Tweets using Twitter datasets. In: WAC-2022: workshop on applied computing, January 27–28, 2022, Chennai, India
5. Agarwal S, Gupta MK (2022) Emotion detection using context-based features using deep learning technique. J Theor Appl Inform Technol 100(19):1817–3195
6. Krommyda M et al (2020) Emotion detection in Twitter posts: a rule-based algorithm for annotated data acquisition. In: International conference on computational science and computational intelligence (CSCI). IEEE. https://doi.org/10.1109/CSCI51800.2020.00050
7. Perikosn I, Hatzilygeroudis I (2016) Recognising emotions in text using ensemble of classifiers. J Homepage. https://doi.org/10.1016/j.engappai.2016.01.0120952-1976/

Government Bidding Security Management System Using Blockchain



Venkata Kishore Kumar Rejeti, G. Rajesh Chandra, T. Venkata Sai Vardhan, T. Manoj Sai, S. Srihas, S. K. Karimulla Saleem, and D. Anand

Abstract Governments and businesses typically utilize contracts or tenders to acquire products or services. When improper procedures are used, mishandled tender management can result in enormous losses. Contractor preference, poor record keeping, a lack of transparency, hacking, data manipulation, and other problems are examples of this. In order to solve this issue, we have employed an obviously block-based design for transaction management in conjunction with a straightforward and secure block chain technology. Here, we use blockchain technology to secure transaction-based documents and transactions, including tender papers, applications, bid proposals, business profiles, historical records, authorizing officer data, and rejection details, in order to ensure a completely transparent bidding process.

Keywords Contractors · Bidders · Tenders · And Blockchain

1 Introduction

Within the current tender management system, there are two discrete sectors: the public sector and the private sector.

Individual sector, certain phases have abbreviations that begin with the letter "R."

Request for Tender, Request for Estimate, Request for Ideas and Request for Proposal. The public sector is structured into three phases:

Interest Expression (IE)

Questionnaire for Pre-qualification (QPQ)

Request for Tender (RT)

There are some stages where the initials start with "R"

Request for Tender Request

V. K. K. Rejeti (✉) · G. R. Chandra · T. V. S. Vardhan · T. M. Sai · S. Srihas · S. K. K. Saleem
Department of CSE, KKR & KSR Institute of Technology and Sciences, Guntur, India
e-mail: mail2vkk@gmail.com

D. Anand
Department of CSE, Koneru Lakshmaiah Education Foundation, Vaddeswaram, AP, India

© The Author(s), under exclusive license to Springer Nature Singapore Pte Ltd. 2025

B. B. V. L. Deepak et al. (eds.), *Recent Advancements in Product Design and Manufacturing Systems*, Lecture Notes in Mechanical Engineering,
https://doi.org/10.1007/978-981-97-6732-8_9

Call for Proposals
Demand for Offer.

As the aforementioned examples demonstrate, there are several industries in which the Indian government frequently invites citizens to engage in bidding processes in order to purchase various commodities for various departments in accordance with how those products will be used. In general, the actual bidding procedure goes like this:

Step 1: Make a proposal request

To start the bidding process, product owners or project teams must first send out a request for proposals (RFP) or invitation to bid (ITB). After that, a tender manager puts together a package with project details. The package should clearly explain the project's objectives, requirements, and priorities to bidders so they know exactly what has to be done.

Step 2: Interested Parties Prepare Their Bids

Interested parties will assess the proposal when an RFP is released. The project manager who draughts the bid is referred to as the bid manager in this context. In addition to coordinating with the company that issued the RFP for clarifications, the bid manager speaks with the project team to confirm that the resources they are going to commit to are available. This procedure can involve arranging for another bidding session with subcontractors or outside vendors if the general contractor is the bidder. The bid can then be forwarded to the entity making the request once all the information has been gathered and arranged.

Step 3: Assessment and Selection of Bids

Tender managers evaluate the bids in relation to each other and the specifications once they have been gathered. Contrary to popular assumption, the lowest offer isn't usually accepted. The MEAT criterion (most economically advantageous tender) is the most widely used method for selecting the best supplier or service provider. MEAT criteria include quality, accessibility, social value, innovation, and other factors into account in addition to price. A two-step procedure of selection may involve shortlisting candidates before choosing.

Some of the Government Agencies involved in Tenders is listed the below table:

S. No.	Ministry
1	Ministry of agriculture
2	Ministry of Panchayati Raj
3	Ministry of chemicals and fertilizers
4	Ministry of Civil aviation
5	Ministry of coal
6	Ministry of commerce and industry
7	Ministry of communications and information technology

(continued)

(continued)

S. No.	Ministry
8	Ministry of consumer affairs, food and public distribution
9	Ministry of cooperation

These are the government agencies mentioned above that are involved in offering bids to Indian residents so they can participate and purchase what they need. Different persons can utilize different sorts of resources from a variety of agencies. Let's now examine the real process that is now being carried out by the federal government as well as state governments.

Bidding procedure in central government

During this phase, it is expected that the buyer and bidders would communicate. For further information, the institution conducting the procurement process may also ask for presentations or interviews.

S. No.	Ministry
10	Ministry of corporate affairs
11	Ministry of culture
12	Ministry of defense
13	Ministry of earth sciences
14	Ministry of environment, forest and climate change
15	Ministry of external aafair
16	Ministry of finance
17	Ministry of food processing industries
18	Ministry of health and family welfare
19	Ministry of AYUSH

1. The builder must complete online enrolment in the portal using the provided user ID and password, as well as the digital signature that was provided during registration.
2. After the enrolment procedure is over, an E- token will be produced; you should take care of it and never want it to be exploited by others.
3. Under the "my document" option, the bidder can update information in advance, such as purchase order details and certifications, and these can be chosen in accordance with the tender criteria during the bidding registration process.
4. The bidding details will be shown as follows in the website in which the user can select the required tender details in which the bidder has to participate.
5. Bidder has to pay some fee before the enrolment of the bidding in the website in advance for the security and due to some resources provided by the government.



Fig. 1 Central government website for bidding

6. Once the payment was done successfully the bidder will receive the document in which they have to carry the hard copy of the document to the place where the bidding has been done physically.
7. The tender inviting Authority will not be responsible for the delay of process and any of the financial and any type of issues.
8. The time will be displayed and notified to you in the website of the bidding process venue and all the details of timing.
9. Now the bidder can actively participate in the auction based on the venue and timings assigned and noted on the website at the time of registration (Fig. 1).

Procedure of bidding in state government

1. The bidder needs to register online using this portal.
2. The bidder then uses the user's name and password they selected when registering to log into the site.
3. The bidder has to create an account if they don't already have one or a password.
4. All of the current auctions will be shown there, and the bidder may obtain information about the auction, such as the start and end times,
5. The winning bidder may reserve a time slot, bring all required paperwork to the designated site, and take part.
6. Before submitting their offer, the bidder reads and agrees to the terms and conditions.
7. The bidder must carefully review the tender schedules after downloading or receiving them, and then submit the papers in accordance with the document; if not, the offer will be rejected.

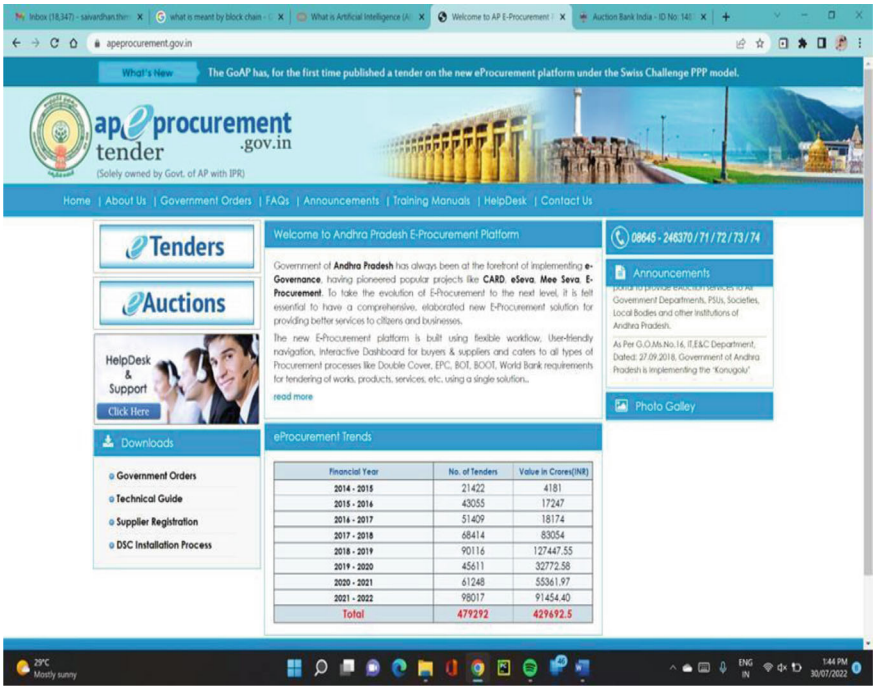


Fig. 2 State government website for bidding

8. Should you want any clarifications; you can get them online via the e-auction portal or by contacting the people listed in the tender document. Before making an online bid, bidders should consider the published corrigendum.
9. As specified in the tender schedule, bidders should prepare their bid materials ahead of time. The documents should be in the PDF, XLS, RAR, or DWF formats. Multiple documents can be grouped together if there are more than one.
10. When a bid is successfully submitted through the system, the bidder's uploaded bids are received and recorded in the system. The system does not attest to its accuracy.
11. If the participant wins, the item can be theirs after the event; if not, it won't be given to them (Fig. 2).

2 Literature Review

Numerous researchers were drawn to the Government Bidding Security Management System that uses blockchain applications. From the journal, we derived the procedure for the suggested system, which will show all of the open tenders in [1]. All website

visitors will be able to see the tender, but only those who have registered as users on the portal will be allowed to submit a bid. The methods are information display, assessment, and storage. Enhance the host organization's efficacy and productivity. Decision-makers frequently combine emotion, subjective assessment based on prior experiences, and intuition while making decisions [2]. Based on the consideration of journal. Often employed in antitrust is deceptive or ineffective. There are several unique characteristics of auctions and bidding processes, such as bid-taker power, common values behaviour, and price creation procedures. It is possible for this to operate in a manner that does not need the deployment of any approach that compromises user security. It is possible for this to operate in a manner that does not need the deployment of any approach that compromises user security.

A contract bidding system was created in [3] according to the journal, using Structured System Analysis and Design Methodology (SSADM). It is planned to create an online application that would allow bidders to register and submit their offers. The increasing realization that bidding procedures that were previously carried out manually must be modified led to the development of apps that would allow bidders to register and submit their bids online. The application's usability may be compromised, and data storage may have an impact on the system's complexity in terms of time and space. In [4], a bidding strategy is assigned at random to each bidder from the examined journal. She uses a uniform distribution to determine her valuation. The results of the trials indicate that the longer the auction lasts, the higher the average predicted utility of the agents using the suggested method. To assess the method in a simulated eBay-like auction environment, we do tests. The suggested bidding strategy is contrasted with five typical ones. The suggested system will include five mechanisms, which will reduce its efficiency and make it seem quite unsettling in general.

Zheng et al. [5], based on observations of the correlation between the length of the bidding period and the price at auction in an online auction. Our findings show that it exhibits clear snip bidding activity on www.taobao.com during online auctions. It mainly demonstrates that comparable snip bidding conduct seen in other nations' mature markets also occurs in the Chinese online auction market. The head person must be aware of the snip bidding process in order to understand the internal workings of the proposed system, which is akin to a snip bidding system. The quick growth of railway transportation building was made possible by the material supplies provided by the railway department in [6]. In addition to saving money and time compared to the traditional method of having employees travel to and from the bidding location, online material procurement bidding also better meets the various demands of railway procurement. Bidders are guided to submit correct and timely bids by the automated cohesiveness of the procurement process, which includes consultation, appraisal, and bidding. The method has several drawbacks, such as the difficulty in using and supplying the bulk materials used by the railway department, which results in more labour and machinery.

Wang et al. [7] uses longitudinal survey data from 12 online reverse auctions across a range of product categories to examine the effects of the supplier's relationship propensity prior to the auction on the supplier's bidding aggressiveness in the auction

(i.e. the quantity, frequency, and price concessions offered) and (2) the impact of bidding behaviours in the auction on the buyer–supplier relationship following the auction. The findings point to several bidders, incumbency, and a readiness to make certain investments as causes of less active bidding. We present a straightforward technique to spot dubious auctions that could be impacted by shill bidding, a type of fraud. This gives us reason to suspect unlawful actions, such as scams, and the harmful effects that are occurring these days. This approach creates a difficult situation where it takes a lot of effort and time to identify fraud and other questionable activity.

3 System Architecture

From Fig. 3, We can have a clear explanation of our proposed system in which it shows the actual process of our system which was very useful actually. At first, the tender officer will release the tender details to the notification centre of the official government website. Now the bidder can clearly know the tender details and he/she can accept the tender. All the details of bidder, tender details will be protected with blockchain technology (Fig. 4).

The tender officer will be released the tender details on the official government website. The details will be encrypted and stored in a database which was established with the blockchain architecture. Now the bidder will get the tender notification details and get registered to bid. The bidder details get encrypted and stored in a database. Now the tender officer will get the decrypted bidder details and make the process of bidding by sending mail to the bidders. After the process of bidding, the tender officer will upload the final bidding results in a database combined with the encryption by using blockchain technology. The bidder will receive the final result of bidding details from the tender officer through secured data encrypted with blockchain. By this we came to know that the secured process of bidding will happen without any hacking and any other attacks. By this we will secure the data in a high manner.

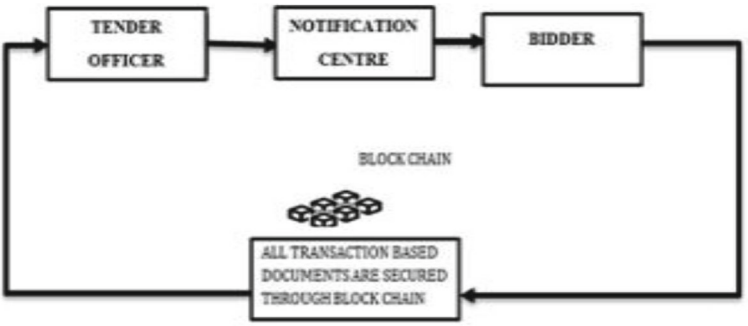


Fig. 3 Block diagram of proposed system

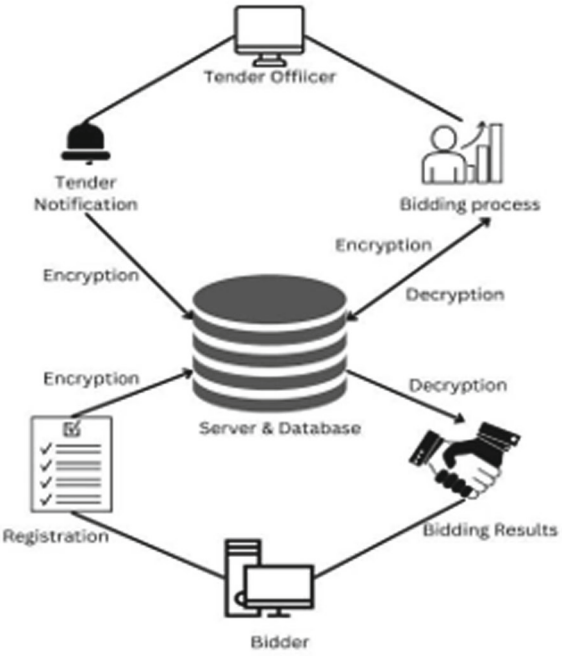


Fig. 4 Architecture of system

4 Proposed System

Blockchain technology is used in the proposed tender management system to provide a safe and effective tender management procedure. Encryption and an unquestionable block-based architecture for transaction management protect a block chain. This enables the system to retain a straightforward, transparent transaction while communicating the essential, need-to-know data. There are huge advantages associated in our proposed system as follows:

1. Reducing the risk of duplicates
2. Simplifying stakeholder management
3. Greater control over documents
4. Proper maintain of rejected records
5. Proper records for applicants
6. Proper records of company profile

The applications for the proposed system are as follows:

- Smart tender management is designed to put the users in the best place.

Algorithm

1. Tender officers have to register as an officer in the official government website.

   a. Details will be secured by using blockchain

2. Bidders have to register as a bidder in the official government website

a. These details will be encrypted by using blockchain and stored in a structured format.

3. Tender officers can login in to the website and release the tender notification details which include all the details of tender in which the bidder has to participate in the official government website.

a. The uploaded details will be secured by using blockchain Technology.

4. After registering, bidders will access the tender notifications by logging into their accounts.
5. Tender officials will download the tender files that we have registered from the bidders and use blockchain technology to decode the data from the downloaded files in order to get bidder information.
6. A confirmation email indicating the bidders' acceptance of the tender applications will be issued to them when the bidders' information is obtained.
7. The bidder will give the bidder officer their information in text files if they are comfortable with the tender description.
8. The bidder can use the official government website to review the tender officer's reaction after submitting their application.

- Beneficial for contractors and customers and tenders.

Modules included in Proposed System

The proposed system includes 3 entities: tender officers, bidders, and blockchain. Let us have a clear explanation about all the above three modules, tender officer and their functionalities and process of securing the data of the tender officer details and also how the notification details will be updated and secured using blockchain technology. And also, we can see what was the main functionality of the bidder and how the bidder details will be secured and how can the bidder see the details of tender notification uploaded by the tender officer and how can the bidder accept the bidding.

The main process which was included as an important concept is how the data will be saved and secured in the databases and how can we encrypt the data and as well as how can we decrypt the data and also how can bidder visualize the data and actual process of the secured data process using block-based architecture will be described clearly.

- **Tender Officer**: After registering, the tender officer will go into the account and update the notice regarding the tender process. The notification part can be edited or removed by them. The bidders' personal information would be obtained by the officer after downloading the tender files they registered for and decoding the data. Following the acquisition of their information, the bidders received a confirmation email including their tender applications.

- **Bidder**: Following registration, bidders will access the tender notifications by logging into their accounts. If the bidder is satisfied with the tender description, they will provide the bidder officer with their information in a text file. After submitting the application, they can see the tender officer's response and can submit data in a text file to the tender officer in order to make a tender.
- **Blockchain**: Data is divided into pieces and stored on the blockchain in an encrypted fashion. In this case, data is encrypted and stored in a database before sections of it are hidden using a hash code.

The proposed system addresses the issue of favouritism like decentralization, immutability, and auditable trial. Improper record maintenance like data integrity, automated record keeping, and secure data storage. Lack of transparency like public ledger, traceability, and reduced information asymmetry. Hacking and data modification lead to cryptographic security, distributed consensus, and immutability. There are specific mechanisms to provide solutions for the above problems like decentralization, immutability, auditable trail and traceability, etc. Here are the more detailed encryption methods. Advanced encryption standard (AES) is used to encrypt sensitive tender information. Elliptic curve cryptography (ECC) is used to secure communication between tender participants. The proposed blockchain-based tender management system employs a combination of cryptographic security measures—symmetric encryption, asymmetric encryption, and digital signature. Distributed consensus mechanisms—Byzantine fault tolerance (BFT) and Proof-of-Stake (PoS), and blockchain architecture—permissioned blockchain and immutability to ensure the security and integrity of tender data and prevent unauthorized access or data tampering.

The key advantages of implementing this in public and private sectors are enhanced transparency and traceability, improved security and data integrity, streamlined processes and reduced cost, enhanced auditability and compliance, and increased efficiency and market access. It improves stakeholder management by enhancing transparency, traceability, real-time access, and immutable audit trails, improves reduced duplicates like automated processes, centralized, secure storage, and standardized tender formats, improves proper record keeping maintaining like immutable record maintenance, audit trail, automated record capturing, and decentralized nature. The article explains the user experience in tender creation and publication, bid submission and evaluation contract award and management in tender officer perspective and tender search and registration, bid preparation and submission, and bid status tracking and communication in the bidders perspective.

The tender officer interaction will be done in the tender creation and publication, bid submission and evaluation, and contract award and management. Bidder interaction will be done in the tender search and registration, bid preparation and submission, and bid status tracking and communication. The proposed blockchain-based tender management system is a relatively new concept with case studies on different sectors like construction tendering in South Korea, supply chain management in the pharmaceutical industry, E-Procurement in the agricultural sectors, and international trade finance like banks. There are several real-world implementations

of blockchain-based tender management systems including the Dubai Government's E-Procurement platform, the South Korean construction company, pharmaceutical company's supply chain management systems, and agricultural co-operative's E-Procurement platform as we discussed in the case studies. Yes, the article provides more details about the encryption methods and blockchain architecture used in the proposed systems like encryption methods like advanced encryption standard (AES), elliptic curve cryptography (ECC), key management, blockchain architecture such as Byzantine Fault Tolerance (BFT), network infrastructure, smart contracts, and integration with existing systems.

5 Results

Let us see the overall outcome of our developed system which was done by using block chain of AES with 128-bit configuration.

According to Fig. 6, we can see the home page in which bidder and tender officer can navigates to their respected pages for registration and login based on the opinion of either bidder or tender officer.

Based on Fig. 7, we can clearly observe the image consists of some technical questions and with the tender officer login details which consists of email and password with constraints based on the field.

According to Fig. 8, we can view the tender notifications in which the bidder can actively participate in the bidder which was updated by the tender officer.



Fig. 6 Home page of developed system

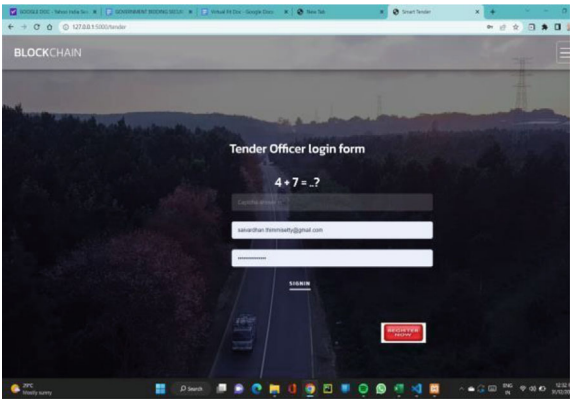


Fig. 7 Tender officer login/ registration page

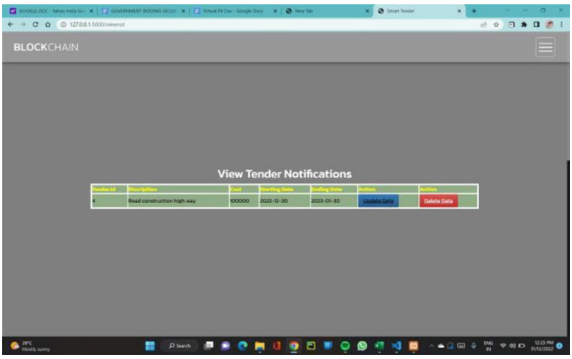


Fig. 8 Tender notification details

From Fig. 9, we came to know that the bidder can register or login through the page and can register for the bidding procedure.

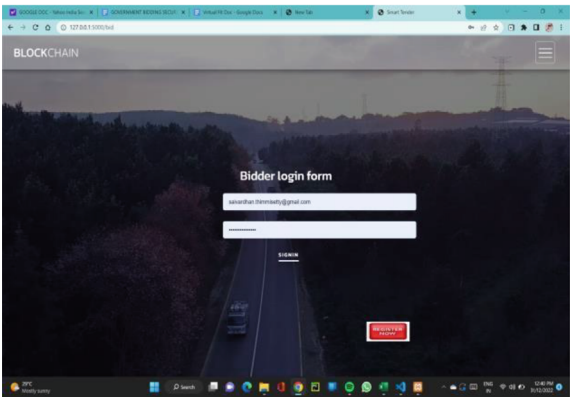


Fig. 9 Bidder login/ registration page

6 Conclusion

Conventional technology and design patterns are incompatible with applications like tender portals, where security and transparency are critical needs that cannot be compromised. As was previously indicated, a tendering framework's security requirements cannot be fully satisfied by using a centralized platform for creating and bidding on contracts. The only way the government can meet this type of application's security and transparency requirements is by leveraging open, transparent, and equitable technology like blockchain and smart contracts. The numerous processes required in the design of such a system are described in this document, along with a basic implementation of those procedures.

References

1. Davis KC (1967) The information act: a preliminary analysis. Univ w Rev 34(4):761–816
2. Ambegaonker A, Gautam U, Rambola RK (2018) Efficient approach for tendering by introducing blockchain to maintain security and reliability. In: 2018 4th International conference on computing communication and automation (ICCCA). IEEE
3. Pal O, Singh S, Blockchain technology and its applications in e-governance services
4. Betts M et al (2006) Towards secure and legal e-tendering. J Inf Technol Constr 11:89–102
5. Zheng Z et al (2017) An overview of blockchain technology: architecture, consensus, and future trends. In: 2017 IEEE international congress on big data (BigData congress). IEEE
6. Pilkington M (2016) Blockchain technology: principles and applications. In: Research handbook on digital transformations. Edward Elgar Publishing
7. Wang W et al (2019) A survey on consensus mechanisms and mining strategy management in blockchain networks. IEEE Access 7:22328–22370

Resource Forecasting of Geographical Area Using Big Data Analytics



Venkata Kishore Kumar Rejeti, G. Rajesh Chandra, V. Mounika, S. K. Thasleema Thanveer, V. Jyothika, Y. Harika, and D. Anand

Abstract Prospective purchasers now deal with location ignorance in a certain area. Here, we want to set up a big data analytics system that can handle different kinds of data processing for a broad variety of uses. Big data analytics (BDA) is an organized method for examining and spotting various relationships, patterns, and trends in a sizable amount of data. In this study, we use BDA to data resources where visualization and trend prediction are achieved by exploratory data analysis. Hadoop-based big data analytics has a useful function. We can extract previously undiscovered, valuable information from structured data by using the big data idea and data mining tools. Here, computer science and the municipality are working together to create a data mining process that will assist people seeking to learn specifics about a certain geographic location. This project may be produced with the aid of data on transportation, utilities, water supply, electricity supply, and other amenities. It is based on location data that our interface will analyses in the past and provide reports to the user.

Keywords Big data · Raw data · Data preprocessing · Machine learning · Data visualization · Classification · Apache Hadoop

1 Introduction

Big data analytics (BDA) is an emerging technique that has gained popularity recently for its ability to analyse data, extract relevant information, and analyse relationships across a broad range of application domains. Cities are becoming increasingly significant and fundamental to our society as a result of ongoing urbanization and population growth. But these advancements have also been followed by a rise in violent

V. K. K. Rejeti (✉) · G. R. Chandra · V. Mounika · S. K. T. Thanveer · V. Jyothika · Y. Harika
Department of CSE, KKR & KSR Institute of Technology and Sciences, Guntur, India
e-mail: mail2rvkk@gmail.com

D. Anand
Department of CSE, Koneru Lakshmaiah Education Foundation, Vaddeswaram, AP, India

© The Author(s), under exclusive license to Springer Nature Singapore Pte Ltd. 2025

B. B. V. L. Deepak et al. (eds.), *Recent Advancements in Product Design and Manufacturing Systems*, Lecture Notes in Mechanical Engineering,
https://doi.org/10.1007/978-981-97-6732-8_10

crimes and the placement of utilities like electricity and water supplies. Sociologists, analysts, and safety organizations have put a lot of work into identifying probable trends and variables in order to address such issues. Yet, managing the vast volumes of data that are available presents several difficulties in terms of public policy. To analyse this heterogeneous and multi-sourced data, new techniques and technologies must be developed. By analysing large amounts of data, we can more efficiently monitor events as they happen, find patterns in incidents, allocate resources, and act quickly when necessary. Additionally, this can deepen our comprehension of both historical and contemporary challenges, ultimately leading to better safety and security, higher standards of living, and more rapid advancements in both the cultural and economic spheres.

The primary obstacles we are dealing with are as follows:

- The growing amount of data that has to be analysed and stored.
- Because the data is inconsistent and fragmentary, data analysis is challenging.
- Restrictions on obtaining data records from government agencies.
- The training set's correctness affects the program's accuracy.

To find additional possible patterns and trends within these datasets, we combine graph mining tools, multivariate visualization, and fine-grained geographical analysis. In addition, we want to carry out more accurate case studies to assess the efficiency and scalability of the various models in our system. To determine the geographical area's percentage rate, a machine learning technique is employed.

The three crime datasets we utilized for our research, which include the Andhra Pradesh cities of Guntur, Vijayawada, and Ongole, are publicly available, as shown in Fig. 1.

As a result, we primarily concentrate on the top 10 offences that occur most frequently, and we exhibit their distributions as percentages in Fig. 1. As can be observed, stealing poses a serious danger to any community, along with other more serious crimes like assaults and burglaries.

We have just information about the resources that are known to exist; thus, we decided to use this approach to determine the resource pattern for a certain location. As a result, a classification method that depends on problems that have already been addressed would not provide accurate predictions for new resources. Additionally,

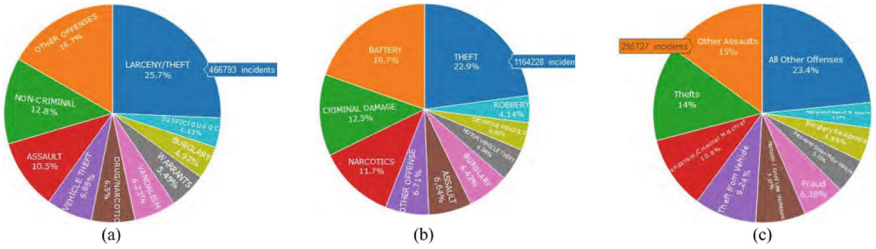


Fig. 1 Top 10 crime cases for cities of **a** Guntur, **b** Vijayawada and **c** Ongole

the nature of resources varies with time; therefore, clustering approaches are more effective at detecting newer and undiscovered patterns in the future.

Analysing involves the following steps:

Data preprocessing, data collection, algorithm classification, geographic data verification, resource classification, and data visualization.

2 Literature Review

Tong et al.'s [1] work uses crime data mining to identify trends in criminal behaviour in an effort to foresee, forecast, and stop illegal conduct. Many crimes that occur annually in a major city may have been perpetrated by the same person or people. Crime-prone zones may be visualized and places with a high chance of crime can be predicted by the system, according to S. Sathayadevan [2]. Crime data analysts are able to assist law enforcement officials in expediting the process of investigating crimes due to the growing use of computerized systems.

Archenaa and Anita [3] state that the purpose of this study is to provide insight into how we might extract more value from the data produced by the government and the healthcare industry. With Hadoop, big data analytics is able to identify critical situations before they arise and do insightful real-time analysis on massive amounts of data. The primary goal of this study, according to Joshi et al. [4], is to use a qualitative and quantitative technique to analyse crime, which includes theft, homicide, and different drug crimes. It also includes suspicious activities, noise complaints, and burglar alarms. We can find vital information through data mining that will assist local authorities in identifying important locations and instances of criminal activity.

Zhon et al. [5] state that the purpose of this research is to examine machine learning approaches within the framework of large data and contemporary computer systems. In particular, we want to look into the benefits and drawbacks of large data machine learning. Nasif et al. [6] state that the current survey's objective is to examine the data mining strategies used by social media networks from 2003 to 2015. Since social media data mining applications are still in their infancy, more work needs to be done in academia and business to properly complete the task. The primary objective of this work, according to Zheng et al. [7].

Niu et al. [8], is to develop an efficient speed prediction model that can anticipate traffic conditions at the city scale, and they suggested a unique spatiotemporal model.

The experimental findings show that our suggested prediction model is capable of accurately predicting the speed of urban traffic by Stopar et al. [9]. They represent temporal dynamics as transitions between the states and summaries the data as conceptual states in order to find such patterns. According to Tamas and Toth, this article illustrates how important it is to determine an indoor location in order to create smart environments [10]. Algorithms for symbolic indoor placement identify the location as a clearly defined space within the building, such a room, hallway, or floor. This research presents a performance analysis of symbolic indoor location techniques based on categorization.

This work aims to bring location awareness intelligence to smart buildings using location-based services (LBS), as stated by Khruahong et al. [11]. One of the LBS for smart city projects will be the use of information and communication technology (ICT) to locate missing properties in complicated structures.

GPS technology is utilized by mobile or online applications to look for misplaced items outdoors. In [12], the spatial arrangement of the vista space is a factor that has not yet been examined by Stulpnagel, R Von, and K Schmid. They demonstrate how to create extremely accurate isovists using laser scans in order to characterize the spatial layout of a vista region [13]. The aim, according to Theodoros Oikonomidis, Konstantinos Fouskas, and Maro Vlachopoulou, is to pinpoint any gaps in the field of LBS for the benefit of both companies and academics. The rapid advancement of technology in relation to smart mobile devices has created new avenues for both commercial and scientific endeavours.

3 Proposed System

In the suggested system, the user chooses a specific neighbourhood where he wishes to purchase a home. Our interface then shows the area's crime rate, needs, and sources, and the user may choose whether or not to purchase a home there. With the aid of data, this project may be produced. Based on the data provided, our interface will examine prior data and provide reports to the user. A comparable but more thorough approach that incorporates statistical analysis, data visualization, and trend prediction has been implemented in our suggested system. We investigated the location's data. To display the statistical associations that have been collected from the massive volume of data pertaining to various qualities, data visualization and mining techniques are employed. Modern machine learning techniques are used to predict patterns and produce highly accurate optimum models.

Benefits of the Proposed System:

- The project is mostly beneficial to those who are not from the area or who are not aware of the location of the property they wish to purchase.
- Those who are going to new places will also benefit from this endeavour.
- Better results.
- Capable of deriving deeper meaning from the outcome.
- Precise outcomes can aid users in understanding the place.

4 System Architecture

Here, Fig. 2 describes the process of proposed system where the user utilizes the data stored in the data storage.

Implementation

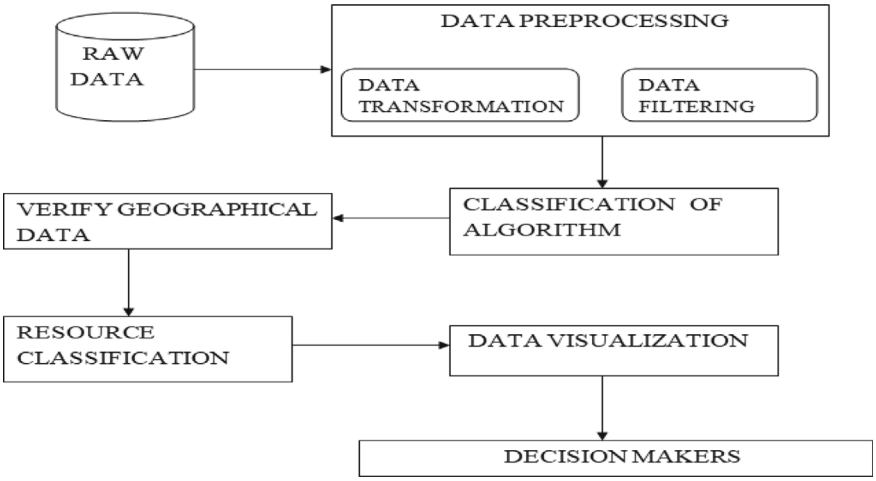


Fig2 Location-based analysis process

1. **Data Collection**

We get information from police and municipal records during the data collection phase. The gathered information is kept in a database for further use. Using Apache Hadoop, the gathered data is organized. One source of raw data that is both organized and available is crime data. Following the data gathering, we proceed to the next phase.

2. **Raw Data**

Raw data is data that hasn't been processed for the following stage and is often referred to as source, atomic, or primary data.

Raw data occasionally finds its way into a database as a result of processing, which improves the data and makes it more available for additional processing and analysis in several contexts.

3. **Data Processing**

Data preprocessing, which is a part of data preparation, refers to any kind of data processing done on raw data in order to get it ready for further data processing steps. It is the idea of transforming unprocessed data into processed data.

(a) Data Filtering

Data filtering facilitates the development of mining models. This subset of data in a mining framework is used in data filtration. Because we may construct a single mining structure based on an extensive data source view, filtering offers us freedom in the design of our data sources and mining structures. Alternatively, we might design filters that let us to utilize a portion of that data for training and testing multiple models, rather than creating new structures and related models for every subset of data.

(b) Data Transformation

We have already started to alter our data in addition to cleaning it, but data transformation will start the process of putting the data into the right format. We will require more procedures and analysis.

This typically occurs in the instances listed below:

Discreditation, aggregation, normalization, feature selection, and concept hierarchy generation.

4. **Classification of Algorithm**

A supervised learning method called the classification algorithm is utilized to find new observations in the training data set. When classifying data, a programmed first learns the observations and dataset provided, after which it divides fresh data into several classes. To assess the model, the data is divided into training and testing models for each instance. This can provide us with a performance estimate relatively quickly, and it is only better to use a given dataset if you have a sizable dataset. Divided percentage: Calculating a percentage is a great way to quickly assess a model's effectiveness. It is not limited to decision-making, unless you have an enormous dataset that adequately captures the issue. For the train and test datasets, a typical split value is 66% to 34%, respectively.

With the use of a machine learning system, we can determine the percentage. An approach for machine learning based on supervised learning is called linear regression. Regression modelling is carried with using independent variables. Finding the relationship between variables is its primary purpose.

5. **Confirm Geographic Information**

Data and information from both internal and external associations in a place are referred to as geographic data. Here, we confirm the information with all of the location's resources before moving on to the next phase.

6. **Classification of Resources**

One popular method used in data mining to divide data points into distinct classes is classification. It enables us to arrange various kinds of datasets, from small and straightforward ones to vast and complicated ones. Here, we categorizes every resource using a method based on location.

7. **Visualization of Data**

Visualization is the process of displaying data and information graphically. Data visualization tools give users a method to observe and comprehend trends, outliers, and patterns in data by utilizing visual components like charts, graphs, and maps. Here, when the user enters the location, we plot the data into pie charts.

8. **Decision Making**

After seeing the location's findings in geographical data resources, the user may determine whether or not he wants to purchase the property. The process of reaching

a choice involves the user identifying all the information obtained and resolves to get to a conclusion.

The proposed method can leverage big data analytics by collecting and analysing a significant amount of information about the utilities and crime rate, such as transportation, electricity supply, and water facilities, in order to reduce the amount of location unawareness among potential buyers in a given region. With this information, ideas and insights specific to the location might be generated, helping prospective buyers make more informed decisions. The main barriers to large-scale, heterogeneous dataset analysis in the context of public policy and urban development are data integration, privacy, scalability, and quality issues. As these datasets often come from several sources, it may be challenging to ensure their quality and consistency. Furthermore, merging multiple datasets may be difficult because of their differences in forms and structures. Data privacy is also a problem as sensitive information needs to be protected. Finally, but just as importantly, scalability of an analytical approach becomes critical when working with large datasets. Data preparation is an important step in preparing raw data for further analysis in the proposed system. The data has to be cleaned and processed in order to be ready for analysis. The process often consists of several stages, such as data reduction, data transformation, and data cleansing.

Data cleaning includes removing outliers, filling in missing figures, and resolving conflicts in the data. Data transformation is the process of changing data into a format or size that is more appropriate. This might include applying mathematical adjustments, normalizing or standardizing numerical data, or encoding category categories in order to improve the data's distribution. By carrying out data preparation, we may enhance the data's quality, get rid of noise and inconsistencies, and get it ready for more analysis. Classifying resources and predicting trends in a given field may be accomplished with a variety of machine learning approaches. Several widely used methods for classification include random forests, decision trees, support vector machines (SVM), and neural networks. Through pattern recognition in labelled data, these algorithms classify resources into many groups or classes. Trends in a certain region can be predicted using techniques for time series analysis. Machine learning methods called recurrent neural networks (RNNs) may be used to analyse historical data and predict future trends. By applying these machine learning approaches, the proposed system may effectively classify resources and forecast trends in the designated region, providing valuable information for planning and decision-making.

To give consumers access to the data, the system employs a number of data visualization techniques. It may generate maps, graphs, charts, and other visual representations to aid users in understanding and interpreting the data. Data visualization plays a key role in supporting individuals in making decisions. It helps users see connections, trends, and patterns in the data that would not be apparent from text or unprocessed numbers. To assist individuals quickly get insights and make informed decisions, data is displayed visually. Visualizations help to clarify complex ideas, highlight important details, and provide a comprehensive picture of the data. They provide the examination and assessment of data from many angles, which aids users in developing a deeper understanding of the underlying patterns and trends.

This is often carried out in the field of supervised machine learning techniques. The accuracy % is calculated by taking the total number of predictions and multiplying it by the number of accurate forecasts. The resulting number is then divided by 100. It gives us a general indication of how well the system predicts the outcome with accuracy. It's important to keep in mind that accuracy alone may not always be the greatest evaluation indication, especially when there are imbalances in the data or false positive costs.

The system uses a range of tools and techniques to provide the data to users. This is the way it functions:

Charts and Graphs: The system can create a wide range of graph types, such as scatter, pie, bar, and line graphs. When these visualizations are used, users may utilize the data to uncover linkages, patterns, and trends. By presenting the facts, the solution speeds up the process of understanding complex information and aids users in reaching well-informed decisions. Visualizations can be used to identify patterns, outliers, correlations, and anomalies that may not be apparent in raw data.

5 Results Analysis

Here, we compare the resources of the dataset that all the resources performed in the previous years of the comparison that we are making the percentages by using percentage accuracy calculation (Fig. 3).

MODELS	YEARS						
	2015-2016	2016-2017	2017-2018	2018-2019	2019-2020	2020-2021	2021-2022
POWER SUPPLY	55	58	61	49	57	63	69
WATER FACILITY	61	64	59	61	66	71	73
TRANSPORTATION	68	73	80	84	88	54	58
CRIME RATE	65	72	76	80	67	48	53
EDUCATION	67.7	68	70	66.4	94.8	67.3	67
STATIONARIES	45.7	54.6	72.3	76	78	52	60
HOSPITALS	70	76	79	80	84.2	85	90

Fig. 3 Resources of the dataset in previous years

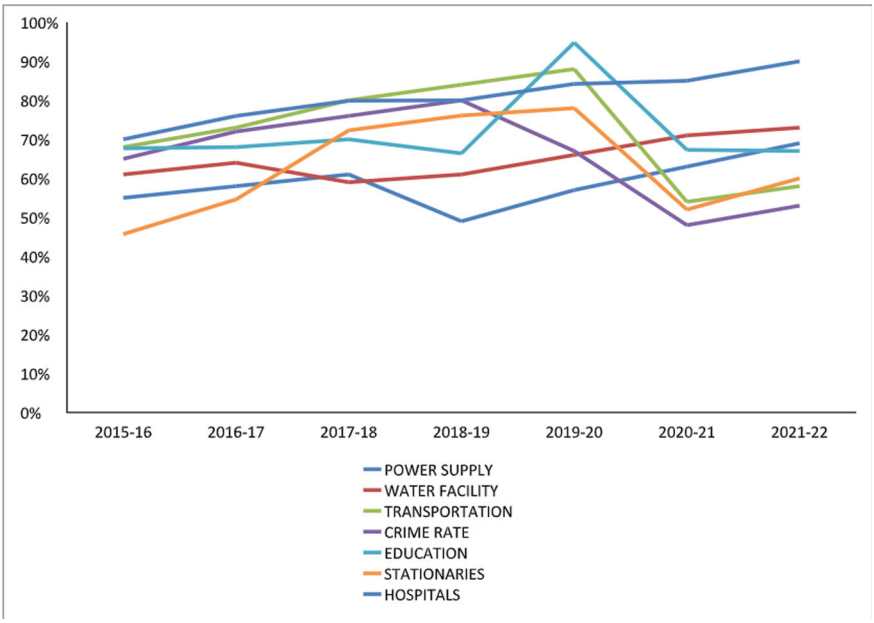


Fig. 4 Graphical representation of resources of previous years

The above table shows the dataset of the previous years of all the resources in a particular city of the system. The resources in the table can be performed by the system of increate and dicrematic nature of the resources based upon situations of the years performed in the resolution of the structure. The resources of the data are performed dramatically in all the years in a city. In pandemic situation, the percentage of the transportation is decreased and the stationary percentage is increased. Now, the graphical representation of all the resources in previous years is as follows (Fig. 4).

In this analysis, the percentage can be calculated by using the accuracy of the system that is performed by all the resources in the table.

The observed value that are calculated by using the all the resources to be presented in the nature of all the resources. The calculation the total percentage of all resources based upon the previous years is as follows (Fig. 5).

The graphical representation of these resources can be referred as follows (Fig. 6).

The representation shows the percentage of all the resources in a city for all the needs of the management.

Fig. 5 Tabular representation of the resources in a city

RESOURCES	RESULT
POWER SUPPLY	25%
WATER FACILITY	10%
TRANSPORTATION	20%
CRIME RATE	5%
EDUCATION	25%
STATIONARIES	15%
HOSPITALS	20%

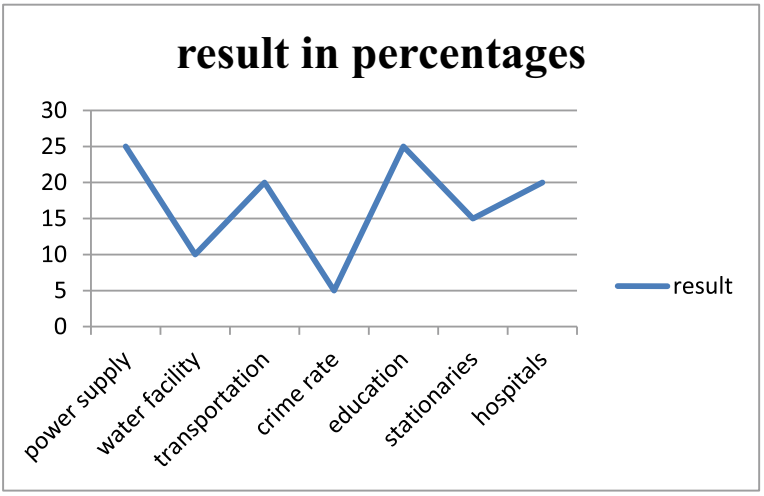


Fig. 6 Chart representation of all resources in a city

6 Conclusion

In this research, we applied the data mining classification technique for the purpose of detecting the crime and resources of the given location by the user. We collect data from all the areas and previous crime rate of that were happened or registered by the police department and municipality department. So, we update the data in such a way that whenever there is an update in the records of government departments. This phase took a considerable effort and time to pre-process and format the data to fit the data mining classifier.

References

1. Wang T, Rudin C, Wagner D, Sevieri R (2013) Detecting patterns of crime with series finder. In: Proceedings of the European conference on machine learning and principles and practice of knowledge discovery in databases (ECMLPKDD 2013)
2. Sathyadevan S, Devan MS, Gangadharan SS (2014) Crime analysis and prediction using data mining. In: 2014 First international conference on networks & soft computing (ICNSC2014), pp 406–412. https://doi.org/10.1109/CNSC.2014.6906719
3. Archenaa J, Anita EAM (2015) A survey of big data analytics in healthcare and government. Procedia Comput Sci 50:408–413
4. Joshi A, Sabitha AS, Choudhury T (2017) Crime analysis using K-means clustering. In: Proceedings of 3rd international conference on computational intelligence and networks (CINE), Odisha, India, pp 33–39
5. Zhou L, Wang J, Vasilakos AV, Pan S (2017) Machine learningon big data: opportunities and challenges. Neurocomputing 237:350–361
6. Injadat M, Salo F, Nassif AB (2016) Data mining techniques in social media: a survey. Neurocomputing 214:654–670
7. Zheng S, Chen S, Yang L, Zhu J, Luo Z, Hu J, Yang X (2018) Big data processing architecture for radio signals empowered by deep learning: concept, experiment, applications and challenges. IEEE Access 6:55907–55922
8. Niu K, Zhang H, Cheng C, Wang C, Zhou T (2019) A novel spatiotemporal model for city-scale traffic speed prediction. IEEE Access 7:30050–30057
9. Stopar L, Skraba P, Mladenic D, Grobelnik M (2019) StreamStory: exploring multivariate time series on multiple scales. IEEE Trans Vis Comput Graph 25(4):1788–1802
10. Tamas J, Toth Z (2018) Classification-based symbolic indoor positioning over the Miskolc IIS data-set. J Location Based Serv
11. Khruahong S, Kong X, Sandrasegaran K, Liu L (2018) Develop an indoor space ontology for finding lost properties for location-based service of smart city. In: 2018 18th International symposium on communications and information technologies (ISCIT), pp 54–59. https://doi.org/10.1109/ISCIT.2018.8588014
12. Von Stülpnagel R, Schmid K (2019) Risk perception during urban cycling in volunteered geographic information and in the lab: effects of the vista space's spatial properties. J Location Based Serv
13. Oikonomidis T, Fouskas K, Vlachopoulou M (2021) Location based services. Research gate

Design Optimization and Aerothermodynamic Analysis Over a Supersonic Vehicle



Divij Arora, R. Balaji, and Amit Kumar Thakur

Abstract This paper presents a comprehensive study on the design optimization and aerothermodynamic analysis of a supersonic vehicle, aiming to enhance its performance and efficiency at the time of re-entry. The distribution of heat over the body can be influenced by varying the shock stand-off distance and intensity over supersonic objects. In this paper, we have modified the blunt body by keeping the double hemispherical disk in the front which will increase the shock stand-off distance and lower the intensity of the shock waves at Mach six. The turbulent module transport equation was used to solve the blunt body with double disk along with Reynolds Navier stoke Equation, according to the aerodynamic performance of the double disk. According to this research analysis, the aero-disk performance is better than the aerospike.

Keywords Shock reduction · Aerothermodynamic · Flow visualization · Aerospike

1 Introduction

High-speed flows are widespread in a variety of engineering applications, including supersonic aircraft, rocket propulsion systems, and gas turbine engines. The tumultuous character of these flows complicates their comprehension and accurate prediction. Chaos and unpredictability in temperature, pressure, density, and other factors are what characterize turbulence, which can lead to increased drag, heat transfer, and noise production. Any flying object must have a nose cone shape because it receives

D. Arora (✉)
Department of Aerospace Engineering, Uttaranchal Institute of Technology, Uttranchal University, Dehradun 248007, India
e-mail: divijarora2000@gmail.com

R. Balaji · A. K. Thakur
School of Aerospace Engineering, Lovely Professoinal University, Phagwara, Punjab 144411, India

© The Author(s), under exclusive license to Springer Nature Singapore Pte Ltd. 2025

B. B. V. L. Deepak et al. (eds.), *Recent Advancements in Product Design and Manufacturing Systems*, Lecture Notes in Mechanical Engineering,
https://doi.org/10.1007/978-981-97-6732-8_11

the most heat loads. There are many different types of nose cones, including blunt cone, parabola, spherical, hemisphere, ogive, and others.

The use of experimental analysis to investigate the turbulent features of high-speed flows is a vital tool. To gather detailed information on the flow field, computational fluid dynamics (CFD) is used. The results of such experiments can be used to evaluate and improve computational models and generate new ideas and concepts for understanding turbulent flows. We give an experimental examination of high-speed flow turbulence features in this work. Using a mix of laser-based flow visualization, we explore the features of turbulence in supersonic flows over a different range of Mach numbers. We investigate the influence of several flow characteristics on turbulence structure and statistics, such as Reynolds number, turbulence intensity, and wall proximity. Our findings shed fresh light on the complicated nature of turbulent flows, with significant implications for the design and optimization of high-speed flow systems. High-speed flow turbulence research is critical for a variety of applications, including the design of high-speed aerospace vehicles, the creation of high-speed machinery, and the optimization of fluid flow in industrial processes. The purpose of this study is to provide an overview of the experimental investigation of high-speed flow turbulence features, including a review of the many experimental techniques utilized and their applications in research and industry.

Learning about high-speed flow turbulence has many real-world applications. For instance, both the development of high-speed machinery and the design of aeronautical vehicles require it. It is also helpful for streamlining fluid flows in industrial operations like mixing and combustion. Re-entry spacecraft are designed with streamlined concepts to protect them from the extreme heat they experience as they return from space into Earth's atmosphere. The primary goal of this work is to apply new geometrical concepts to reduce the aerodynamic heating of re-entry vehicles. This idea executes the surface augmentation of the many traditional nose cones by forming certain spherical protrusions across the nose area. This study investigates how space-entry vehicles' nose portions with spherical structures can lessen aerodynamic heating. To calculate the extent of the reduction in aerodynamic heating, existing and potential re-entry bodies were numerically compared. The spacecraft can only effectively re-enter if the optimal design idea that takes into account aerodynamic drag, air loads, and aerodynamic heating has been selected.

Research attempting to reduce hypersonic drag mostly focused on employing a structural spike that extends upstream and is connected to the blunt body. By creating a zone of reduced dynamic pressure through divided flow over the large volume of the head fairing, the aerospike greatly reduces fore-body drag [1]. Several studies have shown that the conical shock wave the conical spike creates in front of the body lowers pressure on the body's surface, hence reducing overall aerodynamic heating and drag. Metha [2] discovered that as the length of the spike increased, aerodynamic drag and heat transmission were both decreased in the numerical flow stimulations over a conical blunt body. On the other hand, spikes longer than a certain length were useless because the shock structure separated from the tip of the spike and reformed into a strong, normal shock immediately in front of the body. Substantial

recirculation zones close to the nose of the body are found to lower spike friction over the entire length of the body, according to another study [3].

Researchers primarily use computational fluid dynamics to verify the new re-entry vehicle concepts [4]. Researchers found that small variations in flight altitude may have an impact on the aerodynamic forces operating on the capsule in 2012, highlighting the significance of comprehending shock wave effects. Moreover, they discovered that aerodynamic heating might vary significantly even with little modifications to the nose cone's shape [5]. Spikes were mounted in front of the nose cones in 2014, and it was discovered that the aerodynamic heating was reduced by almost 30%. However, this idea causes the exploitation of spikes and the development of shear stresses [6].

Decreasing the aerodynamic heating at the nose cone region is the main goal of this research. In order to accomplish this, instead of using spikes, spherical protrusions are added to the nose sections of traditional re-entry vehicles. Unlike the widely used technique of protecting re-entry vehicles from overheating by using ablative materials, this novel approach seeks to minimize aerodynamic heating. Nevertheless, little thought has been devoted to changing the nose cone's geometry to lessen the impacts of heating. The use of spherical projecting nose cones to lower aerodynamic heating loads at the time of space re-entry is notably lacking in publicly available studies. To advance this topic, it is imperative to comprehend the effects of adding spherical protrusions to the nose cone of different re-entry vehicles [7].

2 Geometry

The steps involved in creating geometry in the SolidWorks program. First, a blunt body with all the dimensions shown in Fig. 1 is created in SolidWorks. The problem statement's base body is created by drawing a curve with a radius of 38.1 mm in front of the baseline in order to give it a blunt nose. The required base body dimensions are used to create a wind tunnel section (pressure far-field region). It is necessary to identify the inlet pressure far-field, wall, and body. Repeating this process results in geometry with various dimensions and various r/d ratios for the cavity, allowing for comparison of the results for the problem statement. To produce an opposing jet in the blunt body with a different r/d ratio, similarly, these steps are repeated. In order to explore the fundamentals of fluid dynamics and heat transmission along the forward-facing spike attached to the heat shield, compressible 3D, a computational simulation of the axisymmetric full Navier–Stokes equations is run [8].

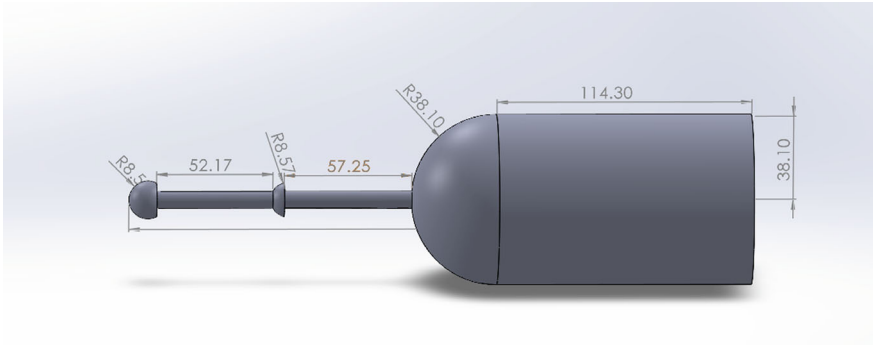


Fig. 1 Dimensions of body

3 Grid Generation

In computational fluid dynamics (CFD), the discretization of the area of interest into an infinite number of cells or points on a grid is known as grid generation. Grid generation aims to produce a mesh that faithfully captures the problem's geometry while preserving a high enough level of resolution to support precise numerical solutions. Grids should be generated with the flow's direction in mind for simulations without side-slip angles. This indicates that the lines of the grid should be parallel to the streamlines, which are the directions of the flow. In a nutshell, the grid must match the fluid flow's velocity vector.

Grid generation uses a variety of grid/cell shapes, including quadrilaterals, triangles, hexahedra, tetrahedra, etc. The mesh produced by the grid generation method for the task will make an effort to match the geometry of the system that is being simulated. Advanced meshing techniques create the mesh and results using interpolation and polynomial curve techniques rather than Cartesian or structured grids. The resolution and accuracy of the simulation results will be determined by the grid used for CFD simulations, which will also influence the calculation time and level of detail in the results.

In this study, a structured grid is used to model the geometry. The flow conditions can be simulated using only a 180-degree grid because the side-slip angle is not involved. The geometries' canters are used to apply the axisymmetric condition. To precisely capture the boundary layer brought on by the effects of viscosity and turbulence, the grid is tightly packed close to the body. Figures 2 and 3 show two different views of a typical structured grid surrounding the spike. Numerical simulations are run on multiple grids of varying sizes to show the results' independence from the grid.

The solver used in this simulation is a density-based solver as in this paper we are working on a supersonic velocity model and the Mach number chosen for the stimulation is 6.

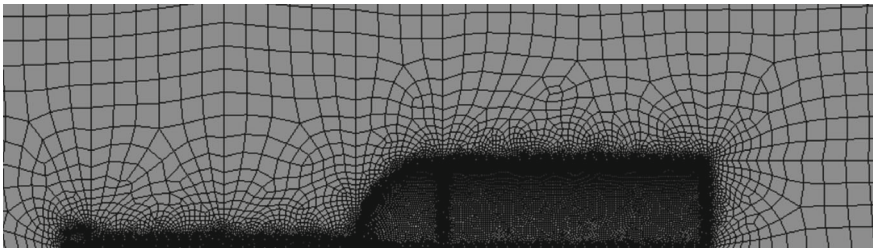


Fig. 2 Meshing of body

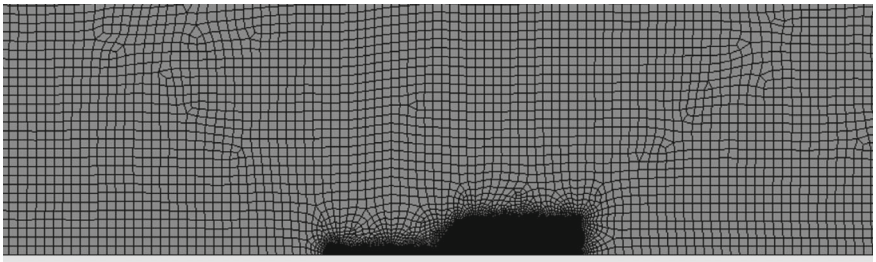


Fig. 3 Meshing of domain

4 Numerical Computations

The axisymmetric form of the Reynolds-averaged Navier–Stokes (RANS) mathematical equations was used in this investigation. Turbulent flows are produced by high Reynolds numbers with significant Mach numbers ($M\infty = 6$ in the current investigation). To solve this, the flow field surrounding the blunt bodies was calculated using a turbulence model and the RANS equations.

A density-based, coupled, double-precision solver was used to computationally solve the equations' stable part. An approach known as second-order upwind solution was used to accomplish the discretization. Publications earlier this year validated the modeling method [9]. Starting from an integral formulation, the governing equations were discretized using the finite-volume discretization technique, without the need for any intermediary mapping. To increase the rate of convergence, the flux function was subjected to the AUSM (Advection Upstream Splitting Method) flux splitting approach. The solver used a time-marching technique to calculate the flow [10]. Local time stepping was used for the steady mode in order to quickly converge to the flow field [10].

Enhancing spatial precision and preventing spurious oscillations were the goals of the second-order flux limiter. If second-order spatial discretization schemes were used, high gradient and shock stream enhancing spatial precision and preventing spurious oscillations were the goals of the second-order flux limiter. If second-order spatial discretization schemes were used, high-gradient streams in the solution's and

shocks domain would cause these oscillations. A fully implicit method, appropriate for compressible viscous flows and stable for linear systems, was used by the solver. Instead of taking the viscosity to be constant, Sutherland's law is used to compute it. The Navier–Stokes equations, which are given by, respectively, signifying the internal energy, body forces, and source term, were the governing equations for this simulation. They were the energy equation, the equation of state, the momentum Equation, and the continuity equation [11].

$$\frac{\partial P}{\partial T} + \nabla \cdot (\rho \vec{v}) = s_m, \tag{1}$$

$$\frac{\partial (\rho \vec{v})}{\partial T} + \nabla \cdot (\rho \vec{v} \vec{v}) = \nabla_P + \rho \vec{g} + \vec{f}, \tag{2}$$

$$\frac{\partial}{\partial T}\left[\rho\left(E + \frac{v^2}{2}\right) + \nabla \cdot \left[\rho\left(l + \frac{v^2}{2}\right)v\right]\right], \tag{3}$$

$$\rho \dot{q} - \nabla \cdot (\rho v) + \rho (f \cdot v) + \dot{Q}_{\text{viscous}} + W_{\text{viscous}}. \tag{4}$$

Since we are working on a supersonic velocity model in this paper, the density-based solver was utilized in the stimulation, and the Mach number selected for the stimulation is 6.

5 Mesh Independence Study

Doing a mesh independence study is one way to find out whether the outcomes of the simulation are independent from the underlying mesh. Making sure the outcomes of computational fluid dynamics (CFD) simulations are accurate and trustworthy is a crucial step. A mesh independence study's goal is to ascertain how much the results depend on mesh density. By executing a few simulations with different mesh resolutions and observing if the results vary, one can determine whether the simulation results are independent of the underlying mesh. The mesh is gradually refined and coarsened in the critical areas of the study, and the outcomes are compared. Plotting a graph of the resultant monitor value vs. the number of cells in the simulation is the best way to determine whether a mesh-independent solution exists. The study finds a trade-off between the accuracy of the simulation and the computation time, which helps to maximize the use of time and effort. Figure 4 represents the mesh study done in this paper.

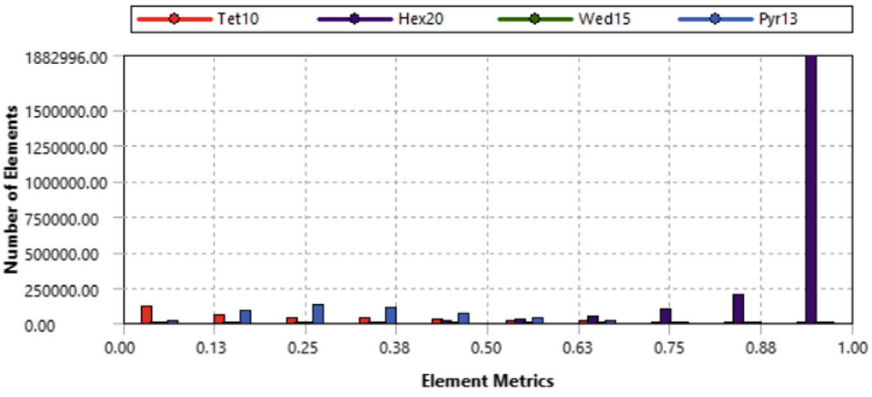


Fig. 4 Orthogonal matrices

6 Boundary Conditions

The following assumptions were made density (ρ), dynamic viscosity, Mach number (M), fluid velocity (v), and dynamic pressure (q) and were all calculated based on measured values of static pressure (p), stagnation temperature (T_0), stagnation pressure (p_0), and static temperature (T). The mean values of the undisturbed flow were also computed, which were $T_0 = 300$ K, Red $= 0.5 \times 106$, and $M = 6$ where Re $=$ ρvd/μ.

In most of the computational situations, a freestream inflow condition with the appropriate Mach number was implemented on the inflow boundary. The pressure was extrapolated from the interior flow on the outflow plane using the extrapolation condition. The nose-cylinder and spike surfaces were exposed to a stationary, adiabatic, no-slip wall condition. The turbulence in these CFD analyses was modeled using the conventional k-ε model. The cross-sectional area of the cylindrical body of the model is its diameter (d), and its reference area (A) is its reference length. The pressure reference value was the dynamic pressure of the undisturbed flow (q). The preliminary boundary conditions are given in Table 1.

Table 1 Boundary conditions used

Boundary conditions	Amount
Mach number	6.0
Free stream pressure	101,325
Temperature	300 K

7 Computational Analysis

In subsonic flow fields, spherical extensions in a flow typically reduce heat transmission, albeit at the expense of a greater pressure drop. Table 2 displays the drag coefficient (CD) and sliding ratio values for a spiked blunt body and a spiked blunt body with disk. When compared to a body with only spikes, the presence of a disk results in higher flow separation in front of the body and a 19% reduction in CD.

The shock stand-off distance has been studied by a large number of researchers. The laminar flow design over a spiky, conical shape with a spherical cap at the end was inspired by the Apollo entrance capsule [12]. The study showed the velocity contour, pressure contour, and density contour at the spike tip as shown in the figure in order to estimate the shock stand-off distance. Figure 5 describes how the coefficient of pressure changes at different positions. The dimensionless pressure coefficient describes the relative pressures over a flow field. A dimensionless static pressure differential, Δp_{stat}, serves as its definition. When dealing with a cold wall, the equation of value $q = P/RT$ causes the boundary layer to become denser. As a result, the boundary layer becomes thinner as the mass flow finds room in a smaller area [13]. According to theoretical study, the separated flow area expands as the temperature of the spike rises due to a small elevation in the angle of separation.

The simulated results are displayed as velocity and pressure contours and graphs in Figs. 7 and 8. The figures show that the strong bow shock that is located close to the body and creates a high-pressure area ahead of it is the source of the large drag force on the body. Figure 6 depicts the variation in skin friction over a cone surface.

The graphs showing the total surface heat flux into the domain from the wall surface show the heating impact brought on by the interaction of the hypersonic shock boundary layer at the reattachment zone.

It is noticeable that the shoulder area, where the shock occurs, exhibits high heat flux values into the body. The density and static pressure are also shown in Figs. 7 and 8.

Table 2 Initial boundary circumstances

Mach No.	AOA	Parameter	Drag coefficient	Sliding ratio
6	1	CD	0.000561996	1.257

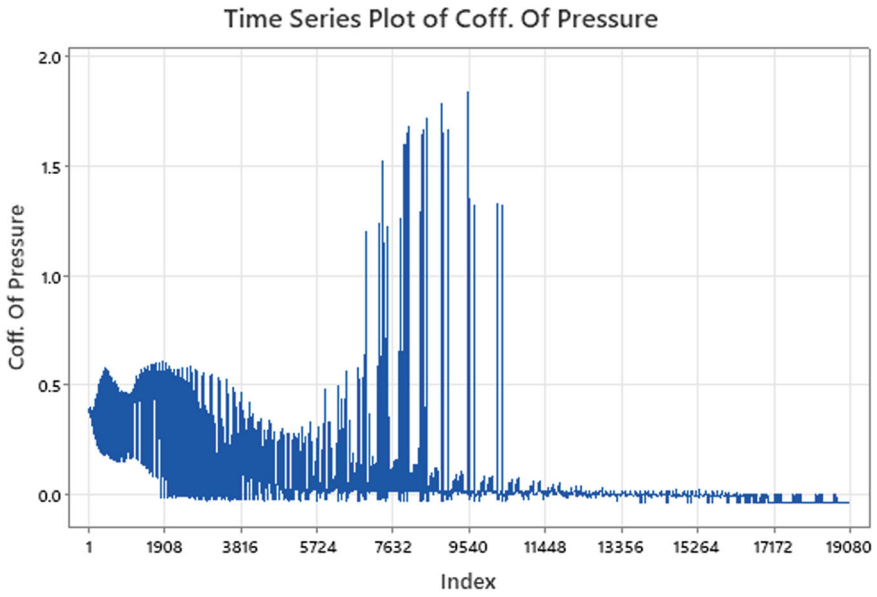


Fig. 5 Coefficient of pressure graph

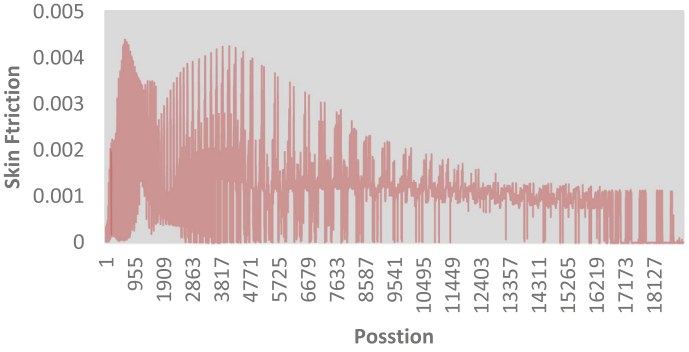


Fig. 6 Skin friction graph



Fig. 7 Static pressure contour

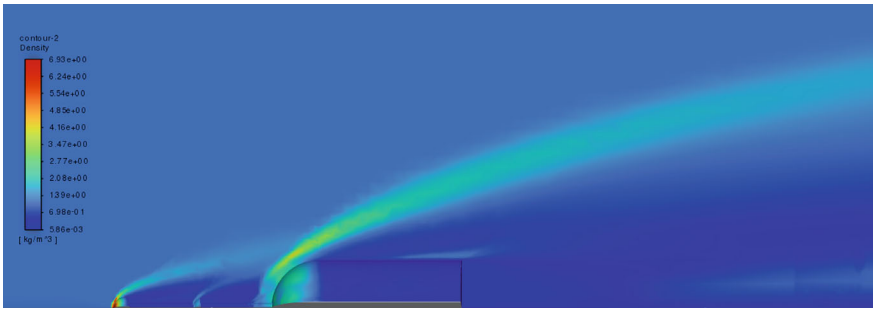


Fig. 8 Density contour

8 Conclusion

For aero-disk tipped spikes, the reattachment point moves in the edge direction of the blunt body. Another significant inference can be made by analyzing the streamlines passing through the bow shock. The aero-disk and its strongly generated bow shock are primarily responsible for deflecting the free stream. We solved the appropriate Reynolds-averaged Navier–Stokes (RANS) equations using the conventional k-omega model. When the coefficient of drag value on the spiked blunt body was compared to a previously published benchmark result, excellent agreement was found. The bow shock and their attachment shock may impinge at the same location if you use the shortest spike. Nevertheless, either hemispherical configuration can produce the best results.

The shorter blunt spike is oftentimes equally as helpful as the longer one, if not more so. When selecting the aero-disk's diameter, consideration must be given to the necessary reduction in drag or heat transmission.

Based on numerical calculations, significant surface augmentation can be used to reduce aerodynamic heating when the vehicle is reentering the air. This novel

strategy to improve the effectiveness of the frontal region of re-entry vehicle nose cones is investigated using a variety of different nose cone designs that are currently on the market.

References

1. Harish P, Naveen HN, Rajagopal DK (2024) Recent advancements in aerothermodynamic design optimization of spiked hypersonic winged re-entry vehicle using CFD. Retrieved 29 Feb 2024. www.ijert.org
2. Mehta RC (2002) Numerical analysis of pressure oscillations over axisymmetric spiked blunt bodies at Mach 6.80. Shock Waves 11(6):431–440. https://doi.org/10.1007/s001930200127
3. Xue Y, Wang L, Fu S (2018) Detached-eddy simulation of supersonic flow past a spike-tipped blunt nose. Chin J Aeronaut 31(9):1815–1821. https://doi.org/10.1016/j.cja.2018.06.016
4. Roychowdhury AP, Unnikrishna (2016) Numerical simulation of hypersonic flow over blunt bodies. Int J Innov Res Technol Sci 2:2321–1156
5. Prasad SU (2012) Flow simulation over re-entry bodies at supersonic & hypersonic speeds. Int J Eng Res Dev 2(4):29–34. Retrieved 29 Feb 2024. www.ijerd.com
6. Ahmed MYM, Qin N (2011) Recent advances in the aerothermodynamics of spiked hypersonic vehicles. Prog Aerosp Sci 47(6):425–449. https://doi.org/10.1016/j.paerosci.2011.06.001
7. Milićev SS, Pavlović MD (2012) Influence of spike shape at supersonic flow past blunt-nosed bodies: experimental study. AIAA J 40(5):1018–1020. https://doi.org/10.2514/2.1745
8. Ahmed M, Qin N, Comparison of response surface and kriging surrogates in aerodynamic design optimization of hypersonic spiked blunt bodies. In: International conference on aerospace sciences and aviation technology, vol 13, no AEROSPACE SCIENCES, pp 1–17. https://doi.org/10.21608/asat.2009.23443
9. Tahani M, Karimi MS, Motlagh AM, Mirmahdian S (2013) Numerical investigation of drag and heat reduction in hypersonic spiked blunt bodies. Heat Mass Transf 49(10):1369–1384. https://doi.org/10.1007/s00231-013-1173-4
10. Chen P, Huang J, Sheng H (2017) Solving steady incompressible Navier-Stokes equations by the Arrow-Hurwicz method. J Comput Appl Math 311:100–114. https://doi.org/10.1016/j.cam.2016.07.010
11. Muthu R, Siva Lakshmi S, Babu S (2022) Aerothermodynamic design and performance analysis of modified nose cones for space reentry vehicles. Int J Ambient Energy 43(1):3282–3293. https://doi.org/10.1080/01430750.2020.1824943
12. Rusanov VV (1976) A blunt body in a supersonic stream. Annu Rev Fluid Mech 8(1):377–404. https://doi.org/10.1146/annurev.fl.08.010176.002113
13. Wood CJ (1962) Hypersonic flow over spiked cones. J Fluid Mech 12(04):614. https://doi.org/10.1017/S0022112062000427

Evaluation of Weldability and Optimization of TIG Welding Process Parameters for Maximized Yield Strength

Guambo Mondo, Bikash Ranjan Moharana, Shoeb Ahmed Syed, and Kamalakanta Muduli

Abstract Often the desired TIG weld quality is not achieved due to the wrong selection of the welding parameters, and as a result, a large number of trial and error runs need to be carried out before the required weld is eventually produced. Hence, this research was conducted to examine how the weld quality and strength of weld joints vary with varying input process parameters and to optimize these process parameters that will provide a good weld in terms of ultimate tensile strength and % elongation. The gray relational analysis-based optimization revealed that optimum combination of process parameters is current 100 A, welding speed 100 mm/min, and gas flow rate 20 lpm. Computation of optimized parameter setting for welding will help in reduce wastage of material leading to reduced cost, increased productivity, reduced fatigue level of the employees, and most importantly reduced energy consumption and environmental hazards.

Keywords Weldability · Gray relational analysis · Dissimilar metal joint

1 Introduction

The welding industry plays a critical role in the growth and development of Papua New Guinea's economy. Applications of this technology can be found in a variety of fields, including mining, manufacturing, and infrastructure, among others; this helps to enhance local industries and employment possibilities. Failures of welded joints are one of the issues that can have a negative impact on the economy. These failures have resulted in economic losses that account for around 1–2% of the country's GDP on an annual basis. However, making strategic investments in welding technology, training, and quality assurance could pave the way for improved productivity,

G. Mondo · B. R. Moharana · S. A. Syed · K. Muduli (✉)
Department of Mechanical Engineering, Papua New Guinea University of Technology, Lae, Morobe Province PMB 411, Papua New Guinea
e-mail: kamalakanta.muduli@pnguot.ac.pg

© The Author(s), under exclusive license to Springer Nature Singapore Pte Ltd. 2025

B. B. V. L. Deepak et al. (eds.), *Recent Advancements in Product Design and Manufacturing Systems*, Lecture Notes in Mechanical Engineering,
https://doi.org/10.1007/978-981-97-6732-8_12

enhanced competitiveness, and continued economic expansion. Effective welding practices lead to less equipment downtime, which in turn lowers the cost of equipment maintenance and extends the lifespan of the equipment. In addition, enhanced welding processes also contribute to the production of high-quality products that meet international standards. This, in turn, opens the door for opportunities for international trade and investment.

In the past, in order to achieve the appropriate level of weld quality, welders were required to carefully examine the input welding parameters and engage in a significant amount of time-consuming trial and error. After that, they checked the welded metal to see whether or not the specified level of quality had been achieved. This can be a process that takes a lot of time and costs a lot of money. In order to achieve optimum values of the process parameters, several researchers have conducted experiments with different input process parameters and optimized these welding parameters using several optimization techniques. In some studies, it was empirically shown that the incorrect selection of process parameters might have a detrimental impact on the quality of welds, potentially leading to the failure of welded connections [1–3] and also could be monitored through simulation and CAD environment [4–6]. In their study, Mahesh and Appalaraju aimed to achieve a high-quality welded joint by optimizing the input process variables that affect the ultimate tensile strength (UTS) of AISI 1050 mild steel [7]. Tesfaye and Getaneh conducted a study that aimed to optimize the input process factors at three levels, specifically the welding voltage, wire feed rate, and welding speed [8]. The findings indicate that the welding voltage is the primary influential factor among the ideal set of parameters. In a recent investigation conducted by Ramarao, the process parameters of gas metal arc welding were utilized and optimized. Specifically, the welding current, voltage, and bevel angle were adjusted in order to combine incompatible materials, namely SA387 grade alloy steel and SS304 stainless steel [9]. The study employed Taguchi and ANOVA optimization methodologies to investigate the impact strength of the welding process. The findings revealed that the welding current exhibited a significant influence on the impact strength, with voltage also playing a notable role. The predominant focus of research endeavors has been directed on the optimization of process parameters in the GMAW welding process. Several researchers are actively working on dissimilar metal joining, such as Al-Steel, Steel-Cu, and AL–Mg alloy, by conventional welding processes [10–13]. Such achievements are really helpful for economic growth of the various industries, as the use of conventional welding processes like TIG or MIG are more (~70%) compared to advanced welding processes. For dissimilar metal joining, the advanced welding processes, such as LBW, EBW, and USW, are more successful than conventional one [14–17] but there are many limitations, such as penetration depth, availability of resources, and high cost. Joining of different grades of Al and galvanized steel are explained by limited researchers [18–22]. After several literature survey, it is found that there is a scarcity of studies that have endeavored to optimize process parameters for various welding processes. Moreover, there is a lack of research conducted within the specific setting of Papua New Guinea (PNG). Hence, this study is conducted with the following objectives.

- To conduct research into the impacts of combining different steel materials using a variety of welding currents, welding voltages, welding speeds, and shielding gas flow rates, and then optimize the process parameters.
- To utilize optical equipment, do an investigation into the quality of the weld as well as any defects.
- To utilize a mechanical testing machine, examination will be conducted on the mechanical properties of the welded specimens.

2 Research Methodology

The research methodology followed in this research is highlighted in Fig. 1.

2.1 Experimental Work

The TIG welding technique is suggested for joining two dissimilar metal couples in the current study project. Table 1 includes the chemical compositions of the materials, such as aluminum alloy and galvanized steel, that were identified via EDS analysis. For all corresponding experimental runs, butt welding is performed with no gap between the two materials. Since no filler material is employed in these experiments, it is preferable to have no groove. The edge of the butt-welding specimen stays flat, forming a 90° angle.

2.2 Design of Experiments

One of the most effective DOEs of all is the Taguchi orthogonal array, according to a wealth of research [23]. With the least number of experiments, the Taguchi design matrix examines each process parameter using a unique orthogonal array. Every factor is assessed independently, and the impacts of one component never interact with the assessment of the influence of another element, according to the principle of orthogonality. Each factor's signal-to-noise (S/N) ratio is examined to determine how much of an impact it has on output responses [24, 25]. Table 2 illustrates three levels of variation for three input process parameters: welding speed, gas flow rate, and current.

The entire set of experiments has been carried out in compliance with the Taguchi L9 (3^3) orthogonal array design matrix, as illustrated in Table 3. The ultimate tensile stress (UTS) is one of the most effective parameters for evaluating welded specimen quality. So, UTS is taken as one of the output responses to assess the effectiveness of process parameters. Tensile tests are carried out at room temperature with the use of

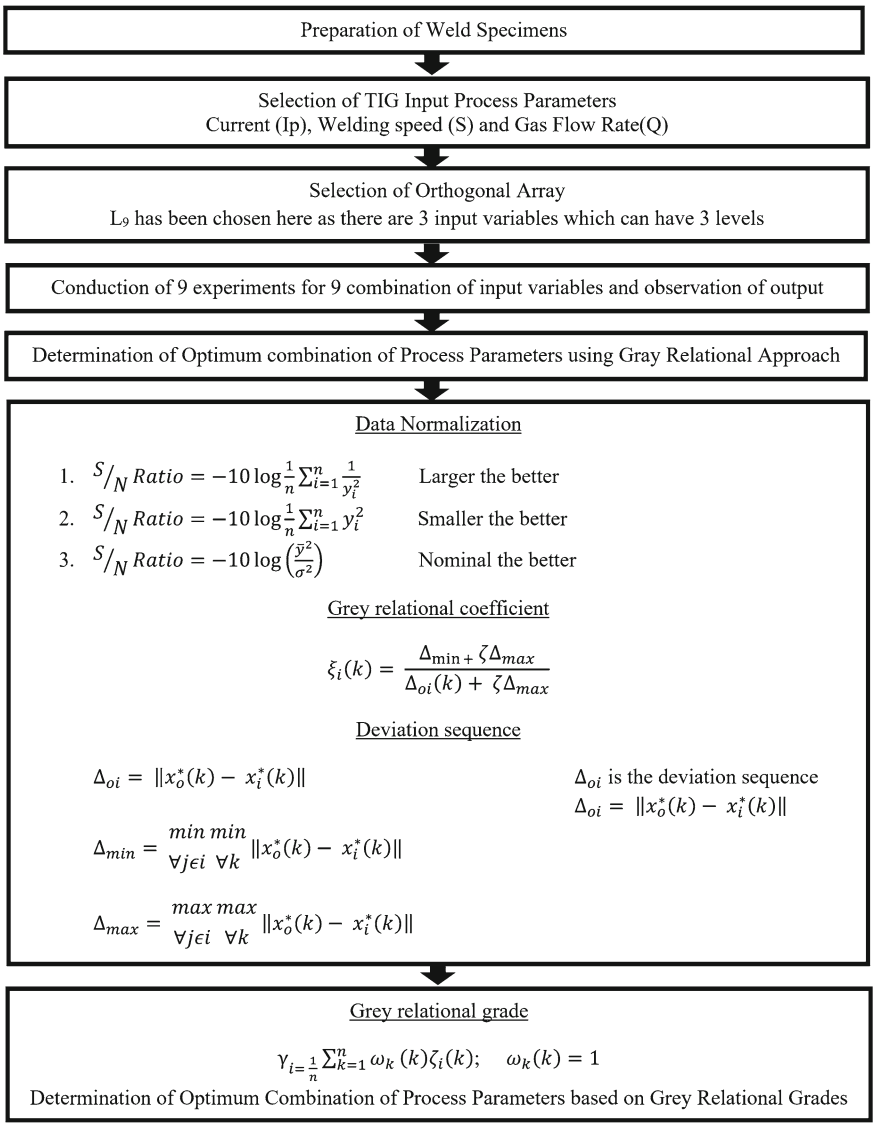


Fig. 1 Research methodology

Table 1 Chemical composition of Al alloy and Galvanized steel (weight fraction, %)

Element	Al	Fe	Cu	Cr	Si	Mn	C	P	Ni	Mg	Ti	Zn
Al alloy	92.65	0.50	4.3	0.10	0.50	0.35	–	–	–	1.2	0.15	0.25
Galvanized steel	0.026	99.67	0.021	0.024	0.025	0.164	0.063	0.016	0.015	–	–	–

Table 2 Welding process parameters for experimentation

Parameters	Units	Levels		
		1	2	3
Current (I_P)	Amp	70	85	100
Welding speed (S)	mm/min	100	125	150
Gas flow rate (Q)	lpm	16	18	20

Table 3 Design matrix with tensile test results

Specimen No.	Current (A)	Welding speed (mm/min)	Gas flow rate (lpm)	UTS (MPa)	Elongation (%)
1	70	100	16	210	1.571
2	70	125	18	232	2.465
3	70	150	20	247	3.342
4	85	100	18	268	1.554
5	85	125	20	295	1.285
6	85	150	16	233	4.195
7	100	100	20	301	2.045
8	100	125	16	280	2.852
9	100	150	18	273	3.246

an automated universal testing machine. In this analysis, the % elongation is used as the second output response, as ductility also plays an important role during failure.

2.3 Optimization of Response Variables

The effect of welding parameters on individual output responses is first investigated, and then a multi-criteria decision-making (MCDM) approach, i.e., gray relational analysis (GRA), is used to optimize the response variables simultaneously. GRA is a widely utilized assessment methodology in the field of MCDM, specifically in situations where decision-making is subject to ambiguity [26]. One notable benefit of the gray system theory lies in its capacity to yield favorable results despite limited information or substantial variations in parameters [27, 28].

3 Result and Discussion

Table 3 shows the experimental design matrix, together with the associated UTS values and % elongations.

3.1 *Influence of Welding Parameters on UTS (Ultimate Tensile Stress)*

The main effect plot of all three process parameters, such as I_p, S, and Q, on the UTS is investigated and is shown in Fig. 2. As UTS should be higher the better criterion, the optimum process parametric combination for UTS is $I_p = 100$ Amps, $S = 125$ mm/min, and $Q = 20$ lpm. Figure 3 illustrates the probability plot. In general, the probability plot describes how well the specified model fits the analysis. All 9 points are close to the normal distribution line, near the middle of the bell curve and additionally all points in between -2 to $+2$ (standardized residuals). This validates the intended model's stability [29]. Table 4 describes the analysis of variance for UTS. The R^2 value 90.55% reflects the adequacy of the design model. This table also provides the influence of each process parameters upon UTS, i.e., "$I_p > Q > S$" (Figs. 4, 5 and Table 5).

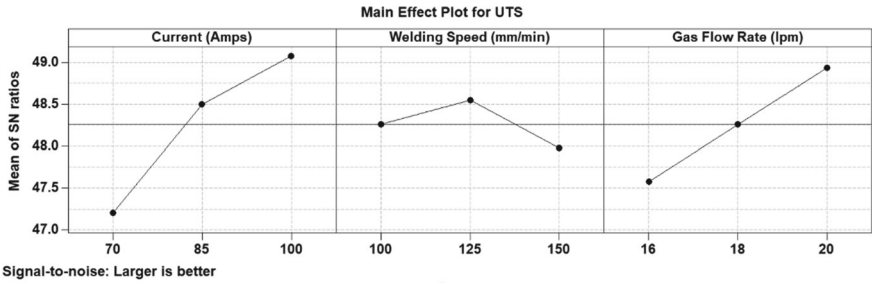
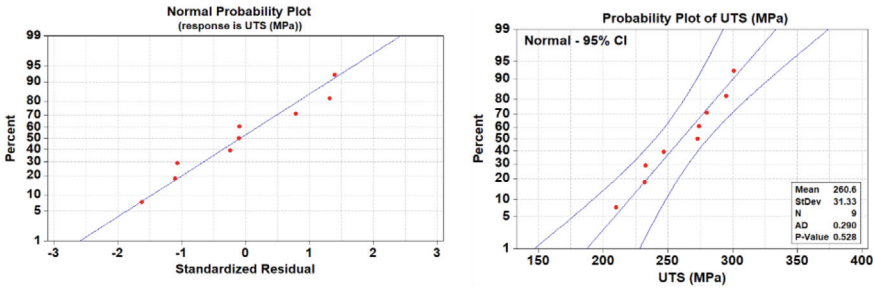


Fig. 2 Main effect plot for UTS



(a) (b)

Fig. 3 Normal probability plot **a** with respect to standardized residual and **b** with respect to UTS

Table 4 Analysis of variance for UTS

Source	DF	Seq SS	*F*	*P*	% Contribution	Rank
Current	1	4537.50	30.5739	0.002652	63.84	1
Welding speed	1	170.67	1.1500	0.332565	2.40	3
Gas flow rate	1	2400.00	16.1713	0.010107	33.76	2
Error	5	742.06				
Total	8	7850.22			100.00	

$S = 12.1824$, $R^2 = 90.55\%$, R^2 (adj) $= 84.88\%$

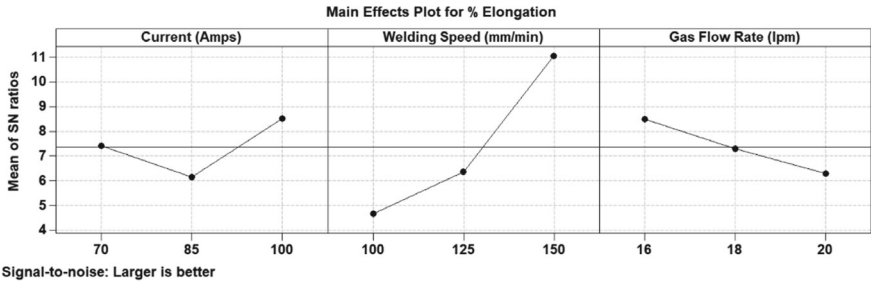
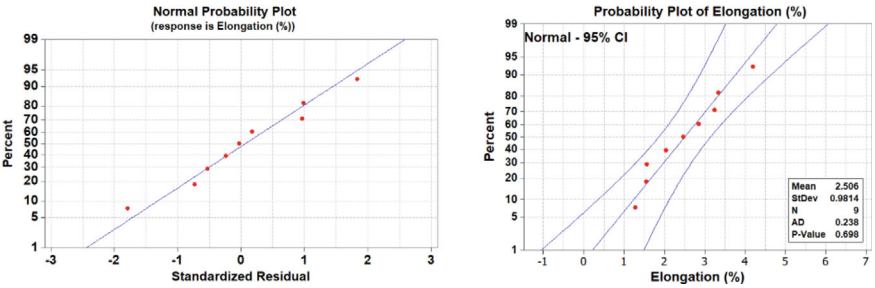


Fig. 4 Main effect plot for % elongation



(a) (b)

Fig. 5 Normal probability plot **a** with respect to standardized residual and **b** with respect to elongation

3.2 Statistical Model for UTS and % Elongation: Gray Relational Analysis (GRA)—A MCDM Approach

It is exceedingly difficult to determine the optimal result from the analysis above because each output response has a unique input parametric condition. In order

Table 5 Analysis of variance for % elongation

Source	DF	Seq SS	*F*	*P*	% Contribution	Rank
Current	1	0.09754	0.2827	0.617677	1.64	3
Welding speed	1	5.25096	15.2215	0.011392	87.81	1
Gas flow rate	1	0.63115	1.8296	0.234127	10.55	2
Error	5	1.72485				
Total	8	7.70450			100.00	

$S = 0.587342$, $R^2 = 77.61\%$, R^2 (adj) $= 64.18\%$

to eliminate uncertainty when determining the best outcome, the GRA method, or MCDM approach, was put into practice. Table 6 displays the results of the multi-objective GRA approach optimization of the output parameters. Table 7 shows rank of the input process parameters to achieve the optimal result, and it is been found that "$I_p > S > Q$". The main effect plot provides the optimum process parametric combination which is $I_p = 100$ Amps, $S = 150$ mm/min, and $Q = 20$ lpm as shown in Fig. 6. Figure 7 shows the probability plot for GRA and confirms the adequacy of design model.

Table 6 Analysis of GRC and GRG from experimental results

Specimen No.	Normalization		GRC		GRG
	UTS	Elongation	UTS	Elongation	
1	1.000	0.902	0.333	0.357	0.345
2	0.758	0.595	0.397	0.457	0.427
3	0.593	0.293	0.457	0.630	0.544
4	0.363	0.908	0.580	0.355	0.467
5	0.066	1.000	0.883	0.333	0.608
6	0.747	0.000	0.401	1.000	0.700
7	0.000	0.739	1.000	0.404	0.702
8	0.231	0.462	0.684	0.520	0.602
9	0.308	0.326	0.619	0.605	0.612

Table 7 Response table for Signal-to-Noise Ratios (GRA)

Level	Current	Welding speed	Gas flow rate
1	−7.308	−6.308	−5.581
2	−4.671	−5.371	−6.086
3	−3.915	−4.215	−4.227
Delta	3.393	2.093	1.859
Rank	1	2	3



Fig. 6 Main effect plot for S/N ratios (GRA)

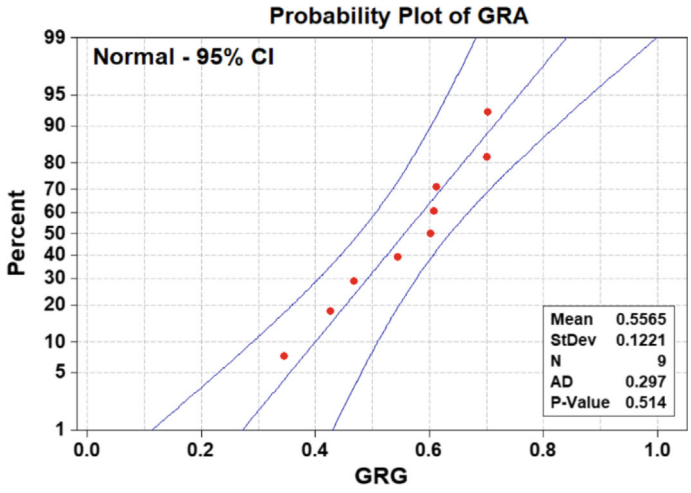


Fig. 7 Probability plot of GRA

4 Implications

- The result of this research provided an optimized parameter setting for producing a high-quality TIG welded joint. This will aid in reducing the waste of material, which will lead to a reduction in costs, an improvement in productivity, a reduction in the level of fatigue experienced by the personnel, and most importantly, a reduction in the amount of energy consumed and environmental hazards.
- It is possible to cut down on both the costs and the risks that come with disposing of waste items. A smaller carbon footprint will be achieved through a reduction in the usage of both energy and virgin materials.
- A smaller carbon footprint will be achieved through a reduction in the usage of both energy and virgin materials, thus contributing to PNG's sustainable development goals (SDGs).

- Our research is primarily focused on the United Nations' Sustainable Development Goal (SDG) #9, which is to promote industry innovation and infrastructure as well as SDG #11, which is to look for solutions for sustainable cities and communities.

5 Conclusions

The majority of failures that occur in welding joints are caused by poor settings for the welding parameters. When using TIG, the quality of the welded joints is determined by a number of input parameters, including the welding current, arc voltage, shielding gas flow rate, angle of the torch or welding gun, wire electrode feed rate, and so on. Hence, evaluation of optimum combination of process parameters for a good weld for joining dissimilar metals employing TIG has been attempted in this research, which is unique in the context of PNG. Optimum combination of the three input process parameters, current, welding speed, and gas flow rate for obtaining optimized value of UTS and % elongation were evaluated using GRA method. Based on the GRG score, it was observed that optimum combination of input parameters for welding in TIG when welding galvanized steel with Al is current 100 A, welding speed 100 mm/min, and gas flow rate 20 lpm. In this research, only 3 input parameters were considered which is one of the limitations of this study. In the future, more input parameters will be considered. Further, fuzzy MCDM techniques could be employed to evaluate optimum parameters in uncertain environment [30].

References

1. Rajkumar V, Arivazhagan N (2014) Role of pulsed current on metallurgical and mechanical properties of dissimilar metal gas tungsten arc welding of maraging steel to low alloy steel. Mater Des 63:69–82
2. Jeet S, Barua A, Parida B, Sahoo BB, Bagal DK (2018) Multi-objective optimization of welding parameters in GMAW for stainless steel and low carbon steel using hybrid RSM-TOPSIS-GA-SA approach. Int J Tech Innov Mod Eng Sci 4:683–692
3. Moharana BR, Sahu SK, Maiti A, Sahoo SK, Moharana TK (2020) An experimental study on joining of AISI 304 SS to Cu by Nd-YAG laser welding process. Mater Today Proc 33:5262–5268
4. Deepak BBVL, Rao CA, Raju BMVA (2016) Weld seam tracking and simulation of 3-Axis robotic arm for performing welding operation in CAD environment. In: CAD/CAM, robotics and factories of the future: proceedings of the 28th international conference on CARs & FoF 2016. Springer India, pp 405–415
5. Deepak BBVL, Bahubalendruni RM, Rao CA, Nalini J (2017) Computer aided weld seam tracking approach. J Eng Des Technol 15(1):31–43
6. Zhou B, Liu Y, Xiao Y, Zhou R, Gan Y, Fang F (2021) Intelligent guidance programming of welding robot for 3D curved welding seam. IEEE Access 9:42345–42357
7. Mahesh S, Appalaraju V (2017) Optimization of MIG welding parameters for improving strength of welded joints. Int J Innov Technol Res 5(3):6453–6458

8. Tesfaye FK, Getaneh AM (2023) Gas metal arc welding process variables enhancement for welding significantly different steels. J Oil Gas Res Rev 3(1):15–20
9. Ramarao M, King MFL, Sivakumar A, Manikandan V, Vijayakumar M, Subbiah R (2022) Optimizing GMAW parameters to achieve high impact strength of the dissimilar weld joints using Taguchi approach. Mater Today Proc 50:861–866
10. Behera RK, Samal BP, Panigrahi SC, Muduli K, Mohamed A, Samal A (2021) Evaluation of magnesium recovery in Al-Mg alloys produced by modified stir casting method using genetic algorithm optimisation technique. Int J Mater Eng Innov 12(2):134–148
11. Moharana BR, Sahoo SK, Biswal DK, Muduli K, Influence of fusion welding processes on microstructure and mechanical properties of dissimilar metal (AISI 304 SS-Copper) weldment. Mater Today Proc. In: Conference on recent advances in mechanical engineering research and development (In Press)
12. Liu LM, Wang SX, Zhu ML (2013) Study on TIG welding of dissimilar Mg alloy and Cu with Fe as interlayer. Sci Technol Weld Joining 11(5):523–525
13. Yu H, Xu Y, Lv N, Chen H, Chen S (2013) Arc spectral processing technique with its application to wire feed monitoring in Al-Mg alloy pulsed gas tungsten arc welding. J Mater Process Technol 213(5):707–716
14. Giri SR, Khamari BK, Moharana BR (2022) Joining of titanium and stainless steel by using different welding processes: a review. Mater Today Proc 66:505–508
15. Magnabosco I, Ferro P, Bonollo F, Arnberg L (2006) An investigation of fusion zone microstructures in electron beam welding of copper-stainless steel. Mater Sci Eng, A 424(1–2):163–173
16. Sahu SK, Moharana BR, Shaibu VB, Sahoo SK (2016) An experimental study on CO_2 laser beam welding of AISI 304SS and Cu dissimilar pipes. Int J Mechatron Manuf Syst 9(4):310–326
17. Moharana BR, Sahoo SK (2014) An ANN and RSM integrated approach for predict the response in welding of dissimilar metal by pulsed Nd: YAG laser. Univ J Mech Eng 2(5):169–173
18. Wallerstein D, Lusquiños F, Comesaña R, Del Val J, Riveiro A, Badaoui A, Pou J (2021) Dissimilar unbeveled butt joints of AA6061 to S235 structural steel by means of standard single beam fiber laser welding-brazing. J Mater Process Technol 291:116994
19. Sierra G, Peyre P, Beaume FD, Stuart D, Fras G (2008) Galvanised steel to aluminium joining by laser and GTAW processes. Mater Charact 59(12):1705–1715
20. Shao L, Shi Y, Huang JK, Wu SJ (2015) Effect of joining parameters on microstructure of dissimilar metal joints between aluminum and galvanized steel. Mater Des 66:453–458
21. Qin GL, Su YH, Wang SJ (2014) Microstructures and properties of welded joint of aluminum alloy to galvanized steel by Nd: YAG laser+ MIG arc hybrid brazing-fusion welding. Trans Nonferrous Metals Soc China 24(4):989–995
22. Shah LH, Mohamad UK, Yaakob KI, Razali AR, Ishak M (2016) Lap joint dissimilar welding of aluminium AA6061 and galvanized iron using TIG welding. J Mech Eng Sci 10(1):1817–1826
23. Ross PJ (1996) Taguchi techniques for quality engineering. Mcgraw-hill International editions
24. Yousefieh M, Shamanian M, Arghavan AR (2012) Analysis of design of experiments methodology for optimization of pulsed current GTAW process parameters for ultimate tensile strength of UNS S32760 welds. Metallogr Microstruct Analy 1:85–91
25. Moharana BR, Sahoo SK, Muduli K (2022) Evaluation of mechanical and metallurgical properties of SS 304-CP copper dissimilar metal joint by innovative pulsed-GTAW process. Int J Mater Eng Innov 13(4):291–305
26. Swain S, Muduli K, Biswal JN, Tripathy S, Panda TK (2017) Evaluation of barriers of health care waste management in India—a gray relational analysis approach. In: Proceedings of the 5th international conference on frontiers in intelligent computing: theory and applications: FICTA 2016, volume 1. Springer Singapore, pp 181–188
27. Muduli K, Pumwa J, Yadav DK, Kumar R, Tripathy S (2018) A grey relation approach for selection of industrial robot. In: 2018 International conference on information technology (ICIT). IEEE, pp 141–144
28. Moharana BR, Patro SS (2019) Multi objective optimization of machining parameters ofEN-8 carbon steel in EDM process using GRA method. Int J Modern Manuf Technol 11(2):50–56

29. Anawa EM, Olabi AG (2008) Optimization of tensile strength of ferritic/austenitic laser welded components. Opt Lasers Eng 46(8):571–577
30. Muduli K, Barve A (2013) Developing a framework for study of GSCM criteria in Indian mining industries. APCBEE Proc 5:22–26

Terahertz-Frequency Propagation for Autonomous Transport Infrastructure



Aezeden Mohamed and Janne Heilala

Abstract Autonomously guided vehicles (AGVs) utilize reconfigurable intelligent surfaces (RISs) for control. The research approach started with selecting a Preferred Reporting Item for Systematic Reviews and Meta-Analyses: Scoping Review (PRISMA-ScR). This was followed by an axiomatic design, defining requirements and parameters. Light Detection and Ranging (LIDAR) and image sensors were integrated for path following and obstacle detection. A computational framework processes environmental data. Motor drivers, combined with digital accelerometers, dictate movement dynamics. Communication is facilitated through a controller area network (CAN) transceiver supported by a power management module. The process concluded with the developing of a printed circuit board (PCB) design, marking a multidisciplinary approach in electronics systems engineering for Software as a Service (SaaS).

Keywords Reconfigurable intelligent surfaces · Terahertz · Trackless autonomous transport · Axiomatic design · Optimization

1 Introduction

Building on the PRISMA-ScR analysis [1], the challenges and needs of the track sector lead to the conceptualization of axiomatic designs for trackless rail. The introduction of autonomously guided vehicle (AGV) systems is noteworthy supply chain for following pattern recognition through autonomous tracking [2]. A significant collision event recently thrust railway safety into sharp focus [3]. Modern transportation concepts, such as hyperloop, have encountered delays due to the concerns [4–6], emphasizing the importance of innovations for safe railroad utilizing smart

A. Mohamed (✉)
Department of Mechanical Engineering, PNG University of Technology, Lae, Papua New Guinea
e-mail: aezeden.mohamed@pnguot.ac.pg

J. Heilala
Faculty of Technology Mechanical Engineering, Turku University, Turku, Finland

© The Author(s), under exclusive license to Springer Nature Singapore Pte Ltd. 2025

B. B. V. L. Deepak et al. (eds.), *Recent Advancements in Product Design and Manufacturing Systems*, Lecture Notes in Mechanical Engineering,
https://doi.org/10.1007/978-981-97-6732-8_13

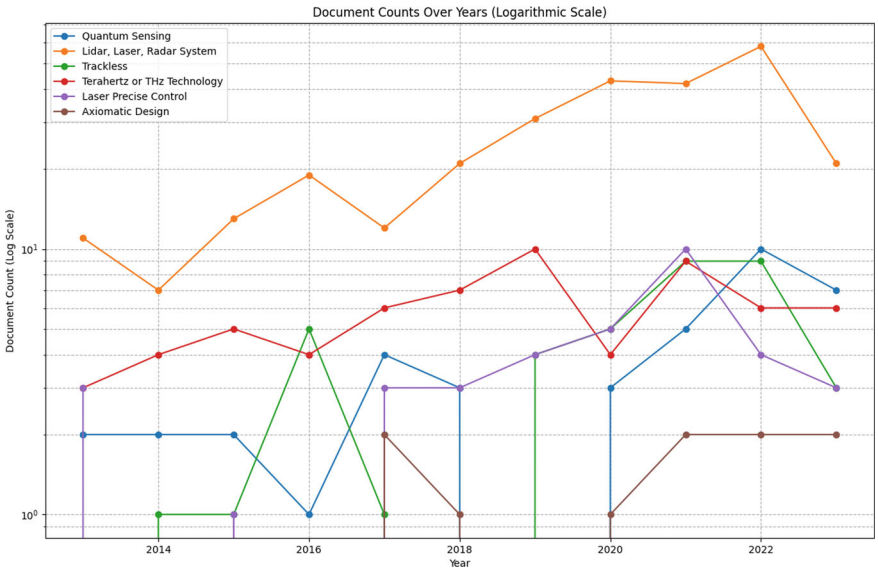


Fig. 1 Scoping documents results (*y*-axle is logarithmic) with the main factor "(locomotive OR tram OR train OR metro)" with the sub-tech given in trend name classes [9]

systems [7]. Scoping with database queries [8], this comprehensive study is guiding by a decade-long Scopus survey spanning 2013–2023. This shows decade's evolution of academic publications related to the railway sector, as depicted in Fig. 1. The primary search string was TITLE-ABS-KEY ("locomotive OR tram OR train OR metro") integrated with distinct technology-centric terms. Specific filters such as date range, subject category, and document type were applied to ensure consistency and reproducibility. A noticeable academic drift toward novel domains such as quantum sensing and axiomatic design was identified. These innovations were particularly observed in the control mechanisms for trackless systems. Over the decade, there were consistent risen trackless autonomous transport, trams, and metros [9].

1.1 Axiomatic Design for Control for Space Debris

The demanding system properties for trackless design are within the given design functional requirements (FRs) for laser-precise trackless semi- to autonomous transport control: achieve precise speed control (FR1) [10–12]; maintain exact track or path following (FR2) [13–15]; ensure immediate obstacle detection and response (FR3) [16–18]; provide smooth acceleration and deceleration (FR4) [19–21], laser precise [22–24]; facilitate real-time monitoring of the system operating environment

(FR5) [25–30]; and offer automatic switching and routing capabilities (FR6) [31–34]. Correspondingly, technologies need hybrid unit responses by design parameters (DPs).

The additional data was scoped for the middle FR3 to ensure the normality of the other as in distribution starting default from binary true unless collision or over-steering probabilities due to the debris on the ground. Data inquired from Scopus with queries (TITLE-ABS-KEY) in RIS-domain with ("reconfigurable intelligent surfaces" OR RIS); on-orbit perspective in designed for the purpose ("debris removal" OR "space debris") for cleansing the road obstacles to enable the deployment; revealing the intersection to capture efforts in the total design optimization of the track. The visualized results from 2013 to 2023 offer insights into the progression and emphasis of study for the domain, a special example in Fig. 2 scoping results for the database findings.

To comprehensively study RIS and metasurfaces connectivity to the actuators, the Scopus queries employ perspective: TITLE-ABS-KEY("reconfigurable intelligent surface"), TITLE-ABS-KEY("intelligent reflecting surface"), combined terms of metasurface with reconfigurable, software-defined, wireless, communications, modeling, fabrication, characterization, and beamforming. These targeted searches spanned specific terminologies to applications, modeling, fabrication techniques, and measurements—filtering by date range, subject area, and document type for replicability to act as enabler for machine vision-aided frameworks.

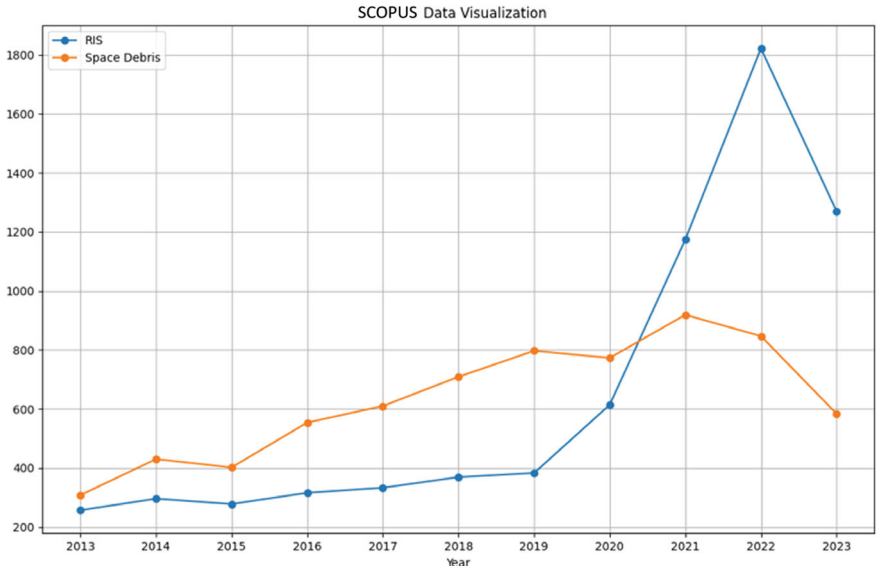


Fig. 2 Scoping documents results (*y*-axle) in function of time (*x*-axle) for RIS for aerospace applications [9]

2 Discussion

LiDAR usability for obstacle detection is outstanding, with few channels [35]. For another component's selection, ranging from different use (in/outdoor), coverage (0–360°), price (low to thousands), the LiDAR usability found decreasing [36–39]. Generally, the components are weighted toward the cost of the sensing antenna. To address each functional requirement and design parameter and achieve laser-precise trackless autonomous transport control using reconfigurable intelligent surfaces (RISs), an assortment of advanced components has been integrated based on their respective functional requirements (FRs) and design parameters (DPs). FR1—Achieve precise speed control: The L298N is a high voltage, high current dual full-bridge driver to this. Designed to accept standard TTL logic levels, this component drives inductive loads, crucially controlling motors to ensure precise speed control [40]. FR2—Maintain exact track or path following with FR3—to ensure immediate obstacle detection and response. The HDL-64E and PUCK HI-RES VLP-16 are both LIDAR systems that provide accurate distance measurements [40, 41]. These systems play a crucial role in allowing the system to maintain track and instantaneously detect obstacles. The HM01B0, a CMOS image sensor that supplements these LIDARs, contributes to visual path tracking and enhanced obstacle detection [42]. FR4—Provide smooth acceleration and deceleration, is played by the ADXL345. This digital accelerometer can measure acceleration across three axes [43]. FR5—Facilitate real-time monitoring of the trackless autonomous transport's operating environment, the BPX65 photodiode augments real-time environmental monitoring by detecting subtle light changes [44]. FR6—Offer automatic switching and routing capabilities: Taking central to this requirement is the M2GL090T-FG484 FPGA, programmed for high-speed data processing and decision-making [45]. This FPGA interfaces efficiently with the STM32H743XIH6, a high-performance ARM Cortex-M7 microcontroller, with routing and switching functionalities [46, 47]. Ensuring streamlined communication with other systems or subsystems, the MCP2551 Module, a high-speed CAN transceiver, is incorporated [48]. Power management for consistent power regulation requires multipass amplifier. Other domains for models of trackless rails, physics dynamics, and business requirements are further developed from traditional buses or trams [49, 50].

3 Results

Laser technology offers axiomatic design independence and information axiom minimization correspondence [51]. Unparalleled precision forms the cornerstone of recent advances in trackless autonomous transport for axiomatic near-coupling in Table 1.

The integration of Terahertz (THz) technology improves control mechanisms such as laser-guided speed control mechanism (DP1); embedded sensors and camera systems for path tracking (DP2); LIDAR or laser radar system for obstacle detection

Table 1 Axiomatic logarithmic minimization

	FR1	FR2	FR3	FR4	FR5	FR6
DP1	X					
DP2		X				
DP3		X	X			
DP4				X		
DP5					X	
DP6		X	X		X	X

(DP3); laser-integrated propulsion and braking system (DP4); onboard monitoring software interfaced with laser sensors (DP5); and automated laser-driven switching system (DP6). The design matrix of the FRs can work uncoupled in trackless autonomous transport operations, while the subsystems challenge concurrent engineering. The enhanced imaging capabilities of structured nonparaxial THz ultrafast imaging is observed for real-time monitoring and navigation. These advancements feed into the functional requirements ensuring adaptability to changing terrains and conditions. The innovations in Terahertz parametric generation with collinear injection of the autonomous system's pulse train wave parametric generation case-by-case basis in artificial intelligence and machine learning algorithms require further studies. The LIDAR or laser radar system for obstacle detection is augmented by imaging technologies accuracy by automated software layers.

4 Conclusions

Certain gaps must be addressed to ensure seamless operation of a reconfigurable intelligent surface (RIS) in a study setting considering the FR3 for the machine vision. These include the need for specialized embedded software and firmware for effective component interfacing, developing a well-designed signal processing, and integrating RF components and antennas for signal transmission. The use of high frequency technologies benchmarking with axiomatic design provides precise control of the transporation during the assembly operations.

5 Further Reasearch

Advancements in THz pulse technology could enhance the environmental awareness of trackless autonomous transport, enabling improvements in electronics manufacturing and beam scanning [52]. Research is underway on autonomous transport designs and systems utilizing pattern recognition for spatial analysis [53]. Integrative studies are being conducted on the synergy of electronics with autonomous systems

and design software [54]. Emphasis is also being placed on developing resilient safety, like IoMT for the multi-industries operation [55]. Additionally, radar systems are being optimized to ensure efficient interfacing with MMIC transceivers, ensuring signal integrity throughout the lifecycle [56, 57].

Acknowledgements No conflicts of interest. Correspondence with Dr. Aezeden Mohamed with gratitude to Janne Heilala on the manuscript preparation.

References

1. Tricco AC, Lillie E, Zarin W, O'Brien KK, Colquhoun H, Levac D, Moher D, Peters MDJ, Horsley T, Weeks L, Hempel S, Akl EA, Chang C, McGowan J, Stewart L, Hartling L, Aldcroft A, Wilson MG, Garritty C et al (2018) PRISMA extension for scoping reviews (PRISMA-ScR): checklist and explanation. Ann Intern Med 169(7):467–473. https://doi.org/10.7326/M18-0850
2. Andersson U (2013) Laser navigation system for automatic guided vehicles: from research prototype to commercial product. Luleå tekniska universitet. http://www.diva-portal.org/smash/get/diva2:995294/FULLTEXT01.pdf https://urn.kb.se/resolve?urn=urn:nbn:se:ltu:diva-22245
3. Analytica O (2023) Crash brings Indian railway safety into sharper focus. Expert Brief. https://doi.org/10.1108/OXAN-ES279529
4. Sakowski M (2016) The next contender in high speed transport Elon Musks hyperloop. J Undergrad Res Univ Illinois Chicago 9:43–47. https://doi.org/10.5210/jur.v9i2.7554
5. Armağan K (2020) The fifth mode of transportation: hyperloop. J Innov Transp. Suleyman Demirel University
6. Premsagar S, Kenworthy J (2022) A critical review of hyperloop (ultra-high-speed rail) technology: urban and transport planning, technical, environmental, economic, and human considerations. Front Sustain Cities 4:842245. https://doi.org/10.3389/frsc.2022.842245
7. Europa (2023) Europe's rail joint undertaking. Flagship project 5: TRANS4M-R—transforming Europe's rail freight. https://projects.rail-research.europa.eu/eurail-fp5/
8. Moher D, Shamseer L, Clarke M, Ghersi D, Liberati A, Petticrew M, Shekelle P, Stewart LA (2015) Preferred reporting items for systematic review and meta-analysis protocols (PRISMA-P) 2015 statement. Syst Rev 4(1):1–9
9. Scopus, Elsevier B V. Available: https://www.scopuscom/. Accessed on 28 Aug 2023
10. Guan K, Moreno J, Ai B, Briso-Rodriguez C, Peng B, He D, Hrovat A, Zhong Z, Kurner T (2020) 5G channel models for railway use cases at mmWave band and the path towards terahertz. IEEE Intell Transp Syst Mag, pp 1–1. https://doi.org/10.1109/MITS.2019.2926371
11. Sapronova S, Tkachenko V, Braykovska N, Kulbovskyi I (2023) Дослідження спрямування екіпажів рейковою колією. Транспортні системи і технології (41):213–221. https://doi.org/10.32703/2617-9059-2023-41-17
12. Cabric N, Branković N, Kalem A (2023) Tram-train system approval procedure
13. Zhang B, Zhang Y, D'Ariano A, Bosi T, Lu G, Peng Q (2023) Optimal platforming, routing, and scheduling of trains and locomotives in a rail passenger station yard. Transp Res Part C Emerg Technol 152:1–35. https://doi.org/10.1016/j.trc.2023.104160
14. Wang Y, Song R, He S, Song Z (2022) Train routing and track allocation optimization model of multi-station high-speed railway hub. Sustainability 14:7292. https://doi.org/10.3390/su14127292
15. Dong J, You P, Tomasino A, Yurtsever A, Morandotti R (2023) Single-shot ultrafast imaging with terahertz radiation. In: CLEO 2023, technical digest series (Optica Publishing Group, 2023), paper SM1N.3

16. Guo J, Hu P, Wang R (2016) Nonlinear coordinated steering and braking control of vision-based autonomous vehicles in emergency obstacle avoidance. IEEE Trans Intell Transp Syst 17(11):3230–3240. https://doi.org/10.1109/TITS.2016.2544791
17. Gao M, Tang J, Yang Y, He Z, Zeng Y (2019) An obstacle detection and avoidance system for mobile robot with a laser radar. In: 2019 IEEE 16th international conference on networking, sensing and control (ICNSC), Banff, AB, Canada, pp 63–68. https://doi.org/10.1109/ICNSC.2019.8743288
18. Brahm A et al (2014) Imaging with a multichannel terahertz time-domain spectroscopy system at 1030 nm excitation wavelength. In: 2014 39th International conference on infrared, millimeter, and terahertz waves (IRMMW-THz), Tucson, AZ, USA, pp 1–2. https://doi.org/10.1109/IRMMW-THz.2014.6956040
19. Sherstobitov VE, Leshchev AA, Soms LN (2003) Nonlinear optical techniques of laser beam control for laser propulsion applications. Beamed Energy Propuls 664:620–633. https://doi.org/10.1063/1.1582148
20. Hauri C, Vicario C, Monoszlai B (2014) GV/m single-cycle terahertz fields from a laser-driven large-size partitioned organic crystal. Phys Rev Lett 112:213901. https://doi.org/10.1103/PhysRevLett.112.213901
21. Kirchner M, Schubert P, Haas C (2014) Characterisation of real-world bus acceleration and deceleration signals. J Signal Inf Process 05:8–13. https://doi.org/10.4236/jsip.2014.51002
22. Vodovozov V, Raud Z, Petlenkov E (2021) Review on braking energy management in electric vehicles. Energies 14(15):4477. https://doi.org/10.3390/en14154477
23. Britten S, Krause V (2019) Industrial blue diode laser breaks 1 kW barrier. PhotonicsViews 16(2):30–33. https://doi.org/10.1002/phvs.201900017
24. Cho J, Na S-J (2009) Three-dimensional analysis of molten pool in GMA-laser hybrid welding. Weld J (Miami, Fla) 88:35s–43s
25. Davor S, Jurum-Kipke J, Petrović D (2012) Ergo-assessment of locomotive drivers' traffic environment. Promet Traffic Traffico 22:439–448. https://doi.org/10.7307/ptt.v22i6.209
26. Brezulianu A, Aghion C, Hagan M, Geman O, Chiuchisan I, Balan A, Balan D, Balas VE (2020) Active control parameters monitoring for freight trains, using wireless sensor network platform and internet of things. Processes 8(6):639. https://doi.org/10.3390/pr8060639
27. Xu K, Pei W, Yang L, Cui G (2014) Precise positioning method and set of mine locomotives (CN104260762A). CITIC HIC Kaicheng Intelligence Equipment Co Ltd.
28. Xu C, Yang Y, Gao W (2020) Skin-interfaced sensors in digital medicine: from materials to applications. Matter 2(6):1414–1445. https://doi.org/10.1016/j.matt.2020.03.020
29. Liang J, Wang LV (2018) Single-shot ultrafast optical imaging. Optica 5(9):1113–1127. https://doi.org/10.1364/optica.5.001113.PMID:30820445;PMCID:PMC6388706
30. Kutas M, Haase B, Bickert P, Riexinger F, Molter D, von Freymann G (2019) Terahertz quantum sensing. ArXiv. https://doi.org/10.1126/sciadv.aaz8065
31. Lei H et al (2023) A low-profile Risley-prism-based 2-D beam-scanning circularly polarized folded transmit array antenna at Ku-band. IEEE Trans Antennas Propag 71(7):6173–6178. https://doi.org/10.1109/TAP.2023.3269102
32. Loughran B, Streeter M, Ahmed H, Astbury S, Balcazar M, Borghesi M, Bourgeois N, Curry C, Dann S, Diiorio S, Dover N, Dzelzanis T, Ettlinger O, Gauthier M, Giuffrida L, Glenn G, Glenzer S, Green J, Gray R, Palmer C (2023) Automated control and optimisation of laser driven ion acceleration. High Power Laser Sci Eng 11:1–11. https://doi.org/10.1017/hpl.2023.23
33. Taghizadeh M, Bozorgzadeh F, Bordbar G (2023) All-optical diffraction and ultrafast switching in a terahertz-driven quantized graphene system. Opt Laser Technol 159:108969. https://doi.org/10.1016/j.optlastec.2022.108969
34. Wang K, Wang X, Ho JD, Fang G, Zhu B, Xie R, Liu YH, Au KW, Chan JY, Kwok KW (2023) A fast-soft robotic laser sweeping system using data-driven modeling approach. IEEE Trans Robot, pp 1–16. https://doi.org/10.1109/TRO.2023.3262118
35. Halterman R, Bruch M (2010) Velodyne HDL-64E LIDAR for unmanned surface vehicle obstacle detection. In: Proceedings of SPIE—the international society for optical engineering, vol 9. https://doi.org/10.1117/12.850611

36. Candrone (2022) The true cost—Implementing lidar into your business. Lidar News. https://lidarnews.com/articles/the-true-cost-implementing-lidar-into-your-business/
37. SICK (2023) 2D laser scanners LMS2xx/LMS291/Outdoor LMS291-S05. https://www.sick.com/es/en/lidar-sensors/2d-lidar-sensors/lms2xx/lms291-s05/p/p109849
38. Lv A, Yuan K, Huang J, Shi D, Zhang S, Yafeng C, He Z (2023) Integrated encapsulation and implementation of a linear-mode APD detector for single-pixel imaging lidar. Photonics 10:970. https://doi.org/10.3390/photonics10090970
39. Zhou B, Xie D, Chen S, Mo H, Li C (2023) Comparative analysis of SLAM algorithms for mechanical LiDAR and solid-state LiDAR. IEEE Sens J, pp 1–1. https://doi.org/10.1109/JSEN.2023.3238077
40. STMicroelectronics (2021) STM32H743xI/G advanced ARM®-based 32-bit MCUs. [Manufacturer datasheet]
41. Velodyne Lidar, Inc. (2021) HDL-64E sensor. [Manufacturer datasheet]
42. Velodyne Lidar, Inc. (2021) VLP-16 Puck. [Manufacturer datasheet]
43. Himax Technologies (2021) HM01B0 ultra-low power CMOS image sensor. [Manufacturer datasheet]
44. Analog Devices, Inc. (2021). ADXL345: 3-Axis, ±2 g/±4 g/±8 g/±16 g Digital Accelerometer. [Manufacturer datasheet].
45. OSRAM Opto Semiconductors (2021) BPX65 silicon PIN photodiode. [Manufacturer datasheet]
46. Microsemi Corporation (2021) SmartFusion2 SoC FPGA family. [Manufacturer datasheet]
47. STMicroelectronics (2021) STM32H743XIH6 ARM Cortex-M7 microcontroller. [Manufacturer datasheet]
48. Microchip Technology Inc. (2021) MCP2551: high-speed CAN transceiver. [Manufacturer datasheet]. Retrieved from https://www.microchip.com/
49. Liu Q, Gordon T, Zhou S, Rahman S, Jin P, Liu X, Xiao L (2022) Lateral control of a trackless road tram 'ART' using multi-axle steering. In: 27th Symposium of the international association of vehicle system dynamics, IAVSD 2021: lecture notes in mechanical engineering. Virtual, Online, pp 783–792. https://doi.org/10.1007/978-3-031-07305-2_73
50. Lawrie I (2020) Transport equity considerations of a 'trackless tram-entrepreneur rail model.' Austr Planner 56(4):270–277. https://doi.org/10.1080/07293682.2020.1854799
51. Suh NP (2001) Axiomatic design: advances and applications. Oxford University Press
52. Tianqi Z, Liu N, Xu J, Liu Z, Zhou Y, Yang Y, Li S, Huang Y, Jiang S (2023) Flexible electronics for cardiovascular healthcare monitoring. The Innovation. 4:100485. https://doi.org/10.1016/j.xinn.2023.100485
53. Won D, Bang J, Choi SH, Pyun KR, Jeong S, Lee Y, Ko SH (2023) Transparent electronics for wearable electronics application. Chem Rev 123:9982–10078. https://doi.org/10.1021/acs.chemrev.3c00139
54. Yudachev S, Sitnikov S, Bosy F (2021) Digitalization of production in Altium Designer software. Glavnyj mekhanik (Chief Mechanic), pp 34–42. https://doi.org/10.33920/pro-2-2106-03
55. Mosallanezhad B, Hajiaghaei-Keshteli M, Smith Cornejo NR, Rodríguez Calvo EZ (2023) An IoMT platform for an integrated sustainable energy-efficient disaster relief supply chain to prevent severity-driven disruptions during pandemics. J Ind Inf Integr 35:100502. https://doi.org/10.1016/j.jii.2023.100502
56. Poole C, Darwazeh I (2016) Microwave transistors and MMICs. In: Microwave active circuit analysis and design, pp 395–437. https://doi.org/10.1016/B978-0-12-407823-9.00012-3
57. Ammar DF, Clark G (2003) Microwave monolithic integrated circuit (MMIC) carrier interface (US Patent No. US6653916B2). United States Patent and Trademark Office

Energy-Efficient Coffee Pulper



Andy Ray and Aezeden Mohamed

Abstract There is an increasing need for a versatile, energy-efficient coffee pulping machine in both the remote and urban coffee-growing areas of Papua New Guinea (PNG). Coffee requires hefty processes from harvesting to processing that involves a lot of human effort and labor. The most energy-draining is the pulping process where the coffee cherry is reduced to coffee beans. The coffee growers in the highlands and some parts of the lowlands of PNG have been using stones, coffee pulping machines, and some other techniques and methods to do the job. However, as more coffee is produced, the need for a more efficient pulping technique emerges. Many farmers resort to using electric motors to drive the pulping machine making the work much faster and more efficient. However, with little consideration, we can see that electricity is dangerous, costly, and only accessible to some privileged urban farmers. Therefore, in this paper, a new technique is proposed by carefully considering the problems encountered by the existing methods. The proposed technique employs a bicycle-driven mechanism that drives the pulping machine via the chains from the bicycle paddle to the back wheel (which acts as a flywheel) and to the pulping machine. The velocity ratio of the system is roughly four; hence, the output velocity and work are four times greater than the conventional pulping using direct effort by hand to pulp the beans. For instance, if you are to spin the wheel (coffee pulping machine) by hand for 36 revolutions per minute, the same work can be done with only nine revolutions per minute using the energy-efficient coffee pulper (the proposed technique). The energy-efficient coffee pulper is very efficient, versatile, safe, sustainable environmentally friendly, and most thrilling; it can be made from waste metals.

Keywords Energy · Efficiency · Coffee pulping machine · Velocity ratio · Work

A. Ray · A. Mohamed (✉)
Department of Mechanical Engineering, PNG University of Technology, Lae, Papua New Guinea
e-mail: aezeden.mohamed@pnguot.ac.pg

© The Author(s), under exclusive license to Springer Nature Singapore Pte Ltd. 2025

B. B. V. L. Deepak et al. (eds.), *Recent Advancements in Product Design and Manufacturing Systems*, Lecture Notes in Mechanical Engineering,
https://doi.org/10.1007/978-981-97-6732-8_14

1 Introduction

Coffee pulping is the third step in coffee processing after picking and floatation [1]. To pulp, berries mean to separate the beans from the pulp and skin. Pulping can be done by hand with a pestle, which breaks the skin and pulp, or with pulping machines [2].

Most PNG coffee farmers and producers used the same method which was pioneered in Brazil around twenty years ago, where it was originally called Cereja Descascada or "peeled cherry." This is because the process involves removing the skin of the fruit before letting the coffee dry with almost all of the pulp still on the beans [3].

The use of a pestle to pulp coffee berries is a very slow and hefty process. On the other hand, the pulping machines have proven very helpful and efficient. The idea is the same though, and that is to remove the pulp and skin. However, time and energy consumption are of the essence here and that is what the paper emphasizes by the proposed system.

The proposed idea of energy-efficient coffee pulper is, as the name states, energy efficient. It integrates a bicycle-driven mechanism and a coffee pulping machine that reduces the energy (effort) and time needed to do the work.

The energy (power) is transmitted through the chains and is amplified by the diametral differences of the pulley wheels making the input effort minimal and maximizing the output work.

2 Literature Survey

A coffee pulping machine is a simple machine used to separate the pulp (skin) of a coffee bean from its seed. The pulper has a knuckled rotating drum that rotates and presses the berries against a larger spoked rotating drum. Both drums are connected to either a belt, gears, or chain pulley system that is driven by a hand crank attached to it. The pressing action squeezes the seeds from the cherries and the pulp is discarded on the other side while the seed is collected on the other side through different channels [4]. Many smallholders utilize a small hand-cranked pulper that uses a two-wheel pulley system for energy transmission.

Coffee undergoes many processes before it is roasted, grounded, and sold on shop shelves. The coffee cherries are processed by disengaging the coffee seeds from their skin and their pulp and are dried from an original moisture content of 63–70% water by weight to 12–13%. According to the Britannica Encyclopedia [5], there are three techniques used to process coffee: the dry or natural process, the wet or washed process, and the hybrid process. The dry method is the oldest, and it requires little use of machinery; it is mostly practiced in places where the climate is dry and has little rainfall. As for the wet process, it is essentially important in this study as it employs the coffee pulper in its initial stage of processing coffee.

Wet processing is very common among many smallholder coffee farmers in the highlands of Papua New Guinea (PNG). Therefore, the first step of processing which is the de-pulping of the coffee cherries is a crucial task. Smallholders who are situated in the remote parts of the country as well as some in urban areas that do not own a mechanized pulping machine resort to using pestles and stones to separate the seeds from their pulp. A handful of smallholders, mostly in the urban centers, alternatively use small motors connected to the hand crank of the pulper to pulp their coffee. Unfortunately, those who do not have access to electricity purely depend on human effort. Therefore, in this paper, we propose a system that can improve the efficiency of the pulper and save time, money, energy, and labor.

According to the literature survey carried out, there were two instances where the idea of amplifying energy through a bicycle-integrated coffee pulping mechanism was used. According to The Smithsonian Magazine [6], six individuals who participated in the month-long MIT International Development Design Summit in Tanzania have developed an idea to integrate a bicycle mechanism. This will enable local coffee producers to reduce labor intensity and energy costs, while also becoming more competitive with commercial coffee producers. Currently, local producers are at a disadvantage and experience significant physical strain when delivering their products. The proposed solution aims to address these challenges effectively and cost-efficiently.

Also, in Peru, a bicycle-propelled pulper was named among three innovations in coffee processing. The article discusses the idea of a bicycle-propelled pulper, which is an adaptation of a bicycle that connects with a belt to a manual coffee pulper for use, vibrating screen sorting machines, and Vetiveria wells [7]. The pedal helps save 50% of time and wages and can pull up to 20 cans of 14 kg of cherries per hour (Fig. 1).



Fig. 1 **a** Ripe coffee cherries, **b** Pulped coffee beans with mucilage

3 Components

See Fig. 2.

3.1 Pulley System

The pulley system comprises the bicycle's back wheel and pedal sprockets connected by the power transmitting bush chains and the coffee pulping machine's spur gear system. These two systems are connected by a third pulley system which utilizes a bush chain link between a sprocket from the back wheel of the bike and another smaller sprocket attached to the pinion of the coffee pulping machine's gear system. The entire pulley system aids in the transfer of energy from the operator to the pulper using several drive pulleys and gears (Fig. 3).

3.2 Frame Structure

The frame structure consists of SHS and RHS galvanized steel structural members mainly 25 × 25 and 50 × 25 welded together to support and house the bicycle frame and the coffee pulper. The structure's design and dimensions largely depend on the type of bicycle frame. The structure is designed to carry loads up to 97 kgs including the weight of the bicycle as well as the coffee pulping machine, thus allowing kids, youth, and adults within this weight range to operate the machine (Fig. 4).



Fig. 2 Energy-efficient coffee pulper model (1) Pulley system, (2) Support frame structure, and (3) Coffee pulping machine. First Prototype—original design (2020)

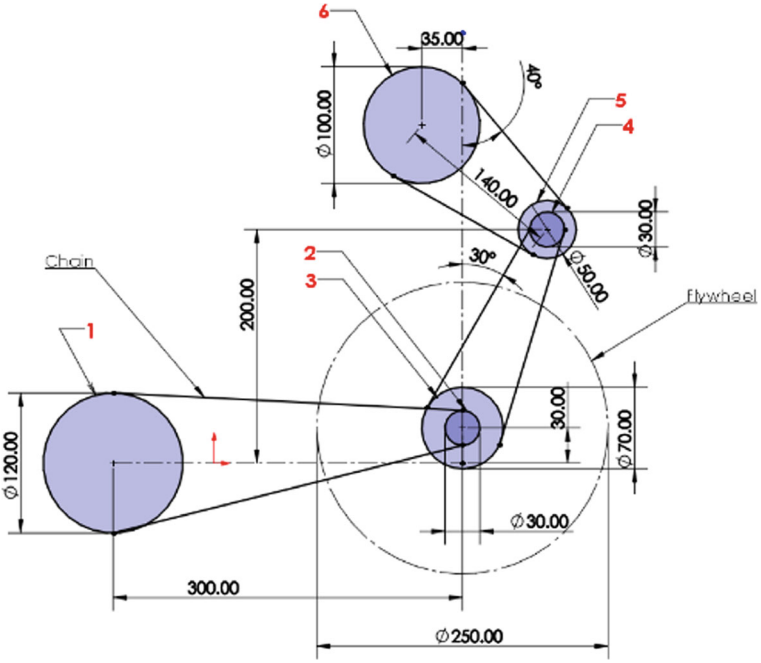


Fig. 3 Diagram of pulley systems. We have drivers or drive gears; 1, 3, 4, and 5, and driven gears; 2, 4, and 6. (SolidWorks drawing, original. ANDY.R. 2023)

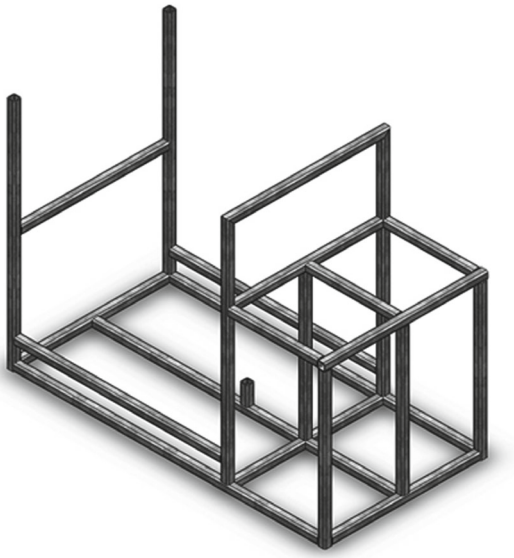


Fig. 4 Solid works model for frame or support structure



Fig. 5 Coffee cherries undergo the pulping process using a conventional hand-crank pulping machine

3.3 Coffee Pulping Machine

The coffee pulping machine comprises a chute, which receives the cherries into a spiked rotating shaft that collects as many cherries as it can gather and presses them against a larger spiked rotating drum where the seeds disintegrate and are separated from the skin and pulp. The coffee pulper employs a two-wheel pulley system that is usually driven by a belt, chain, or (as in our case) gears. This pulley system drives the spiked rotating shaft and the large, spoked rotating drum that does most of the pulping. The pulping machines are in different designs and made with metals ranging from steel to cast iron. For our case, we use a cast iron base pulper to minimize vibrations that the mechanism will generate while in operation. The vibrations can be proven fatal for the pulley system as they can cause misalignment of the chain and pulleys and the gears. In addition, this can lead to increased cyclic stress concentration on the gear pulleys and other critical components of the support structure, and consequently, the system will fail (Fig. 5).

4 Methodology

The approach in which we sought to accomplish the desired output is quite simple. It is derived from the engineering design process and includes several steps as outlined in Fig. 6.

First, we brainstorm ideas about potential ways to recycle scrap metals to create something useful that can benefit people in our community. After brainstorming, we resolved to recycle old bicycle frames and scrap metals to create a mechanism that can help lighten the burden of coffee processing in the coffee-growing areas, especially in the highlands of Papua New Guinea. Hence, we started researching the different coffee pulping techniques that are currently in use in not only PNG but also all around the world.

After weighing out the pros and cons of the existing processing techniques, we came up with a concept that is not only new but also suitable and efficient for our community. We have hand-crank pulping, motor-driven pulping, and pestle, or

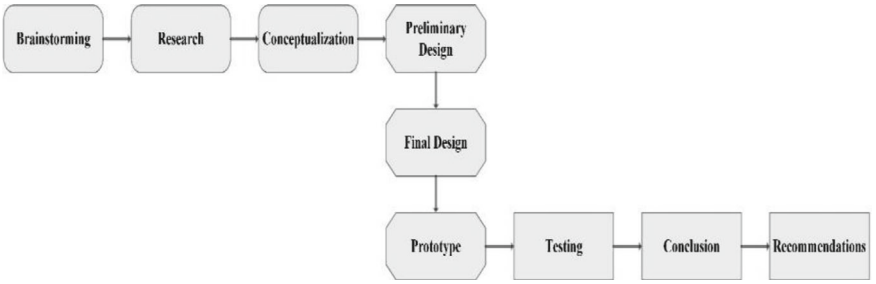


Fig. 6 Methodology flow chart

sometimes stone, pulping techniques. The concept we introduced was bicycle-driven coffee pulping; it does not require power; it is manual but better yet; it saves a ton of energy, labor, and time.

After the concept is ironed out, we jump straight to preliminary designs. The preliminary designs undergo inspections from each member of the group and comments, and corrections were made from time to time. Upon much alterations and corrections, the final design is made ready for implementation.

From the final design, we built the prototype from scrap metals! After the prototype was built, we took it to Kafuku Village in Goroka, Eastern Highlands Province, and did the first testing. The test results were outstanding but we also noticed some potential areas of the design that need altering. Hence, we made conclusions affirming our goal of achieving an energy-efficient output through the system and we noted some areas of improvement and made recommendations for future development. Ideally, we followed the engineering design process where we identified the problem, generated ideas, selected a solution, built the item, evaluated, and then presented the results.

5 Results and Discussion

In this study, the primary goal of the proposed system was to provide an optimized system that can mitigate the hard labor in the pulping process of coffee beans while recycling scrap waste metals and turning them into something useful, and in doing so, we protect the environment. Energy efficiency and energy saving are of great significance in this study as we sought ways to mitigate work done by human labor. Therefore, the energy analysis of the system is done to ensure minimal use of energy and considerable work output.

According to the law of energy conservation, energy is neither created nor destroyed but converted from one form to another. Hence, in the case of a bicycle, the same principle applies. Initially, the chemical energy stored in the cycler's body from food intake is converted to kinetic energy that causes the movement of muscles when the cycler starts applying force on the pedal. Consequently, the kinetic energy is

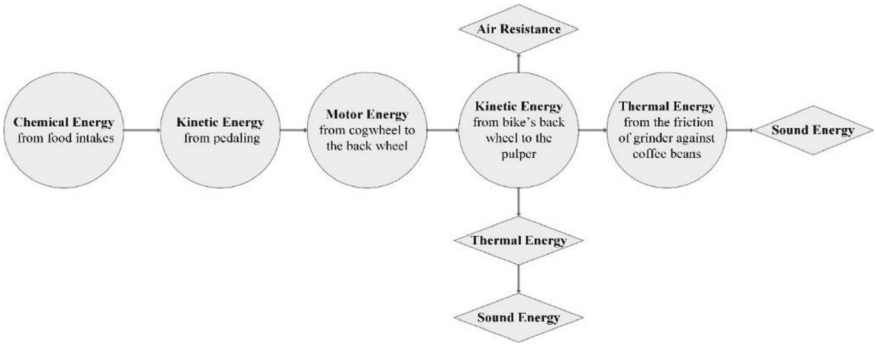


Fig. 7 Energy flow and conservation diagram for coffee pulping mechanism

transferred via the chains to the cogwheel on the backside of the bike. The cogwheel is attached to the back wheel; thus, it introduces output motor energy onto the wheel causing it to rotate [8].

The motor energy from the cogwheel is then converted to kinetic energy and is transferred via another chain link from the cogwheel to a sprocket attached to the gears of the pulping machine. The back wheel of the bicycle does not contact the ground but it is elevated to rotate freely in space sufficing as a flywheel, smoothing out the energy fluctuations and allowing uniform energy flow by lessening the intermittent operation of the machine (Fig. 7).

The system's kinetic energy is converted to motor, sound, and thermal energy from the various stages in the system. The kinetic energy can be calculated from the energy equation;

$$E_k = \frac{1}{2}mv^2.$$

The entire pulley system is a compound chain-drive system where power, which is the rate of work done per unit of time or the rate of energy transfer at any given time, is transmitted from one shaft or axle to another through the pulley systems (Fig. 8).

From the relationship between the pulleys and the gear ratios, we can calculate the velocity ratio of the system and in turn the mechanical advantage (MA) and efficiency (η) of the system. Based on the velocity ratio, provisions are made for the comparison of energy usage in manual pulping and the proposed method of pulping. Hence, by adopting the calculation of the velocity ratio for the compound belt-drive system, we come up with the velocity ratio of the system below [9]:

$$\frac{\text{Speed of last driven}}{\text{Speed of first driver}} = \frac{\text{Product of diameters of drivers}}{\text{Product of diameters of driven}},$$

$$\frac{N_6}{N_1} = \frac{d_1 \times d_3 \times d_5}{d_2 \times d_4 \times d_6}.$$

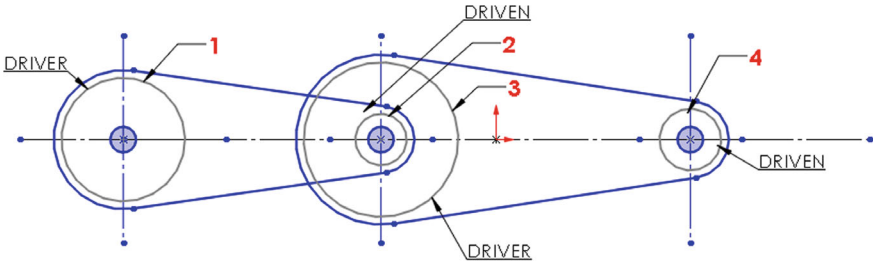


Fig. 8 Drive and driven pulleys in system; 1. Pedal sprocket, 2. Back-wheel sprocket, 3. Larger diameter back-wheel sprocket, 4. Driven sprocket attached to coffee pulping machine

where,

d_1 = diameter of the pulley 1

N_1 = Speed of the pulley 1 in r.p.m

d_2, d_3, $d4$, and N_2, N_3, N_4 = Corresponding values for pulleys 2, 3 and 4.

Hence, by assuming different load applications based on the weight of the operator, we can see how much work is done compared to the conventional method of pulping by hand. The velocity ratio calculated based on the above formula was about 4, which implies that the output is four times the input. So, if we compare this with the output of a conventional hand-crank coffee pulper, 1 revolution of the pedal is equivalent to 4 rotations by hand. This saves energy up to four times, increases productivity in less time, and is very efficient.

The proposed system has countless advantages compared to the existing pulping techniques available. It is very efficient and versatile in that it significantly reduces the energy input for human labor required in pulping compared to conventional pulping. It makes the work faster, and thus, it saves time consequently. It demands less maintenance and is easy to repair, dismantle, and transport from place to place. What is more is that it is made from scrap metals and is environmentally friendly, saving costs while increasing production and efficiency. Cycling is a good exercise as well, thus operating the machine provides a good enough exercise that will contribute to one's well-being as well.

6 Conclusion

Overall, the proposed system employs a bicycle-driven mechanism to drive a conventional coffee pulper. The proposed idea is simple, safe, energy-efficient, and time-saving. There are different methods of pulping used in different settings of places in PNG. We have the electric motor-driven pulpers that some urban farmers use, which is also very efficient.

However, most of the small-scale coffee growers are from the remote parts of the country and do not have access to electricity, and electricity is costly and dangerous.

Thus, in this paper, the idea of a versatile, cost-effective, and energy-efficient coffee pulper is proposed so that the farmers in both the rural and urban centers of PNG can have access to this technology. It saves energy by amplifying the input energy 4 times and saves a tremendous amount of time and energy. What is more, it can be constructed from waste metals.

References

1. Pact Coffee (n.d) Coffee processing methods: pact coffee. Retrieved from Pact Coffee Website: https://www.pactcoffee.com/farms/cherry-processing-methods
2. Food and Agriculture Organization—Agency (n.d) Processing the coffee beans: FAO. Retrieved from Food and Agriculture Organization—Agency Website: https://www.fao.org/3/ad219e/AD219E08.htm
3. Perfect Daily Grind (2016) About us: coffee processing: understanding pulped natural coffee. Retrieved from Perfect Daily Grind Website: https://perfectdailygrind.com/2016/06/coffee-processing-understanding-pulped-natural-coffee/
4. Oil Slick Coffee Company, LLC (2022) Library. Oil slick coffee company, LLC. Retrieved from Oil Slick Coffee Company, LLC Website: https://oilslickcoffee.com/library/coffee-pulper-machine/
5. René C, Myhrvold N (2023) Coffee production. Harvesting and processing. Encyclopedia Britannica. Retrieved from Encyclopedia Britannica Website: https://www.britannica.com/topic/coffee-production
6. Zhou L (2015) Smithsonian Magazine. Retrieved from Smithsonian Magazine Website: https://www.smithsonianmag.com/innovation/farmers-can-shell-coffee-fraction-time-with-this-bike-powered-machine-180954806/
7. Alianza Cafe (2019) Innovations. Alianzacafe. Retrieved from Alianza Café Website: https://alianzacafe.org.pe/en/innovations/
8. Haron T (n.d) Physics of cycling. Energy conservation. Retrieved from Physics of Cycling. Weebly Website: https://timothyharonphysicsproject.weebly.com/energy-conservation.html
9. Khumri R, Gupta J (2015) Theory of machines. S. Chand

Community Perception on Groundwater Quality Versus Analytical Quality in the Coastal Areas of Visakhapatnam, India—Opinion Versus Actuality



Sirisha Korrai, Nallamilli Satish Reddy, Madhavi Earle, Hemanshu Mediboyana, and Bharani Meruva

Abstract With an aim to estimate the quality of ground water and perception of public towards it, a case study was conducted in the selected areas of Visakhapatnam, India. For this study, thirty ground water samples from different locations of coastal Visakhapatnam region (East coast, India) were collected and different physico-chemical parameters of the collected samples were measured. Analysis of the data showed that in all the samples, certain parameters exceeded the tolerable levels set by WHO guidelines for potable water. The study disclosed that total dissolved solids, chlorides, calcium, sodium and hardness were the major parameters and were the predominant contaminants in the sample areas, which crossed the set limits. The high amounts of Cl^{-}(187 mg/L), Ca^{2+} (134 mg/L), NO^{3-}(15.27 mg/L), Na^{+} (232 mg/L) and TDS (1706 mg/L) were observed in S10, S2, S5, S22 and S5 among thirty samples, respectively. In conjunction with the water quality analysis study, a survey regarding the public perception on the ground water quality they regularly use was also conducted. The survey has emancipated that over 96% of people are not satisfied with the quality of available ground water. The analytical report of samples has become an evidential proof and in agreement with the people's conception. The case study is a whistle blower to alert the authorities to take initiatives to curb the health hazards associated with contaminated ground water in those areas.

S. Korrai (✉)
Vignan's Institute of Information Technology, Duvvada, Visakhapatnam, Andhra Pradesh 530049, India
e-mail: sri.siri369@gmail.com

N. S. Reddy · B. Meruva
Department of Environmental Sciences, Andhra University, Visakhapatnam, Andhra Pradesh, India

M. Earle
NSRIT College, Visakhapatnam, Andhra Pradesh, India

H. Mediboyana
Centre for the Environment, Indian Institute of Technology, Guwahati, Assam, India

© The Author(s), under exclusive license to Springer Nature Singapore Pte Ltd. 2025

B. B. V. L. Deepak et al. (eds.), *Recent Advancements in Product Design and Manufacturing Systems*, Lecture Notes in Mechanical Engineering,
https://doi.org/10.1007/978-981-97-6732-8_15

Keywords Quality of ground water · Analytical methods · Contaminants · WHO guidelines · Health hazards · Citizen referendum

1 Introduction

As per the reports of UN Secretary General in World Environmental Day (2003) summit, about 80% of human population is prone to illness and deaths due to water-borne diseases, particularly in the developing countries [1]. The quality of water is said to be safe and potable, when water is set free from disease causing pathogens and hazardous chemicals. Thus, the quality of drinking water assessment is crucial and predetermination of its quality plays a pivotal role in reducing the impact on environment, human health risk as well [2–4]. The UN General Assembly (July 2010) has acknowledged that safe, clean drinking water and sanitation is a privilege along with other human rights to lead a decent life [5]. The malfunctioning activities engulfed with nature and humans, cooperatively or individually are responsible for the malign of quality of water [6–8].

Ground water is indispensable water resource, and unlike surface water, the contamination possibilities are less [9, 10]. Even though it possesses such attributes, ground water is not secure, and its quality is declining day by day at alarming rate. In the present scenario, ground water quality is competing with the surface water in deterioration. Moreover, conservation of limited water available and its quality is important. Reputable studies warn that water scarcity could threaten two-thirds of the world's population by 2025 [11].

Due to exceptional nature, water dissolves almost all kind of chemicals [12]. Infiltration, precipitation, ground water flow pattern and soil characteristics are few activities/processes through which contaminants reach surface water sources level and finally affect the quality of ground water [13, 14]. Chemical contaminants like carbonates, sulphates and chlorides tend to increase the hardness of water and cumulative toxic properties of some elements like mercury, cadmium, lead and other toxic metals are known to cause carcinogenic health problems. Serious health hazards like Fluorosis, Itai-Itai and Blue baby syndrome may be caused due to excess concentrations of fluoride, cadmium and nitrates, respectively.

In broad sense, chloride concentration, electrical conductivity (EC) and total dissolved solids (TDS) are major parameters that reflect the water quality status. The contamination is said to be high, if the samples are showing high values of TDS and EC.

Though the sources of contamination are cut off, the natural ways of groundwater purification might take decades or even more [15].

The inorganic composition of groundwater includes Cl^-, F^-, SO_4^{2-}, Ca^{2+} and Mg^{2+}. Anthropogenic sources of nitrates include domestic waste waters and agricultural runoff that includes fertilizers and manure [16]. Higher levels of Cl^-, F^-, SO_4^{2-}, Ca^{2+} and Mg^{2+} may lead to formation of poisonous substances that reacts

with organic compounds in water, formation of carcinogenic substances like tri-halomethane and causes fluorosis (mottled teeth and damages bones); cathartic and laxative effect; coma and death; nausea, muscle weakness and paralysis in human body when it reaches to about 400 mg/l, respectively [17–21]. If the total dissolved solids (TDS) is more than 2000 mg/l causes laxative effect, sodium portion effects patients afflicted cardiac diseases and women with toxaemia associated with pregnancy.

In the past few decades, the public awareness on quality of drinking water has increased due to widespread publicity on importance of safety of water. The present study evaluates the characteristics of water samples collected at different locations. The study was extended to elicit the opinion of people residing at the areas, where the ground water samples were collected. Three parameters, i.e. general satisfaction (visibility and odour), taste satisfaction and risk perception, were significantly taken as important. Similar surveys have has been reported in literature, who have also taken into account the age, social, cultural and psychological status of people [22–26]. The water quality data and people's responses were compared and analysed.

2 Materials and Methods

2.1 Study Area

Visakhapatnam district is one of the North Eastern Coastal areas of Andhra Pradesh (17°–15′ and 18°–32′ Northern scope and 18°–54' and 83°–30′ in Eastern longitude). The core part of the city territory extends from north to south that resembles a spoon shaped bowl encompassed by hills on three sides with a restricted Eastern Zone jutting into the Bay of Bengal. The present study is focussed on the coastal areas of Visakhapatnam, where maximum commercial activities are taken place (Fig. 1). The climatic conditions in the different parts of the city are dynamic. The city is influenced by the Southwest monsoon and Northeast monsoon; monsoon stretches from September to November, while December to January is the coldest months of the year. The sampling locations along with their latitudes and longitudes is given in Table 1 in Annexure 1.

3 Research Methodology

Thirty groundwater samples were collected from the selected areas of coastal Visakhapatnam, and samples were analysed for twenty physico-chemical parameters using APHA [27] methodologies (Table 2) in Annexure 1. The analysed results were compared with permissible limits suggested by WHO [28].

In continuation of the study, a questionnaire has been organized with the questions relating to different aspects of ground water and the information was cumulated



Fig. 1 Map representing study area

from residents of sample-collected areas. Variety of questions has been circulated among the people, and the data was archived for our future correspondence. The questionnaire contains the general questions like colour, taste and odour to know about the people perception on their usage water.

4 Results and Discussion

4.1 Physico-Chemical Analysis

The analysis report elucidates that pH values of all water samples are in the range from 6.3 to 7.8. This explained that the samples are near to neutral and slightly alkaline in nature. All pH values are within the permissible levels as per IS 10500 (2012), i.e. 6.5 to 8.5, except two samples (S13 and S14), which possess pH 6.4 and 6.3, respectively, lower than the permissible limit of 6.5.

Electrical conductivity (EC) of samples is ranged between 1090 and 2567 μS/cm. Sample S15 and S17 were found to exceed the permissible limits as per WHO [28]. The higher values of EC in some sampling locations may be due to the presence of high concentrations of ionic constituents. The analysis on presence of chlorides stated that 70% of collected water samples were found to exceed the recommended levels of IS 10500 (2012) and WHO [28], which indicates that sampling areas are reported to contaminated with chlorides.

Total hardness (TH) is ranged from 219.9 to 627.2 mg/L in all samples but 16.6% are reported to alter with the permissible level as per WHO [28], i.e. 500 mg/l. WHO

Conference outlines held at Geneva suggested that there were no adverse health threat due to drinking of hard water but few studies has reported that the incessant intake of hard water enhances the calcium and magnesium levels in the human body [29]. The analytical data of the present study expresses that calcium values ranged in between 22.1 and 145.6 mg/L. The results also reveal that 23.3% were found to be exceeding the permissible limits as per WHO [28]. Sodium concentration ranged between 114 and 232 mg/L; approximately, 20% of the samples have exceeded the permissible limits of WHO [28].

Total dissolved solids (TDS) exceed the permissible level, i.e. 500 mg/L as per WHO guidelines. The recorded values are in the range of 587–1706 mg/L. The variations are supposed due to dissolution of salts and minerals at different locations. According to Indirabai et al. [30] the nutrient-rich surface water also causes the TDS enhancement of ground water. Phosphorous content in the collected samples varied between 1.05 and 3.1 mg/L. From recommendations of Canadian Department of National Health and Welfare and European Economic Community [31], the phosphate limits are 0.2 mg/L and 0.54 mg/L, respectively. Based on data, the phosphate content in water samples in the present study was higher than permissible levels. The increased levels of phosphates are attributed that sewage, industrial effluents and agricultural residues, etc., as dissolutions reach the ground water table. Because of non-farming practices in the selected areas, anthropogenic and geological factors might have caused those higher phosphate levels in the water samples.

The iron values ranged between0.08 and 1.01 mg/L. The data reveals that nearly 3.33% of groundwater samples have exceeded the permissible limits as per WHO [28]. The values of turbidity in the study area ranged from 0.03 NTU to 0.09 NTU. All the values of turbidity are within the permissible levels of 5 NTU as both the standards. The concentration of magnesium ranged from 21.1 to 85 mg/L. All the values of Mg^{2+} are within the permissible levels of 150 mg/L as per WHO [28]. The total alkalinity values of the study area ranged from 143 to 263 mg/L. All the TA values are within the permissible levels as per WHO [28]. The concentration of sulphates ranged from 102 to 192 mg/L in the study. All the values of sulphates were found to be within the permissible levels as per WHO [28]. The values of fluoride in the study area ranged from 0.4 to 1.1 mg/L. In all samples, the values of fluoride in the study area are within the permissible levels as per WHO [28]. The results of the study indicate that the values of nitrates ranged between 8.2 mg/L and 15.27 mg/L. All the values of nitrates are within the permissible levels as per WHO [28]. In the present study, the concentration of Cr(VI) ranged between 0.01 mg/L and 0.05 mg/L. All the samples in the study area are within the permissible limits as per WHO [28] that is 0.05 mg/L. The values of bicarbonates in the study area ranged from 221 mg/l to 278 mg/L. All the samples recorded permissible levels of bicarbonates as per BIS standards, i.e. 600 mg/L. The values of phosphorous ranged from 0.02 to 0.09 mg/L. All the samples are within the permissible limit as per WHO (1993), i.e. 0.1 mg/L. Figure 2 illustrates the variability of parameters of collected samples in comparison to standard value. Table 3 (Annexure 1) displays analysed value of all parameters of all collected samples at different locations.

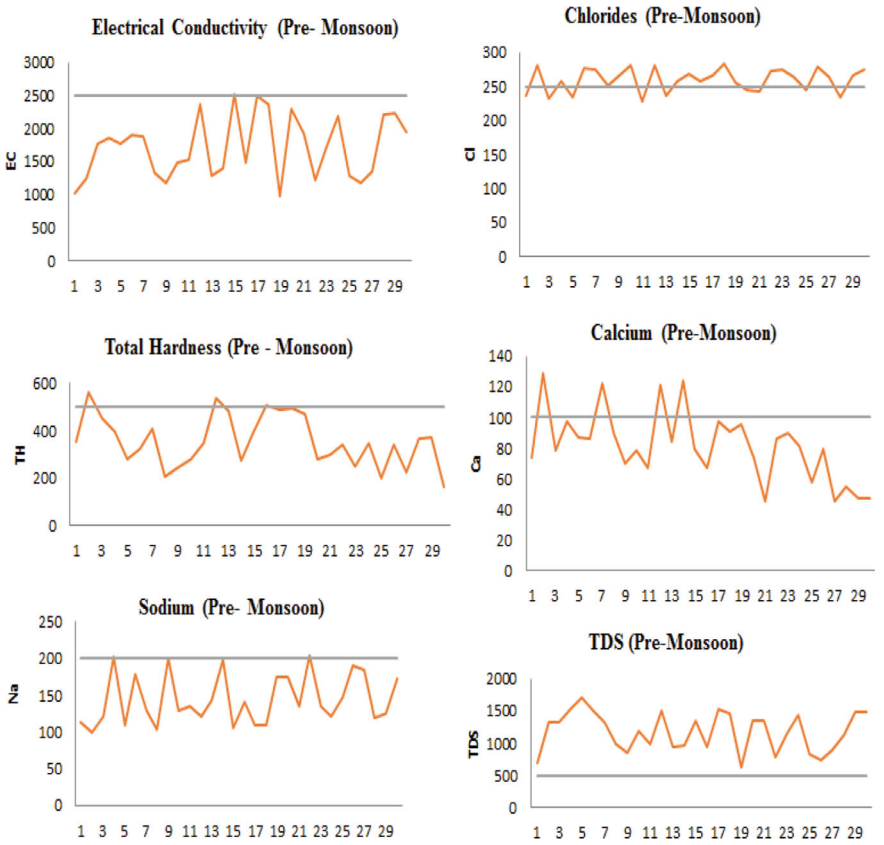


Fig. 2 Trends of parameters with respect to standard (straight line), *X*-axis: Sample number, *Y*-axis: Parameter range in mg/L

4.2 Survey Results

A survey (annexure 1) was conducted, which consisted of general information and main three variables (general satisfaction-colour and odour, taste satisfaction and risk perception). Tables 1 and 3 illustrate the survey details. The general and taste satisfaction variables were scaled from 1 to 3 (1 denotes satisfaction, 2 denotes uncertain and 3 denotes dissatisfied), while the risk perception is scaled from 1 to 4 (1 denotes high risk, 2 denotes medium risk, 3 denotes low risk and 4 denotes no risk). When age factor is considered, respondents were as follows: 20–30 years (54%) and 30–50 years (46%). We have conducted survey by giving more priority to married female respondents with good literary profile. Most of the respondents stated that they could not able to find any visible traces of impurities (i.e. 96% satisfied with the colour); 90% of the respondents are satisfied with the odour and taste (Tables 1 and 2).

Table 1 General profile of study area. *Source* APHA 2005 standards

S. No.	Variables	Profile	Percentage (%)
1	Age	20–30 years	54
		30–50 years	46
2	Gender	Males	08
		Females	92
3	Literacy	Literates	33
		Illiterates	67
4	Marital status	Single	07
		Married	93
5	Family type	Small	86
		Large	14
6	Income	High	0
		Middle	42
		Low (BPL)	58

Table 2 Public perception on quality of groundwater based on general and taste satisfaction

Variable	Profile	Satisfied (%)	Uncertain (%)	Dissatisfied (%)
General Satisfaction	Colourless	96	4	–
	Odourless	90	10	–
Taste satisfaction	Tasteless	90	–	10

Table 3 Risk perception by public

Variable	High risk	Medium risk	Low risk	No risk
Risk perception (%)	10	50	36	4

The risk perception among the people varied widely from no risk to high risk (Table 3). Due to lack of awareness of the problems associated with un-treated water, most of the respondents depended taste and odour to assess the water quality. The data interpreted that risk is under medium level (50% respondents) and low level (36% respondents) and residents close to seashore asserted that risk is very high with their available ground water sources (10% respondents). Only 4% of residents confirmed that no risk associated with water consumption. One more vital point from the survey was that some respondents are utilizing the ground water for domestic purposes only, while drinking water is sourced from municipal water supplies. Few of them boil the ground water before consumption. Figure 3 interprets the responses of people for various questions. The people's perception could be substantiated with analytical data obtained. The results alert the people as well as government officials to take precautionary measurements.

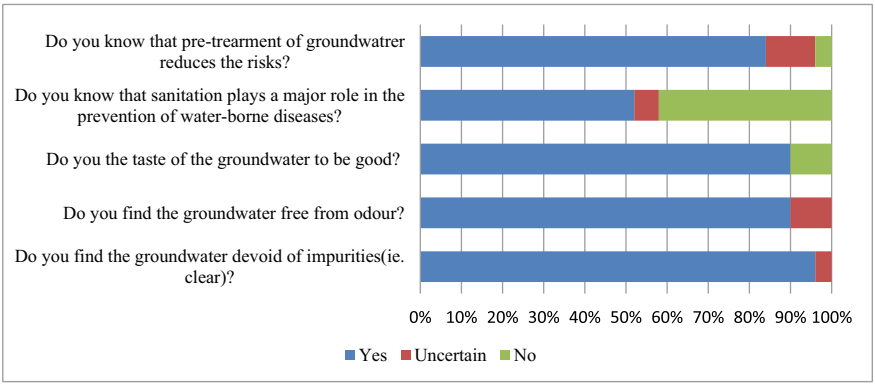


Fig. 3 Respondents' reviews on quality of groundwater in study area

5 Conclusion

Water quality analysis is of priority as many of the diseases are water-born caused with consumption of contaminated water. Basic parameters like hardness, pH, turbidity, Ca^{+2}, Mg^{+2}, Fe^{+2} and other heavy metal analysis are paramount, and their range should be within the standard levels for human consumption. In the present study, the samples collected in coastal region of Visakhapatnam conducted physico-chemical tests and compared the results with the WHO standards. The report revealed that some parameters have crossed the standard limits, and many are within the permissible levels. The survey documented the varied opinions of people, whose concerns were tallying with the quality of ground water in the region. Based on the survey and analytical reports, the ground water hazard is not in peril situation as now. The exceeding limits of parameters like Fe^{+2}, Ca^{+2} and TDS levels make the water non-potable. Overall, the study has brought perception on quality of water in the coastal region of Visakhapatnam, which helps in the implementation of mitigation activities for the safety of ground water in the most affected areas.

Acknowledgements The authors acknowledge Andhra University, Visakhapatnam, for laboratory facilities.

References

1. UN Press release (2003). https://www.un.org/press/en/2003/sgsm8707.doc.htm
2. Olushola MA, Albert CA, Aderonke AO (2014) The physicochemical quality of groundwater in relation to surface water pollution in Majidun Area of Ikorodu, Lagos State, Nigeria. Am J Water Resour 2:26–133
3. Trivedy RK, Goel PK (1986) Chemical and Biological method for water pollution studies. Environ Publ (Karad, India) 6:10–12

4. Udom GJ, Etu- Efeotot JO, Esu EO (1999) Hydrochemical evaluation of groundwater in parts of Port Harcourt and Tai-Eleme Local Government Area, Rivers State. Global J Pure Appl Sci 5:546–552
5. UN Media Release (2010) https:news.un.org/en/story/2010/07/346122
6. Agrawal R (2009) Study of physico-chemical parameters of groundwater quality of Dudu town in Rajasthan. Rasayan J Chem 2:969–971
7. Akoto O, Adiyiah J (2007) Chemical analysis of drinking water from some communities in the Brong Ahafo Region. Int J Environ Sci Technol 4:211–214
8. Appelo CAJ, Postma D (2005) Geochemistry, groundwater and pollution, 3rd edn. CRC Press, Boca Raton, FL; 649
9. Barba MI, Larrechi MS, Coronas A (2019). Quantitative analysis of free water in ionic liquid-water mixtures. Talanta 199:407–414
10. Venkata Rao G, Kalpana P (2016) Assessment of ground water quality in and around Pydibhimavaram Industrial Area, AP, India. Int J Environ Sci Dev 7:703–706
11. Agunbiade FO, Moodley B (2014) Pharmaceuticals as emerging organic contaminants in Umgeni river water system, KwaZulu-Natal, South Africa. Environ Monit Assess 186:7273–7291
12. Momejian N, AbouNajm M, Alameddine I, El-Fadel M (2019) Can groundwater vulnerability models assess seawater intrusion? Environ Impact Assess Rev 75:13–26
13. Fick J, Soderstro H, Lindberg RH, Phan C, Tysklind M, Larsson DGJ (2009) Contamination of surface, ground, and drinking water from pharmaceutical production. Environ Toxicol Chem 28:2522–2527
14. Shah J, Sardar K, Seema AK, Said M, Abdur R, Nisar M (2019) Hydrochemical properties of drinking water and their sources apportionment of pollution in Bajaur Agency, Pakistan. Measurement 139:249–257
15. Tatti F, Papini MP, Torretta V, Mancini G, Boni MR, Viotti P (2019) Experimental and numerical evaluation of groundwater circulation wells as a remediation technology for persistent, low permeability contaminant source zones. J Contam Hydrol 222:89–100
16. Hansen B, Thorling L, Schullehner J, Termansen M, Dalgaard T (2017) Groundwater nitrate response to sustainable nitrogen management. Sci Rep 7:8566. https://doi.org/10.1038/s41598-017-07147-2
17. Bhade DL, Khadsan RE (2014) Physico-chemical analysis of ground water in Sangrampur Tehsil of Buldana District, Maharashtra. Am Int J Res Formal Appl Nat Sci. Available online at http://www.iasir.net
18. Eline B, Gertjan G, Bas Z, Anouk B, Dick V (2019) Water and health: From environmental pressures to integrated responses. Acta Trop 193:217–226
19. Jill EJ, Esther L, Hannah R (2019) Impact of upstream oil extraction and environmental public health: a review of the evidence. Sci Total Environ 657:187–199
20. Tomas M, Slavomir C, Miroslav F, Lucia B, Miroslav G (2019) Pharmaceuticals, drugs and resistant microorganisms—environmental impact on population health, pharmaceuticals, drugs and resistant microorganisms—environmental impact on population health. Curr Opin Environ Sci Health 9:40–48
21. Yan Z, Bin X, Zifang G, Jichang H, Huanhuan L, Lan J, Feng C, Yuqing X (2019) Human health risk assessment of groundwater arsenic contamination in Jinghui irrigation district, China. J Environ Manage 237:163–169
22. Adak MD, Purohit KM (2001) Status of surface and groundwater quality of Mandiakudur, Part-I Physico-chemical parameters. Poll Res 20:103–110
23. Anadu EC, Harding AK (2000) Risk perception and bottled water use. J Am Water Works Assoc 92:82–92
24. Jardine CG, Gibson N, Hrudey SE (1999) Detection of odour and health risk perception of drinking water. Water Sci Technol 40:91–98
25. Larson BA, Gnedenko ED (1999) Avoiding health risks from drinking water in Moscow: an empirical analysis. Environ Dev Econ 4:565–581

26. Yuan L, Dabo G, Shu T, Xuejun W, Kebin H (2018) A review of air pollution impact on subjective well-being: survey versus visual psychophysics. J Clean Prod 184:959–968
27. APHA (2005) https://www.standardmethods.org/doi/book/10.2105/SMWW.2882
28. WHO (2011) Guidelines for drinking-water quality, 4th edn, incorporating the 1st addendum (who.int). https://www.who.int/publications/i/item/9789241549950
29. Galan P, Arnaud MJ, Czernichow S, Delabroise AM, Preziosi P, Bertrais S (2002) Contribution of mineral waters to dietary calcium and magnesium intake in a French adult population. J Am Diet Assoc 102:1658–1662
30. Indirabai WPS, George S (2002) Assessment of drinking water quality in selected areas of Tiruchirappalli town after floods. Poll Res 21:243–248
31. Canadian Department of National Health and Welfare (1969) Canadian drinking water standards and objectives, Canada. https://www.canada.ca/en/health-canada/services/environmental-workplace-health/water-quality/drinking-water/canadian-drinking-water-guidelines.html
32. http://www.un.org/waterforlifedecade/pdf/human_right_to_water_and_sanitation_media_brief.pdf

Simulation Modeling and Analysis for Supply Chain Disruptions: A Case Study from a Process Industry in Kerala



Veedhi Shyam Nishanth, B. Abhiram, Madineni Bhavana, Vani Amrutha Mutyala, Arun Thomas, T. Rathnakaran, and Vinay V. Panicker

Abstract Supply chain disruptions can significantly impact the efficiency and productivity of process industries. This study presents a simulation-based approach to analyze the supply chain of a jackfruit industry. Using Arena software, a simulation model of the supply chain was created and analyzed with disruptions caused by power supply and production bottlenecks. The findings from this study offer crucial recommendations for enhancing the efficiency and supply chain resilience of the jackfruit industry. This study can help process industries deal with supply chain problems before they happen and become more competitive in a market that is always changing.

Keywords Supply chain disruptions · Supply chain resilience · Supply Chain risk · Food supply chain

1 Introduction

Supply chain management encompasses the orchestration of services and processes from raw materials to final products, crucial for cost reduction. Its intricate stages, spanning from suppliers to end users with intermediaries like manufacturers and distributors, heighten complexity and vulnerability to disruptions. These disruptions, whether at the supplier level, during transportation, or due to production delays, can significantly impact operations. Thus, supply chains must be responsive to risks, with businesses conducting thorough disruption analyses to identify weaknesses and fortify their resilience. By doing so, they mitigate the impact of disruptions, ensuring seamless operations and sustained success. Based on the type of raw material, process

V. S. Nishanth · B. Abhiram · M. Bhavana · V. A. Mutyala · A. Thomas · T. Rathnakaran · V. V. Panicker (✉)
Supply Chain and Systems Simulation Laboratory, Department of Mechanical Engineering, National Institute of Technology Calicut, Kattangal, Kerala, India
e-mail: vinay@nitc.ac.in

© The Author(s), under exclusive license to Springer Nature Singapore Pte Ltd. 2025

B. B. V. L. Deepak et al. (eds.), *Recent Advancements in Product Design and Manufacturing Systems*, Lecture Notes in Mechanical Engineering,
https://doi.org/10.1007/978-981-97-6732-8_16

industries are classified into Agro-based, Marine-based, Mineral-based, and Forest-based. This study focused on jackfruit processing firm in the Agro-based category. In India's food supply chain, which encompasses production, processing, distribution, retailing, and consumption, jackfruit stands out as a significant contributor due to its versatility. However, despite being a prominent fruit in India, a considerable portion of jackfruit production is lost due to inadequate storage and transportation facilities, especially in rural areas where most production occurs. This contributes to India's overall food loss and waste issue, with an estimated 40% of food production going to waste. Despite being the world's largest jackfruit producer, India consumes only a small portion of its harvest, leading to significant economic losses for farmers and heightened health risks due to decaying fruit. As a result, there is a pressing need to address storage and transportation challenges to minimize food waste and improve economic outcomes for farmers. The significant contributions of this work are as follows:

- Development of a simulation model for a process industry
- Verification and validation of the simulation model to ensure the accuracy and reliability of the model, making it a valuable tool for process optimization.
- Identification of the key factors and managing them to improve the firm's efficiency.

The novelty of this research lies in the unique application of process industry modeling using Arena software, with a specific focus on disruptions. A module is developed that simulates power disruptions, allowing to study their impact and devise ways to minimize their effects. This research aim is to bolster the robustness of supply chains to disruptions by understanding how the model operates under disruptive conditions. The simulation built offers an accurate representation of a process industry, considering various performance-affecting factors, making it highly relevant to actual industry workings.

2 Literature Review

The relevant articles in the research area are identified from the Scopus database using the keywords "Supply Chain Disruptions," "Supply Chain Resilience," "Supply Chain Risk," and "Food Supply Chain." The systematic methodology followed to determine the relevant research articles is shown in Fig. 1.

Additional refinement with keywords such as "Supply Chain Management," "Supply Chain Optimization," "Simulation Modeling and Analysis," and "Processing Industry" narrowed down the selection to 1,574 articles. Subsequent exclusion of COVID-19- related articles and a focus on engineering further refined the pool to 470 papers, ensuring a targeted selection for the literature review.

The production frequency graph of the research articles is shown Fig. 2 which illustrates trends in the number of articles produced over the past few years. This

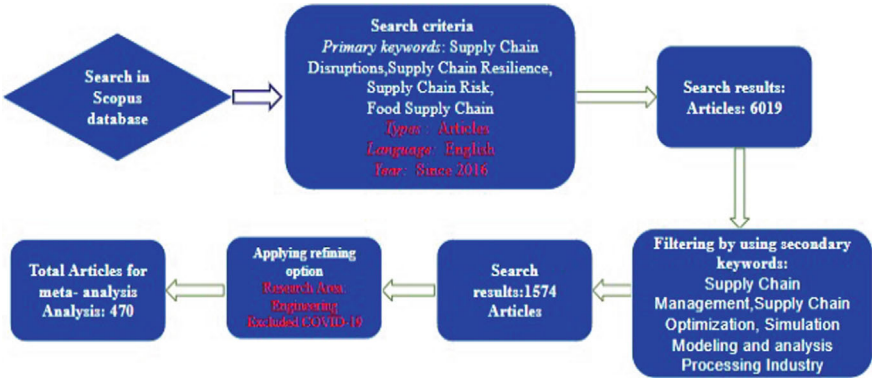


Fig. 1 Flow chart of methodology of literature review

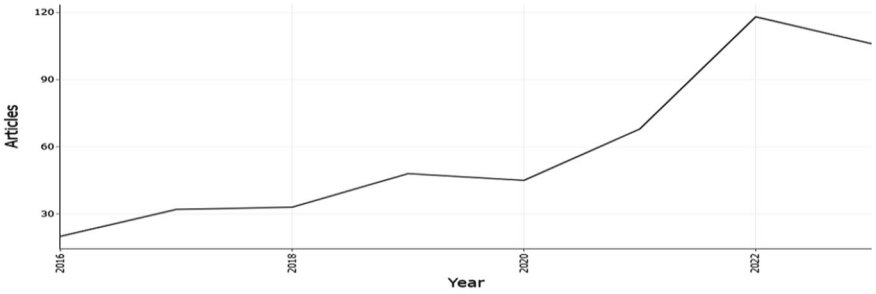


Fig. 2 Articles published over the years 2016–2023. (Image Source: Bibliometric analysis by Biblioshiny software)

graph offers a clear visualization of how article production has evolved over time. There has been a drastic increase in production over the last three years.

Rottenegger et al. [1] examined the bullwhip effect's implications in supply chains, particularly its connection to food waste, utilizing a simplistic model showcasing the potential of Tecnomatix Plant simulation. Badakhshan and Ball [2] aimed to enhance supply chain performance amidst disruptions, offering insights into simulation usage. Logistics feasibility assessment via computer simulation is discussed in [3]. Guo et al. [4] investigated port congestion alleviation through simulation models, highlighting their efficacy in addressing congestion challenges. Resilience strategy impact on supply chain performance is explored in [5], utilizing simulations to test various strategies. Sirisomboonsuk and Burns [6] focused on supply chain sustainability, employing bottleneck simulations and risk-related measures to minimize disruptions. Suryania et al. [7] developed a dynamic model to predict commodity shortages, considering uncertainties like climate change and demand fluctuations.

Collectively, these studies underscore the benefits of simulation modeling in tackling diverse supply chain challenges. Although scalability concerns and simplifications exist, Chen et al. [8] developed a model and algorithm to address disruptions in manufacturing supply chains. Minor production disruptions were studied in [9], focusing on daily output and disruption duration, illustrated through a vehicle manufacturer example, highlighting the broad implications for various industries. Musavi and Bozorgi [10] focused on enhancing efficiency in perishable food supply chains using smart solutions to reduce transportation costs and enhance resilience, which is crucial for managing perishable goods. Badejo and Ierapetritou [11] utilized mathematical programming to guide supply chain decisions during disruptions, weighing both effective and responsive strategies, and providing valuable insights for effective disruption management by decision-makers.

3 Methodology

Beginning by gaining a comprehensive understanding of the processes within the process industry, this involves conducting research, possibly through site visits or interviews with experts, to gather detailed knowledge about how the industry operates. Diving deeper into the specifics of the industry's processes, steps followed in the study are depicted in Fig. 3.

In the production or operational stage, thorough examination involves scrutinizing steps, equipment, materials, and variables, with detailed process flow diagrams and data being pivotal. Utilizing ARENA software, a virtual model is crafted to mirror real- world industry processes, with a focus on defining entities, resources, activities, and their interactions. The simulation aims to closely resemble the actual industry, depicting parts, their functions, and environmental conditions. The aim is to construct a digital twin. Validation is crucial, comparing simulated results with real-world data to ensure accuracy and reliability. Adjustments are made based on validation outcomes, refining parameters, and improving model accuracy to align with industry performance. Regular updates are essential to reflect industry changes, maintaining the model's relevance for decision-making and process enhancement. This research proposes a unique approach to process industry modeling. A power disruptions

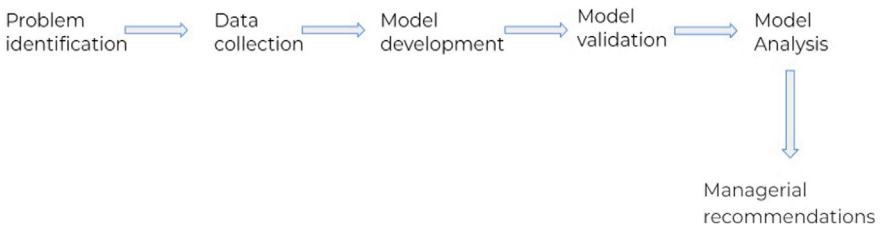


Fig. 3 Steps followed in study

module has been incorporated into the model; a feature not commonly found in traditional models. This allows to simulate and study the impact of power disruptions, enhancing the resilience of the process industry in today's volatile business environment.

4 Simulation Model

The model was constructed with basic and advanced processes in ARENA simulation based on information about the operations in the process industry. The operations involved are described in Table 1. The model is designed to analyze 100 kg of tender jackfruit batched into 8-kg baskets each. Then, at the packaging area, each box contains 3 packs of 1 kg of jackfruit. The model indicates 2:17:13 indicating time in hrs:min:sec for the operations to complete for the whole 100 kg of tender jackfruit. Also, before jackfruit reaches the washing area, the poor-quality fruits are disposed of in the waste room, as can be observed in Fig. 4.

Table 1 Process details for product—tender jackfruit

Sl. No	Process	Description	Workers engaged	Time taken for process minutes
1	Clean and weigh	Collecting 100 kg of tender jackfruit from stacks of stores and bringing it to the wash area. After washing, weigh 8 kg of batches each and transfer them to the cutting area	4	300
2	Cutting	Cutting fruits into small pieces using shear cutter	1	50
3	Skin removal	Then these pieces go to Table 1 for skin and waste removal	4	180
4	Fine cutting	The fine pieces went to Table 2 for slicing into the required size	3	100
5	Blanching	Dipping sliced items in hot water (Steam jet) and holding for minutes using special type containers	2	144
6	Dip in brine	Transfer the blanched batch of fruit slices into a container filled with brine solution and wait for a few minutes	2	100
7	Packing	Long table and a pack sealing machine that is used to seal two packets at a time. Each pack is 1 kg	6	305.2
8	Retort	Complete automation process. All the batches are waiting here for loading in the retort machine (sterilizing)	3	76
9	Pack in box cart	Three packets are inserted in one box. A total of 71 packets requires 27 boxes	2	81

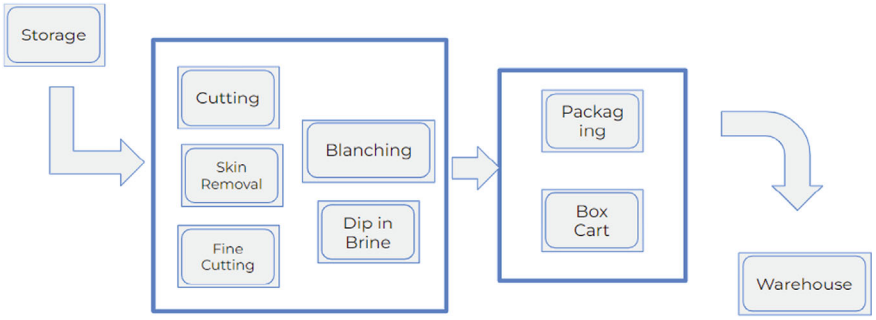


Fig. 4 Process flow diagram: Storage > > Processing Unit > > Packaging Unit > > Warehouse

4.1 Power Disruption Module

A disruption module is developed that behaves as a power house. If jackfruit enters through the power cut module, it holds at the section where there is a power requirement. Rather, if it goes through the power return module (which is a signal that power is back on), all the batches holding at the respective sections start moving forward. (Note: All the items are kept in the warehouse for a 5 days' quarantine period before dispatch.)

The screenshot of the simulation model of process industry developed using the ARENA is shown in Fig. 5.

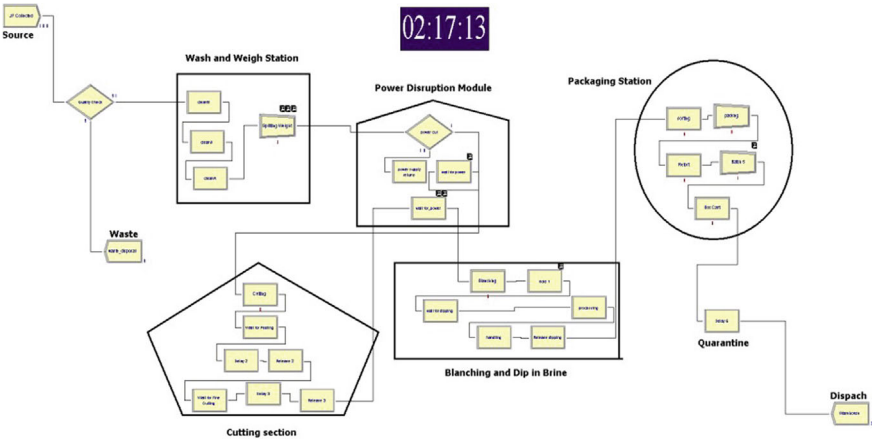


Fig. 5 Screenshot of Simulation model developed using ARENA

5 Results and Discussion

The reports from ARENA gave us information about the time distribution, waiting time, and time utilization of all the workers at each section. These results help us understand the problems with the current scenario and make improvements to the model.

It is well evident that waiting time has covered a good amount of total time. To look into this further, we have taken waiting times at each module in the model and plotted them as shown in Fig. 6. Now, apparently the waiting time is longer in the washing and packaging areas. This can also be identified from Fig. 7, which shows the time utilization of all the workers at each module in the module. Time utilization refers to the ratio of busy resources to all the available resources.



Fig. 6 Time taken for each module to process all batched Jackfruit in hours

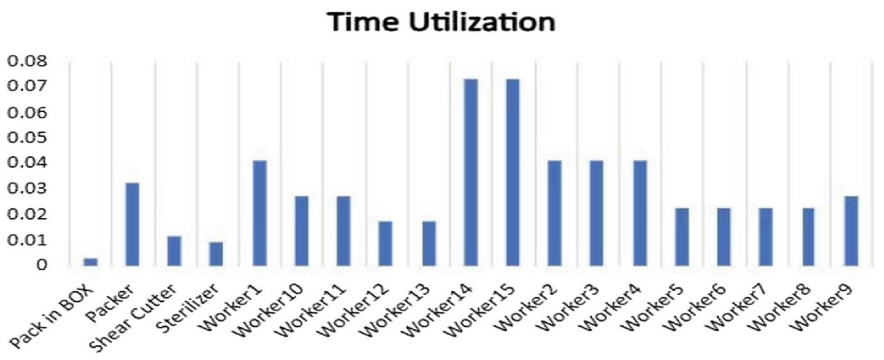


Fig. 7 Fractions of total time divided among workers in process Industry

5.1 Recommendations

Based on the findings of this study, to troubleshoot the wastage of time and manage time utilization, some managerial recommendations are as follows:

- Application of 5S tools (sort, set in order, shine, standardize, and sustain) and other lean manufacturing concepts to keep workspaces clean and reduce waste.
- Use Just-In-Time (JIT) inventory systems to cut down on extra inventory that could cause delays in service.
- Train employees to help them learn new things and get better at what they already know. Skilled workers can get things done faster, which cuts down on wait times.
- Cross-training employees so they can do more than one thing. This will help you assign jobs more efficiently when you are busy.
- Kaizen (constant effort)
- Create an environment where employees are actively seeking out and implementing ways to enhance efficiency and cut down on wait times.

6 Conclusion

In this study, a simulation model of the process industry was developed and analyzed using ARENA software. A tender jackfruit processing company was selected for the study, and the simulation model was developed based on the process information from the company. A power disruption module was incorporated into the simulation model to test the behavior of the model under disruptions. The distribution of the total time taken for different processes, waiting time at each workstation, and worker utilization are analyzed. Managerial recommendations are derived from the results to reduce the impact of disruption.

This work explored the impact of power disruptions in the supply chain of a food processing firm in the Agro-based sector. It helps them understand and plan for power disruptions making their operations more resilient and efficient. This model is suitable for all processing industries where there is a possibility of power supply disruptions.

The study can be extended by considering more scenarios and analyzing each attribute (workers, time, input frequency, number of batches) and its impact on the whole output of the industry. Calculation of revenue loss and making the most possible recommendations in terms of the capabilities of the industry to implement them is also a prominent research direction.

Acknowledgements We express our sincere gratitude to the National Institute of Technology Calicut for their financial support in this research.

Author Contributions Conceptualization: Abhiram B, Madineni Bhavana, Vani Amrutha Mutyala, Veedhi Shyam Nishanth and Arun Thomas; Literature Review: Vani Amrutha Mutyala and Arun Thomas; Methodology: Madineni Bhavana and Arun Thomas; Model preparation: Abhiram

B, Veedhi Shyam Nishanth; Validation and Verification of the model: Veedhi Shyam Nishanth, Rathnakaran T.; Results analysis: Abhiram B. and Rathnakaran T.; Writing—original draft preparation: Madineni Bhavana, Vani Amrutha Mutyala, and Veedhi Shyam Nishanth; Writing—review and editing: Arun Thomas and Vinay V. Panicker; Visualization: Veedhi Shyam Nishanth; Supervision: Vinay V. Panicker. All authors have read and agreed to the published version of the manuscript.

Funding The APC was funded by National Institute of Technology, Calicut.

Data Availability Statement The authors confirm that the data supporting the findings of this study are available within the article.

Conflicts of Interest The authors declare no conflict of interest. The funders had no role in the design of the study; in the collection, analyses, or interpretation of data; in the writing of the manuscript; or in the decision to publish the results.

References

1. Rottenegger D, Öfele M, Braun HM, Braunreuther S (2023) Bullwhip effect: modelling and simulation of a sinusoidal stimulus considering food waste. J Transp Supply Chain Manage 17:1–14
2. Badakhshan E, Ball P (2023) Deploying hybrid modelling to support the development of a digital twin for supply chain master planning under disruptions. Int J Prod Res, pp 1–32
3. Strnad D, Fedorko G, Molnár V, Fialek P (2021) Simulations as an assessment tool for the feasibility of logistics innovations motivated by the emergence of supply chain risk. Adv Sci Technol Res J 15(3)
4. Guo S, Wang H, Wang S (2023) Network disruptions and ripple effects: queueing model, simulation, and data analysis of port congestion. J Marine Sci Eng 11(9):1745
5. Namdar J, Blackhurst J, Azadegan A (2022) On synergistic effects of resilience strategies: developing a layered defense approach. Int J Prod Res 60(2):661–685
6. Sirisomboonsuk P, Burns J (2023) Sustainability in supply chains through rapid capacity increases and minimized disruptions. Sustainability 15(7):5629
7. Suryania E, Hendrawana RA, Muhandhisa I, Dewib LP (2016) Dynamic simulation model of beef supply chain to fulfill national demand. J Teknol 78(9):169–177
8. Chen J, Kang H, Wang H (2023) A product-design-change-based recovery control algorithm for supply chain disruption problem. Electronics 12(12):2552
9. Wu M, Holguin VJ (2022) The impacts of minor disruptions on a production system: Empirical analysis of assembly line data. In: Production planning con trol, pp 1–15
10. Musavi M, Bozorgi-Amiri A (2017) A multi-objective sustainable hub location-scheduling problem for perishable food supply chain. Comput Industr Eng 113:766–778
11. Badejo O, Ierapetritou M (2022) Mathematical programming approach to optimize tactical and operational supply chain decisions under disruptions. Indust Eng Chem Res 61(45):16747–16763

Integrating Hand Gesture Tracking with Physical and Digital Twins of Robotic Arm



Ojas Jain and Krishnaiah Jallu

Abstract Human–robot collaboration has become very important in the industrial areas including the manufacturing domain, as the fixed programming of robot activities is becoming outdated. The main reason for expecting collaboration between humans and robots is due to the dynamic nature of the tasks occurring besides its preprogrammed tasks. However, traditional industrial robots that are controlled by preprogrammed control codes are rigid and they cannot support the emerging needs of human–robot collaboration. To address this, in recent years, many ways of collaboration and communication between humans and robots have been evolving. In this article, two methods, i.e., motion sensor-based hand tracking IR-based sensors and computer vision-based hand tacking are implemented and analyzed in detail for their performance and accuracy.

Keywords IR sensor · Computer vision · Robotic arm · Digital twin

1 Introduction

In recent years, robotic technology has made considerable strides and has integrated itself into a wide range of businesses. Due to their capacity to do repetitive tasks rapidly and correctly, robotic arms are now often used in manufacturing, agriculture, healthcare, and other industries. However, most of the robots are preprogramed to perform certain task, which is getting outdated in today's world where dynamic tasks are in demand. Traditional industrial robots are controlled by preprogrammed control codes that are rigid and cannot support the emerging needs of human–robot collaboration (HRC).

O. Jain · K. Jallu (✉)
IIITDM Kurnool, Kurnool, India
e-mail: krishnaiah@iiitk.ac.in

O. Jain
e-mail: Ojas24012002jain@gmail.com

© The Author(s), under exclusive license to Springer Nature Singapore Pte Ltd. 2025

B. B. V. L. Deepak et al. (eds.), *Recent Advancements in Product Design and Manufacturing Systems*, Lecture Notes in Mechanical Engineering,
https://doi.org/10.1007/978-981-97-6732-8_17

Parallelly, the remote operation of robots has become increasingly popular in various industries due to its efficiency, cost-effectiveness, and safety benefits. The ability to control a robot from a remote location has revolutionized the way tasks are performed. One of the main advantages of remote robot operation is the increased safety it offers, particularly in hazardous or difficult-to-reach environments. In such settings, it is often unsafe for human workers to perform tasks, and the use of robots has become essential to minimize the risks of accidents or injuries. With remote operation, operators can control robots from a safe distance, minimizing the risk of harm. Remote operation of robots has also opened opportunities for telecommuting, reducing travel costs and carbon emissions, and enabling remote access to experts who can oversee operations from afar. Alongside remote operations, collaborative operations between human and robots also have increasing importance in recent times.

One of the ways of HRC is to control it via natural human movements like hand gestures. There are multiple ways of sensing and tracking the hand gestures and performing various activities. Few prominent ones are by using a hand gesture tracking sensors and computer vision recognition. Users may interact with robotic arms in a more natural way because of these sensors and computer vision technology, which can recognize and understand the movements of the human hand. We may design a more logical and user-friendly interface by merging hand gesture tracking sensors with the physical and digital counterpart of the robotic arm. This will provide an interface which will be used to provide dynamic commands to the robotic arm and will also provide constant feedback for better decision making via digital twin.

The goal of this project is to integrate hand gesture tracking sensor and computer vision-based controller with the physical and digital twin of a robotic arm. This will allow users to control the robotic arm using hand gestures, making it easier to perform tasks that require precision and accuracy. The integration of the hand gesture tracking will enable the robotic arm to respond to the user's movements in real time, resulting in a more intuitive and interactive experience.

Although it has been investigated in the past, the integration of hand gesture monitoring with robotic arms is still a relatively new field of study. By creating several systems that can capture hand gestures, interpret them to operate a robotic arm, and analyze their similarity and difference across many dimensions, this project seeks to make a contribution to this field of study. Consider them from a variety of angles and viewpoints.

As part of the project, a software framework is created to collect hand-tracking data from both gesture sensors and computer vision, process it to extract the necessary data, and then translate it into G-code, i.e., CNC machine language code to drive the robotic arm by passing appropriate coordinate position. To provide the user with visual feedback, the software also shows the digital twin of the robotic arm in real-time with appropriate motion involved in the hand gesture.

The project is carried out in multiple stages. Researching and choosing a suitable and workable hand gesture tracking technique is performed in the first phase. A framework based on C# and Unity is developed that integrates hand gestures through hand-tracking sensors and computer vision with the physical twin and digital twin

of the robotic arm. In the subsequent stage, a distant site is connected using socket connectivity to control the robotic arm. The system is synchronized, tested, and validated in the final step to make sure it functions as planned.

In conclusion, the combination of hand gesture monitoring with the actual and virtual twins of robotic arms has the potential to completely change how we engage with these devices by providing a way to control the robots dynamically and in a more human-friendly manner. The goal of this project is to further this field of study by creating a system that can precisely track hand movements and manage a robotic arm in real time.

The resultant approach will make controlling robotic arms simpler and more intuitive, opening new opportunities for their application in many sectors.

The best use cases are listed below:

- Remote operations in hazardous environments.
- Remote surgical operations in the medical domain.
- In an industrial environment where collaboration between human and collaborative robots is essential.

2 Literature Review

By conducting a critical analysis of previous research studies, this literature review aims to make a significant contribution to the existing body of knowledge. It will help in providing a comprehensive understanding of the current state of research in the field of human–computer interaction. Moreover, it will provide a foundation for the study's methodology, guiding the selection of research methods, and data collection techniques.

Yu et al. [1] have investigated the domestic and overseas development status and trends in mechanical arms and remote control, as well as analyzed the issues of remote control of the robot arm, such as distance, latency, a high degree of freedom, and difficulty in controlling. Setting up the remote installation of the KUKA mechanical arm, supporting sensors, and the robot hardware platform, as well as conducting remote operation experiments from any location and at any time via the server/client model. Creating the trajectory on the simulation system, previewing the simulation results, checking the execution effect, and running the KUKA manipulator.

Chung et al. [2] suggested a way called RoSTAR to lessen restrictions like high cost and un-intuitive interface. RoSTAR is a revolutionary open-source HRI system that combines Robot Operating System (ROS) and augmented reality. It allows for user interaction and communication using a robotic arm driven by ROS. The developed model of the robot arm is directly imported into the Unity Game engine and all interactions with this virtual robotic arm are transmitted to the ROS robotic arm. It is demonstrated that their developed technology has the potential to be used for a variety of process operations, such as robotic welding, dispensing, and gluing, as part of a portable, low-cost, interoperable environment.

Duan et al. [3] have developed HRC framework for intelligent assembly systems and experimented with multimodal gesture control instead of only depending on one method of gesture recognition and control. Their experiments are evident that the HRC framework for the intelligent assembly system with multimodal gesture control has realized the human–robot collaborative assembly with the integrally shrouded blade and improved the intelligence of the assembly process.

Similarly, Raheja et al. [4] have described a method for commanding a robotic hand or an individual robot by displaying hand movements in front of a camera. With the help of this technology, a hand gesture in the viewing range of a robot can be posed, and the required action is accomplished by the robotic system. For computer vision, a simple video camera is utilized, which aids in the monitoring of gesture presentation.

Further, the gesture control without camera is demonstrated by Gadalla and team in their research article [5] on the design and implementation of a "Wireless Gesture Controlled Robotic Arm with Vision." Their system design is broken down into three components: the platform, the robot arm, and the accelerometer element. In essence, it is an accelerometer-based system that uses RF signals to wirelessly control a robotic arm with a small, inexpensive 3-axis accelerometer. The Mobile Platform, which is also wirelessly controlled by another accelerometer, is mounted over the Robotic Arm.

Khajone et al. [6], in their research paper, propose an idea and a method to replace buttons and joysticks with a more natural strategy, namely commanding the entire Robotic Arm with the operator's hand gesture. The suggested electronics system recognizes a certain hand gesture made in front of a webcam and wirelessly transmits the corresponding signals via an RF module. The robotic arm, which is controlled by an AVR microcontroller, conducts receptive motions at the receiver portion based on the received signals.

Nair et al. [7] have examined various robotic arm system designs that allow for joint position control by the user with the aim to review current applications and identify promising regions for further study and development. They have studied several types of controls including IoT-based control, smartphone applications, and external hardware modules. The prospective advantages and disadvantages of the various approaches have been compared and listed.

Afzal and Waseem [8] have proposed a robotic arm with gesture control that uses a flex sensor. The robotic arm is designed to mimic human hand movements using a hand glove. Five flex sensors are used in the hand glove to regulate finger movements, and an accelerometer is used to control wrist and elbow movements. Utilizing cables that mimic the tendons in an arm, the finger movements are managed. Using a wireless module, the robotic arm is operated from a distance. They have also built a robotic arm prototype and put it to the test for various hand motions.

Ganesh and Chethan [9] have provided a method for a completely electrical (i.e., devoid of mechanical sensors) human–computer interface. The objective of their study was to replace the outdated methods of manipulating robotic arms with joysticks and buttons with more natural methods, such as using hand motions or gestures.

Dheeban et al. [10] in their paper the gesture-controlled robot with a robotic arm that can carry out any pick-and-place activities via radio frequency transmission is discussed. The Robotic Hand contains specific independent commands for gripper open and close, up and down, forward and backward, base clockwise and counter-clockwise. The displacement of the robotic arm on the chassis is supported by four Omni wheels. Four degrees of freedom are available on the deployed robotic arm. This robot can include additional features like a metal detector, line follower, wall hugger, obstacle avoidance, and more to expand its usefulness.

Artal-Sevil and Montañés [11], in their research paper, discussed how a robotic arm moves and does the task based on human hand gestures, and mimics human hand activities. The arm is adaptable and can be used in environments where humans are not safe, such as the fireworks production business or bomb disposal. Several methods for manipulating the robotic arm were discussed in the article. This work is about using accelerometer-based gesture detection to control the movements of a robotic arm via wireless control using the ZigBee protocol.

3 Problem Definition and Plan of Action

The problem definition and plan of action is stated in this section for both IR sensor-based gesture sensor and computer vision gesture recognition methods that are implemented as part of this work.

3.1 Problem Statement

Build a framework to control the digital and physical twin of the Robotic Arm to do dynamic tasks with hand gestures from a remote location using the gesture sensor and/or computer vision.

3.2 Objective

The aim of the current work is to make a 3D Model of Robotic Arm and then integrate this digital model with the physical Robotic Arm and control with two different hand gesture recognition systems, namely using through IR sensor and Camera by using computer vision. To achieve this, a framework is designed and developed in C# with Unity-based visualization, which will provide an interface to the operator and will recognize hand gestures and control both the digital and physical twin of the robotic arm.

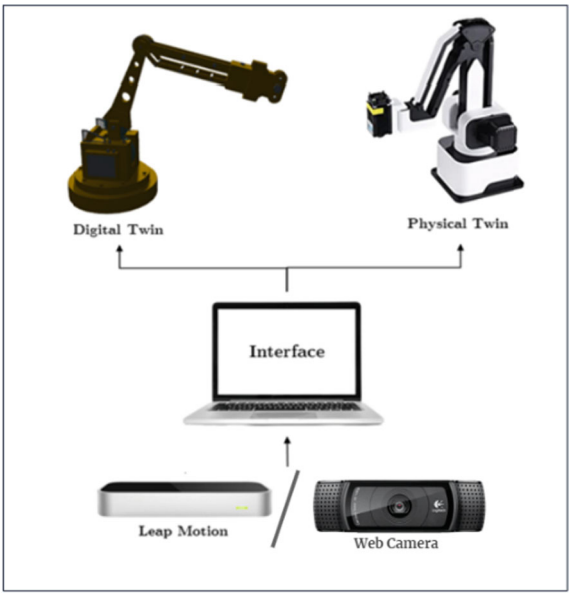


Fig. 1 Design of interface for integration of gesture sensor with digital and physical twin of Robotic Arm

3.3 Architecture

The architecture of the whole framework which is depicted in Fig. 1 is as follows: first the hand gestures and its movements are detected using a motion sensor and computer vision, then these data are sent to the interface that is created using Unity, this interface extracts the required information from the provided data. This extracted information is then formatted and passed through certain checks and then converted to CNC machine code, i.e., G-code. This G-code is sent to the physical twin which results in its movements and motions. This interface constantly gets the hand position in the 3D space, generates the G-code, and sends it to the robotic arm that moves it to that position in physical space. This interface also calculates the angles that are required by the digital twin of the robotic arm to move to the required positions and sends these angles to the digital twin which moves the end effector to the required position.

In this work, both gesture control sensors and computer vision-based methods of gesture recognition and control are explored. Details are discussed in the following sections.

3.4 Implementation Details

Detailed steps in the process flow are shown in Fig. 3. The description of the steps is listed in the following steps:

i. Detect the gestures and motion of the human hand. There are multiple ways for hand gesture detection, two of the ways which are used presently in this work are as follows:
   (a) Using hand tracking and gesture sensors like leap motion, which illuminates the hand with infrared light to get the data. It returns various key points such as palm, thumb end, and wrist for each detected hand.
   (b) Machine learning algorithms to detect the hand skeleton and gestures. A real-time Hand Gesture Recognizer to be made using the MediaPipe framework and Tensorflow in OpenCV and Python. One sample hand gesture is shown Fig. 2.

ii. Send the hand-tracking data to the framework created.
iii. Convert the hand gestures and motion data to G-code.
iv. Set up the serial port communication between the robotic arm and framework.
v. Send the G-code to the robotic arm.

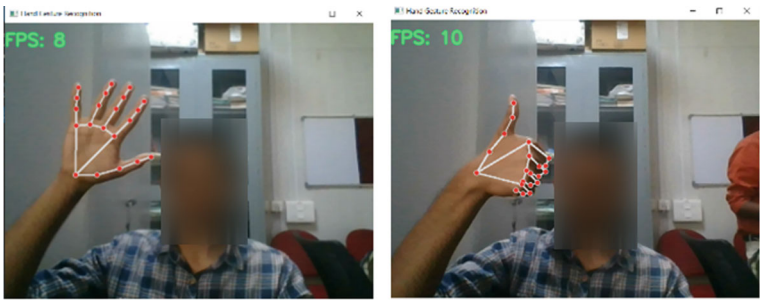


Fig. 2 Hand gestures recognized through computer vision

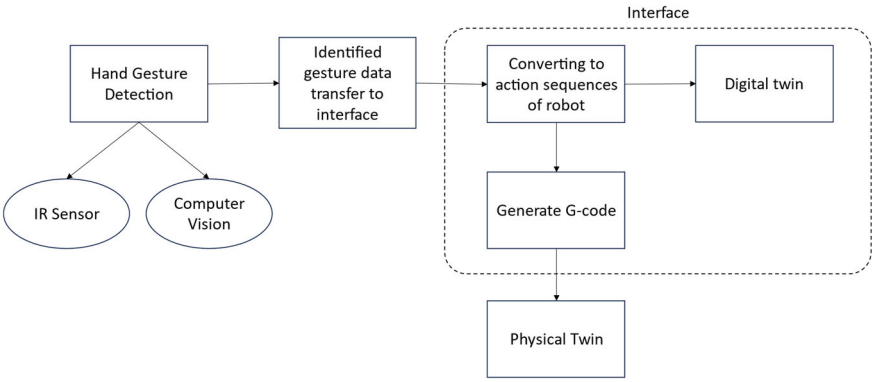


Fig. 3 Detailed process flow of both methods, i.e., IR-based sensor and computer vision

4 Gesture Control Using IR-Based Sensors

The usage of gesture control technology in a variety of devices has seen a phenomenal surge in recent years, enabling a means to communicate with machines that are both convenient and effective. As a result of its low cost and great accuracy, infrared (IR)-based gesture sensors have become one of the most common approaches for deploying technology that enables users to control devices by gesturing. These gesture sensor technologies enable users to interact with devices by merely waving their hands or fingers in front of the sensor. This eliminates the requirement for users to make direct physical contact with the device to perform an action. This technology has the potential to be utilized in a broad variety of fields, including robots, intelligent home automation, and gaming consoles. In this project report, it is investigated that the creation and implementation of control utilizing IR gesture sensors. This will include the design of the hardware and software components, as well as the evaluation of the performance of the system.

The controller is an optical hand-tracking module that captures your hand movements with unrivaled accuracy. The Leap Motion Controller enables engagement with digital content natural and intuitive, from XR to touchless kiosks. It can measure depths ranging from 10 to 60 cm, with a maximum depth of 80 cm and has a standard field of vision of $140 \times 120°$.

Hands are illuminated by IR light from the LEDs. In time with the camera's frame rate, the Lights pulse. The cameras send information to the computer to track your hands each time they perform this. The photos are used by the software of UltraLeap to create a virtual representation of your hand movements. Together with the fingers and palm, UltraLeap also simulates the hand's joints and bones. This means that even if a finger or thumb is concealed from view, we can still anticipate its location with accuracy.

5 Gesture Control Using Computer Vision

Computer vision is a rapidly growing field of computer science that deals with the automated extraction of information from images and videos. The main goal of computer vision is to enable machines to interpret and understand the visual world around them, much in the same way humans do. The field has become increasingly important in recent years, with applications ranging from facial recognition and autonomous driving to medical imaging and augmented reality. The key components of computer vision include image acquisition, image processing, and pattern recognition using machine learning or deep learning. These components work together to enable machines to identify and categorize objects in images, track movement, and recognize patterns and textures. Advancements in computer vision are opening

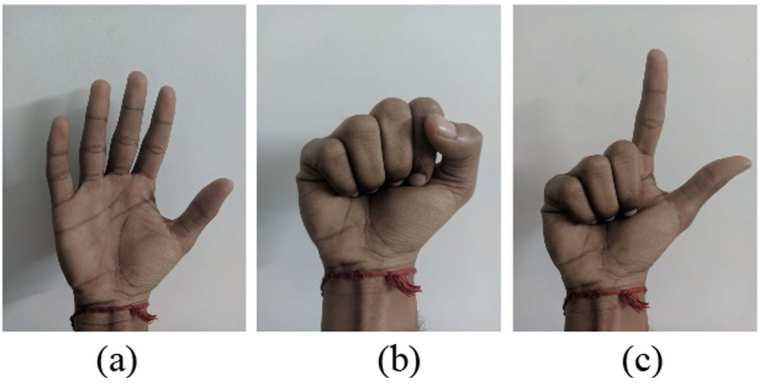


Fig. 4 Three types of gesture visual that are used for performing tasks by the robot. **a** Open palm: hand movements to control the movements for robotic arm. **b** Closed fist: used for Pickup. Starts sucking air from the rubber gripper, which mimics the action of holding. **c** Thumb and first finger open: used for release. Starts releasing air from the rubber gripper, which mimics the action of releasing

exciting new possibilities in fields such as robotics, automation, and digital entertainment. In this work, the MediaPipe, an API of Python for hand gesture recognition, is used which uses deep learning algorithms (Fig. 3).

Figures 4a, b show the three different gesture that are used for human–robot interaction through which certain predefined tasks are achieved. As shown Fig. 4a, the open palm used to control the movements of robotic arm. On recognition of open palm, controller recognizes and tracks the hand and accordingly the movement of the robot is achieved. Figure 4b shows the Closed Fist, which is meant for starts sucking air from the rubber gripper and picking the targeted object by mimicking the action of holding. Similarly, Fig. 4c shows the Thumb and First finger open indicating release.

6 Conclusions

Remote operation of robots has become increasingly popular in various industries due to its efficiency, cost-effectiveness, and safety benefits. The ability to control a robot from a remote location has revolutionized the way tasks are performed. One of the main advantages of remote robot operation is the increased safety it offers, particularly in hazardous or difficult-to-reach environments. In such settings, it is often unsafe for human workers to perform tasks, and the use of robots has become essential to minimize the risks of accidents or injuries. With remote operation, operators can control robots from a safe distance, minimizing the risk of harm. Remote operation of robots has also opened opportunities for telecommuting, reducing travel costs and carbon emissions, and enabling remote access to experts who can oversee operations from afar (Fig. 5).

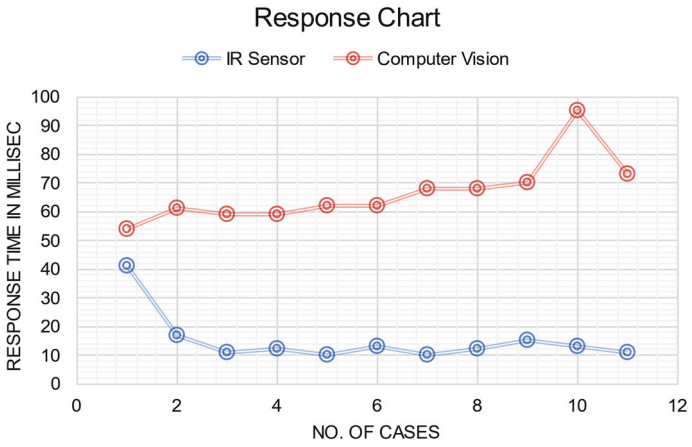


Fig. 5 Comparison of response in detecting the gestures by two methods

References

1. Yu H, Chou W, Dong H, Wang Z (2019) The research of mechanical arm on remote operation system. IOP Conf Ser: Mater Sci Eng 493:012054. https://doi.org/10.1088/1757-899X/493/1/012054
2. Chung S, Murray N, Qiao Y, Henry J, Mcnevin K (2020) RoSTAR: ROS-based telerobotic control via augmented reality. https://doi.org/10.1109/MMSP48831.2020.9287100
3. Duan J, Fang Y, Zhang Q et al (2023) HRC of intelligent assembly system based on multimodal gesture control. Int J Adv Manuf Technol 127:4307–4319. https://doi.org/10.1007/s00170-023-11804-4
4. Raheja JL, Shyam R, Kumar U, Prasad PB (2010) Real-time robotic hand control using hand gestures. In: 2010 second international conference on machine learning and computing, Bangalore, India, pp 12–16. https://doi.org/10.1109/ICMLC.2010.12
5. Gadalla A, Balakrishnan A, Abdulla R (2019) Design and implementation of a wirless gesture controlled robotic arm with vision 86
6. Khajone S, Mohod DR, Harne VM (2015) Implementation of a wireless gesture controlled robotic arm. Int J Innov Res Comput Commun Eng 03:375–379. https://doi.org/10.15680/ijircce.2015.0301031
7. Nair RS, Kumar S, Soumya N, Shanmugasundaram M (2018) A study on gesture controlled robotic arms and their various implementations. Int J Mech Eng Technol 9:425–434
8. Afzal W (2017) Gesture control robotic arm using flex sensor. Appl Comput Math 6:171. https://doi.org/10.11648/j.acm.20170604.12
9. Ganesh Choudhary B, Chethan Ram BV (2014) Real time robotic arm control using hand gestures. In: 2014 international conference on high performance computing and applications (ICHPCA), Bhubaneswar, India, pp 1–3. https://doi.org/10.1109/ICHPCA.2014.7045349
10. Dheeban SS, Dhanasekaran Velayutha Rajan H, Hari A, Marimuthu P, Senthil Kumar N (2016) Gesture Controlled Robotic Arm
11. Artal-Sevil JS, Montañés JL (2016) Development of a robotic arm and implementation of a control strategy for gesture recognition through leap motion device. In: 2016 technologies applied to electronics teaching (TAEE), Seville, Spain, pp 1–9. https://doi.org/10.1109/TAEE.2016.7528373

Performance Enhancement of Pump Parameters Through Innovative Spring Design of Mechanical Seal for a Heat Exchanger

I. Ramu, G. Suresh Bau, N. V. V. Manikanta, and M. Venu

Abstract The present work focuses on optimizing pump performance parameters in heat exchangers by introducing an innovative spring design within mechanical seals. Mechanical seals are crucial components in ensuring fluid containment and system integrity. However, existing seals often struggle with consistent performance, resulting in leakages and reduced pump efficiency. To address these challenges, a novel spring design leveraging modern materials and engineering techniques is proposed. The research methodology involves a comprehensive analysis of current mechanical seals and pump systems to identify areas for improvement. A new spring design is then conceptualized, modeled, and simulated using finite element analysis (FEA) to evaluate its mechanical characteristics and stress distribution. Rigorous testing under simulated and real-world conditions validates the design's effectiveness in enhancing seal reliability and minimizing leakage. The expected outcomes include significant advancements in sealing efficiency, leading to improved overall heat exchanger performance, energy conservation, and extended equipment lifespan. By optimizing pump parameters and minimizing leakage, this innovation promises enhanced system efficiency and cost savings in industrial applications. This research offers a pathway to address the limitations of traditional mechanical seals in heat exchanger pump systems. The proposed innovative spring design holds the potential to revolutionize pump performance, subsequently boosting the efficiency of heat exchange processes across various industries.

Keywords Mechanical seal · Spring design · Pump parameters · Heat exchanger

I. Ramu (✉) · G. Suresh Bau · N. V. V. Manikanta · M. Venu
Department of Mechanical Engineering, Vishnu Institute of Technology (A), Bhimavaram, Andhra Pradesh 534202, India
e-mail: ramu.i@vishnu.edu.in

© The Author(s), under exclusive license to Springer Nature Singapore Pte Ltd. 2025

B. B. V. L. Deepak et al. (eds.), *Recent Advancements in Product Design and Manufacturing Systems*, Lecture Notes in Mechanical Engineering,
https://doi.org/10.1007/978-981-97-6732-8_18

1 Introduction

Industrial equipment such as pumps relies heavily on mechanical seals [1] for fluid containment and leak prevention. Heat exchange systems depend directly on the performance of these seals to maximize efficiency [2], reduce maintenance costs, and reduce environmental impact. To improve mechanical seal design and functionality, continuous efforts are made in the field of mechanical engineering. In order to enhance the performance parameters of pumps used in heat exchangers, this research paper addresses the urgent need for innovation in mechanical seal design.

The mechanical seal, an essential component in pump systems, consists of several key elements, including stationary and rotating parts, a sealing face, and a spring mechanism. These seals are designed to prevent the leakage of fluids and to withstand the extreme conditions commonly found in heat exchange processes, such as high temperatures, aggressive chemicals, and variable pressures [3]. Mechanic seals have a direct impact on the pump's overall efficiency [4], as well as the heat exchange system's reliability.

Many studies have demonstrated the importance of mechanical seal performance in heat exchangers and related industrial processes. Mechanical seals play a critical role in reducing energy consumption and improving overall heat exchanger efficiency. It is evident from Smith and Johnson's [5] discussion that frictional losses and seal wear are significant challenges associated with pump systems [6], and that innovative solutions are essential in order to address them.

Despite many advances in mechanical seal design, there is still room for improvement, especially in the spring mechanism, which is crucial for maintaining alignment between rotating and stationary components. By improving mechanical seal efficiency, reducing maintenance costs, and increasing environmental sustainability, innovative spring designs [7–11] can help improve pump efficiency.

This research paper will explore novel spring designs for mechanical seals and their impact on pump parameters, such as flow rate, head, and energy consumption. Through comprehensive experimentation and analysis, we aim to develop and validate innovative spring designs that can revolutionize the efficiency and reliability of pump systems within heat exchangers. The critical issue of mechanical seal design in heat exchangers by introducing innovative spring designs to enhance pump parameters. By drawing on existing research and methodologies while focusing on experimentation and analysis, we aim to contribute to the ongoing efforts to optimize industrial processes, reduce energy consumption, and minimize environmental impact.

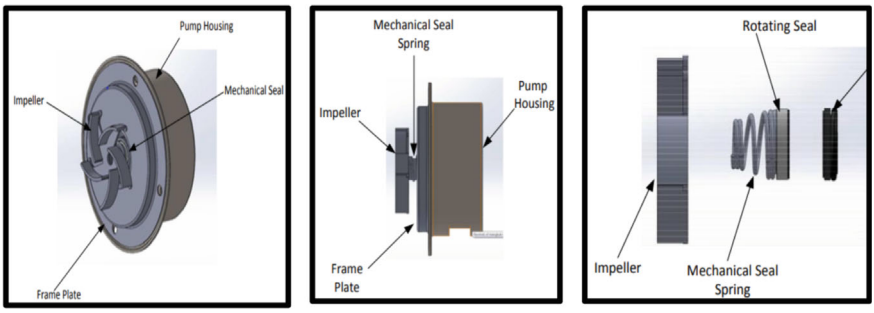


Fig. 1 Existing pump design

2 Materials and Methodology

2.1 Existing Design of Mechanical Seal

In the crystallization plant, we employ rotating machinery, i.e., Kombinator, which facilitates the crystallization of palm oil at extremely low temperatures, resulting in the formation of crystals within the scraper heat exchanger. To avert oil leakage, the scraper shaft is equipped with a mechanical seal. However, it is important to note that the external heating applied to the shaft seal is limited, as excessive temperatures would adversely affect the integrity of the oil crystals. Consequently, this temperature constraint can lead to occasional leakage of crystallized oil from the mechanical seal during production processes. The existing design of mechanical seal with different views is shown in Fig. 1.

2.2 Design of Spring with Enclosure

The new design concept involves enclosing the seal housing to create a barrier that prevents direct contact between the oil and the spring mechanism. This innovative approach aims to eliminate the occurrence of spring seizing, a common issue that arises when the spring comes into contact with oil that has hardened or crystallized within the mechanical seal. To validate this concept on a smaller scale, experimentation will be conducted using an Inoxpa Pump, a pump design that currently exposes the mechanical seal spring to the oil, potentially leading to spring breakdown. The new design of spring is shown in Fig. 2.

The new design involves encasing the lower portion of the spring within the same ceramic seal casing. However, utilizing the top enclosure to encase the spring could potentially limit its free movement. During the initial installation, the pump is expected to remain leak-free. However, we anticipate that after a few months of continuous pump operation, there may be wear and tear on the ceramic seal,

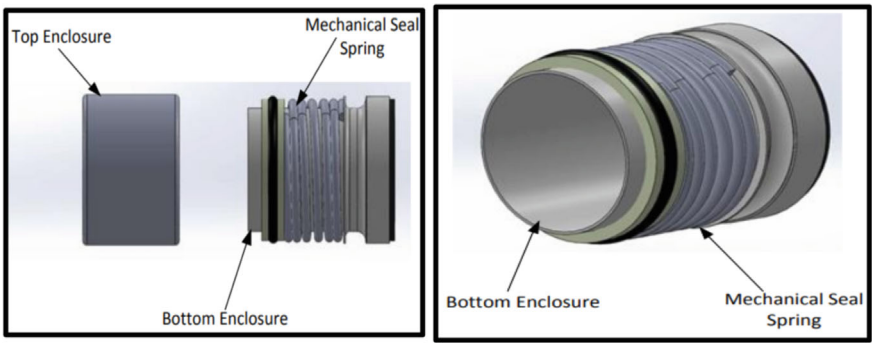


Fig. 2 Spring with enclosure

potentially impeding the spring's ability to exert sufficient force to maintain contact between the rotating ceramic component and the stationary seal.

2.3 Design of Spring with Housing

The design of spring with housing is shown in Fig. 3. Similar to design 1, design 2 comprises two primary components responsible for sealing the spring: a housing where the spring is positioned and a top enclosure that ensures external sealing. Both of these elements serve to encase the spring securely. Design 2 offers enhanced flexibility in achieving superior sealing performance and facilitates the straightforward installation of components within the seal housing. In this research work, we chose design 2 for manufacturing of mechanical seals.

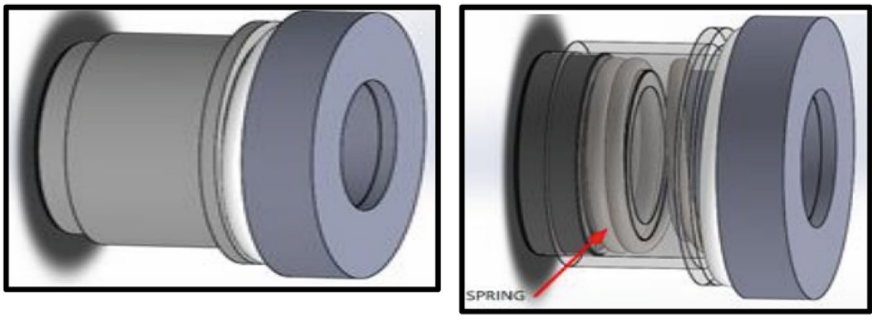


Fig. 3 Design of spring with housing

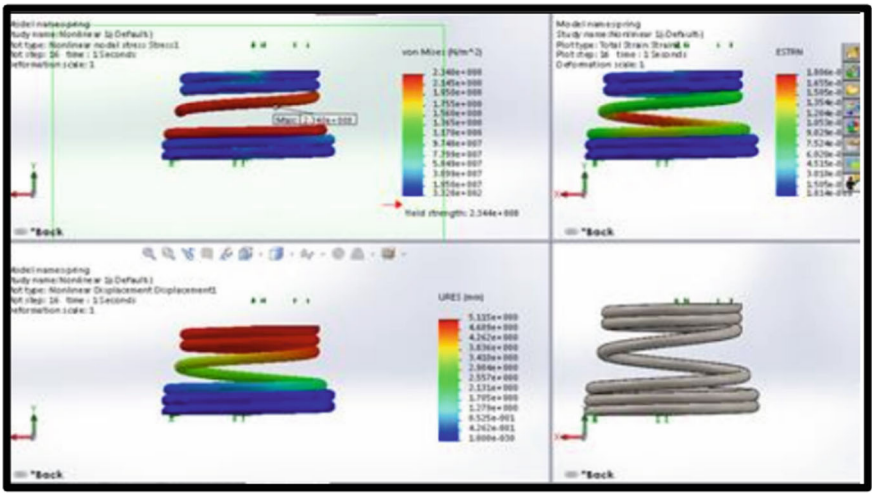


Fig. 4 Shear stress of spring

3 Results and Discussion

3.1 Simulation Results of New and Existing Mechanical Seal

3.1.1 Simulation Results of Existing Mechanical Seal

Stress analysis involves subjecting a tapered spring to compression, with the aim of comparing the resulting stresses to those in a straight spring, which we intend to use in our prototype. It is important to note that both the tapered and straight springs are constructed from stainless steel 304. To compress the ceramic seal jointly, a total displacement of 5 mm is required for both springs. At this 5 mm compression level, the maximum stress observed is 2×10 N/m^2 which is shown in Figs. 4 and 5.

3.2 Simulation Results of Prototype Mechanical Seal

The prototype spring experiences a maximum stress of $1.14 \times 10\text{^}8$ N/m^2 when subjected to deformation, a stress level that is lower than that observed in the original tapered spring is shown in Fig. 6.

During the simulation process, it was observed that the spring remained stable without any buckling.

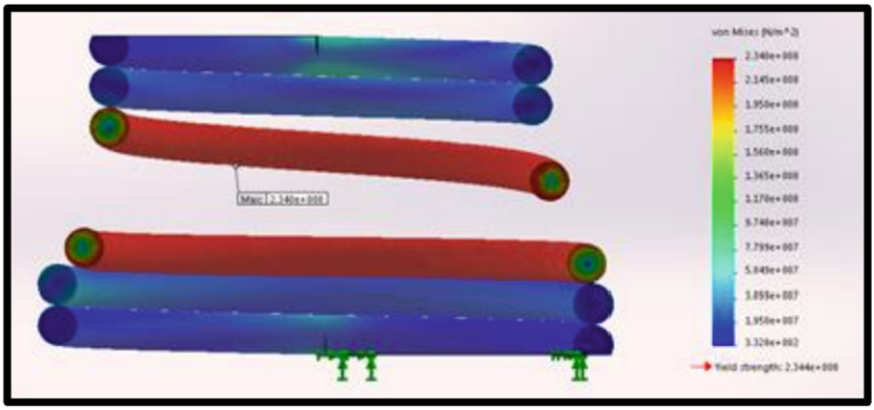


Fig. 5 Shear stress of modified design spring

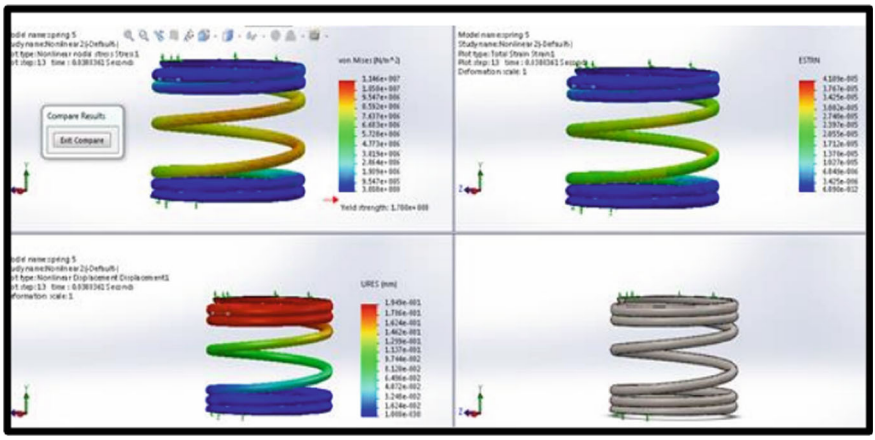


Fig. 6 Shear stress of new spring

3.3 Experimental Results of Existing Mechanical Seal and Designed Prototype Mechanical Sea

In this research, we are considering the pump operating parameters like motor current reading in Amp, temperature in °C, pump discharge pressure in bars, and vibration of pump in mm/sec. The experimental results of pump operating data with original mechanical seal and prototype of designed mechanical seal are given in Tables 1 and 2.

The motor current, motor temperature, pump discharge, and vibration of pump increases with increasing the running time. The pump motor current increases from

Table 1 Pump operating data taken with original mechanical seal and prototype mechanical seal

Measuring parameter	Time intervals	Readings	
		Original seal	Prototype seal
Motor current reading in Amp	Immediate after installation	2.5	2.2
	1 h after installation	2.8	2
	24 h or running	3.2	2
	50 h of running	3.7	2
	100 h of running	4	2
Motor temperature reading in ^{O}C	Immediate after installation	45	40
	1 h after installation	48.5	46.5
	24 h or running	50	46.5
	50 h of running	55	46.5
	100 h of running	58	46.5
Pump discharge pressure in bars	Immediate after installation	2	2
	1 h after installation	2.5	2
	24 h or running	3	2
	50 h of running	3.6	2
	100 h of running	4	2
Measurement of seal face wear surface in mm	50 h of running	9.5	9.49
	100 h of running	9.49	9.49
	150 h of running	9.49	9.49
Vibration of pump in mm/s	50 h of running	0.3	0.8
	100 h of running	0.35	1.2
	150 h of running	0.4	1.4

Table 2 Pump operating data taken with different valve positions

Parameter	Valve positions			
	25% closed	50% closed	75% closed	100% closed
Motor current reading in Amp	1.8	1.5	1.2	3.0
Motor temperature reading in °C	46.5	51	65	80.4
Pump discharge pressure in bars	2.4	3.0	3.8	4.5
Measurement of seal face thickness	9.49	9.49	9.49	9.49
Vibration of pump	0.4	0.4	0.4	0.4

2.5 to 4.0, motor temperature increases from 45 to 58 °C, and the pump discharge pressure is increased from 2.0 to 4.0.

In the course of our prototype mechanical seal testing, we decided to subject it to a series of unconventional operating conditions. Specifically, we gradually throttled the discharge valve in four incremental steps until it was completely closed. It is

essential to note that this type of operational scenario is generally discouraged by pump manufacturers due to its potential to exert undue strain on the mechanical seal and jeopardize the integrity of the motor pump. Prolonged operation under such conditions may also lead to cavitation-related issues and impeller damage within the pump.

3.4 Observation of Pump Parameter Under Different Positions of Valve

It is important to acknowledge that in real-world production scenarios, there is a possibility that operators may inadvertently run the pump under these unusual conditions. To assess the resilience and performance of the mechanical seal and mitigate the risk of motor or mechanical seal damage, we conducted this testing phase in a controlled manner. Each step of valve closure was executed for a short duration of 10 min, with a 30-min interval between each percentage adjustment. Pump operating data taken with different valve positions is given in Table 2. This approach allowed us to gain insights into the mechanical seal's behavior under such conditions without subjecting the system to extended periods of potential stress and damage.

In our experiments, we observed that gradually closing the discharge valve up to 75% led to a reduction in motor current, consistent with typical pump motor behavior. A noteworthy deviation occurred when the valve was fully closed, causing an abnormal increase in motor current due to fluid flow obstruction and heightened resistance in the motor-pump system. Prolonged operation in this state can lead to motor overheating. Thus, cautious monitoring is vital to prevent adverse outcomes when operating under such conditions. By throttling the discharge valve, it would cause the pump casing itself to be very hot. The maximum motor temperature is 80.4 °C, and the pump discharge pressure is 4.5 bars. The temperature and pressure values are rapidly increased with increasing the % of closing of value. Measurement of seal face thickness and vibration of pump were constant at all the above-mentioned valve positions.

When comparison is held between the mechanical oil seal and prototype seal, it was observed that the prototype was far ahead in terms of parameter readings which validate pump performance.

4 Conclusion

In summary, the study addressed several critical issues with the mechanical seal in the context of pump operation for palm oil processing and similar industries. The innovative design successfully eliminated product leakage during startup and operation, while also optimizing material machining and production costs. The direct spring

layout and simplified casing design contributed to ease of assembly and reduced manufacturing expenses. Comparing spring types, the research found that the newly designed spring, with a maximum pressure of 1.14 N/m^2, significantly lowered strain on the ceramic seal compared to the existing spring model bearing 2 N/m^2 maximum pressure. The pump testing, spanning 150 h under normal conditions and 50 h under unusual conditions, demonstrated the prototype's durability and capability to handle a discharge pressure of 2 bar with an open valve (0% Closed).

The innovative mechanical seal success in preventing oil leakage due to spring failure, caused by the seizing of fats, marks a significant advancement. This achievement holds significant implications for applications like palm oil crystallization, where the prevention of oil contact with the spring eliminates leakages during production stoppages and changeover periods. However, with mass production, material and process costs could be further reduced to match the expenses associated with existing mechanical seals. Given the widespread use of the Inoxpa Centrifugal Stainless Steel pump across diverse industries, the newly designed seal has the potential to offer substantial savings in plant design and maintenance costs.

References

1. Cooper J et al (2017) A review of the dynamic modelling of mechanical seals for pumps. J Phys: Conf Ser 789(1):012005
2. Bonhôte P et al (2020) Performance characterization of an electric heat pump for residential heating. Energy Procedia 163:104–109
3. Rasul MG et al (2015) Case study: design and development of an innovative spring mechanism to enhance the performance of industrial pumps. J Mech Eng Autom 5(1):1–9
4. Rahmat MF et al (2016) Development of a mechanical seal test rig for investigating frictional characteristics. Procedia Eng 411–419
5. Smith J, Johnson M (2019) Challenges and innovations in mechanical seal design for pump systems. J Fluid Dyn Tribol 17(2):45–62
6. Bogdana A et al (2011) A Kielce University of Technology, 51–62 XIII th international scientific and engineering conference "HERVICON-2011"
7. Patel RK et al (2019) Enhancing pump efficiency through improved mechanical seal design: a comprehensive study. Chem Eng Res J 28(7):923–938
8. Wang Q et al (2021) Computational analysis of spring mechanisms in mechanical seals: a comparative study. J Fluids Mach 49(9):1101–1120
9. Lee SH et al (2017) Innovative materials for spring design in mechanical seals: a review. Mater Sci Eng, A 52(4):210–228
10. Gupta A et al (2018) Spring dynamics in mechanical seals: modeling and analysis. J Mech Eng Res 36(1):17–34
11. Zhang Y et al (2018) Effect of spring parameters on leakage characteristics of a mechanical seal. Mech Ind 19(5):505

Materials Processing for Product Design

Enhancing Biocompatibility and Performance of Multi-directionally Expanding Materials for Dental Applications: Design and Analysis



M. B. Kumbhar and T. Jagadeesha

Abstract Stents are vital in maintaining artery and duct patency by preventing blockages. However, modern stent types have complications, including thrombosis and bleeding. Our goal is to create a 3D-printed, biocompatible, self-expanding polymer stent to address these issues. Auxetic stents, characterized by their unique mechanical properties, hold promise in addressing these complications. Achieving the Auxetic structure involves a comprehensive exploration of various unit cell designs. In our research, we have meticulously crafted computer-aided design (CAD) models of stents, focusing on the arrowhead unit cell design, utilizing solid works software. Subsequently, we conducted a thorough analysis of the stent-ballooning system using Ansys software, with the stent material modeled as structural steel. This analysis lays the foundation for our upcoming simulations, where we aim to investigate the use of polymer materials, such as PLA. Ultimately, our goal is to discover and refine an optimal stent design, bolstering confidence in the utilization of polymer materials like PLA (polylactic acid) for stent placement and thereby enhancing patient outcomes.

Keywords Cardiovascular stent · PLA (polylactic acid) · Strut · 3D printing

1 Introduction

Over recent years, India has witnessed a rapid increase in coronary heart diseases (CHD), with the National Interventional Council (NIC) reporting a surge in cardiovascular cases from 117,420 in 2010 to 248,152 in 2014. India faces one of the highest burdens of cardiovascular disease (CVD) globally, with CVD-related deaths

M. B. Kumbhar
Department of Mechanical Engineering, Government College of Engineering, Karad, Maharashtra 415124, India

T. Jagadeesha (✉)
Mechanical Engineering Department, National Institute of Technology, Calicut, Kerala 673601, India
e-mail: jagdishsg@nitc.ac.in

© The Author(s), under exclusive license to Springer Nature Singapore Pte Ltd. 2025

B. B. V. L. Deepak et al. (eds.), *Recent Advancements in Product Design and Manufacturing Systems*, Lecture Notes in Mechanical Engineering,
https://doi.org/10.1007/978-981-97-6732-8_20

projected to rise from 2.26 million in 1990 to 4.77 million in 2020. The NIC warns of an alarming 14.5% growth rate in percutaneous coronary intervention (PCI) procedures, with 310,190 stent implants in 2019. The stent market in India is expected to triple by 2021. Stents, described by AIIMS New Delhi as small mesh-like tubes, are vital for keeping coronary arteries open, preventing blockages caused by plaque buildup. When a plaque ruptures, it can lead to blood clotting and artery blockage. Stents are deployed through catheters, inflated to expand and secure the artery, restoring normal blood flow, preventing heart muscle damage, and reducing heart attack risks [1].

The conventional mode of expansion of a stent involved using a balloon. Two major types of stents that used the balloon expansion model were the bare metal stents (BMS) and the drug eluting stents (DES). Nowadays, the polymer-based stents are becoming more popular and are introduced to improve the properties of DES [2]. The complications in the balloon expansion opened the horizon for a new method of expansion, i.e., self-expansion using the shape memory property. Both polymer and metal stents were found compatible with the new mode of expansion [3].

2 Literature Review

Commercially available stents, used for over a decade, were initially made of stainless steel, but they posed risks of vascular tissue damage during expansion. Self-expandable stents emerged as a solution for treating atherosclerotic lesions in carotid, coronary, and peripheral arteries. They rely on the shape memory effect (SME) enabled by shape memory alloys (SMAs) and shape memory polymers (SMPs). The FDA approved coronary stents with balloon expansion in 1994, leading to research into advanced stent materials. Nitinol (NiTi), a shape memory alloy, gained popularity for its excellent properties and biocompatibility, leading to NiTi-based stents in 2003 [4]. These stents rapidly oxidize titanium to create a protective TiO2 film, improving corrosion resistance. Surface modifications are still being explored for further improvements [3].

Biodegradable SMP stents, like the Igaki-Tamai PLA stent, combine PLA and PLGA for biodegradability and use PLA and 3D printing for simplified implantation [5]. SMPs excel due to their biodegradability, flexibility, biocompatibility, chemical stability, and drug delivery potential, making them promising for drug-eluting stents [6]. Bioresorbable polymers like PGA, PLA, and PCL are replacing synthetic materials in medical devices due to improved biocompatibility. However, slow PLA degradation in temporary stents is a concern. SMPs outperform SMAs but need continuous improvement, considering factors like stent hydrophobicity, blood cell activation, and endothelial function. Enhanced experimentation and clinical data analysis can refine polymer-based stents for maximum biocompatibility and mechanical performance [7].

The mechanical properties of temperature-responsive shape memory polymer stents. They developed thermal–mechanical data employing multiple theories,

substantiated by experiments and finite element analysis (FEA) to simulate stent behavior within arteries [8]. Various stent geometries in terms of their mechanical attributes, using FEA to assess radial strength, recoil, and stiffness are analyzed [5]. The cyclic thermo mechanical analysis to explore the shape memory properties of PLA (polylactic acid) are studied [9]. They examined stress–strain–temperature diagrams to understand how temperature changes affected the recovery rate. They found that amorphous PLA chain segments acted as the key components responsible for shape change under external stimuli, memorizing the temporary shape after deformation [10, 11]. The switching temperature for shape change was set at the glass transition temperature (Tg), with a recovery temperature slightly above the Tg of PLA chain segments. They achieved shape recovery ratios of 86.8 and 96.2% for the first and second cycles, indicating excellent shape memory properties for PLA. In another model, thinner strut thickness improved stent structure recovery to its initial shape with external heating [12]. Thin-strut stents reduced restenosis risks by up to 42% in ISAR-STEREO clinical trials [7, 13].

Enhancing stent design and using innovative manufacturing methods like additive manufacturing can address stenting issues. Polymer-based stents, with their superior biocompatibility and potential for bio absorption, surpass metal stents, reducing complexity and risks. Bioabsorbable materials eliminate the need for secondary surgeries. Materials with shape memory enable self-expanding stents, minimizing immediate vessel wall injury upon deployment and facilitating easy deployment and gradual conformation to the vessel wall.

3 Modeling of Stent Crimping

Crimping is a crucial step in stent manufacturing, where a specialized tool uniformly reduces the stent's diameter to improve its deliverability. To speed up computational simulations, we scaled down the stent to 1/16th of its actual size, applying symmetry boundaries. We prevented axial displacement by applying a boundary at one end, using a 0.01-mm-thick cylindrical rigid surface to represent the crimping tool. We aimed to simulate cardiovascular stent delivery by reducing the stent from a 4 to a 1.5 mm diameter. The following steps are done for this analysis.

1. For this analysis we have cut our model into 1/16th size. The full size stent and the cut stent are shown in Fig. 1a and b respectively.
2. Created a surface that will act as the crimping tool. The stent and crimping tool is shown in Fig. 2.
3. The contact between the stent and the crimper is defined as frictional with a friction factor 0.8.
4. Meshed the stent with an element size of 0.09 mm and crimper with element size 0.1 mm. The meshed structure is shown in Fig. 3, and the meshing statistics for a number of nodes is 28323 and for a number of elements is 16643.

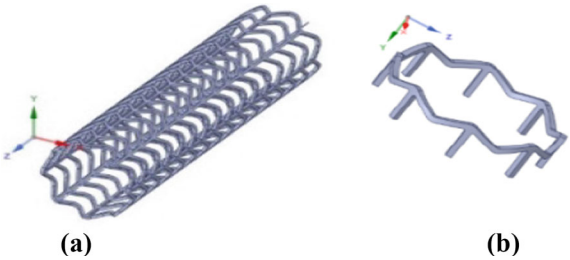


Fig. 1 **a** Full-size stent. **b** Cut stent

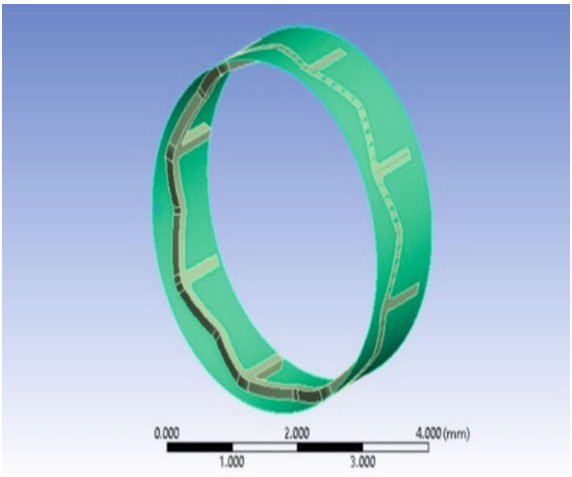


Fig. 2 Crimping tool (green in color)

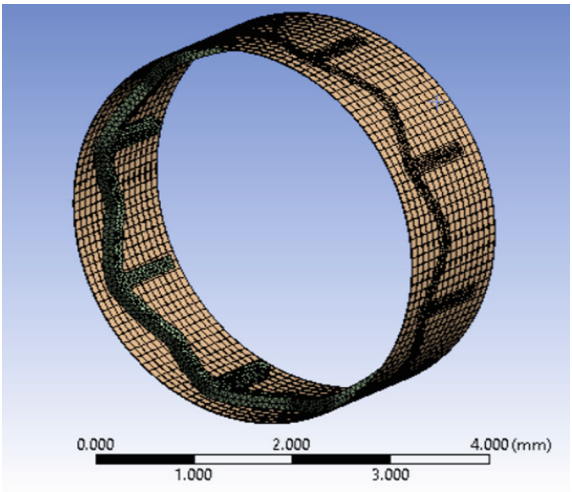


Fig. 3 Meshed stent and crimper

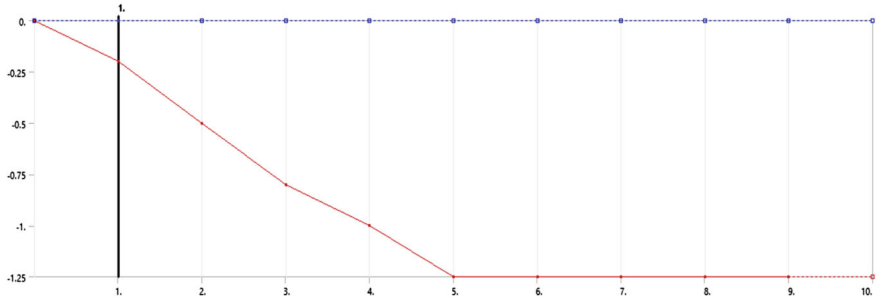


Fig. 4 Displacement given to the crimper with respect to steps

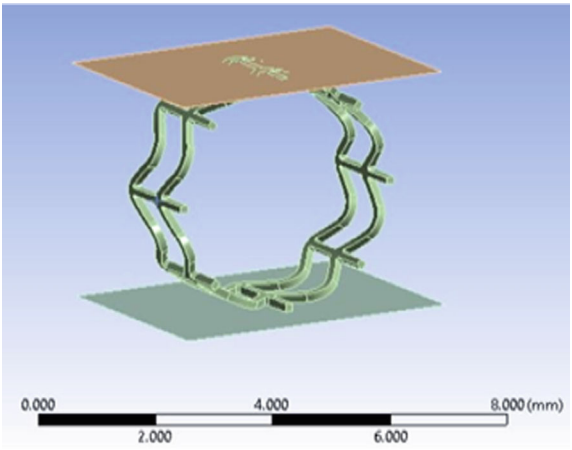
5. The stent is fixed in y direction and unrestricted other movements. A displacement of 1.25 mm in the radially inward direction is given to the crimper in 5 steps as shown in Fig. 4 and solution is generated.

3.1 Modeling of Stent Crushing

The crushing test is intended for checking the radial strength of the stent. The test setup involves stent placed between two rigid plates as shown in Fig. 5. The steps for the test were

1. Creating the rigid plates above and below the stent structure.
2. The between the stent and plates was specified as frictionless contact.
3. Meshed the stent with element size 0.09 and meshed the plates with elements of size 0.2 mm. The meshed structure is shown in Fig. 6.

Fig. 5 Crushing test setup



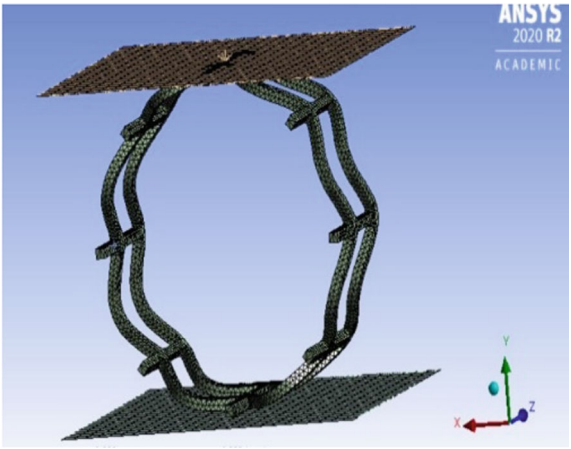


Fig. 6 Generated mesh

4. The displacement of the stent structure is restricted z direction, and all other movements are set as free. The displacement of the lower plate is restricted in every motion to simulate the fixed plate. The upper plate is restricted in every movement but the y axis and given a displacement up to 3 mm in 7 steps as shown in Fig. 7.

Various computational simulation tests were performed on the stent model to check its stability and mechanical strength. The crimping and cruising tests were done, and stress distribution on the stent was determined. A cylindrical structure covering the stent surface is used as a crimping tool in the computational crimp test.

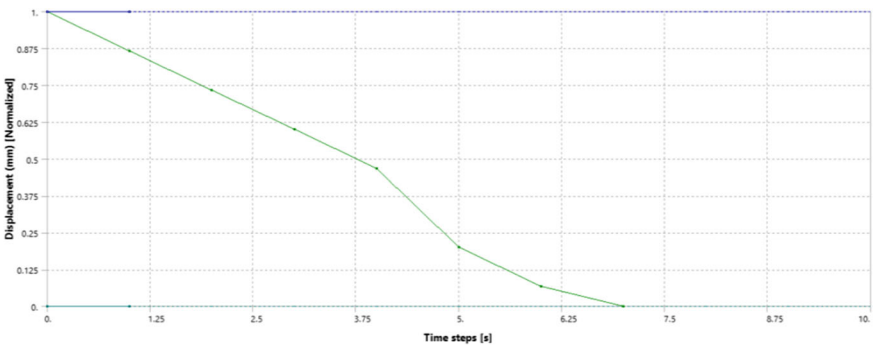


Fig. 7 Displacement of upper plate versus time

4 Result and Discussion

4.1 Equivalent (von-Mises) Stress

The von-Mises stress for a crimping of 1.25 mm radially is obtained. The equivalent von-Mises stress distribution is shown in Fig. 8, and its enlarged view is shown in Fig. 9. The maximum stress is found to occur at crown and at the joining between strut and connecter. The results of maximum stress 96.982 MPa, minimum stress 0.1944 MPa, and average stresses 33.803 MPa.

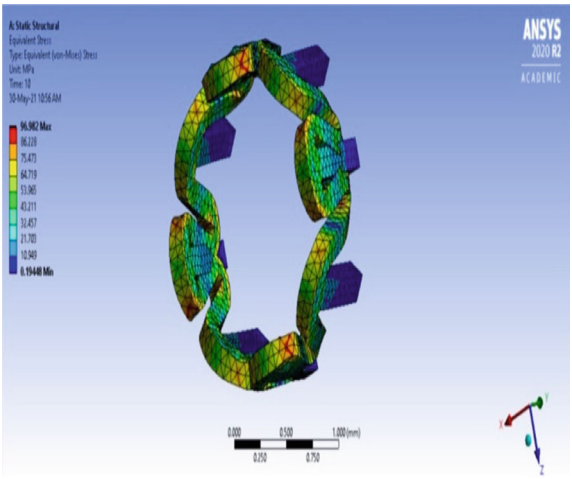


Fig. 8 Stress distributions on stent in crimped state

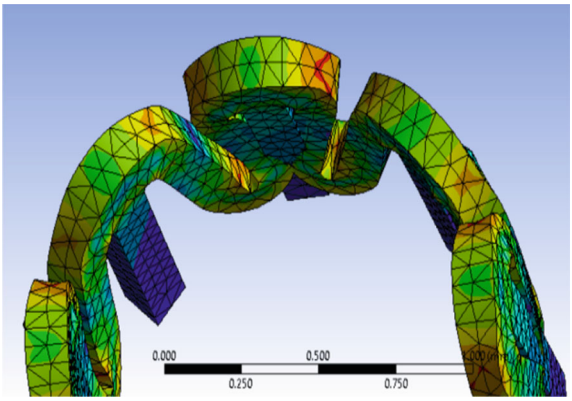


Fig. 9 Enlarged view of stress distribution at the most stressed region

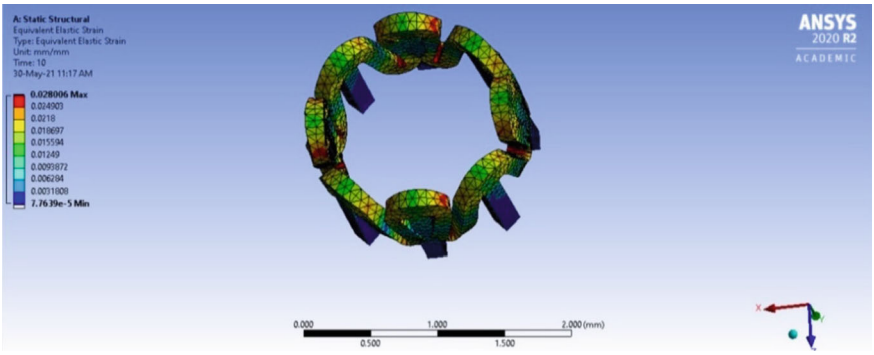


Fig. 10 Equivalent elastic strains

4.1.1 Equivalent (von-Mises) Elastic Strain

The equivalent plastic strain is obtained as shown in Fig. 10. This elastic strain will be recovered by the stent when the crimping tool gets removed. The maximum elastic strain is 0.028, minimum elastic strain is 7.76e-5, and average elastic strains is 0.011.

4.1.2 Equivalent Plastic Strain

The equivalent plastic strain distribution was obtained as shown in Fig. 11; this type of strain is nonrecoverable. The maximum plastic strain is 0.68929, minimum plastic strain is 0.0, and average plastic strain is 0.0596.

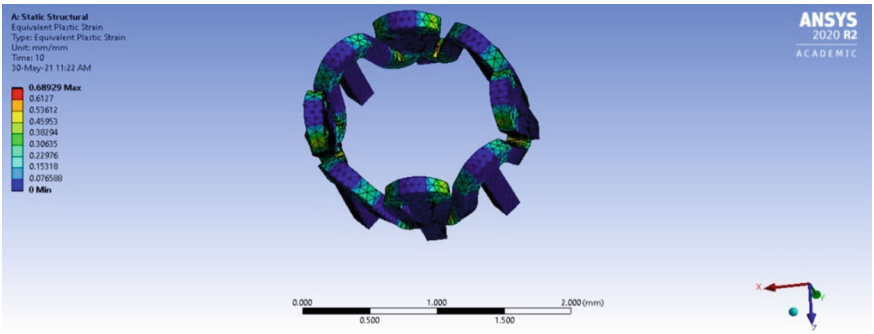


Fig. 11 Equivalent plastic strains

4.2 Computational Crush Test

4.2.1 Equivalent (von-Mises) Stress

The equivalent stresses were obtained as shown in Fig. 12. The maximum stress is 69.908 MPa, minimum stress is 0.002 MPa, and average equivalent stress is 21.267 MPa.

The reaction force that the stent is able to exert onto the plate which is displacing in negative y direction is a direct implication of the radial strength of the stent. The variation of reaction force with respect to the time steps is shown in Fig. 13.

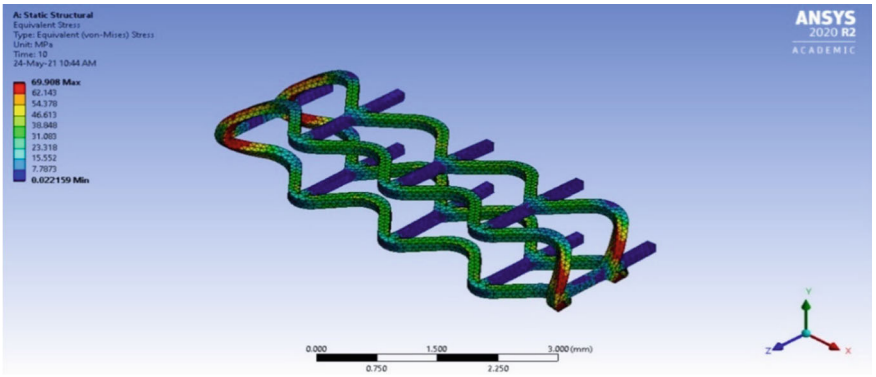


Fig. 12 Stress distribution on stent at the most displaced step

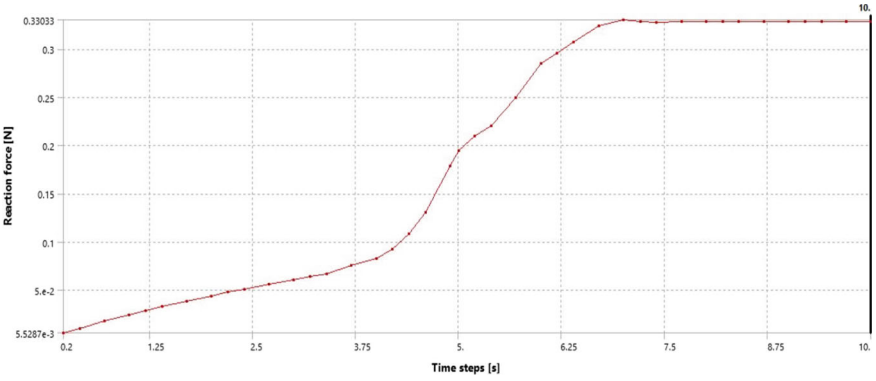


Fig. 13 Reaction force with respect to time

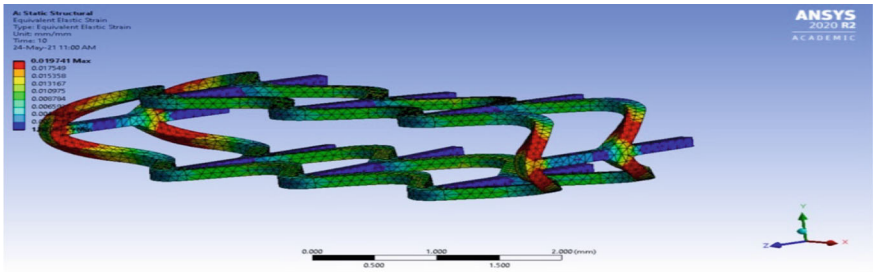


Fig. 14 Equivalent elastic strain distributions

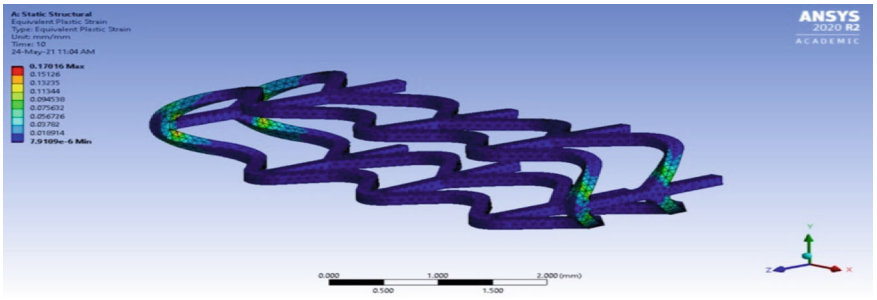


Fig. 15 Equivalent plastic strain distributions

4.2.2 Equivalent (von-Mises) Elastic Strain

The equivalent elastic strain distribution is shown in Fig. 14. The maximum strain is 0.0197, minimum strain is 1.87×10^{-5}, and average strain is 0.007.

4.2.3 Equivalent Plastic Strain

The equivalent plastic strain distribution is shown in Fig. 15. The maximum strain is 0.17, minimum strain is 7.91×10^{-6}, and average equivalent plastic strains are 8.76×10^{-3}.

4.3 Influence of Stent Parameters on Longitudinal Strength

The analyzed stent details are as follows: mean diameter = 4 mm, length = 4 mm, and unit cells per hoop = 8. Figure 16 illustrates the impact of strut thickness on radial strength, highlighting its significant influence. Radial strength is a crucial functional characteristic of a stent. When designing, reducing strut thickness for a

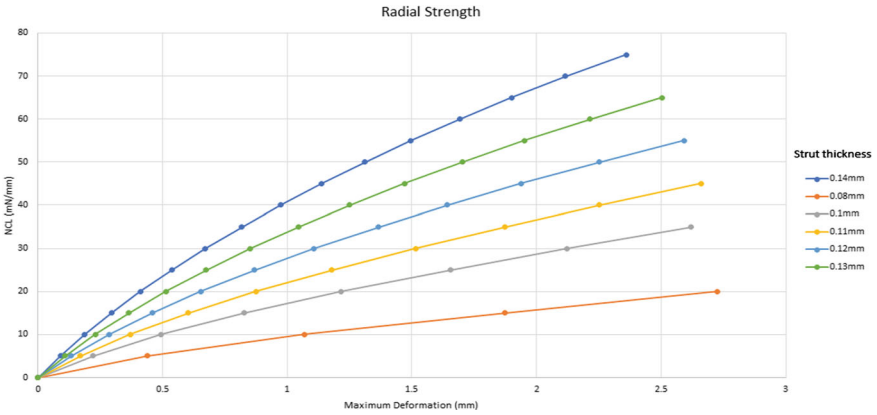


Fig. 16 Radial strength versus strut thickness

lower crimped profile and minimizing effects on blood flow is constrained by the need to maintain radial strength.

4.4 Influence of Stent Parameters on Longitudinal Strength

Figure 17 displays the relationship between longitudinal strength and strut thickness, mirroring the pattern seen in radial strength. Increasing strut thickness enhances longitudinal strength, but this comes at the expense of an enlarged crimped profile.

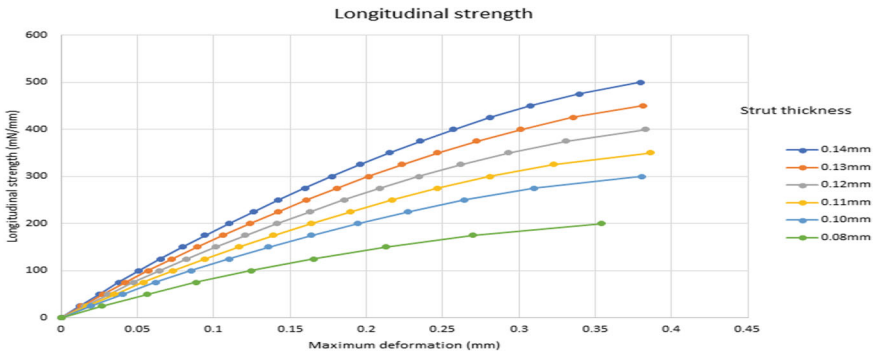


Fig. 17 Longitudinal strength versus deformation for various strut thickness

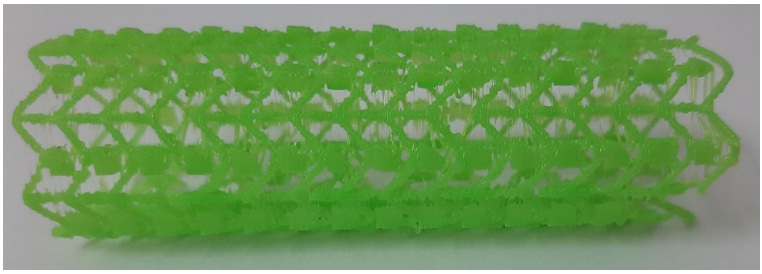


Fig. 18 Fabricated 3D model of stent

5 3D-Printed 5X Prototype Stent

Figure 18 shows a 3D-printed 5X prototype stent based on our final model. While 3D printing PLA-based stents using the FDM technique allowed for rapid production and scaling, it compromised accuracy. This was evident in thinning strands between layers, likely due to high printing speed. Slower speeds could improve layer connection and model strength through better cooling but limited small z-axis structures. For enhanced accuracy, consider using the SLA technique with resin-based printers.

6 Conclusion

We successfully modeled and fabricated a polymer-based smart stent for biomedical applications using software packages. The biocompatible poly lactic acid-based smart stent was developed using computer-aided design methods and is ready for manufacture using 3D printing technology. The proposed stent fabrication process is easy to create complex shapes and structures. The produced smart stent model was investigated in detail through various analyses. Many properties of the model were analyzed. The radial and longitudinal tests conducted on the polymer stents showed more or less comparable strength to the many existing models. We strongly feel that the proposed smart stent will present opportunities to develop the next generation of biomedical devices. The novel stent design proposed would allow for less stress developments at the cross joining parts. The crimping test which was performed on the stent model proved that PLA had good shape recovery property at small deformations.

References

1. Purnama A, Hermawan H, Mantovani D (2014) Biodegradable metal stents: a focused review on materials and clinical studies. J Biomater Tissue Eng 4(11):868–874

2. Iqbal J, Gunn J, Serruys PW (2013) Coronary stents: historical development, current status and future directions. Br Med Bull 106(1):193–211
3. Schmidt T, Abbott JD (2018) Coronary stents: history, design, and construction. J Clin Med 7(6):126
4. Omid SO, Goudarzi Z, Kangarshahi LM, Mokhtarzade A, Bahrami F (2020) Self-expanding stents based on shape memory alloys and shape memory polymers. J Compos Comp 2(3):92–98
5. Pauck RG, Reddy BD (2015) Computational analysis of the radial mechanical performance of PLLA coronary artery stents. Med Eng Phys 37(1):7–12
6. Schiavone A, Zhao LG, Abdel-Wahab AA (2014) Effects of material, coating, design and plaque composition on stent deployment inside a stenotic artery—finite element simulation. Mater Sci Eng, C 42:479–488
7. Kastrati A, Mehilli J, Dirschinger J, Dotzer F, Schühlen H, Neumann FJ, Fleckenstein M, Pfafferott C, Seyfarth M, Schömig A (2001) Intracoronary stenting and angiographic results: strut thickness effect on restenosis outcome (ISAR-STEREO) trial. Circulation 103(23):2816–2821
8. Srivastava V, Chester SA, Anand L (2010) Thermally actuated shape-memory polymers: experiments, theory, and numerical simulations. J Mech Phys Solids 58(8):1100–1124
9. Jia H, Gu SY, Chang K (2018) 3D printed self-expandable vascular stents from biodegradable shape memory polymer. Adv Polym Technol 37(8):3222–3228
10. Torki MM, Hassanajili S, Jalisi MM (2020) Design optimizations of PLA stent structure by FEM and investigating its function in a simulated plaque artery. Math Comput Simul 169:103–116
11. Barletta M, Gisario A, Mehrpouya M (2021) 4D printing of shape memory polylactic acid (PLA) components: investigating the role of the operational parameters in fused deposition modelling (FDM). J Manuf Process 61:473–480
12. Azli AA, Muhammad N, Albakri MMA, Ghazali MF, Abd Rahim SZ, Victor SA (2020) Printing parameter optimization of biodegradable PLA stent strut thickness by using response surface methodology (RSM). IOP Conf Series: Mater Sci Eng 864(1):012154
13. Boutry CM, Beker L, Kaizawa Y, Vassos C, Tran H, Hinckley AC, Pfattner R, Niu S, Li J, Claverie J, Wang Z (2019) Biodegradable and flexible arterial-pulse sensor for the wireless monitoring of blood flow. Nat Biomed Eng 3(1):47–57

Synthesis of Hybrid Nanofluids, Properties, and Its Applications—A Comprehensive Review

Sudhakara Rao Bammidi, Vijay Miditana, and Ravibabu Sajja

Abstract The functional ability of any device lies in its actual thermal management. To augment heat transfer, it is very crucial to identify the best heat transfer liquid available. The field of nanofluids plays a phenomenal role in devices that emit heat during their operation. Nano-sized particles are scattered in base fluid, which then becomes nanofluid for the first time since it was invented in the late twentieth century. A nanofluid synthesized by dispersing two kinds of nanoparticles is called a hybrid nanofluid. These are blended using mechanical stirring, ultrasonication, and surfactants to improve their physical potential. The main reasons the nanofluids work so well are because of their improved stability, pH control, and thermophysical qualities, and they will be used for different thermal applications. The current review is concentrated on nanoscale-level particles used in the synthesis of nanofluids and thermal applications such as electron cooling, heat exchangers, and radiators. The present review of nanofluids summarizes some researchers' progress and discusses challenges and the future scope of nanofluids. Finally, it is concluded that hybrid nanofluids will be synthesized commercially on a large scale and used as next-generation heat transfer fluids for various applications.

Keywords Nanofluid · Surfactant · Ultrasonication · Heat exchanger

S. R. Bammidi · V. Miditana
Department of Mechanical Engineering, Centurion University of Technology and Management, Rajapati, Odisha, India

R. Sajja (✉)
Department of Mechanical Engineering, GMR Institute of Technology, Rajam, India
e-mail: ravibabu.s@gmrit.edu.in

© The Author(s), under exclusive license to Springer Nature Singapore Pte Ltd. 2025

B. B. V. L. Deepak et al. (eds.), *Recent Advancements in Product Design and Manufacturing Systems*, Lecture Notes in Mechanical Engineering,
https://doi.org/10.1007/978-981-97-6732-8_21

1 Introduction

Traditional fluids like water, ethylene glycol, engine oils, and transformer oils are known for having lower thermal conductivity compared to solid metallic or oxide particles. These are blended with nano-powder, which will improve the thermal properties, stability, and constant pH, so that they can be used in different applications like electronic chip devices, biomedical devices, automobile radiators, and refrigeration and air conditioning systems. Energy plays a virtual role in physical, quantitative things that must be transmitted to enter any system that performs mechanical work. The energy is transferred either by heat or work [1]. The heat is moved from one region to another where there are variations in temperature throughout the system. They vary from maximum temperatures to minimum temperatures [2, 3]. Ravi et al. [4] make use of traditional base fluids which have low thermal potential compared to solids. The nano-sized particles (typically 10–100 nm) are dispersed into carrier fluid, which augments thermal characteristics and stability of nanofluid. It is affected by various factors, such as how it is prepared and its concentration, particle type, size, shape, pH of the nanofluid, and fluid temperature. The nanofluid preparation procedures are found to produce altered pH values, particle agglomeration, settling characteristics, and thermophysical properties, in addition to the surfactants, magnetic stirring, and ultrasonication, and this type of technique will be used to propagate the temperature of the liquid progressively. In Fig. 1, thermal conductivities of various frequently used nanoparticles, like metallic oxides and metallics, are depicted.

The main drawback is that nanofluid flows through the pipe and its losses are reduced. Increased viscosity primes for shear stress between the fluid and the adjacent outward wall surface. Moreover, the growing temperature indicates the diffusion of nanofluid into the pipe's inner surface [5, 6]. In order to enhance thermal heat transfer coefficients, Ganji et al. [7] looked into how they might be used in air conditioning systems, heat pipes, electronic cooling, industrial and heating processes,

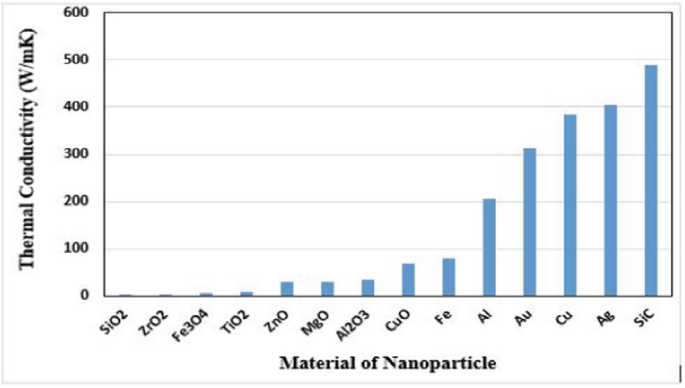


Fig. 1 Thermal conductivity of frequently used nanoparticles

food processing sectors, and automotive heat exchangers. Using an automotive radiator, Nurettin et al. [8] reviewed the growing thermal conductivity as the percentage volume concentration of nanoparticles declined, which was followed by an increase in temperature and a decrease in viscosity. The temperature control of an inspected electrical device [9]. Nurettin et al. [10] reviewed nanoparticles that are not used in industrial applications because the corrosion effect is greater. Several reviews done by researchers [11–21] were analyzed for better understanding of review work. The current review is mainly focusses on synthesis, thermophysical characteristics, and their heat transfer applications.

2 Preparation of Nanofluids

There are one-step and two-step ways for preparing nanofluids. Nanoparticle preparation and base fluid mixing are done simultaneously in the 1-step process. In the two-step process, base fluid is then mixed with the nanoparticles that have first been prepared [22–24]. Figure 2 illustrates the similar procedures needed to manufacture hybrid nanofluid.

Chen et al. [25] described two-step technique used to formulate MWCNT/H_2O nanofluid. They are all synthesized to improve the magnetic stirring and sonication machining processes, which are stable for 2 months. Annie et al. [26] experimentally studied this procedure, which was utilized to enhance the stableness and thermal

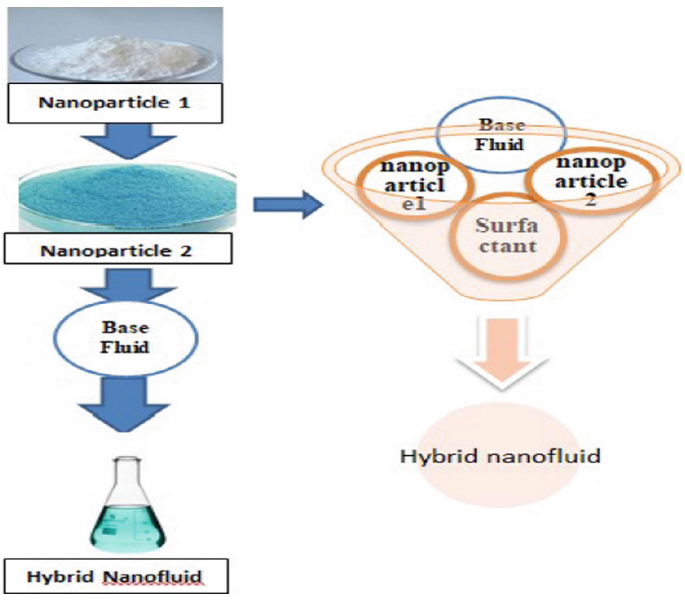


Fig. 2 Steps involved in synthesis of hybrid nanofluid

behavior of MWCNT/water nanofluid with various surface-active agent like SLS and PVP. With the magnetic stirring durations of 60 and 30 min, nanofluids were equipped as stable solutions and were studied with other surfactants such as CTAB, SDBS, ethyl-carbamate, EBT, and APTMS for 6 months. The surfactants are mixed into the proper ratio of working fluid and nanoparticles. Using the Hummers method, Almanassra et al. [27] did experiments to look into a two-step method for making graphite-water that makes nanofluids more stable over three months. Nanofluids were equipped by both magnetic stirring and a sonication bath for 40 min to an hour at different volume fractions of 1–4.5%. Yang et al. [28] used the sol–gel technique to make CuO-water nanofluids, added PVA surfactant in the same ratio, and sonicated the mixture for 1.75 h. It stayed stable for a year.

3 Thermophysical Characteristics of Nanofluids

Thermal characteristics of hybrid nanofluids impact the heat transfer process and its applications in automobiles, industry, and medical devices. The heat transfer device impacts properties like specific heat (C_P), viscosity (υ), thermal conductivity (k), and density (ρ) of nanofluids. Paul et al. [29], Liu et al. [30], Healy et al. [31], Levin et al. [32], Koca et al. [33], and also researchers [34–37] have conducted experiments to prepare and characterize nanofluids. They reported that an experimental investigation of water stability, settling, and time depends on the heat transfer behavior of TiO_2/CNT. When volume 0.3% TiO_2 and volume 0.1% carbon nanotubes (CNT) nanofluids are looked at, the traditional thermal performance gradually goes up from 17.84 to 19.31%. Table 1 provides an overview of a few current works on the synthesis, characterization, and stabilization techniques for nanofluids.

Table 1 Few studies on preparation, stabilization methods

Reference	Base fluid	Nano particle	Synthesis method	Surfactant	Sonication time (hrs)	Stability (days)
[38]	DI water	CuO	Sol–gel	PVA	1.46	360
[39]	Water, EG	GO-SiC (50:50)	–	N/A	0.75	–
[40]	EG, DIW (50:50)	CeO_2	Ball milling	CTAB, CMC	5	> 21
[41]	EG	$COFe_2O_4$	Chemical coprecipitation	SHS	3	–
[42]	PAO oil	Alloy nano	Facile one step nano	Ethyl carbamate	0.5	> 30

Table 2 Thermal conductivity enhancement using hybrid nanofluids

Reference	Base fluid	Nano particle	% Vol fraction	Size of first particle (nm)	Size of second particle (nm)	Thermal conductivity enhancement (%)
[50]	Water	Al_2O_3-Fe	0.05–0.2	29	46	14
[53]	Molten salt	Al_2O_3-SiO_2	1	2–5	12	19
[54]	EG	SiC, CuO	0.82–3.13	45–65	12–28	19.3
[55]	Water	Al_2O_3-Fe	0.05–0.2	29	46	14
[56]	10W40	Al_2O_3, Fe_3O_4	0–4	20	20–40	33

3.1 Thermal Conductivity of Nanofluids

Yu et al. [43], Akhgar et al. [44], Mirsaeidi et al. [45], Essajai et al. [46] and Rahman et al. [47], compared to hybrid nanofluids, CuO-MgO-TiO_2/water nanofluid's the thermal conductivity is increased by 78.6% at a volume concentration of 0.1% [48–52]. Table 2 provides an overview of few works on thermal conductivity of hybrid nanofluids are reported in Table 2.

3.2 Viscosity of Nanofluids

Natividade et al. [57], Dehghani et al. [58], Ye et al. [59], Bahrami et al. [60], and Behrooj et al. [61] carried out tests to identify the rheological characteristics of nanofluids and used magnetic stirring and ultrasonication to significantly boost the viscosity of an oil base fluid. They measured thickness of fluid made of molybdenum sulfate, diesel oil with different particle fractions between 0.1 and 0.7%. It has been observed that the viscosity increases at mass fractions of 0.04–0.7%. In Table 3, recent pilot studies on the rheology of hybrid nanofluids are tabulated and shown.

Specific Heat of Nanofluids. Chen et al. [67], Moldoveanu et al. [68], Wu et al. [69], and Hassan et al. [70] studied the parameters of particle diameter and mass concentration on the specific heat of SiO_2 molten salt. Nanofluids among the traditional nanofluids include SiO_2, Al_2O_3, and TiO_2 nanoparticles. In Table 4, findings of some more studies are summarized [52, 71–73].

Table 3 Viscosity enhancement of hybrid nanofluids

Reference	Base fluid	Nano particle	% vol fraction	Size of first particle (nm)	Size of second particle (nm)	Viscosity enhancement (%)
[62]	Water	MgO-TiO_2	0.1–0.5	25–45	18–23	45
[63]	EG	SiC, CuO	0.82–3.13	45–65	12–28	2.07
[64]	Thermal oil	MWCNT, Al_2O_3	0.125–1.5	15	20	19.3
[65]	EG:PG	Al_2O_3-CuO	0.1–1.5	42	42	102
[66]	Water	MgO-TiO_2	0.1–1.5	25–45	18–23	45

Table 4 Specific heat of hybrid nanofluids

Reference	Base fluid	Nano particle	% vol fraction	Size of first particle (nm)	Size of second particle (nm)	Prediction model
[71]	PEG 400	MWCNT, Fe	0.01–1	25	18	Correlation
[52]	Water	Al_2O_3-TiO_2	1–3	45	30	Correlation
[72]	DW	MgO-TiO_2	0.1–0.5	25–45	18–23	Correlation
[73]	Water	Al_2O_3-Fe	0.05–0.2	29	46	Correlation

4 Heat Transfer Applications of Nanofluids

Nanofluid finds applications in double-pipe concentrated, shell & tube, plate compact heat exchangers. TiO_2/water nanofluid was practically investigated in the DTHE study to observe that heat transfer increased by 14.8% and pressure drop increased by 51.9%. The DTHE has used Al_2O_3/water nanofluid to improve the heat transfer performance by 16% compared to the base fluid water [74]. The rate of heat transfer and pressure drop will be measured, and flow regimes based on nanofluids in the tube will improve the heat transfer coefficient by 7–50% [75]. In Table 5, several authors [76–80] studied about impact of Al_2O_3/water nanofluids on heat transfer coefficient and found that the Nusselt's and Reynolds numbers (Nu, Re) were augmented by 23.2% and 32.23%, respectively. These investigations and their parameters of study are presented.

5 Conclusions and Future Scope

In the past, nanofluids have been used in heat transfer applications. These were looked at to get a better understanding of how nanofluids are made, what their thermal properties are, how stable they are, and how they can be used in mechanical devices to

Table 5 Impact of nanofluids on the performance of heat exchangers

Reference	Base fluid	Nano particle	Type of analysis	Heat exchanger	Perception
[76]	Water, EG	Al_2O_3	Simulation	Double pipe	Spherical and platelet increases to decrease thermal energy and entropy generation
[77]	Water	Al_2O_3-CuO, TiO_2	Simulation	Pillow plate	TiO_2/water at volume concentration is 5% Reynolds number highly performance other nanofluids
[78]	Water	CNT, Al_2O_3	Experimental	PHE	It is large volume of natural fluids such as water and EG are need
[79]	EG:PG	Al-MWCNT	Experimental	PHE	Increases heat transfer rate 15.2% with elimination increases pump work 0.02% and performance index 2.96%
[80]	Water	Al_2O_3	Simulation	PHE	Overall heat transfer performance raises 30–70%. The reduces mass flow rate and pressure drop is 0.75%

make heat transfer more efficient. Various kinds of nanofluids in mechanical system like heat exchangers and radiators are reviewed in preparation for the nanofluid.

- In this review article, it is demonstrated that one-step techniques for preparing nanofluids, as opposed to two-step techniques, improve stability. More studies to analyze the mass production of products used in the one-step technique are needed. The one-step technique that is used to prepare nanofluids is more cost-effective for mass production of nanofluids, whereas the two-step method is suited for laboratory purposes.
- The mechanical stirring and sonication bath processes will reduce the sedimentation of nanoparticles, avoiding a longer period of time and improving thermal properties.

- The increased volume concentrations of nanoparticles will decrease specific heat and increase thermal potential and viscosity.
- The different strategies for obtaining the thermophysical functionality of hybrid nanofluids have increased.
- The enhanced rate of heat transfer with the aid of nanofluids reduces the heat transfer surface area in heat exchangers and radiators. This may result in a reduction in the overall size and volume of these engines. Such advancements would reduce drag forces in vehicles while also increasing engine performance.

There is a need for more investigation into the effects of nanofluid-caused erosion and flow channel corrosion, particularly at high temperatures. The consequences of settling and nanoparticle deposition on heat transfer device efficiency must be studied.

CRediT Authorship Contribution Statement **Sudhakara Rao Bammidi and Vijay Miditana**: Data curation, Formal analysis, Investigation. **Ravibabu Sajja**: Data consolidation, Editing of manuscript.

Declaration of Competing Interest The authors declare that none of the work reported in this study could have been influenced by any known competing financial interests or personal relationships.

References

1. Holman P, Bhattacharyya S (2021) Heat transfer, 10th edn. McGraw-Hill, New York
2. Cengel YA (2002) Heat transfer, a practical approach 2nd edn. McGraw-Hill, New York
3. Kanoglu M (2015) Thermodynamics: an engineering approach, 8th edn. McGraw-Hill, New York
4. Babu SR, Babu PR, Rambabu V (2013) Effects of some parameters on thermal conductivity of nanofluids and mechanisms of heat transfer improvement. Int J Eng Res Appl 3(4):2136–2140
5. Menni Y, Chamkha AJ, Azzi A (2019) Nanofluid flow in complex geometries—a review. J Nanofluids 8(5):893–916
6. Zhao N, Li S, Yang J (2016) A review on nanofluids: data-driven modeling of thermophysical properties and the application in automotive radiator. Renew Sustain Energy Rev 66:596–616
7. Ganji DD, Sabzehmeidani Y, Sedighiamiri A (2017) Nonlinear systems in heat transfer: mathematical modeling and analytical methods. Elsevier
8. Sezer N, Biçer Y, Koç M (2019) Design and analysis of an integrated concentrated solar and wind energy system with storage. Int J Energy Res 43(8):3263–3283
9. Krishna VM, Kumar MS (2019) Numerical analysis of forced convective heat transfer of nanofluids in microchannel for cooling electronic equipment. Mater Today: Proc 17:295–302
10. Sezer N, Koç M (2021) A comprehensive review on the state-of-the-art of piezoelectric energy harvesting. Nano Energy 80:105567
11. Goel N, O'Hern H, Orosz M, Otanicar T (2020) Annual simulation of photovoltaic retrofits within existing parabolic trough concentrating solar powerplants. Sol Energy 211:600–612
12. Bumataria RK, Chavda NK, Panchal H (2019) Current research aspects in mono and hybrid nanofluid based heat pipe technologies. Heliyon 5(5)
13. Cacua K, Buitrago-Sierra R et al (2019) Nanofluids' stability effects on the thermal performance of heat pipes: a critical review. J Therm Anal Calorim 136:1597–1614

14. Sahin AZ, Uddin MA et al (2020) Performance enhancement of solar energy systems using nanofluids: an updated review. Renew Energy 145:1126–1148
15. Qiu L, Ouyang Y, Feng Y, Zhang X (2019) Review on micro/nano phase change materials for solar thermal applications. Renew Energy 140:513–538
16. Bellos E, Tzivandis C (2019) Alternative designs of parabolic trough solar collectors. Prog Energy Combust Sci 71:81–117
17. Xian HW, Sidik NAC (2019) Erosion-corrosion effect of nanocoolant on actual car water pump. In: IOP conference series: materials science and engineering, vol 469, no 1. IOP Publishing, UK, p 012039
18. Elsheikh AH, Sharshir SW et al (2018) Applications of nanofluids in solar energy: a review of recent advances. Renew Sustain Energy Rev 82:3483–3502
19. Ahmadi MH, Ghazvini M et al (2019) Utilization of hybrid nanofluids in solar energy applications: a review. Nano-Struct Nano-Obj 20:100386
20. Farhana K, Kadirgama K et al (2019) Significance of alumina in nanofluid technology: an overview. J Therm Anal Calorim 138:1107–1126
21. Shah TR, Koten H, Ali HM (2020) Performance effecting parameters of hybrid nanofluids. In: Hybrid nanofluids for convection heat transfer. Academic Press, pp 179–213
22. Loni R, Asli-Areh EA et al (2020) Research and review study of solar dish concentrators with different nanofluids and different shapes of cavity receiver: experimental tests. Renew Energy 145:783–804
23. Pak BC, Cho YI (1998) Hydrodynamic and heat transfer study of dispersed fluids with submicron metallic oxide particles. Exp Heat Transf 11(2):151–170
24. Kumar DD, Arasu AV (2018) A comprehensive review of preparation, characterization, properties and stability of hybrid nanofluids. Renew Sustain Energy Rev 81:1669–1689
25. Chen W, Zou C, Li X (2019) Application of large-scale prepared MWCNTs nanofluids in solar energy system as volumetric solar absorber. Sol Energy Mater Sol Cells 200:109931
26. Aureen Albert A, Harris Samuel DG, Parthasarathy V, Kiruthiga K (2020) A facile one pot synthesis of highly stable PVA–CuO hybrid nanofluid for heat transfer application. Chem Eng Commun 207(3):319–330
27. Almanassra IW, Zakaria Y et al (2022) XPS and material properties of raw and oxidized carbide-derived carbon and their application in antifreeze thermal fluids/nanofluids. J Thermal Anal Calorimetry 147(21):11787–11803
28. Yang L, Huang JN, Ji W, Mao M (2020) Investigations of a new combined application of nanofluids in heat recovery and air purification. Powder Technol 360:956–966
29. Paul G, Das PK, Manna I (2016) Synthesis, characterization and studies on magneto-viscous properties of magnetite dispersed water based nanofluids. J Magn Magn Mater 404:29–39
30. Liu WI, Omid M, Seyed AB et al (2019) A new comprehensive experimental work on graphene oxide nanoparticles dispersed in water: synthesis, characterization, measurement of thermal conductivity and a novel approach of RLSF neural network. Int Commun Heat Mass Trans 109:104333
31. Healy JJ, De Groot JJ, Kestin J (1976) The theory of the transient hot-wire method for measuring thermal conductivity. Physica B+ c 82(2):392–408
32. Levin MLV, Miller MAF (1981) Maxwell's treatise on electricity and magnetism. Soviet Phys Uspekhi 24(11):904
33. Koca HD, Doganay S et al (2018) Effect of particle size on the viscosity of nanofluids: a review. Renew Sustain Energy Rev 82:1664–1674
34. Mahian O, Kolsi L, Amani M, Estellé P, Ahmadi G, Kleinstreuer C, Pop I et al (2019) Recent advances in modeling and simulation of nanofluid flows-Part I: fundamentals and theory. Phys Rep 790:1–48
35. Dadhich M, Prajapati OS, Rohatgi N (2020) Flow boiling heat transfer analysis of Al_2O_3 and TiO_2 nanofluids in horizontal tube using artificial neural network (ANN). J Therm Anal Calorim 139:3197–3217
36. Zhou F, Yang L, Sun L, Wang S, Song J, Li X (2023) The preparation, stability and heat-collection efficiency of solar nanofluids. J Therm Anal Calorim 148(3):591–622

37. Shahul Hameed M, Suresh S, Singh RK (2019) Comparative study of heat transfer and friction characteristics of water-based alumina–copper and alumina–CNT hybrid nanofluids in laminar flow through pipes. J Therm Anal Calorim 136:243–253
38. Aureen Albert A, Harris Sam DG, Induja S (2022) Thermal conductivity models for polymer stabilized hybrid nanofluids prepared by one-step method. Int J Nanosci Nanotechnol 18(4):251–264
39. Mahyari AA, Karimipour A, Afrand M (2019) Effects of dispersed added graphene oxide-silicon carbide nanoparticles to present a statistical formulation for the mixture thermal properties. Physica A 521:98–112
40. Taghizadeh A, Taghizadeh M, Azimi M, Alsagri AS, Alrobaian AA, Afrand M (2020) Influence of cerium oxide nanoparticles on thermal conductivity of antifreeze: preparation and stability of nanofluid using surfactant. J Therm Anal Calorim 139:225–236
41. Kharat PB, Kounsalye JS, Shisode MV, Jadhav KM (2019) Preparation and thermophysical investigations of $CoFe_2O_4$-based nanofluid: a potential heat transfer agent. J Supercond Novel Magn 32:341–351
42. Wang C, Chen K, Huang Z, Wang T, Chen F (2020) Effect of polymer-derived silicon carbonitride on thermal performances of polyethylene glycol based composite phase change materials. Sol Energy 208:282–288
43. Yu W, France DM, Singh D, Zhao W (2018) Experimental investigation of subcooled flow boiling of a 50/50 ethylene glycol/water mixture in finned rectangular aluminum channels. Exp Heat Transfer 31(6):482–494
44. Akhgar A, Toghraie D, Sina N, Afrand M (2019) Developing dissimilar artificial neural networks (ANNs) to prediction the thermal conductivity of MWCNT-TiO_2/Water-ethylene glycol hybrid nanofluid. Powder Technol 355:602–610
45. Mirsaeidi AM, Yousefi F (2021) Viscosity, thermal conductivity and density of carbon quantum dots nanofluids: an experimental investigation and development of new correlation function and ANN modeling. J Therm Anal Calorim 143:351–361
46. Essajai R, Tabtab I, Mzerd A, Mounkachi O, Hassanain N, Qjani M (2019) Molecular dynamics study of thermal properties of nanofluids composed of one-dimensional (1-D) network of interconnected gold nanoparticles. Results Phys 15:102576
47. Rehman WU, Bhat AH, Suliamon AA, Khan IU, Ullah H (2016) Effect of volumetric concentration of MWCNTs on the stability and thermal conductivity of nanofluids. In: AIP conference proceedings, vol 1787, no 1. AIP Publishing
48. Yekani Motlagh Y, Nazemi AH, Sadraddini AA, Abbaspour A, Yekani Motlagh S (2013) Numerical investigation of the effects of combining sewer junction characteristics on the hydraulic parameters of flow in fully surcharged condition. Water Enviro J 27(3):301–316
49. Alarifi IM, Nguyen HM, Naderi Bakhtiyari A, Asadi A (2019) Feasibility of ANFIS-PSO and ANFIS-GA models in predicting thermophysical properties of Al_2O_3-MWCNT/oil hybrid nanofluid. Materials 12(21):3628
50. Mousavi SM, Esmaeilzadeh F, Wang XP (2019) Effects of temperature and particles volume concentration on the thermophysical properties and the rheological behavior of CuO/MgO/TiO_2 aqueous ternary hybrid nanofluid: experimental investigation. J Therm Anal Calorim 137:879–901
51. Taherialekouhi R, Rasouli S, Khosravi A (2019) An experimental study on stability and thermal conductivity of water-graphene oxide/aluminum oxide nanoparticles as a cooling hybrid nanofluid. Int J Heat Mass Transf 145:118751
52. Moldoveanu GM, Minea AA, Huminic G, Huminic A (2019) Al_2O_3/TiO_2 hybrid nanofluids thermal conductivity: an experimental approach. J Therm Anal Calorim 137:583–592
53. Nithiyanantham U, Zaki A, Grosu Y, González-Fernández L, Igartua JM, Faik A (2019) SiO_2, Al_2O_3 core-shell nanoparticles based molten salts nanofluids for thermal energy storage applications. J Energy Stor 26:101033
54. Akilu S, Baheta AT, Sharma KV (2020) Characterization and modelling of density, thermal conductivity, and viscosity of TiN–W/EG nanofluids. J Therm Anal Calorim 140:1999–2010

55. Okonkwo EC, Wole-Osho I, Kavaz D, Abid M (2019) Comparison of experimental and theoretical methods of obtaining the thermal properties of alumina/iron mono and hybrid nanofluids. J Mol Liq 292:111377
56. Sulgani MT, Karimipour A (2019) Improve the thermal conductivity of 10w40-engine oil at various temperature by addition of Al_2O_3/Fe_2O_3 nanoparticles. J Mol Liq 283:660–666
57. Natividade PSG, de Moraes Moura G, Avallone E, Bandarra Filho EP, Gelamo RV, Gonçalves JCDSI (2019) Experimental analysis applied to an evacuated tube solar collector equipped with parabolic concentrator using multilayer graphene-based nanofluids. Renew Energy 138:152–160
58. Dehghani Y, Abdollahi A, Karimipour A (2019) Experimental investigation toward obtaining a new correlation for viscosity of WO_3 and Al_2O_3 nanoparticles-loaded nanofluid within aqueous and non-aqueous basefluids. J Therm Anal Calorim 135:713–728
59. Ye X, Kandlikar SG, Li C (2019) Viscosity of nanofluids containing anisotropic particles: a critical review and a comprehensive model. Euro Phys J E 42:1–34
60. Bahrami M, Akbari M, Karimipour A, Afrand M (2016) An experimental study on rheological behavior of hybrid nanofluids made of iron and copper oxide in a binary mixture of water and ethylene glycol: non-Newtonian behavior. Exp Thermal Fluid Sci 79:231–237
61. Ruhani B, Toghraie D, Hekmatifar M, Hadian M (2019) Statistical investigation for developing a new model for rheological behavior of ZnO–Ag (50%–50%)/water hybrid Newtonian nanofluid using experimental data. Physica A 525:741–751
62. Mousavi SB, Heris SZ, Hosseini MG (2019) Experimental investigation of MoS_2/diesel oil nanofluid thermophysical and rheological properties. Int Commun Heat Mass Transfer 108:104298
63. Akilu S, Baheta AT, Chowdhury S, Padmanabhan E, Sharma KV (2019) Thermophysical profile of SiC–CuO/C nanocomposite in base liquid ethylene glycol. Powder Technol 354:540–551
64. Alarifi IM (2021) Advanced selection materials in solar cell efficiency and their properties—a comprehensive review. Mater Today: Proc
65. Kumar V, Sahoo RR (2019) Viscosity and thermal conductivity comparative study for hybrid nanofluid in binary base fluids. Heat Transfer—Asian Res 48(7):3144–3161
66. Mousavi SM, Esmaeilzadeh F, Wang XP (2019) A detailed investigation on the thermo-physical and rheological behavior of MgO/TiO_2 aqueous dual hybrid nanofluid. J Mol Liq 282:323–339
67. Chen Z, Shahsavar A, Al-Rashed AA, Afrand M (2020) The impact of sonication and stirring durations on the thermal conductivity of alumina-liquid paraffin nanofluid: an experimental assessment. Powder Technol 360:1134–1142
68. Moldoveanu GM, Minea AA (2019) Specific heat experimental tests of simple and hybrid oxide-water nanofluids: proposing new correlation. J Mol Liq 279:299–305
69. Wu YT, Ying LI, Lu YW, Wang HF (2017) Novel low melting point binary nitrates for thermal energy storage applications. Sol Energy Mater Sol Cells 164:114–121
70. Hassan MA, Galal A, Sayed M, Dessoki K, Fouad A, Eskarous ET, Khalil A, Elsayed AA (2023) Performance assessment and Pareto front mapping of a novel truncated elliptic cavity solar receiver. Appl Therm Eng 226:120319
71. Marcos MA, Podolsky NE, Cabaleiro D, Lugo L, Zakharov AO, Postnov VN, Semenov KN (2019) MWCNT in PEG-400 nanofluids for thermal applications: a chemical, physical and thermal approach. J Mol Liq 294:111616
72. Esmaelizadeh F, Zarei F, Mousavi SM, Vakili-Nezhaad GR (2020) Prediction of DES' vapor pressure using a new corresponding state model. Phys Chem Res 8(3):471–496
73. Abdellatif YM, Okonkwo EC, Beitelmal AH, Al-Ansari T (2022) Heat transfer analysis of Cu–water nanofluid in a district cooling chilled water loop. J Thermal Sci Eng Appl 14(5):051017
74. Qiu L, Zhu N, Feng Y, Michaelides EE, Żyła G, Jing D, Zhang X, Norris PM, Markides CN, Mahian O (2020) A review of recent advances in thermophysical properties at the nanoscale: from solid state to colloids. Phys Rep 843:1–81
75. Al-Oran O, Lezsovits F, Aljawabrah A (2020) Exergy and energy amelioration for parabolic trough collector using mono and hybrid nanofluids. J Therm Anal Calorim 140:1579–1596

76. Naik BAK, Vinod AV (2020) Natural convection heat transfer in a shell and helical coil heat exchanger using non-newtonian nanofluids. Chem Prod Process Model 15(2):20190058
77. Puspitasari P, Permanasari AA, Shaharun MS, Tsamroh DI (2020) Heat transfer characteristics of NiO nanofluid in heat exchanger. In: AIP conference proceedings, vol 2228, no 1. AIP Publishing
78. Monfared M, Shahsavar A, Bahrebar MR (2019) Second law analysis of turbulent convection flow of boehmite alumina nanofluid inside a double-pipe heat exchanger considering various shapes for nanoparticle. J Therm Anal Calorim 135(2):1521–1532
79. Tian Z, Abdollahi A et al (2019) Turbulent flows in a spiral double-pipe heat exchanger: optimal performance conditions using an enhanced genetic algorithm. Int J Numer Meth Heat Fluid Flow 30(1):39–53
80. Shahsavar A, Godini A, Sardari PT, Toghraie D, Salehipour H (2019) Impact of variable fluid properties on forced convection of Fe_3O_4/CNT/water hybrid nanofluid in a double-pipe mini-channel heat exchanger. J Therm Anal Calorim 137:1031–1043

Application of Hybrid Decision-Making Method in Ranking Polymer Biomaterials for Interim Dental Crowns

Akula Siva Bhaskar and Akhtar Khan

Abstract The main objective of the current study is to rank polymer-based biomaterials used in dental applications using a hybrid multi-criteria decision method (HMCDM), explicitly the fuzzy TOPSIS approach. Seven diverse polymer biomaterials, including polylactic acid (PLA), polycaprolactone (PCL), polylactic-co-glycolic acid (PLGA), poly-methyl-metacrylate (PMMA), acrylonitrile butadiene styrene (ABS), poly ether ether ketone (PEEK), and poly ether ketone ketone (PEKK), were chosen as potential alternatives for the investigation. Ten characteristics, including cost, availability, shore D hardness, melting point, tensile strength, flexural strength, compressive strength, biocompatibility, biodegradability, and Young's modulus, were considered as the main selection criterion. Results revealed that PEKK and PEEK were found to be the best preferential materials for dental interim crowns.

Keywords MCDM · Material selection · Fuzzy TOPSIS · Dental crown

1 Introduction

In industries like the automotive, aerospace, defense, and medical industries, choosing the right material is crucial. This requires a great degree of knowledge. Because inappropriate material choice may result to machinery damage, a great loss in the economy and also a huge influence on human casualties [1, 2]. Since there were not as many materials available in the past, the decision-maker's expertise in the relevant field was heavily weighed while selecting the materials. Recent technological advancements have led to the foundation of a wide variety of materials. This increased the complexity in terms of range, choice, application area, and also converting those materials into final components. Choosing a material for a given

A. Siva Bhaskar (✉) · A. Khan
Indian Institute of Information Technology Design and Manufacturing-Kurnool, Kurnool, Andhra Pradesh 518008, India
e-mail: 319ME0003@iiitk.ac.in

© The Author(s), under exclusive license to Springer Nature Singapore Pte Ltd. 2025

B. B. V. L. Deepak et al. (eds.), *Recent Advancements in Product Design and Manufacturing Systems*, Lecture Notes in Mechanical Engineering,
https://doi.org/10.1007/978-981-97-6732-8_22

application demands thorough understanding of various factors like mechanical, physical, chemical, as well as functional requirements of the material to be selected. Hence, decision-making on the most favorable material from an ample variety of materials considering diverse factors into account is perplexing and trouble-some process [3]. Therefore, to address these technical difficulties, a quantifiable decision support scheme like multi-criteria decision-making (MCDM) method is needed. A potential application of the MCDM method to the problem of material selection is shown in Fig. 1. The most often employed MCDM approaches are analytical hierarchy process (AHP), weighted sum model (WSM), VIekriterijumsko KOmpromisno Rangiranje (VIKOR), Technique for Order Performance by Similarity to Ideal Solution (TOPSIS), Multi-Objective Optimization on the basis of Ratio Analysis (MOORA), elimination and choice translating reality (ELECTRE) and its additional methods, COmplex PRoportional ASsessment (COPRAS), COmbinative Distance-based ASsessment (CODAS), Evaluation based on Distance from Average Solution (EDAS), and preference ranking organization method for enrichment evaluation (PROMETHEE), etc.

Nevertheless, material selection issues have been solved using various MCDM-based techniques, but they have limitations in dealing with issues like rank reversal phenomena and qualitative data and uncertainty [4]. To overcome these limitations, researchers started integrating different MCDM approaches and developed new hybrid multi-criteria decision methods (HMCDM) like AHP-TOPSIS, AHP-VIKOR, AHP-MOORA, etc. [5]. Throughout continuous advancements in techniques, researchers and academicians were able to eliminate rank reversal through new methods like ranking of alternatives through functional mapping of criterion sub-intervals into a single interval (RAFSI) [6]. However, they fell short while handling qualitative variables like good, better, modest, bad, and worst in the decision matrix. At this point, the research community has turned their focus toward the implementation of fuzzy set theory into MCDM approach; thus, the uncertainty in the decision matrix can be resolved enhances the perspective of the decision-maker [7]. The

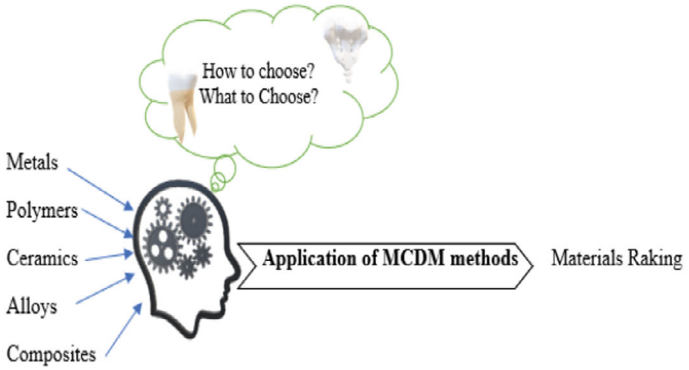


Fig. 1 Application of decision-making in materials

impact of MCDM and HMCDM methods on material selection in a range of industries like manufacturing, energy, construction, automotive, chemical, and medical, etc., is summarized in Table 1.

2 Methodology

2.1 Topsis

Ching-Lai Hwang and Yoon developed the technique for order preference by similarity to ideal solution (TOPSIS) in 1981. The TOPSIS methodology makes use of the idea of closeness to the flawless solution. This method states that the best alternative is one that is close to the positive ideal solution, while the worst alternative is one that is close to the negative ideal solution. The computational process starts with the development of the decision matrix comprising information about alternatives and selection criteria. The most crucial characteristics might be viewed as advantageous and the least advantageous as detrimental. The next stage is to create a normalized decision matrix (NDM), which is then followed by multiplying each criterion's weight to create a weighted NDM. The next step is to identify the ideal negative and positive solutions. The separation between positive and negative ideal solutions must also be determined. Finally, the proximity values must be calculated, and the order of the alternatives must be determined. In general, the best alternative contains the highest relative proximity value and vice versa [41]. Figure 2 shows the framework and step-by-step practice related to the TOPSIS methodology.

2.2 Fuzzy TOPSIS

Dr. Lotfi Zadeh first put forth the idea of a fuzzy set in 1965. The fuzzy set's foundations are derived from set theory. The basic distinction between set theory and fuzzy set theory is how data is represented. For example, consider a binary membership function where the value can be either 0 (no) or 1 (yes). Nonetheless, the fuzzy set has an infinite number of membership functions in the interval [0, 1] for the same binary membership function. This has the advantage that uncertainty can be handled using fuzzy set theory [42]. Thus, decision problems such as material selection, optimal data identification for specific experiments, and multi-criteria decision problems can be more effectively solved using a fuzzy set. In general, four types of fuzzy numbers are commonly available, as listed below:

a. Left–right ordering fuzzy numbers.
b. Trapezoidal fuzzy numbers (TrFN).
c. Gaussian fuzzy numbers (GFN).
d. Triangular fuzzy numbers (TFN).

Table 1 Decision methods used in different applications

Area	Author	Application	Decision method
Automotive	Dev et al. [8]	Automotive component	Entropy-VIKOR
	Manalo and Magdaluyo [9]	Laminated glass interlayer for fuel efficient vehicle	DLM-COPRAS
	Thinh and Mai [10]	Material for transmission rod	PIV and FUCA
	Özakin [11]	Steel sheet	MOORA
	Chami et al. [12]	Corrosion resistance	ELECTRE-I
	Jain et al. [13]	Automotive parts supplier	Fuzzy-based AHP
			TOPSIS
	Jahan et al. [14]	Brake material	MABAC, TOPSIS, CoCoSo
	Gamal and Mohamed [15]	Robot selection	Entropy-MOORA
	Prabhu et al. [16]	Spoiler	PSI
Manufacturing	Pahan et al. [17]	Coating materials	TOPSIS
	Kumar and Kumar [18]	Industrial robot arm	AHP
	Yadav et al. [19]	Tool holder for hard milling	TOPSIS-PSI
	Dhanalakshmi et al. [20]	Pyrolysis process	EDAS, TOPSIS
	Niu et al. [21]	Cutting tool material	COPRAS-G
	Li et al. [22]	Selection of machine tool	Fuzzy DEMATEL
			Entropy VIKOR
	Singh et al. [23]	Hole quality	ARAS, TOPSIS
	Goswami and Behera [24]	Handling equipment	COPRAS-ARAS
	Majumder and Saha [25]	Optimization	MOORA-PCA TOPSIS-PCA
	Abbas et al. [26]	Optimization	Fuzzy TOPSIS
Energy	Venkataramaiah et al. [27]	Solar flat plate collector	AHP
	Shanian and Savadogo [28]	Non-heat treatable cover	AHP
	Martínez Gómez [29]	Tubular packed bed reactor	AHP-TOPSIS, OCRA, ARAS, COPRAS-G
	Rastogi et al. [30]	PCM for domestic heating	Ashby, TOPSIS, and H-TOPSIS
Construction	Do and Kim [31]	Concrete repair	AHP

(continued)

Table 1 (continued)

Area	Author	Application	Decision method
	Ugur and Baykan [32]	Wall material	AHP
	Zhao et al. [33]	Water supply	AHP, GRA(hybrid)
Medical	Bahraminasab and Jahan [34]	Knee joint	VIKOR
	Şenyiğit and Demirel [35]	Dental implant	E-SAW
	Chowdary et al. [36]	Biomaterials	Fuzzy AHP TOPSIS
	Kumar et al. [37]	Making of biocomposite	TOPSIS
Chemical	Dehghan-Manshadi et al. [38]	Material for storing cryogenic fuel	Modified WPM
	Chatterjee et al. [39]		COPRAS EVAMIX(Hybrid)
	Rao and Davim [40]		AHP, TOPSIS

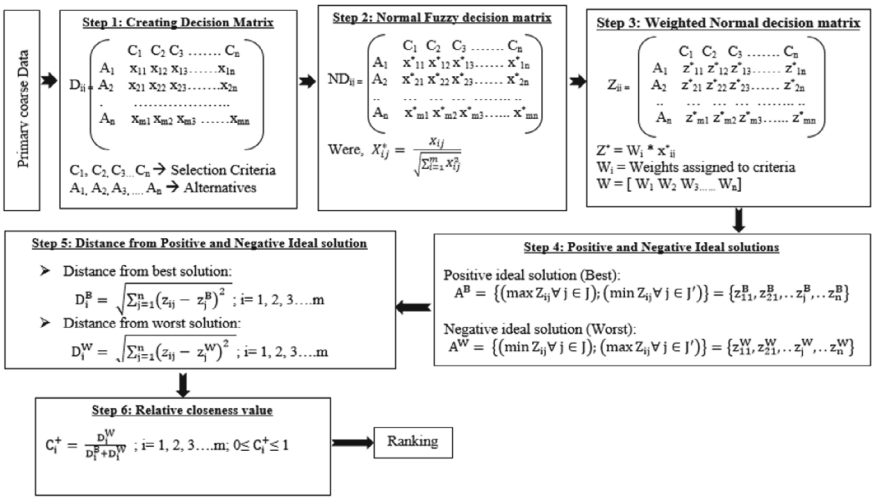


Fig. 2 TOPSIS methodology framework

From above all TFN are most widely used. Equation 1 expresses the membership function of a TFN.

$$\text{Membership function for TFN is, } \mu(z) = \begin{cases} \frac{z-a}{b-a}; & \text{a} \le z \le b \\ \frac{c-z}{c-b}; & \text{b} \le z \le c \\ 0; & \text{otherwise} \end{cases} \tag{1}$$

Consider, $\overline{K} = (X_1, Y_1, Z_1)$ and $\overline{L} = (X_2, Y_2, Z_2)$ are two triangular fuzzy numbers; then, the resultant of arithmetic operations of those two is also a TFN. Following equations through some insight about arithmetic operations on two fuzzy numbers.

i. Fuzzy numbers addition:

$$\overline{K} + \overline{L} = (X_1 + X_2, Y_1 + Y_2, Z_1 + Z_2) \tag{2}$$

ii. Fuzzy numbers subtraction:

$$\overline{K} - \overline{L} = (X_1 - X_2, Y_1 - Y_2, Z_1 - Z_2) \tag{3}$$

iii. Fuzzy numbers multiplication

$$\overline{K} * \overline{L} = (X_1 * X_2, Y_1 * Y_2, Z_1 * Z_2) \tag{4}$$

iv. Distance between them can be calculated from:

$$D(\overline{K}, \overline{L}) = \sqrt{\frac{1}{3}\left[(X_1 - X_2)^2 + (Y_1 - Y_2)^2 + (Z_1 - Z_2)^2\right]} \tag{5}$$

Chen embedded fuzzy concepts into TOPSIS methodology and reformed it to Fuzzy TOPSIS (FTOPSIS). To create a fuzzy decision matrix, the first step in the FTOPSIS process is to give each qualitative variable in the decision matrix a fuzzy number. Then, based on a fuzzy linguistic scale, assign weights to the criteria in the decision matrix. Weighted fuzzy normalized decision matrix and fuzzy normal decision matrix are further modifications of the fuzzy decision matrix. Ultimately, the alternatives are ranked based on the computation of fuzzy positive and fuzzy negative closeness values. The ability of TOPSIS to handle uncertainty in decision-making has increased since fuzzy was associated with it. [43].

3 FTOPSIS Application for Crown Material Selection

Materials used in the fields of manufacturing, automotive, construction, aerospace, and medical industries have their unique functional requirements. In general, biomaterials can be used to make medical devices for complex surgeries and implants, joint surgeries, bone plates, etc., as well as temporary or permanent replacements for human body parts. These materials, which are classified as biomaterials, are widely utilized in a number of biomedical engineering applications as well as in the fields of oral and maxillofacial surgery, orthopedics, cardiology, and tissue engineering, among other medical specialties. Biomaterials fall into three categories:

alloys, metals, and polymers. [44]. However, not all of them can be used as biomaterials. Commercial metals like stainless steel, titanium (Ti), zirconium (Zr), vanadium, and their alloys have already proven their superiority in overall medical as well as in dentistry [45]. All the restorations and implants made out of these materials have long-term reliability. In recent days, polymer-based biomaterials are getting more popular as interim restorations (temporary crowns) in dental applications due to their cost effective and easier to manufacture at the chairside of the doctor [45, 46]. Hence, for the current material selection study, seven polymer-based interim dental restoration materials, namely PLA, PCL, PLGA, PMMA, ABS, PEEK, and PEKK (M-I, M-II, M-III, M-IV, M-V, M-VI, and M-VII) were identified as competitors. A MCDM approach in fuzzy environment has been exploited to identify the most suitable polymer material for temporary dental crowns. Ten different criteria have been used to evaluate these seven materials, namely: biodegradability, shore D hardness, flexural strength, compression strength, tensile strength, Young's modulus, biocompatibility, cost of the material, and availability of the material. Out of the ten criteria listed above, the first seven are beneficial and the final three are non-beneficial [46]. Table 2 summarizes decision matrix framed through the nominated alternatives along with their corresponding criterion for the material selection problem.

All of the decision matrix's quantitative and qualitative data have now been converted into fuzzy numbers by introducing the fuzzy concept. This is achieved by assigning corresponding triangular fuzzy numbers (TFN) to both alternatives and criteria, respectively. Table 3 presents the assigned TFN for each alternative and corresponding weights to criteria. Consider, the biocompatibility data of the first material (PCL) in DM, its corresponding language grade is Very Good (VG) and the biodegradability Very Good (VG). Also, reliable language labels were assigned to the remaining criteria. Table 4 displays the fuzzy decision matrix's linguistic notation. Next, the fuzzy decision matrix's linguistic notations were updated to include the necessary TFN. As an illustration, for PCL, the language notation for biocompatibility is VG and the associated TFN (7, 9, 10). Also, Young's modulus is VVB

Table 2 Decision matrix for the material selection [46]

	Beneficial criteria							Non-beneficial criteria		
Material	C-I	C-II	C-III	C-IV	C-V	C-VI	C-VII	C-VIII	C-IX	C-X
M-I	Acceptable	60	0.34	16	19	1.4	55	Very good	10,000	Average
M-II	Moderate	190	3	60	108	94	88	Very good	6,000	Freely
M-III	Moderate	160	2.4	5.3	85	42	70	Very good	10,000	Average
M-IV	Acceptable	160	1.6	65	90	92	96	Modest	20,000	Average
M-V	Bad	240	2.9	46	75	65	100	Modest	6,000	Freely
M-VI	Exceptional	360	4	105	185	170	95	Bad	30,000	Tough
M-VII	Exceptional	380	5.1	115	200	246	25	Bad	30,000	Tough

and the applicable TFN is (0, 0, 1). The fuzzy decision matrix will be completed by following a similar process for the remaining criteria. The fuzzy decision matrix was then transformed into a normalized version. Using the equation provided in step 3 of Fig. 2, the normalized values of the fuzzy decision matrix were determined.

An example of PCL calculation: the obtained TFN for biocompatibility is (7, 9, 10), i.e., $l = 7, m = 9, n = 10$, and then, its corresponding normalized values are $\left(\frac{l}{n^+}, \frac{m}{n^+}, \frac{n}{n^+}\right) = (0.7, 0.9, 1)$. Also, for continuing criteria, TFN was also transmuted into desired normalized values. The equivalent TFN of NDM was multiplied with the weights allocated to each criterion. For model calculation, regarding PCL, the acquired NDM value is (0.7, 0.9, 1) and its subsequent weightage for biocompatibility is (0.9, 1, 1) obtained from Table 3. Now, multiplying the weightage to NDM value, the resultant WNDM value is (0.63, 0.9, 1). Comparably carryout the same process for outstanding criteria and create necessary weighted normalized decision matrix. The positive and negative ideal solutions, as well as the WNDM, are given in Table 5. Equations given in step 5 of the TOPSIS framework were then used to calculate the distance between the best and worst solutions. When examining the PCL alternative for a sample, the distance from the positive ideal solution

Table 3 Linguistics assigned to alternatives and weights assignment to criteria

Linguistic notation	TFN	Criteria	Linguistic notation	TFN
Very very bad (VVB)	(0, 0, 1)	B.C	Exceptional (E)	(0.9, 1, 1)
Very BAD (VB)	(0, 1, 3)	B.D	Good (Gd)	(0.5, 0.7, 0.9)
Bad	(1, 3, 5)	M.P	Good (Gd)	(0.5, 0.7, 0.9)
Moderate (Mo)	(3, 5, 7)	Y.M	Acceptable (Ac)	(0.7, 0.9, 1)
Good (Gd)	(5, 7, 9)	T.S	Acceptable (Ac)	(0.7, 0.9, 1)
Acceptable (Ac)	(7, 9, 10)	F.S	Acceptable (Ac)	(0.7, 0.9, 1)
Excellent (Ex)	(9, 1, 10)	C.S	Acceptable (Ac)	(0.7, 0.9, 1)
		S.D	Acceptable (Ac)	(0.7, 0.9, 1)
		Cost	Moderate (Mo)	(0.3, 0.5, 0.7)
		Avail	Moderate (Mo)	(0.3, 0.5,0.7)

Table 4 Linguistic notation decision matrix

Material	C-I	C-II	C-III	C-IV	C-V	C-VI	C-VII	C-VIII	C-IX	C-X
M-I	Ac	VVB	VVB	VVB	VVB	VVB	Bd	Ac	Ac	Gd
M-II	Mo	Bd	Gd	Mo	Mo	Bd	Ac	Ac	Ex	Ac
M-III	Mo	Bd	M	VVB	Bd	VB	Gd	Ac	Ac	Gd
M-IV	Gd	Bd	Bd	Mo	Bd	Bad	Ex	Mo	Bd	Gd
M-V	Bad	Mo	Mo	Bd	Bd	VB	Ex	Mo	VVG	Ac
M-VI	Ex	Ex	Ex	Ex	Ex	Gd	Ex	Bd	Mo	Bd
M-VII	Ex	Ex	Ex	Ex	Ex	Ex	Ex	Bd	Mo	Bd

is calculated as: $\left[\sqrt{\frac{1}{3}\left[(0.63-1)^2+(0.9-1)^2+(1-1)^2\right]}=0.221\right]$. Correspondingly, for each criterion, the positive idea solutions were obtained as (0.221, 0.871, 0.967, 0.967, 0.967, 0.967, 0.741, 0.816, 0.639, 0.620). Then, the summation of all individual distances gives the distance from the positive ideal solution, and for PCL, it is 7.781. Similarly, the calculation of distance from the negative ideal solution for first criteria is given as $\left[\sqrt{\frac{1}{3}\left[(0.63-0)^2+(0.9-0)^2+(1-0)^2\right]}=0.769\right]$, and for the remaining all criteria were determined as (0.769, 0.051, 0.057, 0.057, 0.057, 0.057, 0.273, 0.046, 0.041, 0.067), 1.482, the remoteness from the undesirable solution of the PCL alternative, is the result of later adding all of these values. Also, for all the outstanding alternatives, the best and worst values were calculated and tabulated. For instance, consider PCL, closeness value is calculated as 0.160. As well, compute the closeness value for all leftover alternatives. In conclusion, Table 6 displays the alternate with the lowermost closeness value that was noted with the bottommost ranking and the alternate with the peak closeness value that was identified and labeled with the highest rank.

4 Conclusions

In dental applications, several criteria are used to select the best alternative material from available options in decision-making and material prioritization. For this reason, the ideal material selection for temporary dental restorations was proposed using FTOPSIS, a hybrid MCDM technique. After successfully applying the previously mentioned HMCDM technique, it leads to the following inferences. From Table 6, the following conclusion can be drawn:

i. Of all the substitute materials, PEKK has the highest closeness value. In light of the performance parameters examined in this study, PEKK can be deemed the material of choice of greatest significance for temporary dental applications. It might be attributed to its excellent biocompatibility and exceptional mechanical properties which makes it the top choice of material. Nonetheless, the preference order of the selected biomaterials is as follows: PEKK > PEEK > PMMA > PLA > ABS > PLGA > PCL.
ii. PEEK is the second-best choice material for the same application since, no considerable difference between PEKK and PEEK was identified during the study, both the materials belong to a common family namely poly-aryl-ether-ketone (PAEK) [47, 48].
iii. In addition to PEKK and PEEK, PMMA can be recommended as the third best choice of material followed by PLA. Even though ABS has poor biocompatibility, because of its excellent mechanical properties, it has taken fifth position by surpassing PLGA and PCL.

Table 5 Fuzzy-based WNDM

Material	C-I	C-II	C-III	C-IV	C-V	C-VI	C-VII	C-VIII	C-IX	C-X
M-I	(0.63, 0.9, 1)	(0, 0, 0.09)	(0, 0, 0.1)	(0, 0, 0.1)	(0, 0, 0.1)	(0, 0, 0.1)	(0.07, 0.27, 0.5)	(0.05, 0.077, 0.126)	(0.03, 0.055, 0.098)	(0.033, 0.07, 0.14)
M-II	(0.27, 0.5, 0.7)	(0.05, 0.21, 0.45)	(0.35, 0.63, 0.9)	(0.21, 0.45, 0.7)	(0.21, 0.45, 0.7)	(0.07, 0.27, 0.5)	(0.49, 0.81, 1)	(0.05, 0.077, 0.126)	(0.03, 0.05, 0.077)	(0.03, 0.055, 0.098)
M-III	(0.27, 0.5, 0.7)	(0.05, 0.21, 0.45)	(0.21, 0.45, 0.7)	(0, 0, 0.1)	(0.07, 0.27, 0.5)	(0, 0.09, 0.3)	(0.35, 0.63, 0.9)	(0.05, 0.077, 0.126)	(0.03, 0.055, 0.098)	(0.033, 0.07, 0.14)
M-IV	(0.45, 0.7, 0.9)	(0.05, 0.21, 0.45)	(0.07, 0.27, 0.5)	(0.21, 0.45, 0.7)	(0.07, 0.27, 0.5)	(0.07, 0.27, 0.5)	(0.63, 0.9, 1)	(0.07, 0.14, 0.297)	(0.06, 0.165, 0.7)	(0.033, 0.07, 0.14)
M-V	(0.09, 0.3, 0.5)	(0.15, 0.35, 0.63)	(0.21, 0.45, 0.7)	(0.07, 0.27, 0.5)	(0.07, 0.27, 0.5)	(0, 0.09, 0.3)	(0.63, 0.9, 1)	(0.07, 0.14, 0.297)	(0.03, 0.05, 0.077)	(0.03, 0.055, 0.098)
M-VI	(0.81, 1, 1)	(0.45, 0.7, 0.9)	(0.49, 0.81, 1)	(0.63, 0.9, 1)	(0.63, 0.9, 1)	(0.45, 0.6, 0.9)	(0.63, 0.9, 1)	(0.1, 0.231, 0.9)	(0.042, 0.1, 0.231)	(0.06, 0.165, 0.7)
M-VII	(0.81, 1, 1)	(0.45, 0.7, 0.9)	(0.63, 0.9, 1)	(0.63, 0.9, 1)	(0.63, 0.9, 1)	(0.63, 0.9, 1)	(0.63, 0.9, 1)	(0.1, 0.231, 0.9)	(0.042, 0.1, 0.231)	(0.06, 0.165, 0.7)
Ideal positive	(1, 1, 1)	(0.9, 0.9, 0.9)	(1, 1, 1)	(1, 1, 1)	(1, 1, 1)	(1, 1, 1)	(1, 1, 1)	(0.05, 0.05, 0.05)	(0.03, 0.03, 0.03)	(0.03, 0.03,0.03)
Ideal negative	(0.09, 0.09, 0.09)	(0, 0, 0)	(0, 0, 0)	(0, 0, 0)	(0, 0, 0)	(0, 0, 0)	(0.07, 0.07, 0.07)	(0.9, 0.9, 0.9)	(0.7, 0.7, 0.7)	(0.7, 0.7, 0.7)

Table 6 Overall ranking of the materials

Material	Best	Worst	Closeness	Rank
PCL	7.781	1.482	0.160	7
PLA	5.982	3.558	0.384	4
PLGA	6.905	2.546	0.275	6
PMMA	5.916	3.800	0.410	3
ABS	6.472	3.041	0.328	5
PEEK	3.434	6.555	0.708	2
PEKK	3.165	6.799	0.734	1

iv. Finally, PLGA and PCL secured sixth and seventh positions, respectively, due to their lower mechanical properties. But when it comes to the best choice among ABS, PLGA and PCL for dental applications PLGA and PCL were preferred to ABS [49].

Declaration of Interests The authors declare that there is no possibility that the work presented in this study could have been influenced by relationships or known competing financial interests.

Ethical None of the authors of this article have conducted studies on humans or animals.

Conflict of Interest The authors have disclosed no competing interests.

Funding The authors certify that they received no grants, funds, or other forms of support for the preparation of this manuscript.

References

1. Koons GL, Diba M, Mikos AG (2020) Materials design for bone-tissue engineering. Nat Rev Mater 5(8):584–603
2. Zhang L, Yang G, Johnson BN, Jia X (2019) Three-dimensional (3D) printed scaffold and material selection for bone repair. Acta Biomater 15(84):16–33
3. Pitchaiah DS, Hussaian M, Govardhan D (2021) A review on multi attribute decision making for evaluation and selection of supplier for materials. Mater Today: Proc 1(39):296–300
4. Chowdhury P, Paul SK (2020) Applications of MCDM methods in research on corporate sustainability: a systematic literature review. Manag Environ Q: Int J 31(2):385–405
5. Kazimieras Zavadskas E, Antucheviciene J, Adeli H, Turskis Z (2016) Hybrid multiple criteria decision making methods: a review of applications in engineering. Scientia Iranica 23(1):1–20
6. Žižović M, Pamučar D, Albijanić M, Chatterjee P, Pribićević I (2020) Eliminating rank reversal problem using a new multi-attribute model—the RAFSI method. Mathematics 8(6):1015
7. Falak J, Kunjan M, Nagaraju D, Narayanan S (2020) Evaluation of continuous improvement techniques using hybrid MCDM technique under fuzzy environment. Mater Today: Proc 1(22):1295–1305
8. Dev S, Aherwar A, Patnaik A (2020) Material selection for automotive piston component using entropy-VIKOR method. SILICON 12(1):155–169
9. Manalo MV, Magdaluyo Jr ER (2018) Integrated DLM-COPRAS method in materials selection of laminated glass interlayer for a fuel-efficient concept vehicle. In: Proceedings of the world congress on engineering 2018, vol 2. International Association of Engineers London
10. Thinh HX, Mai NT (2023) Comparison of two methods in multi-criteria decision-making: application in transmission rod material selection. EUREKA: Phys Eng 30(6):59–68
11. Özakin B (2022) An application for the selection of steel sheet materials used in automotive construction with the MOORA method. Int J Automotive Eng Technol 11(3):91–95
12. Chami A, El Haji M, Benabbou R, Rais Z, Taleb M (2020) Electre multi-criteria analysis for choosing material concerned by the corrosion problem in automotive industry. J Appl Sci Environ Stud 3(3):3
13. Jain V, Sangaiah AK, Sakhuja S, Thoduka N, Aggarwal R (2018) Supplier selection using fuzzy AHP and TOPSIS: a case study in the Indian automotive industry. Neural Comput Appl 29:555–564
14. Jahan F, Soni M, Wakeel S, Ahmad S, Bingol S (2022) Selection of automotive brake material using different MCDM techniques and their comparisons. J Eng Sci Technol Rev 15(1)

15. Gamal A, Mohamed M (2023) A hybrid MCDM approach for industrial robots selection for the automotive industry. Neutrosophic Syst Appl 8(4):1–1
16. Prabhu SR, Ilangkumaran M, Mohanraj T (2020) 3D Printing of automobile spoilers using MCDM techniques. Mater Test 62(11):1121–1125
17. Pahan F, Dambhare S, Mali A, Nawale S (2018) Implementation of multi-criteria decision making for selection of coating material on AISI 4140 steel. Int Res J Eng Technol 5(12):1514–1517
18. Kumar A, Kumar M (2019) Implementation of analytic hierarchy process (AHP) as a decision-making tool for selection of materials for the robot arm. Int J Appl Eng Res 14(11):2727–2733
19. Yadav S, Pathak VK, Gangwar S (2019) A novel hybrid TOPSIS-PSI approach for material selection in marine applications. Sādhanā 44(3):58
20. Dhanalakshmi CS, Madhu P, Karthick A, Mathew M, Vignesh Kumar R (2020) A comprehensive MCDM-based approach using TOPSIS and EDAS as an auxiliary tool for pyrolysis material selection and its application. In: Biomass conversion and biorefinery
21. Niu J, Huang C, Li C, Zou B, Xu L, Wang J, Liu Z (2020) A comprehensive method for selecting cutting tool materials. Int J Adv Manuf Technol 110:229–240
22. Li H, Wang W, Fan L, Li Q, Chen X (2020) A novel hybrid MCDM model for machine tool selection using fuzzy DEMATEL, entropy weighting and later defuzzification VIKOR. Appl Soft Comput 1(91):106207
23. Singh RP, Tyagi M, Kataria R (2019) Selection of the optimum hole quality conditions in manufacturing environment using MCDM approach: a case study. In: Operations management and systems engineering: select proceedings of CPIE 2018 2019. Springer Singapore, pp 133–152
24. Goswami SS, Behera DK (2021) Solving material handling equipment selection problems in an industry with the help of entropy integrated COPRAS and ARAS MCDM techniques. Proc Integr Optim Sustain 5(4):947–973
25. Majumder H, Saha A (2018) Application of MCDM based hybrid optimization tool during turning of ASTM A588. Decision Sci Lett 7(2):143–156
26. Abbas AT, Sharma N, Anwar S, Luqman M, Tomaz I, Hegab H (2020) Multi-response optimization in high-speed machining of Ti-6Al-4V using TOPSIS-fuzzy integrated approach. Materials 13(5):1104
27. Venkataramaiah P, Rohith B, MohanaReddy P (2012) Material selection for solar flat plate collectors using AHP. Int J Eng Res Appl 2:1181–1185
28. Shanian AA, Savadogo O (2006) A material selection model based on the concept of multiple attribute decision making. Mater Des 27(4):329–337
29. Martínez Gómez J, Material Selection using Multi-criteria decision making methods (MCDM) for design a multi-tubular packed-bed Fischer-Tropsch reactor (MPBR)
30. Rastogi M, Chauhan A, Vaish R, Kishan A (2015) Selection and performance assessment of phase change materials for heating, ventilation and air-conditioning applications. Energy Convers Manage 1(89):260–269
31. Do JY, Kim DK (2012) AHP-based evaluation model for optimal selection process of patching materials for concrete repair: focused on quantitative requirements. Int J Concr Struct Mater 6(2):87–100
32. Ugur LO, Baykan U (2017) A model proposal for wall material selection decisions by using analytic hierarchy process (AHP). Acta Phys Pol, A 132(3):577–579
33. Zhao R, Su H, Chen X, Yu Y (2016) Commercially available materials selection in sustainable design: an integrated multi-attribute decision making approach. Sustainability 8(1):79
34. Bahraminasab M, Jahan A (2011) Material selection for femoral component of total knee replacement using comprehensive VIKOR. Mater Des 32(8–9):4471–4477
35. Şenyiğit ER, Demirel B (2018) The selection of material in dental implant with entropy based simple additive weighting and analytic hierarchy process methods. Sigma: J Eng Nat Sci/ Mühendislik ve Fen Bilimleri Dergisi 36(3)
36. Chowdary Y, Ram VS, Nikhil EV, Krishna PN, Nagaraju D (2016) Evaluation and prioritizing of biomaterials for the application of implantation in human body using fuzzy AHP and topsis 12(1n):21

37. Kumar JS (2021) Multiple decision criterion for material selection by using ranking system. Turkish J Comput Math Educ (TURCOMAT) 12(12):01–06
38. Dehghan-Manshadi B, Mahmudi H, Abedian A, Mahmudi R (2007) A novel method for materials selection in mechanical design: combination of non-linear normalization and a modified digital logic method. Mater Des 28(1):8–15
39. Chatterjee P, Athawale VM, Chakraborty S (2011) Materials selection using complex proportional assessment and evaluation of mixed data methods. Mater Des 32(2):851–860
40. Rao RV, Davim JP (2008) A decision-making framework model for material selection using a combined multiple attribute decision-making method. Int J Adv Manuf Technol 35(7):751–760
41. Çelikbilek Y, Tüysüz F (2020) An in-depth review of theory of the TOPSIS method: an experimental analysis. J Manag Anal 7(2):281–300
42. Kahraman C, Öztayşi B, Çevik OS (2016) A comprehensive literature review of 50 years of fuzzy set theory. Int J Comput Intell Syst 9(sup1):3–24
43. Palczewski K, Sałabun W (2019) The fuzzy TOPSIS applications in the last decade. Procedia Comput Sci 1(159):2294–2303
44. Babaie E, Bhaduri SB (2018) Fabrication aspects of porous biomaterials in orthopedic applications: a review. ACS Biomater Sci Eng 4(1):1–39
45. Iftikhar S, Jahanzeb N, Saleem M, ur Rehman S, Matinlinna JP, Khan AS (2021) The trends of dental biomaterials research and future directions: a mapping review. Saudi Dental J 33(5):229
46. Bhaskar AS, Khan A (2022) Comparative analysis of hybrid MCDM methods in material selection for dental applications. Expert Syst Appl 15(209):118268
47. Zhao Y, Zhao K, Li Y, Chen F (2020) Mechanical characterization of biocompatible PEEK by FDM. J Manuf Proc 1(56):28–42
48. Alqurashi H, Khurshid Z, Yaqin SA, Habib SR, Rokaya D, Zafar MS (2020) Polyetherketoneketone (PEKK): an emerging biomaterial for oral implants and dental prostheses. J Adv Res
49. AL-Rabab'ah M, Hamadneh WA, Alsalem I, Khraisat A, Abu Karaky A (2019) Use of high performance polymers as dental implant abutments and frameworks: a case series report. J Prosthodontics 28(4):365–72

Analysis on Mechanical Properties of Aluminium MMC with Graphite and Boron Nitride Powder



Neelapu Madhu Latha and I. N. Niranjan Kumar

Abstract Aluminium alloys continue to be a popular choice in the automotive, naval building, and aviation industries due to their superior corrosion and wear resistance in comparison with conventional metals and alloys, as well as their favourable mechanical characteristics, low density, as well as low coefficient of thermal expansion. Furthermore, composites have attracted substantial attention due to their adaptability in a variety of technological applications, as well as their cost-effective manufacture and increased mechanical properties. Researchers used varying particle proportions in the composite mixture to develop metal matrix composites composed of aluminium. The fundamental goal of this present study is to create aluminium-based metal matrix composite materials, particularly by employing the stir casting technique and the UNSA92618 supplemented with boron nitride and graphite. The created specimens were tested for hardness, compressive along with tensile strengths, in addition to XRD, SEM, and also optical microscope analyses, to evaluate the characteristics of the metal matrix.

Keywords MMC · UNS A92618 · Mechanical characteristic · BN · And Gr

1 Introduction

Aluminium alloys have gotten a lot of interest from manufacturers and designers over the last few decades because of its exceptional properties, including low density, affordability, and a high ratio of strength to weight [1]. These alloys have a wide range of technical uses, including the automotive, aerospace, along with biomedical

N. Madhu Latha (✉)
Department of Mechanical Engineering, College of Engineering, Dr. B. R. Ambedkar University, Srikakulam, India
e-mail: neelapu.madhulatha@yahoo.in

I. N. Niranjan Kumar
Department of Marine Engineering, Andhra University College of Engineering, Vishakapatnam, India

© The Author(s), under exclusive license to Springer Nature Singapore Pte Ltd. 2025

B. B. V. L. Deepak et al. (eds.), *Recent Advancements in Product Design and Manufacturing Systems*, Lecture Notes in Mechanical Engineering,
https://doi.org/10.1007/978-981-97-6732-8_23

sectors [2]. However, it is crucial to remember that, despite their remarkable qualities, aluminium alloys are not especially successful in corrosion and wear applications. Because the wear along with corrosion properties of engineering materials have a substantial influence on component effectiveness and durability, they should be carefully studied in the creation of components for engineering [3].

MMCs, or metal matrix composites, became known as a notable alternative for improving the mechanical as well as wear characteristics of aluminium alloys by generating a homogeneous structure containing refined grains to meet these difficulties [4, 5]. MMCs are well-known for their high hardness, abrasion resistance, as well as their light weight [6]. They are strong, corrosion resistant, wear resistant, fatigue resistant, stiff, and have other desired features [7]. These composites consist of a mixture of numerous elements, particularly metals or alloys that are to produce certain properties which metals in their pure form or alloys cannot supply alone [8]. MMCs are often made up of fibres, whiskers, or particles that are scattered inside a metallic matrix [9]. MMCs are manufactured using a variety of processes, such stir casting, centrifugal moulding, powder metallurgy, compensating casting, infiltration, or in squeeze casting, among others [10–14]. Powder metallurgy along with stir casting have proven to be the most often used procedures [15]. Recent research has concentrated on aluminium matrix composites (AMCs) and several testing with magnesium matrix composite (Mg-MMCs) [16].

2 Experiment Details

2.1 Materials

The aim of this research was to create a matrix of metal composite utilising aluminium UNSA92618 being the base material and reinforcements made of boron nitride as well as graphite powder. The aluminium alloy was split into tiny ingots which were able to be easily inserted into the furnace to aid the melting process.

2.1.1 Aluminium UNS A92618

Because of its beneficial properties, such as outstanding corrosion resistance, excellent electrical as well as thermal insulation, low density, as well as machinability, aluminium UNS A92618 distinguishes out as a notable matrix material of metal matrix composites. Through the introduction of extra particles, the mechanical characteristics of this alloy may be improved. Aluminium oxide, silicon carbides, silicon dioxide, graphite, and boron nitride, along with boron carbide are common reinforcements for this alloy.

2.1.2 Boron Nitride (BN)

Boron nitride is well-known for its outstanding hardness as well as heat and chemical resistance. Boron nitride particles having particle sizes that range from 7 to 11 microns was employed in this investigation. The sort of boron nitride used was HCV, a critical grade required for the manufacturing of numerous sophisticated products.

2.1.3 Graphite (Gr)

Because of its laminar structure, graphite improves the anti-friction qualities of the composite, essentially acting in the role of self-lubricating reinforcement. Furthermore, the addition of graphite to the matrix improves the accuracy of the composite. For these goals, graphite particles having a particle size measuring 260 microns were used in this investigation.

2.1.4 Composite Preparation

Metal matrix components are prepared using the stir casting process. To achieve homogeneous dispersion of the reinforcing elements inside the metal matrix, a vortex is created within the molten metal. The reinforcing particles Bn (boron nitride) along with Gr (graphite) are mixed using the base material UNS A92618 to create the hybrid metal matrix composite. The technique begins with 600 g of aluminium alloy being placed inside a graphite crucible, which then undergoes heating inside a high temperatures electric furnace. In the electric furnace, the aluminium alloy has been heated beyond its melting point (650 °C) for one hour. At the same time, the particles that reinforce Bn and Gr undergo heating to 450–550 °C to eliminate any moisture content.

After melting the aluminium alloy, a mechanical stirrer serves to stir up the molten metal at speeds that vary from 550 to 1100 RPM. The Bn as well as Gr particles are progressively injected through the molten metal as well as continually spun inside the vortex phase throughout this stirring procedure. The stirring rate is raised after a consistent 5-min period. The heated metal is subsequently allowed to cool down and also solidify inside a prepared mould, yielding the casting material (Fig. 1).

Heat treatment is performed on the casting with composite ingots in a muffle furnace. The ingots are meticulously heated to an exact temperature of 535 °C, employing a 1.5 °C precision level. Following that, the composite material is subjected to a water treatment procedure to complete the treatment phase, following that it is matured for 7 h at 160 °C. Following the completion of the heat treatment procedure, the casting materials is processed to the requisite standards for testing.

Four sets of specimens are created using the aforementioned process. As shown in the samples, these examples are made of UNS A92618 alloy having various weight proportions on BN along with Gr (Table 1).



Fig. 1 Stir casting process

Table 1 Samples with percentages in composition

	UNS A92618 (%)	Bn (%)	Gr (%)
Sample A	100	0	0
Sample B	96	3	1
Sample C	94	5	1
Sample D	92	7	1

2.2 Mathematical Modelling

Equations (1)–(3) depict the mathematical relationships governing the ultimate tensile strength, microhardness, and compressive strength. In these models, the coefficients linked to components A, B, and C exhibit positive values. A signifies the proportion of UNS A92618, B denotes the percentage of Bn, and C stands for the percentage of Gr. Through these coefficients, experimental findings have been utilised to establish correlation equations representing the tensile strength, compressive strength, and hardness.

The equation for calculating the tensile strength (TS) is as follows:

$$\begin{aligned} \mathrm{TS(tensile\,strength)} = {} & 98.3 + 25.4\,\mathrm{A} + 25.4\,\mathrm{B} + 25.4\,\mathrm{C} + 24.9\,\mathrm{AB} + 24.9\,\mathrm{AC} \\ & + 24.9\,\mathrm{BC} + 25.4\,\mathrm{A2} + 24.9\,\mathrm{B2} + 24.9\,\mathrm{C2} \end{aligned} \tag{1}$$

The equation for calculating the compressive strength (CS) is as follows:

$$\begin{aligned} \mathrm{CS(compressive\,strength)} = {} & 102.9 + 26.3\,\mathrm{A} + 25.5\,\mathrm{B} + 27.3\,\mathrm{C} + 10.13\,\mathrm{AB} \\ & + 24\,\mathrm{AC} + 18.1\,\mathrm{BC} + 12.88\,\mathrm{A2} + 24\,\mathrm{B2} + 31.22\,\mathrm{C2} \end{aligned} \tag{2}$$

The equation for calculating the hardness (HD) is as follows:

$$\begin{aligned}\text{HD(Hardness)} = {} & 94.3 + 33\,\text{A} + 28.2\,\text{B} + 28.1\,\text{C} + 9.39\,\text{AB} + 26.2\,\text{AC} \\ & + 18.2\,\text{BC} + 15.8\,\text{A2} + 23.9\,\text{B2} + 26.9\,\text{C2} \end{aligned} \quad (3)$$

2.3 Testing Methods

Five distinct processes are used to test the composite specimen. The four categories include hardness testing, tensile strength testing, compressive testing, and XRD, SEM, along with optical microscopy tests.

2.3.1 Tensile Testing

An EDM cutting device is used to manufacture a tensile sample for testing. The specimen for tensile testing is produced in accordance with ASTM E8 criteria. The specimen is 100 mm in length along with 5 mm in thickness. The specimen's exact specs and drawing are supplied Fig. 2.

Following the selection of measurements, the rectangular sample is then sliced into dumbbell form using an EDM cutting machine. The cutting machinery is seen Fig. 3.

Several steps are involved in the method of cutting tensile specimens employing an EDM cutting machine, which includes developing the sample via a CAD programme, developing the material, putting it on the EDM device, setting up the machine based to its specifications of the design, doing the cutting by employing electrical discharges, and then cleaning and removing the finished specimen. This technology is well-known for its speed, accuracy, and capacity of cutting complicated forms, making it an appealing option for material testing for analysing mechanical qualities under stress.

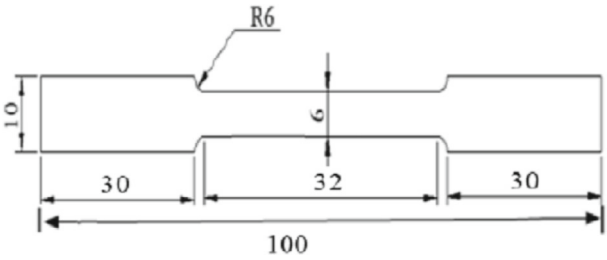


Fig. 2 Specimen dimension



Fig. 3 EDM cutting machine

The specimen is 100 mm long and conforms to ASTM E 08 criteria. The sample's maximal tensile strengths (UTS) was evaluated utilising a computerised universal testing device.

The following are the final tensile specimens' specifications (Fig. 4):

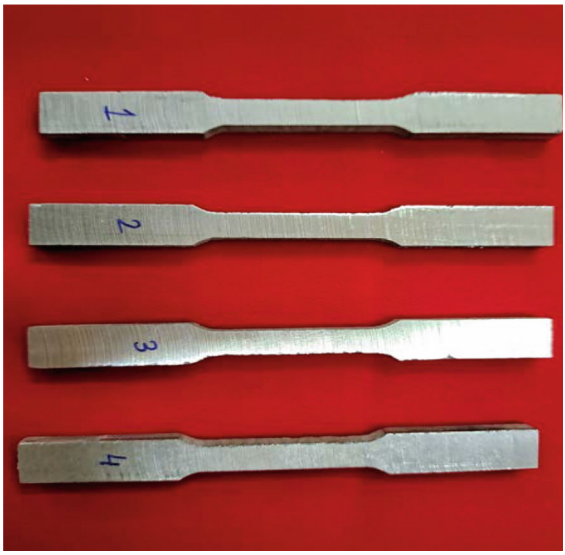


Fig. 4 Tensile testing specimens

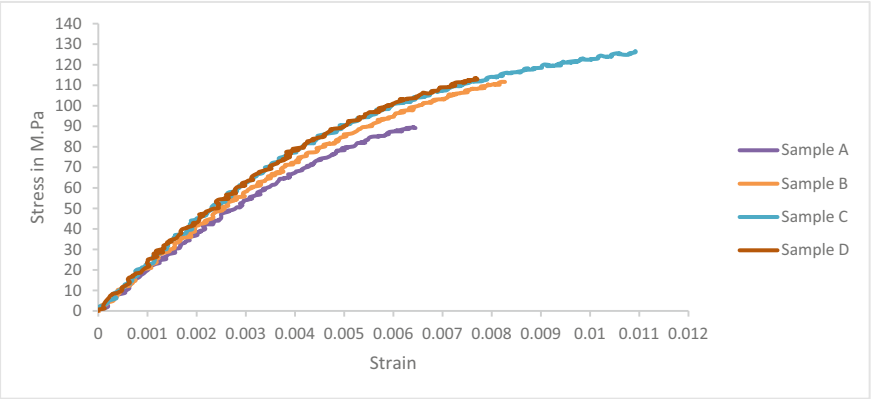


Fig. 5 Stress and strain curve for different specimen

2.3.2 Testing of Composites

The specimens were polished using different supplies including emery paper, aluminium paste, along with diamond paste throughout the preparation process. They were then etched via Keller's reagents and viewed using an optical microscope. The water displacement method was used to estimate the density of both basic metals and diverse composite compositions. Vickers testing for hardness was performed to determine the hardness of the basic metal as well as the composites. Tensile and compressive tests were performed in accordance with ASTM standards using a universal tests machine (UTM) to determine tensile strength and % elongation (Fig. 5).

The graphic above depicts a stress–strain curve in addition to its connection, where the x-axis represents tensile strain and the y-axis represents tensile stress for all specimens (Fig. 6).

Based on tests performed using a UTM testing instrument, the graph above demonstrates the effect of reinforcements on high metal matrix composite (HMMC) samples. The findings were collected and shown on a graph, demonstrating clearly that increasing the reinforcement % leads to increased strength. After a total of eight per cent reinforcement, a strength in 159.67 MPa was obtained.

2.3.3 Compressive Testing

A UTM is used for compression testing, and cylindrical samples are created for this purpose. These samples are 12 mm tall and 8 mm in diameter. They are precisely manufactured on a lathe machine in accordance with ASTM E9 specimen measurements. The specimens are shown in Figs. 7 and 8.

The graph shown here depicts compressive strength across multiple samples. While there is just no reinforcement at all (0%), and the compressive strength equals

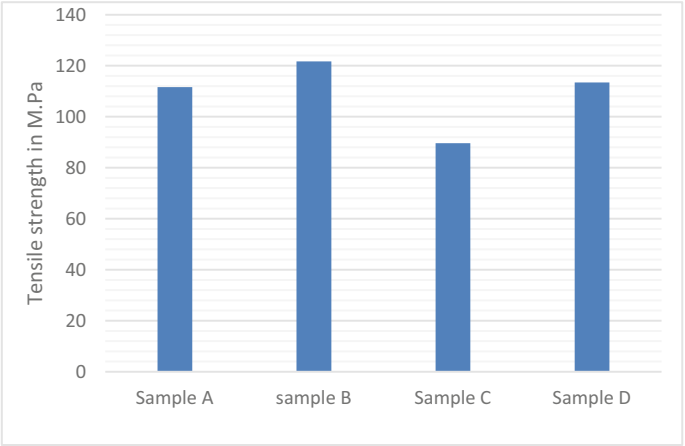


Fig. 6 Effect of Bn and Gr on tensile strength

Fig. 7 Compressive testing specimens



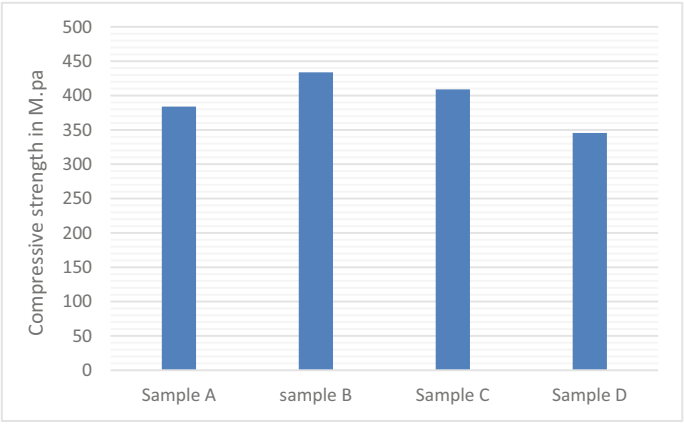


Fig. 8 Compressive strength

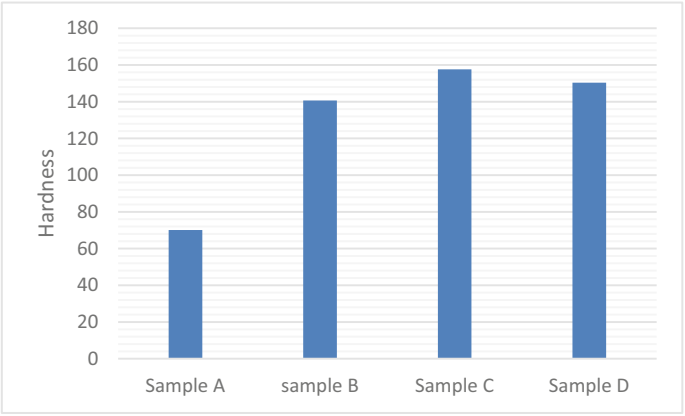


Fig. 9 Hardness test

433 MPa, but with 8% reinforcement, it increases dramatically to 546 MPa. This data clearly shows that increasing the reinforcement correlates to increasing the compressive strength.

2.3.4 Hardness Test

Vickers microhardness test was performed using cast composite specimens with different weight fractions in line with ASTM E384. A HXD-1000TM/LCD digital hardness measurement apparatus was used, with a diamond indenter using a force applied of 100 gf and a dwell duration of 15 s. Ten measurements of hardness were collected and averaged to achieve reliable findings.

The Fig. 9 depicts the outcomes from the hardness test on varying amounts of reinforcing. According to the graph, the higher the proportion of reinforcement, the hardness to the specimens.

2.4 XRD Analysis

The use of XRD analysis, or X-ray diffraction, to investigate the crystal structures of material is a helpful approach. In this research, an X-ray beam strikes at a material, allowing the X-rays to disperse in different ways depending on the atomic arrangement of the substance. The angles and intensities of the scattered X-rays may be used to derive essential data regarding the crystal's structure, such as lattice spacing and orientation. XRD analysis is widely used in the identification and characterisation of crystalline structures in a variety of domains such as the science of materials, geophysical sciences, the field of chemistry and physics(Fig. 10).

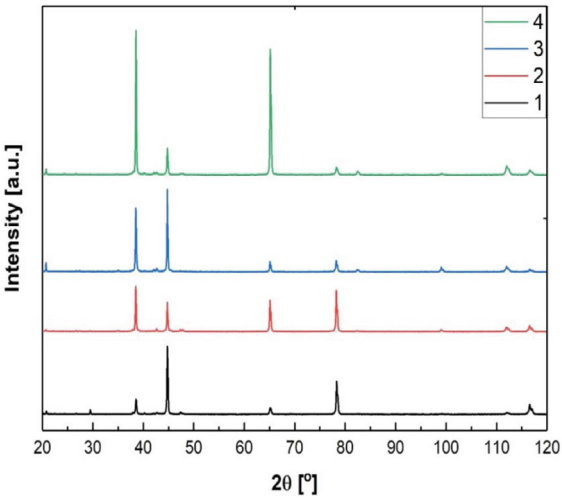


Fig. 10 XRD analysis of aluminium and composite

The XRD spectrum in the picture depicts the principal peak regions of hybrid composites made of metal matrix reinforced with boron nitride (Bn) along with graphite (Gr). The figure shows peak height changes related to varied percentages of Bn as well as Gr composition. With corresponding as-synthesised HMMC peaks, the nearly equivalent two values had been 37, 44, 64, and 77°, respectively.

3 Microstructural Studies

All of these phases was thoroughly examined using the Xpert Highscore programme. The insertion of Bn as well as Gr within the aluminium matrix caused minor modifications in the two values. For example, in a Bn reinforced composite, the 2θ value went between 37 and 35°, but in a Gr reinforced composite, the 2θ value moved between 37 and 33°.

An SEM, or scanning electron microscope, creates pictures of a specimen by using a high-energy stream in electrons which communicate with atoms as well as produce unique signals that transmit information about the sample. Figure depicts the morphology of a produced metal matrix composites (MMC) with a weight composition of graphite and boron nitride. The particles in this picture are evenly dispersed inside the matrix substance. Each composite has particles that are firmly packed and have a constant spatial distribution.

3.1 Scanning Electron Microscopy (SEM)

SEMs create pictures of specimens by utilising a strong stream of electron which combine with atoms and produce unique signals providing data regarding the sample. Figure [Insert Figure Number] depicts the morphology of a manufactured MMC having a composition of graphite as well as boron nitride by weight. Throughout the matrix material, the particles are equally dispersed, and each composite has densely packed particles having a constant spatial distribution.

The particle dispersion is represented in the picture, with white particles indicating boron nitride along with smaller black particles identifying graphite. SEM is used to identify porosity, which can be a source of mechanical flaws and failures. SEM was used to examine the microstructure between cast Al-Gr as well as boron nitride particle composites, demonstrating a balanced distribution of the graphite as well as boron nitride particles inside the UNS A92618 matrix at varied weight fractions ranging from 6 to 2%.

The micrographs also show indicate the reinforcing particles are round and rectangular in form, and are dispersed evenly over each specimen. Excessive reinforcing, on the other hand, can cause disparate dispersion and agglomeration, particularly among specimens with greater volume percentages, leading in increased mechanical defects in the composite.

The spatial distribution of particulate reinforcements seems to be constant, with the aluminium matrix seeming to be a continuous substance and the reinforcement particles being tiny in size with obvious grain boundaries. Higher amounts of reinforcement might result in structural alterations, bigger and oval-shaped grains, increased porosity, and mechanical defects.

Figure 11 depicts UNS A92618, which reveals an elaborate and linked boundary structure as well as a coarse grain texture.

Figure 12 shows non-refined grain structures as well as a nonuniform distribution of Bn and Gr particles on the base material UNS A92618.

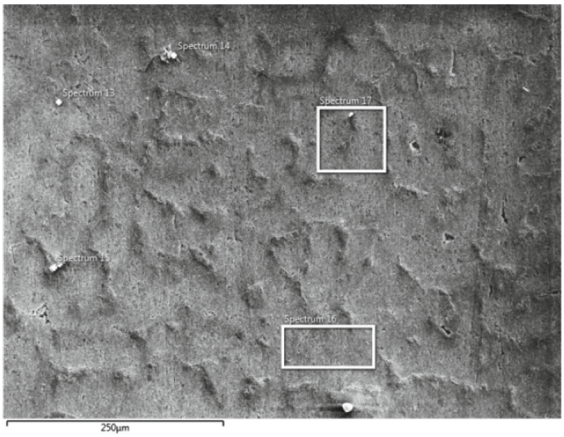


Fig. 11 Specimen ASEM micrograph of MMC's

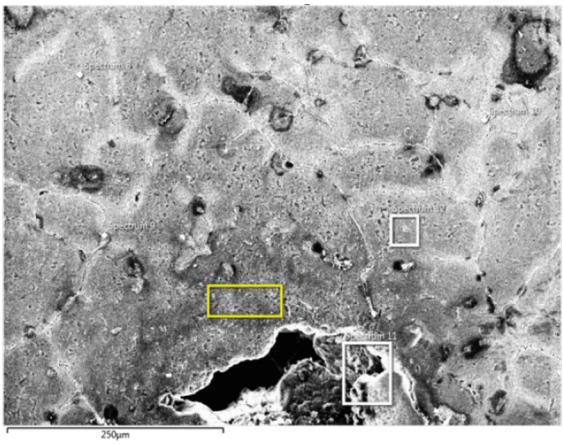


Fig. 12 Specimen BSEM micrographs of MMC'

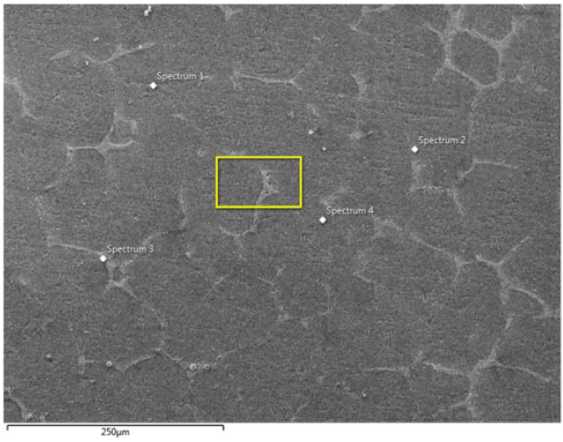


Fig. 13 Specimen C SEM micrographs of MMC's

Figure 13 shows a homogeneous distribution of Bn and Gr particles for reinforcement in the base of UNS A92618.

According to the Fig. 14, the Bn and Gr particles in base UNS A92618 were fine grain and uniformly dispersed.

3.2 Optical Microscopic Structure

In overall, an optical microscope picture from MMC may provide important information regarding the distribution, orientation, along with other properties of the reinforcing elements, and also the bonding within the matrix and reinforcement. This information is critical for understanding the material's mechanical as well as

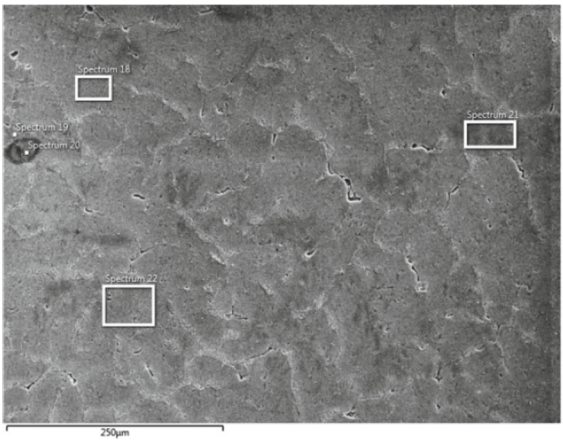


Fig. 14 Specimen D SEM micrographs of MMC's

physical characteristics, as well as optimising its performance in industries such as aerospace, automotive, and defence.

Figure 15 depicts the microstructure of UNS A92618 (Fig. 16).

Various optical microscopic structures that represent different metal matrix configurations are found, and they are shown below at a magnification of 20 µm (Fig. 17).

Figure 18 depicts the distribution produced inside the composite as a result of the addition of boron nitride (Bn) along with graphite (Gr) reinforcement at percentages of weight of 5 and 1%, each, throughout a UNS A92618 aluminium matrix.

The composite reinforced using Bn and Gr (7 and 1% in weight) within a UNS A92618 aluminium matrix has a homogeneous distribution, as illustrated in the figure above.

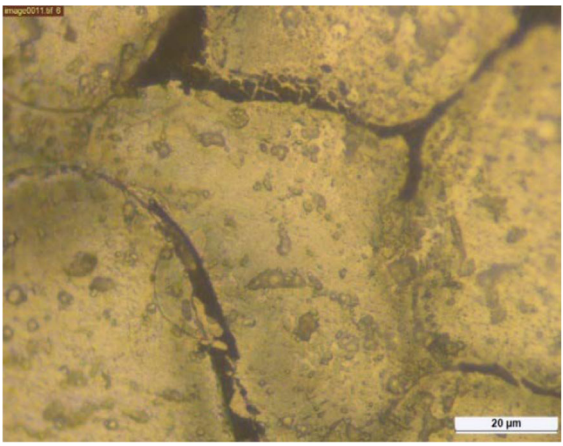


Fig. 15 Microscopic structure for Sample A

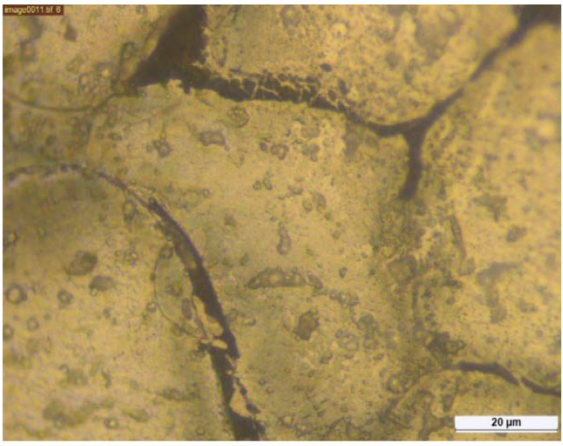


Fig. 16 Microscopic structure for Sample B

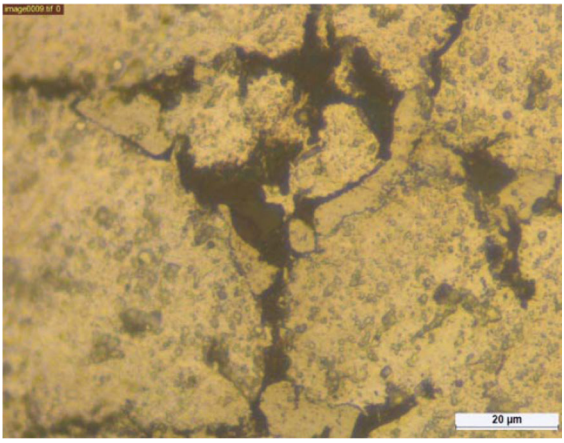


Fig. 17 Microscopic structure for Sample C

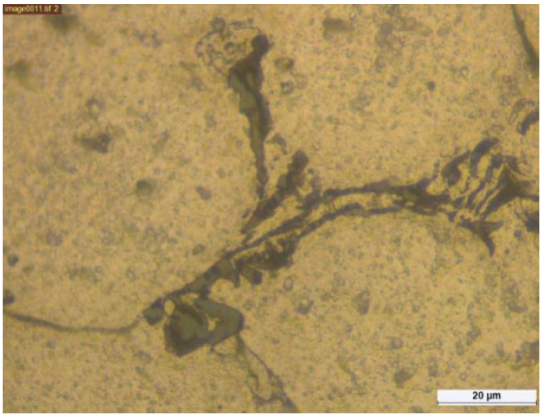


Fig. 18 Microscopic structure for Sample D

4 Conclusion

The composite reinforced using Bn and Gr (7 and 1% in weight) within a UNS A92618 aluminium matrix has a homogeneous distribution, as illustrated in the figure above.

(1) Stir casting yields samples with a homogenous microstructure and good mechanical characteristics.
(2) Boron nitride (Bn) increases yield strength, hardness, along with compressive strength when compared to pure aluminium.
(3) With Sample D, the maximum measured tensile strength was 159 MPa, the highest possible compressive strength was 546 MPa, as well as the hardness value is 170.
(4) Sample D has a high intensity, according to XRD analysis.
(5) The distribution of aluminium, boron nitride, as well as graphite components is revealed by microstructural investigation. A homogenous distribution is found in the Sample D.

References

1. Jiang J, Saleh B, Xu Q, Fathi R, Ma A, Li Y, Wang L (2020) Statistical analysis of dry sliding wear process parameters for AZ91 alloy processed by RD-ECAP using response surface methodology. Met Mater Int
2. Ma A, Li Y, Xu Q, Li Y, Saleh B, Yuan Y, Jiang J (2019) Enhancement of mechanical properties and rolling formability in AZ91 alloy by RD-ECAP processing. Materials (Basel) 12(21):3503
3. Jiang J, Wang L, Saleh B et al (2020) Controlling corrosion resistance of a biodegradable Mg–Y–Zn alloy with LPSO phases via multipass ECAP process. Acta Metall Sin (Engl Lett) 33:1180–1190
4. Ma A, Xu Q, Saleh B, Li Y, Yuan Y, Jiang J, Ni C (2020) Enhancement of strength and ductility of SiCp/AZ91 composites by RDECAP processing. Mater Sci Eng A 771:138579
5. Asgari A, Sedighi M, Krajnik P (2019) Magnesium alloy-silicon carbide composite fabrication using chips waste. J Clean Prod 232:1187–1194
6. Amuthakkannan P, Raja MA, Manikandan V, Rajesh S (2018) Wear resistance of basalt particulate-reinforced stir-cast Al7075metal matrix composites. J Australian Ceramic Soc 54:119–128
7. Gao Y, Xiao P, Xu F, Yang C, Li Y, Liu Z, Zheng Q (2018) Tribological behavior of in situ nanosized TiB2 particles reinforced AZ91 matrix composite. Tribiol Int 128:130–139
8. El-Galy IM, Ahmed MH, Bassiouny BI (2017) Characterization of functionally graded Al-SiCp metal matrix composites manufactured by centrifugal casting. Alex Eng J 56:371–381
9. Kim C, Cho K, Manjili MH, Nezafati M (2017) Mechanical performance of particulate-reinforced Al metal-matrix composites (MMCs) and Al metal-matrix nano-composites (MMNCs). J Mater Sci 52:13319–13349
10. Saleh B, Jiang J, Ma A, Song D, Yang D (2019) Effect of main parameters on the mechanical and wear behaviour of functionally graded materials by centrifugal casting: a review. Met Mater Int 25:1395–1409
11. Jiang J, Saleh B, Ma A, Song D, Yang D, Xu Q (2020) Review on the influence of different reinforcements on the microstructure andwear behavior of functionally graded aluminum matrix composites by centrifugal casting. Met Mater Int 26:933–960

12. Hua H, Ling Y, Yuhong Z, Xiaomin Y (2016) Microstructure and mechanical properties of squeeze casting quasicrystal reinforced AZ91D magnesium matrix composites. Rare Met Mater Eng 45:1978–1982
13. Yılmaz S, Kalkanlı A (2008) Synthesis and characterization of aluminum alloy 7075 reinforced with silicon carbide particulates. Mater Des 29:775–80
14. Saleh BI, El-galy IM, Ahmed MH (2019) Functionally graded materials classifications and development trends from industrial point of view. SN Appl Sci 1:1–23
15. Looney L, Hashim J, Hashmi MSJ (1999) Metal matrix composites: production by the stir casting method. J Mater Process Technol 93:1–7
16. Ma A, Fathi R, Saleh B, Xu Q, Jiang J (2020) Investigation on mechanical properties and wear performance of functionally graded AZ91-SiCp composites via centrifugal casting 24:101169

Development of Battery Case Design Using Banana Fibre



G. Manikandan, M. Boopathi, S. Narasimmabharathi, S. Vimal, M. K. Rithik, and T. S. Sanjay

Abstract As the demand for portable electronic devices continues to rise, so does the need for efficient and sustainable energy storage solutions. The proposed battery case leverages the unique properties of banana fibre, such as its high tensile strength, lightweight nature, and biodegradability, to address the growing concerns associated with traditional battery cases made from non-renewable resources. Banana fibre, derived from agricultural waste, offers a promising alternative that not only reduces environmental impact but also promotes rural livelihoods through the utilisation of readily available resources. Through a combination of material engineering and manufacturing techniques, the banana fibre battery case exhibits excellent mechanical properties, ensuring robust protection for the battery while minimising weight and bulk. The inherent flexibility of banana fibre allows for seamless integration with various battery sizes and shapes, providing a versatile solution for different electronic devices. Moreover, the banana fibre battery case demonstrates remarkable thermal insulation capabilities, protecting the enclosed battery from temperature fluctuations and optimising its performance and lifespan. Additionally, the high moisture absorption properties of banana fibre help mitigate the risks associated with moisture-induced damage to the battery, ensuring its longevity. By incorporating banana fibre as a primary material for battery cases, the proposed solution offers a sustainable and renewable alternative that minimises the reliance on fossil fuel- based resources. The utilisation of banana fibre not only reduces waste and environmental pollution but also supports local economies by creating value from agricultural by-products.

Keywords Banana fibre · Epoxy resin · Battery case

G. Manikandan (✉) · M. Boopathi · S. Narasimmabharathi · S. Vimal · M. K. Rithik · T. S. Sanjay
Department of Automobile Engineering, Kongu Engineering College, Perundurai, Erode, Tamil Nadu 638060, India
e-mail: manikandan.auto@kongu.edu

© The Author(s), under exclusive license to Springer Nature Singapore Pte Ltd. 2025

B. B. V. L. Deepak et al. (eds.), *Recent Advancements in Product Design and Manufacturing Systems*, Lecture Notes in Mechanical Engineering,
https://doi.org/10.1007/978-981-97-6732-8_24

1 Introduction

Fibres play a crucial role in enhancing material properties by reinforcing the matrix. Initially, glass fibres were the primary choice for reinforcement, succeeded by ceramic and metal fibres, known for their increased stiffness and heat resistance. However, fibres come with limitations that impact their performance [1]. A fibre composite's strength depends on factors like fibre length, shape, orientation, composition, and the matrix's mechanical properties. Optimal performance is achieved when the load direction aligns with the fibre's longitudinal direction, and deviations can significantly weaken the composite [2–4]. To accommodate various load directions, composites use a mix of fibre orientations, particularly in high-stress situations. Monolayer tapes can be unidirectional or stacked into plies, with customised orientations through computer projections [1, 5]. This enables planar composites to approach isotropic properties, while angle-plied composites may deviate from quasi-isotropy. In cases with strong matrices and non-longitudinally oriented fibres, the longitudinal strength can be calculated considering reduced effective strength. Composites can be constructed using continuous or short fibres. Continuous fibres offer precise orientation but do not guarantee improved performance. Short fibres, when properly oriented, can provide higher strength [2]. Filament winding is a common method for joining continuous fibres, ensuring favourable orientation and load distribution. Short fibres integrated through open- or closed-mould processes are cost-effective but less efficient [4]. While most fibres today have solid, circular cross-sections, unconventional shapes and hollow fibres show potential for enhancing composite properties [6]. Smaller fibre diameters increase strength by minimising surface defects [7]. Rectangular cross-section fibres offer options for high-strength applications [8]. Hollow fibres, despite challenges in production and processing, excel in composites prioritising stiffness and compressive strength, unless the hollow section exceeds 50% of the total fibre diameter [9, 10].

The major goals of this addition of banana to epoxy are to greatly increase stiffness and reduce density, and for every weight percent of banana added to epoxy (up to 4 wt.%), density and elastic modulus are increased by 3% and 4%, respectively. By employing banana-epoxy in place of conventional interior materials in aircraft, designers can reduce weight by up to 20% [2, 3, 6]. Studies on how slip morphology affects banana-epoxy's monotonic and cyclic ductility reveal that ductility is governed by strain localisation, which is dependent on the degree of work softening on the glide plane. Shearable precipitates localise monotonic strain in dense regions of deformation as ageing progresses from underaged to peak strength, resulting in stress concentrations and reduced ductility.

2 Design Considerations

The availability and cost of raw materials, the necessary expertise and processing technology, rejection rates and waste recycling of finished components, unknown risks related to the application area chosen, performance uncertainties, frequency of damage tolerance maintenance, replacement procedures, as well as other factors like increased profitability and margins, must all be considered when designing a new material for the aircraft industry.

The following factors should be taken into consideration when choosing an application area:

- Raw material availability and cost.
- Required skills and processing technology.
- Finished component rejection rates and waste recycling.
- Unknown risks when choosing an application area.
- Performance uncertainties.
- Damage tolerance maintenance frequency and replacement procedures.
- Other factors, such as an increase in profitability and margins**.**

Design considerations for a battery case encompass multiple factors to ensure optimal performance, safety, and efficiency. These considerations include material selection, mechanical design for impact and vibration resistance, thermal management to prevent overheating, electrical isolation to prevent short circuits, enclosure design for secure housing and easy access, incorporation of safety features like pressure relief valves, adherence to manufacturing feasibility and cost-effectiveness, compliance with regulatory standards, and awareness of environmental impact through recyclability. By addressing these factors, a well-designed battery case can be achieved, promoting reliable battery operation, and mitigating potential risks.

3 Design of Battery and Dimensions

Battery cases made using banana fibre offer a promising scope due to their eco-friendly and sustainable nature. Banana fibre, derived from agricultural waste, can be used as a renewable and biodegradable material for producing lightweight and durable battery cases [11, 12]. Its high tensile strength, thermal stability, and low production cost make it an attractive option for creating environmentally friendly battery enclosures, reducing reliance on non-renewable materials, and minimising ecological impact (Fig. 1).

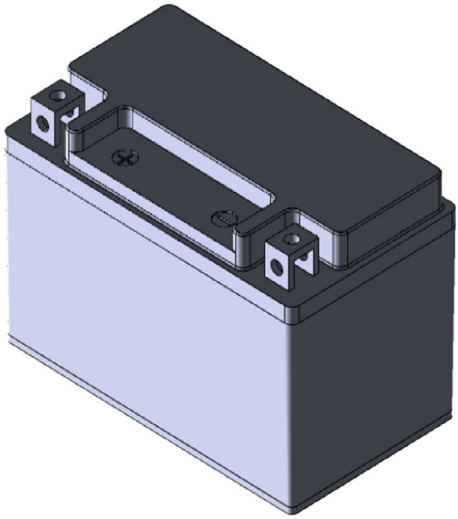


Fig. 1 CAD design for battery case. Dimensions: 113 × 87 × 105 mm, capacity: 9 Ah

4 Experimental Details

4.1 Material Required

- Banana fibre,
- Epoxy resin,
- Battery case for measurement.

4.2 Banana Fibre

Bananas, often mistaken for trees, are tall herbs that can grow up to 15 feet in height. They are self-renewing perennials, developing from bulbs or rhizomes rather than seeds. It takes about 9–12 months from planting a banana to harvesting the bunch, with blossoming typically occurring in this more than six or seven month. In tropical locations with average highs of 80 °F (27 °C) and highs of 78–98 inches (200–250 cm) of rainfall, bananas can be found year-round. However, they do require well-draining, damp soil [2, 3, 11]. Regions within 30 degrees of the equator are the source of most banana exports.

Successful banana cultivation demands individualised care, including clearing away overgrowth, providing support to prevent bending under the weight of fruit, and irrigation during dry spells. Bananas are grown in more than 120 tropical and subtropical nations worldwide; the largest producers being the Democratic Republic of the Congo, India, Uganda, Ecuador, Brazil, Colombia, the Philippines, China, Indonesia, and Costa Rica. India, alone contributing almost 17% of global production,



Fig. 2 Banana fibre

produces around 13.5 million tonnes of bananas annually, primarily in states like Gujarat, Kerala, Karnataka, Andhra Pradesh, Maharashtra, and Tamil Nadu. Banana plants offer additional utility by providing banana fibres from their pseudo stems, which are often discarded as agricultural waste [11]. An estimated 1.5 million tonnes of dry banana fibre can be produced each year from the pseudo stems. It is anticipated that output and pseudo stem biomass waste will rise in response to the growing demand for bananas both domestically and globally [2, 3]. Utilising the pseudo stem is profitable, with banana fibre extraction involving decorticating the stem with a blunt knife. However, low recovery rates hinder the adoption of this technology, leading to higher transport costs. The banana plant produces fibres from its several sections, each having unique qualities, colours, and uses (Fig. 2).

4.3 Process of Banana Fibre

In various parts of the world, such as India, banana fibre harvesting remains a largely manual and unprofitable endeavour. Traditional methods involve hand scraping the banana pseudo stem, yielding only a small amount of fibre. However, there is a promising shift in this landscape with the introduction of the banana fibre separator machine, known as the raspatory. This machine mechanises the extraction process, making it more practical and efficient. Countries like the Philippines, Uganda, China, and Indonesia have recognised the value of banana fibre and implemented systematic extraction methods [11, 12]. After harvesting, the banana plants are cut down, and the cleaner, white portion of the trunk is retained for fibre processing. The pseudo stem's sheaths are removed to obtain different grades of fibres. These fibres are extracted using hand extraction machines, dried in the sun for a whiter appearance, and then knotted for various uses. Notably, the development of the banana fibre separator machine represents an environmentally friendly approach, as it utilises agricultural waste from banana harvests to create high-grade silk-grade fibre. This innovation holds the potential to revolutionise banana fibre production, offering a more sustainable and commercially viable future for this industry (Fig. 3).

To make a battery case using banana fibre, the following steps can be followed:

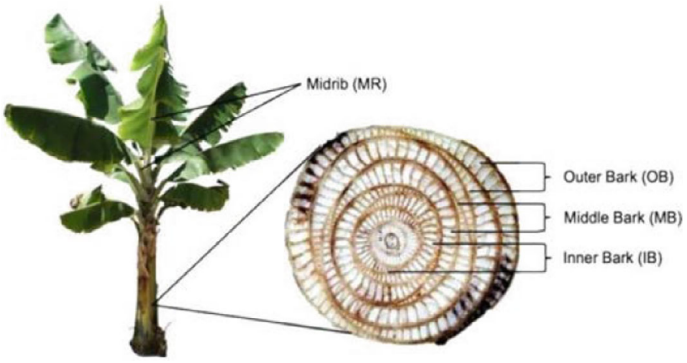


Fig. 3 Banana stem

Fibre Extraction: To soften the fibres, the stem of the banana plant is chopped into tiny pieces and submerged in water. After that, the fibres are either manually or mechanically removed off the stem.

Fibre Preparation: The extracted banana fibre needs to be cleaned, dried, and processed to remove impurities and align the fibres.

Resin Preparation: The banana fibre is then impregnated with a resin to create a composite material. The resin can be made of a variety of materials, including plant-based materials like soybean oil or animal-based materials like gelatine.

Moulding: The composite material is then melded into the desired shape for the battery case. The moulding process can be done using compression moulding, injection moulding, or other moulding techniques.

Post-processing: Once the battery case is moulded, it can be sanded, painted, or coated to provide additional protection and aesthetic appeal.

4.4 Characteristics of Banana Fibre

Except for Kerala, where it is partially utilised to produce household products, most of India discards these banana trunks as agricultural waste due to ignorance about the fibre's extraction and application. This section of the article evaluates the yield, structure, and characteristics of banana fibres derived from a few commercially grown varieties. The findings show that the fibre structure and characteristics vary depending on the trunk's thickness and length. One kind of natural leaf fibre is banana fibre. It is a high-quality fibre because of its unique chemical, physical, and other qualities [2, 3]. Banana fibres resemble those of bamboo and ramie fibres.

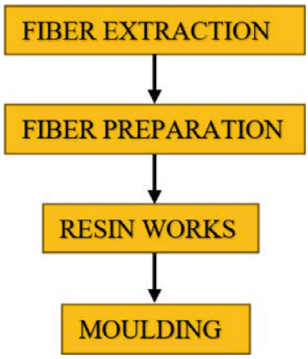


Fig. 4 Banana fibre process flow

- Banana fibre contains cellulose, hemicelluloses, and lignin as its main chemical components.
- The fibre is robust.
- The elongation is less.
- Depending on the extraction, it appears to be slightly sparkly.
- It is portable.
- It has excellent moisture-absorbing capabilities. It quickly absorbs and releases moisture.
- It may be categorised as an eco-friendly fibre because it is biodegradable and has no adverse effects on the environment.
- Its typical fineness ranges from 4 to 15 tex.

4.5 Flowchart

See Fig. 4.

4.6 Specification of Banana Fibres

See Table 1.

4.7 Epoxy Resin

When referring to epoxy resins, also known as polyoxides, the term "epoxy" can be used to describe both their constituent parts and their finished cured products Epoxide-group polymers and reactive prepolymers combine to form epoxy resins [5, 6]. They can form cross-links with a range of co-reactants, such as polyfunctional

Table 1 Banana fibre specifications

S. No.	Properties	Values
1	Linear density (D)	4.03
2	Average strength (cN/tex)	39.3
3	Strength unevenness (%)	34.3
4	Average elongation at break (%)	5.4
5	Elongation unevenness (%)	19.7
6	Break strength (cN/tex)	2.3

Table 2 Composition of case

S. No.	Material	Usage percentage (%)
1	Banana fibre	20
2	Epoxy resin	80

amines, acids (including acid anhydrides), phenols, alcohols, and thiols (also known as mercaptans) by catalytic photopolymerisation. Often referred to as hardeners or curatives, these co-reactants aid in the healing process. A thermosetting polymer that generally has favourable mechanical characteristics, strong heat resistance, and chemical resistance is created by the interaction of polyoxides with hardeners. Paint brush manufacturing, fibre-reinforced plastics, structural adhesives, electronics, electrical components, LEDs, high-tension electrical insulators, metal coatings, and structural adhesives are just a few of the industries that use epoxy extensively. On rare occasions, epoxy is also utilised as an adhesive or glue. To combine the banana fibre and create a rigid casing, epoxy resin is employed.

5 Preparation

5.1 Composition of Case

See Table 2

5.2 Preparation of Moulding

See Figs. 5, 6 and 7.

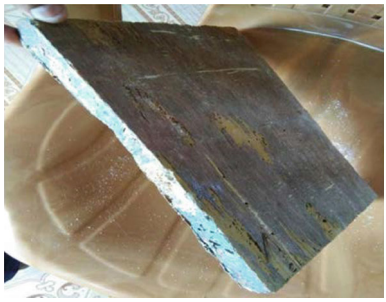


Fig. 5 Compression moulding preparation

Fig. 6 Surface finishing of moulding



Fig. 7 Fabricated composite material



6 Test and Result

6.1 Test to Be Performed

- Tensile test,
- Hardness test.

- **Equipment**
  - Tensile specimens,
  - Micrometre or Vernier callipers,
  - Universal testing machine,
  - Stereoscope.
- **Test Experimental Procedure**
  1. For calculating engineering stress and engineering strain, measure the composite material specimens' diameter and gauge length and enter the data in the accompanying table. Mark the gauge length position along each specimen's parallel length as well to make it easier to see necking and quantify strain.
  2. Execute the test by securely positioning the samples on the universal testing machine (UTM). During the testing process, accurately record the load and extension data to produce the stress–strain curve for each tested specimen.
  3. Using the information gathered, determine each specimen's Young's modulus, yield strength, ultimate strength of tensile, fracture strain, percent elongation, and percentage area reduction. Put these calculated figures in the provided table.
  4. Examine the fracture surfaces of the broken specimens using a stereoscope, and then meticulously sketch and explain your results.
  5. Provide a detailed description of the experimental results, making deductions from the data acquired. Analyse the mechanical characteristics and fracture behaviour of the composite materials considering the measured stress–strain curves and fracture surface features.

6.2 Tensile Strength of Composites Result

The composite specimens are put through a tensile test on a universal testing machine, and the results are displayed in the Table 3.

Table 3 Tensile stress of composition

	CS area (mm^2)	Peak load	Elongation %	UTS (N/mm^2)
Minimum	200.00	1031.796	2.850	5.160
Maximum	200.00	1031.796	2.850	5.160
Average	200.00	1031.796	2.850	5.160
Std. dev	0.00	0.00	0.00	0.00
Variance	0.00	0.00	0.00	0.00
Median	200.00	1031.796	2.850	5.160

Table 4 Microhardness

S. No.	Microhardness (vickers) average HV(H)
1	14.80

6.3 Hardness Strength of Composites Result

The values are furnished in Table 4. The value of flexural strength obtained is 14.80 HV.

6.4 Graph for Tensile Test Result

Battery casings are important components of electric vehicles, as they protect the batteries from external damage and provide structural support. One of the materials that can be used to make battery casings is a composite of epoxy resin and banana fibre. Epoxy resin is a thermosetting polymer that has high strength, stiffness, and chemical resistance. Banana fibre is a natural fibre that is extracted from the stem of the banana plant. It has high tensile strength, flexibility, and biodegradability. The slope of the graph is the modulus of elasticity, which measures the stiffness of the material. The point where the graph deviates from a straight line is the yield point, which indicates the onset of plastic deformation. The point where the graph reaches its maximum is the ultimate strength, which is the maximum stress that the material can withstand. The point where the graph drops to zero is the fracture point, which is the point of failure of the material. The stress and strain graph of a unidirectional composite can be obtained by applying a tensile load along the direction of the fibre. The graph will have different regions, depending on the behaviour of the fibre and the matrix (Fig. 8).

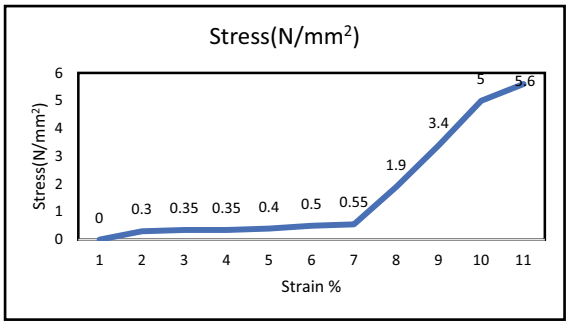


Fig. 8 Graph of tensile stress test



Fig. 9 Battery case using banana fibre

6.5 Image of Battery Case

See Fig. 9.

7 Conclusion and Future Scope

7.1 Conclusion

In conclusion, the utilisation of banana fibre in battery cases demonstrates several advantages over other materials. The use of banana fibre offers enhanced durability and strength, as well as improved thermal and electrical properties. Additionally, banana fibre is a renewable and sustainable resource, making it an environmentally friendly alternative. Furthermore, the cost-effectiveness and availability of banana fibre make it as a viable option for large-scale production. Therefore, it can be concluded that the incorporation of banana fibre in battery cases provides a superior

solution compared to other materials, benefiting both the performance of the battery and the environment.

7.2 Future Work

As we have done the tensile and hardness test for our battery case using banana fibre, next work is to test them in the following manner.

Thermal Test

The battery cases can be subjected to various temperature conditions, and their ability to resist heat and provide insulation can be monitored. This test assesses how well the cases dissipate heat and protect the battery from excessive temperatures.

Electrical Conductivity Test

The battery case materials can be connected to an electrical circuit, and their ability to conduct electrical current can be evaluated. This test typically involves measuring the resistance or voltage drop across the cases to assess their conductivity.

References

1. Agarwal G, Patnaik A, Sharma RK (2013) Thermo-mechanical properties of silicon carbide filled chopped glass fiber reinforced epoxy composites. Int J Adv Struct Eng 5:1–8
2. Kumar A, Choudhary D (2013) Development of glass/banana fibers reinforced epoxy composite. Int J Eng Res Appl 3(6):1230–1235
3. Prasanna P, Gopinath V, Rao D (2017) Synthesis, characterization of banana/glass fiber reinforced epoxy based hybrid composites. Int J Eng Res Appl 7(9) (Part-6):47–57. ISSN: 2248-9622
4. Kumar KN, Prasanth Kumar M, Krishna V, Srinivasa Rao D (2013) Experimental investigation on mechanical properties of coal ash reinforced glass fiber polymer matrix composites. Int J Emerg Technol Adv Eng 3(8):250–258
5. Devendra K, Rangaswamy T (2013) Strength characterization of E-glass fiber reinforced epoxy composites with filler materials. J Min Mater Char Eng 1(06):353–357
6. Sapuan SM, Leenie A, Harimi M, Beng YK (2006) Mechanical properties of woven banana fiber reinforced epoxy composites. Mater Des 27(8):689–693
7. Herrera-Franco PJ, Valadez-Gonzalez A (2004) Mechanical properties of continuous natural fiber-reinforced polymer composites. Compos A Appl Sci Manuf 35(3):339–345
8. Wambua P, Ivens J, Verpoest I (2003) Natural fibers: can they replace glass in fiber reinforced plastics? Compos Sci Technol 63(9):1259–1264
9. Venkateshwaran N, ElayaPerumal A, Jagatheeshwaran MS (2011) Effect of fiber length and fiber content on mechanical properties of banana fiber/epoxy composite. J Reinf Plast Compos 30(19):1621–1627
10. Ochi S (2008) Mechanical properties of kenaf fibers and kenaf/PLA composites. Mech Mater 40(4–5):446–452
11. Mukhopadhyay S, Fangueiro R, Arpac Y, Şentürk Ü (2008) Banana fibers–variability and fracture behaviour. J Eng Fibers Fabr 3(2):155892500800300200
12. Gururaja MN, Hari Rao AN (2012) A review on recent applications and future prospectus of hybrid composites. Int J Soft Comput Eng 1(6):352–355

Data Simulation: Creep Behavior in Ti–6Al–4V Alloy



Jones Woya, Malachi Mai, and Aezeden Mohamed

Abstract This paper describes the development of a computer model for titanium alloys. JMAT Pro and ANSYS Granta Selector are utilized to further understand and depict the creep behavior of Ti–6Al–4V under extreme conditions in both a controlled and uncontrolled environment. These data can be used as replacement to the constitutive equations in computer-aided-engineering simulation.

Keywords Creep · Failure · Simulation · Titanium alloy · Ti–6Al–4V

1 Introduction

Modern aircrafts in the aviation business today are made to be light. Modern passenger airplanes are being innovatively designed to be lightweight in order to be more economical in terms of fuel usage [1–4].

The high strength to lightweight ratio of titanium alloys makes them one of the numerous metal alloys frequently employed in the production of aircraft parts [1]. Titanium is widely employed in many other applications due to its high strength, low modulus, and low density, as well as its superior corrosion resistance when compared to other metals. Failures caused by low temperature creep are probably a result of applying a sustained load (tension) for an extended period of time [4].

The Ti–6Al–4V alloy has these characteristics in addition to being a two-phase alloy, which often displays a variety of microstructures or grain structures depending on the manufacturing and thermal treatment processes. These key elements that guarantee the material's ultimate intended mechanical qualities, including its strength, ductility, resistance to fracture propagation, and many more, are attained through the components. The tensile and fatigue behavior of the Ti–6Al–4V alloy will be considered. Ti–6Al–4V is very sensitive to temperature and strain rate. Therefore, fracture

J. Woya · M. Mai · A. Mohamed (✉)
Department of Mechanical Engineering, PNG University of Technology, Lae, Papua New Guinea
e-mail: aezeden.mohamed@pnguot.ac.pg

© The Author(s), under exclusive license to Springer Nature Singapore Pte Ltd. 2025

B. B. V. L. Deepak et al. (eds.), *Recent Advancements in Product Design and Manufacturing Systems*, Lecture Notes in Mechanical Engineering,
https://doi.org/10.1007/978-981-97-6732-8_25

to the shank of the titanium alloy (Ti–6Al–4V) occurred due to the uncontrolled process parameters during its manufacturing [3, 5].

This paper provides a simulation and model data of the Ti–6Al–4V alloy with its certain properties and how the material behaves under certain conditions in both a controlled and uncontrolled environment.

2 Methodology

The software package known as JMatPro, sometimes known as Java-based materials characteristics software, is utilized here.

Simulation is done as per [6] for the following properties of the Ti–6Al–4V alloy which are

- Solidification behavior and properties, e.g., Scheil calculations,
- Mechanical properties, e.g. tensile strength, hardness, flow curves,
- Thermophysical and physical properties, e.g., Young's (E), shear (G), and bulk (K) moduli, Poisson's ratio, thermal conductivity, thermal expansion coefficient, density, specific heat,
- Phase transformations, e.g., TTT/CCT/diagrams.

This property is then cross-referenced to ensure and prove the working and creep conditions for the mentioned material. Additionally, a data simulation analysis of the material properties is extracted using ANSYS Granta selector, a material-based selection software. Properties calculated in Granta are tensile strength, yield strength, compression strength, and fatigue strength. Other properties calculated include Young's modulus.

3 Results and Discussion

Calculation of Ti–6Al–4V properties.

3.1 Phase Transformations (TTT, CCT, TTA)

See Figs. 1 and 2.

3.2 Thermophysical Properties

See Fig. 3.

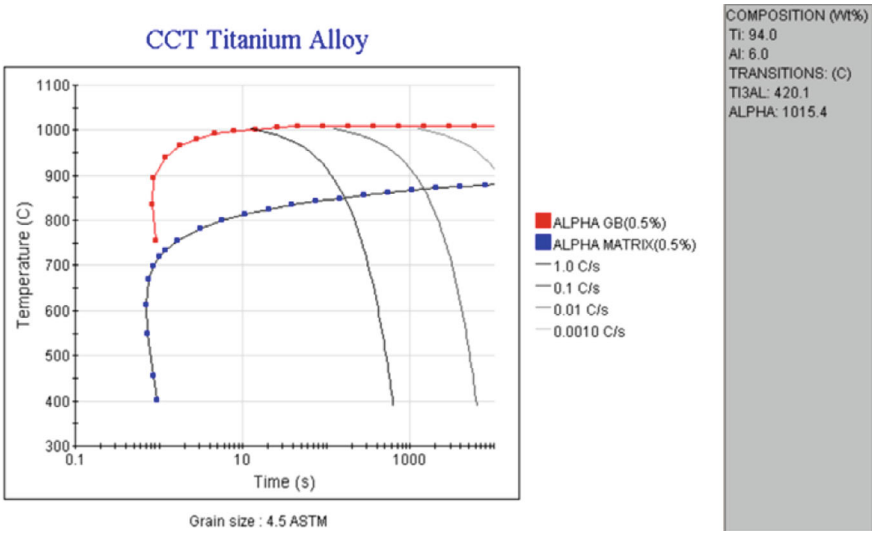


Fig. 1 Isothermal temperature (TTT) diagram for titanium alloy with grain size 4.5 ASTM

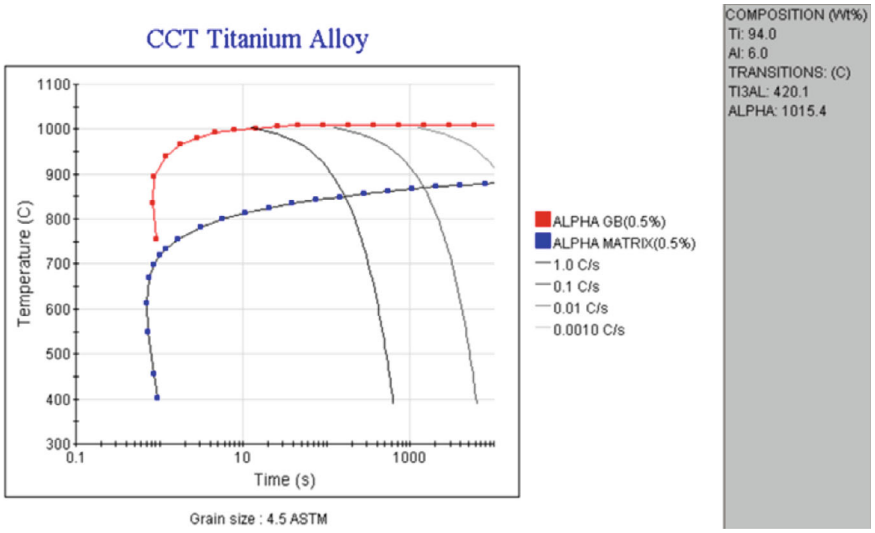


Fig. 2 Continuous cooling temperature (CCT) diagram for titanium alloy

A graph depicting the shear modulus (also known as the elastic modulus) as a function of temperature for a material, in this case, Ti–6Al–4V, provides valuable insights into the material's mechanical behavior under varying thermal conditions. The shear modulus represents the material's resistance to shear deformation. At low temperatures, the shear modulus of Ti–6Al–4V is relatively high. This is indicative

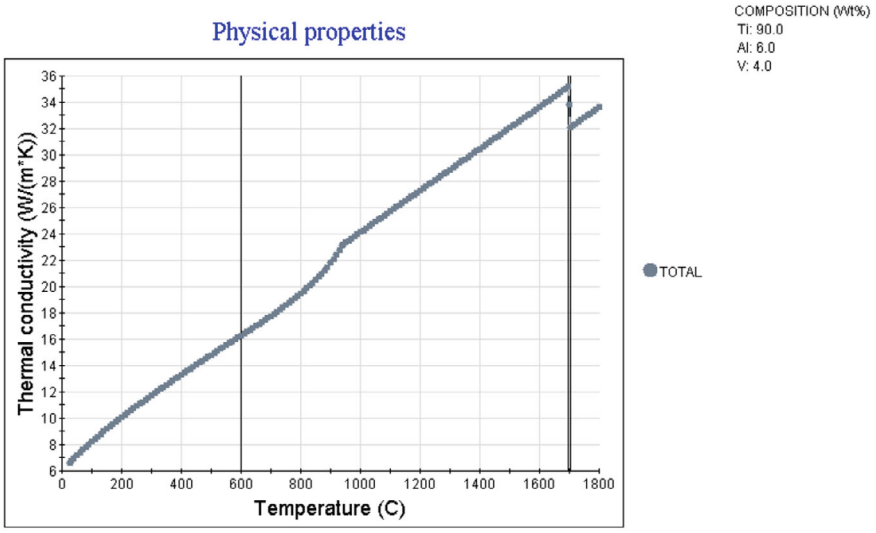


Fig. 3 Thermal conductivity of Ti–6Al–4V, dependent on temperature and quenching rate at fixed composition and grain size

of its strong resistance to shear deformation when exposed to low thermal energy conditions. This property makes it suitable for applications in aerospace. So, based on this, it can be said that the bolt should have a relatively high shear modulus (Fig. 4).

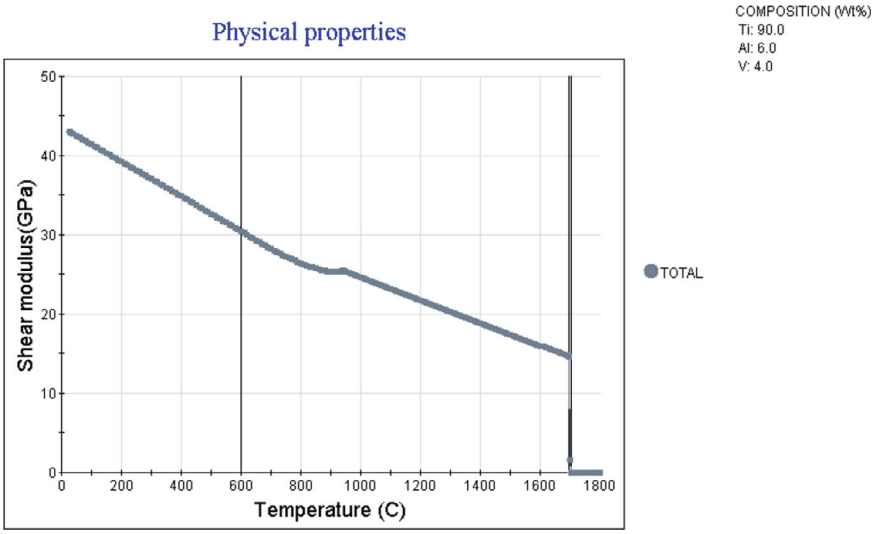


Fig. 4 Shear modulus at different temperatures for Ti–6Al–4V

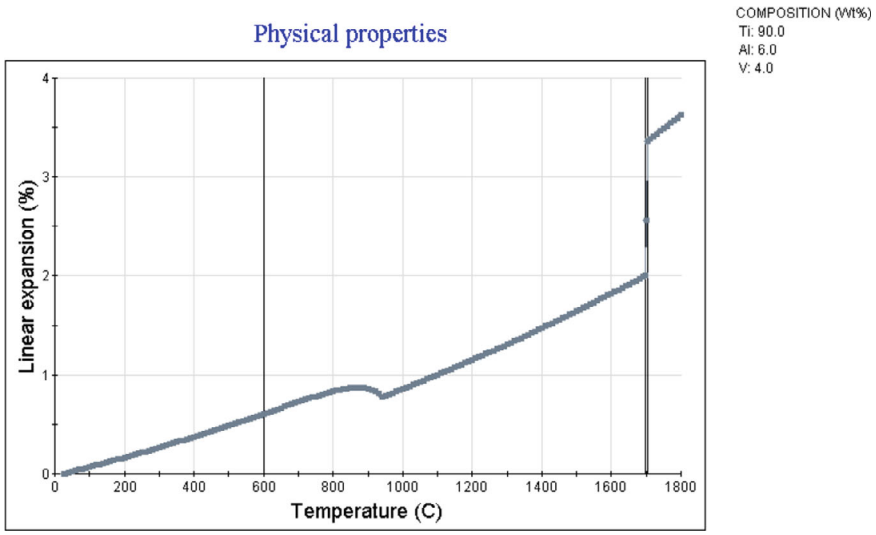


Fig. 5 Linear expansion at different temperatures for Ti–6Al–4V

Another useful property calculated is the linear expansion for Ti–6Al–4V. Shown below is a graph depicting how the material's length changes as a function of temperature. This is crucial information in engineering and construction because it helps us understand how materials expand or contract with temperature fluctuations, which is essential for designing structures and components that can withstand temperature variations. This include the bolts used in this case study (Figs. 5, 6, 7, 8, 9 and 10).

The Ti–6Al–4V alloy can creep with low stress values as low as 20 MPa. The creep rate of the material increases from as low as these stress values and can last to about 10,000 h before rupture. However, the rate at which creep occurs may not be steady due to the fact that stresses may not be constant, and there may be other factors that can alter the rate of creep, for instance temperature and corrosion. Figure 11 is the graph depicting the creep rate for the material Ti–6Al–4V at different stress levels.

3.3 Mechanical Properties

The conventional Hall–Petch equation and solid solution hardening are taken into consideration when calculating the yield or proof stress of materials. The strength of each microstructure is determined by the grain size and cooling rate using phase transformation data.

Below is the transition phase graph for the material as it transits into different phases with respect to temperature. At higher temperatures, the material transits into the liquid phase as indicated by the blue line. Therefore, the bolts failed at

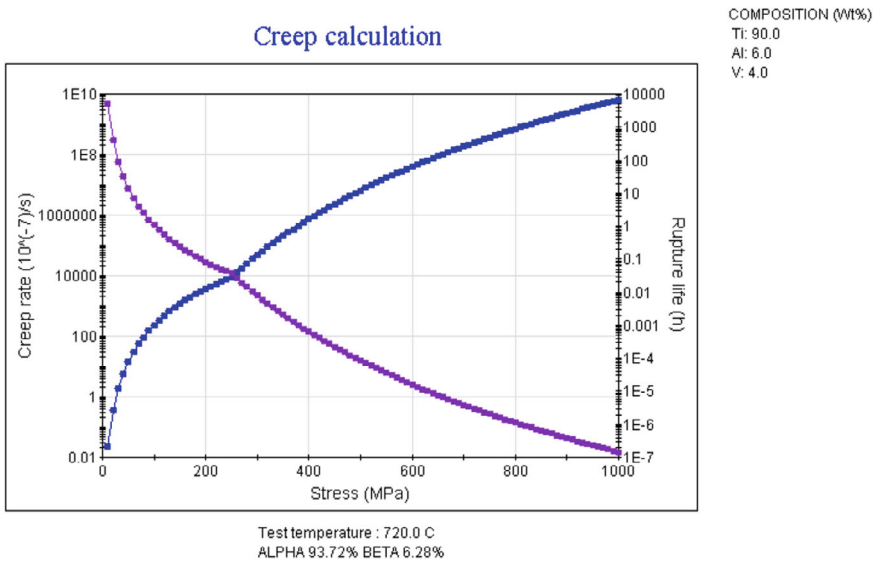


Fig. 6 Creep rate for Ti–6Al–4V at a test temperature of 720 °C

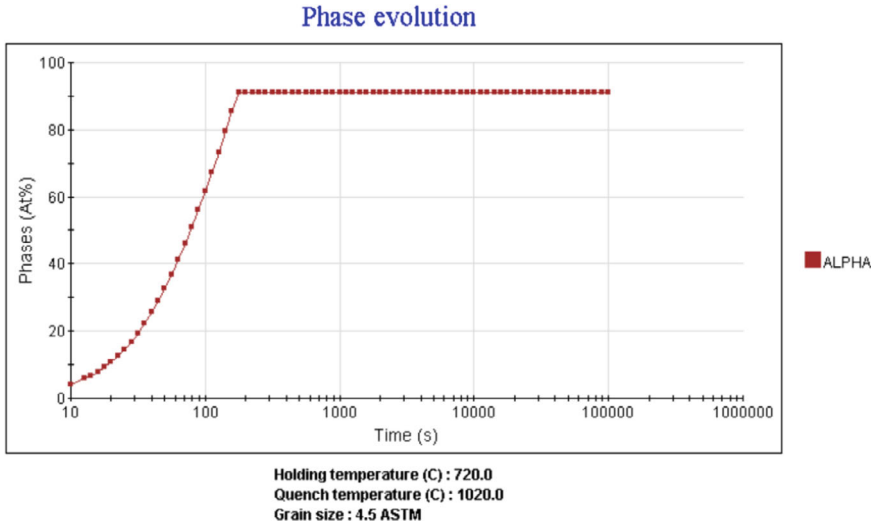


Fig. 7 Phases of Ti–6Al–4V at holding temperature and quench temperature with a grain size of 4.5 ASTM

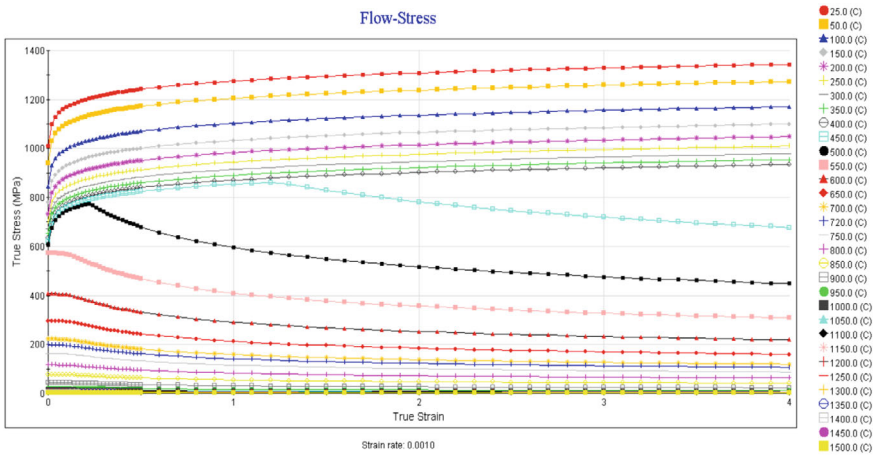


Fig. 8 Exemplary flow stress analysis of Ti–6Al–4V at a strain rate of 0.001/s

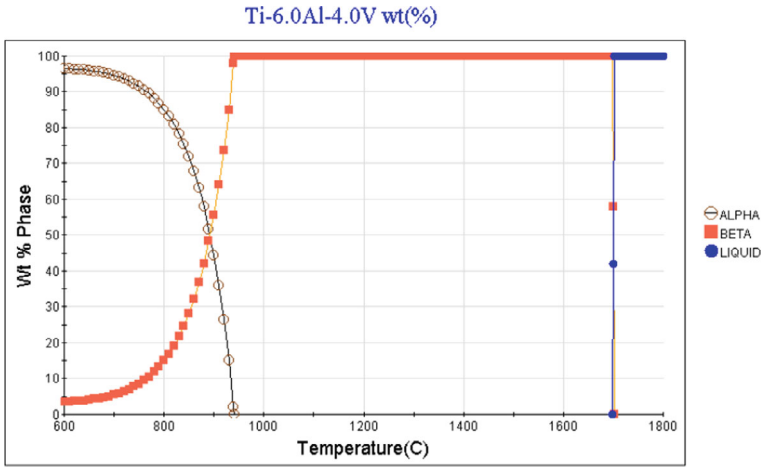


Fig. 9 Wt% of Ti–6Al–4V at different phases, alpha, beta, and liquid, with respect to increasing temperature

temperatures less than 1000 °C as it is the materials property to fail under these given temperatures, respectively, with their transition phases.

Ti–6Al–4V has a yield strength or elastic limit of 1080 MPa without temperature and 1070 MPa with temperature. Figure 10 shows rate at which yield strength decreases with increasing temperature. The simulation data was calculated at a temperature of 23 °C. The tensile strength on other hand is 1270 MPa without temperature and 1200 MPa with temperature. This is depicted in Figs. 11 and 12.

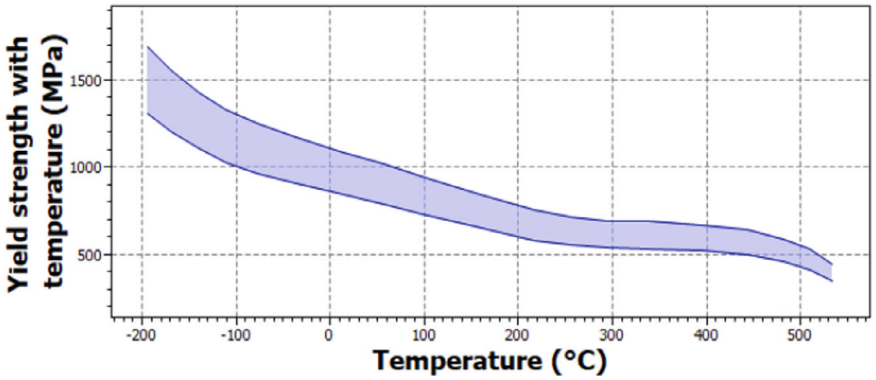


Fig. 10 Yield strength with temperature (MPa)

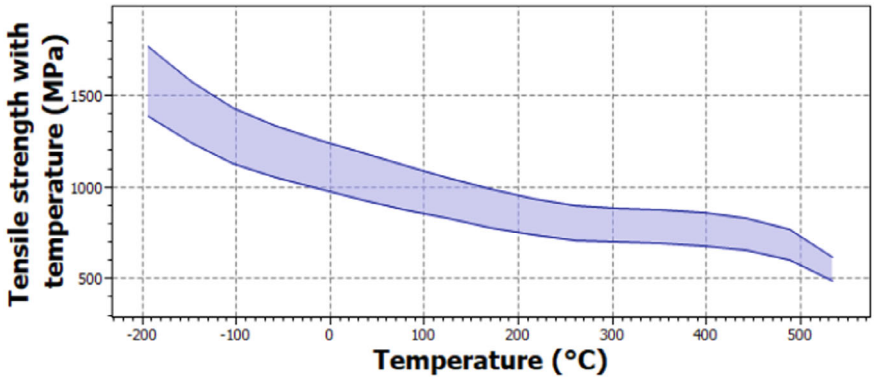


Fig. 11 Tensile strength with temperature

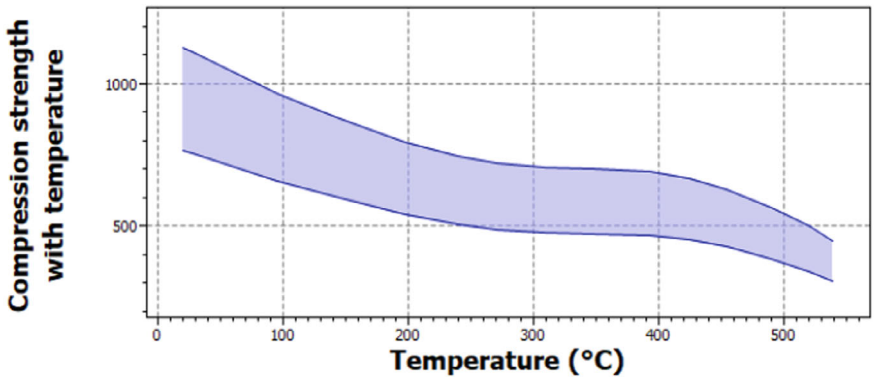


Fig. 12 Compression strength with temperature

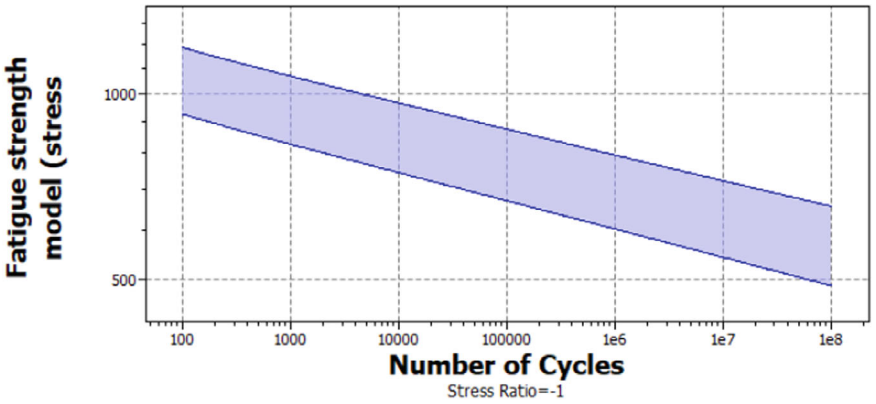


Fig. 13 Fatigue strength model

Ti–6Al–4V has a maximum compression strength of 1150 MPa and decreases with increasing temperature by about 30 MPa which is seen in Fig. 12.

Additionally, flexural modulus and strength are determined to be 119GPa and 1100 MPa, respectively. Fatigue strength at 107 cycles is found to be 638 MPa. The model itself in Granta accounts to about 722 MPa assuming a minimum stress ratio of 1 (Fig. 13).

4 Conclusion

To conclude, at high temperatures, creep deformation is associated with the synergistic effect of both microstructural changes and strain accumulation which leads to nucleation of voids, growth, and coalescence and subsequently to failure [5, 7, 8]. The tensile and fatigue behavior of the Ti–6Al–4V is highly influenced by its microstructure and the process applied during manufacturing [6]. Unalloyed Ti has the best corrosion resistance and is lowest in cost but is also low strength compared to other alloys. However, alloyed titanium such as the Ti–6Al–4V has high strength-to-weight ratio, low density, exceptional corrosion resistance, and a good creep resistance up to 550–600 °C with a fracture toughness of 100 MPa $m^{0.5}$ [9]. Despite being expensive, its remarkable properties have resulted in a growth in demand.

References

1. Alloys A (2023) Titanum for aviation. Retrieved from Titanum for Aviation Corp. www.avionalloys.com

2. Debashhish T, Rajagopal K, Tharian T, Venkitachalam Venkitakrishnan P (2013) Failure analysis and optimization pf thermo-mechanical process parameters of Titanium alloy (Ti–6Al–4V) fasteners for aerospace applications. Elsevier, Trivandium
3. Lutjering G, Albrecht J, Ivasishin O (1994) In: Ankem S, Hall J (eds) The Minerals Metals & Materials Society, Warrendale, pp 65–74
4. Iordanius S, Kyriakos K, Koutsomichalis A (2018) Investigation of in-service creep failures of aircraft Ti–6Al–4V bolts. EDP Sciences
5. Gammon L, Briggs R, Packard J, Batson K, Boyer R, Domby, C (2004) ASM handbook, volume 9: metallography and microstructures Vander Voort GF (ed), pp 899–917
6. https://docplayer.net/26778495-Calculation-of-steel-data-using-jmatpro-uwe-diekmann.html
7. Venkateswarlu V, Tripathy D, Rajagopal K, Thomas K, Venkitakrishnan T (2013) Case Stud Eng Fail Anal 1:49–60
8. Cui Y, Meng Q, Zhang B, Yan F (2006) Eng Fail Anal 13:669–672
9. Spyroglou I, Kourousis K, Koutsomichalis A (2018) Investigation of in-service creep failures of aircraft Ti–6Al–4V bolts. In: MATEC web of conferences, vol 188. EDP Sciences, p 04008

Influence of Stability Improvement Methods Over the Thermal Conductivity of Al_2O_3-DI Nanofluids



Ravi Kiran Mudidana, Vijay Miditana, and V. Rambabu

Abstract Stability has a dominant role over preserving the thermophysical properties of nanofluids for longer durations from their development. Rapid decrement in the balance between repulsive and attractive forces of nanoparticles can promote the agglomeration in the suspension and deteriorate the thermal performance with the drastic loss of colloidal characteristics. Various techniques such as magnetic stirring, ultrasonication, surfactants, and pH modifiers are applied to improve the chemical stability of nanofluids. But the stability improvement techniques can have significant influence over the thermal conductivity of nanofluids with the effect of intermolecular reactions. The study is aimed to investigate the influence of stability enhancement techniques over the thermophysical properties such as thermal conductivity, viscosity, and density. The nanofluid at different volume fractions such as 0.03, 0.06, 0.09, and 0.12% are developed by dispersing 35 nm sized Al_2O_3 nanoparticles into deionized (DI) water, and stability improvement techniques are applied. The observations made from the performed experimentation are discussed with suitable illustrations.

Keywords Nanofluids · Magnetic stirring · Ultrasonication · Thermophysical properties

R. K. Mudidana (✉) · V. Miditana
Centurion University of Technology and Management, Paralakhemundi, Odisha, India
e-mail: ravikiranmudidana335@gmail.com

V. Rambabu
GMR Institute of Technology, Rajam, Andhra Pradesh, India

© The Author(s), under exclusive license to Springer Nature Singapore Pte Ltd. 2025

B. B. V. L. Deepak et al. (eds.), *Recent Advancements in Product Design and Manufacturing Systems*, Lecture Notes in Mechanical Engineering,
https://doi.org/10.1007/978-981-97-6732-8_26

1 Introduction

Nanofluids are popularized to exhibit higher heat transfer capacity than the conventional fluids such as water, diesel, and ethylene glycol due to achievement of greater thermal conductivity with the addition of nanosized metallic and non-metallic particles/fibers/tubes [1–3]. The thermal, oxidative stabilities of these nanofluids to maintain higher thermophysical properties for longer durations are dependent over the chemical stability. Pang et al. stated that the chemical stability of nanofluid can be expressed the ability to withhold the dispersed nanoparticles in the suspension without sedimentation due to gravitational force [4]. Ilyas investigations revealed that the agglomeration initiated with the effective drop in the repulsive forces between the nanoparticles and the downward velocity get increased by associating with the gravitational force [5]. Researchers developed and applying various methods such as mechanical, agent, and medium control to improve the chemical stability by reducing the coagulation of nanoparticles in the base fluid [6–8]. However, these chemical stability improvement techniques can have significant influence over the thermophysical properties of the nanofluids due to the possible chemical interactions in the suspension.

Khan et al. survey over the nanofluids revealed that the magnetic stirring, ultrasonication, pH modifiers, and surfactant addition are the various methods existed to improve stability through mechanical, agent, and medium control [9]. Choi et al. obtained the produced AIN nanoparticles and attempted to develop nanofluids at different volume fractions by dispersing them into the ethylene glycol. The magnetic stirring is given at 700 rpm for 50 min, and the aqueous solution is kept under ultrasonicator for 15 min [10]. Suresh et al. followed two-step preparation method to develop nanofluids by dispersing $CuNO_3$ into the deionized water. The solution is given magnetic stirring for 60 min under the magnetic force and kept under 20 kHZ ultrasonicator about 35 min to improve the stability through mechanical energy-based stability enhancement techniques [11].

Madathil et al. stated that the agglomeration is an effect occurred in the nanofluids by eliminating the boundaries between droplets which are in contact to each other. It is observed that the reduction in the total surface area of the droplets due to tremendous changes appeared in the shape of a droplet in the bulk phase [12]. Xuan et al. stated that the surfactants create a coating layer over the surface of a nanoparticle which reduce the surface tension of the base fluid in order to increase the steric repulsive forces against the agglomeration [13]. Zawrah et al. dispersed SDBS along with the Al_2O_3 into the RO water to increase the stability of nanofluids and observed that the attained increase in distance between the nanoparticles prolong coagulation with the reduction in tendency of attraction [14]. Rashmi et al. preferred gum Arabic as the surfactant for their nanofluids obtained by dispersing CNT into the deionized (DI) water and attained the improvement in chemical stability for 36 h without greater sedimentation [15].

Umar stated that the stability of the suspension can be improved by promoting the strong repulsive forces with the modification of pH of a nanofluid [16]. Samal

et al. added oleic acid to modify the pH of nanofluid developed by dispersing Al_2O_3 particles into the DI water and observed that the strong acid–weak base combination can offer the desired repulsive force for improving the chemical stability [17]. Wang and Dong studied the influence of pH modification over the chemical stability by performing an experimental investigation over the NaOH added Al_2O_3-RO water nanofluids [18]. It is observed that the kinetic properties of the fluids are modified by reducing the velocity of particles. Ghanbarpour et al. added different pH modifiers such as NaOH and HCl to improve the stability of the Al_2O_3 nanoparticles in the suspension and stated that the stability is improved for 60 h than the addition of single pH modifier into the solutions [19].

The studied literature is revealed that the majority of research is focused to attain the improvement in chemical stability of nanofluids through various controlling methods. However, the influence of chemical stability modifiers over the thermo-physical properties is required to select the suitable method for avoiding the loss in thermal properties. Although the selection of suitable pH modifier or surfactant can also have significant influence, the current research is confined to study with most preferred reagents such as NaOH and CH_3COOH for Al_2O_3 nanofluids in order to reduce the complexity of research.

2 Preparation of Nanofluids and Measurement

Two-step method is used to develop the nanofluids at different volume fractions such as 0.03, 0.06, 0.09, and 0.12% in this study. The criteria for preferring the volume fractions are the constant rate of weight addition for the development of nanofluids by dispersing the nanoparticles. It might be expected that the trend of increase or decrease can be observed from the experimentation with this approach. Deionized water at pH of 6.9 is selected as base fluid and a 35 nm sized alumina (Al_2O_3) nanoparticles which produced from the chemical vapor deposition technique are procured from the standard suppliers, Jharkand, India. The weight of nanoparticles is measured by using digital weight machine and dispersed in the base fluid in the concise environment to avoid the trap of dust, atmospheric moisture, and other foreign materials existed at microscale. Figure 1 represents the weighing of nanoparticles with a digital weighing machine and dispersion into the deionized water for the development of Al_2O_3 nanofluids.

Thermal conductivity of the nanofluids is measured by using KD2 pro thermal analyzer at the room temperature under steady-state conditions as per the ASTM C518 standards. The device is initially calibrated with the known fluids such as water, ethylene glycol, and diesel. The samples taken from the various volume fractions are loaded into the cylindrical shaped glass vessel and pulse of heat waves are supplied to obtain the readings about the thermal conductivity of nanofluids.



Fig. 1 Development of Al_2O_3 nanofluids

3 Application of Stability Improvement Methods

The nanofluids of various volume fractions are allowed to expose individually to the each of the stability improvement methods such as magnetic stirring, ultrasonication, pH modifiers, and surfactants.

The magnetic stirrer is set under 600 rpm at the room temperature in order maintain the degree of uniformity in the temperature along with the other methods. The knob is placed in the nanofluid contained glass beaker and allowed to rotate for 30 min under the influence of centrifugal force with the effective conversion of electromagnetic energy. The foam formed over the surface of the magnetic stirrer is cleared by using a filter paper which is commonly preferred for laboratory purpose.

The ultrasonicator which can produce the shock waves with a frequency of 20 kHZ is allowed to flow in the different volume fractions of developed nanofluids for 30 min individually. The probe is cleaned with a dry cloth to prevent the entry of foreign elements from the previous studies and set to dip in the nanofluid without allowing to make contact over any edge or surface or walls of the glass beaker, because it is essential to the respective precaution for avoiding break of the beaker glasses and the entry of glass particles into the nanofluids.

The pH modifying technique is applied by adding equal quantity of drops of 1% NaOH reagent into the various volume fractions of developed nanofluids. CH_3COOH is found as the most preferred surfactant to improve the stability of nanofluids, and it is taken as surfactant and 2 wt% to the actual nanoparticle weight added into the base fluid for the development of different volume fractions. Hand stirring for 5 min is applied over the both the medium and agent control stability modifying technique implemented nanofluid samples to get the uniformity of dispersion. The samples of mechanical, agent, and medium control are kept in a moisture-free environment by tightly sealing the container with the aluminum foil for 24 h prior to the measurement.

4 Results and Discussions

KD2 pro thermal analyzer is used to test the thermal conductivity of the samples taken from the developed nanofluids for different volume fractions. The calibration is performed to maintain the accuracy in the measurement and necessary precautions are taken to avoid the data discrepancy. Table 1 enlists the data obtained about thermal conductivity measured at 30 °C (room temperature) of various samples developed by applying different stability improvement methods.

The thermal conductivity of base fluid is measured to calibrate the device and mentioned as 0.00% (pure deionized water). The measurements are taken at 30 °C to study the thermal conductivity behavior the samples under the absence of temperature influence. Later, the experimentation is conducted from 30 to 70 °C for study the thermal conductivity of the taken samples under the influence of temperature.

4.1 Thermal Conductivity with Magnetic Stirring

The response of thermal conductivity of magnetic stirring applied Al_2O_3 nanofluids for volume fractions such as 0.03, 0.6, 0.09, and 0.12% is plotted against temperature, and it is represented in Fig. 2.

It can be observed from Fig. 2 that the thermal conductivity is increased from 40 to 70 °C for lower volume fractions such as 0.03 and 0.06, and gradual decrease is started with the increase of nanoparticles addition. The increment in thermal conductivity at 70 °C is exhibited by all samples of Al_2O_3 nanofluids, and the highest thermal conductivity with 0.65 W/mK is observed for the 0.0.6% by 1.2, 2.56, 3.42% than the 0.03, 0.06, 0.09% volume fractions. The expose of higher temperatures revealed the ability of nanofluid to carry the heat without any interruptions for lower volume fractions. Although the decrement in thermal conductivity for higher volume fractions at elevated temperatures is found greater, still it exhibited higher thermal conductivity than the samples taken at room temperature. It is understood that the centrifugal force given by the magnetic stirrer can hold lower volume fractions and this stability improvement technique is not suitable for higher volume fractions [20].

Table 1 Thermal conductivity (W/mK) of Al_2O_3-DI nanofluids at 30 °C

Method	Volume fraction				
	0.00%	0.03%	0.06%	0.09%	0.12%
Magnetic stirring	0.59	0.609	0.62	0.61	0.592
Ultrasonication	0.6	0.61	0.628	0.654	0.67
pH modifier	0.57	0.59	0.61	0.58	0.572
Surfactant	0.58	0.61	0.63	0.603	0.59

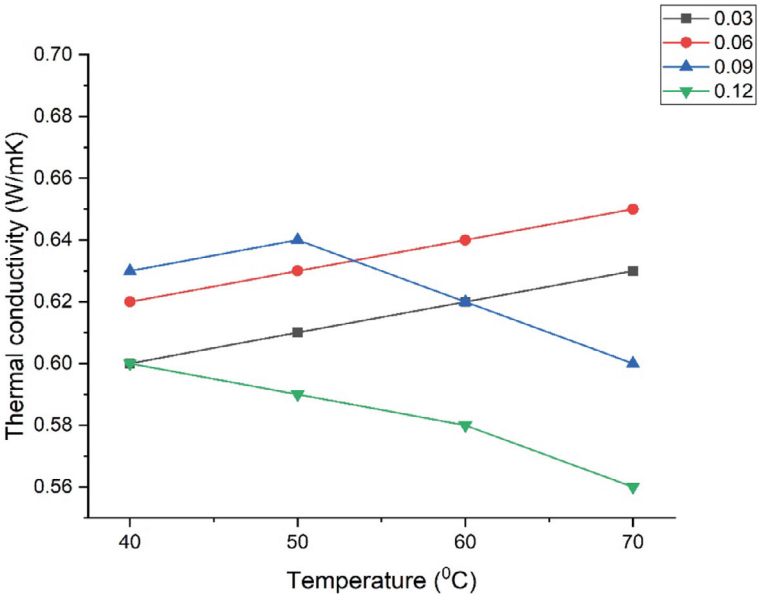


Fig. 2 Thermal conductivity of magnetic stirring applied Al_2O_3-DI nanofluids

4.2 Thermal Conductivity with Ultrasonication

The response of thermal conductivity of ultrasonication applied Al_2O_3 nanofluids for volume fractions such as 0.03, 0.6, 0.09, and 0.12% is plotted against temperature, and it is represented in Fig. 3.

It can be observed from Fig. 3 that the thermal conductivity is increased from 40 to 70 °C for all volume fractions such as 0.03, 0.06, 0.09, and 0.12%. The highest thermal conductivity with 72 W/mK is observed for the 0.12% at 70 °C by 1.8, 2.84, 4.21% than the 0.03, 0.06, 0.09% volume fractions. The entry of sonic vibrations into the nanofluids penetrated the clusters and restricted the formation of dendrite like structures from the nanoparticles with the low electrostatic repulsions of Al_2O_3. The particles become activated and electrically charged by receiving the sonic vibrations for 30 min of duration. However, the studies are showing that the optimum sonication time should be chosen to avoid the loss of thermal properties, because it can cause severe reduction in the surface area of the nanoparticles and discharge of metallic particles from the sonicator's probe [21]. It is understood that this stability improvement technique is suitable for generation of stable nanofluids at higher volume fractions.

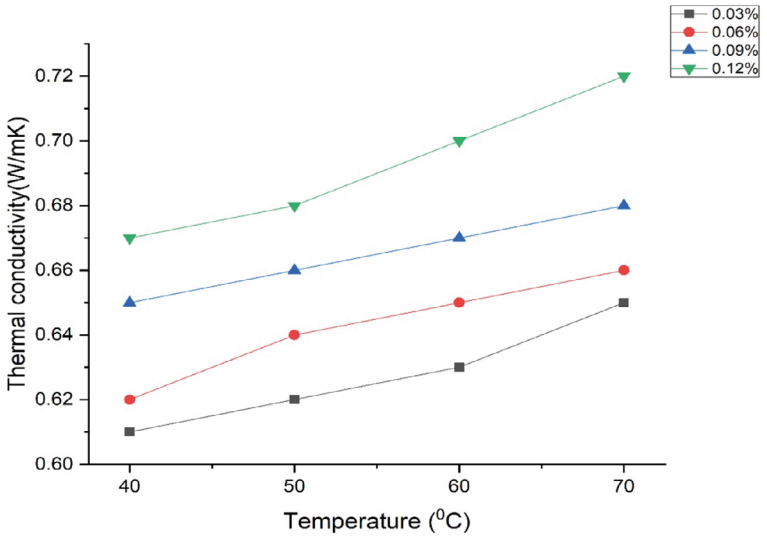


Fig. 3 Thermal conductivity of ultrasonication applied Al_2O_3-DI nanofluids

4.3 Thermal Conductivity with pH Modifier

The response of thermal conductivity of pH modifier applied Al_2O_3 nanofluids for volume fractions such as 0.03, 0.6, 0.09, and 0.12% is plotted against temperature, and it is represented in Fig. 4.

It can be observed from Fig. 4 that the thermal conductivity is increased for lower volume fractions and gradual decrease is started from the further addition of nanoparticles. The highest thermal conductivity with 0.63 W/mK is observed for the 0.06% at 70 °C by 1.18, 2.1, 2.89% than the 0.03, 0.06, 0.12% volume fractions. The formation of electrical double layer on the surface of the nanoparticles and the electrostatic stabilization achieved with the adsorption ions is responsible for the increase of thermal conductivity. Consequently, it shown the lower thermal conductivity with rise of temperature from 40 °C for the volume fraction greater than 0.06%. It is expected that the addition of higher amount of pH modifier can alter the situation and understood the quantity of NaOH is not sufficient to create necessary repulsive force to withhold the nanoparticles in the suspension [22]. Significant research is required in this direction to examine the electrophoretic behavior with respect to nanoparticle's diameter, surface area, and charge.

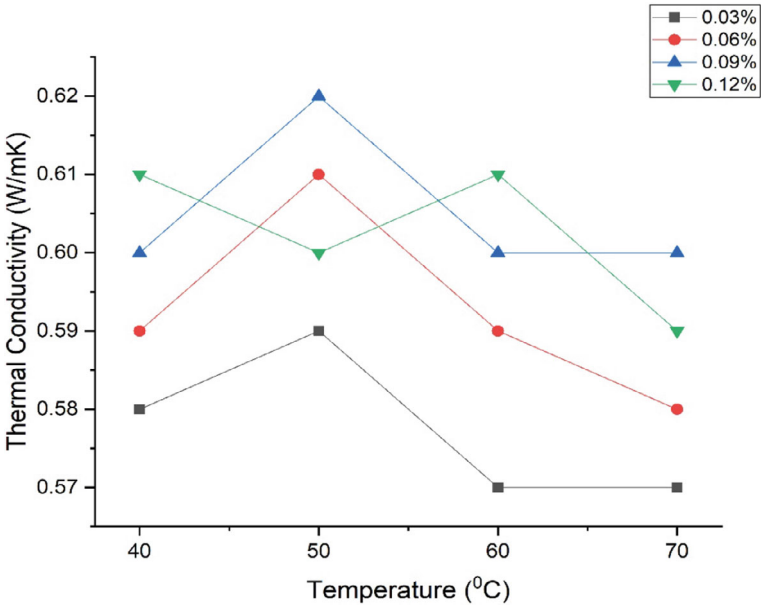


Fig. 4 Thermal conductivity of pH modifier applied Al_2O_3-DI nanofluids

4.4 Thermal Conductivity with Surfactant

The response of thermal conductivity of surfactant applied Al_2O_3 nanofluids for volume fractions such as 0.03, 0.6, 0.09, and 0.12% is plotted against temperature, and it is represented in Fig. 5.

It can be observed from Fig. 5 that the thermal conductivity is increased at the initial increment of temperature from 40 to 50 °C and gradual decrease is started from the further rise of temperature to 70 °C. The brakeage of bonds established by the surfactants at the elevated temperatures can lead to sedimentation of nanoparticles with the gravitational force. The loss of suspension characteristics can create the effective drop in the thermal conductivity for various volume fractions. The catastrophic fall in the thermal conductivity is observed for the higher volume fractions such as 0.09 and 0.12% which can be caused with rapid bond brakeage. The reduction in surface tension and kelvin barrier shifts is become limited for low volume fractions and increase in particle size with the loss of repulsive force for the further increase of nanoparticles rather than room temperature. The generation of fumes in the nanofluids samples at higher volume fractions is observed at higher temperatures applied in the study [23]. The catastrophic fall in thermal conductivity might be appeared due to increase of thermal resistance created by the sedimentation of nanoparticles with loss of surfactant.

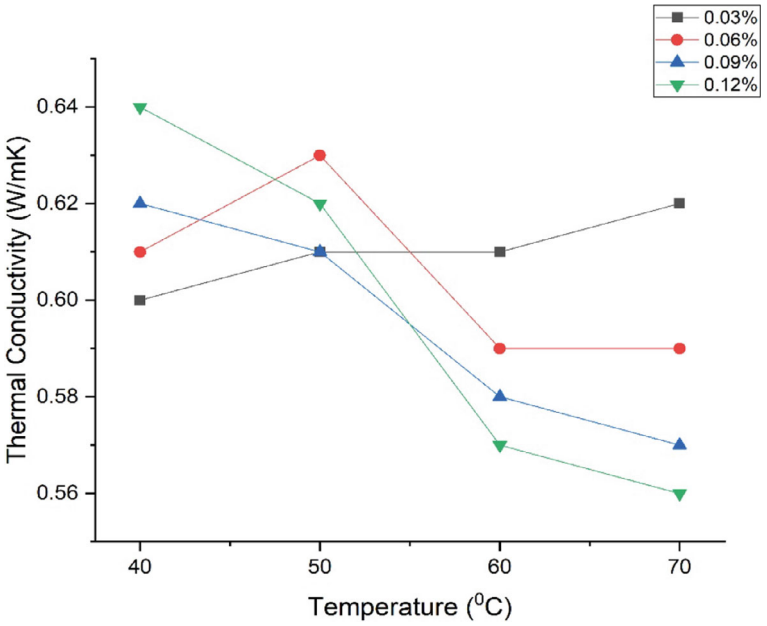


Fig. 5 Thermal conductivity of surfactant applied Al_2O_3-DI nanofluids

5 Conclusion

The study is focused to investigate the influence of stability improvement methods over the thermal conductivity of the nanofluids. Two-step method is followed for the development of nanofluids and Al_2O_3 nanoparticles are dispersed in the deionized water at different volume fractions such as 0.03, 0.06, 0.09, and 0.12%. The stability improvement methods such as magnetic stirring, ultrasonication, surfactant addition, and pH modifiers are applied over the various samples of the nanofluids. Magnetic stirring at 600 rpm and ultrasonication at 20 kHZ are applied for 30 min individually, whereas 1, 2% of CH_3COOH, NaOH is used as surfactant, pH modifier over the all different nanofluids. The samples are kept under observation for time period of 24 h, and stability of nanofluids is measured through the naked eye test. The thermal conductivity of the samples is measured by using the transient hot-wire method.

- The increment in thermal conductivity of the developed nanofluid with application of magnetic stirring is limited for the lower volume fractions such as 0.03, 0.06% with respect to the rise of temperature.
- Ultrasonication found as most probable stability improvement method to achieve the increased thermal conductivity for higher volume fractions, and optimum time should be employed to avoid the reduction in the surface area of the nanoparticles.

- The increment in thermal conductivity of the developed nanofluid with application of pH modifier is limited for the lower temperatures such as 40 and 50 °C, and significant study is essential to analyze the electrophoretic behavior at higher temperatures.
- Surfactant addition can improve the chemical stability of the nanofluid, but it is negotiating to achieve the enhancement in thermal conductivity at higher volume fractions limited for lower volume fractions and fume generation is observed at highest temperature such as 70 °C applied in this study.

The future scope of this research is to investigate the influence of these stability improvement methods over the other thermophysical properties such as viscosity, density, and thermal diffusivity.

References

1. Saidur R, Leong KY, Mohammed HA (2011) A review on applications and challenges of nanofluids. Renew Sustain Energy Rev 15(3):1646–1668
2. Wong KV, De Leon O (2010) Applications of nanofluids: current and future. Adv Mech Eng 2:519659
3. Sarkar J, Ghosh P, Adil A (2015) A review on hybrid nanofluids: recent research, development and applications. Renew Sustain Energy Rev 43:164–177
4. Pang C et al (2012) Thermal conductivity measurement of methanol-based nanofluids with Al_2O_3 and SiO_2 nanoparticles. Int J Heat Mass Transf 55(21–22):5597–5602
5. Ilyas SU, Pendyala R, Marneni N (2017) Stability of nanofluids. Eng Appl Nanotechnol: Energy Drug Deliv, 1–31
6. Mukherjee S, Paria S (2013) Preparation and stability of nanofluids—a review. IOSR J Mech Civ Eng 9(2):63–69
7. Chakraborty S, Panigrahi PK (2020) Stability of nanofluid: a review. Appl Therm Eng 174:115259
8. Hwang Y et al (2007) Stability and thermal conductivity characteristics of nanofluids. Thermochim Acta 455(1–2):70–74
9. Khan AI, Valan Arasu A (2019) A review of influence of nanoparticle synthesis and geometrical parameters on thermophysical properties and stability of nanofluids. Therm Sci Eng Prog 11:334–364
10. Choi SUS et al (2001) Anomalous thermal conductivity enhancement in nanotube suspensions. Appl Phys Lett 79(14):2252–2254
11. Suresh S et al (2011) Synthesis of Al_2O_3–Cu/water hybrid nanofluids using two step method and its thermo physical properties. Colloids Surf, A 388(1–3):41–48
12. Madathil PK et al (2016) Preparation and characterization of molten salt based nanothermic fluids with enhanced thermal properties for solar thermal applications. Appl Therm Eng 109:901–905
13. Xuan Y, Li Q, Tie P (2013) The effect of surfactants on heat transfer feature of nanofluids. Exp Therm Fluid Sci 46:259–262
14. Zawrah MF, Khattab RM, Girgis LG, El Daidamony H, Abdel Aziz RE (2016) Stability and electrical conductivity of water-base Al_2O_3 nanofluids for different applications. HBRC J 12(3):227–234
15. Rashmi W, Ismail AF, Sopyan I, Jameel AT, Yusof F, Khalid M, Mubarak NM (2011) Stability and thermal conductivity enhancement of carbon nanotube nanofluid using gum arabic. J Exp Nanosci 6(6):567–579

16. Umar S, Sulaiman F, Abdullah N, Mohamad SN (2018) Investigation of the effect of pH adjustment on the stability of nanofluid. In: AIP conference proceedings, vol 2031(1). AIP Publishing
17. Samal S, Satpati B, Chaira D (2010) Production and dispersion stability of ultrafine Al–Cu alloy powder in base fluid. J Alloy Compd 504:S389–S394
18. Wang X-j, Zhu D-S (2009) Investigation of pH and SDBS on enhancement of thermal conductivity in nanofluids. Chem Phys Lett 470(1–3):107–111
19. Ghanbarpour M, Bitaraf Haghigi E, Khodabandeh R (2014) Thermal properties and rheological behavior of water based Al_2O_3 nanofluid as a heat transfer fluid. Exp Therm Fluid Sci 53:227–235
20. Murshed SMS, Leong KC, Yang C (2008) Investigations of thermal conductivity and viscosity of nanofluids. Int J Therm Sci 47(5):560–568
21. Shahsavar A et al (2015) An experimental study on the effect of ultrasonication on thermal conductivity of ferrofluid loaded with carbon nanotubes. Thermochim Acta 617:102–110
22. Liu M, Jia K, Liu X (2015) Effective thermal conductivity and thermal properties of phthalonitrile-terminated poly (arylene ether nitriles) composites with hybrid functionalized alumina. J Appl Polym Sci 132(10)
23. Xia G et al (2014) Effects of surfactant on the stability and thermal conductivity of Al_2O_3/de-ionized water nanofluids. Int J Therm Sci 84:118–124

Development of High-performance Welding Consumables and Filler Materials: A Review

Anish K. Raj, Bikash Ranjan Moharana, Sunita Routray, and Kalinga Simant Bal

Abstract Welding is a vital process in various industries such as power generating, oil and gas, automotive, and aerospace. The quality and reliability of welded joints depend not only on skilled welders, but also on the materials used. High-performance welding consumables and filler materials play a crucial role in ensuring strong and durable welds. In the realm of welding, a profound shift is underway, ushering in an era of innovation and environmental consciousness. As our world pivots toward sustainability, welding consumables are being reinvented with a greener touch. The focus is on reducing the use of hazardous materials while embracing recycling and waste management strategies, paving the way for cleaner and safer welding practices. The welding industry is riding the wave of digitalization and automation. Cutting-edge technologies like artificial intelligence, robotics, and data analytics have become integral to the welding process. This infusion of advanced technology demands that high-performance consumables keep pace, ensuring efficiency and productivity reach unprecedented heights. In this article, we will explore the development of such materials, their importance, and their applications in different industries.

Keywords High-performance welding consumables · Filler materials · Advanced techniques

A. K. Raj (✉) · S. Routray
Department of Mechanical Engineering, C. V. Raman Global University, Bhubaneswar, Odisha 752054, India
e-mail: anishonfire2015@gmail.com

B. R. Moharana
Mechanical Engineering Department, Papua New Guinea University of Technology, Lae 411, Papua New Guinea

K. S. Bal
Department of Mechanical Engineering, National Institute of Technology, Raipur, Chhattisgarh 492010, India

© The Author(s), under exclusive license to Springer Nature Singapore Pte Ltd. 2025

B. B. V. L. Deepak et al. (eds.), *Recent Advancements in Product Design and Manufacturing Systems*, Lecture Notes in Mechanical Engineering,
https://doi.org/10.1007/978-981-97-6732-8_27

1 Introduction

The development of high-performance welding consumables and filler materials has revolutionized the field of welding, offering enhanced properties and capabilities for creating strong and durable welds. The quality and reliability of welded joints not only depend on the skills of the welder but also on the materials used. High-performance welding consumables and filler materials are essential to maintaining the longevity and integrity of these junctions [1, 2]. Welding consumables, such as wires and electrodes, and filler materials are essential components of the welding process. They provide the necessary material to form the weld joint and contribute to its strength and durability. High-performance welding consumables offer numerous advantages over conventional ones, including improved mechanical properties, higher resistance to corrosion, and enhanced heat resistance, may fulfilling the demands of contemporary industries [3, 4].

The performance of welding consumables is influenced by various factors. The development of high-performance welding consumables involves optimizing these factors to achieve superior performance in specific welding applications, in an additional study shown in [5]. There are different types of high-performance welding consumables and filler materials available, each suited for specific welding processes and applications. Solid wires, flux-cored wires, stick electrodes, and gas tungsten arc welding (GTAW) filler rods are among the commonly used options. According to Hosseini et al., these materials provide exact control over the welding process and yield high-quality welds with few flaws [6]. Advancements in welding consumable development have been made possible through the use of advanced techniques. Alloy design and optimization, microstructural control, coating technology, and specialized additives are some of the methods employed to enhance the properties and performance of welding consumables [7, 8]. Manufacturers and researchers work tirelessly to advance these materials, pushing the limits of what they can do.

The applications of high-performance welding consumables and filler materials are vast and varied. Industries such as power developing, oil and gas, aerospace, and transportation rely on these materials for constructing critical components and structures. Their application guarantees the endurance, dependability, and safety of welded structures in demanding conditions [9, 10]. Even though there has been a lot of advancement in the growth of high-performance welding consumables, there are still challenges to address and future trends to explore. Environmental sustainability, digitalization and automation, and the incorporation of nanostructured materials are some of the areas that researchers and industry professionals are focusing on. In the upcoming years, these developments will significantly enhance the functionality and effectiveness of welding consumables [11–13].

With this background, the present study was conducted to answer the following research questions.

1. What are the possibilities to enhance the performance of high-performance welding consumables?

2. How we can achieve the expected level of high-performance welding consumables for different applications?

To answer these research questions, the study was conducted with the following objectives.

1. How high-performance welding consumables and filler materials show better performance when compared with ordinary welding consumables and filler materials.

Importance and application of high-performance welding consumables and filler materials over ordinary welding consumables.

1.1 Importance of Welding Consumables and Filler Materials

Welding consumables, such as wires and electrodes, and filler materials are essential components in the welding process. They provide the necessary material to form the weld joint and ensure its integrity. High-performance welding consumables offer several advantages over conventional ones, including improved mechanical properties, higher corrosion resistance, and enhanced heat resistance and may support the overall improvement of weld quality [9, 12, 14].

1.2 Factors Affecting the Performance of Welding Consumables

Several factors influence the performance of welding consumables and filler materials. These factors need to be carefully considered during the development process to ensure optimal performance in specific applications.

1.2.1 Composition

The chemical composition of welding consumables greatly impacts their mechanical properties. The selection of suitable alloying elements and their proportions can enhance strength, toughness, and corrosion resistance. For instance, it was demonstrated that incorporating components like chromium and nickel into stainless steel consumables increases their resistance to oxidation at high temperatures and corrosion [14–17].

1.2.2 Strength and Toughness

Welding consumables must exhibit adequate strength and toughness to withstand mechanical stresses and prevent weld joint failure. Excellent tensile strength, yield strength, and impact toughness are provided by high-performance consumables, which produce welds that can endure large loads and dynamic stresses [18–20].

1.2.3 Resistance to Corrosion

Many applications require welded structures to withstand corrosive environments. High-performance consumables are designed to offer superior corrosion resistance, preventing the formation of rust, pitting, or other forms of degradation. This is particularly important for the oil and gas, chemical processing, and maritime industries [21–23].

1.2.4 Heat Resistance

Some welding operations involve high temperatures, such as those encountered in the aerospace and power generation sectors. High-performance consumables are formulated to retain their mechanical properties even under extreme heat conditions. They guarantee the integrity of the welds in tough settings because of their exceptional creep resistance and thermal stability [24, 25].

2 Types of High-Performance Welding Consumables and Filler Materials

A wide range of high-performance welding consumables and filler materials are available to meet diverse welding requirements. Here are some commonly used types:

2.1 Solid Wires

Solid wires are widely used in various welding processes, including gas metal arc welding (GMAW) and gas tungsten arc welding (GTAW). They consist of solid metal wire with a uniform diameter and are suitable for both mild steel and alloy welding applications. With solid filler wires, concerns such as heat input and distortion can be addressed through proper techniques. According to many researchers that the solid

wires offer excellent control over the welding process and result in high-quality welds with little spatter [25–27].

2.2 Flux-Cored Wires

Flux-cored wires are similar to solid wires but have a flux-filled core. Flux-cored wires come in different types, primarily categorized as self-shielded and gas-shielded. The flux acts as a shielding gas and provides additional protection to the weld pool, reducing the risk of defects. Flux-cored wires are frequently utilized in applications that call for deeper penetration and higher deposition rates [23].

2.3 Stick Electrodes

Stick electrodes, also known as shielded metal arc welding (SMAW) electrodes, are widely used in industries where versatility and portability are essential. They consist of a metal core wire coated with flux. In order to prevent contamination and guarantee high-quality welds, the flux coating creates a protective gas shield throughout the welding process [28]. To provide a clear and concise overview of the differences between stick electrode, MIG, and TIG welding, let us explore them in Table 1.

3 Advanced Techniques in Welding Consumable Development

The development of high-performance welding consumables and filler materials involves advanced techniques that optimize their properties and performance. Some of these techniques include:

3.1 Alloy Design and Optimization

Researchers and manufacturers focus on developing new alloy compositions or optimizing existing ones to enhance specific properties. Computational modeling and simulation are examples of advanced alloy design approaches that aid in the prediction of material behavior and in customizing it to satisfy the requirements [29].

Table 1 Differences between stick electrode, MIG, and TIG welding

Aspect	Stick electrode welding	MIG welding	TIG welding
Process overview	Involves a flux-coated electrode that melts to form the weld. The flux creates a protective gas shield during welding	Uses a wire electrode on a spool, fed through a welding gun. A continuous flow of inert gas provides shielding	Uses a non-consumable tungsten electrode to create the arc. A separate filler metal may be added manually
Suitability for outdoor use	Ideal for outdoor applications due to its self-shielding nature, making it less sensitive to wind and atmospheric conditions	Can be affected by wind and requires a controlled environment due to its reliance on external shielding gas	–
Versatility	Highly versatile, suitable for various metals and welding positions	Versatile but may require different shielding gases for different materials	–
Ease of learning	Considered more forgiving for beginners due to its simplicity and ability to tolerate variations in technique	Relatively easy to learn, with a shorter learning curve compared to some other methods	–
Precision and control	Offers less precision compared to TIG welding, making it better suited for robust and structural welds	–	Provides superior control and precision, suitable for intricate and critical welds
Weld appearance	Generally produces a more substantial and rugged appearance in the weld	–	Yields a cleaner and aesthetically pleasing weld, making it preferred for applications where appearance matters
Applications	Commonly used in construction and heavy fabrication where the structural integrity of the weld is paramount	–	Ideal for applications requiring high-quality and visually appealing welds, such as aerospace and automotive industries

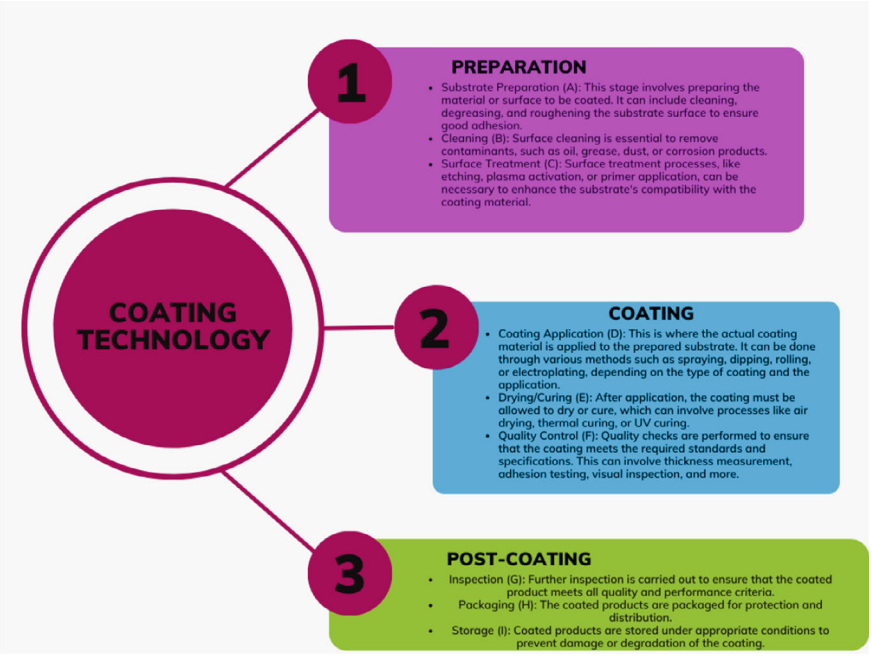


Fig. 1 Process involved in the coating process

3.2 Coating Technology

Coating plays a significant role in welding consumables, providing protection against environmental factors and enhancing performance. The flowchart given in Fig. 1 shows the process involved in the coating process. By improving resistance to wear, corrosion, and high temperatures, advanced coating technologies, such as ceramic and alloy-based coatings, extend the service life of the welding consumables [30].

3.3 Specialized Additives

Additives are incorporated into welding consumables to achieve specific properties or performance enhancements. For example, adding rare earth elements can improve the arc stability and mechanical properties of welding consumables. Nanoparticles are also used as additives to enhance the material's strength and corrosion resistance. Some of the added elements used to improve welding consumables with their unique qualities are displayed in Table 2, as described by the researchers [31].

Table 2 Additive elements used for enhancing welding consumables with their specific properties

Alloying element	Specific properties
Nickel (Ni)	1. Increases the corrosion resistance of the weld
	2. Enhances the robustness and resilience of the welded metal
	3. Often used in stainless steel and nickel-based alloys
Chromium (Cr)	1. Improves the resistance to corrosion and oxidation
	2. Enhances high-temperature strength and durability
	3. Commonly found in stainless steel and certain high-alloy steels
Molybdenum (Mo)	1. Increases the resistance to pitting and crevice corrosion
	2. Enhances the high-temperature strength of the weld
	3. Often used in stainless steel and alloy steel welding
Vanadium (V)	1. Enhances the strength and wear resistance of the weld
	2. Used in some low-alloy and high-strength steel applications
Titanium (Ti)	1. Improves the weldability of certain materials
	2. Helps reduce the risk of embrittlement during welding
Zirconium (Zr)	1. Enhances resistance to corrosion and oxidation
	2. Used in the welding of certain stainless and nickel alloys
Aluminum (Al)	1. Deoxidizes the molten metal, reducing porosity in the weld
	2. Enhances the mechanical characteristics of aluminum-based alloys
Silicon (Si)	1. Deoxidizes the weld metal and enhances fluidity
	2. Frequently employed while welding carbon and stainless steels
Manganese (Mn)	1. Acts as a deoxidizer and enhances the strength of the weld
	2. Often used in conjunction with silicon in carbon steel welding
Copper (Cu)	1. Improves electrical conductivity and thermal properties
	2. Used in various applications, including electrical welding
Tungsten (W)	1. Increases the melting temperature of the electrode tip
	2. Maintains a stable arc in TIG (Tungsten Inert Gas) welding
Boron (B)	1. Enhances hardenability and strength in some steel applications
	2. Particularly useful in the welding of certain tool steels

4 Applications of High-Performance Welding Consumables and Filler Materials

High-performance welding consumables and filler materials find applications in various industries, including:

4.1 Automotive Industry

In the automotive sector, high-performance welding consumables are crucial for manufacturing lightweight yet strong structures. They are used in the fabrication of vehicle frames, chassis components, exhaust systems, and other critical parts. High-performance components are utilized to ensure the durability and security of the automotive structures [32].

4.2 Aerospace Industry

Aerospace applications demand exceptional quality and performance from welding consumables. High-performance materials are used in the fabrication of aircraft components, such as airframes, engine parts, and landing gears. To endure the severe operating conditions, the aircraft sector needs welds with high strength, fatigue resistance, and exceptional corrosion resistance [22, 26, 33].

4.3 Oil and Gas Industry

The oil and gas industry operates in challenging environments that expose welded structures to corrosive substances and extreme temperatures. High-performance welding consumables are used in the construction of pipelines, offshore platforms, storage tanks, and refinery equipment. Researchers have noted that they offer dependable welds that are resistant to the severe circumstances found in oil and gas operations [15, 18, 23, 34].

5 Challenges and Future Trends in Welding Consumable Development

While significant advancements have been made in the development of high-performance welding consumables, several challenges and future trends deserve attention:

5.1 Environmental Sustainability

There is a growing emphasis on developing welding consumables that are environmentally friendly. In addition to investigating recycling and waste management

techniques, researchers are attempting to decrease the amount of toxic and hazardous components used in consumables [35–39].

5.2 Nanostructured Materials

Nanotechnology holds great promise for the future of welding consumables. The incorporation of nanoparticles in welding materials can lead to improved mechanical properties, enhanced corrosion resistance, and better performance at high temperatures. The development of sophisticated welding consumables will be fueled by ongoing research into nanostructured materials [12, 36–42].

6 Implications of this Research

- Welding consumables, encompassing items such as wires and electrodes, in conjunction with filler materials, constitute indispensable constituents within the welding procedure. Their primary function lies in supplying the requisite materials essential for the formation of the weld joint, thereby safeguarding its structural integrity.
- It is noteworthy that high-performance welding consumables confer a multitude of advantages when juxtaposed with their conventional counterparts. These benefits encompass the augmentation of mechanical properties, heightened resistance to corrosion, and increased capacity to endure elevated temperatures.
- The collective effect of these characteristics is a substantive enhancement in the overall quality and durability of welded structures, thereby making a substantial contribution to the field of welding technology.
- It is noteworthy that the welding industry is currently riding the crest of the digitalization and automation wave. State-of-the-art technologies, including artificial intelligence, robotics, and data analytics, have now assumed pivotal roles within the welding domain.

7 Conclusion

The development of high-performance welding consumables and filler materials has revolutionized the welding industry. These materials offer improved mechanical properties, higher resistance to corrosion and heat, and enhanced performance in various industries. The continuous research and development in alloy design, microstructural control, coating technology, and additive incorporation are paving the way for further advancements in welding consumable technologies. By using

high-performance welding consumables, industries can ensure the reliability, safety, and durability of welded structures.

References

1. Hensel J, Kromm A, Nitschke-Pagel T, Dixneit J, Dilger K (2020) Capability of martensitic low transformation temperature welding consumables for increasing the fatigue strength of high strength steel joints. Mater Test 62(9):891–900
2. Thomas M, Vollert F, Weidemann J, Gibmeier J, Kromm A, Kannengießer T (2020) Surface- and volume-based investigation on influences of different Varestraint testing parameters and chemical compositions on solidification cracking in LTT filler metals. Weld World 64:913–923
3. Vollert F, Thomas M, Kromm A, Gibmeier J (2020) Solidification cracking assessment of LTT filler materials by means of Varestraint testing and μCT. Materials 13(12):2726
4. Feng Z, Ma N, Tsutsumi S, Di X (2021) Size effect on residual stress in low transformation temperature welded joints. Mar Struct 78:103001
5. Wang H, Woo W, Kim DK, Em V, Lee SY (2018) Effect of chemical dilution and the number of weld layers on residual stresses in a multi-pass low-transformation-temperature weld. Mater Des 160:384–394
6. Hosseini SA, Gheisari K, Moshayedi H, Ahmadi MR, Warchomicka F, Enzinger N (2021) Assessment of the chemical composition of LTT fillers on residual stresses, microstructure, and mechanical properties of 410 AISI welded joints. Weld World 65:807–823
7. Wu S, Wang D, Zhang Z, Li C, Liu X, Zhou Z, Di X (2019) Effect of dilution on fatigue behaviour of welded joints produced by low-transformation-temperature fillers. Sci Technol Weld Joining 24(7):601–608
8. Choi S, Lee J, Lee JY, Kang SK, Kim YC, Lee SJ, Kwon D (2021) Effect of low transformation temperature welding consumable on microstructure, mechanical properties and residual stress in welded joint of A516 carbon steel. Korean J Metals Mater 59(8):524–532
9. Feng Z, Ma N, Tsutsumi S, Lu F (2021) Investigation of the residual stress in a multi-pass T-welded joint using low transformation temperature welding wire. Materials 14(2):325
10. Dixneit J, Vollert F, Kromm A, Gibmeier J, Hannemann A, Fischer T, Kannengiesser T (2019) In situ analysis of the strain evolution during welding using low transformation temperature filler materials. Sci Technol Weld Joining 24(3):243–255
11. Igwemezie V, Shamir M, Mehmanparast A, Ganguly S (2022) A review of LTT welding alloys for structural steels: design, application and results. J Adv Join Process 5:100110
12. Wang H, Woo W, Kim DK, Em V, Karpov ID, An GB, Lee SY (2018) Effect of tailored martensitic transformation in a thick weld: residual stresses mitigation, heterogeneous microstructure, and mechanical properties. Mater Charact 144:345–355
13. Dixneit J, Kromm A, Boin M, Wimpory RC, Kannengiesser T, Gibmeier J, Schroepfer D (2017) Residual stresses of LTT welds in large-scale components. Weld World 61:1089–1097
14. Hosseini SA, Gheisari K, Moshayedi H, Warchomicka F, Enzinger N (2020) Basic alloy development of low-transformation-temperature fillers for AISI 410 martensitic stainless steel. Sci Technol Weld Joining 25(3):243–250
15. Harati E, Karlsson L, Svensson LE, Dalaei K (2017) Applicability of low transformation temperature welding consumables to increase fatigue strength of welded high strength steels. Int J Fatigue 97:39–47
16. Moat RJ, Ooi S, Shirzadi AA, Dai H, Mark AF, Bhadeshia HKDH, Withers PJ (2018) Residual stress control of multipass welds using low transformation temperature fillers. Mater Sci Technol 34(5):519–528
17. Shirzadi AA (2019) Modelling and design of new stainless-steel welding alloys suitable for low-deformation repairs and restoration processes. Procedia Manuf 37:627–632

18. Jiang W, Chen W, Woo W, Tu ST, Zhang XC, Em V (2018) Effects of low-temperature transformation and transformation-induced plasticity on weld residual stresses: numerical study and neutron diffraction measurement. Mater Des 147:65–79
19. Feng Z, Aung TL, Shao C, Lu F, Tsutsumi S, Ma N (2020) A design method of tensile triangles and low transformation temperature weld metal for reduction of stress concentration and residual stress of welded joints. Mar Struct 72:102759
20. Hashimoto T, Fujishiro Y (1958) An experiment of line heating designed with the table orthogonal array L32 (231). Journal of Zosen Kiokai 1958(104):201–225
21. Chen X, Wang P, Pan Q, Lin S (2018) The effect of martensitic phase transformation dilation on microstructure, strain–stress and mechanical properties for welding of high-strength steel. Crystals 8(7):293
22. Kromm A, Dixneit J, Kannengiesser T (2014) Residual stress engineering by low transformation temperature alloys—state of the art and recent developments. Welding in the World 58:729–741
23. Ooi SW, Garnham JE, Ramjaun TI (2014) Low transformation temperature weld filler for tensile residual stress reduction. Mater Des (1980–2015) 56:773–781
24. Novotný L, de Abreu HFG, de Miranda HC, Béreš M (2016) Simulations in multipass welds using low transformation temperature filler material. Sci Technol Weld Joining 21(8):680–687
25. Ramjaun TI, Stone HJ, Karlsson L, Kelleher J, Ooi SW, Dalaei K, Bhadeshia HKDH (2014) Effects of dilution and baseplate strength on stress distributions in multipass welds deposited using low transformation temperature filler alloys. Sci Technol Weld Joining 19(6):461–467
26. Kromm A, Kannengießer T (2014) Stress build-up during multilayer welding with novel Martensitic filler materials. HTM J Heat Treat Mater 69(2):80–88
27. Kromm A, Kannengiesser T (2014) Effect of martensitic phase transformation on stress build-up during multilayer welding. In: Materials science forum, vol 768. Trans Tech Publications Ltd., pp 660–667
28. Wu S, Wang D, Zhang Z, Li C, Liu X, Meng X, Di X (2019) Mechanical properties of low-transformation-temperature weld metals after low-temperature postweld heat treatment. Sci Technol Weld Joining 24(2):112–120
29. Sridharan N, Bunn J, Kottman M, Fancher CM, Payzant A, Noakes M, Babu SS (2021) Consumable development to tailor residual stress in parts fabricated using directed energy deposition processes. Addit Manuf 39:101837
30. Gibmeier J, Held E, Altenkirch J, Kromm A, Kannengiesser T, Buslaps T (2014) Real time monitoring of phase transformation and strain evolution in LTT weld filler material using EDXRD. J Mater Process Technol 214(11):2739–2747
31. Ramjaun TI, Stone HJ, Karlsson L, Gharghouri MA, Dalaei K, Moat RJ, Bhadeshia HKDH (2014) Surface residual stresses in multipass welds produced using low transformation temperature filler alloys. Sci Technol Weld Joining 19(7):623–630
32. Martinez-Lombardia E, Lapeire L, Maurice V, De Graeve I, Klein L, Marcus P, Terryn H (2017) Use of local electrochemical methods (SECM, EC-STM) and AFM to differentiate microstructural effects (EBSD) on very pure copper. Corros Sci Technol 16(1):1–7
33. Aydinyan S, Kirakosyan H, Niazyan O, Tumanyan M, Nazaretyan K, Kharatyan S (2016) Reaction pathway in the WO3-CuO-Mg-C system at nonisothermal conditions. Armenian J Phys 9(1)
34. Khomskaya IV, Kheifets AE, Zel'dovich VII, Korshunov LG, Frolova NYYY, Abdullina DN (2018) The formation of friction-induced nanocrystalline structure in submicrocrystalline Cu–Cr–Zr alloy processed by DCAP. Lett Mater 8(4):410–414
35. Majdanchuk T (2014). Electrode and filler materials for surfacing and welding of cast tin bronzes
36. Chembarisova RG (2020) Influence of grain boundaries on the electrical conductivity of copper alloys. Tech Phys 65:593–601
37. Gupta A, Singh J, Chhibber R (2023) Dissimilar welding of austenitic and ferritic steels using nickel and stainless-steel filler: associated issues. Proc Inst Mech Eng, Part E: J Process Mech Eng, 09544089231159776

38. Jose B, Manoharan M, Natarajan A, Muktinutalapati NR, Madhusudhan Reddy G, Meshram SD (2023) Current research and developments in welding of 18% nickel maraging steel. Proc Inst Mech Eng, Part L: J Mater: Des Appl 237(6):1295–1318
39. Liu D, Zha X, Wang W, Tang Y, Jiao H, Hu Y, Zhang J (2023) Microstructure and mechanical properties of welded joints of stainless steel clad sheets using Cr-Ni–Cu–Al multi-principal filler wires. J Mater Eng Perform 32(5):2029–2040
40. Yibowei ME, Adekoya JG, Adediran AA, Adekomaya O (2021) Carbon-based nano-filler in polymeric composites for supercapacitor electrode materials: a review. Environ Sci Pollut Res 28:26269–26279
41. Rout A, Deepak BBVL, Biswal BB (2019) Advances in weld seam tracking techniques for robotic welding: a review. Robot Comput-Integr Manuf 56:12–37
42. Rout A, Deepak BBVL, Biswal BB, Mahanta GB (2021) Weld seam detection, finding, and setting of process parameters for varying weld gap by the utilization of laser and vision sensor in robotic arc welding. IEEE Trans Industr Electron 69(1):622–632

Frictional and Wear Behavior of Polyol Ester—Commercial Motorbike Engine Oil Blend under Boundary Lubrication Conditions



B. Koteswara Rao, V. Srinivas, S. Jai Kumar, L. S. Pradeep, and M. S. Srikar

Abstract The objective of this study is to investigate the effects of blending a bio-lubricant, specifically pentaerythritol ester, with a motor oil that is widely available in the market. The focus is on analyzing the changes in frictional properties when operating under conditions of boundary lubrication. The objective of this study was to optimize the synthesis of pentaerythritol ester (PE ester) with the aim of attaining a complete conversion to long-chain tetraesters. Furthermore, significant emphasis was placed on the meticulous formulation of the bio-lubricant to mitigate the risk of any potential deterioration in its physicochemical properties upon its incorporation with conventional oil. The research entailed the combination of commercially available motor oil with pentaerythritol (PE) ester obtained from *Calophyllum inophyllum*. The blending was conducted using proportions of 10 and 20%. The primary idea of this study was to investigate the anti-wear and anti-friction characteristics of the test oils utilizing a pin-on-disc tribometer under boundary lubrication conditions. The bio-lubricant—motor oil blends have demonstrated a substantial decrease in both friction coefficient and wear, particularly when the blending percentage reaches 20%.

Keywords Boundary lubrication · Pin on disc tribometer · Friction · Wear · Bio lubricant · Motor oil

1 Introduction

Technology and industrial modernization have increased petroleum use during the past century. To reduce friction, wear, heat, and corrosion, engine oil is essential. Numerous scientists [1–20] have studied bio-based lubricants in various industrial applications. Karuna et al. (2013) and Ting et al. (2011) found that esters from oil-bearing tree species may benefit new lubricant compositions. This approach

B. Koteswara Rao · V. Srinivas (✉) · S. Jai Kumar · L. S. Pradeep · M. S. Srikar
Department of Mechanical Engineering, GITAM (Deemed to be University), Visakhapatnam, India
e-mail: svadapal@gitam.edu

© The Author(s), under exclusive license to Springer Nature Singapore Pte Ltd. 2025

B. B. V. L. Deepak et al. (eds.), *Recent Advancements in Product Design and Manufacturing Systems*, Lecture Notes in Mechanical Engineering,
https://doi.org/10.1007/978-981-97-6732-8_28

has shown promise in reducing lubricant toxicity and increasing biodegradability. Imran et al. (2013) and Lathi et al. (2007) showed that bio-lubricants could replace petroleum-based oils. These materials also offer excellent tribological properties, including high viscosity index and low volatility. Bio-based lubricants and their blends may replace mineral and synthetic lubricating oils because their chemical composition is similar. Controlled combustion technologies and lightweight materials have been used to find alternatives to mineral-based oils in IC engines, but only a few researchers (Zulkifli et al., 2015; Jayadas et al. 2006) have suggested ester-based bio-lubricants. Mobarak et al. [11] found that petroleum-based engine oils are used in residential, automobile, aviation, metal forming, and manufacturing industries. Yunus et al. (2015) tested plant oil-based bio-lubricants in mineral oil-based lubricants. The study found that these bio-lubricants are as poisonous, biodegradable, and cost-effective as commercial oils. Ponnekanti et al. (2012) suggested that vegetable oils can reduce wear and friction by interacting strongly with lubricated surfaces. Elongated fatty acid chains with polar groups make vegetable oil effective in boundary and hydrodynamic lubrication conditions.

Ester molecules are limited in cooler temperatures due to oxidation from hydrogen atoms on the β-carbon atom, despite their benefits such high stearic and oleic acid content, renewability, and biodegradability. Ting et al. (2011), Imran et al. (2013), Zulkifli et al. (2015), and Havet et al. (2001) also found that these materials' load-bearing capacity decreases, causing collapse under larger loads. This renders them unsuitable for automotive use. The high temperature stability of vegetable-based lubricants can be increased by employing sugar per-esters instead of glycerol esters. Numerous studies (Imran et al., 2013; Zulkifli et al., 2015; Havet et al., 2001) have shown that replacing glycerol with alcohol improves oxidation resistance and thermal stability. Jayadas et al. (2006), Salih et al. (2011), Masjuki et al. (2003), and Patel et al. (2017) investigated polyol esters, specifically TMP and PE, as bio-lubricants. The above research shows that polyol ester composition and fatty acid chain length affect border lubrication wear and friction. Vegetable oils' lubrication depends on ester group content, fatty acid chain length, and polyol linearity.

1.1 Present Studies

The present study is centered around the investigation of the lubricating properties of a blend of bio-lubricant (specifically esters) obtained from *Calophyllum inophyllum* oil, in conjunction with a lubricant that is commercially available. The rationale for choosing pentaerythritol (PE) ester as bio-lubricants in this work is grounded on their unique characteristics, specifically the presence of four ester groups and an extended chain length. Prior studies have extensively investigated the composition and tribological properties of pentaerythritol (PE) ester. This particular ester is comprised of around 50–60% tetraester, with the remaining constituents consisting of trimester, diester, and monoester constituents. In the present study, the synthesis

procedure entails carrying out the reaction until a full conversion of the reactants into a long-chain tetraester is attained.

The chosen commercial lubricant is a fully formulated four-stroke motorbike oil that contains additives based on zinc dialkyl dithiophosphate (ZDDP). The process of extracting *C. inophyllum* oil entails the acquisition of oil from its seeds which predominantly flourishes in coastal areas. The bio-lubricant is considered to be a viable choice owing to its advantageous composition, comprising enough proportions of oleic acid (38%) and stearic acid (16%), as well as exhibiting physicochemical properties that fall within the desired range. Polyester esters, namely those derived from Tamanu seed oil, were produced in this study. The investigation focused on assessing the influence of additives found in commercial oil and esters included in bio-lubricants on the tribological properties. The blending procedure is carried out at several volumetric proportions, from 10 to 25% v/v. The inclusion of additives in commercial motor oil facilitates the achievement of higher blending ratios. Considerable focus was dedicated to the determination of an ideal blending ratio with the aim of attaining optimal performance.

There is a necessity to evaluate tribological qualities in the context of boundary lubrication

Boundary lubrication is a phenomenon that occurs in many scenarios when there is a lack or absence of a continuous fluid layer to establish a boundary between moving surfaces, leading to direct contact between such surfaces. While hydrodynamic lubrication is generally more effective than boundary lubrication in reducing friction and wear, the latter nonetheless serves a crucial role under specific circumstances. Boundary lubrication might manifest in several scenarios. Boundary lubrication is observed in automotive engines, specifically during the initiation of engine operation or when exposed to substantial mechanical stresses. In a similar vein, gears undergo boundary lubrication, particularly when subjected to elevated loads or abrupt shock loads. Furthermore, it is worth noting that the valve train in internal combustion engines experiences boundary lubrication during certain operational circumstances. Adhesive wear is a prominent phenomenon observed in the domain of boundary lubrication, wherein it arises as a result of the direct connection between two surfaces. The observed phenomena is distinguished by the fusion and subsequent separation of small surface irregularities or micro-contacts, resulting in the exchange of material and the manifestation of degradation.

Therefore, it is crucial to investigate the tribological characteristics of lubricants in boundary lubrication systems. The objective of this study is to evaluate the tribological characteristics of lubricant-bio-lubricant blends in the presence of boundary lubrication conditions. The present study utilizes a pin-on-disc tribometer for the purpose of measuring the friction and wear characteristics. The pin-on-disc tribometer exhibits the characteristics of boundary lubrication when the pin and disc establish a singular point of contact under conditions of limited lubrication. The methodology is utilized to assess the relative performance of test oils in terms of their friction and wear characteristics.

2 Materials and Methods

The seeds of *C. inophyllum* are easily obtainable in the surrounding area. The chemicals utilized in the preparation of bio-lubricant samples were of extreme pure (EP) quality and were obtained from Fisher Scientifics, a supplier based in Mumbai, India. The procurement of aluminum oxide of AR grade, as well as hexane, toluene, and ethyl acetate, was carried out from Finar, a provider based in India. The chemical compound p-TSA, which is often referred to as para toluene sulphonic acid, was obtained by AVRA labs, situated in Hyderabad, India.

2.1 Preparation of Bio-lubricant Samples

The nuts of *C. inophyllum* underwent a drying procedure, thereafter being pulverized into a finely ground powder. The oil was subsequently extracted from the powdered nuts utilizing a soxhlet apparatus, wherein hexane was utilized as the solvent. The production process of TMP ester- Calophyllum fatty acids entailed the use of 270 g (1.0112 mol) of Calophyllum fatty acids, 43.76 g (0.3262 mol) of trimethylolpropane, 2.7 g of p-TSA (equivalent to 1% of the weight of fatty acid), and 250 ml of toluene. The reaction mixture was subjected to agitation at the temperature of reflux. To synthesize the PE ester, a mixture comprising 238 g (0.8432 mol) of Calophyllum fatty acid, 28 g (0.2056 mol) of pentaerythritol, 2.5 g of p-TSA (equivalent to 1% weight of fatty acid), and 220 ml of toluene was subjected to stirring at reflux temperature.

Following the completion of the reaction, the mixture is permitted to attain the surrounding temperature, commonly referred to as ambient temperature. Subsequently, the toluene is evaporated from the mixture utilizing a vacuum. The reaction mixture is augmented with an aqueous solution of sodium bicarbonate, in conjunction with ethyl acetate, and exposed to agitation for a period of thirty minutes. The organic layer that was obtained as a result of the chemical reaction was separated and underwent a sequence of purification procedures. The initial step involved a double washing with water in order to eliminate any potential contaminants. Afterward, the sample was subjected to dehydration by employing anhydrous sodium sulfate in order to remove any residual moisture. Subsequently, the organic layer was subjected to vacuum concentration in order to eliminate any surplus solvent.

The purification of the crude ester was carried out using a conventional alumina column chromatography method. The eluent used for this purpose was a mixture consisting of 95% hexane and ethyl acetate. The reaction was permitted to progress until the desired quantity of water was accumulated within a Dean Stark apparatus. Prior study undertaken by several scholars [4, 8, 15] has examined analogous subject matter. The present investigation, however, centers on the synthesis of PE ester with a purity level of 100%, which is subsequently blended with commercially accessible oil.

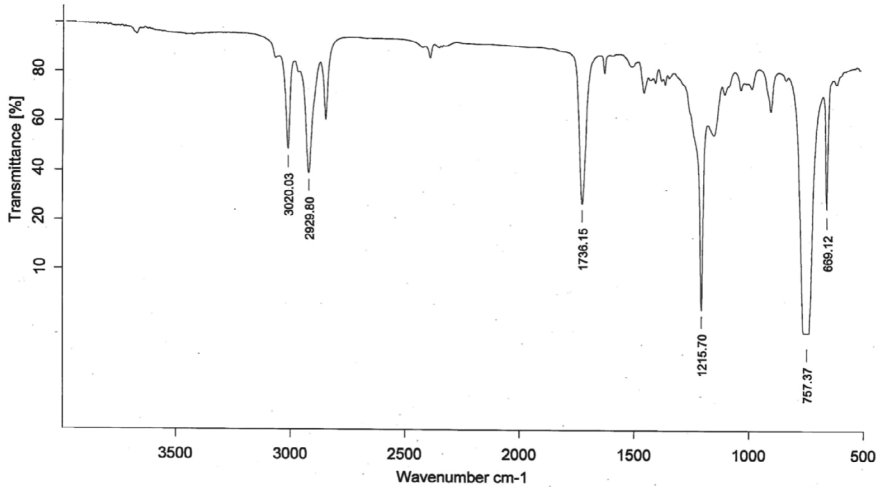


Fig. 1 FTIR spectrum of PE ester

The ester that has been synthesized is subjected to characterization through the use of infrared (IR) spectrum investigations, as well as analysis of its physicochemical properties. In this study, the researchers utilized a 1600 FT-IR Perkin–Elmer spectrometer (located in Norwalk, CT) to acquire infrared (IR) spectra. The measurements were conducted using a liquid film positioned between the NaCl cells. As depicted in Fig. 1, the infrared (IR) spectrum of the polyethylene (PE) ester exhibited a C=O stretching band at a wavenumber of 1736 cm^{-1}, whereas a C–O stretching band was observed at 1215 cm^{-1}. Tetraesters will manifest numerous peaks in the carbonyl stretching area as a consequence of the existence of four ester groups. The polyol ester compound is characterized by the presence of hydroxyl groups (O–H) within the spectral range of 3200–3600 cm^{-1}. The synthesis procedure is adjusted and refined to enhance the physicochemical characteristics.

2.2 The Process to Produce Mixtures of Bio-lubricants and Commercially Available Lubricants

The lubricant utilized in the current investigation is a developed SM grade four-stroke motorbike engine oil that incorporates additives based on zinc and phosphorus. Pentaerythritol (PE) ester-based bio-lubricants are blended with commercially available lubricants at volumetric ratios of 10 and 20%. Following the combination of the mixture, it is subjected to sonication for a duration of 5 min within a bath sonicator, thereby achieving a homogeneous dispersion.

2.3 Assessment of Tribological Properties

A comprehensive examination and evaluation of tribological properties, including friction, wear, and lubrication, is conducted in accordance with the ASTM G99 standard using a pin-on-disc apparatus. The pin-on-disc device is a highly adaptable tool used to measure the friction coefficient of material combinations in both dry and lubricated circumstances. The pin-on-disc tribometer is a multifunctional device that comprises a revolving disc and a pin subjected to a predetermined load. Its purpose is to assess the friction and wear characteristics of material combinations in both dry and lubricated environments. This test replicates the linear movement of a piston in both reciprocating piston engines and Wankel engines. The diagram illustrating the structure of the tribometer is depicted in Fig. 1. In the current investigation, the lubricant is applied via spraying into the contact area between the disc and pin, thereby establishing a boundary lubrication system. This experimental setup aims to replicate the conditions experienced in real-time lubrication systems seen in internal combustion engines. Two distinct experiments are performed to ascertain the friction coefficient and wear rate, under specific conditions. The experiments are conducted at varying speeds and magnitudes of force while operating in a lubricated environment. Before commencing the experiment, the discs undergo a grinding process using a grinding machine to achieve a consistent and smooth surface. The surface roughness of all discs undergoing testing is assessed to ensure they fall within the specified range of 0.2–0.4 μm Ra (Fig. 2).

The test conditions are enumerated as follows.
The applied loads are 50, 75, and 100 N.
The rotational speed observed—1000 revolutions per minute (RPM).



Fig. 2 **a** Pin-on-disc tribometer **b** pin sliding over disc with lubricant spray

3 Results and Discussion

3.1 Physicochemical Properties of Bio-lubricant and Blends

The retention of tribological properties heavily relies on the physicochemical characteristics of bio-lubricants. Insufficient synthesis of bio-lubricant may lead to a decrease in its characteristics, thereby impacting performance in a negative manner. The optimization of the synthesis technique is accomplished by the analysis of properties. The aforementioned features have undergone evaluation utilizing approved procedures for testing and have been ascertained to be within the permissible range.

All tested lubricants have acid numbers that are below the threshold of 1.5 mg/KOH/g, as specified by the SAE standard. When the blending percentages exceed 20%, there is a slight decrease in both viscosity and viscosity index. Nevertheless, it is important to highlight that the viscosity index continues to exceed the prescribed minimum threshold of 90, as stipulated for engine oils. The observed phenomena can be ascribed to the elongation of the polyethylene ester's chain.

A corrosion test on a copper strip was conducted under controlled conditions, with a temperature of 50 °C maintained throughout the experiment and a length of 3 h. The findings of the study suggest that the corrosion prevention shown exceptional efficacy up to a blending ratio of 15%, aligning with the performance of lubricants currently available in the market. The satisfactory corrosion resistance of the blended mixture, including 20 and 25% proportions, has been established through the attainment of a corrosion rating of 1b on the corrosion standard (Table 1).

Table 1 Physicochemical properties of PE ester bio-lubricants and commercial oil blends

S. No.	Properties	Methods	PE ester	Motor oil	Oil + 10 % PE ester	Oil + 15 % PE ester	Oil + 20% PE ester	Oil + 25% PE ester
1	Acid number (mgKOH/g)	ASTM D664	0.27	1	0.94	0.9	0.92	0.88
2	Viscosity at 40 °C (cSt)	ASTM D2245	22.66	130.36	118.11	114.2	108.78	103.43
3	Viscosity at 100 °C (cSt)	ASTM D2245	6.35	14.93	14.07	13.64	13.21	12.79
4	Viscosity index	ASTM D2270	249	114	113	111	110	105
5	Coppers strip corrosion	ASTM D130	1b	1a	1a	1a	1a	1b

3.2 Tribological Properties

Boundary lubrication is distinguished by the presence of a restricted or sporadic lubrication coating between the surfaces that slide or roll against one other, resulting in direct contact between the metal surfaces. This phenomenon commonly manifests itself during the initiation, cessation, or when operating under conditions of substantial demand and reduced velocities.

During the initiation of an internal combustion engine, a transient phase ensues wherein the complete establishment of the lubricant film is momentarily delayed, hence potentially leading to the occurrence of boundary lubrication. During this crucial stage, it is possible for some components such as cylinder liners, piston rings, and camshaft surfaces to undergo direct contact between metal surfaces until the lubricant film has reached its complete development.

Mixed lubrication displays characteristics that are representative of both boundary and hydrodynamic lubrication regimes. The phenomenon of this regime arises when there is sporadic interaction between surfaces, and the lubricating film is in a state of partial establishment or incomplete loss. Mixed lubrication is a common occurrence in situations, especially IC engines characterized by varying operating circumstances and fluctuations in the thickness of the lubricant coating. The boundary friction coefficient values and stabilized values of friction coefficient signifying hydrodynamic lubrication are shown in Table 2.

The following graphs show the variation of friction and wear with time during a test on pin-on-disc tribometer. As can be seen from Figs. 3 and 4, at lower loads, the boundary friction is small, and as the load increases, there is an increase in boundary friction for all cases. The incorporation of PE ester at concentrations of 10 and

Table 2 Results of friction test under boundary lubrication and hydrodynamic lubrication conditions

Test oil	Coefficient of friction in boundary lubrication	Coefficient of friction in hydrodynamic lubrication
At 50 N load		
Motor oil (SM grade)	0.1443	0.103
Motor oil + 10 % PE ester	0.117	0.083
Motor oil + 20 % PE ester	0.105	0.075
At 75 N load		
Motor oil (SM grade)	0.124	0.091
Motor oil + 10 % PE ester	0.118	0.086
Motor oil + 20 % PE ester	0.116	0.073
At 100 N load		
Motor oil (SM grade)	0.158	0.086
Motor oil + 10 % PE ester	0.128	0.077
Motor oil + 20 % PE ester	0.118	0.053

20% in a commercially available lubricant results in a reduction in both boundary lubrication friction and mixed lubrication friction. There exists a notable similarity between commercial lubricants and their mixes in relation to both frictional force and coefficient of friction.

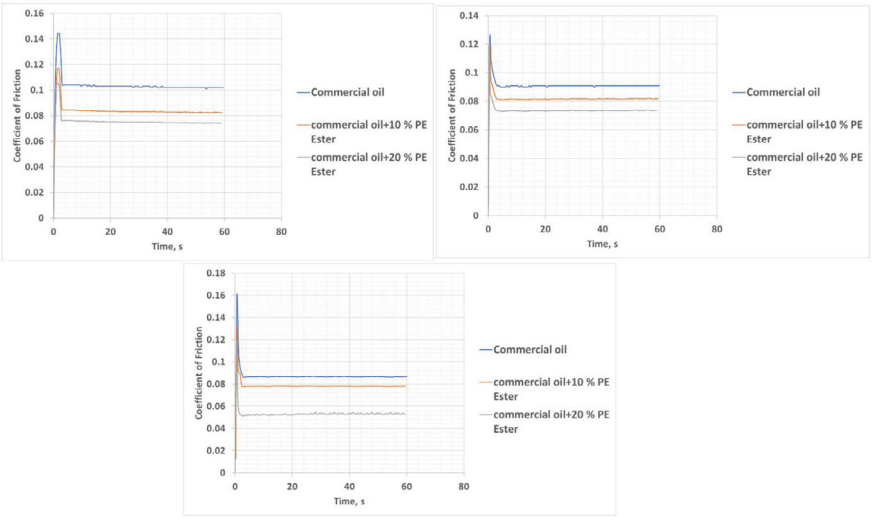


Fig. 3 Variation of friction coefficient with time for different test oils

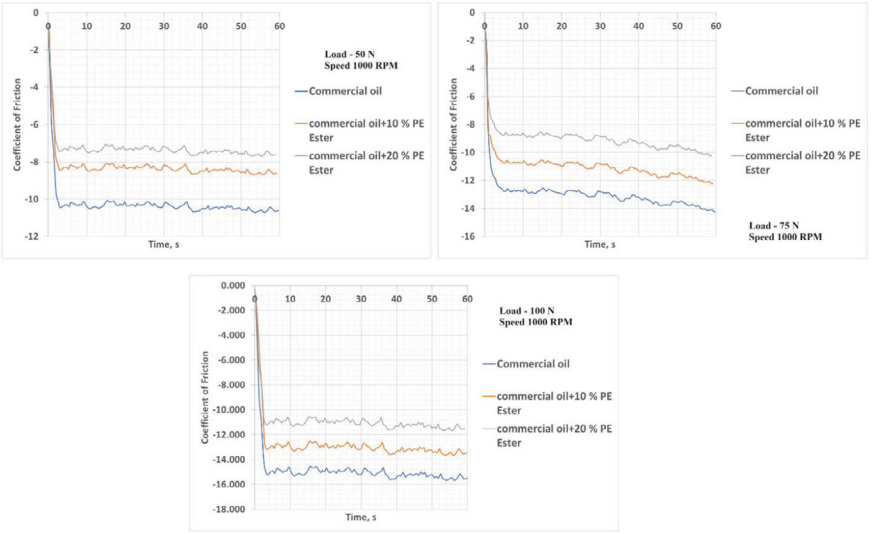


Fig. 4 Variation of wear with time for different test oils

In Figs. 3 and 4, the wear in the boundary lubrication and mixed lubrication is shown. In the context of boundary lubrication, the wear processes is heightened due to the heightened probability of metal-to-metal contact. In mixed lubrication, both fluid film and asperity contact coexist, and hence, a slight reduction in wear is observed. The wear and friction have stabilized one hydrodynamic lubrication condition set in. Due to a decline in the coefficient of friction, a significant reduction in the wear is observed with blending of PE ester. The enhanced lubricating performance exhibited by esters, resulting in reduced friction and wear, can be attributed to several factors, including an increase in the quantity of ester groups, the length of fatty acid chains, and the linearity of the polyol.

4 Conclusions

The experimental findings indicate that the incorporation of 100% long-chain tetraesters into commercial engine oil at concentrations of 10% and 20% by volume resulted in improved tribological qualities, while maintaining the physicochemical properties.

The blending of PE ester results in a significant decrease in both wear and friction coefficient of the test oils.

At all levels of load, it can be noticed from Figs 3 and 4 that bio-lubricant–motor oil blends exhibit a lower friction coefficient in comparison with commercial oil.

To achieve optimal outcomes, it is recommended to maintain a blending percentage that is lower than 20%.

An increase in the blending percentage leads to a fall in both viscosity and viscosity index, hence potentially causing premature engine oil failure.

Acknowledgments The authors gratefully acknowledge the support received from Hindustan Petroleum Corporation Ltd., for conducting the tests. The authors acknowledge the assistance from GITAM (Deemed to be university) in characterization.

References

1. Awang NW, Ramasamy D, Kadirgama K, Najafi G, Sidik NAC (2019) Study on friction and wear of cellulose nanocrystal (CNC) nanoparticle as lubricating additive in engine oil. Int J Heat Mass Transf 131:1196–1204
2. Aziz NAM, Robiah Y, Umer R, Nurin W, Zulkifli M (2016) Temperature effect on tribological properties of polyol ester-based environmentally adapted lubricant. Tribol Int 93:43–49
3. Cecilia JA, Ballesteros Plata D, Alves Saboya RM, Tavares de Luna FM, Cavalcante CL, Rodriguez-Castellon E (2020) An overview of the biolubricant production process: challenges and future perspectives. Processes 8(3):257
4. Doll KM, Cermak SC, Kenar JA, Walter EL, Isbell TA (2017) Derivatization of castor oil based estolide esters: preparation of epoxides and cyclic carbonates. Ind Crops Prod 104:269–277

5. Owuna FJ (2020) Stability of vegetable based oils used in the formulation of ecofriendly lubricants—a review. Egypt J Petrol 29(3):251–256
6. Habibullah M, Masjuki HH, Kalam MA, Ashraful AM, Habib MA, Mobarak HM (2014) Effect of bio-lubricant on tribological characteristics of steel. Procedia Eng 90:740–745
7. Hamid H, Yunus T, Rashid U, Choong TSY, Ali S, Syam AM (2016) Synthesis of high oleic palm oil-based trimethylolpropane esters in a vacuum operated pulsed loop reactor. Fuel 166:560–566
8. Heikal EK, Elmelawy MS, Salah AK, El-basuny NM (2017) Manufacturing of environment friendly biolubricants from vegetable oils. Egypt J Pet 26:53–59
9. Joshi JR, Bhanderi KK, Patel JV (2023) Waste cooking oil as a promising source for bio-lubricants- a review. J Indian Chem Soc 100(1):100820
10. Kamalakar K, Rajak AK, Prasad RBN, Karuna MSL (2013) Rubber seed oil-based biolubricant base stocks: a potential source for hydraulic oils. Ind Crops Prod 51:249–257
11. Mobarak HM, Niza Mohamad E, Masjuki HH, Kalam MA, AlMahmud KAH, Habibullah M, Ashraful AM (2014) The prospects of biolubricants as alternatives in automotive applications. Renew Sustain Energy Rev 33:34–43
12. Panchal TM, Patel A, Chauhan DD, Merlin T, Patel JV (2017) A methodological review on bio-lubricants from vegetable oil based Resources. Renew Sustain Energy Rev 70:65–70
13. Ponnekanti N, Kaul S (2012) Development of eco-friendly /biodegradable lubricants: an overview. Renew Sustain Energy Rev 16:764–774
14. Shah R, Woydt M, Zhang S (2021) The economic and environmental significance of sustainable lubricants. Lubricants 9(2):21
15. Shafi WK, Charoo MS (2020) Rheological properties of hazelnut oil mixed with zirconium-dioxide nanoparticles. Mater Today Proc 26:745–749
16. Singh Y, Farooq A, Raza A, Mahmood MA, Jain S (2017) Sustainability of a non-edible vegetable oil based bio-lubricant for automotive applications: a review. Process Saf Environ Prot 111:701–713
17. Sulgani MT, Karimipour A (2019) Improve the thermal conductivity of 10w40-engine oil at various temperature by addition of Al_2O_3/Fe_2O_3 nanoparticles. J Mol Liq 283:660–666
18. Uppar R, Dinesha P, Kumar S (2023) A critical review on vegetable oil-based bio-lubricants: preparation, characterization, and challenges. Environ Dev Sustain 25:9011–9046
19. Singh Y, Sharma A, Singh N, Singla A, Rastogi PM (2020) Prospects of inedible plant oil-driven bio-lubricants for tribological characteristics—a review. Int J Green Energy 41(13):1534–1547
20. Zaid M, Kumar A, Singh Y (2021) Lubricity improvement of the raw jojoba oil with TiO_2 nanoparticles as an additives at different loads applied. Mater Today Proc 46:3165–3168

Investigation of Turning Parameters on AL7075 Alloy Reinforcement with Silicon Carbide for a Surface Roughness of Composite Material

S. Padmanabhan, Ch. Siva Ramakrishna, A. Lalitha Saravanan, Ramesh Bokde, S. Venugopal, V. Manikkavasakan, and Krishna Kant Pandey

Abstract Presently, manufacturing sector largely depends on the utilization of alloys and composite materials in the fabrication of a diverse array of components. Both the automotive and aerospace sectors are actively seeking materials and solutions with exact surface characteristics that enable them to effectively showcase their respective goods. The investigation of the surface finish of novel alloy materials is of utmost importance in order to effectively cater to the requirements of various industries. The significance of the output reactions offered by these materials is essential for industrial applications. In the current study, the alloy Al7075 is exposed to reinforcement with silicon carbide at three distinct percentages. In order to determine the influence of several constraints on the surface roughness of composite materials, variations will be made to the machine feed rate, cutting spindle speed, depth of cut, and the

S. Padmanabhan
School of Mechanical and Construction, Vel Tech Rangarajan Dr. Sagunthala R&D Institute of Science and Technology, Chennai, Tamil Nadu 600062, India

Ch. Siva Ramakrishna
Department of Mechanical Engineering, Vignan's Institute of Information Technology, Visakhapatnam, Andhra Pradesh 530049, India

A. Lalitha Saravanan
Deptartment of Mechanical Engineering, SRM Institute of Science & Technology, Vadapalani Campus, Chennai, Tamil Nadu 600026, India

R. Bokde
Department of Mechanical Engineering, IES Institute of Technology & Management, IES University, Bhopal, Madhya Pradesh 462044, India

S. Venugopal · V. Manikkavasakan
Department of Automobile Engineering, Vels Institute of Science Technology and Advanced Studies, Chennai, Tamil Nadu 600117, India

K. K. Pandey (✉)
Department of Mechatronics Engineering, Manipal University Jaipur, Jaipur, Rajasthan 303007, India
e-mail: kknitrkl@yahoo.in

© The Author(s), under exclusive license to Springer Nature Singapore Pte Ltd. 2025

B. B. V. L. Deepak et al. (eds.), *Recent Advancements in Product Design and Manufacturing Systems*, Lecture Notes in Mechanical Engineering,
https://doi.org/10.1007/978-981-97-6732-8_29

reinforcement of silicon carbide. The results revealed that spindle speed of 600 rpm, machine feed of 0.175 mm/rev, depth of cut of 0.4 mm, and SiC addition of 5% produce the better surface finish on the Al7075 material.

Keywords Aluminium alloy · Al7075 · CNC turning · Surface roughness · Silicon carbide · Optimization

1 Introduction

Metal matrix composites have a range of benefits in situations that need elevated levels of particular strength, stiffness, and wear resistance. The combination of aluminium and silicon carbide (SiC) particles, known as metal matrix composites, holds great importance in several industries such as aerospace, automobile engineering, and other applications [1]. Aluminium metal matrix composites (MMC), particularly those incorporating SiC particulates, are experiencing a growing utilization in extensive engineering applications, encompassing automotive and aeronautical components.

Various manufacturing procedures can be employed to achieve the production of near net form composite components of superior quality. Regrettably, due to factors such as the intricacies of component design and the necessity for precise dimensional tolerances, the entire eradication of machining is unattainable [2].

In recent years, numerous vehicle industries have experienced significant profitability due to the high quality of their products. The assurance of quality can be achieved by the utilization of the paper inspection method. Achieving higher levels of accuracy in surface roughness is particularly crucial, particularly in the context of engine components. Typically, industries exhibit a preference for utilizing stylus probes in the measurement of surface roughness, albeit at the cost of increased inspection duration [3].

In an investigation, the study was focused on examining the impact of machining process parameters on the average roughness (Ra) of the machined surface and the rate of material removal (M) in a turning operation involving a metal matrix composite composed of Al7075 reinforced with silicon carbide (SiC) particles [4]. The optimization of Ra was conducted using a Taguchi-based grey relational analysis technique. The molten Al7075 was mixed with varying amounts of fibre glass and tungsten carbide according to the application-specific strength parameters of the rule of mixtures. The final compound was poured into the mould, and a hybrid composite casting was produced. Taguchi technique was applied for optimization of surface roughness [5]. During the machining of Al7075, the influence of the cutting parameters on surface roughness and spindle vibration was studied, along with the link between the two. According to the findings, feed rate is one of the most important cutting parameters for influencing both spindle vibration and surface roughness. With a higher cutting feed, machine vibration amplitude and roughness

values rose noticeably. Both spindle vibration and cutting speed were found to be minimally affected by depth of cut and cutting speed, respectively [6].

Many modern industries use metals and composites for components. To meet industrial output requirements, new materials' surface roughness and material removal rate must be evaluated. Many studies have been carried out on Al6061/SiC/Gr composite samples using a CNC lathe with a carbide single-point cutting tool to know which machining parameters effect surface imperfection, metal removal rate, and material durability at high temperatures. The Taguchi approach considers input and level factors while designing experiments. Two multi-performance characteristics optimized by grey relational analysis were metal removal factor and surface irregularity [7]. The study employed analysis of variance (ANOVA) method, grey relational approach and examined the interactions among parameters to examine the effects of machining constraints on CNC turning of AA6061 alloy using Minitab 16 software. ANOVA is a statistical method employed to investigate the impact of different independent variables on the probable results [8]. The investigation's rationale has been anticipated by the comparison of ideal parameters with confirmation tests. In order to optimize the performance of the turned component, it is imperative to allocate the most suitable cutting constraints. Utilizing a blend of multi-linear optimization approaches to control input variables with the aim of producing an optimal solution is more advantageous compared to relying solely on a single linear optimization strategy [9–11].

The geometric characteristics of a tool, such as the nose radius and depth of cut, have a significant impact on cutting forces, material removal rate, and various other parameters. Various statistical techniques can be employed to examine the impact of these variables. It is feasible to examine the output parameters in relation to the different combinations of input parameters [12, 13]. Aluminium-based MMC are very desirable in the industrial sector as a result of their low density, high strength, and low wear resistance [14]. Several challenges may develop while operating a CNC machine when dealing with MMC. The utilization of different tool inserts has an impact on several machining characteristics, such as surface roughness, cutting force, and machining time [15]. Various types of cutting tool inserts, including as carbide, CBN, tungsten carbide, and cemented carbide, are commonly employed in the CNC turning process of aluminium alloy. Each of these inserts has its own distinct impact on both the material removal rate and the resulting surface roughness [16, 17]. The manufacturing industry, specifically, exerted significant efforts to decrease production durations and expenses in order to sustain its expansion. Aluminium alloys, renowned for their exceptional material properties, have been extensively utilized in various industrial applications. The cutting process is widely recognized as a cost-effective stage in the production process, characterized by minimal expenses. Consequently, a variety of efforts were undertaken with the objective of enhancing the efficiency of machining techniques [18].

The aerospace, aviation, marine, and automotive industries could all benefit from Al7075. Therefore, Al7075's strength and wear resistance should be enhanced. Composites, which consist of many types of ceramic particles, can also increase the material's strength and wear resistance. This study therefore incorporates three

distinct reinforcing weights of silicon carbide (SiC) ceramic particles into an Al7075 matrix. The manufactured Al7075-SiC composites' turning properties are analysed. Optimization of the surface roughness is performed via a desire function analysis based on a response surface. The present study investigates the impact of machining parameters on AA7075, with a specific emphasis on surface roughness as the key outcome variables. The Al7075 alloy is reinforced with varying quantities of silicon carbide (SiC), namely 5, 10, and 15%. The specimens of Al-SiC composite were processed using a CNC turning centre equipped with a carbide single-point cutting tool. The aim of this study is to investigate the impact of machining factors, including machine feed rate, depth of cut, cutting spindle speed, and SiC reinforcement, on surface roughness.

2 Materials and Methods

Aluminium 7075-T6 has exceptional mechanical and physical characteristics, particularly in terms of its impressive strength-to-weight ratio, when compared to alternative materials commonly employed in structural applications. Zinc serves as the primary alloying element in Al7075, imparting enhanced strength properties that surpass those of numerous steel alloys. The material exhibits favourable fatigue resistance and displays average qualities in terms of machinability [19]. The tensile strength of the aluminium alloy is estimated to be over 570 MPa, making it one of the most durable alloys among aluminium materials. The density of Al7075 is around 2.81 g/cm^3, which indicates its high strength-to-weight ratio. Despite exhibiting favourable corrosion resistance, Al7075 does not exhibit the same level of corrosion resistance as numerous other aluminium alloys. Figure 1 depicts the scanning electron microscopy (SEM) image of Al7075. This is attributed to the capacity of the material to combine strength, lightness, and favourable machining properties into a unified entity. Within the range of different grades of aluminium, the 7xxx series has the desirable characteristic of being heat treatable.

This particular series is notable for its utilization of zinc as the principal alloying element. It finds extensive application in industries such as aircraft manufacturing, vehicle production, and the construction of structural components, where exceptional strength is a crucial requirement. The material exhibits a high strength-to-weight ratio as a result of its favourable combination of specific tensile strength and ultimate elongation. The Al7075 alloy possesses a unique combination of high strength and excellent resistance to corrosion, making it a highly sought-after material for many applications such as machine components and artillery [20]. Because of its high fatigue resistance, the Al7075 alloy is ideally suited for use in situations with cyclic loading and stress, such as the building of aircraft structures.

Especially in its heat-treated form, the alloy's machinability falls short of that of other aluminium alloys. As a heat-treatable aluminium alloy, Al7075 may be manipulated to take on a variety of hardnesses and other characteristics through controlled heating and cooling. Currently, T6 is the most common temper, and it is

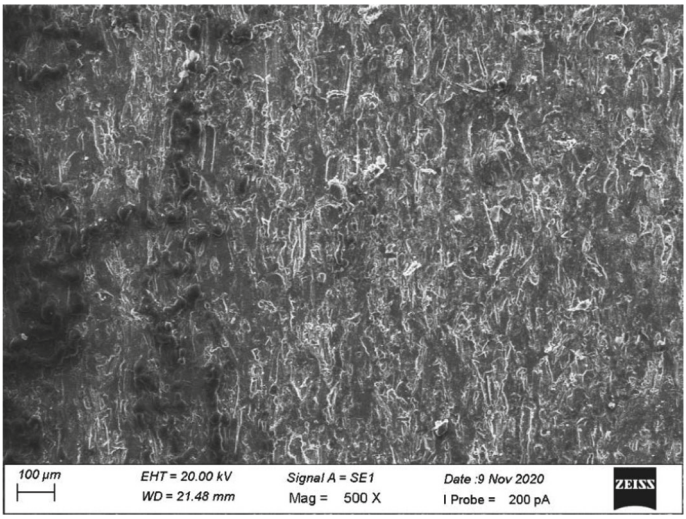


Fig. 1 SEM analysis of Al7075 alloy

achieved through a process of solution heat treatment followed by artificial ageing. When it comes to strength and toughness, this alloy is unparalleled. When compared to other aluminium alloys, Al7075's electrical conductivity is modest, making it a candidate for some uses. Al7075's high strength-to-weight ratio makes it a popular choice for a wide variety of aerospace and military applications, such as airplane and missile parts and even bicycle frames. It is also used in the production of high-performance parts for industries like racing [21, 22].

Silicon carbide is widely recognized as a highly durable material that exhibits exceptional resistance to mechanical wear, abrasion, and scratching. This property renders it advantageous for applications involving cutting tools, abrasive materials, and coatings that resist wear. Silicon carbide exhibits superior heat dissipation capabilities compared to silicon as a result of its elevated thermal conductivity. Silicon carbide possesses distinctive and advantageous properties that render it highly valued across various applications. Silicon carbide exhibits superior thermal stability compared to silicon, enabling it to withstand elevated temperatures without undergoing degradation. This characteristic renders it very suitable for demanding environments such as vehicle engine components, aircraft systems, and high-temperature electronics [23]. The incorporation of silicon carbide particles into an aluminium matrix has been seen to result in significant enhancements in both the mechanical strength and stiffness of the resultant composite material. Previous studies have demonstrated that the addition of SiC as a reinforcing agent in composites of aluminium alloys leads to improved mechanical, thermal, and wear properties in comparison with the base aluminium alloy. Silicon carbide particles exhibit a notable resistance to deformation and fulfil a pivotal function in the dispersion of loads over the material. Silicon carbide demonstrates a significant attribute of possessing a

high thermal conductivity, hence improving the overall thermal performance of the composite material [24, 25].

3 Turning Experimental Details

The present study employs the stir casting technique for the fabrication of the raw material into a cylindrical rod configuration. The stir casting technique is used to fabricate composites using Al7075 as the matrix material and silicon carbide particles as the reinforcing agent. The Al7075 material is augmented with reinforced material at three discrete weight percentages, specifically 5%, 10%, and 15%. The rotational speed of the stirring apparatus is consistently maintained at a fixed value of 600 rpm, while the temperature of the stirring process is consistently maintained at around 800 °C. The duration of the procedure varies between 25 and 35 min. The samples are fabricated using a computer numerical control turning machine. The specimens are depicted in Fig. 2, exhibiting a maximum diameter of 250 mm and a maximum length of 500 mm. Table 1 displays the machining parameters alongside their respective levels. A full factorial design encompasses all conceivable combinations of treatment doses for every component. To undertake an examination involving "m" components at two separate levels, it is required to carry out a total of "2 m" research. The 2 m complete factorial design is a useful tool in the early stages of experimental research, particularly when the number of process parameters or design parameters is limited to less than four. When considering 2-level factors, it is justifiable to make the assumption of a linear relationship between the response variable and the levels of the factor. A drawback associated with full factorial designs is that the experimental size exhibits a proportionate increase as the number of elements being investigated expands. It is recommended to employ a full factorial design when the quantity of factors or process parameters to be examined is four or less. The CNC turning process entails the determination of distinct machining parameters, notably spindle speed (SS), machine feed rate (MF), and depth of cut (DC). The evaluation of the machinability output was conducted in relation to the surface roughness (SR) as the measured response. The trials were identified by conducting an application of a full factorial design using Minitab 19. Table 2 presents the trial design and its associated response.

4 Results and Discussion

The assessment of surface roughness was carried out in order to ascertain the machinability performance. The study investigates the impact of various production parameters on the Al7075-SiC reinforcement by utilizing a full factorial design methodology in Minitab 19 software. Optimization and contour plots are utilized for the purpose



Fig. 2 Experimental turning samples

Table 1 CNC turning parameters and its level

Turning parameters	Notation	Unit	Low Level	High level
Spindle speed	SS	RPM	600	1000
Machine feed rate	MF	mm/rev	0.075	0.175
Depth of cut	DC	mm	0.4	1.2
Reinforcement	RF	%	5	15

of analysing the outcomes. Figure 3 displays a contour map that depicts the correlation between spindle speed and SiC reinforcement, with a specific focus on their influence on the surface finish. The results suggest that lower spindle speeds and the addition of 5–10% SiC reinforcement are correlated with the most desirable surface roughness results. The minimal spindle speed was discovered to occur within the region of 600–700 rpm.

The contour curve depicted in Fig. 4 shows the correlation between the machine feed rate and the SiC reinforcement. It has been discovered that in order to attain the lowest possible surface roughness, it is necessary to utilize a machine feed rate ranging from 0.145 to 0.175 mm/rev, along with a SiC reinforcement level beyond 9%. The augmentation of the feed rate yields a favourable effect on the minimum surface finish. Just like the influence of cutting speed, an overly high feed rate can lead to inadequate surface finishing and a decreased longevity of the cutting tool. Achieving a harmonious equilibrium between the feed rate, tool capabilities, and material qualities is of utmost importance. From the contour plot portrayed in Fig. 5, it is apparent that the achievement of the lowest surface roughness occurred while utilizing a depth of cut equal to or less than 0.75 mm, in combination with a SiC

Table 2 Experimental input parameters and its response

Std order	Run order	SS	MF	DC	RF	SR
3	1	600	0.175	0.4	5	0.78040
16	2	1000	0.175	1.2	15	2.02785
11	3	600	0.175	0.4	15	0.66587
13	4	600	0.075	1.2	15	0.91632
15	5	600	0.175	1.2	15	1.39064
5	6	600	0.075	1.2	5	0.97533
7	7	600	0.175	1.2	5	0.74320
6	8	1000	0.075	1.2	5	2.34210
1	9	600	0.075	0.4	5	0.76780
10	10	1000	0.075	0.4	15	1.97261
12	11	1000	0.175	0.4	15	1.31147
9	12	600	0.075	0.4	15	1.57780
4	13	1000	0.175	0.4	5	0.95561
2	14	1000	0.075	0.4	5	1.95034
8	15	1000	0.175	1.2	5	0.68825
14	16	1000	0.075	1.2	15	1.63644

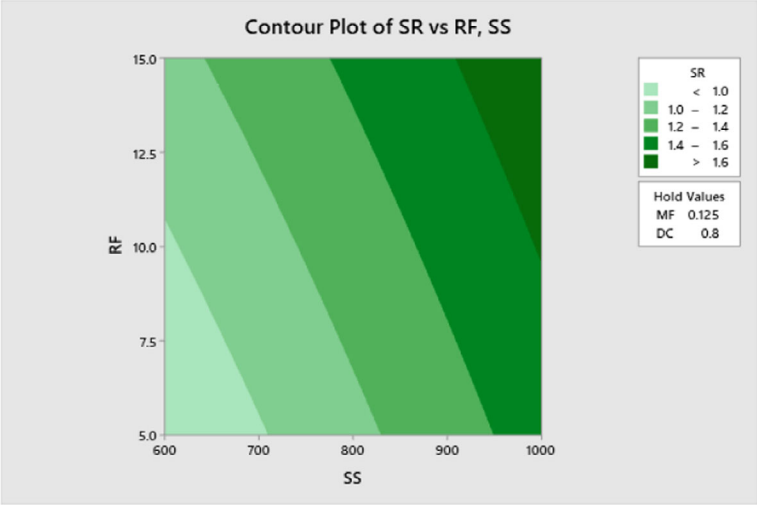


Fig. 3 Contour plot of SR with RF and SS

reinforcement ranging from 5 to 10%. Figure 6 displays a contour plot illustrating the relationship between different machining parameters.

The optimal surface roughness was attained through the utilization of decreased spindle speeds in combination with elevated feed rates. The experimental investigation identified a range of spindle speeds, specifically between 600 and 700 rpm, which resulted in the smallest surface roughness. Additionally, it was observed that

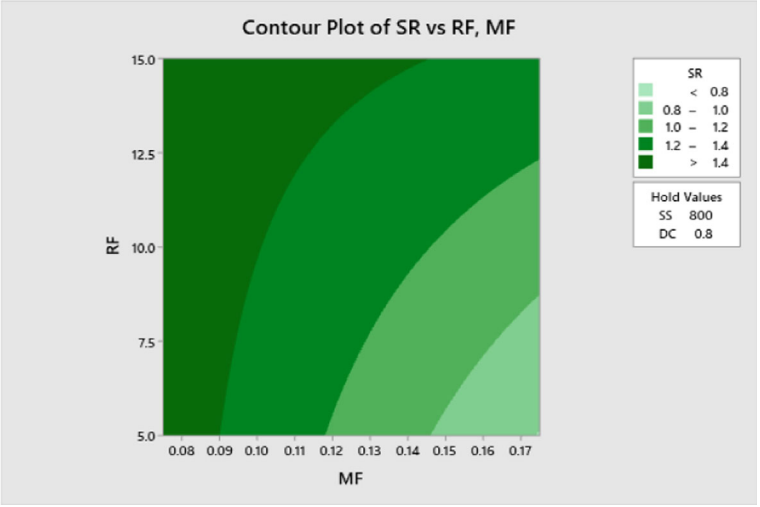


Fig. 4 Contour plot of SR with RF and MF

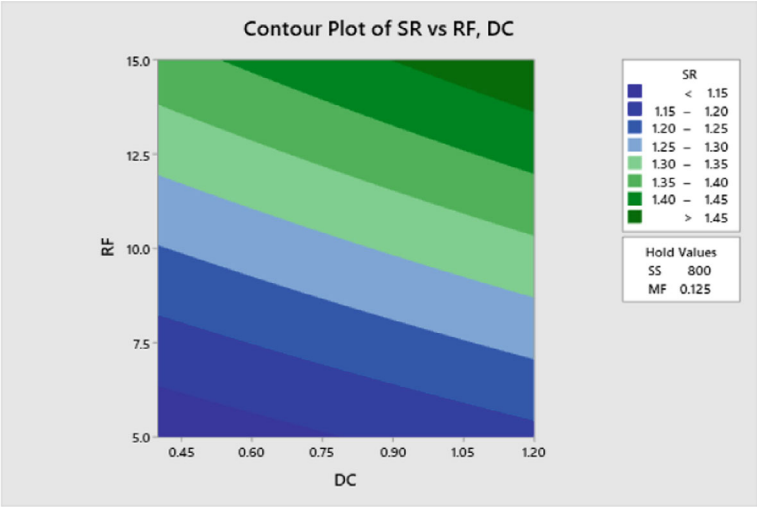


Fig. 5 Contour plot of SR with RF and DC

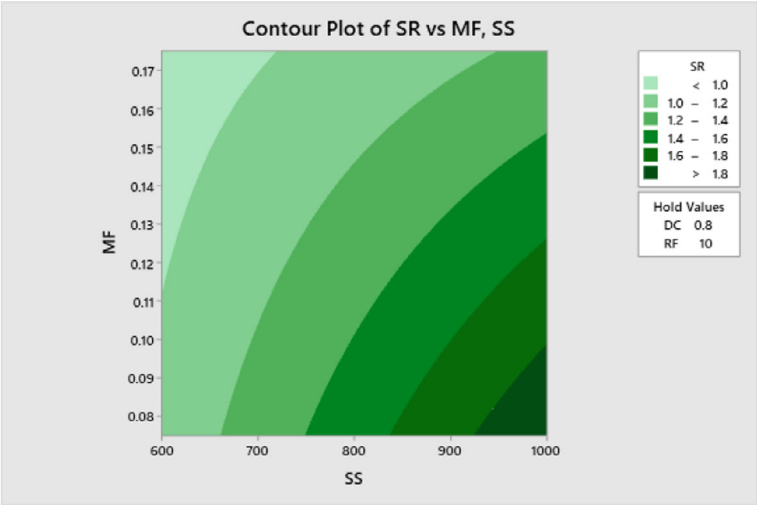


Fig. 6 Contour plot of SR with MF and SS

the corresponding feed rate required to achieve this minimum surface roughness exceeded 0.12 mm/rev. Based on the contour plot depicted in Fig. 7, it can be observed that the attainment of the optimal surface roughness was achieved by the utilization of a depth of cut equal to or below 0.75 mm, in conjunction with a spindle speed below 700 rpm. The contour map depicted in Fig. 8 illustrates the relationship between the machine feed rate and the depth of cut. To obtain minimum surface roughness, it is necessary to ensure that the machine feed rate falls within the range of 0.15–0.17 mm/rev, while also ensuring that the depth of cut remains below 0.6 mm. Table 3 shows the response optimization results of surface roughness. It shows that spindle speed of 600 rpm, machine feed of 0.175 mm/rev, depth of cut of 0.4 mm, and SiC addition of 5% produce the better surface finish of 0.66.

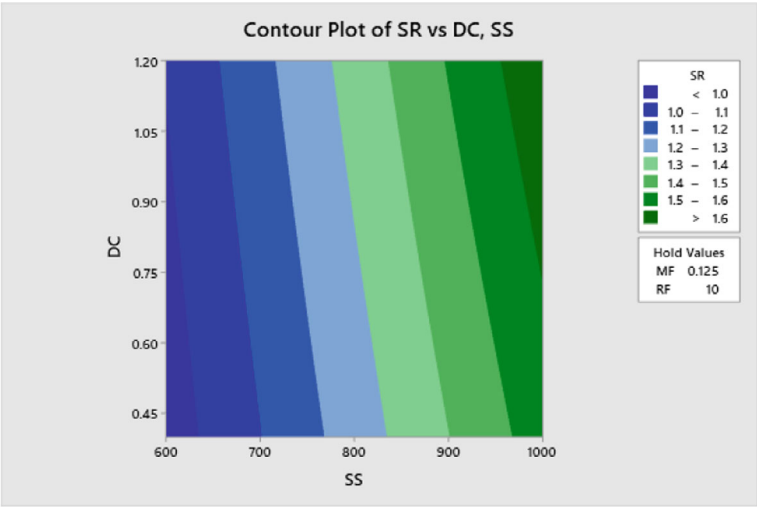


Fig. 7 Contour plot of SR with DC and SS

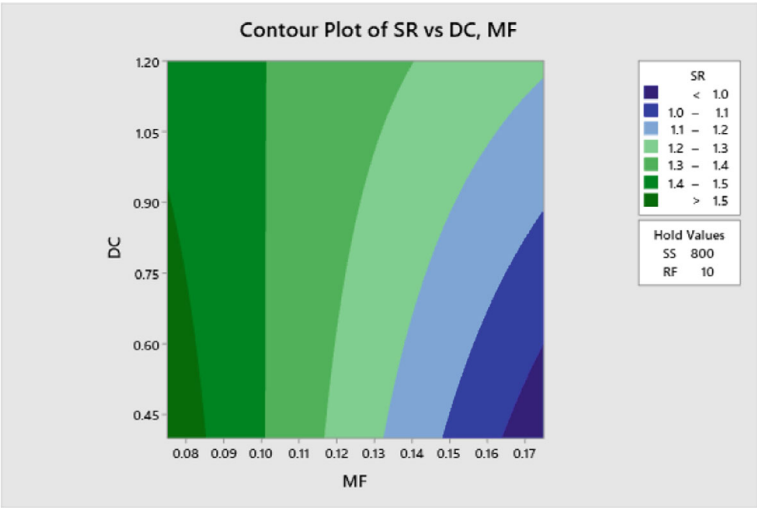


Fig. 8 Contour plot of SR with DC and MF

Table 3 Response optimization results of surface roughness

Solution	SS	MF	DC	RF	SR fit	Composite desirability
1	600	0.175000	0.40000	5.0000	0.665866	1.00000
2	600	0.174395	0.41429	4.9962	0.684216	0.98905

5 Conclusion

The technocrats have done many works in investigating the machinability of aluminium alloys in directive to optimize the rate of material subtraction and attain the desired surface qualities during the machining process. The importance of these materials' output responses stems from the vital role they play in industrial applications. One of the three experimental settings in this work involves reinforcing Al7075 by including various quantities of SiC. The objective of this study is to recognize the utmost influential machining parameters on surface roughness, such as cutting speed, feed rate, depth of cut, and the use of SiC. According to the results, the optimal spindle speed for producing a high-quality surface was between 600 and 700 revolutions per minute. This happened when the reinforcement percentage was more than 7.5%, the cutting feed rate was 0.175 mm/rev, and the depth of cut was 0.75 mm or less. The optimization findings revealed that the best surface finish, 0.66 R_a, is achieved with a spindle speed of 600 rpm, a machine feed of 0.175 mm/rev, a depth of cut of 0.4 mm, and reinforcement of 5% SiC. Because of their many desirable properties, including low density and great mechanical and thermal capabilities, aluminium alloys are frequently favoured in an extensive technical application.

References

1. Gopalakannan S, Senthilvelan T, Ranganathan S (2012) Modeling and optimization of EDM process parameters on machining of Al 7075–B4C MMC using RSM. Procedia Eng 38:685–690
2. Kumar R, Chauhan S (2015) Study on surface roughness measurement for turning of Al 7075/10/SiCp and Al 7075 hybrid composites by using response surface methodology (RSM) and artificial neural networking (ANN). Measurement 65:166–180. https://doi.org/10.1016/j.measurement.2015.01.003
3. Veluchamy B, Karthikeyan N, Krishnan BR, Sundaram CM (2021) Surface roughness accuracy prediction in turning of Al7075 by adaptive neuro-fuzzy inference system. Mater Today Proc 37:1356–1358. https://doi.org/10.1016/j.matpr.2020.06.560
4. Das D, Chapagain A, Nayak RK, Routara BC (2018) Multiple-response optimization for surface quality and productivity during turning Al 7075/SiCp composite in spray cooling environment. Mater Today Proc 5:18052–18060. https://doi.org/10.1016/j.matpr.2018.06.139
5. Raghu Tilak Reddy M, Sanjay Kumar SM (2022) Machinability studies of Aluminium-7075 alloy based hybrid composites. Mater Today Proc 50:2515–2521. https://doi.org/10.1016/j.matpr.2021.10.506
6. Şahinoğlu A, Karabulut Ş, Güllü A (2017) Study on spindle vibration and surface finish in turning of Al7075. Solid State Phenom 261:321–327. https://doi.org/10.4028/www.scientific.net/SSP.261.321
7. Srinivas Kumar G, Mohana Reddy YV, Mohana Reddy BC (2022) Experimental study on the influence of turning process parameters on surface texture and material removal rate of composites by using Grey relational Taguchi technique. Mater Today Proc. https://doi.org/10.1016/j.matpr.2022.11.163
8. Raguraman D, Balu P, Manavalan S, Raja E (2023) Multi-linear optimization of machining parameters of CNC turning of AA6061alloy using GRA method. Mater Today Proc. https://doi.org/10.1016/j.matpr.2023.03.271

9. Abbas AT, Sharma N, Alsuhaibani ZA, Sharma A, Farooq I, Elkaseer A (2023) Multi-objective optimization of AISI P20 mold steel machining in dry conditions using machine learning—TOPSIS approach. Machines 11:748
10. Padmanabhan S, Chandrasekaran M, Ganesan S, Khan Patan MN, Navakanth P (2017) Optimal solution for an engineering applications using modified artificial immune system. In: IOP Conference series: materials science and engineering. https://doi.org/10.1088/1757-899X/183/1/012025
11. Mohanty S, Rath K, Ranjan Sikha M, Kumar Patra U, Kumar Gope A (2022) Optimization of process parameters during turning of fly ash reinforced aluminum MMC in CNC machine. Mater Today Proc 62:6049–6054. https://doi.org/10.1016/j.matpr.2022.04.1005
12. Pradeep Devaneyan S, Ganesh R, Senthilvelan T (2017) On the mechanical properties of hybrid aluminium 7075 matrix composite material reinforced with SiC and TiC produced by powder metallurgy method. Indian J Mater Sci 2017:1–6. https://doi.org/10.1155/2017/3067257
13. Kumar Tripathy S, Kumar Senapati A, Krushna Mohanty G (2022) Parametric optimizination of machining parameter in CNC turning of al based hybrid metal matrix composites. Mater Today Proc 62:6232–6245. https://doi.org/10.1016/j.matpr.2022.05.201.
14. Sharma N, Sharma VS, Sharma RC, Arora R, Sharma A (2022) Development of quality micro-holes by electrical discharge drilling on Al/SiC composite using of grey-desirability approach. Int J Light Mater Manuf 5:267–277
15. Choubey M, Maity KP, Sharma A (2020) Finite element modeling of material removal rate in micro-EDM process with and without ultrasonic vibration. Grey Syst Theory Appl 10:311–319. https://doi.org/10.1108/gs-11-2019-0047
16. Alam ST, Tomal ANMA, Nayeem MK (2023) High-speed machining of Ti–6Al–4V: RSM-GA based optimization of surface roughness and MRR. Results Eng 17:100873. https://doi.org/10.1016/j.rineng.2022.100873
17. Khanna R, Sharma N, Kumar N, Gupta RD, Sharma A (2022) WEDM of Al/SiC/Ti composite: a hybrid approach of RSM-ARAS-TLBO algorithm. Int J Light Mater Manuf 5:315–325
18. Chamarthi P, Nagadolla R (2019) Grey fuzzy optimization of CNC turning parameters on AA6082/Sic/Gr hybrid MMC. Mater Today Proc 18:3683–3692. https://doi.org/10.1016/j.matpr.2019.07.302
19. Sharma A, Sharma N, Singh RP, Arora R, Gill RS, Singh G (2022) Micro-drill on Al/SiC composite by EDD process: an RSM-MOGOA based hybrid approach. Int J Light Mater Manuf 5:564–575
20. Ramakrishnan H, Balasundaram R, Selvaganapathy P, Santhakumari M, Sivasankaran P, Vignesh P (2019) Experimental investigation of turning Al 7075 using Al_2O_3 nano-cutting fluid: ANOVA and TOPSIS approach. SN Appl Sci 1:1639. https://doi.org/10.1007/s42452-019-1664-0
21. Kumar ST, Srinivasan S, Raffic NM, Babu KG (2022) Experimental investigation on turning process parameters for AA7075 by Taguchi's orthogonal array. AIP Conf Proc 2446:40026. https://doi.org/10.1063/5.0108097
22. Srivastava VS, Gupta TK, Srivastava AK, Chauhan S, Chauhan PK (2021) Effects of cutting parameters on aluminium alloys—a review. Mater Today Proc 47:3823–3827. https://doi.org/10.1016/j.matpr.2021.03.091
23. Khan MA, Jani SP, Kumar AS, Rajesh S (2021) Machining parameter optimization using Adam—gene algorithm while turning lightweight composite using ceramic cutting tools. Int J Light Mater Manuf 4:262–267. https://doi.org/10.1016/j.ijlmm.2020.12.005
24. Das D, Sharma M, Samal C, Kumar Nayak R (2019) Investigation of mechanical properties of SiCp reinforced Al7075 metal matrix composites: a case study. Mater Today Proc 18:3958–3965. https://doi.org/10.1016/j.matpr.2019.07.337
25. Faisal N, Kumar D, Kumar A, Ansu AK, Sharma A, Jain AK, Alkahtani MQ, Yunus Khan TM, Almakayeel N (2024) Experimental analysis for the performance assessment and characteristics of enhanced magnesium composites reinforced with nano-sized silicon carbide developed using powder metallurgy. ACS Omega

Design and Analysis of Gudgeon Pin to Minimize Stress Concentration by Selecting Different Material Through FEA

J. Kumaraswamy, Ch. Siva Ramakrishna, S. Ramasubramanian, Rahul Mishra, D. T. Sakhare, K. Karthik, S. Baskar, and Krishna Kant Pandey

Abstract The gudgeon pin is one of the engine's most stressed components. Gudgeon pins are used in automotive engines to link the piston and connecting rod. Stress concentration is a critical concern in the design of mechanical components, as it can lead to premature fatigue failure and, consequently, catastrophic consequences. To mitigate this risk, engineers continually seek ways to optimize the design of components like the gudgeon pin, and one avenue of exploration is the judicious choice of materials. This study looks at the detailed design and analysis of existing gudgeon pins in order to detect the pin's stress concentration and

J. Kumaraswamy
Department of Mechanical Engineering, R. L. Jalappa Institute of Technology, Doddaballapur, Karnataka 561203, India

Ch. Siva Ramakrishna
Department of Mechanical Engineering, Vignan's Institute of Information Technology, Visakhapatnam, Andhra Pradesh 530049, India

S. Ramasubramanian · S. Baskar
Department of Automobile Engineering, Vels Institute of Science Technology and Advanced Studies, Chennai, Tamil Nadu 600117, India

R. Mishra
Department of Mechanical Engineering, IES Institute of Technology & Management, IES University, Bhopal, Madhya Pradesh 462044, India

D. T. Sakhare
Department of Chemistry, Shivaji, Art's, Commerce & Science College Kannad, Aurangabad, Maharashtra 431103, India

K. Karthik
Department of Mechanical Engineering, Vel Tech Rangarajan Dr. Sagunthala R&D Institute of Science and Technology, Chennai, Tamil Nadu 600062, India

K. K. Pandey (✉)
Department of Mechatronics Engineering, Manipal University Jaipur, Jaipur, Rajasthan 303007, India
e-mail: kknitrkl@yahoo.in

© The Author(s), under exclusive license to Springer Nature Singapore Pte Ltd. 2025

B. B. V. L. Deepak et al. (eds.), *Recent Advancements in Product Design and Manufacturing Systems*, Lecture Notes in Mechanical Engineering,
https://doi.org/10.1007/978-981-97-6732-8_30

then minimize it by making necessary changes to the pin's design and mounting. The current work involved constructing a gudgeon pin and then using finite element analysis (FEA) software to examine and minimize stresses on the pin. This comprehensive study delves into the intricate world of gudgeon pin design and analysis, with a specific emphasis on minimizing stress concentration by selecting different materials through FEA.

Keywords ANSYS · Finite element analysis · Gudgeon pin · Material · Stress concentration

1 Introduction

In the dynamic realm of engineering, where innovation and advancement drive progress, the quest for optimization is perpetual. In this pursuit, one critical area of focus lies in the design and analysis of mechanical components that can withstand the ever-increasing demands of modern machinery.

The gudgeon pin, a seemingly inconspicuous component of internal combustion engines, plays a pivotal role in the functioning of these machines. Its primary function is to connect the connecting rod and piston, allowing for the transfer of reciprocating motion into rotational motion. However, despite its seemingly straightforward role, the gudgeon pin's performance can greatly affect the overall efficiency and longevity of an engine [1]. The significance of gudgeon pins within internal combustion (IC) engines cannot be overstated. These engines power a vast array of vehicles, machinery, and equipment, making them the heartbeat of modern industry. As engines become more powerful and efficient, the components within them must also evolve to withstand the increased stresses and pressures [2]. The gudgeon pin, being subjected to both tensile and compressive loads, represents a prime candidate for investigation and improvement. In this pursuit, finite element analysis (FEA) emerges as an invaluable tool. FEA is a computational technique that allows engineers to simulate the behavior of complex mechanical systems under various conditions. It aids in the prediction of stress distribution, deformation, and other critical factors, enabling designers to make informed decisions about geometry, material selection, and manufacturing processes [3]. By employing FEA, engineers can gain profound insights into how different materials and design parameters influence stress concentration in the gudgeon pin [4]. Material selection, a fundamental aspect of engineering, profoundly impacts a component's performance. The gudgeon pin, typically made of steel or alloy materials, requires careful consideration when it comes to selecting the most suitable material. The choice of material influences properties such as strength, stiffness, and durability, all of which are critical in minimizing stress concentration. Through meticulous analysis and simulation, engineers aim to identify materials that not only meet the mechanical requirements but also offer cost-effective solutions. The motivation behind this study lies in the urgent need to enhance the reliability and longevity of IC engines. As these engines power everything from automobiles

to industrial machinery, any improvement in their efficiency can have significant economic and environmental ramifications [5–7]. A well-designed gudgeon pin, optimized to minimize stress concentration, can contribute to reduced maintenance costs, increased fuel efficiency, and decreased emissions.

The piston's job is to create mechanical energy that is useful by absorbing the energy generated during combustion. The heavy diesel engine cylinder experiences a rise in temperature and pressure as a result of the fuel burning [8, 9]. The piston experiences tremendous thermal and structural strains due to its high speed and load [10]. According to the findings, one of the primary causes of fatigue failure is stress concentration, where the piston's upper end experiences the most stress. Cracks typically form in the upper end of the piston as a result of high thermal load and concentrated tension. The piston can possibly split due to this crack. The analysis was done using a variety of techniques, including analytical methods and finite element analysis (FEA).

By identifying the root causes of stress concentration, engineers can better devise strategies to minimize its impact. FEA often referred to as the "virtual laboratory" of engineering will be a central focus of this investigation. Through FEA, simulation of the behavior of the gudgeon pin under various load conditions, providing valuable insights into stress distribution and concentration areas can be done. This allows for a deeper understanding of how different materials and design parameters can influence stress levels, paving the way for informed decision-making in the design process. The selection of materials is another critical aspect to be scrutinized in the previous study. By evaluating a range of materials, including traditional steel alloys and advanced composite materials, it was aimed to identify those that offer superior resistance to stress concentration. To establish their appropriateness for gudgeon pin applications, material parameters such as yield strength, ultimate tensile strength, Young's modulus, and fatigue resistance were examined [11]. Furthermore, the study acknowledged the environmental and sustainability implications of material choices. In an era of increasing environmental consciousness, the selection of materials that not only perform well but also have a reduced ecological footprint is of paramount importance. Hence, not only mechanical properties but also the environmental impact of materials was considered in previous studies. The design and analysis of gudgeon pins to minimize stress concentration via material selection and FEA is a varied and critical subject of study within mechanical engineering [12]. The objective of the present study is designing of gudgeon pin and determine the pin's stress concentration through design and analysis of the current gudgeon pin, and then reduce stress concentration by modifying the mounting and design of the gudgeon pin as needed.

2 Methodology

The process makes sure that the gudgeon pin's design is both theoretically sound and useful for actual engine applications by combining computational analysis with hands-on experimentation. The ultimate goal of this research is to lower stress

Table 1 Selection of material

Material	Titanium alloy	Nickle alloy	Silicon nitride
Density (g/cc)	4.43	8.83	2.37
Yield strength (MPa)	970	59.0	–
Yield tensile strength (MPa)	880	59.0	60
Yield ultimate strength (MPa)	950	45.0	–
Modulus of elasticity (GPa)	113.8	179	166
Poisson ratio	0.34	0.30	0.23

concentrations in a crucial component, which will increase the dependability and efficiency of internal combustion engines. Three materials were chosen for this investigation: silicon nitride, nickel alloy, and titanium alloy. Table 1 shows that of these three materials, silicon nitride displayed the lowest density and least amount of deformation. Higher performance is necessary for IC engines to have a longer lifespan.

It is observed that the operating load and piston pin temperature have increased significantly as a result of high cylinder pressure.

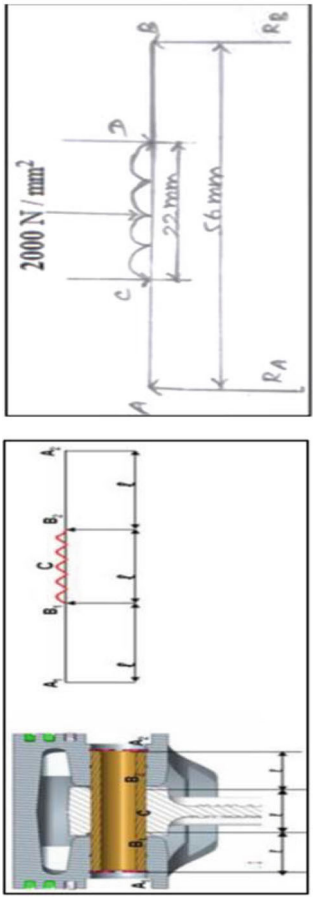
3 Analytical Method

The topic of the presentation is the analysis of a hollow cylindrical gudgeon pin under bending and shear pressures. A uniformly distributed load (UDL) at 2000 N was applied to a gudgeon pin or piston pin with a length of 56 mm, an outer diameter of 22 mm, and an inner diameter of 11 mm. The following theoretical formulas are used to evaluate the stress concentration factor. When comparing the three materials, silicon nitride, nickel alloy, and titanium alloy, silicon nitride has the lowest density and the least amount of deformation. Figure 1 shows piston's pin arrangement under UDL acting on the simply supported beam.

3.1 Theoretical Calculations

Let consider

Load (F)	=	2000 N
Inner diameter (d)	=	11 mm
Outer diameter (D)	=	22 mm
UDL length	=	22 mm
Length (L)	=	56 mm



(a) Piston arrangement (b) Diagram for Force

Fig.1 Piston's pin arrangement (**a**) under UDL acting on the simply supported beam (**b**)

The theoretical computation for structural analysis uses an assumed simply supported beam.

Taking momentum,

R_B * 56	=	2000 * 22 * ((22/2) + 17))
	=	22,000 N
$R_A + R_B$	=	2000 * 22
R_A	=	22,000 N

The values of shear force (SF) at B, D, C, and A are calculated as − 22,000 N, − 22,000 N, 22,000 N, and 22,000 N, respectively.

Bending momentum calculation.

BM at B	=	0
BM at D	=	R_B * 17
	=	374 × 10^3 N mm
BM at C	=	R_B * 39−(2000 * 22 * (22/2))
	=	374 × 10^3 N mm
BM at A SF has (−) sign	=	0
SF	=	− 22,000 N + (2000(X−17))
X	=	28 mm

The shear force diagram, bending moment diagram, stress distribution, and deformation of the silicon nitride are shown in Figs. 2, 3, 4, and 5, respectively. The analytical calculation for selected materials is shown in Table 2.

Gudgeon pin is modeled in design modeler application of Ansys. The pin is modeled, and the face is split at the location where it is held in piston for giving cylindrical support. The gudgeon pin is held at both ends into the piston; hence two cylindrical supports are given. In this radial and axial movement are fixed, whereas tangential movement is made free. One of the ends of pin (face) was given displacement, where displacement in x, y, and z direction is made zero because pin is firmly held in piston and there is no relative movement between piston and pin. As there is small clearance in pin and piston, hence pin acts as a simply supported beam where it is supported by piston bore at two ends with line contact. Gudgeon pin is also held in small end of connecting rod. Hence, contact area of connecting rod and pin is considered as loading zone. So pin is given load at middle area with pressure of 7 bar (Maximum pressure in the cylinder at the end of combustion).

As the pin is uniform and is sweep able body, the sweep type meshing is carried out, so that all hexagonal brick mesh can be formed. Brick type of meshing gives accurate results, and also, brick mesh was densely arranged in the model. Brick mesh is suitable when volume-to-surface area ratio is high as like the gudgeon pin. Total 1824 number of elements and 10,224 numbers of nodes were formed in the meshing. The global mesh size was 5 mm. The above setup is solved in Ansys workbench; the

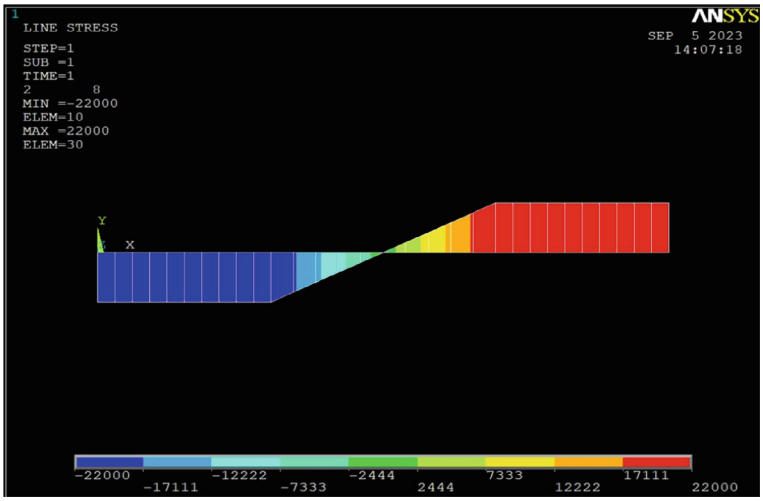


Fig. 2 Shear force diagram

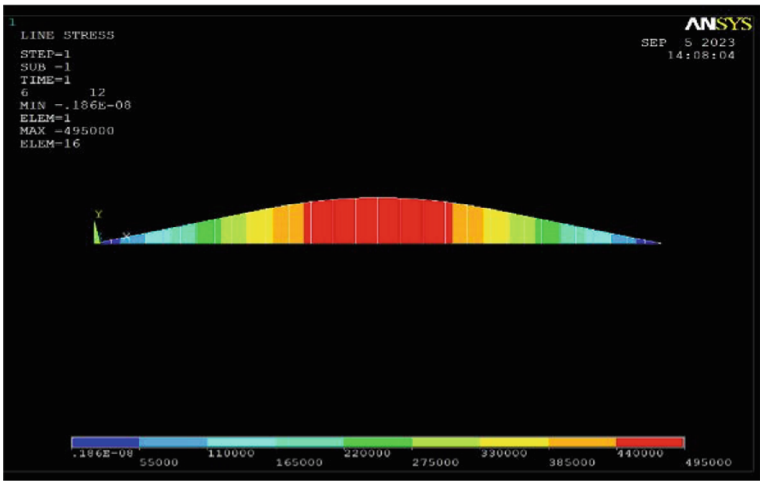


Fig. 3 Bending moment diagram

total CPU time was 15 s. Here, mathematical model is prepared, and it is solved for given boundary conditions, constraints, and loads.

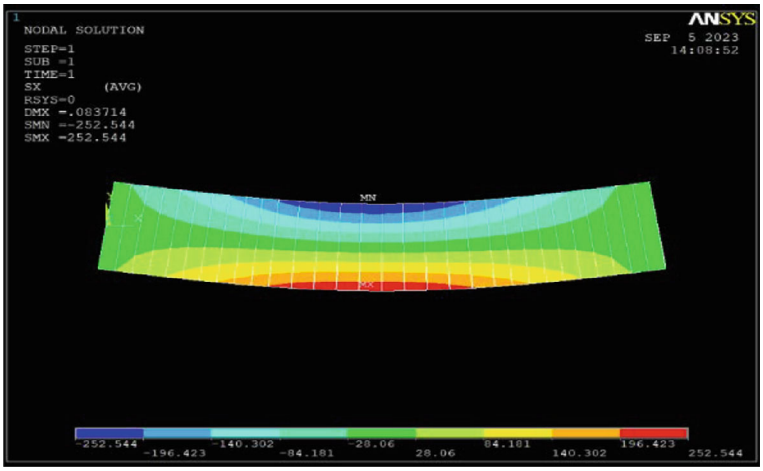


Fig. 4 Stress distribution

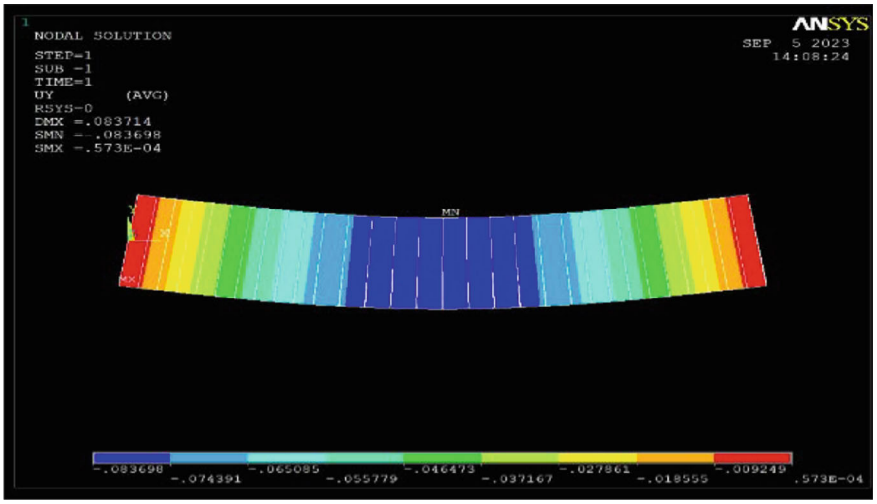


Fig. 5 Deformation of the silicon nitride

Table 2 Analytical calculation for selected materials

Material	Stress (N/mm^2)	Strain	Maximum deflection (mm)	Shear stress (N/mm^2)
Silicon nitride	28.57	0.00017	0.0048	14.03
Titanium alloy	27.74	0.00029	0.0059	11.58
Nickle alloy	27.743	0.000186	0.0038	11.581

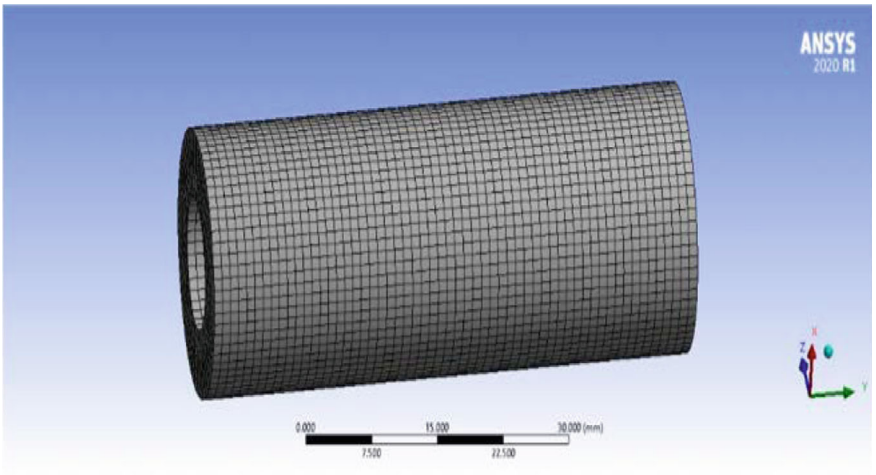


Fig. 6 Design of piston pin in SolidWorks

4 Results and Discussions

4.1 Analysis of Titanium Alloy

The finite element analysis of titanium alloys is shown from Figs. 6, 7, 8 and 9. As shown in Fig. 6, the geometric entity was meshed using a 3D hexahedral element to create a FEM entity. As shown in Fig. 7, the boundary condition was applied to lessen the tensile test by anchoring one end and applying an axial tensile load to the other. Additionally, it was allocated the material's characteristics, such as the Young's modulus value, which came from the experimental data.

4.2 Analysis of Nickle Alloy

The analysis of nickel alloy of equivalent stress 27. 86 MPa, 0.00020 elastic strain, and shear stress 11.62 MPa is almost equal to theoretical calculation of nickel alloy as shown in Figs. 10, 11, and 12.

4.3 Analysis of Silicon Nitride

Analysis of silicon nitride material undergoes less deformation, when compared to titanium alloy and nickel alloy as shown in Figs. 13, 14, and 15.

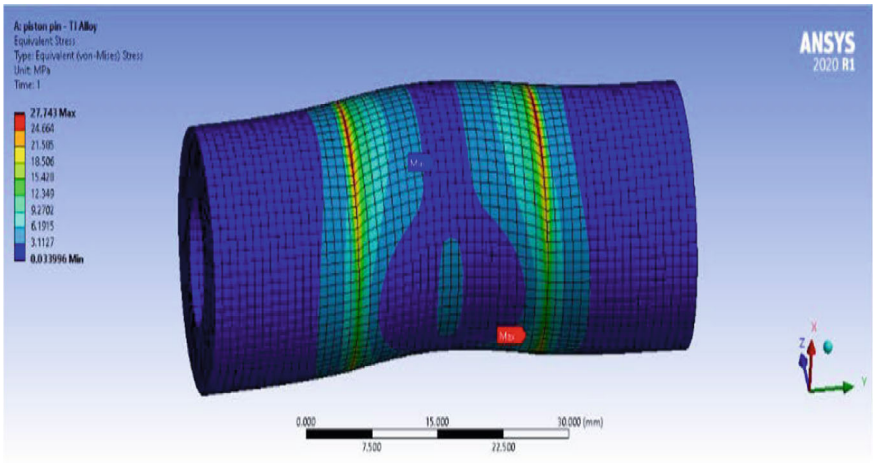


Fig. 7 Equivalent stress on titanium alloy

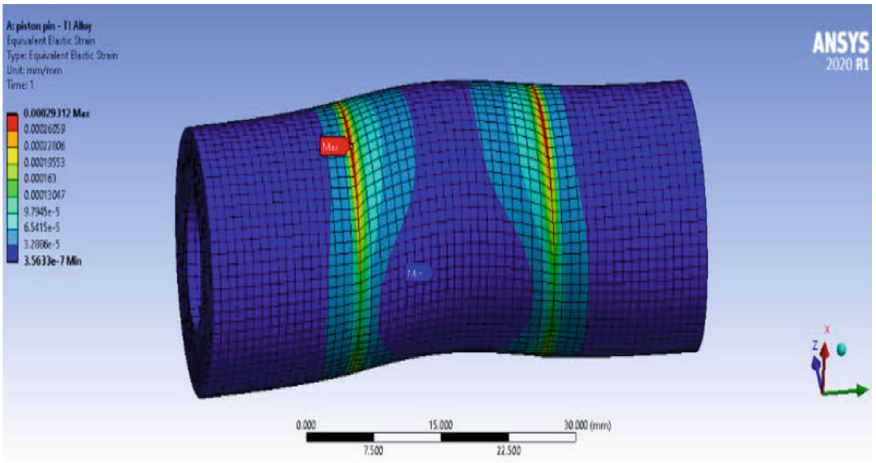


Fig. 8 Equivalent elastic strain on titanium alloy

According to the aforementioned theoretical computation and the analytical calculation performed by Ansys R 2021 V, a material that is resistant to corrosion, shear, and wear is a good fit for a piston pin, which can only improve performance. It can be concluded that the material "silicon nitride" deforms less under different stresses. To resist shear and wear, it also has a high yield strength. In addition to the performance factor, it also has lower availability, cost, and manufacturing/machining methods. The substance known as "silicon nitride" meets all the requirements and is superior to the two other materials, namely "titanium alloy and nickel alloy."

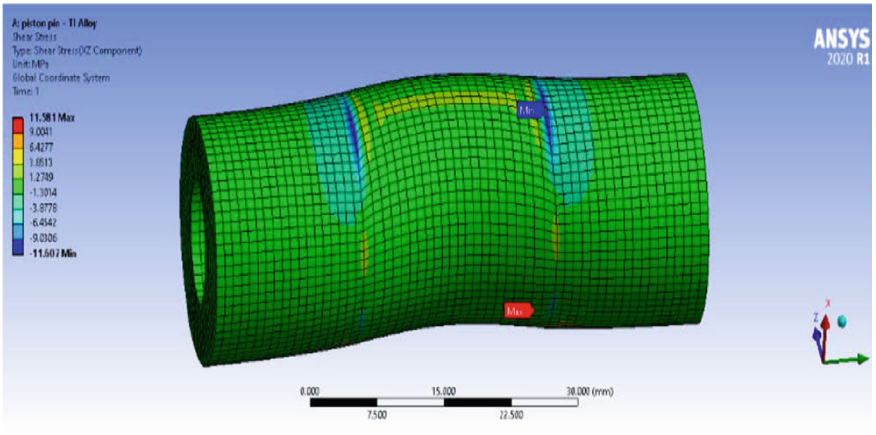


Fig.9 Shear stress on titanium alloy

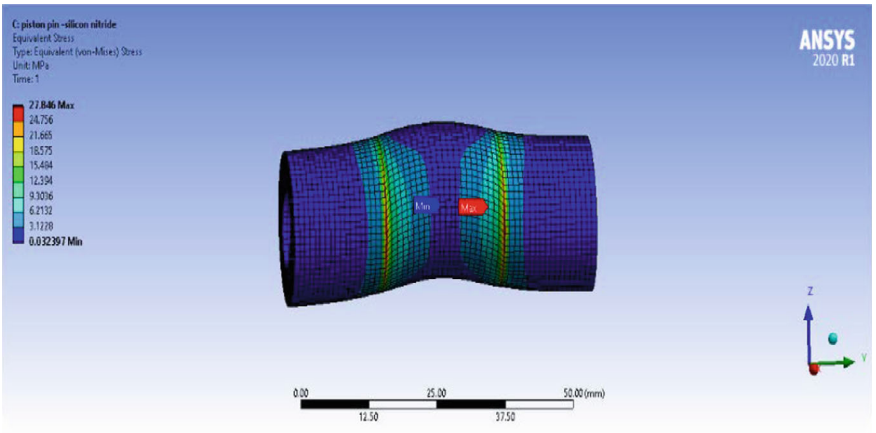


Fig. 10 Equivalent stress on nickel alloy

5 Conclusions

This study's objectives encompass a broad spectrum of engineering challenges. Firstly, it aims to explore the fundamental principles of gudgeon pin design and its role within IC engines. Understanding the mechanics and operating conditions is crucial for designing components that can withstand real-world stresses. Secondly, the study will delve into the intricate details of stress concentration and its detrimental effects on mechanical components. In the current study, titanium alloy, nickel alloy, and silicon nitride materials to construct a piston pin for an I.C. engine were considered. It was discovered that nickel alloy deforms less than the other two materials. By

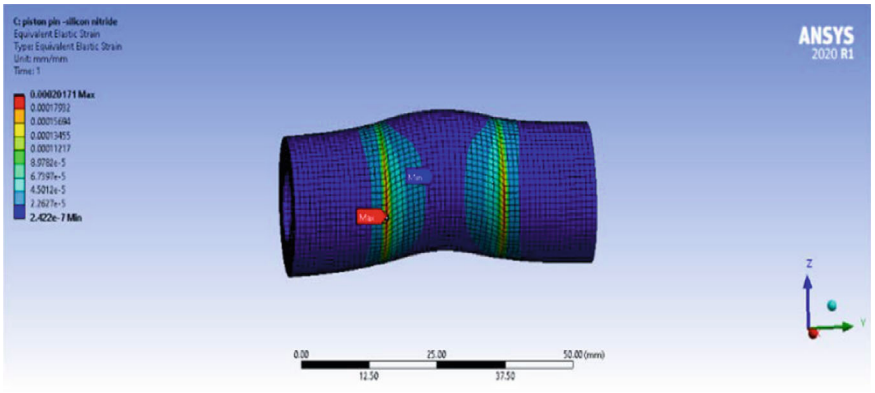


Fig. 11 Equivalent elastic strain on nickel alloy

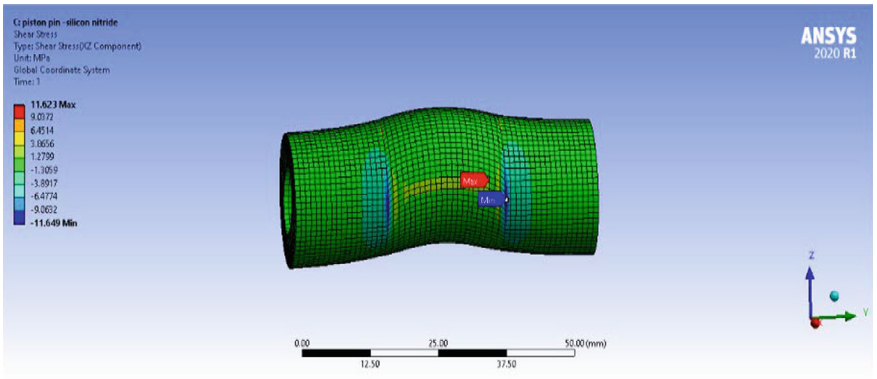


Fig.12 Shear stress on nickel alloy

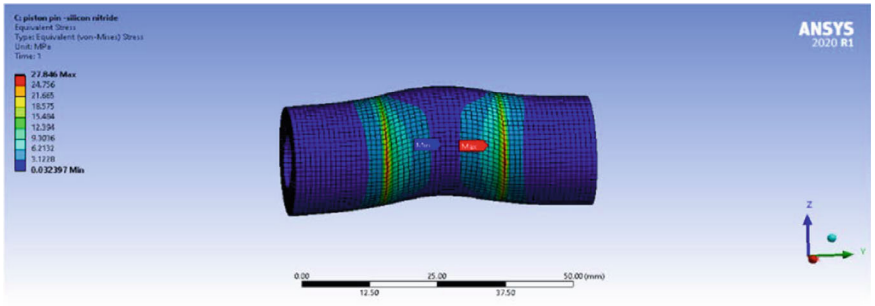


Fig. 13 Equivalent stress on silicon nitride

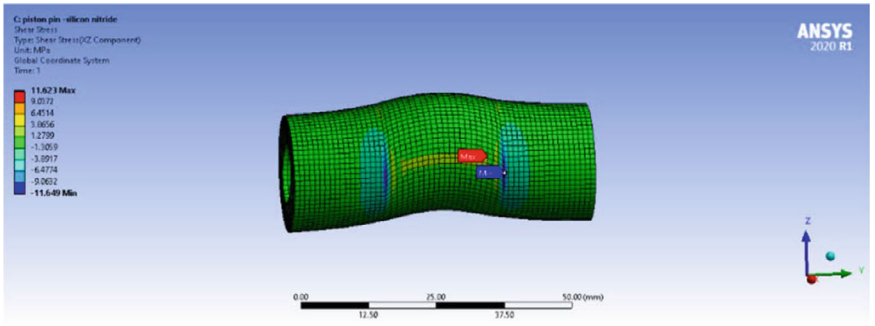


Fig. 14 Shear stress on silicon nitride

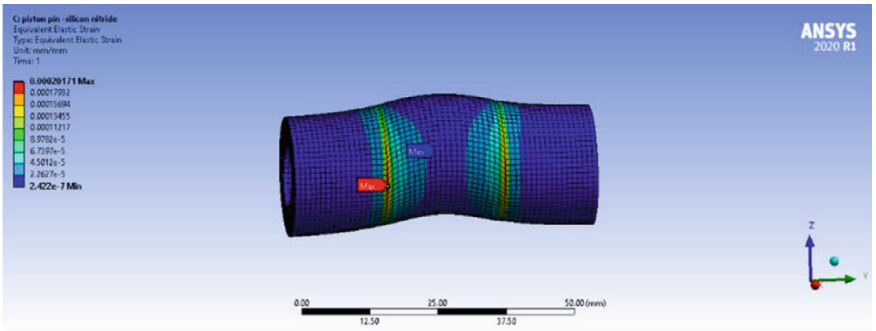


Fig. 15 Equivalent elastic strain on silicon nitride

assimilating the theoretical, analytical findings, and von Mises stress theory, silicon nitride material deformation was reduced. Finally, based on the above results, it was concluded that silicon nitride is a good material to use when making piston pins.

References

1. Robinson JE (1964) The design and development of pistons for automobile engines. Proc Inst Mech Eng Automob Div 179:181–211
2. Guzzomi AL, Hesterman DC, Stone BJ (2008) Variable inertia effects of an engine including piston friction and a crank or gudgeon pin offset. Proc Inst Mech Eng Part D J Automob Eng 222:397–414
3. Fessler H, Hyde TH (1997) Stress distribution in gudgeon pins. J Strain Anal Eng Des 32:375–386
4. Bianco L, Barbieri SG, Mangeruga V, Giacopini M, Capoccia G (2022) Influence of the thermal deformation on the lubricating performance of the piston-gudgeon pin interface in an internal combustion engine. Tribol Int 174:107719

5. Strozzi A, Baldini A, Giacopini M, Bertocchi E, Mantovani S (2018) A repertoire of failures in gudgeon pins for internal combustion engines, and a critical assessment of the design formulae. Eng Fail Anal 87:22–48
6. Wang Y, Gao H (2011) Research on optimization for the piston pin and the piston pin boss. Open Mech Eng J 5
7. Sharma A, Murugan S (2015) Potential for using a tyre pyrolysis oil-biodiesel blend in a diesel engine at different compression ratios. Energy Convers Manag 93:289–297. https://doi.org/10.1016/j.enconman.2015.01.023
8. Sharma A, Murugan S (2017) Effect of nozzle opening pressure on the behaviour of a diesel engine running with non-petroleum fuel. Energy 127:236–246. https://doi.org/10.1016/j.energy.2017.03.114
9. Sharma A, Murugan S (2015) Combustion, performance and emission characteristics of a di diesel engine fuelled with non-petroleum fuel: a study on the role of fuel injection timing. J Energy Inst 88:364–375. https://doi.org/10.1016/j.joei.2014.11.006
10. Sharma A, Murugan S (2017) Durability analysis of a single cylinder DI diesel engine operating with a non-petroleum fuel. Fuel 191:393–402. https://doi.org/10.1016/j.fuel.2016.11.086
11. Najafi M, Dastani H, Abedini M, Pirani S (2019) Stress analysis and fatigue life assessment of a piston in an upgraded engine. J Fail Anal Prev 19:402–411
12. Soong K, Thompson BS (1990) A theoretical and experimental investigation of the dynamic response of a slider-crank mechanism with radial clearance in the gudgeon-pin joint

Identifying the Influence of the WEDM Process Variable on Performance Indicators: MRR During the Machining of Inconel X-750



Smita Padhan, Sudhansu Ranjan Das, and Pankaj Charan Jena

Abstract This study attempted to identify the influence of the WEDM process variable on performance indicators such as material removal rate during the machining of Inconel X-750. The primary objective of this study is to examine the impact of process variables, understand their effect on material removal rate (MRR), and concurrently optimize MRR using the desirability function analysis (DFA) approach. The results of the experiment have led to the outcomes, as the regression model for MRR developed using RSM is statistically significant. Because of its modest *p*-value (<0.05) and greater R2 value (0.8799), the response surface methodology (RSM)-based prediction model proposed for MRR is sufficient, statistically significant, and probabilistically validated. The MRR surface plots show that MRR increases with increasing peak current and T_{on} time while decreasing with increasing servo voltage and pulse-off time. It is observed that the estimated optimum value for MRR using the DFA technique is 4.0998 mm^3/min with optimum parameters setting (i.e., $T_{on} =$ 120 μs, $T_{off} = 50$ μs, $I_p = 12$A, and $S_v = 40$ V).

Keywords WEDM process · Inconel X-750 · Machining · MRR

1 Introduction

Wire electro-discharge machining (WEDM) has gained popularity because it is unaffected by material hardness, exerts no cutting force, provides high accuracy, and enables the production of intricate shapes and profiles. WEDM employs electrical

S. Padhan (✉) · S. R. Das · P. C. Jena
Department of Production Engineering, Veer Surendra Sai University of Technology, Burla, Odisha 768018, India

S. R. Das
e-mail: das.sudhansu83@gmail.com

P. C. Jena
e-mail: pcjena_pe@vssut.ac.in

© The Author(s), under exclusive license to Springer Nature Singapore Pte Ltd. 2025

B. B. V. L. Deepak et al. (eds.), *Recent Advancements in Product Design and Manufacturing Systems*, Lecture Notes in Mechanical Engineering,
https://doi.org/10.1007/978-981-97-6732-8_31

discharge cutting, relying on physical processes like heating and cooling. Repeated rapid releases of electrical current between two electrodes, separated by a dielectric liquid and subjected to an electrical voltage, result in the removal of material from the workpiece [1]. WEDM finds extensive application in the tool and die manufacturing industry, particularly for producing high-precision items such as sheet metal press dies, stamping dies, extrusion dies, and wire drawing dies [2]. Several process parameters, including wire tension, wire feed speed, servo voltage, open voltage, pulse off and on time, and dielectric pressure, influence three critical performance metrics in WEDM. These metrics are surface roughness, determining finished part quality; MRR, impacting process economics and, kerf, deciding dimensional accuracy [3].

Nickel-based superalloys are widely preferred in manufacturing industries over titanium-based alloys due to their inherent properties and advantages. Nickel-based superalloys offer crucial benefits, including heat resistance with the ability to retain intended characteristics at elevated temperatures, a high melting temperature, and a high resistance to corrosion [4].

Amitesh and Jatinder conducted an experimental investigation on the impact of process parameters while machining Nimonic-80A alloy in WEDM. The study considered WT, WF, I_P, S_V, T_{off}, and T_{on} as input variables, with MRR and Ra as the observed responses. The results indicate that, among the varied input parameters, T_{on} and T_{off} have a significant influence, accounting for nearly 80% of the variation in MRR, while S_V and T_{on} have a more prominent impact on surface roughness. So, it suggests a correlation between the quality of the worked surface and the rate of energy input. Higher energy input conditions result in the generation of a rougher surface, while a lower density of energy input to the cutting zone produces smooth surface integrity [5]. Another study was conducted on WWR, surface integrity, and MRR in the WEDM process for Nimonic 80A. They utilized the grey relational analysis (GRA) and Taguchi method to analyze the factors influencing the process. Their findings revealed that T_{on} had the most substantial impact on MRR, contributing 46%, T_{off}, on the other hand, was responsible for 33% of the variance in MRR. Additional machining variables, such as I_p and gap voltage, were identified as relatively less significant [6]. In an another study, the research emphasizes the creation of multiple regression equations to predict performance aspects in Wire-cut EDM of Stellite. Input variables include I_p, Pulse-on and off time, with MRR as the performance metric. The application of Taguchi's design and optimization techniques improves machining performance. Through multiple regression analysis, empirical relationships among process parameters are established, providing manufacturers with insights to optimize production rates and product quality in WEDM. The close alignment between experimental and predicted values validates the credibility of the study's findings [7].

The existing literature highlights a noticeable absence of research on identifying optimal machining characteristics for machining Inconel X-750 on WEDM with zinc-coated brass wire as the electrode with efficient machining performance. In this study, we conduct an experimental study on Inconel X-750 while machining it in wire-cut EDM, with a specific emphasis on evaluating the material removal rate as a crucial performance metric. Experiments are performed following the RSM,

and modeling with regression analysis is conducted to assess the material removal rate (MRR). The primary objective of this study is to examine the impact of process variables, understand their effect on material removal rate, and concurrently optimize MRR using the desirability function analysis (DFA) approach.

2 Section Materials and Methodology

In this present study, the experiments are performed on Inconel X-750 using the ELECTRONICA Ecocut (e-pulse) four-axis CNC wire electrical discharge machining (WEDM) machine employing deionized water as dielectric fluid. In this study, a stratified brass wire coated with zinc is employed to cut the work material, with a wire diameter of 0.25 mm. In the present investigation, Inconel X-750 (rectangular slab, having the dimension of 150 * 50 * 12.5 mm) is selected as the work material. The nickel-based superalloy, Inconel X-750, finds primary applications in thrust chambers of rocket engines, in gas turbines (bolts, wheels, rotor blades, and other structural members), extrusion dies, forming tools, rocket-engine thrust chambers, heat treating fixtures, and nuclear reactor components. Its widespread utility across diverse fields makes it the chosen work material for this study [8]. The weight % of chemical constituents and physical characteristics of Inconel X-750 are shown in Tables 1 and 2. The machining parameters selected for investigation included I_P, S_V, T_{off}, and T_{on}.

Table 3 illustrates the values for the input factors, which were chosen through a literature review and a preliminary study employing a single factor at a time methodology. In each experimental run, the material was cut to a length of 10 mm, and cutting time was recorded. The thickness of the work was measured using digital Vernier calipers, while Kerf was measured using a toolmaker microscope.

The MRR has been calculated manually using the following Eq. 1:

$$(\text{MRR}) = \frac{l * w * t}{T} \text{ mm}^3/\text{min} \tag{1}$$

where l = length of cut in mm, w = Kerf width in mm, h = thickness of workpiece in mm, and T = machining time in min.

The experiments were systematically planned and executed using the RSM. The choice of suitable model and the creation of response surface models were accomplished with the assistance of statistical software, specifically "Minitab 16." Regression equations for MRR were derived for the chosen model. The regression equation was constructed based on the data collected from the experiments (as shown in Table 4) and was visualized to explore the influence of input machining factors on MRR. Statistical analysis, specifically ANOVA, was conducted to assess the results.

The graphical representation of the procedure used for the wire-cut EDM machining setup and analysis of the test data is shown in Fig. 1.

Table 1 Chemical constitution of INCONEL X-750

Elements	Al	C	Si	Nb + Ta	Fe	Cr	Ni	Ti	Co	Cu	S	Mg
% of wt	0.40–1.00	0.08	0.50	0.70–1.20	5.0–9.0	14.0–17.0	70.00	2.25–2.75	~ 1.00	~ 0.05	~ 0.01	~ 1.00 max

Table 2 Physical properties of INCONEL X-750

Properties	Poisson's ratio	Specific heat	Modulus of elasticity	Modulus of rigidity	Co-efficient of expansion	MP	Density	Electrical resistivity
Value	0.29	431.24 J/Kg °C	212.4 kN/mm^2	75.8 kN/mm^2	12.6 μm/m °C	1393–1427 °C	8.28 g/cm^3	μΩ m

Table 3 Selected input variables and their levels

Variables	Levels		
	1	2	3
T_{on} (μs)	100	110	120
T_{off} (μs)	50	55	60
I_p (amp)	10	11	12
S_v (volt)	40	50	60

The help of Minitab 16 software performed analysis of variance (ANOVA) for MRR. The fit summary is explained in Table 5. Only the factors identified as significant from the ANOVA test (as indicated in Table 1) were taken into account for creating the main effects as well as interaction plots. The ANOVA table for MRR includes the following components: SS, degrees of freedom (DoF), mean of square, *F*-value, and probability value. *P*-value and *F*-value are utilized as statistical tools to assess the adequacy as well as statistical significance of the constructed regression model. For a specific input parameter if the *P*-value is below 0.05 (indicating a 95% confidence level), it is thought to positively affect the corresponding output statistically, which is preferable. On the other hand, a parameter is considered to have no impact on the outcome if the estimated Fischer value is less than the standardized F-value or if the probability value for that parameter is greater than 0.05. The regression model for MRR developed using RSM is statistically significant. The *F*-value of the regression model was 51.58. The probability of having a large *F*-value arising due to random noise is only 0.01%. A *P*-value of less than 0.05 suggests that the model terms are significant. In this case, the factor I_P, S_V, T_{off}, and T_{on} and the interaction terms ($T_{on} \times I_P$ and $I_P \times I_P$) are significant terms of the model. The model terms whose *P*-value exceeds 0.1 are considered insignificant. The "lack of fit *F*-value" of 3.21 suggests that when compared to pure error, lack of fit does not seem significant. There is only a 10.50% probability that a "lack of fit *F*-value" of this magnitude could arise from random noise. The model fits well when there is a non-significant lack of fit, which is ideal.

Regression equation of MRR

$$\begin{aligned}\mathrm{MRR} = (&-52.78729 + 0.10245 * T_{on} + 0.20961 * T_{off} + 8.49311 * I_P \\ &- 0.027151 * S_v - 6.11472E - 004 * T_{on} * T_{off} \\ &- 0.011945 * T_{on} * I_P + 2.40093E - 004 * T_{on} * S_v \\ &- 5.75895E - 003 * T_{off} * I_P + 3.48474E - 005 * T_{off} * S_v \\ &+ 1.46105E - 003 * I_P * S_v + 1.03430E - 004 * T_{on}^2 \\ &-6.07456E - 004 * T_{off}^2 - 0.33128 * I_P^2 - 1.11943E - 004 * S_v^2\big)^{-2} \end{aligned} \quad (2)$$

For the purpose of preventing misleading conclusions, various diagnostic tests were conducted for the suggested regression model (MRR), including adequacy, efficacy, and goodness of fit. With a difference of less than 0.2, the "Pred R-Squared"

Table 4 Experimental results

EXPT No.	Input parameters				Output response
	T_{on} (μs)	T_{off} (μs)	I_P (A)	S_V (V)	MRR (mm^3/min)
1	110	55	11	50	0.361416
2	110	50	11	50	0.366032
3	120	50	12	40	4.78146
4	110	55	11	50	0.355523
5	100	55	11	50	0.28133
6	100	60	10	40	0.263308
7	120	50	12	60	2.32384
8	110	55	12	50	0.869243
9	110	55	11	50	0.348123
10	100	60	12	60	0.429287
11	100	50	12	60	0.494045
12	110	55	11	60	0.340928
13	120	60	12	60	1.8542
14	110	55	11	50	0.304974
15	100	50	10	60	0.349246
16	120	60	10	40	0.396323
17	120	55	11	50	0.413582
18	100	60	10	60	0.216965
19	100	60	12	40	0.501995
20	110	55	10	50	0.352422
21	110	55	11	50	0.345642
22	110	55	11	50	0.342006
23	120	50	10	60	0.369781
24	120	50	10	40	0.546998
25	110	60	11	50	0.331676
26	100	50	10	40	0.313215
27	110	55	11	40	0.352383
28	120	60	12	40	2.32384
29	100	50	12	40	0.589666
30	120	60	10	60	0.387438

of 0.8799 and the "Adj R-Squared" of 0.9607 are in close agreement (Table 6). The signal-to-noise ratio is measured by Adeq Precision. A ratio that is higher than 4 is preferred. An appropriate signal is shown by the ratio of 26.125, which implies that the quadratic model can be utilized to analyze the design space.

Since the residuals of the MRR regression model are distributed linearly, as the normal probability plot shows (see Fig. 2), where the associated errors were found to

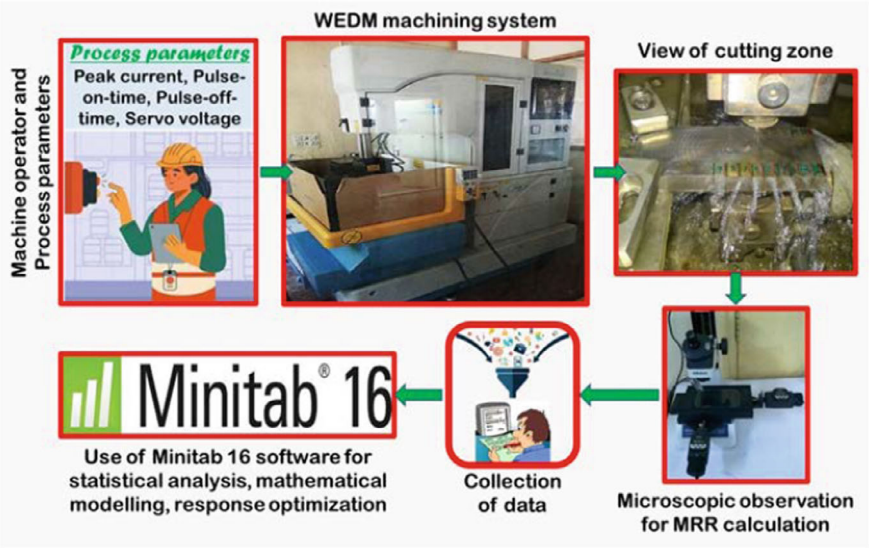


Fig. 1 Graphical representation of the methodology and analysis of the results

be normally distributed, so, all of the model's contributing elements are statistically significant.

The surface plot for MRR clearly demonstrates that an extended pulse-on time leads to a greater material removal rate (MRR). It can have observed that the duration of the spark rises along with the pulse-on time. So the frequency of energy discharge increases, as a result MRR increases [9]. However, when servo voltage increased, the gap between two electrodes increased. Due to which the energy density between the electrodes decreased. As a result, MRR was decreased (refer, Fig. 3a). Similarly, when pulse-off time increased, time interval in-between two consecutive sparks also increased which lead to decrease in MRR, while with the increase in peak current, the electrical pulse generated was more. i.e., energy utilization was more [10]. So, the intensity of spark was more. As a result, MRR was increased (refer, Fig. 3b).

Optimization of MRR using the desirability function.

The desirability function methodology of RSM is utilized in this experimental investigation to maximize the material removal rate. A statistical technique known as desire function analysis converts each predicted response into a desirability value, which is a scale-free value between 0 and 1. The weighted geometric mean of each desirability value is then composited to create a desirability function for optimization [11]. The goal of this is to maximize, minimize, or reach a target value for the given response in both single- and multi-response problems. The possible value of any response is considered unwanted when the desirability rating for that response is close to 0. Alternatively, a desirability value of any response equal to or approaching 1 indicates a higher level of desirability. Many desirability functions d_i can be utilized depending on whether a given response X_i is to be minimized, maximized, or given a

Table 5 Results obtained after ANOVA for MRR

Response			MRR			
Transform			Inverse squrt			Constant:0
Source	SS	df	MS	*F*-value	*p*-value	
Model	4.90	14	0.35	51.58	< 0.0001	Significant
T_{on}	1.39	1	1.39	205.25	< 0.0001	
T_{off}	0.087	1	0.087	12.85	0.0027	
I_p	2.24	1	2.24	329.74	< 0.0001	
S_v	0.066	1	0.066	9.72	0.0071	
$T_{on} * T_{off}$	0.015	1	0.015	2.20	0.1584	
$T_{on} * I_p$	0.23	1	0.23	33.63	< 0.0001	
$T_{on} * S_v$	9.223 E−003	1	9.223 E−003	1.36	0.2619	
$T_{off} * I_p$	0.013	1	0.013	1.95	0.1824	
$T_{off} * S_v$	4.857 E−005	1	4.857 E−005	7.156 E−003	0.9337	
$I_p * S_v$	3.415 E−003	1	3.415 E−003	0.50	0.4890	
$T_{on} * T_{on}$	2.772 E−004	1	2.772 E−004	0.041	0.8426	
$T_{off} * T_{off}$	5.975 E−004	1	5.975 E−004	0.088	0.7708	
$I_p * I_p$	0.28	1	0.28	41.89	< 0.0001	
$S_v * S_v$	3.247 E−004	1	3.247 E−004	0.048	0.8298	
Residual	0.10	15	6.787 E−003			
Lack of fit	0.088	10	8.809 E−003	3.21	0.1050	Not significant
Pure error	0.014	5	2.744 E−003			
Cor total	5.00	29				
Model	4.90	14	0.35	51.58	< 0.0001	Significant

Table 6 Model summary for MRR

Std. dev.	0.082	R^2 value	0.9797
Mean	1.50	Adj R^2 value	0.9607
C.V. %	5.49	Pred R^2 value	0.8799
Press	0.60	Adeq precision	26.125

goal value. According to Derringer and Suich [12], if the objective (T_i) is to maximize a response, the individual desirability (d_i) is computed as Eq. 3:

$$d_i = \begin{cases} 0 & \text{if } X_i < (X_i)_{max} \\ \left(\frac{X_i - (X_i)_{min}}{T_i - (X_i)_{min}}\right)^w & \text{if } (X_i)_{min} \le X_i \le T_i \\ 1 & \text{if } X_i > T_i \end{cases}. \quad (3)$$

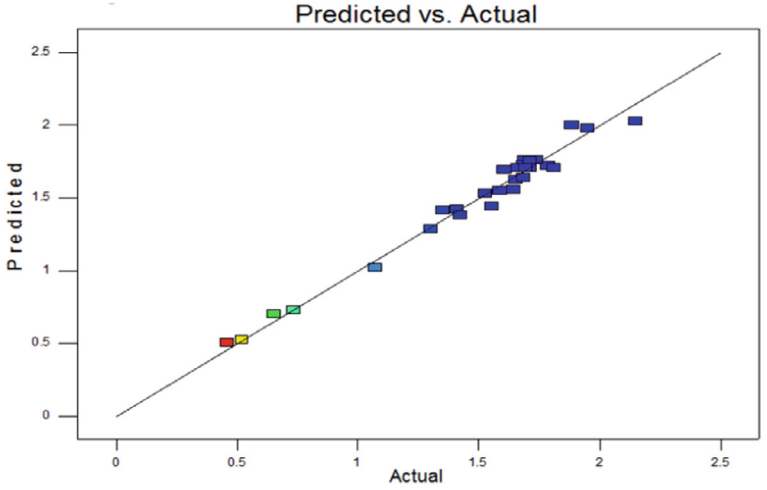


Fig. 2 Normal probability plot for MRR

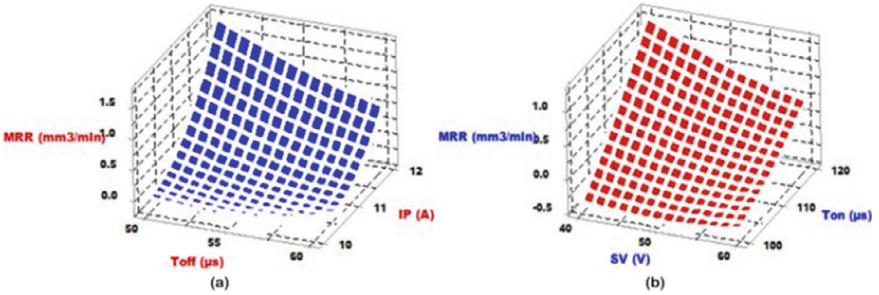


Fig. 3 3D surface plots to analyze the influence of machining parameters on MRR

Figure 4 depicts the optimization plot for MRR utilizing desirability function analysis, highlighting optimal machining conditions with a T_{on} of 120 µs, $T_{off\ of}$ 50 µs, I_p of 12A, and S_v of 40 V. The estimated optimum value for MRR using the DFA technique is 4.0998 mm^3/min.

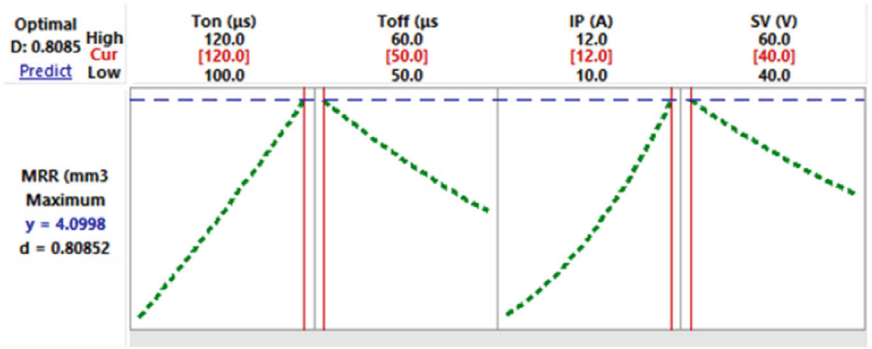


Fig. 4 Optimization chart for MRR employing DFA technique

3 Conclusion

This study attempted to identify the influence of the WEDM process variable on performance indicators such as material removal rate during machining of Inconel X-750. The results of the experiment have led to the following conclusions:

- The regression model for MRR developed using RSM is statistically significant. Because of its modest *p*-value (<0.05) and greater R^2 value (0.8799), the RSM-based prediction model proposed for MRR is sufficient, statistically significant, and probabilistically validated.
- The MRR surface plots show that MRR increases with increasing peak current and Ton time while decreasing with increasing servo voltage and pulse-off time.
- The estimated optimum value for MRR using DFA technique is 4.0998 mm^3/min with optimum parameters setting (i.e., $T_{on} = 120$ µs, $T_{off} = 50$ µs, $I_p = 12$A, and $S_v = 40$ V).

Further, the work may be extended to find out morphological analysis of the machine surface, and a multi-objective algorithm may be fitted to identify the optimum value of machining parameters.

References

1. Kneubühler F, Wiessner M, Wegener K (2020) Analysis of WEDM process with respect to wire wear and wire consumption. Procedia CIRP 95:313–318. https://doi.org/10.1016/J.PROCIR.2020.03.151
2. Maruda RW, Krolczyk GM, Nieslony P, Wojciechowski S, Michalski M, Legutko S (2016) The influence of the cooling conditions on the cutting tool wear and the chip formation mechanism. J Manuf Process 24:107–115. https://doi.org/10.1016/J.JMAPRO.2016.08.006
3. Ikram A, Mufti NA, Saleem MQ, Khan AR (2013) Parametric optimization for surface roughness, kerf and MRR in wire electrical discharge machining (WEDM) using Taguchi design of experiment. J Mech Sci Technol 27(7):2133–2141. https://doi.org/10.1007/s12206-013-0526-8

4. Satyanarayana K, Mounika M, Raj Kiran K (2021) Experimental studies and optimization of WEDM process in machining of Inconel 600 using zinc wire. Mater Today Proc 44:2431–2434. https://doi.org/10.1016/J.MATPR.2020.12.475
5. Goswami A, Kumar J (2014) Optimization in wire-cut EDM of Nimonic-80A using Taguchi's approach and utility concept. Eng Sci Technol Int J 17(4):236–246. https://doi.org/10.1016/J.JESTCH.2014.07.001
6. Goswami A, Kumar J (2014) Investigation of surface integrity, material removal rate and wire wear ratio for WEDM of Nimonic 80A alloy using GRA and Taguchi method. Eng Sci Technol Int J 17(4):173–184. https://doi.org/10.1016/J.JESTCH.2014.05.002
7. Binoj JS, Manikandan N, Thejasree P, Varaprasad KC, Prem Sai N, Manideep M (2021) Machinability studies on wire electrical discharge machining of Nickel alloys using multiple regression analysis. Mater Today Proc 39:155–159. https://doi.org/10.1016/J.MATPR.2020.06.407
8. Şirin Ş, Yıldırım ÇV, Kıvak T, Sarıkaya M (2021) Performance of cryogenically treated carbide inserts under sustainable cryo-lubrication assisted milling of Inconel X750 alloy. Sustain Mater Technol 29. https://doi.org/10.1016/j.susmat.2021.e00314
9. Kumar M, Singh H (2016) Multi response optimization in wire electrical discharge machining of Inconel X-750 using Taguchi's technique and grey relational analysis. Cogent Eng 3(1). https://doi.org/10.1080/23311916.2016.1266123
10. Divya Sadhana A, Udaya Prakash J, Ananth S, Jebarose Juliyana S, Sarala Rubi C (2022) Effect of process parameters for wire EDM of AISI H13 tool steel. Mater Today Proc 52:1870–1874. https://doi.org/10.1016/j.matpr.2021.11.508
11. Costa NR, Lourenço J, Pereira ZL (2011) Desirability function approach: a review and performance evaluation in adverse conditions. Chemom Intell Lab Syst 107(2):234–244. https://doi.org/10.1016/J.CHEMOLAB.2011.04.004
12. Derringer G, Suich R (1980) Simultaneous optimization of several response variables. J Qual Technol 12(4):214–219. https://doi.org/10.1080/00224065.1980.11980968

Experimental Investigation of Corrosion Effect of Automotive Fuel Tank for Biofuels



T. Vinod Kumar, M. Chandrasekaran, R. Pugazhenthi, Abhishek Sharma, Anil Singh Yadav, Rahul Kumar, and Gopal Kaliyaperumal

Abstract The present research work investigates the corrosion deformation of carbon steel materials at various temperatures such as 50, 60 °C, and ambient temperature. Stabling absorption tests were conducted in pure diesel, biodiesel in 50% diesel, and pure biodiesel for 720 h. After the tests were finished, the corrosion performance qualities were evaluated by using assessment weight loss methods to expose the metal surface. Microscopic and computational fluid dynamic oxidation analyzers were used to analyze biofuels of fuel's acidity and oxidation. Morphological tests were studied on the fuel tank surface by using SEM images and dispersive gauging. Results monitoring that the corrosion of automotive mild steel material increase of worm heating, the water content, and oxidation products are increased or decreased are evaluated with processing simulation with the experiment.

Keywords Biofuel · Corrosion · Fuel tank · SEM · Pungamia

T. Vinod Kumar · M. Chandrasekaran · R. Pugazhenthi
Department of Mechanical Engineering, Vels Institute of Science, Technology & Advanced Studies, Chennai, Tamil Nadu 600117, India

A. Sharma (✉)
Department of Mechanical Engineering, B I T Sindri, Dhanbad, Jharkhand 828123, India
e-mail: drasharma58@gmail.com

A. S. Yadav
Department of Mechanical Engineering, Bakhtiyarpur College of Engineering (Science, Technology and Technical Education Department, Govt. of Bihar), Bakhtiyarpur, Patna, Bihar 803212, India

R. Kumar
School of Mechanical Engineering, Lovely Professional University, Phagwara, Punjab 144001, India

G. Kaliyaperumal
Department of Mechanical Engineering, New Horizon College of Engineering, Bangalore, Karnataka 560103, India

© The Author(s), under exclusive license to Springer Nature Singapore Pte Ltd. 2025

B. B. V. L. Deepak et al. (eds.), *Recent Advancements in Product Design and Manufacturing Systems*, Lecture Notes in Mechanical Engineering,
https://doi.org/10.1007/978-981-97-6732-8_32

1 Introduction

The need of reduction of carbonated fuel pollution reduction is one of the most crucial issues in current trends of research the alternative fuels are the way to control air pollution. Alternate fuel is one of the most effective methods to control air pollution in the automotive industry. Biofuels are becoming more important as a whole or partial replacement for diesel fuel. However, a key problem is the corrosion of modern materials in biodiesel, which might lower vehicle efficiency. The degrading attack (or degradation) of a metal caused by a chemical (or electrochemical) reaction with its surroundings is known as corrosion. Iron will corrode even in the absence of a separate cathodic metal because corrosion is an electrochemical process that affects metals. On a steel surface, anode–cathode pairs can be arranged at various electrochemical potentials or oxidation inclinations. In a galvanic cell, oxygen and moisture are present while two dissimilar metals, such as iron and copper, are brought into electrical contact. At the surfaces of the two metals, distinct chemical processes occur, resulting in an electron flow across the connecting wire. The following anodic reaction occurs at the iron surface, or anode, when the iron is oxidized:

$$2\mathrm{Fe} - 4\ \text{electrons} \rightarrow 2\mathrm{Fe}^{++} \tag{1}$$

The following cathodic reaction takes place at the copper surface, or cathode, when oxygen is reduced:

$$\mathrm{O_2} + 2\mathrm{H_2O} + 4\ \text{electrons} \rightarrow 4\mathrm{OH}^- \tag{2}$$

According to Eq. 1.1, the anode is where the process's actual metal loss occurs. In the solution around the anode, the iron atoms are changed into ferrous ions (Fe++), which dissolve. According to the following net redox reaction, they may diffuse and mix with the hydroxyl ions (OH–), leading to the precipitation of ferrous hydroxide [$\mathrm{Fe(OH)_2}$]:

$$2\mathrm{Fe} + \mathrm{O_2} + 2\mathrm{H_2O} \rightarrow 2\mathrm{Fe(OH)_2} \tag{3}$$

Rust is created by further oxidizing the hydrous ferrous oxide (FeOH20) created by Eq. 3 to create hydrous ferric oxide (Fe203. nH20). The most prevalent type of steel corrosion is general corrosion, also known as rusting. Numerous micro corrosion cells are triggered at the corroded area in what might be considered a uniform corrosion process. Small granules that typically have the anode as their boundary might be the cells, for instance.

2 Literature Review

When compared to gasoline-diesel, biodiesel offers the most benefits and is the ideal substitute because it is environmentally benign. It was discovered that using biodiesel in compression ignition engines and subsequently replacing non-renewable fossil fuels was crucial [1]. The main sources of biodiesel are vegetable oil and animal fats used as feedstock. Low volatility and high viscosity are the two main reasons why vegetable oil and animal fat cannot be utilized directly as fuel in a diesel engine [2]. This also leads to severe engine deposits, piston ring sticking, and injector checks. Triglycerides are prohibited from being used directly in diesel engines due to these factors. The catalyzed transesterification of triglycerides with alcohol to produce a mono alkyl is one of the greatest ways to advance the fuel characteristics of triglycerides. Esters of long-chain fatty acids, or biodiesel, are similar to hydrocarbon-based diesel fuels in that they provide equivalent engine performance while emitting fewer pollutants [3]. The primary biodiesel-producing ingredients are canol, palmoils, soyabean, cotton seed, and repacked seeds; these ingredients have some of the greatest heating values (HHV) of any fuel. The notions of biodiesel changed from 39 to 49 mg/kg and are significantly less [4].

The gasoline, which has a 46 mg/kg concentration in all types of vegetable oils, can be used to substitute diesel oil, although palm and grape seed oils are best for use as a diesel fuel extender or additive [5]. Biodiesel is referred to as a clean fuel because its sulfur concentration is comparably lower than that of petroleum diesel and it contains no genetic chemicals. When used in CI engines, the capability of biodiesel to be extremely biodegradable plus its superior oiling quality make it a wonderful fuel. Petrol and diesel have many physiochemical characteristics, which have disclosed their potential and practical usage as a fuel to replace petroleum diesel in the near future [6]. If the physical and chemical characteristics of biodiesel meet the requirements of the international standard biofuel specification. It might serve as a substitute fuel for compression ignition diesel engines. Before being used as an alternate fuel, biofuel must meet the requirements set forth by (ASTM), BS71-3, and EN14214 [7]. The characteristics of biofuel include higher heating value (HHV), distillation range, total glycerine content, copper common flash point, free glycerine content, sulfur content cloud carbon residue acid value, ash content, and viscosity density center [8].

Biodiesel and petroleum diesel fuel have equivalent physiochemical properties. The most coveted differentiating characteristic of biodiesel fuel is its viscosity since it significantly affects how fuel injection equipment functions, especially at lower temperatures. The fuel's fluidity is reduced when viscosity increment. Otherwise, the higher viscosity of the fuel spray results in poor atomization. The accuracy of the operation is directly impacted by this. However, because biodiesel naturally has a lower viscosity, it has made it simpler to pump, automate, and generate finer droplets [9]. The atomizer of fuel in the ignition chamber, the stickiness of fuel, and the lubricating properties of engines are all hampered by higher viscosity values. The

range of the international standard specification should therefore be maintained for biodiesel values [10].

The methyl or ethyl esters are linked to triglycerides through the transesterification process and have a molecular weight that is roughly eight times smaller than that of vegetable oil [11]. Viscosity fuels made from animal fats, such as those derived from land animals, display the same bias at temperatures greater than those of ordinary diesel and necessitate significant engine modification. Because vegetable oil burns uncleanly in a diesel engine, unwanted substances like acrolein and organic acid are formed. Burning of vegetable oil is the primary cause of the detrimental impacts on the longitudinal engine's performance. Fuel for diesel engine applications can be made without significant alterations if the fatty acid methyl esters are made from vegetable oil using the transesterification process [12].

Storage is very interested in the position of the feature of biodiesel throughout the process of oxidization and the chemical action of biodiesel provided at the phase of combustion. These issues cause the acid version of this environmentally favorable fuel to transform into sediments and gum that will not dissolve, which can block carbon filters. However, oxidation and polymerization happen because unsoaked fatty acid chains are nearby and the parent molecule has strong double bond properties, which rapidly react with oxygen as soon as it is exposed to air [13].

Many methods are used to oxidize the chain of fatty acids, which is a difficult process, according to Jain and Sharma (2010b). Numerous elements, such as light, temperature, unrelated substances, peroxides, and the size of the surface area between the biodiesel and air, contribute to the oxidation growth of the biodiesel. The greatest ways to boost the oxidative firmness of biodiesel, according to the authors, include consciously increasing antioxidants and changing the fatty ester strikingness [1].

3 Fuel Tank Material

Diesel fuels should not be utilized with zinc, either as plating or as a significant alloying component. In the presence of sulfur, zinc is unstable, especially if the fuel contains moisture. The internal engine parts are severely harmed by the sludge created by chemical reactions. Steel's resistance to corrosion in fuel tanks for automobiles has been questioned by automakers. Some additives that may be used in the manufacturing of biodiesel may hasten the development of corrosion. Figure 1 is an example of a common gasoline tank leak brought on by corrosion. Two bench-scale simulative tests were utilized to evaluate the resistance to external corrosion: the neutral salt spray test (ASTM B117) with exposures up to 2000 h and the cyclic corrosion test (SAE J2334) with exposures up to 120 and 160 cycles. The latter exposures were chosen to represent a 15- and 20-year road life, respectively. The failure criterion of perforation was adopted. To examine the quantitative development of corrosion, pit depths were measured over the coating integrity, the entire specimen was determined by chip ratings, and creep back at the scribe line was determined after gravel contact.



Fig. 1 Prototypical seepage of an automobile fuel tank

An aggressive gasoline was built in deep drawn cups with flat tops to test the internal corrosion resistance (CE10A). (Automakers' recommendations to SASFT and their prior expertise led to the selection of this fuel.) Clamping rings and an inert gasket sealed the fuel-cup assembly. To replenish contaminated ions, prevent oxygen loss, and imitate repeated fuel tank filling, the fuel was changed every four weeks. By documenting the breadth and location of rust, as well as quantitatively by weight changes and pit depths, the extent of corrosion was assessed.

4 Problem Identification

4.1 Corrosion: Is the Deterioration of a Metal as a Result of Slow Oxidation

With the abnormality of gold, all metal elements are found as compounds rather than on their own. This is because most metals as oxidized by their automotive environment.

Metals like zinc, copper, and aluminum form a protective coating when they oxidized Copper forms a green tough protective layer. Iron on the other hand forms rust is porous and flakes off of the iron exposing a new layer of iron, which causes further rusting. In a galvanic cell, where the anode and cathode are located at various locations on the same metal surface, the metal is corroding. Electrons can shine from the anode to the cathode because metal is a conducting substance. The anode is located where there are more impurities in the metal. The presence of moisture and oxygen causes the electrons to be released (Fig. 2).



Fig. 2 Degradation of a metal–automobile fuel tank

4.2 Causes of Fuel Tank Rust

Water is a necessary reactant for corrosion to take place. The electrolyte in road salt raises the water's conductivity. The salt also aids in charge neutralization, creating an environment very similar to that of the salt bridge. As a result of losing electrons to the less reactive metal, the more reactive metal oxidizes. Bending shaping or cutting metals can stress the metal. This would then become a corrosion site.

Hydrocarbon impermeability makes it the ideal material for PZEV applications. In terms of cost, comparable to those of the co-extruded blow-molded plastic fuel tanks that are now in use. Road environments-resistant to corrosion. Suitable for all fuels. Decent design adaptability. Readily producible using tried-and-true, traditional, affordable, and broadly accessible methods. Over a century of performance and safety history. Totally recyclable the annual recycling of steel from autos is close to 15 million tons. Steel gasoline tanks are not indestructible structures. They have to put up with ongoing corrosion brought on by stored products and the external atmosphere, which reduces the construction's thickness and harms its overall integrity. The detrimental effects of foundation geometrical deviation must be recorded by qualified individuals. Correct tank analysis and expert repair reduce the chance of accidents and environmental damage and extend the time they can be used.

5 Experimental Setup

The experimental setup parameters needed for the fuel tank with empty area data were obtained from journals that were cited by fuel tanks with empty systems and have shown promise in helping vehicles meet pollution regulations. The inlet diffuser is among the fuel tank's most crucial components. The distribution flow at the internals' entrance face is significantly impacted by the input diffuser. Maldistribution flow is one of the most significant issues that can arise in the fuel tank. Because of the non-uniform entrance velocity distribution flow caused by large diffuser cone angles, the

turbulent exhaust gas flow from the exhaust pipe into the diffuser tends to detach from the walls and enter the internal channels [1].

As a result, the majority of the exhaust flow is permitted through the center of the internal at a crucially higher velocity than in the perfect form. In a perfect converter, the flow that emerges from the intake diffuser would be consistent throughout, meaning that it would be dispersed evenly throughout all of the internal channels. The geometry of a particular design of an intake diffuser, as seen in drawings and modeled in computer programmers, is what decides how the flow is distributed across the internal frontal area. We begin by performing numerical analyses of models used in experiments. The data collected include:

1. Transformation of data in inches to metrics.
2. Dimensions for a full-flow setup.
3. Reengineering the scaling measure.

5.1 Product Size After Complete Assembly

The parameters and their descriptions are listed below.

The width of the flow channel, the depth of the fuel tank, and other design parameters are all gleaned from the assembled system.

The engine was connected to a swirl current dynamometer in order to conduct experimental tests. The goal of the test bed is to simulate realistic vehicle operating conditions. To generate airflow over a moving vehicle, two axial fans with ducting were used, as shown in Fig. 3 L-4, SI type, 1.3 L engine with multi-point fuel injection (MPFI). The fuel tank was a 3-way fuel tank model, the properties of which are summarized in Table 1. The experiment used Ni–Cr thermocouples with a thickness of 1 mm. Several thermocouples protruded 5 mm from the channels to measure the temperature of the inflow gas. They were found at r coordinates of 0.2R, 0.5R, and 1R along the radial direction. A digital differential pressure transducer with a diaphragm sensor calibrated between 0 and 50 mbar was used. The velocity of the exhaust gas was measured using a vane. The Eddy current dynamometer was used to measure torque and engine speed. Conversion efficiency was calculated by measuring the number of pollutants absorbed before and after the fuel tank using an AVL model 4000 gas analyzer at varying loads and speeds. Thermocouples, a differential pressure transducer, and a gas analyzer are shown in a simplified configuration in Fig. 3.

It is a methodical approach to determining the best possible outcomes from a set of possible values. It has played an important role in accelerating technological progress in all fields in recent years. At each level of the selection process, this method improves the method of selecting parameters. It helps the auto industry make better use of the wide variety of materials and geometrical structures at their disposal.

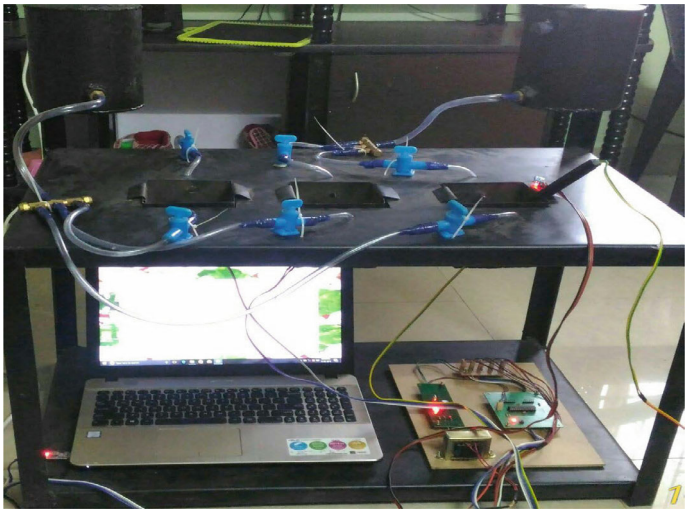


Fig. 3 Fuel tank original design schematic—test station

Table 1 Fuel tank design specifications

Description	Details	Units
Wash coat	45	gr/m^2
Precious metals	Mild steel	–
Channel density	200–400	channel/cm^2
Surface area	2.41	m^2
Length	900	Mm
Diameter	265	Mm

5.2 Biofuel Material Enhancement

The primary focus is on using the material's performance characteristics to determine which one is the greatest fit for a given task. In order to get the results, you want from your project, material choice is of the utmost importance. To attain these lower emission values, laminating materials are utilized to absorb carbon particles within the fuel tank (Fig. 4).

An alternative to the traditional light microscope is the scanning electron microscope (SEM). Compared to a light microscope, a scanning electron microscope (SEM) offers many benefits. Because of the SEM's deep depth of field, a sizable section of the sample can be in sharp focus at the same time. The SEM's high-resolution pictures also facilitate the detailed inspection of small, closely-spaced structures. The preparation of samples for most SEMs is straightforward because only conductive samples are required. Given its increased magnification, better depth of focus, higher resolution, and simplicity of sample observation, the SEM has become

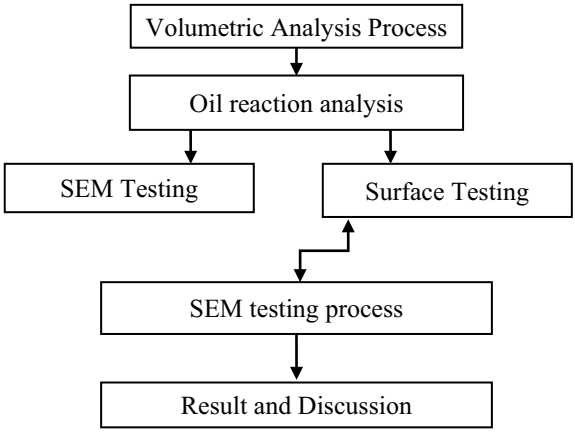


Fig. 4 Experimental flow

one of the most extensively utilized devices in modern research. An energy dispersive X-ray analysis (EDX) equipment can be added to a scanning electron microscope (SEM) in order to do compositional analysis on samples. The energy dispersive X-ray spectroscopy (EDX) method can be used to determine the composition of a specimen's surface and to make relative concentration estimates of any pollutants present.

6 Results and Discussion

6.1 Experimentation Analysis

Exhaust The speed of the air was measured by the velocity of the air. We were able to gauge both engine speed and torque with the help of the eddy current sensor. Before and after the fuel tank, an STI model 2000 biofuel analyzer measured high concentrations to evaluate conversion performance over a range of engine loads and speeds.

As shown in Table 2 and Fig. 5, a schematic installation of thermocouples and a differential pressure transducer was used to measure corrosion (Figs. 6, 7, 8 and 9).

6.2 Scanning Electron Microscopy (SEM)—Biofuel-Pungamia B50

Figures show that a fine film is visible, which reduces corrosion of the material, implying that the lubricating property of the material is increased. The MoS2 is

Table 2 Experimentation analysis

Solution ID#	Mass change at 1 month (g)	Mass change at 2 months (g)	Mass change at 3 months (g)
STI-1	− 0.1023 ± 0.0921	− 0.0279 ± 0.00495	− 0.0353 ± 0.0077
STI-2	0.0049 ± 0.0031	− 0.0061 ± 0.017	0.0091 ± 0.0007
STI-3	− 0.0144 ± 0.0697	0.0131 ± 0.0099	0.0138 ± 0.0117
STI-4	0.0067 ± 0.0449	− 0.0480 ± 0.0840	− 0.0079 ± 0.0241
STI-5	− 0.0231 ± 0.0309	− 0.00175 ± 0.0008	− 0.0005 ± 0.0008
STI-6	0.0069 ± 0.0051	− 0.0126 ± 0.0556	− 0.0455 ± 0.0612
STI-7	0.0013 ± 0.0047	0.0063 ± 0.0090	0.0054 ± 0.0094
STI-8	− 0.0193 ± 0.0157	0.3100 ± 0.4397	− 0.0171 ± 0.0291
STI-9	− 0.0073 ± 0.0027	0.0578 ± 0.0869	− 0.0004 ± 0.0027
STI-10	− 0.0405 ± 0.0479	− 0.0429 ± 0.0532	− 0.0392 ± 0.0571
STI-11	0.4078 ± 0.5791	0.0060 ± 0.0035	0.0090 ± 0.0008
STI-12	$-0.0049 \pm 6.93X10^{-5}$	0.0038 ± 0.0043	0.0059 ± 0.0025
STI-13	− 0.0029 ± 0.0031	− 0.0361 ± 0.0059	− 0.0337 ± 0.0017
STI-14	− 0.0018 ± 0.0065	0.0025 ± 0.0019	0.0049 ± 0.0021
STI-15	− 0.3221 ± 0.4889	0.0029 ± 0.0045	0.0019 ± 0.0011
STI-16	− 0.0068 ± 0.0121	− 0.0267 ± 0.0340	− 0.0218 ± 0.0332

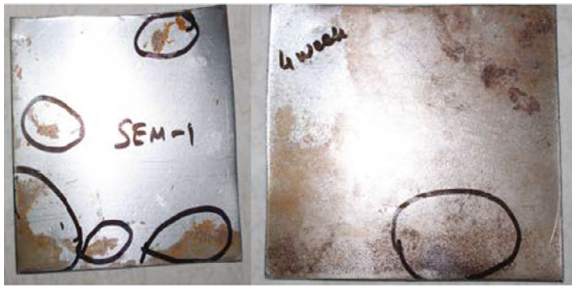


Fig. 5 Experimentation analysis visual effects

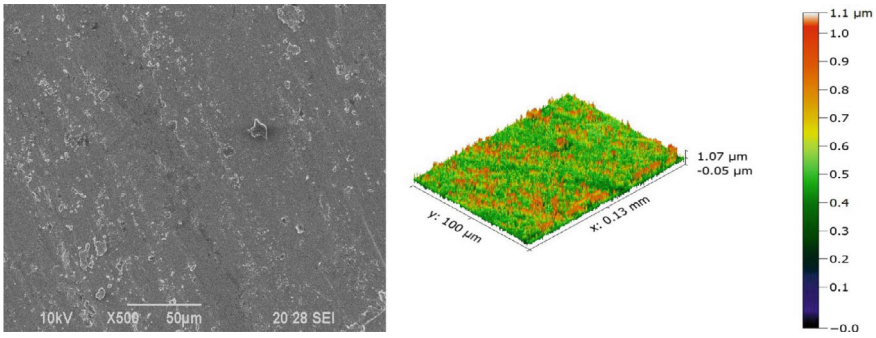


Fig. 6 SEM images of brass alloy 50 µm × 500

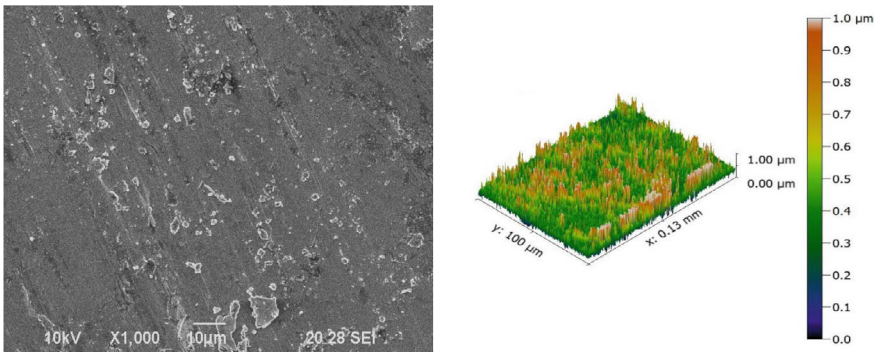


Fig. 7 SEM images of brass alloy 10 µm × 1000

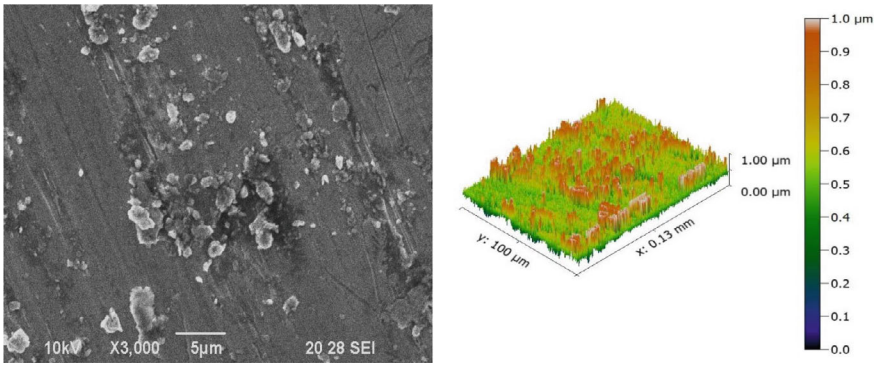


Fig. 8 SEM images of brass material 5 µm × 3000

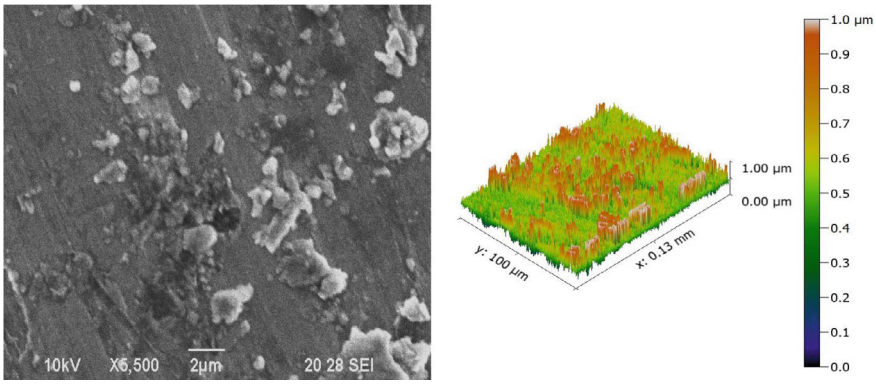


Fig. 9 SEM images of brass material 2 µm × 5500

represented by the black portions. Furthermore, the SEM image demonstrates the uniformity of the distribution.

The image depicts the unevenness of the specimen, as evidenced by the white patches visible here and there. The hard particles in the SEM create voids, which are visible in the image.

7 Conclusion

The fuel tank internal corrosion was studied for B50 pugamia blended biodiesel in mild steel. The mechanical properties such as hardness and tensile strength were tested on the mild steel material. They are also tested for adhesive wear with a plate and various corrosion-resistance apparatuses. SEM and numerical analysis were used to characterize the developed Mild steel material with corrosion without corrosion resistance. When compared to base mild steel material bonding, reinforcement improves mild steel material hardness by 15%. The results of the SEM images confirm the presence of reinforcement and uniform distribution. Finally, we compare the numerical results of using bonded material causes in better performance analysis in aluminum at room temperature, perfectly bonded under varying loads, with those of using the same amount of old cause material in an aluminum alloy but without a coating in the process of spontaneous heat transfer.

References

1. Mishra BK, Kumar R (2012) The production of biodegradable fuel from nonedible oilseed in India: a review. IOSR J Appl Chem (IOSRJAC) ISSN: 2278-5736 1(1), pp 43–46
2. Rashid U, Anwar F (2010) Amer Jamil and Haq Nawaz Bhatti Jatropha Curcas seed oil as a viable source for biodiesel Pak. J Bot 42(1):575–582
3. Jain S, Sharma MP (2011) Study of oxidation stability of Jatropha curcas biodiesel/diesel blends 2(3):533–542
4. Berchmans HJ, Hirata S (2008) Biodiesel production from crude Jatropha curcas L. seed oil with a high content of free fatty acids. Bioresour Technol 99:1716–1721
5. Akbar E, Yaakob Z, Kamarudin SK, Ismail M, Salimon J (2009) Characteristic and composition of Jatropha Curcas Oil Seed from Malaysia and its potential as biodiesel feedstock. Feedstock, Eur J Sci Res 29(3):396–403, ISSN 1450-216X
6. Mazumdar P, Borugadda VB, Goud VV, Sahoo L (2013) Effect of storage parameters on stability of Jatropha-derived biodiesel Mazumdar et al. Int J Energy Environ Eng 4:13
7. Nandi S, Performance of C.I Engine by Using Biodiesel-Mahua Oil. Am J Eng Res (AJER) e-ISSN: 2320-0847 p-ISSN: 2320-0936 02(10):22–47
8. Ramning Amol M, Dhote Priya S, Ganvir VN (2013) Production of Neem Oil Methyl Ester (NOME) from Oscillatory Baffled Reactor Res J Recent Sci 2(ISC-2012):223–228
9. Awolu OO, Layokun SK (2013) Optimization of two-step transesterification production of biodiesel from neem (Azadirachta indica) oil Awolu and Layokun. Int J Energy Environ Eng 4:39

10. Muthu H, SathyaSelvabala V, Varathachary TK, Kirupha Selvaraj D, Nandagopal J, Subramanian S (2010) Synthesis of biodiesel from neem oil using sulfated zirconia via Tranesterification 27(04):601–608, ISSN 0104-6632
11. Heroor SH, Rahul Bharadwaj SD (2013) Production of bio-fuel from crude neem oil and its performance. Int J Environ Eng Manag 4(5):425–432, ISSN 2231-1319
12. Anbumani K, Singh AP (2010) Performance of mustard and neem oil blends with diesel fuel in C.I. engine. ARPN J Eng Appl Sci 5(4), ISSN 1819-6608
13. Bobade SN, Khyade VB (2012) Detail study on the Properties of Pongamia Pinnata (Karanja) for the production of biofuel. Res J Chem Sci 2(7):16–20

Dynamic Instability of a Sandwich Revolving Beam Non-uniform Along Width and Depth Under Pulsating Load



Nabakishor Dang, Madhusmita Pradhan, Madhumita Mohanty, Prasanta Kumar Pradhan, and Pusparaj Dash

Abstract The parametric instability of a revolving sandwich beam with an axially pulsing load operating at a position along the cross-sectional centroid has been studied in this study. For the system, the consequence of transverse shear stress is neglected for the calculation of strain energy. All the energy expressions that are for bending deformation, axial deformation and kinetic energy in addition to strain energy due to transverse shear stress have been neglected. The system's differential equations and conditions for extremes are then determined using Hamilton's principle and then these are non-dimensionalised. Series solutions for each co-ordinate of the system are chosen from previous study, which satisfy the differential equations and boundary conditions. Finally, by using Galerkin's energy principle, the matrix expressions for mass, stiffness, etc. are obtained for the system. From these matrices, the eigen values are utilised to find out the parametric instability of the system by means of Saito and Otomi conditions. The results are expressed by number of graphs for different system parameters.

Keywords Asymmetric sandwich beam · Axial pulsating load · Dynamic stability · Shear parameter · Taper parameter

1 Introduction

In order to reduce noise and vibration, sandwich beams are often used in the automotive, aerospace, and marine industries. The strength to weight ratio of Timoshenko sandwich beams is higher than that of solid straight beams. In order to reduce noise and vibration, it is necessary to look at the needs in numerous industries and extensive study has been done on sandwich beams. It was shown by Hansen et al. [1] that

N. Dang · M. Pradhan (✉) · P. K. Pradhan · P. Dash
Department of Mechanical Engineering, VSSUT, Burla, Sambalpur 768018, India
e-mail: madhusmitapradhan_me@vssut.ac.in

M. Mohanty
School of Mechanical Engineering, KIIT DU, Bhubaneswar 751019, India

© The Author(s), under exclusive license to Springer Nature Singapore Pte Ltd. 2025

B. B. V. L. Deepak et al. (eds.), *Recent Advancements in Product Design and Manufacturing Systems*, Lecture Notes in Mechanical Engineering,
https://doi.org/10.1007/978-981-97-6732-8_33

the sandwich beams with outer elastic layers and middle visco-elastic layer show greater dynamic stability. The vibrations of pre-twisted blading were subjected to a matrix displacement analysis by Dokumaci et al. [2]. The theoretical as well as experimental analysis of lateral and torsional vibration of pre-twisted blades was carried out by Carnegie [3]. Further, he obtained the vibrational frequency and for the first five modes results and verified the results experimentally. Again, the same author [4] analysed a straight cantilever beam of symmetric configuration under centrifugal force. Following the derivation of the production of work done by the centrifugal force, the free vibrational frequencies and mode shapes were identified. Rao and Carnegie [5] examined the vibration of a cantilever beam that was mounted on the disc and rotated and found that there exists a component of Coriolis acceleration which was the major factor for the nonlinearity of the partial differential equations. They observed that when angular velocity of rotation increases, the nonlinearity in response increases. The method of finite element and the fifth-degree polynomial for the displacement function was used to analyse the vibration of the radial beam fitted on a disc by Putter and Manor [6]; Putter and Manor analysed the presence of tip mass of their work, that is the presence of shroud in turbine blades. For different boundary conditions, Bauer and Eidel [7] examined the Euler beam revolving about an axis perpendicular to its length axis. He studied the effect of angular velocity of rotation, spin rate of beam and aspect ratio for the beam stability. He found that the angular velocity of rotation increases the natural frequencies for some boundary conditions and decreases for others. There was stiffening and softening effect when increased and decreased ratio of hub radius and length. The dynamic Timoshenko beam under periodic force was investigated by Sabuncu and Evran [8]. The researchers concluded that as the distance between the centroid and the centre of flexure rises, the coupled bending dominant frequency grows. Kerwin [9] created the sandwich beam, which consists of two elastic layers on top and bottom and one visco-elastic layer in the middle. The authors also said that the loss of energy in the core of visco-elastic material is only because of shear. Many researches took under consideration the axial displacements of the upper and lower layers, and there was no error discovered in doing so, particularly for the lower frequencies. Ray and Kar [10] explored the instability of the beams under innumerable boundary conditions under parametric vibration in the dynamic instability of revolving sandwich beams using MRE as the core material was done by Nayak et al. [11]. When a strong magnetic field is present, MRE stabilises the system. The spinning pre-twisted sandwich beam was examined by Lin and Chen [12] utilising the harmonic balancing method and FEM. It was discovered that if pre-twist is present but absent, increasing spinning could destabilise a beam and stabilise a beam. The stability of a non-uniform uneven sandwich beam on a Pasternak base in a thermal grade was investigated by Pradhan et al. [13]. In [14], Chand et al. looked at the dynamic instability of a revolving beam with a parabolic taper under conditions of varying temperature, and they came to the conclusion that the non-uniformity parameters reduce the stability of the system. The parametric response of beams supported by visco-elastic material was examined by Saito and Otomi [15]. Ditaranto and Blasingame [16] found generalised results for composite loss factor and natural frequencies. The forced vibration was

analysed by Mead and Marcus [17] for different boundary conditions by using the solutions provided by Ditaranto and observing different uncoupled complex modes. Banerjee [18] presented the problem-solving approach by dynamic stiffness method for sandwich beam. Nayak et al. [19] investigated a tapered beam of exponential variation, pre-twisted system on a Pasternak foundation supported visco-elastically and a temperature grade. A functionally graded, an examination of pre-twisted thick cantilever beams was conducted by Mohanty et al. [20], into its vibration and dynamic stability. They discovered that a low index damages the system's stability when power levels rise. Pradhan et al. [21] examined the stability of an uneven sandwiched beam on a foundation of Pasternak type with a temperature grade. Kar and Sujata [22] investigated the impact of temperature on a non-uniform under parametric vibration.

After going through literatures, it was found that the effect of spinning is not considered for a revolving sandwich beam non-uniform along width and depth. The above-mentioned parameters are essential for turbine, helicopter blades and other automobile industries which must be analysed. As a result, the stability analysis of rotating sandwich beams that are non-uniform throughout width and depth is the focus of this work.

2 Problem Formulation

Figure 1 shows the isometric view of a three-layer Timoshenko sandwiched beam with pre-twisted angle α, sinusoidal taper, rotating at an angular velocity Ω and a periodic axial load acting at a point p other than centroid of cross section of the beam. The periodic axial load is denoted by $P(t) = P_0 + P_1 \cos \omega t$. In this analysis, a three-layer sandwich beam is constructed using plywood as the visco-elastic middle layer, with structural steel and Cu-Al alloy being considered for the top and bottom sheets, respectively. Using the right adhesive, the layers are joined.

3 List of Symbols

b	Span between axis of rotation and nearer end of the beam
α_b	Non-uniformity parameter width-wise
γ_2	Middle layer shear strain
$2h_i$ $(i = 1, 2, 3)$	Depth of the layers, $i = 1$ for top layer
l	Beam length
lh_{10}	$l \big/ (h_1)_0$
$\overline{m}$	Mass per unit of beam length
$\overline{P_1}$	Anomaly without dimensions for the dynamic loading
$w\,(x, t)$	Deflection of beam in transverse direction
ω	Force function frequency
$\overline{\omega}$	Frequency of non-dimensional forcing

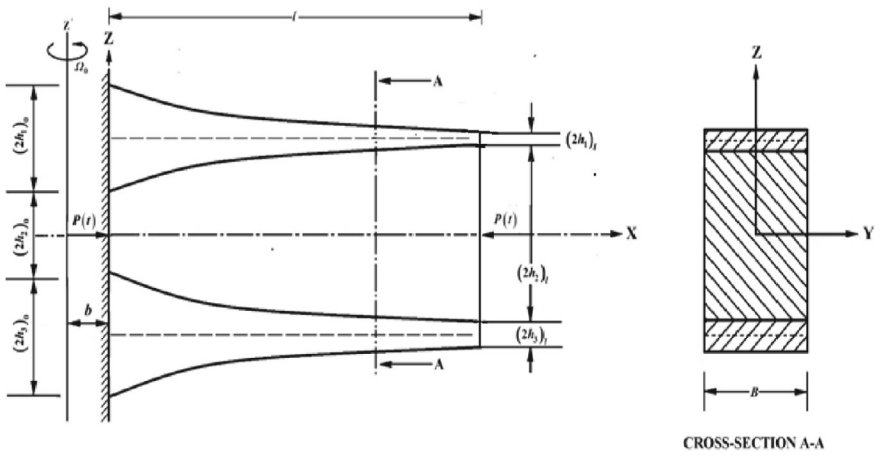


Fig. 1 System configuration

Ω_0 Rotational velocity of the beam about z' axis

3.1 Numerical Modelling

The system's overall work output can be expressed as follows:

$$T = \frac{1}{2}\int_0^l \overline{m} w_t^2, \mathrm{d}x + \frac{1}{2}\Omega_0^2 \int_0^l \left[\overline{m}(b+x)\int_0^x w_x^2\,\mathrm{d}x\right]\mathrm{d}x + \frac{1}{2}\int_0^l \overline{m}\Omega_0^2 w^2 \mathrm{d}x \tag{1}$$

One can express the system's total potential energy as follows:

$$V = \frac{1}{2}\int_0^l E_{1,x}A_{1,x}U_{1,x}^2\mathrm{d}x + \frac{1}{2}\int_0^l E_{3,x}A_{3,x}U_{3,x}^2\mathrm{d}x + \frac{1}{2}\int_0^l \left(E_{1,x}I_{1,x} + E_{3,x}I_{3,x}\right)W_{xx}^2, \mathrm{d}x + \frac{1}{2}G_2^*\int_0^l A_{2,x}\gamma_2^2\mathrm{d}x \tag{2}$$

The total work done of the system can be written by

$$W_p = \frac{1}{2}\int_0^l p(t)w_x^2, \mathrm{d}x \tag{3}$$

Energy principle by Hamilton $\delta \int_{t_1}^{t_2} (T - V - W)\mathrm{d}t = 0$
The differential equations that govern the system are as follows:

$$\begin{aligned}
&\bar{m}\bar{w}_{,\bar{t}\bar{t}} + \left[1 + \frac{\lambda_0^2\left(1 + E_{31}h_{i31}^3\right)}{(lh_{10})^2(1 + E_{31}h_{i31})}\left\{\frac{f}{l^2} - \left(\bar{x} + \bar{b}\right)^2\right\}\right]\bar{W}_{,\bar{x}\bar{x}\bar{x}\bar{x}} \\
&- \frac{2\lambda_0^2\left(1 + E_{31}h_{i31}^3\right)}{(lh_{10})^2(1 + E_{31}h_{i31})}\left(\bar{x} + \bar{b}\right)\bar{W}_{,\bar{x}\bar{x}\bar{x}} \\
&+ \left[-\frac{\lambda_0^2\left(1 + E_{31}h_{i31}^3\right)}{(lh_{10})^2(1 + E_{31}h_{i31})} - \lambda_0^2\left\{\frac{f}{l^2} - \left(\bar{x} + \bar{b}\right)^2\right\}\right. \\
&\left. -3g_{11}^*\left(1 + \frac{h_{i12} + h_{i32}}{2}\right)^2 + \bar{p}(\bar{t})\right]\bar{W}_{,\bar{x}\bar{x}} \\
&+ \lambda_0^2\left(\bar{x} + \bar{b}\right)\bar{W}_{,\bar{x}} + \frac{3}{2}g_{11}^* lh_{i10}h_{i12}\left(1 + \frac{h_{i12} + h_{i32}}{2}\right)(1 + \alpha)\frac{2(h_2)_0}{C}\gamma_{2,\bar{x}} = 0
\end{aligned} \tag{4}$$

$$\begin{aligned}
&\frac{2(h_2)_0}{C}\gamma_{2,\overline{x}\overline{x}} - \frac{g_{11}^*}{4}h_{i12}^2\left(\frac{1 + E_{31}h_{i31}^3}{1 + \alpha^2 E_{31}h_{i31}}\right)(1 + \alpha) \\
&\left[(1 + \alpha)\frac{2(h_2)_0}{C}\gamma_2 - \left(\frac{2\left(1 + \left((h_{i12} + h_{i32})/2\right)\right)}{(lh_{i10}h_{i12})}\right)\overline{W}_{,\bar{x}}\right] = 0
\end{aligned} \tag{5}$$

$$\begin{aligned}
\overline{m} = b_0\left(1 + e^{\alpha_b\bar{x}}\right) &\left(e^{-\alpha_1\bar{x}} + \left(\frac{\rho_2}{\rho_1}\right)\left(\frac{2(h_2)_0 + \left((h_1)_0 - (h_1)_0e^{-\alpha_1\bar{x}}\right) + \left((h_{i31})_0 - (h_{i31})_0e^{-\alpha_3\bar{x}}\right)}{2(h_1)_0}\right)\right. \\
&\left. + \left(\frac{\rho_3}{\rho_1}\right)\left(\frac{(h_3)_0e^{-\alpha_3\bar{x}}}{(h_1)_0}\right)\right)
\end{aligned}$$

The end conditions are as follows:

$$\begin{aligned}
&\left[1 + \frac{\lambda_0^2\left(1 + E_{31}h_{i31}^3\right)}{(lh_{10})^2(1 + E_{31}h_{i31})}\left\{\frac{f}{l^2} - \left(\overline{x} + \overline{b}\right)^2\right\}\right]\overline{w}_{,\overline{x}\overline{x}\overline{x}} \\
&- \frac{2\lambda_0^2\left(1 + E_{31}h_{i31}^3\right)}{(lh_{10})^2(1 + E_{31}h_{i31})}\left(\overline{x} + \overline{b}\right)\overline{w}_{,\overline{x}\overline{x}} = 0
\end{aligned} \tag{6}$$

Or

$$\overline{w}_{,\bar{x}} = 0 \tag{7}$$

$$\left[\frac{\lambda_0^2\left(1 + E_{31}h_{i31}^3\right)}{(lh_{10})^2(1 + E_{31}h_{i31})} - \lambda_0^2\left\{\frac{f}{l^2} - \left(\overline{x} + \overline{b}\right)^2\right\} - 3g^*\left(1 + \frac{h_{i12} + h_{i32}}{2}\right)^2 + \overline{p}_1(\bar{t})\right]$$

$$\overline{w}_{1,\bar{x}} = 0 \tag{8}$$

Or

$$\overline{w}_1 = 0 \tag{9}$$

$$\frac{3}{2} g_{11}^{*} l h_{i10} h_{i12} \left(1 + \frac{h_{i12} + h_{i32}}{2}\right)(1+\alpha)\frac{2(h_2)_0}{C}\gamma_{2,\bar{x}} = 0 \tag{10}$$

Or

$$\gamma_2 = 0 \tag{11}$$

3.2 Solution by Variational Method

The system's solution was estimated through the use of the following set of equations

$$\overline{W}_1(\bar{x}, \bar{t}) = \sum_{i=1}^{i=p} \overline{W}_i(\bar{x}) f_i(\bar{t}) \tag{12}$$

$$\overline{\gamma}_{21}(\bar{x}, \bar{t}) = \sum_{k=p+1}^{k=2p} \gamma_{21k}(\bar{x}) \tag{13}$$

Hence generalised coordinates are f_i and f_k.

As a result, different boundary conditions are given along with the appropriate approximation functions in [10].

After non-dimensionalising, the extended Galerkin principle is applied to the energy equations for finding the following matrix equation:

$$[M_1]\{\ddot{Q}_{11}\} + [K_{111}]\{Q_{11}\} + [K_{121}]\{Q_{21}\} = \{0\} \tag{14}$$

$$[K_{211}]\{Q_{11}\} + [K_{221}]\{Q_{21}\} = \{0\} \tag{15}$$

$$M_{ij} = \int_0^1 \overline{m} w_i w_j \mathrm{d}\bar{x} \tag{16}$$

$$K_{11ij} = \int_0^1 \left[1 + \lambda_{11}\left\{\frac{f}{l^2} - \left(\bar{x} + \bar{b}_1\right)^2\right\}\right] w_{1i}'' w_{1j}'' \, \mathrm{d}\bar{x}$$

$$+\lambda_{10}^2\int_0^1\left\{\frac{f}{l^2}-\left(\bar{x}+\bar{b}_1\right)^2\right\}w'_{1i}w'_{1j}\,\mathrm{d}\bar{x}$$

$$+\left\{3g_{11}^*\left(1+\frac{h_{i12}+h_{i32}}{2}\right)^2-\bar{p}(\bar{t})\right\}\int_0^1 w_{1i}{}'w'_{1j}\,\mathrm{d}\bar{x} \tag{17}$$

$$K_{12jl}=-\left(\frac{3}{2}\right)g_{11}^*lh_{i10}h_{i12}(1+\alpha)\left(1+\frac{h_{i12}+h_{i32}}{2}\right)\left(\int_0^1 u_{1l}w'_{1i}d\bar{x}\right) \tag{18}$$

$$K_{22kl}=3\times(lh_{i10})^2\frac{\left(1+\alpha^2E_{31}h_{i31}\right)}{\left(1+E_{31}h_{i31}^3\right)}\left(\int_0^1 u_{1k}{}'u'_{1l}\,\mathrm{d}\bar{x}\right)$$

$$+\frac{3}{4}g_{11}^*(lh_{i10})^2h_{i12}^2(1+\alpha)^2\left(\int_0^1 u_{1k}u_{1l}\mathrm{d}\bar{x}\right) \tag{19}$$

$$[K_{21}]=[K_{12}]^{\mathrm{T}} \tag{20}$$

Equations (14) and (15) are further simplified to

$$[M_1]\left\{\ddot{Q}_{11}\right\}+\left[[K]-\overline{P}_0[H_{11}]\right]\{Q_{11}\}-\overline{P}_1\cos\left(\overline{\omega}\bar{t}\right)[H_{11}]\{Q_{11}\}=\{0\} \tag{21}$$

3.3 Parametric Instability

Referring [15], from above the following equations can be derived

$$\ddot{u}_{N1}+\omega_{N1}^{*2}U_{N1}+2\varepsilon\cos\overline{\omega}\bar{t}\sum_{M_1=1}^{M_1=p}b_{1NM}u_M=0\quad\text{where}\,N_1=1,2,3\ldots P$$

where b_{NM} are the matrix's components $[B_{11}]$, ω_N^* are the system's distinct eigen values $\varepsilon=\frac{\overline{P}_1}{2}<1$ and $[B_{11}]=-[L_1]^{-1}[M_1]^{-1}[H_{11}][L_1]$, where L denotes the modal matrix $[M_1]^{-1}\left[[k]-\overline{P}_0[H_{11}]\right]$

So $\{Q_{11}\}=[L_1]\{u\}$, where is a $\{u\}$ new set of system's generalised coordinates. As a result, the following usages are $\omega_{N1}^*=\omega_{N1,R}+j\omega_{N1,I}$ and $b_{N1M1}=b_{N1M1,R}+jb_{N1M1,I}$ where $\mu=1,2,3.....N1$.

Saito and Otomi [16], utilising all of the previously described conditions, determine the boundaries of the zone where the primary and combination resonances are unstable.

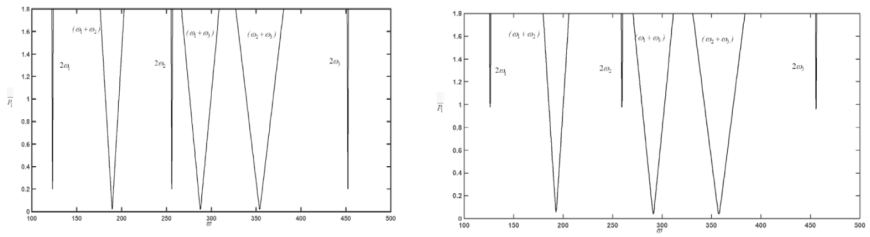
4 Result and Discussion

The study of dynamic stability of system for clamped-free boundary conditions is depicted below.

Figure 2 represents the impact of the shear parameter g_{11} on the parametric instability zone. When comparing the figures, it can be found that increasing (g_{11}) improves the system's dynamic stability by relocating the instability zone to a higher value of (ω). Along with simple resonance, combination resonance was seen in this situation $(\omega_1 + \omega_2)$, $(\omega_1 + \omega_3)$, $(\omega_2 + \omega_3)$ parametric instability zones are reducing.

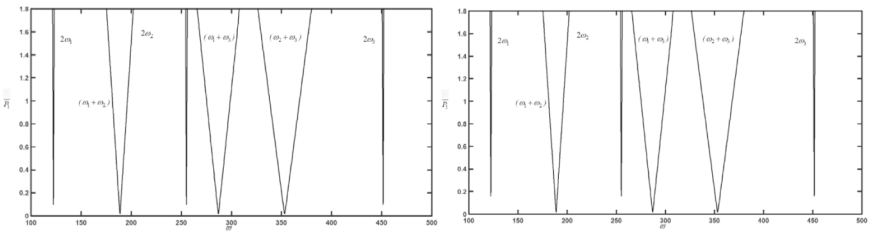
Figure 3 represents the effect of the core loss parameter (η) on the parametric instability zone. When evaluating the figures, it can be discovered that increasing (η) improves the system's dynamic stability by relocating the instability zone to a higher value of ω.

Figure 4 represents the impact of the taper parameter on the parametric instability zone. When comparing the figures, it can be found that increasing improves the system's dynamic stability by relocating the instability zone to a higher value of frequency. The similar results are obtained for taper parameter α_1 but due to space limitation, the graph is not presented here.



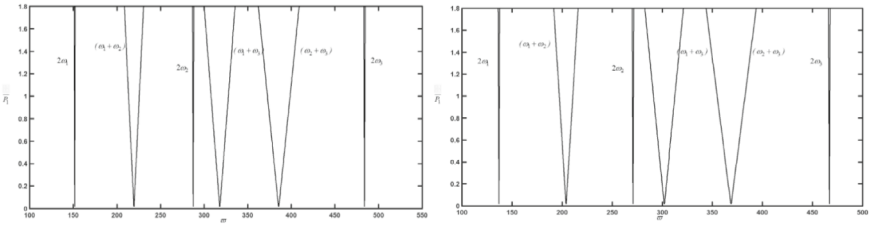
(a). Responses of zones of instabilities for g_{11} =0.1 **(b).** Responses of zones of instabilities g_{11}=0.5

Fig. 2 **a** Responses of zones of instabilities for $g_{11} = 0.1$. **b** Responses of zones of instabilities $g_{11} = 0.5$



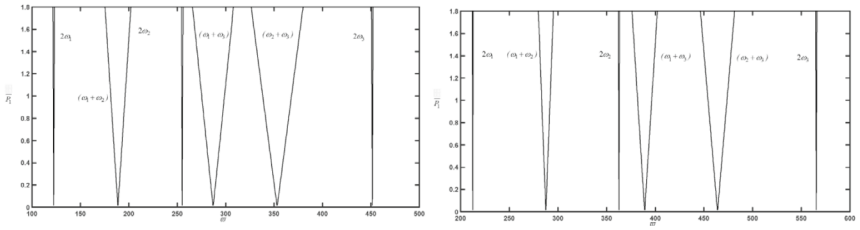
(a). Responses of zones of instabilities for η=0.5 **(b).** Responses of zones of instabilities for η=0.8

Fig. 3 **a** Responses of zones of instabilities for $\eta = 0.5$. **b** Responses of zones of instabilities for $\eta = 0.8$



(a). Responses of zones of instabilities for $\alpha_3 = 0.1$ **(b).** Responses of zones of instabilities for $\alpha_3 = 0.5$

Fig. 4 **a** Responses of zones of instabilities for $\alpha_3 = 0.1$. **b** Responses of zones of instabilities for $\alpha_3 = 0.5$



(a). Responses of zones of instabilities $\Omega = 10$ **(b).** Responses of zones of instabilities for $\Omega = 15$

Fig. 5 **a** Responses of zones of instabilities $\Omega = 10$. **b** Responses of zones of instabilities for $\Omega = 15$

The impact of rotational speed (Ω) on the zone of parametric instability is shown in Fig. 5. When comparing figures, it can be found that increasing (Ω) improves the system's dynamic stability by relocating the instability zone to a higher value of ω.

5 Conclusion

The analysis of the dynamic stability of rotating pre-twisted Timoshenko sandwich beams with periodic axial loads operating at points other than the cross-sectional centroid has been done in this work. Studies of the stabilities are based on a number of different parameters, including pre-twisted angle, angular rotational velocity, modulus ratio, core loss factor, offset distance, width to length ratio, taper parameters and temperature gradient parameters.

From dynamic stability analysis, it is concluded that for our system dynamic stability increases with increase in angular velocity of rotation, pre-twisted angle. For increasing pre-twist angle, the stability increases with a very slow rate. However, it is discovered that the stability increases dramatically for the breadth to length ratio. The system's stability is very marginally enhanced by the modulus ratio and core loss factor. The system becomes more stable as the taper parameters are increased

and becomes more unstable as the temperature gradient parameters are increased. For the studied values, the system's stability deteriorates offset for distances in the y, z directions.

References

1. Hansen MOL, Sørensen JN, Voutsinas S, Sørensen N, Madsen HA (2006) State of the art in wind turbine aerodynamics and aeroelasticity. Prog Aerosp Sci 42(4):285–330
2. Dokumaci E, Thomas J, Carnegie W (1967) Matrix displacement analysis of coupled bending-bending vibrations of pretwisted blading. J Mech Eng Sci 9(4):247–254
3. Carnegie W (1959) Vibrations of rotating cantilever blading: theoretical approaches to the frequency problem based on energy methods. J Mech Eng Sci 1(3):235–240
4. Carnegie W, Dawson B (1969) Vibration characteristics of straight blades of asymmetrical aero foil cross-section. Aeronaut Quart 20(2):178–190
5. Rao JS, Carnegie W (1970) Non-linear vibrations of rotating cantilever beams. Aeronaut J 74(710):161–165
6. Putter S, Manor H (1978) Natural frequencies of radial rotating beams. J Sound Vib 56(2):175–185
7. Bauer HF, Eidel W (1988) Vibration of a rotating uniform beam, part II: orientation perpendicular to the axis of rotation. J Sound Vib 122(2):357–375
8. Sabuncu M, Evran K (2005) Dynamic stability of a rotating asymmetric cross-section Timoshenko beam subjected to an axial periodic force. Finite Elem Anal Des 41(11–12):1011–1026
9. Kerwin EM Jr (1959) Damping of flexural waves by a constrained viscoelastic layer. J Acoust Soc Am 31(7):952–962
10. Ray K, Kar RC (1995) Parametric instability of a sandwich beam under various boundary conditions. Comput Struct 55(5):857–870
11. Nayak B, Dwivedy SK, Murthy KSRK (2013) Vibration analysis of a three-layer magnetorheological elastomer embedded sandwich beam with conductive skins using finite element method. Proc Inst Mech Eng C J Mech Eng Sci 227(4):714–729
12. Lin CY, Chen LW (2005) Dynamic stability of spinning pre-twisted sandwich beams with a constrained damping layer subjected to periodic axial loads. Compos Struct 70(3):275–286
13. Pradhan M, Dash PR (2016) Stability of an asymmetric tapered sandwich beam resting on a variable Pasternak foundation subjected to a pulsating axial load with thermal gradient. Compos Struct 140:816–834
14. Chand RR, Behera PK, Pradhan M, Dash PR (2019) Parametric stability analysis of a parabolic-tapered rotating beam under variable temperature grade. J Vibr Eng Technol 7(1):23–31
15. Saito H, Otomi K (1979) Parametric response of visco elastically supported beams. J Sound Vib 63(2):169–178
16. DiTaranto RA, Blasingame W (1967) Composite damping of vibrating sandwich beams 633–638
17. Mead DJ, Markus S (1969) The forced vibration of a three-layer, damped sandwich beam with arbitrary boundary conditions. J Sound Vib 10(2):163–175
18. Banerjee JR (2003) Free vibration of sandwich beams using the dynamic stiffness method. Comput Struct 81(18–19):1915–1922
19. Nayak DK, Dubey A, Nayak CR, Dash PR (2020) Stability analysis of an exponentially tapered, pre-twisted asymmetric sandwich beam on a variable Pasternak foundation with viscoelastic supports under temperature gradient. J Braz Soc Mech Sci Eng 42(3):1–19
20. Mohanty SC, Dash RR, Rout T (2015) Vibration and dynamic stability of pre-twisted thick cantilever beam made of functionally graded material. Int J Struct Stab Dyn 15(04):1450058

21. Pradhan M, Dash PR, Pradhan PK (2016) Static and dynamic stability analysis of an asymmetric sandwich beam resting on a variable Pasternak foundation subjected to thermal gradient. Meccanica 51(3):725–739
22. Kar RC, Sujata T (1988) Parametric instability of a non-uniform beam with thermal gradient resting on a Pasternak foundation. Comput Struct 29(4):591–599

Application of AI/ML

Low Birth Weight Prediction Using Machine Learning

G. Harika, T. Venkata Lakshmi, P. Santhosh Prudhvi Raj, U. D. Prasan, and M. Jayanthi Rao

Abstract In recent decades, machine learning has its increased problem solving methodologies and applications in various fields of business, marketing, education and medical diagnostics. Among all the ML techniques, some have been employed in the fields of medical sciences to predict various health conditions which require complete analysis of the patient's health by considering some parameters which impact the health condition of an individual. Low birth weight of infants has been a constant recurring problem which has its visible impacts only after the birth of the baby. It acts as an indicator of sickness in newborn baby's weight. This can be avoided using suitable ML techniques which predict required values from the information passed to the trained model. The prediction algorithm is implemented using random forest regression algorithms. We are aiming to develop a website which considers the health indicators as inputs from the user and provides them with estimated value by the trained ML model. The measures of metrics used here are the number of gestational days, age of mother, height, weight, plurality, and smoking status of the mother. All of these parameters can be used to estimate the accurate value of the weight of the baby within the web application.

Keywords Machine learning · Python · LBW prediction · HTML · CSS

1 Introduction

Babies born with a birth weight under 2500 grams are often categorized as having a low birth weight. It's important to note that while a low birth weight doesn't necessarily mean the baby is unhealthy, it can increase the risk of various health issues. Premature birth (born before 37 weeks of pregnancy) and fetal growth restrictions are two primary causes of low birth weight. While some of these babies may be

G. Harika · T. Venkata Lakshmi · P. Santhosh Prudhvi Raj · U. D. Prasan · M. Jayanthi Rao (✉)
Department of Computer Science & Engineering, Aditya Institute of Technology and Management, Tekkali 532201, India
e-mail: jayanth.mtech@gmail.com

© The Author(s), under exclusive license to Springer Nature Singapore Pte Ltd. 2025

B. B. V. L. Deepak et al. (eds.), *Recent Advancements in Product Design and Manufacturing Systems*, Lecture Notes in Mechanical Engineering,
https://doi.org/10.1007/978-981-97-6732-8_34

perfectly healthy, others might require medical attention and care to address potential health challenges associated with their lower birth weight. Early diagnosis and appropriate medical support are essential in such cases to ensure the well-being of these newborns. Risk during delivery arises when the growth of the baby is slow, and if there is any abnormality in its health condition, a baby born with low weight has high mortality rate within one year and is vulnerable to chronic diseases as the body cannot be developed to function fully. Some diseases like infections, breathing problems such as respiratory disease of prematurity caused by immature lungs, etc. will show an immediate impact on baby's health [1]. Some developmental /behavioral problems may be visible along the growing years or in adulthood which can't be corrected at later stages and have a huge impact on the life of an individual. There is no direct method to predict the birth weight of a baby before the delivery. It can be only predicted by doctor's experience and people from remote areas will not be able to always visit professional healthcare specialists [2].

Normal birth weight baby =2.5kg

Low birth weight baby <2.5kg–2.0kg

Very low birth weight baby <1.5kg

Extreme low birth weight baby <1.0kg.

ML algorithms can be deployed for the prediction of low birth weight before the delivery of the baby. Regression problem (predicted weight) focuses on the accurate prediction of the weight [2]. The algorithms such as random forest regressor and linear regression have accurate values of the birth weight which are close to the previous data collected in the datasets. The classification (low weight/normal weight/very low weight) happens by calculating whether the predicted value is in range of normal weight ($w > 2500$ grams), low weight ($w > 1500$ grams and $w < 2500$ grams) and very low birth weight ($w < 1000$ grams). All of these can be implemented using the trained machine learning algorithm which is designed using Visual Code Studio and which includes Flask Framework for module implementation [2].

2 Literature Survey

Study

Babies with extremely low birth weights (ELBW) often exhibit characteristics that set them apart from babies with normal birth weights. Risk factors for low birth weight in Nigeria: evidence from 2013 Nigeria demographic and health survey [1, 3]. They are significantly smaller in size, and in cases of ELBW, their head may appear disproportionately larger compared to their body. ELBW babies typically have very low body fat percentages, which can make them look thin and fragile. Diagnosing this condition is common in infants with such distinctive physical traits, and it is crucial to provide specialized medical care to address their unique needs and challenges due to their extremely low birth weight. Using machine learning algorithms, infant birth weight estimation and low birth weight classification are carried out in the United

Arab Emirates [2]. It reduces unwanted frequent visits to health care to monitor the weight of the baby. It helps in maintaining a graph of change in the predicted weight over time. It helps in upgrading to necessary diet changes if the weight is low. It indicates the need of checkups if the observed birth weight is less than the normal weight.

It helps in assessing the condition and analyzing the health conditions related to it. It saves the time for arrangement of the required equipment which can help at the time of the birth of the baby. In our system, we build a web application with all these features. Low birth weight prediction is an interface designed to predict the possible birth weight of the baby before the actual delivery of the baby happens. It can help the family to previously anticipate the birth weight and check whether the baby's health is at risk or not. It also helps in intimating them with certain actions if the birth weight falls in the abnormal range. Every mother has similar attributes like age, gestational days, plurality of the baby. Mother's weight, physically measurable parameters such as smoking conditions, lifestyle choices, which are associated with the birth weight and have a lasting impact on it. These parameters can be very well attributed in predicting the birth weight of the newborn baby.

3 Methodology

Predictive LBW models were applied in this study using information from the dataset. The purpose of this study was to evaluate and determine which of the following classifiers—logistic regression, decision tree, Naive Bayes, K-nearest neighbor and random forest (RF)—was most appropriate for predictive classification. Gradient boosting, support vector machine and extreme gradient boosting [4–6].

3.1 Support Vector Machin:

Cortes introduced support vector machines (SVM), an efficient technique based on statistical learning for binary classification, regression, or ranking functions. Because of its numerous appealing features, which allow it to unravel intricate nonlinear data points, it is widely used by researchers in the healthcare industry for classification.

3.2 Logistic Regression

Logistic regression in machine learning is a statistical model used for binary or multi-class classification. It models the probability of an input belonging to a specific class and is particularly effective when predicting outcomes that fall into distinct categories

3.3 Naïve Bayes

The "Naive" assumption is that features are conditionally independent and the Bayes theorem serves as its foundations. Naive Bayes is efficient in many text and document classification applications, spam detection and other areas despite its simplification. It is a strong and effective classification tool because it determines the likelihood that a data point belongs to a specific class based on its features.

3.4 Decision Tre:

A decision tree in machine learning is a hierarchical tree-like structure used for both classification and regression tasks. It breaks down data into smaller subsets based on the most important features, effectively mapping a series of decisions. Decision trees are appreciated for their simplicity and interpretability, making them a valuable tool for understanding the decision-making process.

3.5 Random Forest

Random forest is a well-liked ensemble learning technique. Although it is based on decision trees, it incorporates more than one tree to increase prediction accuracy. Random forest is renowned for its capacity to manage high-dimensional data, minimize overfitting and offer insightful information about the significance of individual features. It is extensively employed in many different tasks, such as regression and classification.

Algorithm Prediction Evaluation Steps
Step 1: Consider the dataset according to the requirements.

Step 2: Use the input data from the dataset to make predictions based on our use case.

Step 3: If the input data is not in the same format as the data used for training, then apply data preprocessing techniques like data cleaning.

Step 4: Remove unwanted data and noisy data to improve accuracy.

Step 5: Split the data into training and testing datasets.

Step 6: Apply the model to the testing data.

Step 7: Perform evaluation and select the best model.

Step 8: Now the model is read.

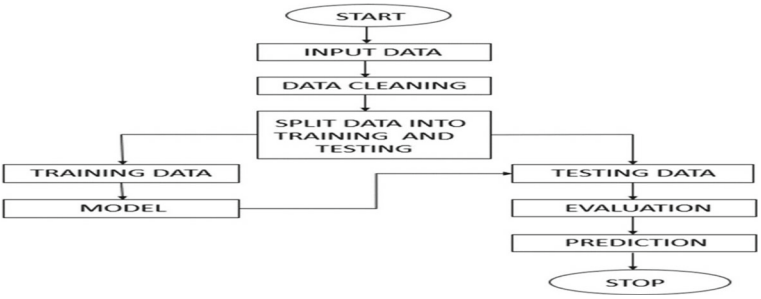


Fig. 1 Algorithm working process

We use the above Fig. 1 algorithm for the implementation of a prediction algorithm [7]. We aim to achieve an accuracy above 75%. We tested the accuracy of all the algorithms on our dataset. We have come to a conclusion that the random forest algorithm and linear regression are the best ones to implement the project.

Accuracy obtained from the algorithms:

Accuracy of random forest: 81%

Accuracy of linear regression: 78%.

Based on accuracy, the random forest algorithm is the optimal choice for implementing the low birth weight prediction process. The final model employs the "random forest algorithm."

3.6 Working Process of Random Forest Algorithm

1. Randomly select some data points from the training set.
2. Build decision trees using the randomly selected data.
3. Examine the outcomes of each tree.
4. Make the final prediction by either counting the majority votes or calculating the average.

Working Model
See Fig. 2.

3.7 Comparative Study Existing System

We referred to almost all websites and YouTube videos for existing birth weight prediction applications [8]. Very few applications are designed to predict the birth weight before the actual birth occurs.

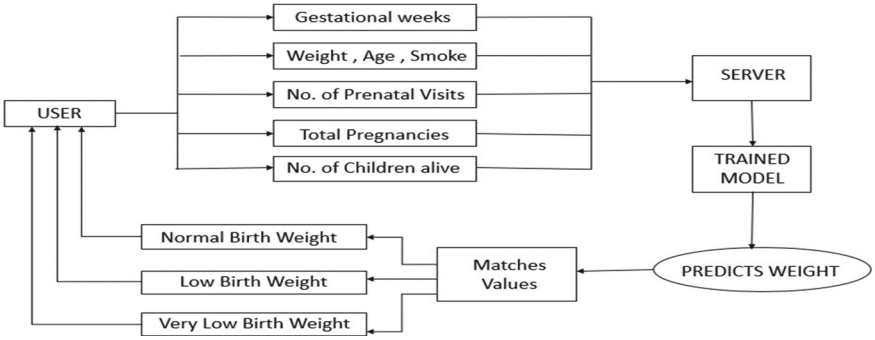


Fig. 2 Model representation

Most of the applications directly provide results in a format that is challenging for common users to understand. It requires healthcare professionals to comprehend the input data types and the output from the predicted algorithm [9–13]. These applications primarily focus on files only.

Disadvantages

There is no web API available to predict the birth weight according to the user's flexibility. Accurate prediction of the weight using parameters with a low impact on birth weight is lacking. In our proposed system, we provide users with the measurable parameters that help in accurate and faster prediction of the baby's weight [14]. It reduces the repetitive checkups only to know the weight of the baby. It helps in maintaining track of the fluctuations in growing weight. It increases usability as the web API is easier to use and deploy.

4 Results

We improve the accuracy in prediction by increasing the number of parameters used in the prediction of the birth Weight of the baby. We are also aiming to work on other modules of the website which can provide a medium to guide the user about the nutritional information and the possible pre-natural care for the baby during the early stages of development of the baby in the mother's womb. We plot graphs based on dataset we defined. Dataset is the key information that consists of features and target outcomes of our theme. Based on machine learning algorithms, we designed a web API to measure the weight of the baby in the womb.

Dataset Description
The dataset contains information about crucial input parameters for pregnant women, including:

Mother's age in years (MAGE)

Father's age (FAGE)

Weight gained during the last pregnancy (gained)

Number of prenatal visits (VISITS)

Total number of pregnancies (TOTALP)

Number of children, whether alive or deceased (BDEAD)

Number of terminations (TERMS)

Outcome of the last delivery (LOUTCOME)

Completed weeks of gestation (WEEKS)

Infant birth weight (BWEIGHT).

The ultimate measure of infant well-being is their birth weight.

Sample Dataset

AGE	GAINED	VISITS	MAGE	TOTALP	BDEAD	TERMS	LOUTCOME	WEEKS	BWEIGHT
33	26	10	34	2	1	0	1	35	4.375
19	40	10	18	1	0	0	9	41	6.9375
33	16	14	31	2	0	0	1	39	8.5
25	40	15	28	3	1	0	1	38	8.5
21	60	13	20	2	0	0	1	40	9
21	30	15	21	1	0	0	9	42	8
29	20	11	32	2	0	0	1	39	7
23	41	15	21	1	1	0	9	41	7.375
27	0	12	26	1	0	4	9	38	8.1875

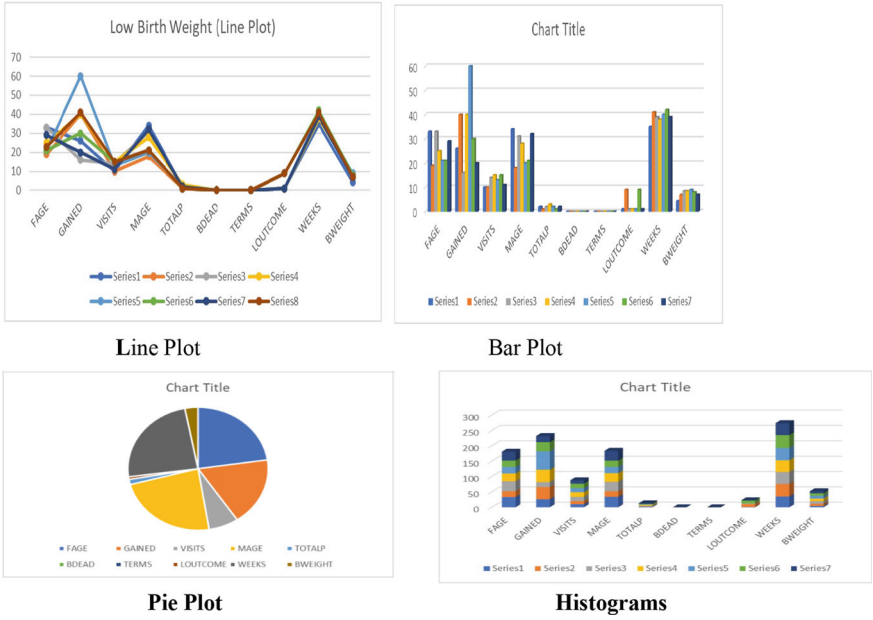


Fig. 3 Plots represent the output of the working model

These plots represent the output of the working model.

Future Enhancement

We will improve the accuracy in prediction by increasing the number of parameters used in the prediction of the birth weight of the baby. We are also aiming to work on other modules of the website which can provide a medium to guide the user about the nutritional information and the possible prenatal care for the baby during the early stages of development of the baby in the mother's womb [15] (Fig. 3).

We will collect more data values for different cases of the birth where several other factors like hereditary diseases, mother and father's health history have a huge impact on the growth of the baby during pregnancy. We will also check for ancestral cases of abnormalities in the birth weight which can help in deciding possible alternatives for baby's health.

5 Conclusion

The low birth weight prediction project is all completed. Because the system was constructed precisely and error-free, it is fast and efficient. The goal of this project was to develop a web application that, with the correct parameters, provides users with an enhanced interface for precisely forecasting when a child will be born. With

this project, we were able to gain practical knowledge and expertise on a number of topics, such as building predictive models using machine learning algorithms and HTML and CSS web pages. Every system is safeguarded. As a result, it was easier for us to comprehend the phases of project development and the software development life cycle.

References

1. Senthilkumar D, Paulraj S (2015) Prediction of low birth weight infants and its risk factors using data mining techniques. In: International conference on industrial engineering and operations management, Dubai, United Arab Emirates (UAE), 3–5 Mar 2015
2. Khan W, Zaki N, Masud MM, Ahmad3 A, Ali1 L, Ali N, Ahmed LA (2020) Infant birth weight estimation and low birth weight classification in United Arab Emirates using machine learning algorithms
3. Dahlui M, Azahar N, Oche OC, Aziz NA (2016) Risk factors for low birth weight in Nigeria: evidence from 2013 Nigeria demographic and health survey. Global Health Action 9:28822
4. Bekele WT (2022) Machine learning algorithms for predicting low birth weight in Ethiopia
5. Faruk A, Cahyono ES, Eliyati N, Arifieni I (2018) Prediction and classification of low birth weight data using machine learning techniques. Indonesian J Sc Technol 3(1):18–28
6. Arayeshgari M, Najafi-Ghobadi S, Tarhsaz H (2020) Machine learning based classifier of low weight
7. Akhtar F et al (2018) Effective large for gestational age prediction using machine learning techniques with monitoring biochemical indicators
8. Bian J, Ali L, Masud MM, Ghenimi N, Ahmed LA (2020) Infant low birth weight prediction using graph embedding features
9. Jayanthi Rao M, Kiran Kumar R (20202) Follicle detection in digital ultrasound images using bemd and adaptive clustering algorithms. In: Lecture notes in mechanical engineering, pp 651–659
10. Jayanthi Rao M, Kiran KR, Harikiran J (2019) Method for follicle detection and ovarian classification in digital ultrasound images using geometrical features. J Adv Res Dyn Control Syst 11(2):1249–1258
11. Jayanthi Rao M, Apparao D, Ramakrishna B, Durga Prasad KG, Ramana BV, Ramanaiah M (2023) Intelligent Traffic Monitoring System Using Vehicular Ad Hoc Network. Int J Recent Innov Trends Comput Commun 11(10):629–635
12. Jayanthi Rao M, Prasanthi P, Suresh Patnaik P, Divya M, Sureshkumar J, Ramanaiah M (2022) Forecasting systems for heart disease using advanced machine learning algorithms. Int. J. Food Nut Sci 11(7):1257–1268
13. Jayanthi Rao M, Divya M, Ratnan Mohitha M, Prasanthi P, Paparao S, Ramanaiah M (2022) Analyzing the effectiveness of convolutional neural networks and recurrent neural networks for recognizing facial expression. Int J Food Nut Sci 11(7):1269–1282
14. Surya Pavan Kumar G, Sourav KumarB, Soumya Ranjan N, Amit Verma (2022) DI-ADS: a deep intelligent distributed denial of service attack detection scheme for fog-based IoT applications. Math Probl Eng 2022:1–17
15. Donders ART, van der Heijden GJMG, Stijnen T, Moons KGM (2006) Review: a gentle introduction to imputation of missing values J Clin Epidemiol
16. Di Laurea T (2016) Predicting mortality in low birth weight infants: a machine learning perspective

Complaint Management System for State Government Authority



A. Siva Sankar, Venkata Kishore Kumar Rejeti, Shaik Thanda Moddinsha, S. Rakesh, V. Himanish, M. Vinod, and D. Anand

Abstract Population growth is causing a severe deterioration in the state of cleanliness and waste management. The disarray of trash in public spaces leads to unsanitary conditions in the immediate vicinity. The neighbouring population may get many deadly diseases as a result of it. It also lowers the area's valuation. In this project, "a compliant management system using web technologies" is suggested as a way to prevent this and improve cleaning. Under the suggested system, the administrator generates a garbage bin ID and gives it to the driver so that he or she may pick up the trash and provide a way for individuals to file complaints about the waste that is lying about. Anybody may easily utilize this system because it is so user-friendly.

Systems for managing complaints that are error-free, secure, dependable, and rapid can be achieved with web-based solutions. It assists the user in shifting their attention from maintaining records to other duties. As a result, it will help the organization utilize its resources more effectively. The organization can retain computerized records without having to enter duplicate data. This suggests that one need not get distracted by unrelated information in order to obtain the knowledge. The objective is to suit the needs of the organization and enable the long-term storage of their irreplaceable data and information with easy access and modification by automating their current manual process with computerized hardware and sophisticated software.

Keywords Complaint · Computerized records · Garbage management · Garbage bin · Admin · Driver · User

A. S. Sankar · V. K. K. Rejeti (✉) · S. T. Moddinsha · S. Rakesh · V. Himanish · M. Vinod
Department of CSE, KKR & KSR Institute of Technology and Sciences, Guntur, India
e-mail: mail2rvkk@gmail.com

D. Anand
Department of CSE, Koneru Lakshmaiah Education Foundation, Vaddeswaram, AP, India

© The Author(s), under exclusive license to Springer Nature Singapore Pte Ltd. 2025

B. B. V. L. Deepak et al. (eds.), *Recent Advancements in Product Design and Manufacturing Systems*, Lecture Notes in Mechanical Engineering,
https://doi.org/10.1007/978-981-97-6732-8_35

1 Introduction

The world is upgrading right now, but there's one major issue that has to be resolved. Sewage! We frequently see images of trash cans being overfilled to the point that everything spills out. There are thus more diseases, pests, and mosquitoes that breed there. In most other countries, including India, solid waste management is a significant problem in urban areas. Thus, it is necessary to devise a strategy that may either totally eradicate or significantly reduce this problem. Garbage collection process is critical to service providers.

The antiquated practice of physically inspecting the trash cans to make sure nothing is missing is a labour-intensive, time-consuming process that is incompatible with contemporary technologies. We are presenting the idea of a waste management system that enables trash management with the least amount of human intervention in order to maintain a clean environment in order to handle all of these problems. To provide a comfortable place for people to live, smart cities combine a variety of online or mobile applications. Providing an eco-friendly, effective, and efficient waste management system is one of these answers. In addition to not covering every area of the city, the existing waste collection system involves regular garbage trucks making rounds once a day or once a week. This is a very inefficient use of public funds (Fig. 1).

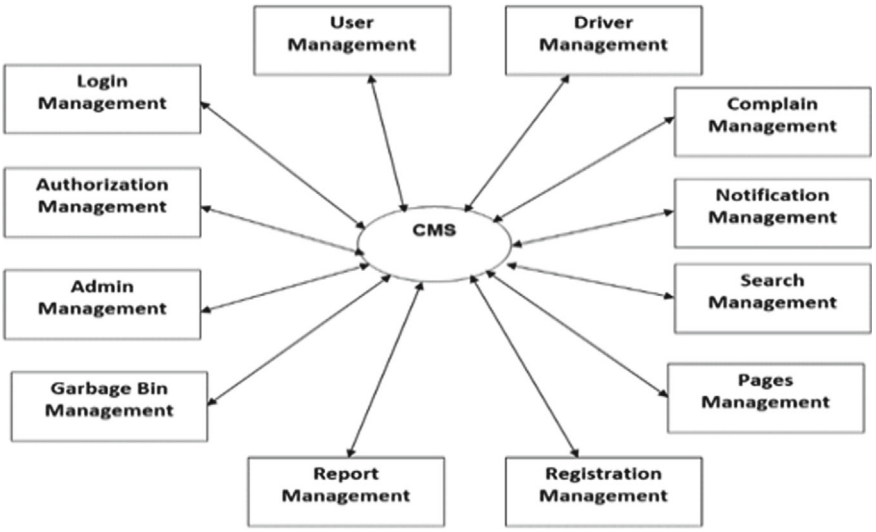


Fig. 1 Complaint management system

2 Literature Review

In [1], a waste management system called "cleanv" is suggested in this study to prevent pollution and inappropriate trash disposal. Features like the ability to report careless garbage dumping, connect with waste collection businesses, specify waste disposal regions within a certain locality, and allow waste collection firms to connect with recycling companies would all be included in the planned system. In [2], the authors made the decision to begin a systematic literature study in order to work on a preliminary mapping of the existing academic literature and perspectives on waste management systems in order to report quantified waste stream data. This decision was made based on research findings in other research disciplines. Based on the authors' prior study on other academics as well as their personal experience, a list of keywords was developed for this project. Academic articles with waste management systems, computations, and/or reporting capabilities were found using keywords.

These studies quantified and displayed in numerical form the quantity of various waste components that operations produce, handle, and process based on actions that the system is able to see.

According to [3], there is a great amount of rubbish piled up in many locations due to the massive expansion in population. Trash that accumulates in public areas causes social unrest. This unsanitary setting makes it simple for illnesses to spread to those in the vicinity. It also lessens the splendour of the natural world. As a result, cleanliness becomes imperative. In order to have a clean and germ-free society, proper waste management must be established. We must use some technologically based solutions to address the garbage that is growing daily. This study suggests an affordable, web-based waste management solution. We can save time and human labour by introducing this document now. From [4], researchers and specialists from a variety of sectors are paying close attention to the steadily increasing amounts of waste and rubbish that are produced. Because it must be gathered and treated as quickly as possible, the administration and collection of this enormous and dispersed volume of garbage offer a difficulty.

Garbage must be collected as soon as possible since it may be a major source of hazardous gas emissions and toxic material production into the soil, which can have fatal repercussions for the environment and seriously affect human health. In order to address this situation, the research suggested an online waste management system that would allocate and schedule available garbage trucks based on the amount of rubbish being created throughout smart cities. To handle the organization of these wastes and make it easier for the drivers to collect the rubbish, the suggested solution offers a mobile application and a web-based system. From [5], the amount of garbage created on a daily basis appears to be endless; it is continuously growing from tiny to huge size. We learn that we lack an appropriate system for dumping and disposing of waste from a variety of sources. These result from improper waste disposal management and insufficient use of technology. Additionally, many don't take it seriously since they either don't know about it or don't accept responsibility for it. We have suggested a Smart Trash model as a way to change the present situation. Here, we automated

the process so that people would not have to exert themselves further than filling the trash can with waste.

Additionally, we suggested a management system that would notify the appropriate authorities if the garbage was full and wasn't emptied on time. From [6], researchers and specialists from a variety of sectors are paying close attention to the steadily increasing amounts of waste and rubbish that are produced. Because it must be gathered and treated as quickly as possible, the administration and collection of this enormous and dispersed volume of garbage offers a difficulty. Waste must be collected as soon as possible since it may accumulate and become a major source of hazardous material and harmful gas emissions into the soil, which can have fatal effects on the ecosystem and seriously harm human health. In order to address this situation, the research suggested an online waste management system that would allocate and schedule available garbage trucks based on the amount of rubbish being created throughout smart cities. The suggested solution makes it easier for the driver to collect rubbish by offering a web-based system and a mobile application to handle the organization of these wastes.

Citizens' involvement in the process of city development is crucial, as stated in [7]. The public can contribute by lodging grievances, offering information, or offering counsel in order to establish democracy and good government. While speed and accuracy are required, complaints are currently handled manually by one or two operators under the present system. The issue is that the manual process of addressing complaints leads to mistakes when determining which government entities should handle the complaint. In order to minimize human error, this research will provide a method that uses the K-nearest neighbour (KNN) algorithm to identify the relevant government agency for complaints submitted by citizens. This text classification method is one of the ones employed in this study to categorize complaints with texts written in Indonesian. A citizen's complaint is the system's input, and its output is the name of the relevant government agency that has been informed of the complaint's details.

This is in [8]. One of the elements influencing the people's degree of satisfaction with government performance is public service. The expectations and requirements of the public are ascertained via complaints. Comprehending the grievances offers an opportunity to enhance the calibre of public services. In today's world, microblogging is popular on Twitter. Through the internet, society may simply and instantly express itself through its experiences, activities, and grievances. In this study, tweeters are used to categorize concerns from society about roads, energy, and water. Utilizing the K-nearest neighbour (KNN) method, Twitter is classified. In this study, term frequency (TF), document frequency (DF), information gain, and chi-square are used in the feature selection process. A mix of characteristics from the preceding feature selection was used in this study. The outcome of the experiment demonstrates that KNN can categorize complaints. The achieved accuracy rates for both the detection and categorization of complaints were 83.75% and 77.08%, respectively. The average values generated for each parameter in the classification of categories of water complaints are 87.5% for precision, 87.8% for recall, and 87.49% for F-measure testing.

3 Proposed System

In this project, we use PHP and MySQL databases. It has three modules

1. Admin
2. Driver
3. User.

3.1 Architecture of Admin Module:

Figure 2b shows the architectural system of admin module, which consists of the following.

1. Dashboard
2. Pages
3. Complain
4. Driver complain response
5. Driver bin response
6. Search
7. Reports.

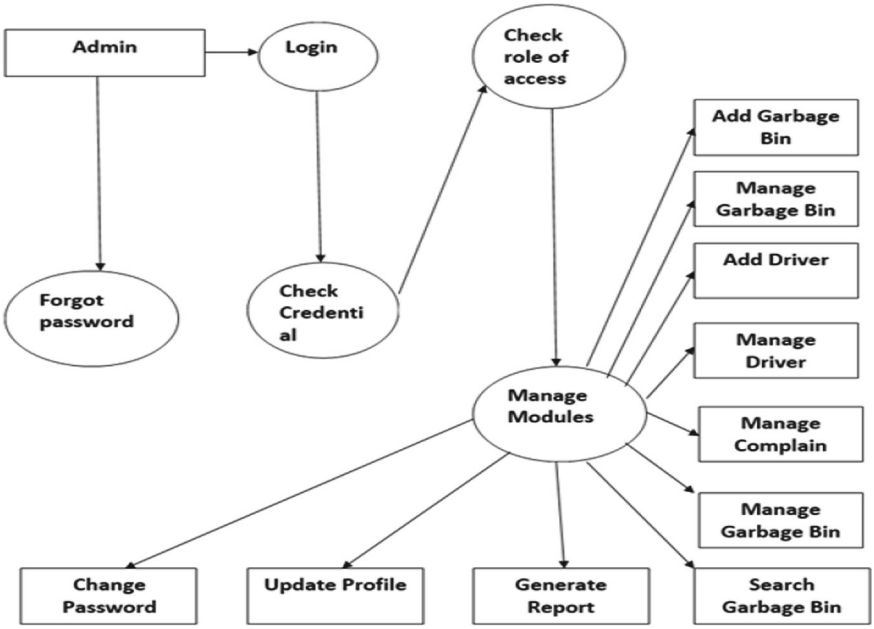


Fig. 2 Architectural diagram of admin module

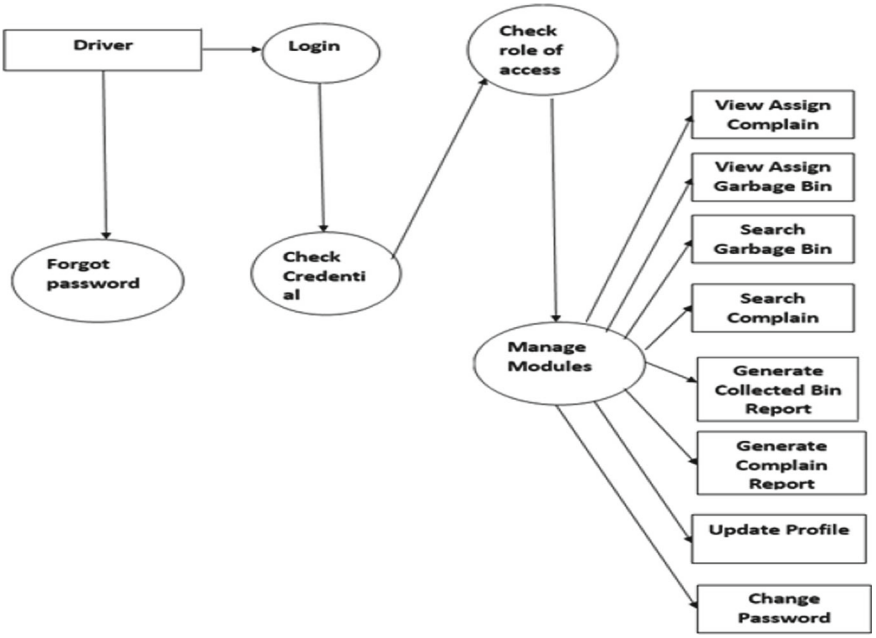


Fig. 3 Architectural diagram of driver module

Architecture of Driver Module
The following picture depicts that architectural design of driver module which consists of the following submodules (Fig. 3).

Architecture of User Module
The following picture depicts that architectural design of user module consists of the following submodules (Fig. 4).

4 Methodology

The "Garbage Management System" implements various technological solutions to tackle the challenges caused by rapid population growth and industrialization. One of the key solutions is the use of web technologies to automate and streamline the waste collection process. This includes modules for administrators, drivers, and users, allowing for efficient management, complaint handling, and tracking of garbage bins. The system also utilizes PHP and MySQL databases for data storage and management, ensuring accurate and secure records. Additionally, web and SMS notifications are integrated to enhance efficiency and reliability. These technological solutions aim to reduce human effort, save time, and ensure proper resource allocation in waste management practices.

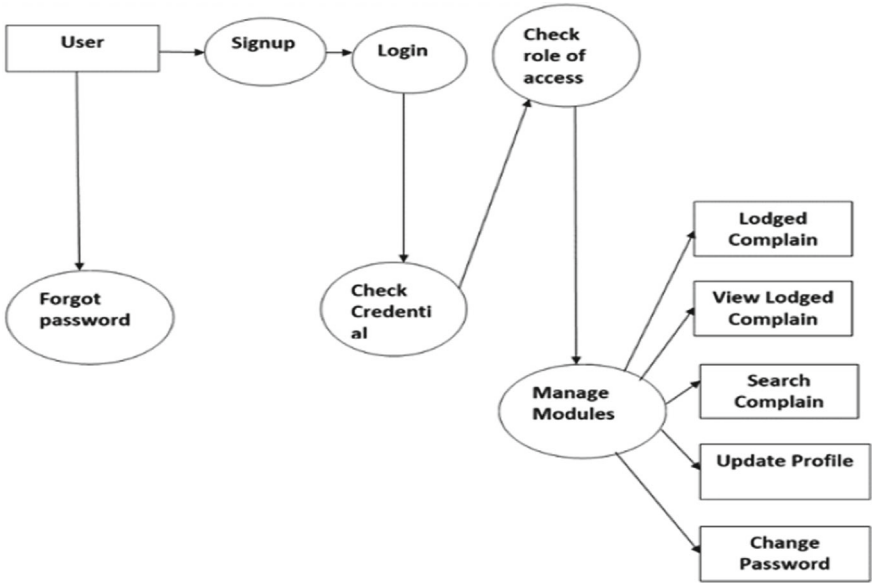


Fig. 4 Architectural diagram of user module

The "Garbage Management System" stands out from other waste management solutions due to its utilization of web technologies, PHP, and MySQL databases to automate and streamline the waste collection process. This system includes modules for administrators, drivers, and users, allowing for efficient management, complaint handling, and tracking of garbage bins. It also incorporates web and SMS notifications to enhance efficiency and reliability. Furthermore, the system aims to reduce human effort, save time, and improve resource allocation in waste management practices. These features make it a user-friendly and effective solution for garbage management, setting it apart from other waste management solutions. Summary: The "Garbage Management System" differentiates itself through its use of web technologies, automation, and efficient modules for various stakeholders. It aims to streamline waste collection, improve resource allocation, and enhance efficiency in garbage management practices.

The management system makes use of web technologies to create a user-friendly system that allows users to lodge complaints and for the admin to assign tasks to drivers for garbage collection. The system aims to streamline the process of addressing user complaints efficiently by creating an error-free, secure, reliable, and fast platform. The system aims to improve the management of garbage collection and address complaints from the public regarding garbage in their surroundings.

The system uses web and SMS notifications in the Complaint Management System to improve waste management. Web notifications can be used to inform users about the progress of their complaints, such as when their complaint has been received or when it has been resolved. This allows for transparency and keeps users updated

on the status of their complaints. SMS notifications can be sent to drivers to assign them tasks for garbage collection, ensuring efficient allocation of resources and timely garbage collection. These notification mechanisms, as highlighted in previous research, enhance the overall waste management process by improving communication, increasing efficiency, and providing better supervision. Summary: The system incorporates web and SMS notifications in the complaint management system to enhance waste management. These notifications improve communication, increase efficiency, and provide better supervision in the overall waste management process.

The "Garbage Management System" aligns with smart city initiatives by utilizing web technologies and automation to improve waste management practices. It addresses the challenges posed by rapid population growth and industrialization by streamlining the process of addressing user complaints about garbage in their surroundings. The system incorporates web and SMS notifications to enhance communication and improve the overall waste management process. By automating and digitizing waste management practices, the system contributes to the development of a smart city and promotes urban sustainability and cleanliness. The "Garbage Management System" aligns with smart city initiatives by utilizing web technologies and automation to streamline waste management practices and address user complaints efficiently. It promotes urban sustainability and cleanliness by automating and digitizing waste management processes.

worked together with more than 200 local authorities and other stakeholders to collect requirements and guarantee adherence to industry standards and operational requirements. Using PHP and MySQL, an integrated garbage management system was created to improve communication, optimize waste collection, and cut operating costs by 20%.

In the description of the admin module and dashboard, it would be helpful to understand the specific features and functionalities available to the admin for complaint management. Describe the various features provided to admin. The website's administrator is the super user with complete control over everything on the site. Using the login page, the admin can log in. Dashboard: The administrator can view all the details in this part, including the number of drivers, the total number of complaints filed, the number of complaints assigned, the number of complaints rejected, the number of completed complaints, and the total number of bins cleaned or in progress. Pages: The administrator can manage the contact and about us pages in this section. Complain: The administrator can see and allocate user-submitted complaints to drivers in this section. Driver complaint response: The administrator can examine the status of complaints that the driver has marked or completed in this section.

The "Garbage Management System" streamlines the process of addressing user complaints efficiently through the use of web and SMS notifications. Web notifications allow users to easily lodge complaints about garbage in their surroundings, which are then automatically assigned to drivers for collection. This automation eliminates manual intervention and ensures timely garbage collection. SMS notifications complement the web notifications by providing real-time updates to users about the status of their complaints and the estimated collection time. These notification mechanisms enhance communication between users and the system, improving the overall

waste management process by enabling faster response times and increasing user satisfaction. It is mentioned that this project addresses the concept of a smart city. Could you discuss in more detail how the "Garbage Management System" aligns with smart city initiatives and contributes to urban sustainability and cleanliness. The "Garbage Management System" aligns with smart city initiatives by incorporating web technologies and automation to improve waste management practices. This system addresses the challenges posed by rapid population growth and industrialization, which are common in smart cities. By allowing users to lodge complaints about garbage in their surroundings, the system ensures timely garbage collection through efficient allocation of tasks to drivers. It also utilizes web and SMS notifications to enhance communication and improve the overall waste management process. This automation and digitization contribute to the development of a smart city and promote urban sustainability and cleanliness.

5 Result

The two main factors contributing to pollution are thought to be the growing population and industry. People in the vicinity are seriously at risk for health problems when there is trash on the streets and overstuffed trash cans. Technology advancements can be used to solve these issues. The goal of this initiative is to improve the neighbourhoods and support the idea of a smart city. It runs on dependable, low-cost software. Additionally, it uses SMS and web notifications to improve system dependability and efficiency. The "Garbage Management System" project underwent extensive research and analysis in order to create the code and put it into use. Under the direction of the knowledgeable project guide, it was completed. Since every company uses the "Complaint Management System for State Government Authority" in its daily operations to preserve cleanliness in its region, all current requirements and possibilities have been addressed during the project period (Fig. 5).

Figure 6 shows the login page of the admin module which consists of username and password fields. The admin should provide valid and authenticated values to enter into the dashboard.

The above diagram depicts the dashboard design of all modules. Particularly above one shows the dashboard of admin module through which the admin can manage all the complaints that are received by the user.

Figure 7 shows the bin management by the admin by assigning the bin id through which the admin can easily identify the place from where the complaint is received.

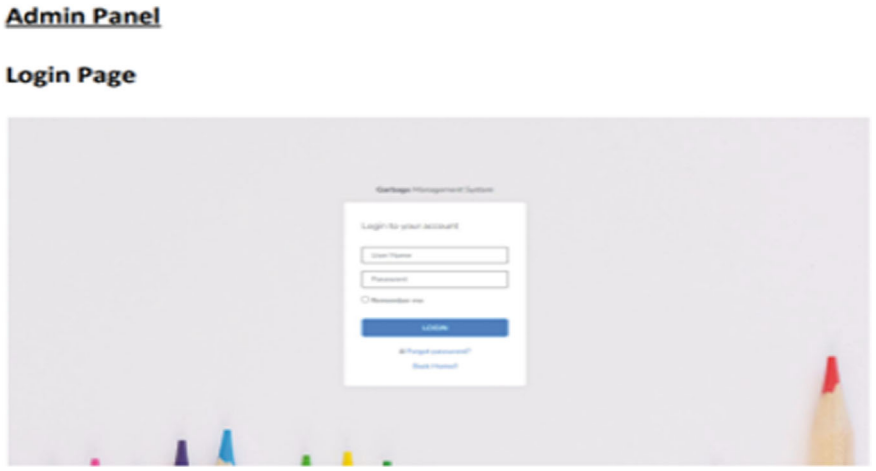


Fig. 5 Log in page of admin module

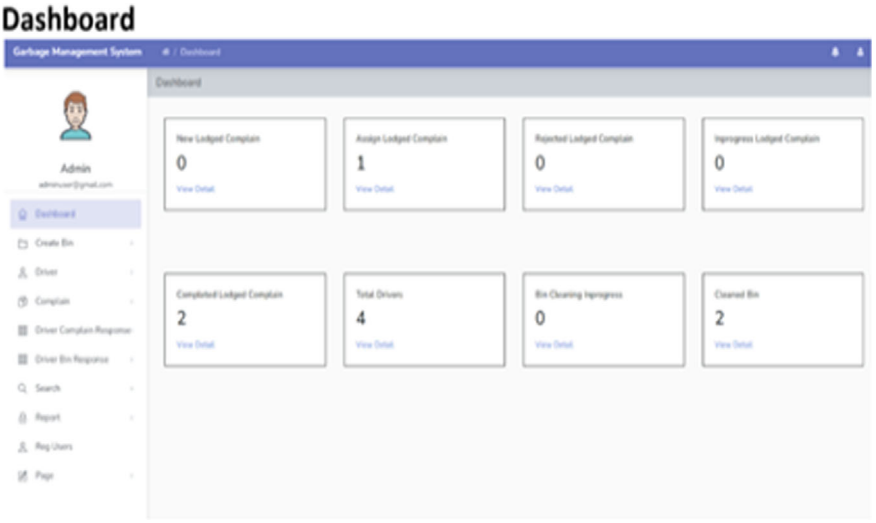


Fig. 6 Dashboard of all modules

6 Conclusion

The two main factors contributing to pollution are said to be the growing population and industry. People in the vicinity are seriously at risk for health problems when there is trash on the streets and overstuffed trash cans. Technology advancements can be used to solve these issues. The goal of this initiative is to improve the neighbourhoods and support the idea of a smart city. It runs on dependable, low-cost software.

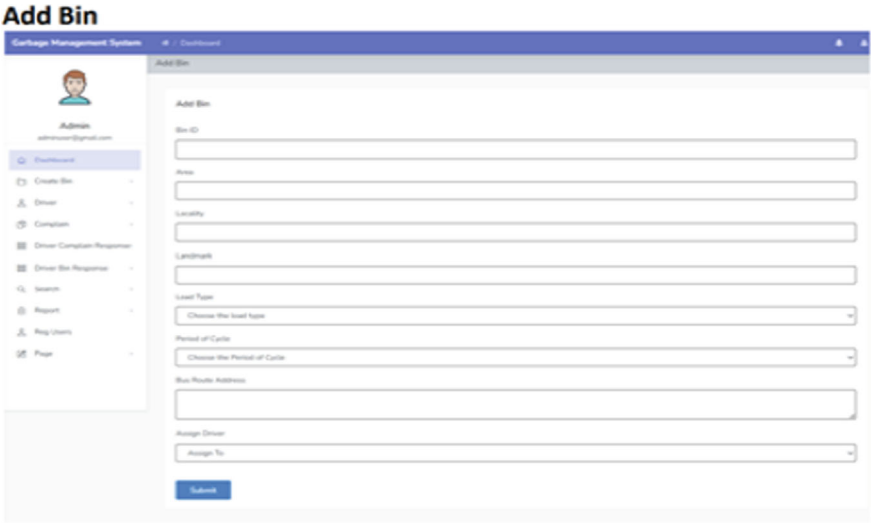


Fig. 7 Bin management by the admin

Additionally, it uses SMS and online notifications to improve system dependability and efficiency.

The "Garbage Management System" project underwent extensive research and analysis in order to create the code and put it into use. Under the direction of the knowledgeable project guide, it was completed. As the "Garbage Management System" is utilized for everyday operations in any organization to maintain cleanliness in their region, all current requirements and possibilities have been taken care of during the project period.

References

1. Odhiambo G (2022) Waste management system. https://www.researchgate.net/publication/360835841_waste_management_system
2. Geethamani R, Rakshana P, Raveena P, Ragavi R (2021) Garbage management system. In: 2021 7th International Conference on Advanced Computing and Communication Systems (ICACCS), pp 1190–1192. https://doi.org/10.1109/ICACCS51430.2021.9441922
3. Jajoo P, Mishra A, Mehta S, Solvande V (2018) Smart garbage management system. In: 2018 International conference on smart city and emerging technology (ICSCET), pp 1–6. https://doi.org/10.1109/ICSCET.2018.8537390
4. Mishra A, Patel DK, Singh T, Singh A, Gawre SK (2020) Garbage management with Smart trash using IoT. In: 2020 IEEE international students' conference on electrical, electronics and computer science (SCEECS), pp 1–6. https://doi.org/10.1109/SCEECS48394.2020.98
5. Jabar H, Hassan R, Sadeq AS (2020) A new smart waste managing system. In: 2020 International conference on computer science and software engineering (CSASE), pp 209–214. https://doi.org/10.1109/CSASE48920.2020.9142068

6. Srilatha M, Abhinav C, Balaram M, Sanjana A (2021) Smart monitoring and collection of garbage system using Internet of Things. In: 2021 Third international conference on intelligent communication technologies and virtual mobile networks (ICICV), pp 335–342. https://doi.org/10.1109/ICICV50876.2021.9388438
7. Tjandra S, Warsito AAP, Sugiono JP (2015) Determining citizen complaints to the appropriate government departments using KNN algorithm. In: 2015 13th international conference on ICT and knowledge engineering (ICT & knowledge engineering 2015), pp 1–4. https://doi.org/10.1109/ICTKE.2015.7368461
8. Kandhari VK, Mohinani KD (2014) GPS based complaint redressal system. In: 2014 IEEE Global humanitarian technology conference—South Asia Satellite (GHTC-SAS), pp 51–56. https://doi.org/10.1109/GHTC-SAS.2014.6967558

Implementing a Support Vector Machine Algorithm on Social Media Flat Forms to Detect and Restrict Cyberbullying Conversations

M. Jayanthi Rao, P. Prasanthi, B. Ramakrishna, K. G. Durga Prasad, and M. Ramanaiah

Abstract In contemporary times, there has been a significant prevalence of communication that is subject to abuse inside the realm of social media. According to a recent survey research, it has been substantiated that over 80% of online social networks exhibit instances of abusive or obscene communication within their user accounts. These forms of communication are mostly disseminated on the personal profiles of users with the intention of subjecting adolescents, preadolescents, and other minors to harassment through the dissemination of offensive content. To date, no existing program has successfully addressed the issue of preventing the dissemination of offensive cybercontent on social media platforms. This lack of a viable solution has served as a catalyst for my motivation to develop a novel application aimed at curbing indecent communication within online social networks. This suggested application primarily aims to introduce a novel representation learning approach for addressing the issue of identifying and preventing the dissemination of abusive communications in online chat platforms. In this study, we employ widely recognized machine

M. J. Rao
Department of Computer Science and Engineering, Aditya Institute of Technology and Management, Tekkali-532201, India

P. Prasanthi
Department of Information Technology, Aditya Institute of Technology and Management, Tekkali 532201, India

B. Ramakrishna (✉)
Department of Mechanical Engineering, Aditya Institute of Technology and Management, Tekkali 532201, India
e-mail: brkbtech@gmail.com

K. G. D. Prasad
Department of Mechanical Engineering, Vignan's Institute of Information Technology (A), Visakhapatnam 530049, India

M. Ramanaiah
Department of Chemistry, Aditya Institute of Technology and Management, Tekkali 532201, India

© The Author(s), under exclusive license to Springer Nature Singapore Pte Ltd. 2025

B. B. V. L. Deepak et al. (eds.), *Recent Advancements in Product Design and Manufacturing Systems*, Lecture Notes in Mechanical Engineering,
https://doi.org/10.1007/978-981-97-6732-8_36

learning algorithms, such as support vector machine, to categorize communications into two categories: abused messages and regular messages. Additionally, we utilize the Porter Stemming algorithm to preprocess the text messages. The Porter Stemming algorithm is a widely recognized component of the Natural Language Toolkit (NLTK) package. It functions by segmenting the entire text into distinct units and subsequently assigning tokens to each individual word. In this study, the cyberbullying discourse is categorized into five distinct classifications, drawing upon existing research on hate speech, vulgarity, offensiveness, sexual content, and violence.

Keywords Cyberbullying · Communication · Natural language toolkit · Support vector machine · Porter stemming · Vulgar · Offensive

1 Introduction

Online social media encompasses a range of internet-based platforms that facilitate the creation and dissemination of content provided by users. These platforms are built upon the fundamental principles and technological foundations of web 2.0 [1]. Most of this information can be exchanged through social media, where users have access to a wealth of knowledge, convenient communication tools, and other things. Social media may, however, have certain unintended consequences, such cyberbullying, which can have a severe impact on people's lives, particularly those of children and teenagers. Because they do not have to confront anyone and can hide behind the internet, bullies are free to hurt their peers' feelings. Because we are all always connected to the Internet or social media, especially young people, victims are easily exposed to harassment. According to [2], victimization rates for cyberbullying range from 10 to 40%. Nearly 43% of teenagers in the USA have experienced cyberbullying at some point [3]. Similar to traditional bullying, cyberbullying has detrimental, pervasive effects on kids [4–6], as shown in Fig. 1. The results of cyberbullying for victims may even be devastating, such as the prevalence of self-harming behavior or suicides. Automated detection and fast reporting of bullying communications is one strategy for combating the issue, allowing for the right action to be done to avert potential catastrophes. Natural language processing and machine learning are effective techniques for studying bullying, according to earlier computational studies [7–9]. The problem of detecting cyberbullying can be expressed as supervised learning.

The major goal of the current study is to create a unique technique that can train discriminative and robust representations to address the aforementioned issues with cyberbullying detection. In order to address these issues, expert knowledge is incorporated into feature learning [10]. Generally speaking, when we use certain words in sentence building, some words give positive meaning in one way while the same words give negative meaning in another way. To train a support vector machine for online cyberbullied detection, Dynacare g. Yin et al. proposed combining BoW features, sentiment features, and contextual features. They used label-specific

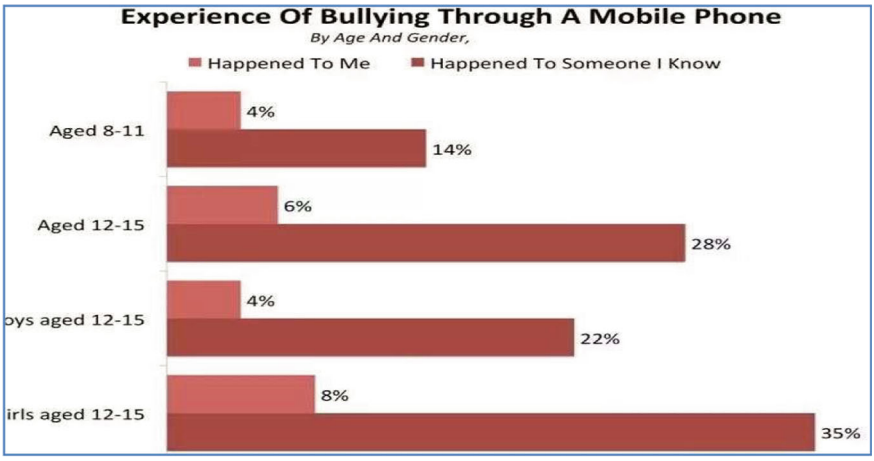


Fig. 1 Percentage of users who are getting bullying messages

features to extend the general features, where the label-specific features are learned by linear discriminative analysis [11]. Additionally, we attempt to discover the weighted TF-IDF scheme by scaling bullying-like features by a factor of two using a mechanism from a toolkit for natural language processing [12]. In addition to content-based data, such as gender and history messages, we also try to find out the other information such as extracting the features [13, 14] and then form a new bullying set. In this current work, we only design the model for English literature words, and in the future, we want to derive some more new methods which can be applied on multilanguages.

2 Literature Survey

The literature review is the most crucial phase in the software development process. Before designing a new application or model, it is vital to calculate the timeline, budget, and company's strength. Once all of these elements have been reviewed and approved, application development can commence. The literature review focuses mostly on all of the past work performed by multiple users, as well as the benefits and drawbacks of those models. This literature review serves primarily to establish the list of resources that will be used to create this suggested application.

2.1 Motivation

Kaplan and Haenlein [15] proposed that the concept of social media is top of the agenda for many business executives today. Decision makers, as well as consultants, try to identify ways in which firms can make profitable use of applications such as social media flat forms. This article intends to provide some clarification. Begin by describing the concept of social media, and discuss how it differs from related concepts such as web 2.0 and user-generated content. Finally, present 10 pieces of advice for companies which decide to utilize social media.

Reynolds et al. [16] reported a language-based system for identifying online bullying in a small sample of form spring data; we were able to correctly identify 78.5% of the posts that contain cyberbullying by keeping track of the proportion of swear and insult terms within a post. Our findings show that while our features can detect cyberbullying in form spring postings to a respectable degree, there is still much space for advancement in this timely and significant use of machine learning to web data. Hani et al. [17] suggested uses of machine learning to identify cyberbullying. We used TF-IDF and sentiment analysis algorithms to extract features and two classifiers, SVM and neural networks, to evaluate our model. The categorizations were assessed using several n-gram language models.

2.2 Proposed SVM Algorithm for Cyberbullying Detection in Online Social Networks

The provided figure illustrates a fundamental graph for SVM classification. Support vector machines (SVM) can be categorized into two main types: linear SVM and nonlinear SVM. Linear support vector machines (SVMs) are capable of linearly separating data by use of a line. Conversely, nonlinear SVMs are employed when the data cannot be separated using a linear boundary. In certain instances, the complexity of data may render linear support vector machines (SVM) inadequate for data separation. In such cases, a kernel function is employed to facilitate nonlinear SVM. A variety of data classes that exhibit nonlinear separability can be transformed into higher-dimensional spaces, where they can be rendered linearly separable, by the utilization of a kernel function. On one side of the margin, there is a set of data of one type, while on the other side, there is a corresponding set of data of another type. Support vector machines (SVM) can be utilized for the purposes of prediction and classification. In the context of predicting cyberbullying, it is possible to classify classes into distinct categories using a hyperplane. This hyperplane effectively separates instances with a higher likelihood of experiencing cyberbullying from those with a lower likelihood. The SVM algorithm successfully classified a linear line for instances of internet bullying and a nonlinear line for instances of non-cyberbullying (Figs. 2 and 3).

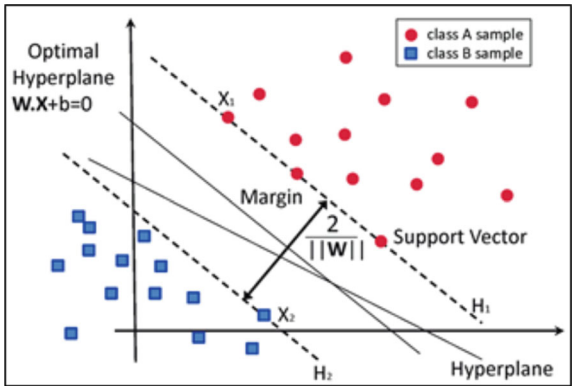


Fig. 2 Illustration of support vector machines (SVM)

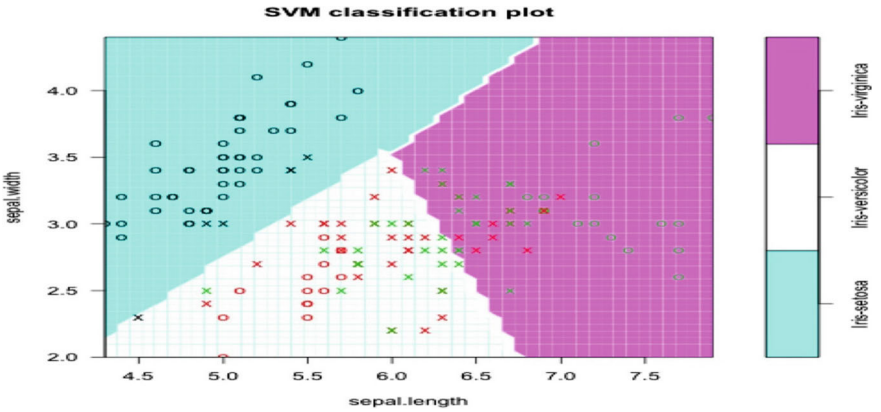


Fig. 3 Flow of proposed model for cyberbullying detection

There are numerous machine learning techniques [18–22] for text classification with machine learning platforms in general. Support vector machines, which we employ in our current application, are one of the best. Support vector machines are algorithms that find the best decision border between vectors that belong to a particular group (or category) and vectors that do not. To transform text messages into vectors, we can assume vectors on any type of data. Vectors are thought of as lists of integers that represent a collection of coordinates in space. By dividing the complete list into two halves, the SVM algorithm performs best in classifying text messages into two or more subgroups. We attempt to apply the SVM method to text categorization issues and achieve excellent results (Fig. 4).



Fig. 4 Different social media flat forms for datasets

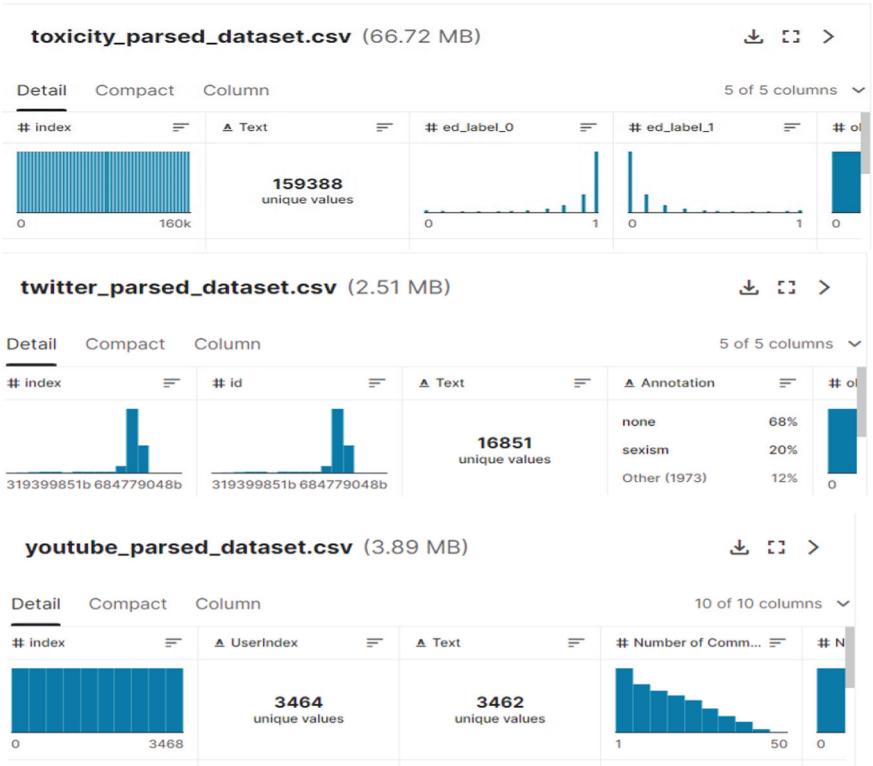


Fig. 4 (continued)

Statistics of the Datasets

Total number of conversations	1800
Number of cyberbullying	900
Number of non-cyberbullying	900
Number of distinct words	6300
Number of tokens	54,675
Maximum conversation size	865 Characters
Minimum conversation size	66 Characters

2.3 Step-By-Step Procedure

The step-by-step procedure of SVM classification algorithm in order to detect cyberbullied messages from online social networks are as follows:

Step 1: Choose the Model

Initially, we need to choose which type of model we want to design with SVM algorithm. There mainly three types of models are such as:

1. Classifier model
2. Extractor model
3. Workflow model.

In our current work, we try to use SVM as classification model to classify the tweets into cyberbullied or not.

Step 2: Choose Classification Type

At this stage, we need to choose the type of classification task what we would like to perform. Based on the topic, we need to choose the type of classification type. Here in our current work, we try to classify the text messages and find out cyberbullied and normal messages. The content classification is divided into three types such as:

1. Topic classification
2. Sentiment analysis
3. Intent classification.

Step 3: Import the Data

In this stage, we try to import necessary data which is required for the current application. In this current application, we try to import the tweets data either collected from well-known social media or directly from social user profiles. Here, the data can be imported either from Excel file, CSS file or data library.

Step 4: Load the Inputs for Feature Extraction

In this stage, we try to load the input by taking some sample keywords such as cyberbullied words and these words are matched with feature extraction. Here, we try to identify these features extracted from sentences and then try to load these features to match with the corresponding bag of words(BOW) which is present in the database.

Step 5: Train the Model

In this stage, we try to train the model by using SVM classifier and then try to divide the messages into parts and then verify the message whether comes under cyberbullied category or normal category. Here, we try to train the model with more than hundreds of cyberbullied words and then make the model ready to classify any type of messages.

Step 6: Test the Model

In this stage, we try to test the model by giving some sample inputs which contain both cyberbullied words and also normal meanings and then test the efficiency of our current application by using SVM algorithm.

2.4 Implementation Phase

The implementation stage is where the theoretical design is translated into a programmed format. At this point, the program will be divided into modules and coded for deployment. The front end of the application uses JSP, HTML, and Java Beans, and the back end data base is My SQL. The application is broken into the five parts listed below. They are listed below.

1. Now Network construction module
2. User registration module
3. Bag of words construction module
4. Identify the bullying feature set module
5. Cyberbullied detection module.

Let us discuss each and every module in detail as follows:

1. **Network Construction Module**

In this lesson, the initial task is constructing a network comprising a solitary administrator and multiple users. The administrator possesses the capability to append a set of terms to each BoW database, contingent upon specific categories. The administrator is responsible for manually inputting each unique word into the database. The addition of a word to one category should preclude its addition to any subsequent categories. Hence, it is imperative for the administrator to execute this procedure prior to incorporating new terms into the database. Furthermore, the administrator has the ability to grant authorization to individual users throughout the registration process. Access to a user's profile on the website is restricted to the individual for whom the administrator has granted activation privileges. This is achieved by requiring the user to log in. Individuals who are not granted permission are categorically prohibited from accessing their personal accounts, regardless of any conditions.

2. **User Registration Module**

In this module, the users need to register with all their basic details and once the user gets registered then they need to request for activation by the admin or server. Once the server activates the users, then only the user can able to login into their account and try to perform the operations such as: Login into their account, send friend requests and receive responses, add posts, receive comments and send replies and so on.

3. **Bag of Words Construction Module**

Here in this section, we try to construct a bag of words (BOW) model in which the admin try to add all the set of abused or vulgar words into the database. Here, the admin try to categorize the cyberbullied communication into five categories such as vulgar, hate, violence, offensive, and sex. Based on the type of word, the admin try to add those words into that appropriate category and finally try to maintain the words in the BoW for classification using support vector machine classification algorithm.

4. **Identify the Bullying Feature Set Module**

The characteristics of bullying have a significant influence and should be carefully considered. The processes for building the bullying feature set Zb are provided here, with the first layer and the other layers being discussed separately. Word embedding and expert knowledge are employed for the first layer. Discriminative feature selection is carried out for the other layers.

5. **Cyberbullied Detection Module**

Here, we try to apply support vector machine and PT Stemmer method to divide the messages into parts and then classify which message contain cyberbullied content and which messages contain normal content. Based on the words which are present in the message, the system tries to identify the cyberbullied users and normal users separately. Finally, the admin try to maintain all the log information about cyberbullied users and normal users and then present that information for end users.

3 Experimental Results

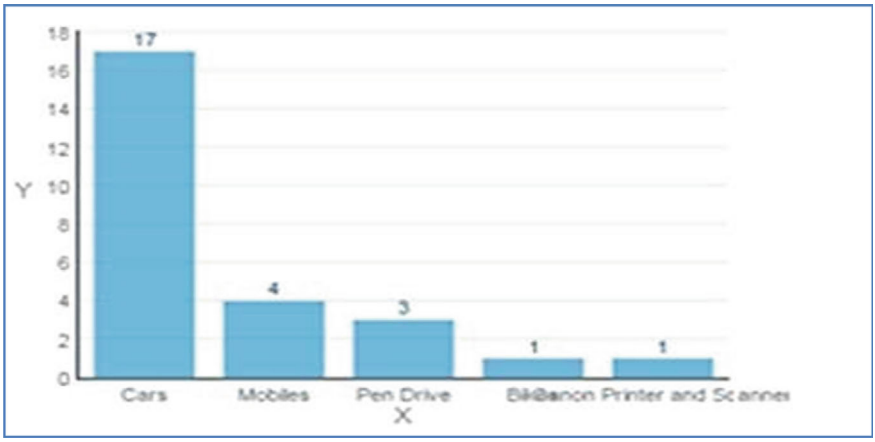
In this section, we try to design our current model using JAVA as programming language and taking MY-SQL as storage database. Here, we try to construct the application in the form of online social networks simulated with the same functionalities and then test the current application on that current model. In order to test the efficiency using SVM algorithm, we try to maintain bag of words (BOW) model and then add all sets of cyberbullying words inside the database.

All Filter Words..

Violence	[attack, wildness, storm, fury, clash, assault, abondon, acuteness, terrorism, scum, kill, idiot]
Vulgur	[unworthy, low, crude, boorish, raw, malicious, improper, nasty, gripe, fuck]
Offensive	[frog, honky, spade, whitey, rude, off-color, evil, annoying, embarrasing, hell]
Hate	[horror, disgust, mislike, objection, spite, trouble, hatred, hostility, bad]
Sexual	[coupling, lovemaking, screw, union, douchebag]

Bag of Words

Cyber Bulled Users Graph



From the above figure, we can clearly find out the set of cyberbullied users who try to post cyberbullied messages on several post.

4 Conclusions

In the present study, we have ultimately determined that our model is capable of providing precise outcomes for distinguishing between cyberbullied users and non-cyberbullied users with a high level of accuracy. These forms of communication are mostly disseminated on the personal profiles of users with the intention of subjecting adolescents, preadolescents, and other minors to harassment through the dissemination of offensive content. In this study, we aim to develop a model utilizing support vector machine (SVM) and Porter's Stemming approaches to classify tweets based on a bag of words (BOW) model. The objective is to distinguish between tweets that exhibit cyberbullying behavior and those that are considered normal. In this study, the cyberbullying conversations are categorized into five distinct classifications as identified in existing literature: hate speech, vulgar language, offensive content, sexual references, and violent content. Through the implementation of several experiments on our proposed model, utilizing online social networks as a simulated environment, our simulation outcomes unequivocally indicate the high efficacy of our model in accurately recognizing instances of cyberbullying inside communications.

References

1. Yin D, Xue Z, Hong L, Davison BD, Kontostathis A, Edwards L (2009) Detection of harassment on web 2.0. In: Proceedings of the content analysis in the WEB, vol 2, pp 1– 7
2. Dinakar K, Reichart R, Lieberman H (2011) Modeling the detection of textual cyberbullying in the social mobile web
3. Nahar V, Li X, Pang (2012) An effective approach for cyberbullying detection," Communications in Information Science and Management Engineering, 2012.
4. Dadvar M, de Jong F, Ordelman R, Trieschnigg R (2012) Improved cyberbullying detection using gender information. In: Proceedings of the 12th—Dutch-Belgian information retrieval workshop (DIR2012). ACM, Ghent, Belgium
5. Dadvar M, Trieschnigg D, Ordelman R, de Jong F (2013) Improving cyberbullying detection with user context. Adv Inf Retrieval. 693–696 (Springer)
6. Vincent P, Larochelle H, Lajoie I, Bengio Y, Manzagol P-A (2010) Stacked denoising autoencoders: learning useful representations in a deep network with a local denoising criterion. J Mach Learn Res 11:3371–3408
7. Baldi P (2012) Autoencoders, unsupervised learning, and deep architectures, unsupervised and transfer learning challenges in machine. Learning 7:43
8. Chen M, Xu Z, Weinberger K, Sha F (2012) Marginalized denoising autoencoders for domain adaptation. arXiv:1206.4683
9. Jayanthi Rao M, Kiran Kumar R (2020) Follicle detection in digital ultrasound images using BEMD and adaptive clustering algorithms. In: Lecture notes in mechanical engineering, pp 651–659
10. Jayanthi Rao M, Kiran KR, Harikiran J (2019) Method for follicle detection and ovarian classification in digital ultrasound images using geometrical features. J Adv Res Dyn Control Syst 11(2):1249–1258
11. Jayanthi Rao M, Apparao D, Ramakrishna B, Durga Prasad KG, Ramana BV, Ramanaiah M (2023) Intelligent traffic monitoring system using vehicular ad hoc network. Int J Recent Innov Trends Comput Commun 11(10):629–635
12. Jayanthi Rao M, Prasanthi P, Suresh Patnaik P, Divya M, Sureshkumar J, Ramanaiah M (2022) Forecasting systems for heart disease using advanced machine learning algorithms. Int J Food Nut Sci 11(7):1257–1268
13. Jayanthi Rao M, Divya M, Ratnan Mohitha M, Prasanthi P, Paparao S, Ramanaiah M (2022) Analyzing the effectiveness of convolutional neural networks and recurrent neural networks for recognizing facial expression. Int J Food Nut Sci 11(7):1269–1282
14. Griffiths TL, Steyvers M (2004) Finding scientific topics. Proc Natl Acad Sci USA 101:5228–5235
15. Blei DM, Ng AY, Jordan MI (2003) Latent dirichlet allocation. J Mach Learn Res 3:993–1022
16. Hofmann T (2001) Unsupervised learning by probabilistic latent semantic analysis. Mach Learn 42:177–196
17. Bengio Y, Courville A, Vincent P (2013) Representation learning: a review and new perspectives. Pattern Anal Mach Intell. IEEE Trans 35:1798–1828
18. McLaughlin BL, Braga AA, Petrie CV, Moore MH (2002) Deadly lessons: understanding lethal school violence. National Academies Press
19. Kaplan AM, Haenlein M (2010) Users of the world, unite! The challenges and opportunities of social media. Bus Horizons 53:59–68
20. Reynolds K, Kontostathis A, Edwards L (2011) Using machine learning to detect cyber bullying. In: 2011 10th international conference on machine learning and applications and workshops, Honolulu, HI, USA, pp 241–244

21. Hani J, Nashaat M, Ahmed M, Emad Z, Amer E, Mohammed A (2019) Social media cyberbullying detection using machine learning. Int J Adv Comput Sci Appl 10(5):703–707
22. Chauhan S, Reddy DE, Vijayasree B, Jayanthi Rao M, Ramalingaswamy C, Soumya Ranjan N, Sheshikala M, Lavanya K, Debebe TD (2024) Nigat detection of COVID-19 using edge devices by a light-weight convolutional neural network from chest X-ray images. BMC Med Imaging 24:1

Multi-objective Optimal Power Flow Using Krill Herd Algorithm



Bondalapati Devasahayam and B. Venkateswara Rao

Abstract In this paper, a different biologically enthused Krill Herd algorithm is used for optimal power flow (OPF) with the four objectives reduction of power loss, reduction of emission, minimization of voltage deviation and reduction of generation cost is considered. The proposed Krill Herd algorithm approach is accepted on the standard IEEE 30 bus to solve four objectives and simulation results are related with PSO and NSGA2. The imitation results are compared with the dominance of the proposed tactic and confirm it is likely to solve the OPF problem.

Keywords Active power loss · Krill Herd · Emission · Voltage deviation · Optimal power flow · Generation cost

1 Introduction

In today's world, the consumption of electricity is increasing day by day, so the demand for electricity is increasing, resulting in voltage instability, line overload, congestion and power system blackouts. Therefore, the various resources of electric grids should be optimally planned to reduce costs and improve performance. You need this smart optimization technique. OPF problem is one of the most researched topics in the community of power systems. The objective of optimum power flow (OPF) is to find the optimal combination of the actual output level, voltage value and tap position of the load-changing transformer (LTC) and minimize the sum. This reduces the actual power loss while removing the physical and technical limitations of the network. A KHA is used to solve the four single objectives of cost of power generation, voltage deviation, emissions and power loss. The NSGA algorithm is used for renewable energy sources embedded in IEEE 30 buses to minimize generation costs, active power losses, voltage deviations and emissions [1]. Proposed to use PSO algorithm in IEEE 6th bus, where the main objective functions are to minimize

B. Devasahayam · B. Venkateswara Rao (✉)
Department of EEE, V R Siddhartha Engineering College, Kanuru, AP, India
e-mail: bvrao.eee@gmail.com; drbvrao@vrsiddhartha.ac.in

© The Author(s), under exclusive license to Springer Nature Singapore Pte Ltd. 2025

B. B. V. L. Deepak et al. (eds.), *Recent Advancements in Product Design and Manufacturing Systems*, Lecture Notes in Mechanical Engineering,
https://doi.org/10.1007/978-981-97-6732-8_37

power loss and maximize power generation [2]. Explained forecasting probabilities of generation planning, transmission planning and long term [3]. Explained here how minimized fuel cost, power loss and thermal unit emissions were in this IEEE 30 bus system by using Mayfly algorithm [4]. Explained the integrated renewable energy of wind into IEEE 30 bus system. Minimized generation cost and improvement of reactive power [5]. Explained minimization of generation cost with adaptive modified gravitational search algorithm [6]. Explained the minimization of generation cost and minimization of transmission losses applied differential evolution algorithm [7]. The use of the Weibull possibility distribution purpose is to demonstrate the use of wind power generation and model of stochastic nature. Uncertainty is considered as a limitation for systems with random variables. [8]. PSO algorithm for the finest situations of OPF problem regulator variables tested on the IEEE 30 bus system [9]. The extensive review of the KH algorithm in the area of submissions and crossings across these arenas is discussed [10]. Proposed to solve optimization tasks and solve a wide range of benchmark optimization problems [11]. Minimization of voltage deviation and generation cost and performed on IEEE 30, IEEE 57 and IEEE 118 using KHA [12].

The novelty of this work can be summarized as below:

- KH algorithm is proposed for OPF problem, which results in accurate solutions;
- MATLAB was applied to solve the optimization problem with different case studies.

2 Problem Formulation

2.1 Mathematical Formulation of Multi-objective

The MOOPF is a nonlinear optimization tricky is the main objective to optimize control variables with respect to two or more objective functions to satisfy constraints. In these two objectives are converted into single objective by taking weighting factors into consideration.

2.2 Objectives of the Problem Formation:

Minimization of the generation cost:

$$C_{\mathrm{t}} = \sum_{i=1}^{N_{\mathrm{G}}} a_i + b_i P_{G_i} + c_i P_{G_i}^2 + |d_i * \sin(e_i * (P_{\mathrm{G}_i} - P_{\mathrm{G}_i}))| \tag{1}$$

a_i, b_i, c_i—cost coefficients of ith generator and d_i, e_i ith generator with loading effects

Minimization of real power loss:

$$P_{\text{loss}} = \sum_{i=1}^{\text{nl}} \sum_{j \neq i}^{\text{nl}} G_{ij} \left[V_i^2 + V_j^2 - 2V_i V_j \cos\left(\delta_i - \delta_j\right) \right] \tag{2}$$

G_{ij} denotes the transfer-conductance between bus i and j.

Minimization of voltage deviation:

$$\text{VD} = \sum_{m=1}^{\text{NL}} |V_{\text{Lm}} - 1.0| \tag{3}$$

Minimization of emission:

$$\text{emission} = \sum_{i=1}^{\text{NG}} \propto_i + \beta_i P_{\text{G}_i} + \gamma_i P_{\text{G}_{2i}} + \varsigma_i e\left(\varphi_i P_{\text{G}_i}\right) \tag{4}$$

where $\propto_i$, β_i, γ_i, ς_i, φ_i is the emission coefficients of the ith gen.

The OPF obtains ideal settings of regulated variables to reduce a chosen objective function of satisfying the other constraints. The chosen optimization objective is often a specific objective, such as production cost, or a single objective transformed by several objectives using a weighted summation approach. This method gives only one solution. However, multi-objective optimization techniques allow you to simultaneously optimize several different objectives and select multiple feasible solutions.

In general, multi-objective OPF problem can be formulated as

$$\text{Minimize} f(x, y) = \{f_1(x, y), \ldots, f_{\text{m}}(x, y)\} \tag{5}$$

$$\text{S.t.} \quad g(x, y) \tag{6}$$

$$h(x, y) \leq 0 \tag{7}$$

where $f(x, y)$ represents optimization objective, m is number of optimization objective. $g(x, y)$ represents constrains and $h(x, y)$ is the inequality limitations. x denotes control variables and y denotes state variables correspondingly [1].

2.3 Constraints

In general, OPF problems have two main constraints, including equation constraints and inequalities. In particular, parity constraints are mainly due to the balance of input and output power, while inequality constraints arise by considering some operational constraints. For OPF power system networks, generator active power, i.e., reactive power, must be equal to active load demand and active power losses. Therefore, the equality constraint of OPF can be formulated as

$$P_{G_i} = P_{D_i} + V_i \sum_{j=i}^{NB} V_j \left[G_{ij} \cos(\delta_i - \delta_j) + B_{ij} \sin\left(\delta_i - \delta_j\right) \right] \tag{8}$$

$$Q_{G_i} = Q_{D_i} + V_i \sum_{j=i}^{NB} V_j \left[G_{ij} \cos(\delta_i - \delta_j) + B_{ij} \sin\left(\delta_i - \delta_j\right) \right] \tag{9}$$

where P_{D_i} is the demand for active load and Q_{D_i} is the reactive load. Q_{D_i} is ith bus voltage angle. G_{ij}—conductance and B_{ij}—susceptance between buses i and j. NB—number of buses [1].

3 Methodology

The KH is an innovative efficient biology encouraged population constructed optimization method introduced by Gandomi and Alavi in 2012. Based on individual krill grazing behavior, each krill moves in a multidimensional search space to find food density.

Objective function for krill migration is restrained by the unswerving distance from individual krill prey and the highest crowding density. Krills move in multidimensional space, and each krill moves the other krill to adjust its position, searching for migration and random diffusion. Flow char for KH is provided in Fig. 1.

Step 1: Randomly set the population for N krills.

Step 2: Estimate appropriateness value for apiece krill.

According their fitness value, we find which one is best and which one is worst

Step 3: Perform motion calculations

Movement of other individuals: For krill individual movement calculated as

$$N_i^{\text{new}} = N^{\max} \alpha_i + \omega_n N_i^{\text{old}} \tag{10}$$

where $N^{\max}$ = maximum induced motion, ω_n = inertia weight {0, 1}, N_i^{old} = last induced motion

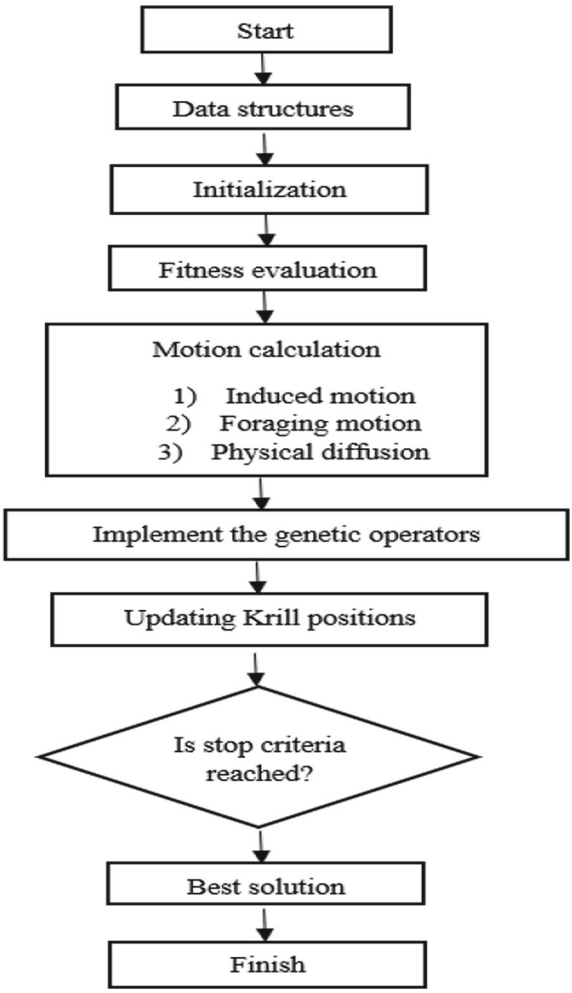


Fig. 1 Flow chart for KHA

Foraging activity: Foraging activity is formulated by feeding point and prior knowledge about the location.

$$F_i = V_f \beta_i + \omega_f F_i^{\text{old}} \tag{11}$$

$$\beta_i = \beta_i^{\text{food}} + \beta_i^{\text{best}} \tag{12}$$

$$X^{\text{food}} = \frac{\sum_{i=1}^{N} \frac{1}{K_i} X_i}{\sum_{i=1}^{N} \frac{1}{K_i}} \tag{13}$$

Random physical diffusion: The random carnal diffusion of krill computed as diffusion is equal to net movement.

$$D_i = D^{\max}\delta \tag{14}$$

where $D^{\max}$ is the maximum dissemination speed, δ is the arbitrary steering vector

$$D_i = D^{\max}\left(1 - \frac{I}{I_{\text{ma}}}\right)\delta \tag{15}$$

Step 4: Update each krill position.

$$\frac{\mathrm{d}_{x_i}}{\mathrm{d}t} = N_i + F_i + D_i \tag{16}$$

Step 5: Discovery new-fangled position $(t + 1)$ for apiece krill.

Step 6: Assess each krill rendering to their novel position.

Cross-over component: Each associate of krill updates its existing position using situation of other

$$X_{i,m} = \{X_{r,m} \quad \text{rand}_{i,m} < C_r\} \tag{17}$$

$$X_{i,m} \quad \text{else}$$

$$C_r = 0.2K_{i,\text{best}}$$

$r \in [1, 2,\ldots, i - 1, i + 1, \ldots, N]$. With this new-fangled crossover possibility, the global best crossover possibility is zero and increases as fitness decreases.

Mutation: Measured by mutation restriction. Modification in best solution for the adaptive mutation arrangement used here is verbalized as:

$$X_i, = \{X_{\text{gbes}}, m + \ (X_p, m - X_q, m)\text{rand}_i, m < \text{Mu}\} \tag{18}$$

$$X_i\, m \quad \text{else}$$
$$\text{Mu} = 0.05/K_{i,\text{best}}$$

4 Results and Discussion

Four cases were taken to optimize objective functions. Case 1 is a solo objective function and remaining Case 2 to Case 4 were multi-objective functions. KHA is performed on an IEEE 30 bus system, and results are related with NSGA2 and PSO. Results were discussed in detail below.

Results for Case 1 Reduction of generation cost is a single objective function; here KHA algorithm is applied to IEEE 30 bus system for test case and those results were compared with PSO in Table 1; in PSO test case, the generation cost is 800.41 $ whereas KHA obtained 795.0311 $ compared with PSO, and KHA got best optimization value. Figure 2 shows convergence characteristics for both KHA and PSO. Total iterations were 500 but convergence was taken between 50 and 180 iterations only.

Table 1 Comparison between KHA and PSO for Case 1

Minimization of generation cost		
Algorithm	PSO	KHA
Control variables		
P_{g2} (MW)	75.165	79.013
P_{g3} (MW)	20.546	25.249
P_{g4} (MW)	17.986	15.008
P_{g5} (MW)	27.786	28.537
P_{g6} (MW)	36.076	34.608
V_1 (pu.)	1.0821	1.0500
V_2 (pu.)	1.0636	1.0441
V_3 (pu.)	1.0259	1.0398
V_4 (Pu.)	1.0389	1.0301
V_5 (Pu.)	1.0921	1.0436
V_6 (Pu.)	1.0584	1.0187
State variables		
P_{g1} (MW)	108.256	100.9061
Q_{g1} (MVAr)	− 17.895	− 11.8066
Q_{g2} (MVAr)	20	16.9098
Q_{g3} (MVAr)	25.486	24.7413
Q_{g4} (MVAr)	30	40
Q_{g5} (MVAr)	17.963	18.1981
Q_{g6} (MVAr)	26.789	23.5463
Objective		
Cost ($)	800.41	**795.0311**

Bold indicates the objective function value

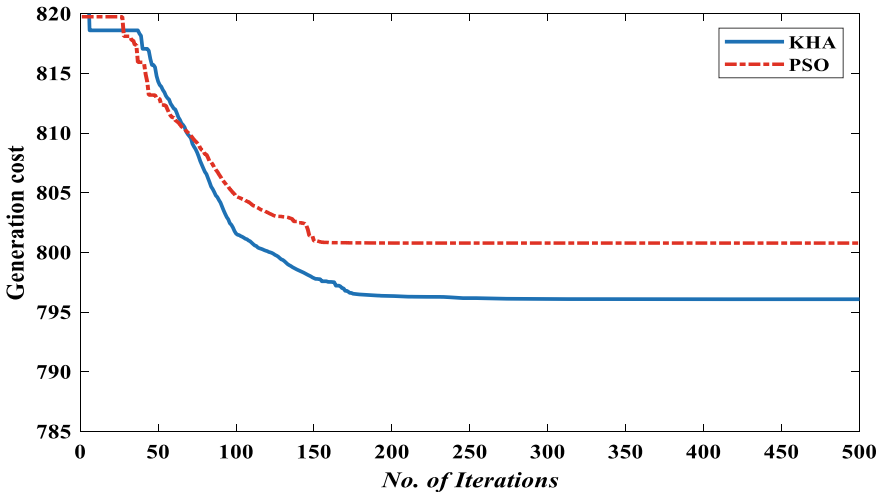


Fig. 2 Generation cost convergence of KHA and PSO

Results for Case 2 It is a multi-objective case. Minimization of generation cost and real power loss is considered as objective function and both algorithms tested IEEE 30 bus system from observing Table 2 the comparison of KHA with NSGA2, KHA obtained best optimal solution for both generations cost 837.6054 $ and real power losses 5.6925 MW were as NSGA2 obtained cost 870.249 $ and power loss 7.002 MW. Figure 3 explains about convergence for generation cost and Fig. 4 explains convergence for power losses, between KHA and NSGA2.

Results for Case 3 Reduction of generation cost and voltage deviation was multi-objective functions. Comparison for both KHA and NSGA2 is shown in Table 3. Compared to Case 2 in Case 3, generation cost is reduced because pg1 + pg2 generated less than Case 2; in Case 3, cost value is 813.172 $ which is less than 837.605 $ in Case 2. KH obtained better solutions compared with NSGA2 as shown in Fig. 5. Figure 6 shows the convergence curve for generation cost and voltage deviation.

Result for Case 4 Here in this case, all four objective functions were taken to optimization—voltage deviation, cost, emission and real power losses, whereas in previous cases, only two objectives were considered but, in this case, all four objectives were taken and tested results were KHA obtained best results compared with NSGA2; Table 4 gives the comparison and values for four objectives, real power losses, cost, emission, voltage deviation and all are significantly better values compared with NSGA2; Figs. 7 and 8 show the convergence for cost, power loss between KHA and NSGA2; Figs. 9 and 10 show the voltage deviation and emission convergence curves.

Table 2 Minimization of real power losses between NSGA2 and KH

Algorithm	NSGA2	KH
Control variables		
P_{g2} (MW)	61.385	62.599
P_{g3} (MW)	46.785	58.878
P_{g4} (MW)	29.447	29.101
P_{g5} (MW)	29.243	25.433
P_{g6} (MW)	37.518	38.783
V_1 (pu.)	1.061	1.097
V_2 (pu.)	1.032	1.095
V_3 (pu.)	1.031	1.070
V_4 (Pu.)	1.095	1.081
V_5 (Pu.)	1.089	1.059
V_6 (Pu.)	1.098	1.008
State variables		
P_{g1} (MW)	119.298	139.121
Q_{g1} (MVAr)	14.222	− 20
Q_{g2} (MVAr)	5.197	44.796
Q_{g3} (MVAr)	6.635	32.381
Q_{g4} (MVAr)	40	40
Q_{g5} (MVAr)	27.862	− 5.280
Q_{g6} (MVAr)	25	25
Objective		
P_{Loss} (MW)	**7.002**	**5.692**
Cost ($)	870.249	837.605

Bold indicates the objective function value

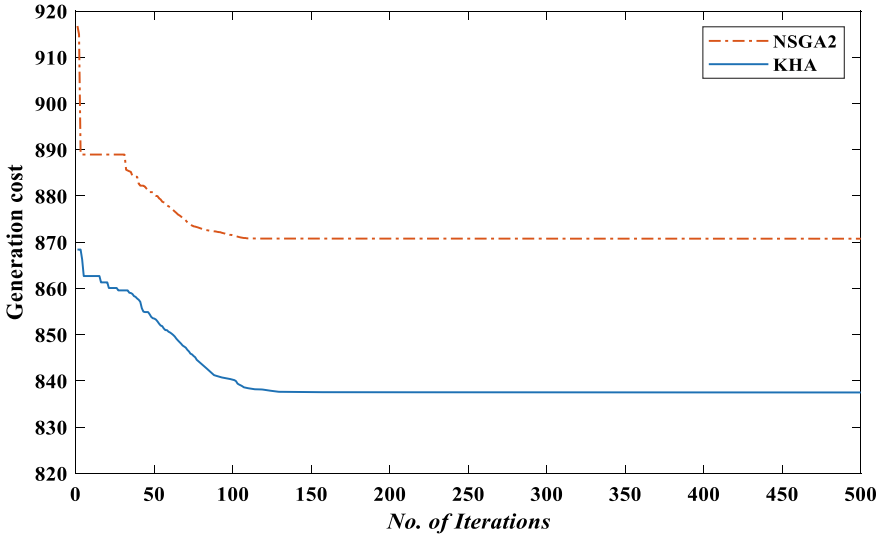


Fig. 3 Generation cost convergence of KH and NSGA2

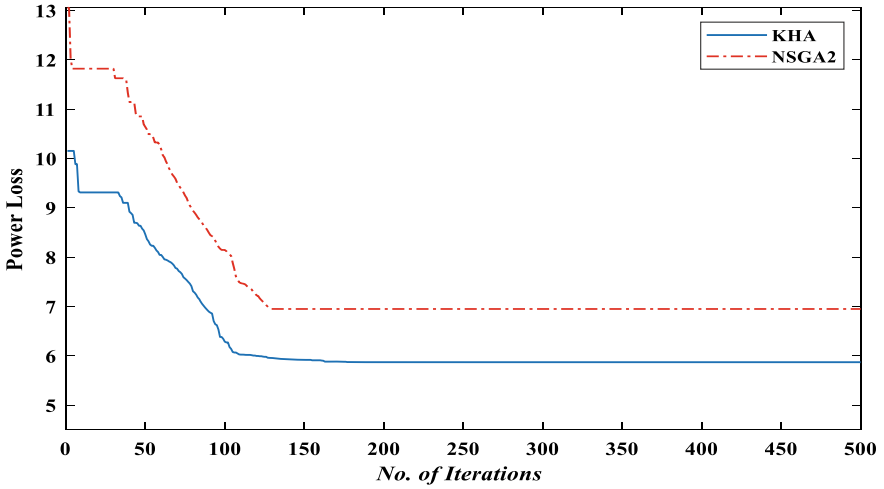


Fig. 4 Convergence of power loss for KH and NSGA2

Table 3 Minimization of voltage deviation for NSGA2 and KH

Minimization of generation cost and VD		
Algorithm	NSGA2	KH
Control variables		
P_{g2} (MW)	34.56117	39.316
P_{g3} (MW)	44.79807	46.987
P_{g4} (MW)	26.88086	25.669
P_{g5} (MW)	26.57122	16.303
P_{g6} (MW)	21.38556	25.682
V_1 (pu.)	1.065365	1.0273
V_2 (pu.)	1.046806	1.0386
V_3 (pu.)	1.019496	1.0901
V_4 (Pu.)	1.022423	1.0748
V_5 (Pu.)	1.028592	1.0662
V_6 (Pu.)	1.024107	1.0491
State variables		
P_{g1} (MW)	136.548	138.864
Q_{g1} (MVAr)	− 6.243	− 20
Q_{g2} (MVAr)	60	60
Q_{g3} (MVAr)	− 13.752	14.725
Q_{g4} (MVAr)	40	40
Q_{g5} (MVAr)	18.566	11.695
Q_{g6} (MVAr)	25	13.529
Objective		
Generation cost ($)	849.078	813.172
VD (p.u)	**0.986**	**0.785**

Bold indicates the objective function value

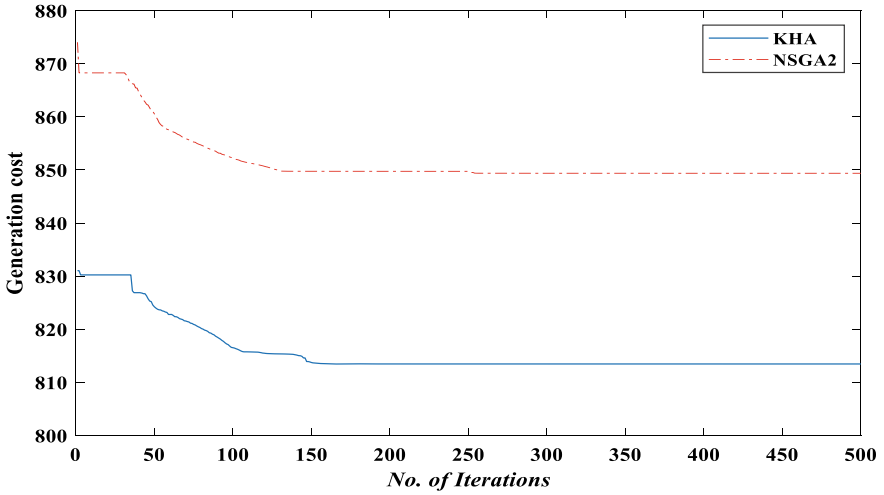


Fig. 5 Convergence of generation cost for KH and NSGA2

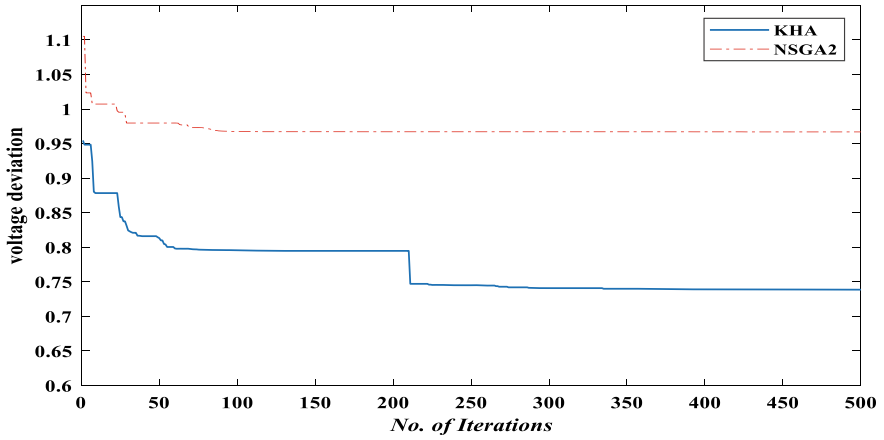


Fig. 6 Convergence of voltage deviation for KH and NSGA2

Table 4 Minimization of emission for NSGA2 and KH

Algorithm	NSGA2	KH
Control variables		
P_{g2} (MW)	70.13275	67.383
P_{g3} (MW)	45.7283	25.295
P_{g4} (MW)	13.21745	25.836
P_{g5} (MW)	23.2357	33.449
P_{g6} (MW)	19.07768	20.261
V_1 (pu.)	1.060323	1.0721
V_2 (pu.)	1.089842	1.0363
V_3 (pu.)	1.015922	1.0384
V_4 (Pu.)	1.068323	1.0814
V_5 (Pu.)	1.093595	0.97772
V_6 (Pu.)	1.009302	1.0535
State variables		
P_{g1} (MW)	100.551	66.027
Q_{g1} (MVAr)	− 19.246	− 20
Q_{g2} (MVAr)	60	60
Q_{g3} (MVAr)	35	− 21.880
Q_{g4} (MVAr)	16.559	40
Q_{g5} (MVAr)	3.992	30
Q_{g6} (MVAr)	25	25
Objective		
Cost ($)	**894.216**	**833.610**
Power loss (MW)	**6.970**	**6.809**
Emission (t/h)	**0.280**	**0.116**
VD (p.u)	**1.033**	**0.550**

Bold indicates the objective function value

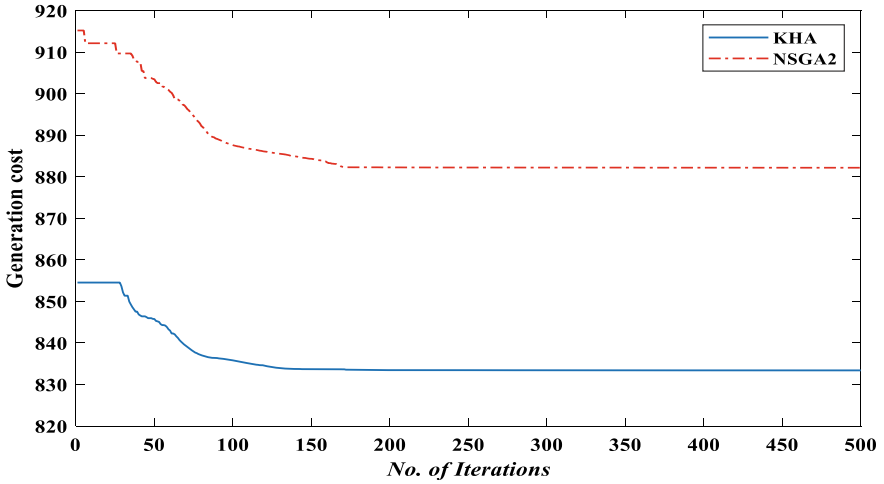


Fig. 7 Convergence of generation cost for KHA and NSGA2

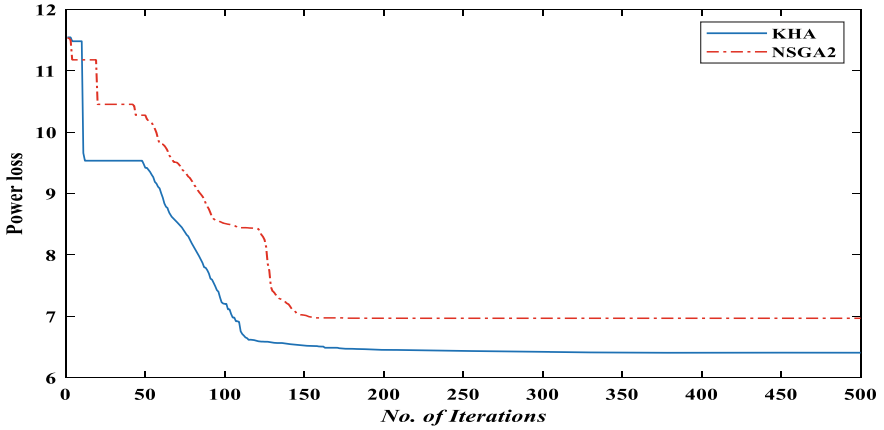


Fig. 8 Convergence of power loss for KHA and NSGA2

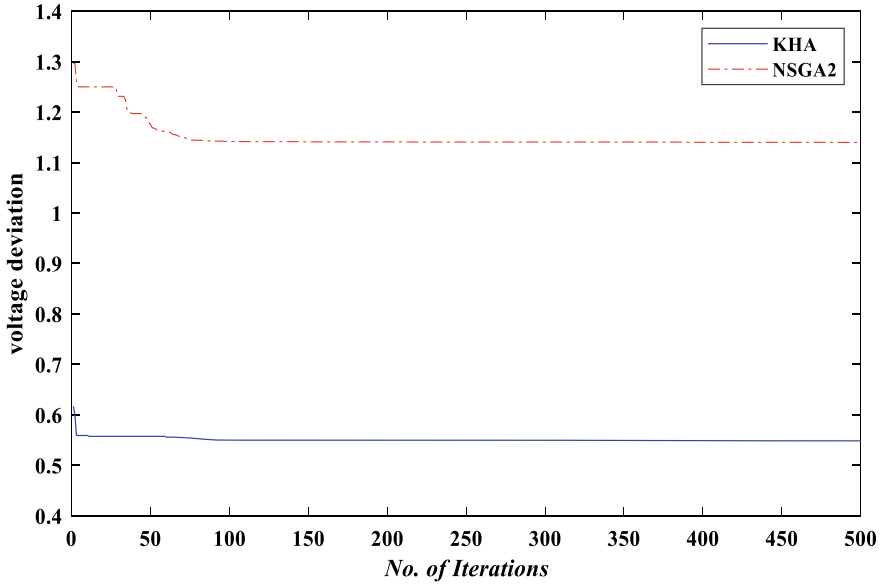


Fig. 9 Convergence of voltage deviation for KHA and NSGA2

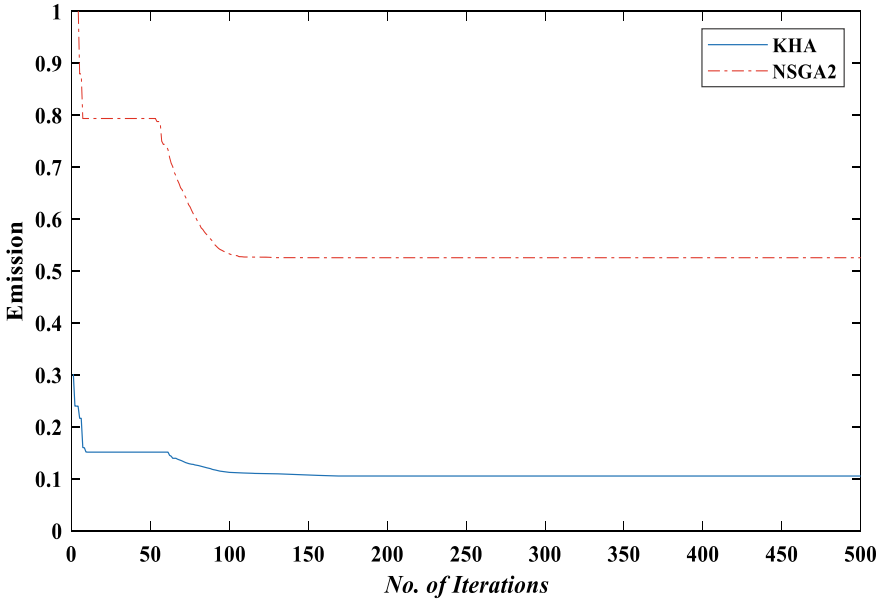


Fig. 10 Convergence of emission for KHA and NSGA2

5 Conclusion

In this paper, OPF is performed to minimize the objective functions in Case 1; it is single objective function minimizing generation cost and remaining cases where multi-objective functions include power loss, voltage deviation, and emission, along with generation cost. From the results, in each test case, the applied KHA provides better voltage deviation, power loss, emission and generation cost compared with the PSO and NSGA2. In future Incorporating renewable energy sources, such as wind and solar, at different generator buses and can be tested on IEEE 57 bus, IEEE 30 bus and IEEE 118 bus systems. And FACTS devices also can be added to obtain less power loss.

References

1. Li S, Gong W, Wang L, Gu Q (2022) Multi-objective optimal power flow with stochastic wind and solar power, vol 114. Elsevier, p 108045. https://doi.org/10.1016/j.asoc.2021.108045
2. Lakshmi P, Rao BV, Devarapalli R, Rai P (2020) Optimal power flow with Bat algorithm for a power system to reduce transmission line losses using SVC. In: 2020 ICEFEET, pp 1–5. https://doi.org/10.1109/ICEFEET49149.2020.9186964
3. Milligan M, Donohoo P, O'Malley M. Stochastic methods for planning and operating power systems with large amounts of wind and solar power. National Renewable Energy Laboratory (NREL), Golden
4. Khameles AK, Abdelaziz AY, Eskaros MR, Alhelou HH. Stochastic modeling for wind energy and multi-objective optimal power flow by novel meta-heuristic method. IEEE Access https://doi.org/10.1109/ACCESS.2021.3127940
5. Chaitanya SNVSK, Ashok Bakkiyaraj R, Venkateswara Rao B (2021) Optimal reactive power dispatch of interconnected power system using firefly algorithm. In: Komanapalli VLN, Sivakumaran N, Hampannavar S (eds) Advances in automation, signal processing, instrumentation, and control. Lecture notes in electrical engineering, vol 700. Springer, Singapore. https://doi.org/10.1007/978-981-15-8221-9_22
6. Biswas PP, Suganthan PN, Amaratunga GAJ (2017) Optimal power flow solutions incorporating stochastic wind and solar power. Energy Conserv Manage 148:1194–1207. https://doi.org/10.1016/j.enconman.2017.06.071
7. Niknam T, Massrur HR. Stochastic mid-term generation scheduling incorporated with wind power. Electr Power Energy Syst (Elsevier). 10.1016 /j.ij.epes.2014.07.076
8. Qu BY, Liang JJ, Zhu YS, Wang ZY, Suganthan PN (2016) Economic emission dispatch problems with stochastic wind power using summation based multi-objective evolutionary algorithm. Inf Sci 351 (Elsevier). https://doi.org/10.1016/j.ins.2016.01.081
9. Abido MA (2020) Optimal power flow using particle swarm optimization. Int J Electr Power Energy Syst 24(7) (Elsevier). https://doi.org/10.1016/S0142-0615(01)00067-9.
10. Bolaji AL, Al-Betar MA, Awadallah MA, Khader AT, Abualigah LM (2016) A Comprehensive review: Krill Herd algorithm and its applications. Appl Soft Comput 49 (Elsevier). https://doi.org/10.1016/j.asoc.2016.08.041
11. Gandomi AH, Alvi AH (2012) Krill Herd: A new bio-inspired optimization algorithm. Commun Nonlinear Sci Numer Simul 17(12) (Elsevier). https://doi.org/10.1016/j.cnsns.2012.05.010
12. Roy PK, Paul C. Optimal power flow using krill herd algorithm. Int Trans Electr Energy Syst 25(8). https://doi.org/10.1002/etep.1888

Optimal Reactive Power Dispatch Using Improved Grey Wolf Algorithm



K. Bhaskara Sandhya, S. N. V. S. K. Chaitanya, B. Venkateswara Rao, and R. Ashok Bakkiyaraj

Abstract This paper proposes the meta-heuristic algorithm as an answer to optimal reactive power dispatch (ORPD) in a power system. Single (or) multi-objective functions are used to solve ORPD. In this case, the multi-objective function is specially used. The purpose is to reduce the actual electricity consumption and voltage deviation, instead of limiting the technical equality and inequality. This segment consists of voltage management for generator buses, transformer taps, and reactive power compensators. The IEEE 30-bus system is used to test the proposed improved Grey Wolf Optimizer for multi-objective optimization using MATLAB software.

Keywords Optimal reactive power · Active power · Reactive power · Improved grey wolf · Multi-objective

1 Introduction

Modern energy companies face many demanding situations due to the increasing call for energy; however, the growth of transmission and power generation has been constrained by resources, environmental constraints, and right-of-way issues [1]. The main cause of such instability is due to heavy system load. Other causes of instability of voltage are (1) insufficient reactive power, (2) line failure, (3) generator shutdown, and (4) poor coordination between device and control. Optimal redistribution of reactive power generation provides a very robust solution to voltage instability [2].

K. Bhaskara Sandhya · B. Venkateswara Rao (✉)
Department of EEE, V R Siddhartha Engineering College, Vijayawada, India
e-mail: drbvrao@vrsiddhartha.ac.in

S. N. V. S. K. Chaitanya
VR Siddhartha Engineering College, Vijayawada, India

R. A. Bakkiyaraj
EE Department, Annamalai University, Chidambaram, Tamil Nadu, India

© The Author(s), under exclusive license to Springer Nature Singapore Pte Ltd. 2025

B. B. V. L. Deepak et al. (eds.), *Recent Advancements in Product Design and Manufacturing Systems*, Lecture Notes in Mechanical Engineering,
https://doi.org/10.1007/978-981-97-6732-8_38

Optimal distribution of reactive power can be a nonlinear optimization problem. The principle purpose of ORPD is to lessen the energetic power consumption of the gadget and hold the voltage profile in the positive limits and maintain voltage within system reliability limits and minimize active power losses [3]. At certain stages in the configuration of typical networks, generator bus voltages and passive components, including transformers, must be considered [4].

To overcome this ORPD problem, a few meta-heuristics optimization techniques were implemented, improved slime mould algorithm [5], moth-flame optimizer algorithm [6], modified sine cosine algorithm [7], artificial bee colony algorithm [8], sunflower algorithm [9], a novel optimization algorithm [10], particle swarm optimization and LP approach [11], PSO with time carrying acceleration coefficients [12], particle swarm optimization [13], modified stochastic fractal seek set of rules [14], improved GSA-based set of rules with novel techniques to address constraints [15], chaotic Krill Herd algorithm [16], hybrid Nelder-Mead simplex-based firefly algorithm [17], used new multi-objective strategy [18], SBDE and DE strategy algorithm [19], gravitational search optimizer [20], JAYA algorithm [21], sine–cosine algorithm [22], those all papers are minimizing the real electricity losses, and minimize overall voltage deviation using unique strategies and examined one of a kind bus systems.

The problem of ORPD increases as the size and complexity of the network increase and as the problem becomes significantly more difficult to solve. Industries also helped expand the use of electrical energy. In past decades, energy companies owned relatively few generators compared to the numbers installed today due to the rise of independent power producers. Demand response programmes, on the other hand, add variables to the burden side of the ORPD problem.

The novelty of this work can be summarized:

- IGWO algorithm is proposed for ORPD problem, which results in accurate solutions compared to GWO;
- MATLAB has been applied to solve the optimization problem with different case studies.

2 Problem Structure

The proposed work presents a new technique, an improved Grey Wolf Optimization, to solve the ORPD problem. ORP flow, transmission losses are considered as performance indices. The main objective functions are:

1. Active power losses
2. Total voltage deviation.

Subject to constraint of equality is power balance equation. Constraints of inequality are generator constraints, reactive compensation sources, and voltage limits parameter limits.

1. Active power losses minimization:

Equation (1) is used to limit the energetic strength loss in an ORPD problematic transmission line.

$$F_1 = F_L = \text{Min}(P_L) = \sum_{k=1}^{N_l} G_K \left[V_m^2 + V_n^2 - 2V_m V_n \cos(\delta_m - \delta_n) \right), \tag{1}$$

where k denotes the branch of buses between m and n; FL represents the power losses minimization function; P_L and G_K are the mutual conductance of department k. The voltage angles δ_m and δ_n on buses m and n, N_l are transmission lines generally numbered.

2. Total voltage deviation (TVD) minimization

To reduce the voltage, collapse so that the voltage is properly maintained. So, improve the voltage profile and reduce voltage sags. In Eq. (2), minimize voltage deviation.

$$F_2 = \sum_{m=1}^{N_B} |V_m - 1|, \tag{2}$$

where N_B is the number of buses, V_m is the voltage magnitude on buses 1 to n.

3. Multi-objective optimization

This function combines transmission line loss target and voltage deviations optimized simultaneously by considering the same age weighting factor for both targets.

$$F = w_1 f_1 + w_2 f_2, \tag{3}$$

- w_1, w_2 are the optimized weights
- f_1 is the power loss minimization function.
- f_2 is the voltage deviation function.

2.1 Equality Restrictions

Using the ORPD, the equality constraints clear up the subsequent Eqs. (4–5).

$$P_{Gm} - P_{Dm} - V_m(G_{mn} \cos(\delta_m - \delta_n) + B_{mn} \sin(\delta_m - \delta_n)) = 0 \tag{4}$$

$$Q_{Gm} - Q_{Dm} - V_m(G_{mn} \sin(\delta_m - \delta_n) + B_{mn} \cos(\delta_m - \delta_n)) = 0, \tag{5}$$

where P_{Gm} and Q_{Gm} are the energetic and reactive strength generation of bus m. P_{Dm} and Q_{Dm} are lively and reactive power load necessities for bus m. B_{mn} is the mutual susceptance and G_{mn} is the mutual conductance.

2.2 Inequality Restrictions

1. Generator Limitation: The voltage generator V_{Gm} is limited by upper and lower limits in a given Eq. (6)

$$V_{Gm,minimum} \leq V_{Gm} \leq V_{Gm,maximum,} \tag{6}$$

   where N_G is generator numbers.
2. Tap setting restrictions of transformer: Transformer tap positions are within the tolerance specified in Eq. (7).

$$T_{m,minimum} \leq T_m \leq T_{m,maximum,} \tag{7}$$

3. Switchable VAR compensator: The reactive power offered by the variable VAR sources; they are limited via the minimal and maximum limits in Eq. (8).

$$Q_{Gm,minimum} \leq Q_{Gm} \leq Q_{Gm,maximum}. \tag{8}$$

3 Methodology

- The ORPD solution methodologies are often broadly classified into two types; those are conventional (classical) methods and intelligent methods.
- The conventional (standard) methods are supported mathematical programming approaches and are accustomed to solve different sizes of ORPD problems.
- The intelligent methods supported meta-heuristic optimization developed within the recent past can eliminate the drawbacks in conventional methods.
- Deterministic ORPD aboard configurations using MATLAB programming language of IEEE 30 bus systems using new improved grey wolf optimization technique.

4 Optimization Techniques

4.1 Grey Wolf Optimization (GWO)

This technique depends on the behaviour of wolf nature. Mainly consider three leader wolves are α, β, and δ for effective solutions and remaining wolves are ω wolves towards promising areas. GWO is implemented in three methods [23].

4.1.1 Encircle

Grey wolves are modelled in chase position as shown in Eqs. (9–10).

$$D = |C \times X_c(p) - X(p)| \tag{9}$$

$$X(p+1) = X_c(p) - A \times D. \tag{10}$$

X_c Is chase position of wolf's, X denotes vector position of grey wolf, and p is the present iteration.

C and A are coefficient directions computed by the usage of Eqs. (11–12).

$$A = 2 \times r_1 - a(p) \tag{11}$$

$$C = 2 \times r_2. \tag{12}$$

r_1, r_2 is randomly chosen vectors in [0, 1], the 'a' vector is decreasing to zero depending on the number of circles Eq. (13).

$$a(p) = 2 - \frac{2 \times p}{\text{MaxIter}}. \tag{13}$$

4.1.2 Hunting

Mathematically modelled in the hunting behaviour of wolves. α, β, and δ of the position of 3 perfect solution positions are considered. The following formula (14–20) hunting behaviour is described.

$$D_\alpha = |C_1 \times X_\alpha - X(p)| \tag{14}$$

$$D_\beta = \left|C_2 \times X_\beta - X(p)\right| \tag{15}$$

$$D_\delta = |C_3 \times X_\delta - X(p)|. \tag{16}$$

Use Eq. (12) to calculate C_1, C_2, and C_3.

$$X_{i1}(p) = X_\alpha(p) - A_{i1} \times D_\alpha(p) \tag{17}$$

$$X_{i2}(p) = X_\beta(p) - A_{i2} \times D_\beta(p) \tag{18}$$

$$X_{i3}(p) = X_\delta(p) - A_{i3} \times D_\delta(p). \tag{19}$$

The best solutions of the primary are X_α, X, and X In Eq. (11) calculating the A_1, A_2, and A_3, and Eqs. (14–16) calculated D_α, D, and D.

$$X(p+1) = \frac{X_{i1}(p) + X_{i2}(p) + X_{i3}(p)}{3}. \tag{20}$$

4.1.3 Attack

In this case, the process of hunting is finished to stop the moving to chased position, and wolfs attacking is started.

4.2 Improved Grey Wolf Optimizer (IGWO)

To overcome GWO problem, this section proposes IGWO. Compared to GWO, IGWO contains three additional steps: initializations, movement, select, and update [24].

4.2.1 Initialization

Wolves are randomly allotted in the specified region $[i_j, u_j]$ in keeping with to Eq. (21).

$$X_{ij} = i_j + \text{rand}_j[0, 1] \times \left(u_j - i_j\right), i \in [1, N], j \in [1, D]. \tag{21}$$

4.2.2 Movement Phase

IGWO includes another strategy of movement called dimensional learning search strategy (DLH). Using DLH, every wolf is learning from its neighbours of new position of next candidate $X_i(p)$ Eqs. (17–19). The first candidate wolf's new position $X_i(p)$ is calculated using Eq. (20).

The selected wolf is picked randomly by its various neighbours from pop. To this end, first calculate radius $R_i(p)$ and then distance of the present locality of $X_i(p)$ using Eq. (22).

$$R_i(p) = X_i(p) - X_{i\text{ - gwo}}(p+1). \tag{22}$$

The neighbours of $X_i(p)$ denoted by $N_i(p)$ are determined by Eq. (23)

$$N_i(p) = \left\{X_j(p) | D_i\left(X_i(p), X_j(p)\right) \le R_i(p), X_j(p) \in \text{Pop}\right\}. \tag{23}$$

In Eq. (24), different multi-neighbours learning for performed in the d-th dimension.

$$X_{i-\text{DLH},d}(p+1) = X_{i,d}(p) + \text{rand} \times \left(X_{n,d}(p) - X_{r,d}(p)\right). \tag{24}$$

4.2.3 Selected and Updated Phase

The fitnesses of two candidates are best candidates; first they are selected $X_{i\text{ - gwo}}(p+1)$ and $X_{i\text{ - DLH}}(p+1)$ using Eq. (25).

$$X_i(p+1) = \begin{cases} X_{i\text{ - gwo}}(p+1), & \text{if } f\left(X_{i\text{ - gwo}}\right) < f\left(X_{i\text{ - DLH}}\right) \\ X_{i\text{ - DLH}}(p+1) & \text{otherwise} \end{cases}. \tag{25}$$

Then, look at $X_i(p+1)$ the new position of the updated value. If it is not updated, it will not change, so it will be calculated after the position.

5 Simulation Results

Test system: IEEE 30 bus device.

The test system details for the IEEE 30 bus of managed variables are 6 numbers of generator gadgets, 4 tapping transformers, 41 numbers of transmission lines, and 2 reactive power compensation devices. Electricity loss is 17.598 MW, reactive energy loss is 22.244 MVAR, and the voltage deviation is 0.896 p.u. The most and minimum barriers are proven in Table 1.

Table 1 Boundary values settings

Variable quantity	Min. in p.u	Max. in p.u
Generator voltages	0.90	1.10
Transformer tap position	0.95	1.05
Shunt capacitors	0.00	0.20

Studied for IEEE 30 bus system is carried out, and divided into three categories.

Case 1: Minimize active power loss

Case 2: Minimize voltage deviation

Case 3: Multi-objective function.

MATLAB programming is used to carry out these procedures.

5.1 Case 1: Minimize Active Power Loss

In this case, the power loss is constant on the minimum position. The total active power loss for GWO and IGWO includes the optimum values related to the controlled variables as shown in Table 2, and the convergence plots also are proven in Fig. 1.

5.2 Case 2: Minimize Voltage Deviation

In this case, the voltage deviation will be fixed to minimum position. Figure 2 shows the total voltage deviation of GWO and IGWO for the IEEE 30 bus systems as shown in Table 3 and the corresponding plots are seen on diagram.

5.3 Case 3: Multi-objective Function

In this situation, the electricity losses and voltage deviation may have the same weights. The optimal values of GWO and IGWO, strength loss, voltage deviation, and each convergence charts for the IEEE 30 bus device shown in Table 4 are shown in Fig. 3.

Comparison results of GWO and IGWO

In Table 5 the power losses and voltage deviation are compared between GWO and IGWO we observed that if real power losses are minimized, the losses are minimum but voltage deviation is not reduced, same way voltage deviation is minimized, the total voltage deviation is reduced and power losses are high, multi-objective function

Table 2 Active power loss and control variables

Control variables	GWO	IGWO
$V1$	1.1	1.0999
$V2$	1.0953	1.0943
$V5$	1.0744	1.0760
$V8$	1.0808	1.0811
$V11$	1.1	1.0998
$V13$	1.1	1.0993
$T_{6–9}$	1.0765	1.0568
$T_{6–10}$	0.9015	0.9022
$T_{4–12}$	1.0400	0.9877
$T_{27–28}$	0.9790	0.9886
Q_{c10}	2.8402	4.9318
Q_{c12}	1.0829	4.8697
Q_{c15}	2.7984	4.9039
Q_{c17}	1.1400	4.9548
Q_{c20}	0.7208	3.4675
Q_{c21}	3.9210	4.9387
Q_{c23}	0.16239	3.4902
Q_{c24}	0.42126	4.9122
Q_{c29}	3.3967	2.9235
PLoss (MW)	**4.425**	**4.122**
Voltage deviation	1.3265	1.8663

The bold text indicates the main objectives in the objective function

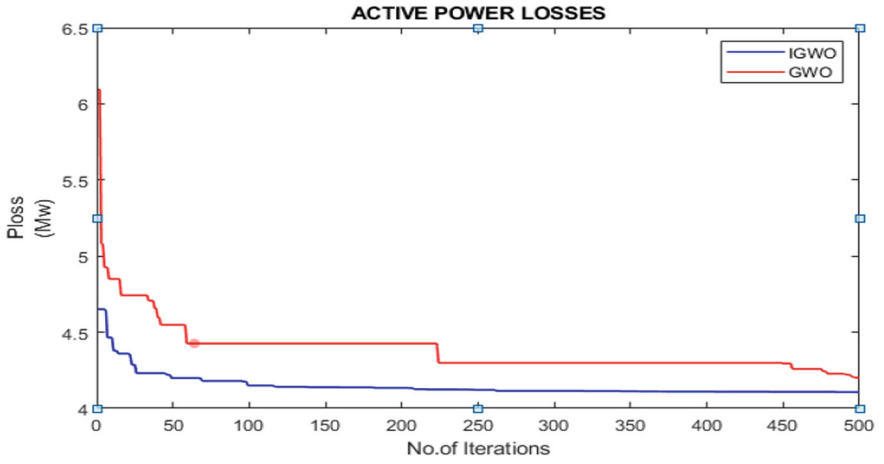


Fig. 1 Convergence curves of minimization of active electricity losses

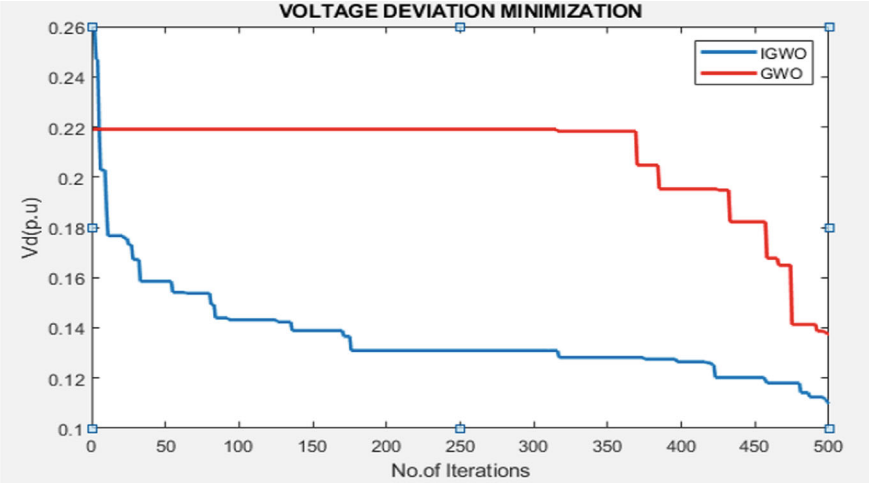


Fig. 2 Convergence curves of minimize voltage deviation

Table 3 Minimize voltage deviation and control variables

Control variables	GWO	IGWO
$V1$	0.9596	0.9954
$V2$	0.9880	1.0880
$V5$	1.0173	1.0148
$V8$	1.0108	0.9922
$V11$	1.06952	1.0611
$V13$	1.0816	0.9545
$T6$–9	1.0658	1.0541
$T6$–10	0.9028	0.9035
$T4$–12	1.0871	0.9046
$T27$-28	0.9390	0.9575
Q_{c10}	3.5774	2.1590
Q_{c12}	0.6716	4.4579
Q_{c15}	1.1298	4.7899
Q_{c17}	1.5059	0.2953
Qc20	3.5168	4.7322
Q_{c21}	3.0760	2.4179
Q_{c23}	1.1962	4.6748
Qc24	0.7344	4.8888
Q_{c29}	0.0239	4.4486
PLoss (MW)	6.859	5.357
Voltage deviation	**0.1432**	**0.1187**

The bold text indicates the main objectives in the objective function

Table 4 Multi-objective functions and control variables

Control variables	GWO	IGWO
V_1	1.0999	1.0999
V_2	1.0909	1.0918
V_5	1.0678	1.0675
V_8	1.0727	1.0740
V_{11}	1.0897	1.0355
V_{13}	1.0401	1.0328
$T_{6–9}$	1.0948	1.0743
$T_{6–10}$	0.9971	1.0289
$T_{4–12}$	1.0649	1.0755
$T_{27–28}$	1.0181	1.0391
Q_{c10}	0.6871	2.6082
Q_{c12}	1.1919	1.3394
Q_{c15}	0.1967	2.5011
Q_{c17}	0.7921	4.2416
Q_{c20}	2.6009	4.1718
Q_{c21}	3.5140	4.6834
Q_{c23}	0.9620	4.6665
Q_{c24}	0.4532	4.5641
Q_{c29}	1.5879	3.7746
PLoss (MW)	**4. 321**	**4.295**
Vd (p.u)	**0.5875**	**0.5251**
Optimal value	**2.4544**	**2.4101**

The bold text indicates the main objectives in the objective function

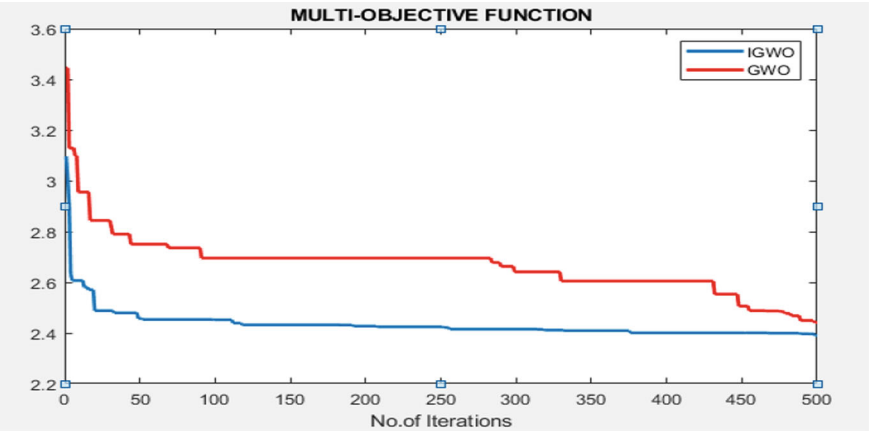


Fig. 3 Convergence properties of multi-objective functions

Table 5 Comparison of GWO and IGWO

Technique	Minimize active power loss (MW)		Minimize total voltage deviation (p.u)		Multi-objective function	
	Ploss (MW)	Vd (p.u.)	Ploss (MW)	Vd (p.u.)	Ploss (MW)	Vd (p.u.)
GWO	**4.425**	1.3265	6.859	**0.1432**	**4.321**	**0.5875**
IGWO	**4.112**	1.8663	5.375	**0.1187**	**4.295**	**0.5251**

The bold text indicates the main objectives in the objective function

is both the Ploss and Vd are minimum so, mainly considered the multi-objective function.

6 Conclusion

In this paper, an improved GWA is implemented at the IEEE 30 bus gadget. IGWO has been effectively carried out to clear up the ORPD problem, minimizing active power loss and voltage deviation for the single and multi-goal functions. In my end result, multi-objective is best. The IEEE 30 bus has a power loss of 4.295 MW and a voltage deviation of 0.5251 p.u. The effects received by way of imposing the IGWO set of rules have been compared with the ones from the Newton–Raphson technique, and his IGWO algorithm into located suitable for ORPD.

Future Work The work is extended with the FACTS device, wherein the energetic energy loss and voltage deviation are determined after placement of the FACTS device.

References

1. Chaitanya SNVSK, Ashok Bakkiyaraj R, Venkateswara Rao B (2021) Optimal reactive power dispatch of interconnected power system using firefly algorithm. In: Komanapalli VLN, Sivakumaran N, Hampannavar S (eds) Advances in automation, signal processing, instrumentation, and control. Lecture notes in electrical engineering, vol 700. Springer, Singapore. https://doi.org/10.1007/978-981-15-8221-9_22
2. Ramkee P, Chaitanya SNVSK, Venkateswara Rao CB, Ashok Bakkiyaraj R (2021) Optimal reactive power dispatch under load uncertainty incorporating solar power using firefly algorithm. In: Advances in energy technology 2021, lecture notes in electrical engineering, vol 766. Springer. https://doi.org/10.1007/978-981-16-1476-7_39
3. Nadakuditi G, Mohan Rao U, Bathina V, Pandi S (2018) Economic load dispatch in microgrids using real-coded genetic algorithm. In: Soft computing in data analytics advances in intelligent systems and computing book series, vol 758. Springer, Singapore, pp 377–386. https://doi.org/10.1007/978-981-13-0514-6_38

4. Lakshmi P, Rao BV, Devarapalli R, Rai P (2020) Optimal power flow with Bat algorithm for a power system to reduce transmission line losses using SVC. In: 2020 ICEFEET, pp 1–5. https://doi.org/10.1109/ICEFEET49149.2020.9186964
5. Wei Y, Zhou Y, Luo Q, Deng W (2021) Optimal reactive power dispatch using an improved slime mould algorithm. Elsevier.https://doi.org/10.1016/j.egyr.2021.11.138,2352-4847/2021
6. Anbarasan P, Dr. Jayabarathi T (2017) Optimal reactive power dispatch using moth-flame optimization algorithm, vol 12, no 13. Research India Publication, pp 3690–3701. ISSN 0973-4562. ORCID: 0000-0001-7417-2102
7. Abdel-Fatah S, Ebeed M, kamel S (2022) Optimal reactive power dispatch using modified sine cosine algorithm. IEEE Xplore. 978-1-5386-5261-9/19
8. Ettappan M, Vimala V, Ramesh S, Thiruppathy Kesavan V (2020) Optimal reactive power dispatch for real power loss minimization and voltage stability enhancement using Artificial Bee Colony Algorithm. Elsevier.https://doi.org/10.1016/j.micpro.2020.103085. 0141-9331
9. Duong V-T, Nguyen T-T, Duong T-L, Truong A-V (2021) Optimal reactive power dispatch using sun flower algorithm. IEEE Xplore. https://doi.org/10.1109/ICSSE52999.2021.9538483. 978-1-6654-4848-2/21
10. Roy R, Das T, Mandal KK (2021) Optimal reactive power dispatch using a novel optimization algorithm. Springer. https://doi.org/10.1186/s43067-021-00041-y
11. Rayudu K, Ali M, Yesuratnam G, Jayalaxmi A (2022) Optimal reactive power dispatch based on particle swarm optimization and LP technique. IEEE Xplore. 978-1–5090-3751-3/16
12. Nguyen TT, Vo DN, Van Tran H, Van Dai L (2019) Optimal dispatch of reactive power using modified stochastic fractal search algorithm, vol 2019, Article ID 4670820. Hindawi Complexity, 28 p. https://doi.org/10.1155/2019/4670820
13. Chen G, Liu L, Zhang Z, Huang S (2016) Optimal reactive power dispatch by improved GSA-based algorithm with the novel strategies to handle constraints. 1568-4946/2016. https://doi.org/10.1016/j.asoc.2016.11.008 (Elsevier)
14. Mukherjee A, Mukherjee V (2015) Solution of optimal reactive power dispatch by chaotic krill herd algorithm, vol. 9, issue 15. IET Generation, Transmission& Distribution, pp. 2351–2362. https://doi.org/10.1049/iet-gtd.2015.0077. ISSN 1751 8687
15. Rajan A, Malakar T (2014) Optimal reactive power dispatch using hybrid Nelder-Mead simplex based firefly algorithm. Elsevier. https://doi.org/10.1016/j.ijepes.2014.10.041. 0412-0615/2014
16. Ghasemi A, Valipour K, Tohidi A (2013) Multi objective optimal reactive power dispatch using a new multi objective strategy. Elsevier Ltd. https://doi.org/10.1016/j.ijepes.2013.11.049. 0142-0615/2013
17. Suresh V, Semthil Kumar S (2020) Optimal reactive power dispatch for minimization of real power loss using SBDE and DE-strategy algorithm. Springer. https://doi.org/10.1007/s12652-020-02673-w.
18. Duman S, Sonmez Y, Guvenc U, Yorukeren N (2012) Optimal reactive power dispatch using a gravitational search algorithm. IET Generation, Transmission & Distribution. https://doi.org/10.1049/iet-gtd.2011.0681
19. Roy R, Das T, Mandal KK (2022) Optimal reactive power dispatch for voltage security using JAYA algorithm. IEEE Xplore. https://doi.org/10.1109/ICCDW45521.2020.9318700,978-1-7281-4635-5/20
20. Medani KBO, Sayah S (2022) Optimal reactive power dispatch using particle swarm optimization with time carrying acceleration coefficients. IEEE Xplore. 978-0-9567157-6-0
21. Saddique MS, Habib S, Bhatti AR, Ahmed EM (2022) Optimal solution of reactive power dispatch in transmission system to minimize power losses using sine-cosine algorithm. IEEE Access.https://doi.org/10.1109/ACCESS.2022.3152153

22. Pandya S, Roy R (2015) Particle swarm optimization based optimal reactive power dispatch. IEEE Xplore. 978-1-4799-6085-9/15
23. Mirjalili S, Mirijalili SM, Lewis A (2014) Grey wolf optimizer. Adva Eng Softw 69:46–61. IEEE Xplore. https://doi.org/10.1016/j.advengsoft.2013.12.007
24. Liu J, Wei X, Huang H (2021) An improved grey wolf optimization algorithm and its application in path planning. IEEE Access. https://doi.org/10.1109/ACCESS.2021.3108973

Construction of Cascaded Deep Neural Network with Optimization-Based Feature Selection in CT Images for Detecting Laryngeal Cancer

P. Naga Padmavathi, M. Sree Devi, V. V. R. Maheswara Rao, and Amara S. A. L. G. Gopala Gupta

Abstract A sin laryngeal carcinoma is the most common kind of head and neck cancer to damage the soft tissues of the larynx. To prevent further medical difficulties and to provide better patient care, early stage laryngeal cancer identification is essential. The primary objective of this research is to provide computer-aided cancer diagnosis driven by deep learning. In order to do this, we create a brand-new Optimization-Based Cascaded Deep Neural Network (OCDNN) that distinguishes between good and unhealthy/cancerous tissues. Additionally, we also provide cascaded patch-based CNN (CP-CNN) picture segmentation. The models are assessed using accepted measures that are unique to the biomedical field. When compared to other models, the performance of our suggested OCDNN architecture was exceptional. Additionally, it fared better than other cutting-edge CNN models applied to medical domain challenges. The findings suggest that the suggested method is quite successful in identifying early indications of laryngeal cancer. The results demonstrate that the suggested strategy may help doctors identify laryngeal carcinoma early and precisely. The suggested OCDNN is discovered to attain 98.4% accuracy, 94% precision, 97.5% recall, and 98% F1-score.gle paragraph of about 100 words to give a brief introduction to your work.

P. Naga Padmavathi (✉) · M. Sree Devi (✉)
Department of Computer Science and Engineering, Amrita Sai Institute of Science and Technology, Paritala, AP, India
e-mail: padmavathi481@gmail.com

M. Sree Devi
e-mail: srivijaysujay@gmail.com

V. V. R. Maheswara Rao
Department of Computer Science and Engineering, Shri Vishnu Engineering College for Women, Bhimavaram, AP, India

A. S. A. L. G. Gopala Gupta
Department of Computer Science and Engineering, KoneruLakshmaiah Education Foundation, Vaddeswaram, AP, India

© The Author(s), under exclusive license to Springer Nature Singapore Pte Ltd. 2025

B. B. V. L. Deepak et al. (eds.), *Recent Advancements in Product Design and Manufacturing Systems*, Lecture Notes in Mechanical Engineering,
https://doi.org/10.1007/978-981-97-6732-8_39

Keywords Laryngeal cancer · Convolution neural network (CNN) · Optimization · CT images · Feature selection

1 Introduction

Every year, the number of people who are diagnosed with laryngeal carcinoma, one of the most prevalent cancers that may present in the head and neck region, increases [1]. Laryngeal preservation, 87–90% rates of local control, and a favorable prognosis have all been connected to precancer [2]. And also advanced-stage cancer demands multimodal therapies, which have significant side effects and an inferior level of life. Despite having the best possible treatment programs, studies reveal significant recurrence rates and a five-year general survival of 33–61% [3, 4]. For the early diagnosis and screening of laryngeal malignant and precancerous lesions, endoscopic imaging methods are increasingly frequently employed in clinical settings [5, 6]. The combination of contact endoscopy (CE) and narrow-band imaging (NBI), which is one of these approaches, may produce a better and enlarged picture of changes in the morphology and three-dimensional orientation [7, 8]. Another one of these methods is the combination of narrow-band imaging (NBI) and contact endoscopy (CE). However, using CE-NBI for diagnosis heavily depends on the otolaryngologists' expertise and takes years of training. This may lead to a subjective decision-making process, which is then followed by over- or under-treatment planning [9, 10]. Furthermore, the otolaryngologist's practice, which requires several years of training, has a considerable impact on how well CE-NBI images are used in early prognosis [11]. Additionally, this might result in results for the highly subjective decision procedure after under-treatment or even over-treatment procedures. At the moment, advanced-level feature engineering expansion, deep learning, and machine learning procedures in the area of healthcare applications provide a variety of paths for supporting medical specialists and conquering these types of obstacles inside clinical trial settings in real time [12, 13]. Currently, neck and head cancer patients undergo standard staging and prognostic procedures that include the use of positron emission tomography (PET), magnetic resonance imaging (MRI), and contrast-improved computed tomography (CT) images [14]. Investigative radiomic assessment might be greatly aided by this enormous dataset that was gathered using a variety of image modalities inside the current medical data. Non-invasive techniques might be used to capture this diverse structure of head and neck malignancies, which could serve as an essential adjunct for real-time medication decision-making. The main contributions are:

- In addition, a cascade CNN technique is used to effectively segment the features following the preprocessing stage. To make our model adaptable to changes in the tumor's size and location, the CNN mode employs a novel distance-wise attention method.

- The hybrid pooling approach, which stochastically chooses the maximum or average pooling in each pooling layer. Each convolutional layer's pooling model selection probability may be controlled.

The other sections of this chapter are organized as follows: A few prior research studies are discussed in Sect. 2, the proposed technique and strategy are shown in Sect. 3, the experiment's findings and analysis are presented in Sect. 4, and a conclusion and recommendations for next research are provided in Sect. 5, which wraps up the paper.

2 Literature Survey

National cancer planning places a major emphasis on cancer research. Investment in cancer research is economically viable given the high cost of cancer therapy at advanced stages of the illness. Data mining and artificial intelligence methods have been employed extensively in numerous fields in recent years, and the findings have shown that these approaches may be used with great assurance when discussing medical diagnosis.

They developed a technique [15] for automatically identifying cancerous and benign vocal lesions in 2179 laryngoscopy photographs from six hospitals using five different types of laryngoscopy equipment. The most accurate method for differentiating between benign and malignant vocal lesions was pathological investigation. The Bayesian networks (BN) model used in [16] combines patient-specific data with incorporated causalities from expert sources to recommend the best course of therapy and hence possibly aid in the treatment of laryngeal cancer decisions. Present a unique and improved Mask R-CNN model for the real-time detection of laryngeal cancer and its associated symptoms using a variety of image datasets and CT scans in [17]. Our proposed methodology also reduces time for the physicians, enabling more patient screenings each day, and is capable of catching and identifying small laryngeal cancers in a substantial and quicker way during real-time patient screening. In [18], authors propose a novel UNet dubbed the Efficient Exception UNet (EFX-UNet), which trains and predicts using the two channels Nos. 13 and 14 from each cube. The EFX-UNet generates an initial segmentation and forecasts the likelihood that the patient has a malignant tumor. Following that, a further in-depth analysis is conducted for the identified patients utilizing our modified Deep UNet and channels 9 through 16 to accurately segment the tumor. In [19], images are classified as cancerous or normal using convolutional neural networks (CNN), support vector machines (SVMs), and transfer learning (TL) with an average accuracy of 93%. With 10 data, transfer learning produced superior results, with an average accuracy of 94.18%, significantly outperforming SVM and itself. This study uses a suggested Adaptive Spotted Hyena Optimizer-based Deep Quantum Neural Network (ASHO-based Deep QNN) to propose an effective model for classifying laryngeal cancer. With the help of features like the histogram of gradients (HOG), gradient binary

pattern (GBP), and spider local image feature (SLIF), the preprocessing is successfully completed here utilizing Gaussian filtering. The deep QNN is used to do classification toward the end, and it is tuned using the newly developed ASHO. Narrow-band imaging (NBI) endoscopy has been used to construct a deep convolutional neural network (CNN) model for pathological diagnosis of LSCC. The model was tested and validated using 4591 laryngeal NBI scans from patients (1,927 benign and 2664 LSCC). Additionally, the pathological diagnostic training and validation employed 3,443 pathological pictures from the hematoxylin and eosin-stained slides of 1228 patients (318 benign and 910 LSCC). In [20] by fusing the Resnet and Inception models, the improved network model (RICN model) is created. The effectiveness of these three network models is assessed and contrasted utilizing the classification of laryngeal cancer pictures using the Resnet model, Inception model, and RICN model.

3 System Model

Figure 1 depicts the overall block design for the proposed categorization of laryngeal cancer using a CT image dataset. The dataset is first uploaded and then preprocessed using a wiener filter. Next, segmentation is carried out using cascaded patch-based CNN (CP-CNN), and feature selection is based on the dolphin optimization approach. Classification of pictures using an improvised backbone follows feature selection CNN. The time-consuming daily screening of many individuals by professionals is making earlier diagnostic technologies worthless in the present day. The authors of this article provide an innovative and more efficient method for patient screening employing a variety of photos to address the aforementioned issues. An improvised technique is proposed in this study for the real-time detection of laryngeal cancer and its symptoms. In contrast to the other models, this strategy uses a deep learning method and takes very minimum time.

3.1 Data Preprocessing

Building a segmentation and classification model for laryngeal carcinoma requires careful data preparation. By reducing noise and artifacts, adjusting for data biases, and ensuring that the pictures are in a uniform format, this stage tries to prepare the acquired CT images for analysis. To obtain greater accuracy, several preprocessing and normalizing methods were used. The initial stage in data preparation is to improve the pictures' quality by eliminating any noise, artifacts, or other distortions that might compromise the analysis's precision. Due to changes in the imaging procedure, CT pictures may have varied degrees of intensity. To make it simpler to compare photos from various sources, intensity normalization methods are used to put the intensities of the images into a similar range. An picture is enhanced using a filtering

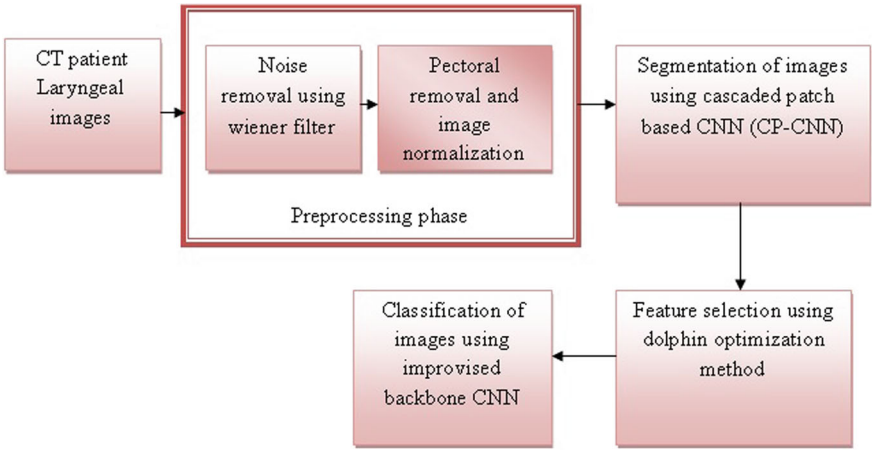


Fig. 1 Overall architecture for laryngeal cancer detection

approach where the filters are mostly used to suppress the high frequencies or the low frequencies, or to enhance or detect the edges in the image. For instance, you may filter a picture to highlight some elements while removing others. There are several approaches, and the best ones may vary depending on the picture and its intended application. Edge detection, noise reduction, sharpening, and edge smoothing are just a few of the uses for image filtering. Based on a stochastic framework, the method is used. According to the orthogonality principle, the Wiener filter in the Fourier domain may be written as follows.

Our main goal in doing this study was to cost-effectively remove the pectoral muscle from the neck region, which is superfluous. The areas of the pectoral muscles have the brightest pixels. The removal of the pectoral muscles should be done well to prevent making erroneous assumptions about favorable outcomes. Based on the front side image of the specified laryngeal area, the left or right pectoral muscles are determined. The RANSAC method was used to pick the most efficient component of the quadratic curve fitting, and the pectoral muscle was interpolated using the data of the candidate objects. By excluding inactive elements, the suggested technique yields results that are more accurate than those produced by the linear RANSAC method.

The algorithm is as follows:

- Choose data at random from the data points for interpolation.
- Set the k (iterations) initial value to 1.
- Import n points at random from the collection and then calculate the model.
- To save the model in the tolerance, compute the incoming data model.
- In increments of 1, increase the number of iterations (k). Repeat the procedure from step (3) if the chosen maximum number of iterations (k) is such that ($k < K$. The model has the largest consensus set among the interpolation models if (k) is equal to.

3.2 Segmentation of Images

In this paper, we describe a multimodal CP-CNN architecture for laryngeal malignancies in CT images that is based on big data analysis. The distance-wise attention (DWA) module and patch extraction are two essential components of the CP-CNN architecture. We use a sliding window approach to extract tiny sub-images (i.e., patches) from the main picture during the patch extraction process. The patches are subjected to a number of convolutional layers before a series of learnable filters are used to extract features from the patches. Next, the data in each feature map is compressed, and the resulting feature maps are then routed via pooling layers to reduce their dimensionality. After pooling, fully connected layers are used to categorize the features into separate groups, reducing the dimensionality of the feature maps.

3.3 Patch Extraction Module

Patch extraction is the technique of dividing the preprocessed laryngeal CT images into smaller regions or patches. In this stage, the deep learning model's training costs are reduced, and the model is given the opportunity to learn from the small, local details in the images. Each patch is often a tiny, square or rectangle-shaped sub-image of the laryngeal CT that has a defined size, such 64×64 or 128×128 pixels. Depending on the size of the tumor and the computing capabilities, the patch size is determined. For all photos, the patch size and stride were set at $64 \times 64 \times 64$ and $32 \times 32 \times 32$, accordingly. Across 224 and 289 patches were retrieved, varying across pictures.

3.4 Feature Selection Using Dolphin Optimization Method

Techniques for features selection will eliminate redundant and pointless characteristics from the data. Feature ranking and subset selection are the two main types of feature selection algorithms [21]. All features are scored according to certain criteria in feature ranking, and those that fall short of a predetermined score are eliminated. When choosing a subset, the best possible subset is sought for, and qualities are chosen depending on ranking. The search stage, the call stage, the reception stage, and the predation stage are the four essential steps that dolphins use to carry out their predation algorithm. The optimal solution to the issue is produced by continuous iteration, and the associated search connections are created utilizing the behavior of four joint stages.

3.4.1 Initialization

Each dolphin in the optimization problem symbolizes a feasible solution. The dolphin in this study is defined as $\mathrm{dp}_i = \left[y_1, y_2, \ldots y_D\right]K(i = 1, 2, \ldots J)$, namely a feasible D-dimensional solution, where J is the number of dolphins and $y_j(j = 1, 2 \ldots \mathrm{com})$ is the component of each dimension to be optimized.

In this research, the dolphin is defined as $\mathrm{dp}_i = \left[y_1, y_2, \ldots y_D\right]K(i = 1, 2, \ldots J)$, which is a workable D-dimensional solution, where J is the number of dolphins, and $y_j(j = 1, 2 \ldots \mathrm{com})$ is the component of each dimension that has to be optimized.

Two variables related to the dolphin are the individual optimal solution (I) and neighborhood optimum solution (N).

There are two associated variables Li (i = 1,2,…J) and Ni (i = 1,2,…J) for each $\llbracket \mathrm{dp} \rrbracket$ i (i = 1,2,…J), where Li stands for the optimal solution that the $\llbracket \mathrm{dp} \rrbracket$ i discovers once, and Ni represents the optimal solution that the $\llbracket \mathrm{dp} \rrbracket$ i finds independently or obtains from others.

The standard for determining if the answer is superior is fitness fit. Three directions are best for bootlenose dolphin locomotion. The first is the distance between dp_i and dp_j known $\mathrm{dis_dp}_{ij}$ and known as $\left|\mathrm{dp}_i - \mathrm{dp}_j\right|, i, j = 1, 2 \ldots J, i \neq j$. The second is the distance between dp_i and N_i, known as dist_N_i and $\mathrm{dist}_{N_i} = \left|\mathrm{dp}_i - N_i\right|, i = 1, 2, \ldots J$. The third is the distance between I_i and N_i, known as dist_IN_i and $\mathrm{dist}_{IN_i} = I_i - N_i, i = 1, 2, \ldots J$.

3.5 Classification of Images

In our suggested model, in order to detect laryngeal cancer and its signs in a timely manner, we opted for a hybrid deep learning-based approach. In this case, the input is varied, the testing image data does not have a category label, the class label shows a collection of varied images, and FP shows a list of testing image datasets. This output is a collection of varied class image datasets that have been trained and verified.

3.5.1 Vector Pooling Block

Let $C \times H \times W$ represent the number of channels, height, and width, respectively, of the input layer Input.

Two parallel vertical and horizontal pooling layers are initially used to route the input. The output of each pooling route is then subjected to a 1×1 convolutional layer with the same number of kernels as the layer before it. Using a 1×1 convolutional layer, the attributes with the greatest abundance are retrieved. A RELU layer is added after the element-by-element summing to speed up convergence. The block for vector pooling is shown in Fig. 2 and is stated as follows:

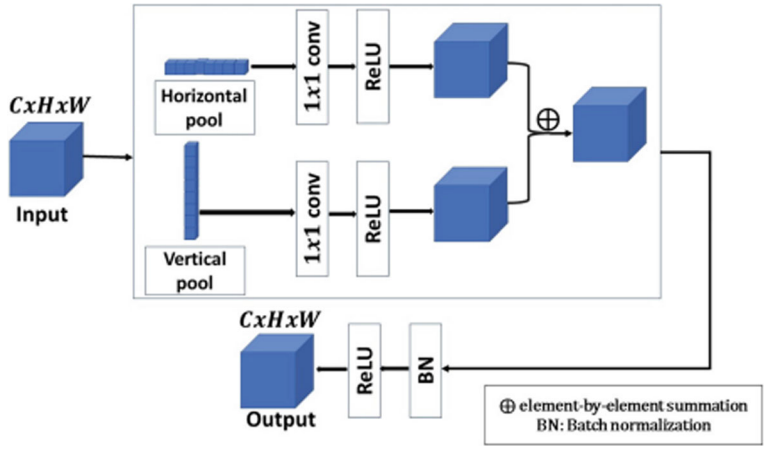


Fig. 2 Vector pooling block

$$y_{\text{vertical}} = \text{RELU}\left(\text{conv}_{1\times 1}\left(\text{pool}_{1\times N}\left(I_{\text{input}}\right)\right)\right)$$

$$y_{\text{horizntal}} = \text{RELU}\left(\text{conv}_{1\times 1}\left(\text{pool}_{N\times 1}\left(I_{\text{input}}\right)\right)\right)$$

$$y_{\text{output}} = \text{RELU}(y_{\text{vertical}} + y_{\text{horizontal}})$$

where + is the summation of element-by-element.

The methods used in CNNs are max-pooling and average pooling. The max-pooling parameter determines the highest possible value inside the pooling region. When things are pooled together, the average is calculated as the sum of their individual values. The right side calculates the maximum and average pooling using a filter of size 2 × 2 and stride 2, while the left side represents the input matrix of size 4 × 4. The computation of the maximum pooling and average pooling for each color from the input matrix is shown by the color of each cell on the right side. AVG-MAX with the notion of VPB, which can be shown as follows, a pooling block is created by VPB that may gather useful features by employing max-pooling and average pooling:

$$y_{\text{MAX_vertical}} = \text{ReLU}\left(\text{conv}_{1\times 1}\left(\text{max pool}_{1\times N}\left(I_{\text{input}}\right)\right)\right)$$

$$y_{\text{MAX_horizontal}} = \text{ReLU}\left(\text{conv}_{1\times 1}\left(\text{max pool}_{N\times 1}\left(I_{\text{input}}\right)\right)\right)$$

$$y_{\text{AVG_vertical}} = \text{ReLu}\left(\text{conv}_{1\times 1}\left(\text{max pool}_{1\times N}\left(I_{\text{input}}\right)\right)\right)$$

$$y_{\text{AVG_horizontal}} = \left(y_{\text{MAX}_{\text{horizontal}}} + y_{\text{MAX}_{\text{vertical}}} + y_{\text{AVG}_{\text{vertical}}}\right)$$

3.6 Convolution Module

The training set had nearly 2.5 times as many clinical photos of benign laryngeal disorders as there were of cancer and OPMD, a problem known as "class imbalance." This may induce bias into CNN training, which would result in poor testing results. To reduce the effect of "class imbalance," we used "weighted cross entropy loss" function that takes into consideration the quantity of samples in each class (e.g., the contribution of each photo of cancer or OPMD to the training error is 2.5 that of each picture of benign tongue diseases). During the course of training, a total of two callbacks were used. The first feedback was "early stopping," a technique that terminates training if there is no further improvement in the validation loss. The second callback was a "model checkpoint," a function of the Keras toolkit that allows the model to be saved with little validation loss at any stage in the training process.

4 Performance Analysis

The performance of our proposed Optimization-based Cascaded Deep Neural Network (OCDNN) is carried out using parameters such as accuracy, precision, recall, and F1-score.The comparison is done with existing methods such as Bayesian networks (BN) [16], Adaptive Spotted Hyena Optimizer-based Deep Quantum Neural Network (ASHO-based Deep QNN) [22], deep convolutional neural network (DCNN) [23]

The laryngeal dataset.tar [24] contains 1320 patches from normal and early stage cancer laryngeal tissues. Patches (100 × 100 pixels) were manually excised from 33 narrow-band laryngoscopic CT images of 33 individual individuals with laryngeal spinocellular cancer. Specifically, 330 patches from each of four different types of tissue were considered: He (healthy tissue), Hbv (tissue with hypertrophic vasculature), Le (tissue with leukoplakia), and IPCL (tissue with intrapapillary capillary loops).

4.1 Accuracy

The accuracy demonstrates the model's propensity to make broad predictions (Table 1).

$$\text{Accuracy} = \frac{\text{TP} + \text{TN}}{\text{TP} + \text{TN} + \text{FP} + \text{FN}}.$$

The suggested OCDNN technique and the existing methods are compared in Fig. 3 where the *Y*-axis shows the accuracy attained in percent and the *X*-axis represents the quantity of data. When analyzing Fig. 3, the existing BN, ASHO-DQNN, and

Table 1 Comparison of accuracy

Number of data	BN	ASHO-DQNN	DCNN	OCDNN
100	87	90	84.7	97.4
200	88.5	90.5	85	98
300	89	89.9	85.7	98.3
400	85.7	89	86	98.4
500	88	91	85	97.9

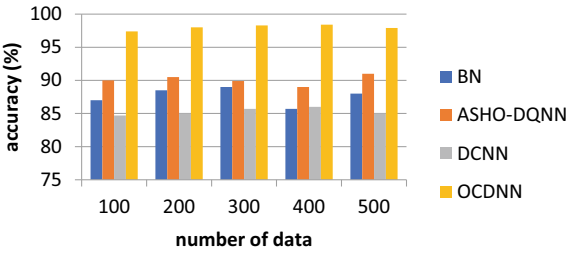


Fig. 3 Comparison of accuracy

DCNN achieve 89, 91, and 85% of accuracy, where the suggested OCDNN achieves 98.4% which is 9.4, 7, and 13.4% better than aforementioned existing methods.

4.2 Precision

The ratio of a positive sample size determines the accuracy rate. Rather precision represents the proportion of the prediction models when cancer is actually present (Table 2).

$$\text{Precision} = \frac{\text{TP}}{\text{TP} + \text{FP}}.$$

The suggested OCDNN technique and the existing methods are compared in Fig. 4 where the *Y*-axis shows accuracy attained in percent and the *X*-axis represents

Table 2 Comparison of precision

Number of data	BN	ASHO-DQNN	DCNN	OCDNN
100	78	87	89	93
200	77.9	86.4	86.4	93.4
300	77	84	89	94
400	76.3	86.3	86.3	94.2
500	75.2	87	87	95

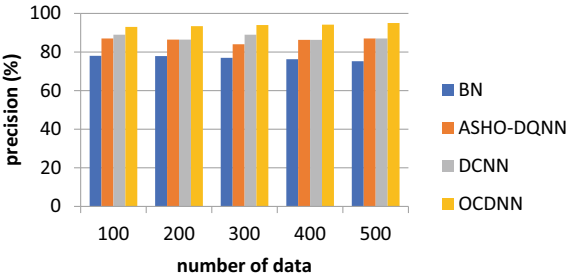


Fig. 4 Comparison of precision

the quantity of data. When analyzing the existing BN, ASHO-DQNN, and DCNN achieves 78, 86, and 89% of precision, where, the suggested OCDNN achieves 94% which is 16, 8, and 5% better than aforementioned existing methods.

4.3 Recall

Since it is impossible to redo a test, results that are too close to call must be ignored, and so must the samples that yielded such results. The ability to accurately detect cancer in data sets is at issue (Table 3).

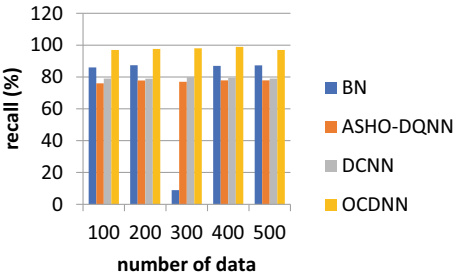
$$\text{Recall} = \frac{\text{TP}}{\text{TP} + \text{FN}}$$

The suggested OCDNN technique and the existing methods are compared in Fig. 5. When analyzing the existing BN, ASHO-DQNN, and DCNN achieves 87.3, 76.5, and 79% of recall, the suggested OCDNN achieves 97.5% which is 10.2, 22, and 17% better than aforementioned existing methods.

Table 3 Comparison of recall

Number of data	BN	ASHO-DQNN	DCNN	OCDNN
100	86	76	79	97
200	87.4	77.8	78.9	97.6
300	8.9	77	79.9	98
400	87	77.9	79.4	98.9
500	87.3	77.9	79	97

Fig. 5 Comparison of recall



4.4 F1-Score

It is used to evaluate the performance of predictions. An equal weight is given to both accuracy and recall. The best is determined by the number 1, and the poorest by the value 0 (Table 4).

The suggested OCDNN technique and the existing methods are compared in Fig. 6. When analyzing the existing BN, ASHO-DQNN, and DCNN achieves 85, 77, and 87% of F1-score, the suggested OCDNN achieves 98% which is better than aforementioned existing methods (Table 5).

Table 4 Comparison of F1-score

Number of data	BN	ASHO-DQNN	DCNN	OCDNN
100	81.8	78	84.6	97.65
200	86.4	77	87.4	96.58
300	87.4	78.9	84.5	98.32
400	84.6	76	87.5	97.48
500	82.6	77	86.4	98.25

Fig. 6 Analysis of F1-score

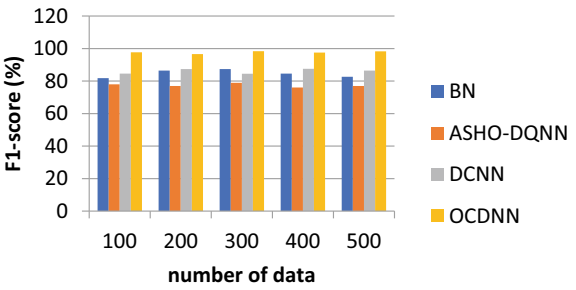


Table 5 Overall comparative analysis

Parameters	BN	ASHO-DQNN	DCNN	OCDNN
Accuracy (%)	89	91	85	98.4
Precision (%)	78	86	89	94
Recall (%)	87.3	76.5	79	97.5
F1-score (%)	85	77	87	98

5 Conclusion

Clinicians must perform the diagnosis and different types of laryngeal cancer, especially in the early stages of malignant as well as benign tumors developing in patients' head and neck regions. Since laryngeal cancer is a serious condition, a timely and precise diagnosis during the early stages is crucial to save lives. In this study, the scientists created a brand-new, for the identification and diagnosis of laryngeal cancer, an adapted deep learning model, particularly in the early stages. In contrast to other models, our suggested model is one of the most innovative and appropriate ones since it can more accurately and quickly diagnose laryngeal cancer and the symptoms that go along with it using CT image datasets. The model also demonstrates a large medical effect and improved rates of early laryngeal carcinoma detection. Future research on the detection of laryngeal cancer utilizing a variety of datasets has a great deal of promise for reducing screening times and enhancing model accuracy, particularly for larger datasets.

References

1. Wang JY, Zhang QW, Wen K, Wang C, Ji X, Zhang L (2021) Temporal trends in incidence and mortality rates of laryngeal cancer at the global, regional and national levels, 1990–2017. BMJ Open 11:e050387. https://doi.org/10.1136/bmjopen-2021-050387
2. Guimarães AV, Dedivitis RA, Matos LL, Aires FT, Cernea CR (2018) Comparison between transoral laser surgery and radiotherapy in the treatment of early glottic cancer: a systematic review and meta-analysis. Sci Rep 8:11900. https://doi.org/10.1038/s41598-018-30218-x
3. García-León FJ, García-Estepa R, Romero-Tabares A, Borrachina JGM (2017) Treatment of advanced laryngeal cancer and quality of life. Systematic review. Acta Otorrinolaringol 68:212–219. https://doi.org/10.1016/j.otorri.2016.11.005
4. Elicin O, Giger R (2020) Comparison of current surgical and non-surgical treatment strategies for early and locally advanced stage glottic laryngeal cancer and their outcome. Cancers 12:732. https://doi.org/10.3390/cancers12030732
5. Missale F, Taboni S, Carobbio ALC, Mazzola F, Berretti G, Iandelli A, Fragale M, Mora F, Paderno A, Del Bon F et al (2021) Validation of the European Laryngological Society classification of glottic vascular changes as seen by narrow band imaging in the optical biopsy setting. Eur Arch Oto-Rhino-Laryngol 278:2397–2409. https://doi.org/10.1007/s00405-021-06723-7
6. Lauwerends LJ., Galema HA, Hardillo JA, Sewnaik A, Monserez D, van Driel PB, Verhoef C, Baatenburg de Jong RJ, Hilling DE, Keereweer S (2021) Current Intraoperative imaging

techniques to improve surgical resection of laryngeal cancer: a systematic review. Cancers 13:1895. https://doi.org/10.3390/cancers13081895.
7. Davaris N, Lux A, Esmaeili N, Illanes A, Boese A, Friebe M, Arens C (2020) Evaluation of vascular patterns using contact endoscopy and barrow-band imaging (CE-NBI) for the diagnosis of vocal fold malignancy. Cancers 12:248. https://doi.org/10.3390/cancers12010248
8. Puxeddu R, Sionis S, Gerosa C, Carta F (2015) Enhanced contact endoscopy for the detection of neoangiogenesis in tumors of the larynx and hypopharynx. Laryngoscope 125:1600–1606. https://doi.org/10.1002/lary.25124
9. Mannelli G, Cecconi L, Gallo O (2016) Laryngeal preneoplastic lesions and cancer: challenging diagnosis. Qualitative literature review and meta-analysis. Crit Rev Oncol/Hematol 106:64–90. https://doi.org/10.1016/j.critrevonc.2016.07.004
10. Mehlum CS, Døssing H, Davaris N, Giers A, Grøntved ÅM, Kjaergaard T, Möller S, Godballe C, Arens C (2020) Interrater variation of vascular classifications used in enhanced laryngeal contact endoscopy. Eur Arch Oto-Rhino-Laryngol 277:2485–2492. https://doi.org/10.1007/s00405-020-06000-z
11. Kim H, Jeon J, Han YJ, Joo Y, Lee J, Lee S, Im S (2020) Convolutional neural network classifies pathological voice change in laryngeal cancer with high accuracy. J Clin Med 9:3415
12. Jena L, Mishra S, Nayak S, Ranjan P, Mishra MK (2021) Variable optimization in cervical cancer data using particle swarm optimization. In: Advances in electronics, communication and computing. Springer, Singapore, pp 147–153
13. Bhattacharjee S, Xu W (2022) VoiceLens: a multi-view multi-class disease classification model through daily-life speech data. Smart Health 23:100233
14. Unger J, Lohscheller J, Reiter M, Eder K, Betz CS, Schuster M (2015) A noninvasive procedure for early-stage discrimination of malignant and precancerous vocal fold lesions based on laryngeal dynamics analysis. Cancer Res 75:31–39
15. Yan P, Li S, Zhou Z, Liu Q, Wu J, Ren Q, Chen Q, Chen Z, Chen Z, Chen S, Scholp A., Ge P (2023) Automated detection of glottic laryngeal carcinomain laryngoscopic images from a multicenter databaseusing a convolutional neural network. Clin Otolaryngol
16. Hikal A, Gaebel J, Neumuth T, Dietz A, Stoehr M (2023) A treatment decision support model for laryngeal cancer based on Bayesian networks. Biomedicines 11(1):110
17. Sahoo PK, Mishra S, Panigrahi R, Bhoi AK, Barsocchi P (2022) An Improvised deep-learning-based mask R-CNN model for laryngeal cancer detection using CT images. Sensors 22(22):8834
18. Meyer-Veit F, Rayyes R, Gerstner AO, Steil J (2022) Hyperspectral endoscopy using deep learning for laryngeal cancer segmentation. In: Artificial neural networks and machine learning–ICANN 2022: 31st international conference on artificial neural networks, Bristol, UK, September 6–9, 2022, Proceedings; Part IV, pp 682–694. Cham: Springer Nature Switzerland.
19. Kadirappa R, Amaranageswarao G, Deivalakshmi S (2022) Convolutional neural network models for throat cancer classification using histopathological images. In: Distributed computing and optimization techniques: select proceedings of ICDCOT 2021. Springer, Singapore, pp 263–271
20. Wu F, Wu P, Hou Y, Shang H (2021) Neural network for image classification of laryngeal cancer. In: 2021 International conference on networking systems of AI (INSAI). IEEE, pp 239–243
21. Gangula R, Vutukuru MM, Kumar R (2024) Hybridization of bottlenose dolphin optimization and artificial fish swarm algorithm with efficient classifier for detecting the network intrusion in Internet of Things (IoT). Int J Intell Syst Appl Eng 12(6s):220–232
22. Sachane MN, Patil SA (2022) Adaptive spotted hyena optimizer-enabled deep QNN for laryngeal cancer classification. In: 2022 International conference on edge computing and applications (ICECAA). IEEE, pp 1025–1032
23. He Y, Cheng Y, Huang Z, Xu W, Hu R, Cheng L, He S, Yue C, Qin G, Wang Y, Zhong Q (2021) A deep convolutional neural network-based method for laryngeal squamous cell carcinoma diagnosis. Ann Transl Med 9(24)
24. https://zenodo.org/record/1003200#.ZG4N9HZBzIU

Smart Voting System Using Deep Learning

P. Prasanthi, K. Aneesha, P. Sujith, S. Deepika, S. Sai Vamsi, and M. Jayanthi Rao

Abstract The world's largest democratic nation is India, where we live. Therefore, it is imperative to guarantee that a fair election is used to elect the governing body. India exclusively employs an offline voting system, which is characterized by inefficiency and substandard performance due to the substantial manpower requirements and the extended duration for processing and disseminating the results. Therefore, a change that addresses these drawbacks is necessary for the system to become effective. The new procedure makes voting easier by not requiring a voter's physical appearance. This study focuses on a two-step authentication system that uses face recognition and an OTP mechanism to enable voters to cast their ballots remotely from any location using a computer or mobile device. If the user finds it more comfortable, this product also lets them vote offline. Prior to the election, voters' faces are recorded using a face scanning technique that is helpful while voting. RFID tags, not voter ID the offline voting method. In order to use this method, voters must snap a photo of themselves prior to the election and compare it to the original before casting their vote.

Keywords RFID · Computer vision · Deep learning · Haar cascading · Open CV · CNN

1 Introduction

In a democratic society, elections are an unavoidable event, and it is the duty of both the government and the people to ensure that they are conducted smoothly and in a safe and secure manner. This approach requires the voter to take a picture

P. Prasanthi · K. Aneesha · P. Sujith · S. Deepika · S. Sai Vamsi
Department of Information Technology, Aditya Institute of Technology and Management, Tekkali 532201, India

M. Jayanthi Rao (✉)
Department of Computer Science and Engineering, Aditya Institute of Technology and Management, Tekkali 532201, India
e-mail: jayanth.mtech@gmail.com

© The Author(s), under exclusive license to Springer Nature Singapore Pte Ltd. 2025

B. B. V. L. Deepak et al. (eds.), *Recent Advancements in Product Design and Manufacturing Systems*, Lecture Notes in Mechanical Engineering,
https://doi.org/10.1007/978-981-97-6732-8_40

of themselves before the election, which is then compared before casting a ballot. After the microcontroller has read the information, the data that was recorded offline is transferred to the Web. Utilizing a serial terminal for application, the individual database is administered by the Web application's software. After a voter casts, the website confirms that the vote was correctly registered by sending a notification that reads, "voted successfully" when casting their votes, expressing their opinions, or articulating their choices. This project's primary objective is to ensure that a voting system that uses face recognition technology and an OTP system is created so that voters can cast their ballots from any location with Internet access. The server database contains the voting data. The world is changing daily, and in order to thrive and adhere to international norms, one must learn to live in the computer age. This innovative technology, known as electronic voting systems, utilizes a central database to ease data transfers and result computation. It enables both online and offline voting. Therefore, in order to have a fair election, an electronic voting system must be created and used.

2 Literature Survey

In the paper titled "SEVEP: Verifiable, Secure and Privacy Preserving Remote Polling with Untrusted Computing Devices," author Amna Qureshi explains the process of designing a versatile polling system. This system incorporates fingerprint devices to enhance authentication, enables voters to utilize different devices, eliminates the need for polling sheets, and generates poll tags [1]. The article titled "Secure and Hassle Free EVM Through Deep Learning Face Recognition" by author Ishani Mondal utilized neural networks to extract facial characteristics of voters and utilize these attributes as a basis for casting votes in an election. If the details correspond to the ones currently on record [2], the user is eligible to vote. The paper "VOT-EL: Three Tier Secured State-of-the-art EVM Design Using Pragmatic Fingerprint Detection Annexed with NFC Enabled Voter-ID Card," written by Anosmia Das, explores the use of NFC technology and biometrics. The user's text is "[3]." Se-VEP is an Internet-enabled electronic polling system that has been described by authors AMNA QURESHI, DAVID MEGÍAS, and HELENA RIFA-POUS. This system ensures the integrity and security of voters, their unique details, and the integrity of the polls. It also prevents third-party breaches, double voting, and coercion. Additionally, it protects against devices with viruses that could manipulate users' voting decisions and produce false results [4].

2.1 Motivation

- Election integrity*:* The motivation to develop smart voting systems using deep learning arises from the need to enhance election integrity and ensure fair and

secure elections. Deep learning can play a crucial role in detecting and preventing various forms of election fraud.
- Efficiency and accessibility: Smart voting systems aim to make the voting process more efficient and accessible. Deep learning can help automate various aspects of voting, such as voter identification, ballot processing, and result tabulation.
- Data-driven decision making: Deep learning techniques can analyze vast amounts of election-related data to provide valuable insights to election officials and policy-makers. This can lead to data-driven decision-making for improving the electoral process.

2.2 Creators

- Andrew Ng: In the fields of deep learning and machine learning, Andrew Ng is well-known. The dissemination of deep learning knowledge has been greatly aided by his work on deep learning and online learning environments like Coursera.
- Yann LeCun: Convolutional neural networks (CNNs), which are extensively employed in image processing applications, are the result of Yann LeCun's groundbreaking research. His contributions are pertinent to any study on intelligent voting systems based on images.
- Geoffrey Hinton: Geoffrey Hinton is a pioneer in deep learning and neural networks. His work on deep belief networks and backpropagation algorithms has been influential in the development of deep learning models.
- Ian Goodfellow: Ian Goodfellow authored the book "Deep Learning," which has become a foundational resource in the deep learning community. His contributions to generative adversarial networks (GANs) may also be relevant to smart voting system research.
- Fei-Fei Li: Fei-Fei Li is known for her work in computer vision and image analysis. Her research in image recognition and object detection can be highly relevant in the context of smart voting system (Fig. 1).

3 Methodology

3.1 Existing System

Electronic voting machines (EVM) and secret ballot voting are the two current voting methods; both involve labor-intensive and time-consuming procedures. Voting is available to those who are older than eighteen. Voters' IDs and other information are manually verified, and they are not permitted to cast ballots unless those data are confirmed. Everywhere in the nation where an election is held, the EVMs must be inspected and moved. It also requires security and manual power. Ballot voting is done entirely by hand, and the counting of votes cast in electronic voting machines

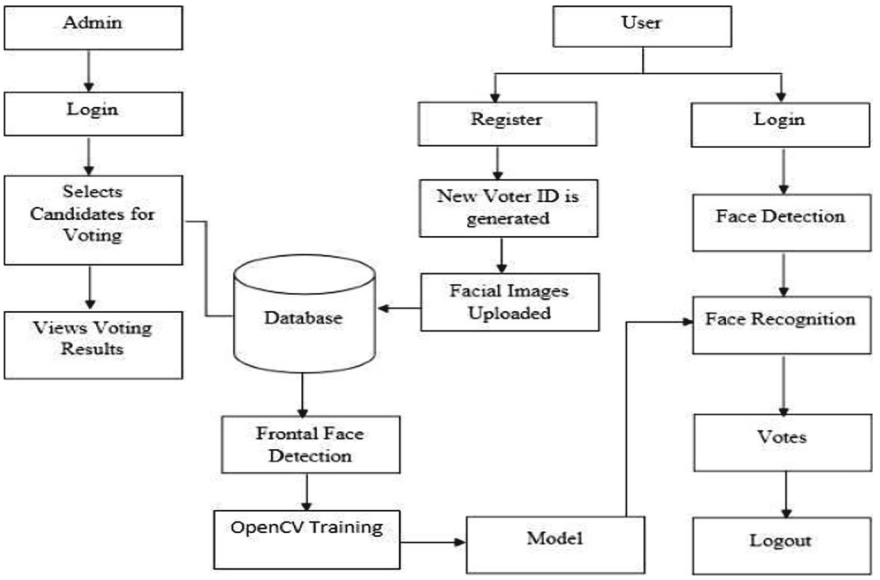


Fig. 1 System architecture

(EVMs) requires labor and takes a whole day. Thus, there are numerous ways for the vote and counting process to be tainted. Therefore, there is room to improve and streamline the current method.

3.2 Limitations

- Cybersecurity risks: [5–7] Smart voting systems are vulnerable to cyberattacks. Ensuring robust cybersecurity measures to protect against hacking attempts and data breaches is essential
- Education and training: Voters, poll workers, and election officials may require training to use and manage the smart voting system effectively. Providing adequate education and training can be a logistical challenge.
- Limited resources: In some regions or countries, limited resources, both financial and technological, may hinder the implementation of advanced smart voting systems.
- Unforeseen technical issues: Like any technology-based project, smart voting systems can encounter unexpected technical issues or glitches that disrupt the voting process.
- Public perception and trust: Building public trust in the new system and ensuring that voters have confidence in the security and fairness of the elections conducted using the smart voting system is crucial.

3.3 Proposed System

We have made an effort to create a safe online voting environment for voters to use in the proposed system, one that is impervious to illegal access [8, 9]. The suggested system's server features a distribution of authority that prevents the server from manipulating the votes. It is anticipated that the suggested online voting mechanism will improve the electoral system's dependability and openness.

3.3.1 Advantages

- Reduced time consumption.
- Fraud/gambling's can be minimized.
- Private and safe.
- Extremely practical.
- Simple to expand.
- Cheap.

3.4 Algorithm Implementation

The current study follows the algorithm using deep learning technology [10].

3.4.1 Haar Cascade

Algorithm: The initial step is to compile the Haar features. In essence, Haar features are just calculations performed on neighboring areas at a specific place within a different detecting window. The computation mostly consists of adding the brightness of each pixel in each sector and in between the total differences computations.

3.4.2 CNN Algorithm

A convolutional neural network is a primary method used for image recognition and categorization. CNNs are extensively utilized in various domains like as object identification and facial recognition. Our current project involves utilizing a CNN algorithm to identify and categorize drones within video footage. Input the image into the convolutional layer. Select parameters and apply filters using strides, and add padding if necessary. Conduct convolution on the picture and implement ReLU activation on the matrix. Apply pooling technique to decrease the size of the dimensions. Increase the number of convolutional layers. Flatten the output and input it into a fully connected layer, also known as an FC Layer. Utilize an activation function to generate the output of the class and classify images.

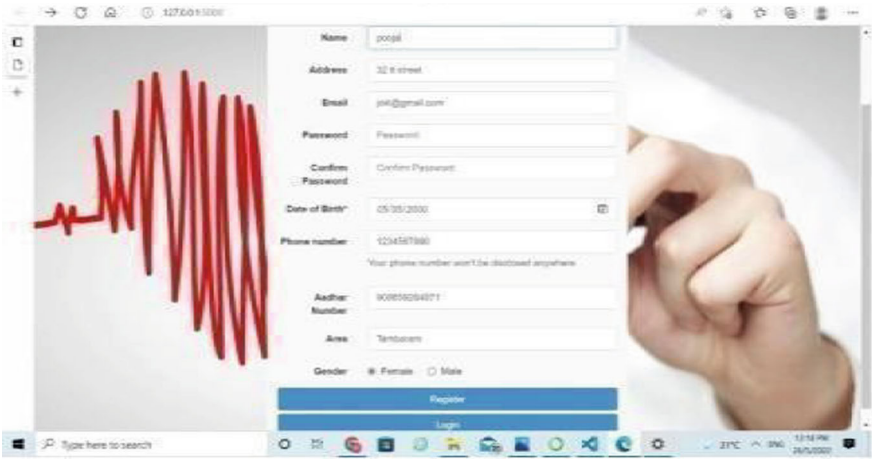


Fig. 2 Registration process

3.5 Working Process

The registration process for an online voting system typically involves several steps to verify the identity of the voter and ensure the integrity of the election. Here is a simplified explanation of the process [11–14].

3.5.1 User Registration

The registration process for an online voting system typically involves several steps to verify the identity of the voter and ensure the integrity of the election. Here is a simplified explanation of the process (Fig. 2).

3.6 Verification of Identity

The system verifies the provided information against government databases or other trusted sources to ensure the person is eligible to vote.

3.6.1 Account Creation

If the identity is verified successfully, the voter's account is created, and they are assigned a unique username or voter ID.



Fig. 3 Face recognition

3.6.2 Authentication

To access their account, voters need to log in using their username or voter ID and a secure password. Some systems might also require two-factor authentication for added security [15, 16].

3.6.3 Face Recognition

Face recognition is a technique that uses patterns and features on the face to identify and authenticate people [3, 4]. This particular kind of biometric technology is now widely used in many different applications (Fig. 3).

4 Results and Discussions

The data involved in an online voting system is highly sensitive and must be treated with utmost care to maintain the integrity, security, and privacy of the voting process. Here are some key aspects of the data in an online voting system (Figs. 4, 5, 6 and 7).

	Voter_Name	Aadhar_No	Gender	Age	city	Eligibility_Criteria
0	Suresh	624867091254	Male	39	Vishakapatnam	Yes
1	Ram	654787905467	Male	24	Srikakulam	Yes
2	Bhanu	904598713245	Male	38	Guntur	Yes
3	Shalini	679085349021	Female	22	Chittor	Yes
4	Nikhita	653490008124	Female	16	Tekkali	No
5	Christy	934509761435	Female	17	Palasa	No
6	Vasu	809574461834	Male	29	Vizayanagaram	Yes
7	Shankar	609835218008	Male	44	Vijayawada	Yes
8	Roshini	6456723456	Female	15	Vishakapatnam	No
9	Sriya	8097634267	Female	21	Srikakulam	Yes
10	Varshitha	6540983124	Female	34	Guntur	Yes
11	Swetha	9087634678	Female	23	Chittor	Yes
12	Srija	8025698762	Female	19	Tekkali	Yes

Fig. 4 Data set

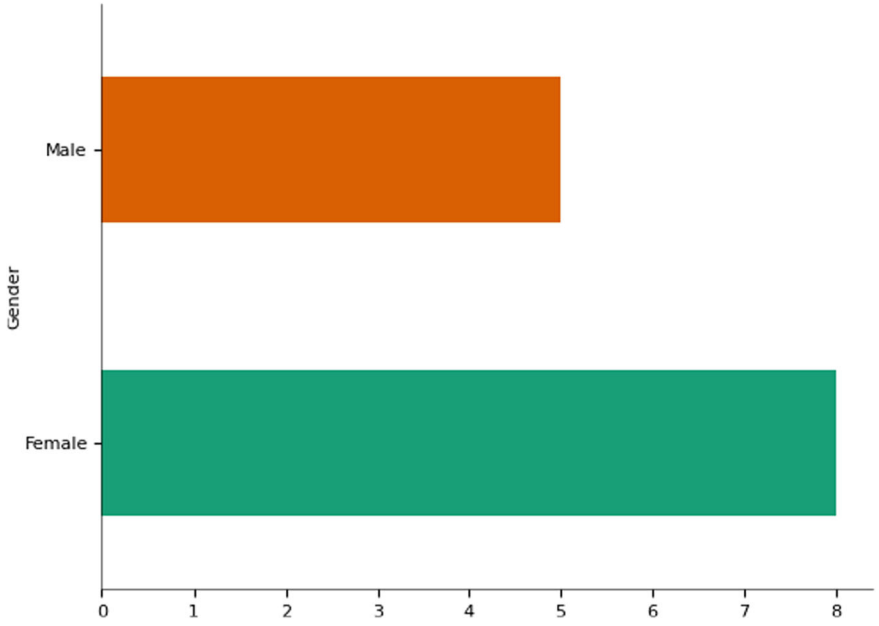


Fig. 5 Graph based on the data of voter's gender

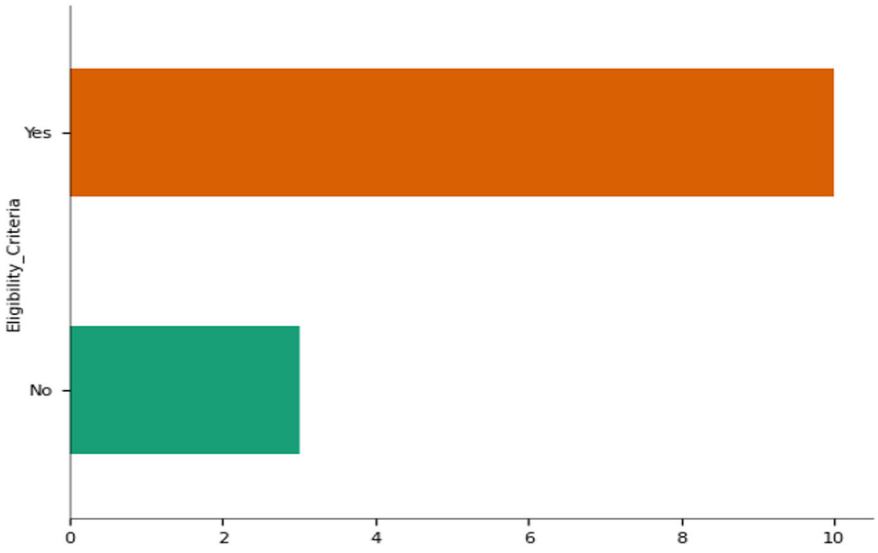


Fig. 6 Graph based on the data of voter's eligibility criteria

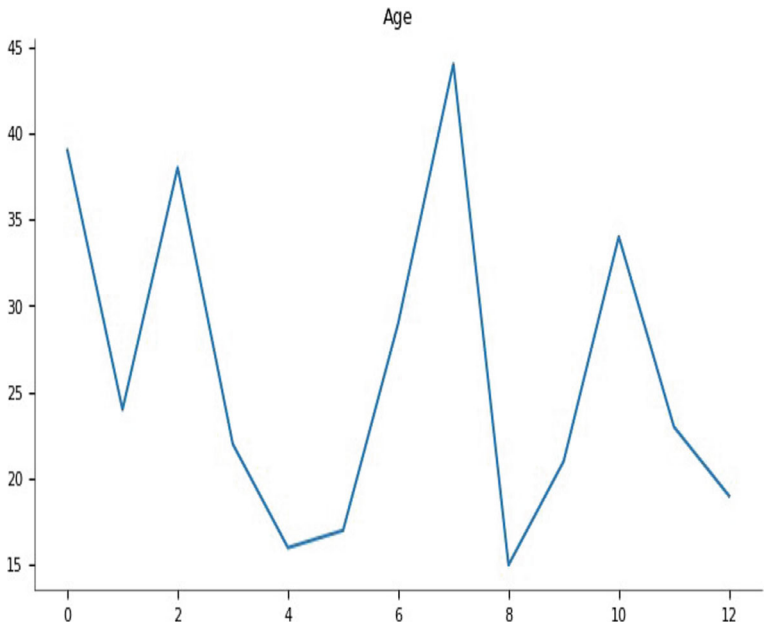


Fig. 7 Graph based on the data of voter's age

5 Conclusion

The suggested approach aims to address every flaw in the conventional or existing voting system by creating a safe online voting system based on facial recognition. Numerous strong points, such as accuracy, verifiability, convenience, characterize the suggested method. With this approach, voting is possible from anywhere that is secure as long as there is an Internet connection and face scanners. No election officer, paper ballot, or electronic voting equipment is needed.

References

1. Qureshi A, Megías D, Rifà-Pous H (2018) VSPReP: verifiable, secure and privacy-preserving remote polling with untrusted computing devices. In: Doss R, Piramuthu S, Zhou W (eds) Future network systems and security. In: FNSS 2018. Communications in computer and information science, Springer, Cham, p 878
2. Prabhu SG, Shalini S, Rachel AS, Roshinee AR (2020) Tracking real time vehicle and locking system using labview applications. In: 2020 6th International conference on advanced computing and communication systems (ICACCS), Coimbatore, India, pp 55–57
3. Annoshmitha Das F (2016) VOT-EL: three tier secured state-of-the-art EVM design using pragmatic fingerprint detection annexed with NFC enabled voter-ID card. IEEE
4. Mondal I, Chatterjee S (2019) Secure and hassle-free EVM through deep learning based face recognition. In: 2019 International conference on machine learning, big data, cloud and parallel computing (COMITCon), Faridabad, India, pp 109–113
5. Thirrunavukkarasu RR, Meeradevi T, Ravi A, Ganesan D, Vadivel GP (2019) Detection R peak in electrocardiogram signal using Daubechies wavelet transform and Shannon's energy envelope. In: 2019 5th International conference on advanced computing & communication systems (ICACCS), Coimbatore, India, pp 1044–1048
6. Prabhu SG, Vinotha K, Shanthala M, Subhashini SR, Vishnu S (2017) IOT based home automation and security system. SSRG Int J Electron Commun Eng (SSRG-IJECE) **4**(3):19–22
7. Kohno T, Stubblefield A, Rubin AD, Wallach DS (2004) Analysis of an electronic voting system. In: IEEE Symposium on security and privacy, 2004. Proceedings. Berkeley, CA, USA, 2004, pp 27–40
8. Keerthana G, Priyanka P, Alise Jenifer K, Rajadharashini R, Aruna Devi P (2017) Impressive smart card based electronic voting system. Int J Res Eng Technol 3:284–288
9. Malathy S, Rastogi R, Maheswar R et al (2020) A novel energy-efficient framework (NEEF) for the wireless body sensor network. J Supercomput 76:6010–6025
10. Pooja NP, Anuja T (2022) Smart voting system using deep learning techniques. Int J Eng Res Technol (IJERT) ETEDM 10(08):25–28
11. Chaum D (2004) Secret-ballot receipts: true voter-verifiable elections. IEEE Secur Priv 2(1):38–47
12. Evans F, Paul S (2004) Election security: perception and reality. IEEE Security Privacy Mag 2(1):24–31
13. Jefferson F, Rubin AS, Wagner T (2004) Analyzing internet voting security. Commun ACM 47(10):59
14. Evans D, Paul N. Election security: perception and reality. IEEE Secur Privacy 2(1):24–31
15. Shekhar Mishra F, Roja Y, Peter S (2018) Electronic voting machine using biometric finger print with Aadhar Card authentication. Int J Eng Sci Comput (2018)
16. Maheswar R, Kanagachidambaresan GR (2020) Sustainable development through Internet of Things. Wireless Netw 26:2305–2306

Mechanism of Data Sharing Using Secured Keyword Search in Cloud Computing



Umamaheswararao Mogili, Aezeden Mohamed, and Collettah Kasup

Abstract Cloud computing has revolutionized the ability to store and analyze vast quantities of data in a manner that is both economical and adaptable. Keyword search is an important mechanism for users to retrieve information from the cloud, but traditional keyword search techniques are vulnerable to attacks from cloud service providers or malicious users. The proposed mechanism uses a combination of encryption, data fragmentation, and user authentication to guarantee that only approved users can search for and retrieve the data, and user authentication is implemented. At the same time, the data remains confidential and secure. The results present a prototype implementation of the mechanism and evaluate its performance in a real-time scenario.

Keywords Cloud computing · Encryption · Decryption · Cipher text

1 Introduction

Cloud computing is a widely recognized computing design that enables end-users to conveniently retrieve and store their information and applications via the Internet. However, the security of cloud computing has been a significant concern for many organizations and individuals who want to protect their sensitive data from unauthorized access and disclosure. Secure keyword search and data sharing mechanisms

U. Mogili (✉)
Department of Computer Science and Engineering, Avanthi's St Theressa Institute of Engineering and Technology, Chepurapally, Andhra Pradesh, India
e-mail: umajrfnit@gmail.com

A. Mohamed
Department of Mechanical Engineering, PNG University, Lae, Papua New Guinea
e-mail: aezeden.mohamed@pnguot.ac.pg

C. Kasup
Department of Business Studies, PNG University, Lae, Papua New Guinea
e-mail: 22800315coka@pnguot.ac.pg

© The Author(s), under exclusive license to Springer Nature Singapore Pte Ltd. 2025

B. B. V. L. Deepak et al. (eds.), *Recent Advancements in Product Design and Manufacturing Systems*, Lecture Notes in Mechanical Engineering,
https://doi.org/10.1007/978-981-97-6732-8_41

have been proposed as solutions to these security issues in cloud computing. Searchable encryption is a popular approach for achieving secure keyword searches in cloud computing. It allows users to encipher their information before uploading to the cloud and perform keyword searches on the encrypted data without revealing the plaintext to the cloud service provider [1]. Symmetric searchable encryption enables the user and the cloud service provider to jointly possess a confidential key, which is utilized for both searching and enciphering the information (data). At the same time, public key searchable encryption involves the use of a public key to encipher the information file and a private key to search the data file [2].

Homomorphic encryption is another approach for ensuring confidential keyword searches and secure data sharing in cloud computing. This approach enables secure data sharing and keyword search while preserving data privacy [3]. However, Fully Homomorphic Encryption (FHE) is computationally expensive and is not suitable for all types of data and applications. Secure multi-party computation (MPC) and secure two-party computation (MTC) protocols are other approaches for achieving data sharing and secure keyword search in cloud computing [4]. MPC and two-party computation protocols are computationally expensive and require a high level of coordination among the parties. However, they provide a high degree of security and privacy for data sharing and keyword searches. Researchers have also proposed application-specific protocols. These protocols are outlined to meet the specific security and privacy requirements of different application domains such as healthcare, social media, and financial systems.

1.1 Fuzzy Identity-Based Cryptography

Fuzzy identity-based cryptography (FIBC) can be used in data sharing and secure keyword search mechanisms in cloud computing environments. In cloud computing, data is stored on remote servers, and users access it over the Internet. This poses various security and privacy concerns, including unauthorized entry, information disclosure, and data manipulation. FIBC can be used to address these challenges by allowing for fine-grained access control and secure data sharing [5, 6]. In a secure keyword search system, users can encrypt their data with FIBC, ensuring that solely authorized individuals can search for and access the information. To achieve this, the user first generates a private key using its imprecise identity and a set of attributes. The user then encrypts the data using FIBC, such that only users with the same attributes can access and decrypt the data. When a user desires to look for a specific keyword, they transmit a search query to the cloud server [7]. The server then retrieves the relevant encrypted data, which it decrypts using FIBC and returns to the user [8]. In a data sharing mechanism, the utilization of FIBC guarantees that solely authorized users can modify and access the information. For example, in the healthcare setting, FIBC can be used to encrypt medical records such that only doctors with the appropriate specialty and experience level can access and modify the records [9, 10]. To achieve this, each authorized user is allocated a set of attributes that correspond to

their specialty and experience level. The data is then encrypted using FIBC, such that only users with the appropriate attributes can modify and access the information. The data is safeguarded against unauthorized access and alteration, guaranteeing its protection [11].

1.2 Attribute-Based Cryptography for Cipher Text-Policy

Cipher text-policy attribute-based cryptography (CP-ABE) is another cryptographic mechanism that can be used to enhance privacy and security features in cloud computing environments. CP-ABE is a type of access control mechanism that uses attributes to specify who can access and decrypt data. In a secure keyword search system, CP-ABE can be used to essential that only authenticated users can retrieve and search data [12]. For example, in a healthcare setting, CP-ABE can be used to encrypt medical records such that only doctors with the appropriate specialty and experience level can access and search the records. To achieve this, each authorized user is assigned a set of attributes that correspond to their specialty and experience level [13]. The data is then encrypted using CP-ABE, ensuring that only users who wish to search for a specific keyword, will transmit a search query to the cloud server. The server then retrieves the relevant encrypted data, which it decrypts using CP-ABE and returns to the user. For example, in a financial setting, CP-ABE can be used to encrypt financial data such that only users with the appropriate clearance level and job role can access and modify the data [14]. The information is subsequently encoded utilizing CP-ABE in a manner that solely individuals possessing the suitable attributes can decipher and retrieve the information. This guarantees that the data remains safeguarded against unauthorized entry and alteration. The exploitation of privacy-preserving personal health records involves the utilization of multi-authority attribute-based cryptography with revocation.

Privacy-preserving personal health record (PHR) exploitation multi-authority attribute-based cryptography (MA-ABE) with revocation is a more advanced cryptographic mechanism that can be used to enhance security, safety, and privacy in cloud computing environments for personal health records [15, 16]. In this mechanism, a user generates a private key using attributes such as their name, age, gender, and medical conditions. The data is then encrypted using MA-ABE, which involves multiple authorities who issue credentials based on different attributes. This ensures that the data can only be accessed by users with the appropriate attributes. In addition, the mechanism includes a revocation mechanism that allows for the revocation of access to data in case of any changes to the user's attributes. For example, if a user's medical condition changes, their access to certain data can be revoked [17]. The server then decrypts the data using the appropriate private keys issued by the authorities. In a data sharing mechanism, the same principles apply. Each user is assigned a set of attributes, and the data is encrypted using MA-ABE, such that only users with the appropriate attributes can access and modify the information. The revocation mechanism is also used to ensure that access to data can be revoked in

case of any changes to the user's attributes [18, 19]. The recent technology of artificial intelligence and machine learning applications is increasing the efficiency of the cloud computing architecture automatically [20].

In summary, privacy-preserving PHR exploitation MA-ABE with revocation is a powerful cryptographic mechanism that can be used to enhance security and privacy in cloud computing environments for personal health records. By using multiple authorities to issue credentials based on different attributes and including a revocation mechanism, the mechanism ensures that the information (data) can only be gained access by end-users with the congruous attributes and that access can be revoked in case of any changes to the user's attributes. Based on the above research practices, the present paper describes the data sharing and secured key search mechanism for cloud computing. The section describes the introduction part of the presented work and the section describes the literature review of the present work. Section 3 presents the methodology used to create the security key in the process of decryption and encryption. The fourth section presents the esteemed results and discussions of the final output of the work. The last section ends with the conclusion following references.

2 Methodology

The cloud computer server reserves the encipher data with accumulation C and the searchable enciphered tree I index for the data keeper. Upon reception of the trap door (TD) from the data user, the server analyzes the index tree I and subsequently provides the appropriate collection of top-k ranked encoded documents. Moreover, after obtaining the revised data from the data owner, the cloud server must reform both indexes I and document collection C under the information obtained. A scheme for generating dynamic keys plays a crucial role in achieving the current multi-keyword-ranked search scheme that utilizes parallelism. The process of sending data to multiple users involves several steps. Initially, when multiple users request data, each user will receive a unique dynamic key to access the enciphered cloud data. Furthermore, the data can only be accessed by the user upon entering the correct dynamic key. This not only enhances privacy but also enables a simultaneous search process. In our system, we have chosen the B-tree as the indexing data structure to create a connection between the data documents and the search query.

The evaluation of the similarity between a document and a search query involves analyzing the internal data correspondence, particularly focusing on the frequency at which the query keywords appear within the document. To facilitate this evaluation, each document is transformed into a balanced B-tree based on the keywords and then encrypted using the cloud service risk assessment (CRSA) model. When a user initiates a search, a trapdoor is generated for the keywords, enabling efficient retrieval of relevant documents. Our objective is to develop and evaluate various keyword-ranked search methods by utilizing the commutative Rivest-Shamir-Adleman (RSA) algorithm and the searchable index trees of the B-tree data structure re-used. We have

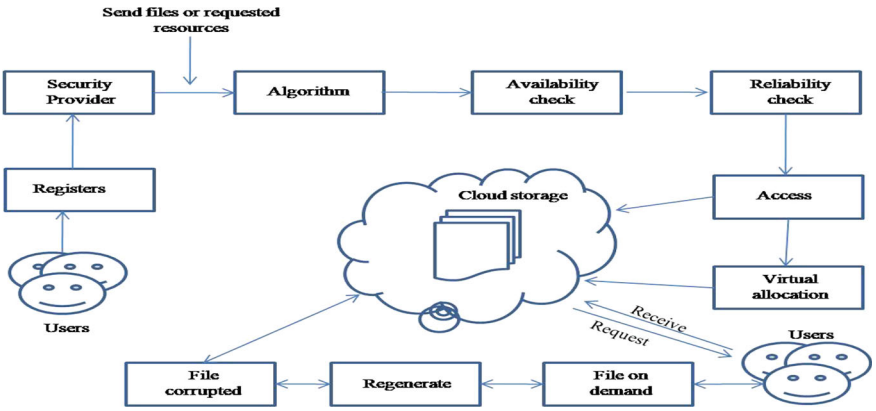


Fig. 1 Resource allocation and secure data storing architecture of the system [17]

devised a secure ranked multiple-keyword search approach for encrypted cloud data using CRSA. Additionally, the author has examined its efficiency on a searchable index tree that is based on B-trees. The system's configuration is depicted in Fig. 1. The implementation process involves the following steps.

2.1 Requirement Analysis

The first stage is to identify the user requirements and source requirements for the project. A crucial aspect involves grasping the project's objectives, outlining its extent, and pinpointing the stakeholders engaged in it.

2.2 System Design

It is the next stage in system design to design the system architecture. This includes identifying the components or applications of the system, defining their roles and responsibilities, and determining how they will interact with each other.

2.3 Data Model Design

Once this system architecture is designed, the next stage is to design the data model. This may include identifying the types of data that will be stored, defining the data schema, and determining how the data will be accessed and shared.

2.4 Encryption

To ensure data security, encryption should be used to protect the data while it is stored and transmitted. This includes selecting the appropriate encryption algorithms and implementing them in the system.

2.5 Implementation

After the design has been finalized, the subsequent step involves the implementation of the system. This encompasses the process of coding, establishing the required infrastructure, and conducting thorough testing of the system.

2.6 Encryption-Based Approach

Before saving the data in the cloud storage is encrypted using an encryption-based approach. To ensure the data is protected from unauthorized access, only authorized users can access it. To search for the data, the user provides the search keyword, and the search is performed on the encrypted data. This approach provides security, but it can be slow and may not be suitable for large data sets.

2.7 Homomorphic Encryption

This approach provides privacy and security, but it can be computationally intensive.

This approach allows computation on encrypted data the data is encrypted, and the encrypted data can be searched by the user without the need for decryption. The search result is also encrypted, and the user can decrypt the result using a decryption key. This approach provides privacy and security, but it can be computationally intensive.

2.8 Secure Multiparty Computation

This approach allows multiple parties to compute the same data without sharing the data. The data is encrypted, and each party holds a decryption key. The parties can perform a search on encrypted data, and the result is computed without any party knowing the data. This approach provides security and privacy, but it can be complex to implement.

2.9 Attribute-Based Encryption

In this approach, the data is encryption based on attributes. The user can search for data based on the attributes, and the information is decrypted only when the user has the required attributes. This approach provides security and privacy, but it requires a careful full design of the attribute-based access control system.

2.10 Trusted Third-Party Approach

This party is the approach that is responsible for performing the search of the data. The data is encrypted, and the third party holds the decryption key. The user provides the search keyword to the third party, and the search is performed on the decrypted data. This approach provides security, but it requires trust in the third party.

3 Results and Discussions

To attain a reliable method for conducting keyword searches and sharing data in cloud computing, the utilization of the following techniques is necessary.

3.1 Encryption

The act of converting plain text or data into an illegible format, referred to as ciphertext, to safeguard the information from unauthorized access, is known as encryption. Encryption can be employed to protect data while it is stored and while it is being transmitted.

3.2 Searchable Encryption

This encryption method enables searching through encrypted data without disclosing the original text. This approach proves valuable in preserving data confidentiality while granting authorized users the ability to conduct searches.

3.3 Access Control

The process of controlling who has access to what resources in a system. Access control is a crucial process that encompasses authentication, authorization, and accounting. Authentication verifies the user's identity, authorization determines access based on identity and permissions, and accounting maintains a record of user activity. The primary objective of access control is to safeguard sensitive data and resources by allowing only authorized users to access them.

3.4 Data Sharing

Data sharing involves the exchange of data between two or more parties. For the security and privacy of the data being shared, it is imperative to incorporate encryption and access control mechanisms into the system.

3.5 Auditing and Logging

Logging and auditing are the processes of monitoring and recording system events, user activity, and access to resources. This information is used to identify and investigate security incidents, monitor compliance with policies and regulations, and detect anomalies or unauthorized access attempts.

Navigate to w.w.w.sample.com. Validation should be as below please entering a valid username and password to get the secure keyword search and data sharing shown in Fig. 2. At that time browser asks to upload the encrypted file to create the keyword for encrypting shown in Fig. 3. In the next step, user file request console will open, and in that select the user name to get the details shown in Fig. 4.

After that, the key generation console will open in enter the security key to encrypt the data. The key assigned to the user console is detailed in Fig. 5. Figure 6 presents the cloud user information. The cloud information of the user should be displayed in this console such items are user ID, user name, mobile no, email ID, city, registered date, and time.

Finally, the decrypted file download console will be displayed with the details of the name, file name, and security key. Then click the download button to download the decrypted file which will be displayed in Fig. 7.

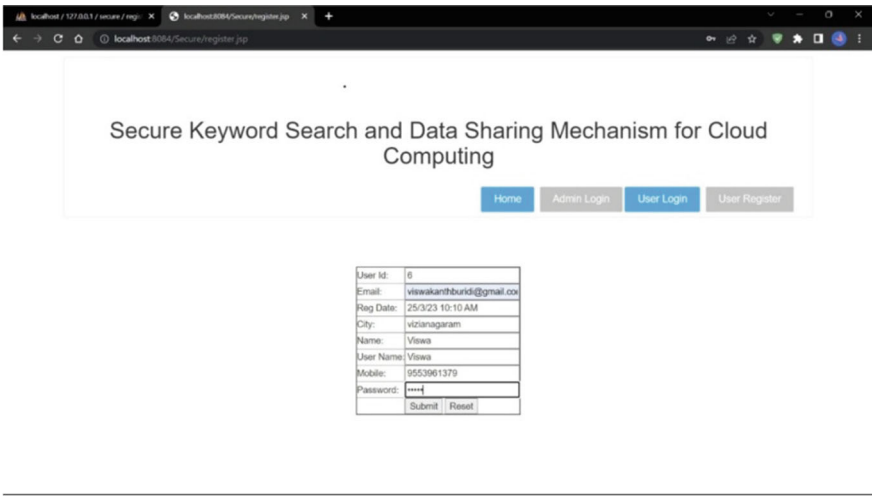


Fig. 2 User registration

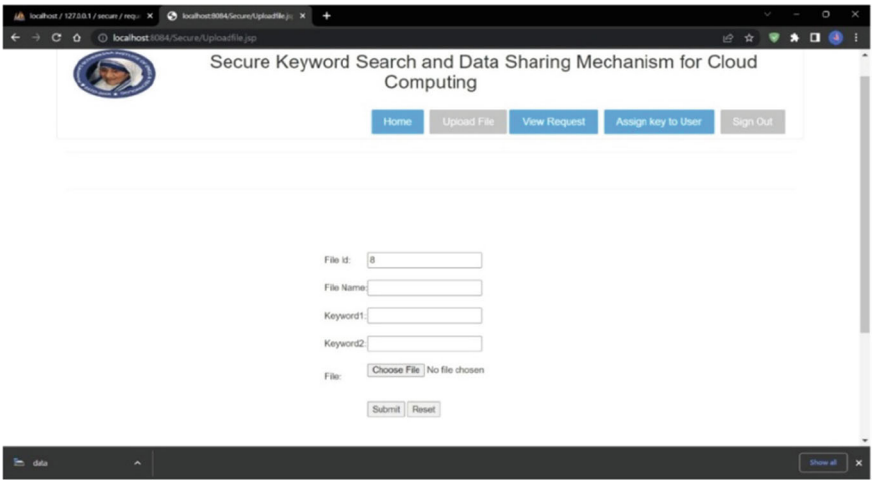


Fig. 3 Upload file

4 Conclusion

In conclusion, our proposed data sharing and keyword search mechanism using cloud computing addresses the security and privacy concerns associated with traditional keyword search techniques in cloud computing. The mechanism employs a combination of encryption, data fragmentation, and user authentication to make sure that authorized users only can access and search the information while maintaining

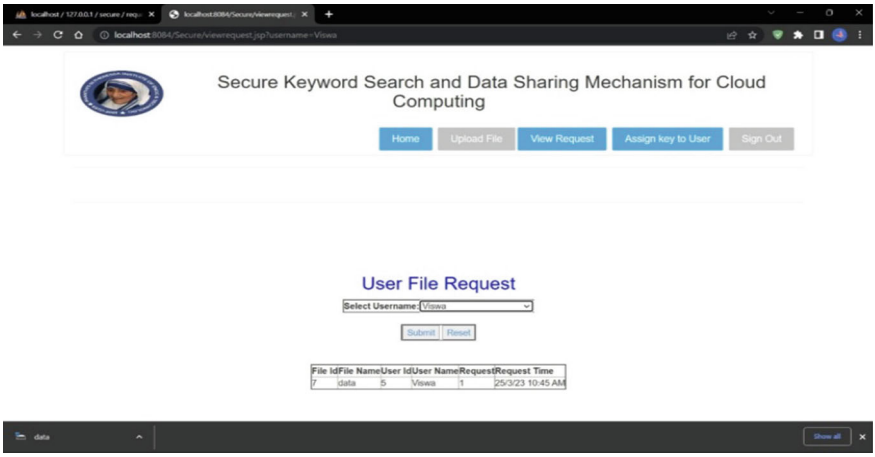


Fig. 4 View requisition

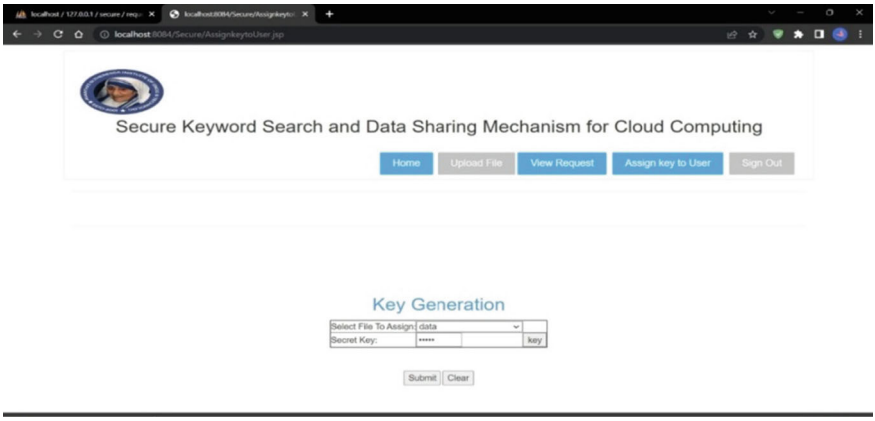


Fig. 5 Assign a key to the user

confidentiality and security. The implementation of our prototype demonstrates that our mechanism is efficient and effective in providing secure keyword search and data sharing capabilities. Our evaluation shows that the mechanism is scalable, and the search time is acceptable even for large data sets. Furthermore, the mechanism provides resistance to various attacks, including keyword guessing, statistical analysis, and dictionary attacks, thereby ensuring the security of the data. Our proposed mechanism offers a viable solution for ensuring secure keyword search and data sharing in the realm of cloud computing technology. With the ever-increasing adoption of cloud computing, it becomes imperative to have mechanisms in place that guarantee the confidentiality and privacy of sensitive data. Our contribution to this

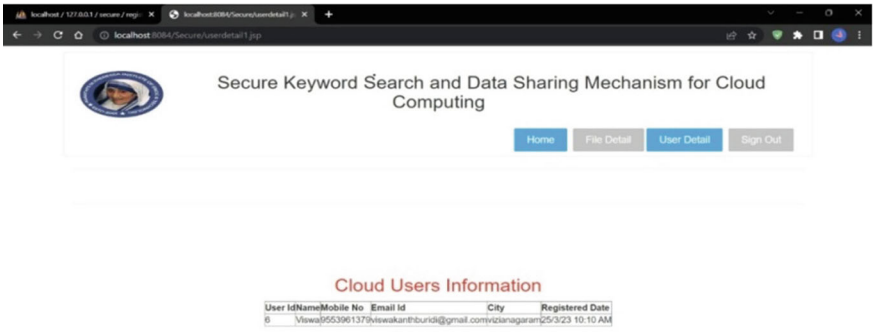


Fig. 6 Cloud user information

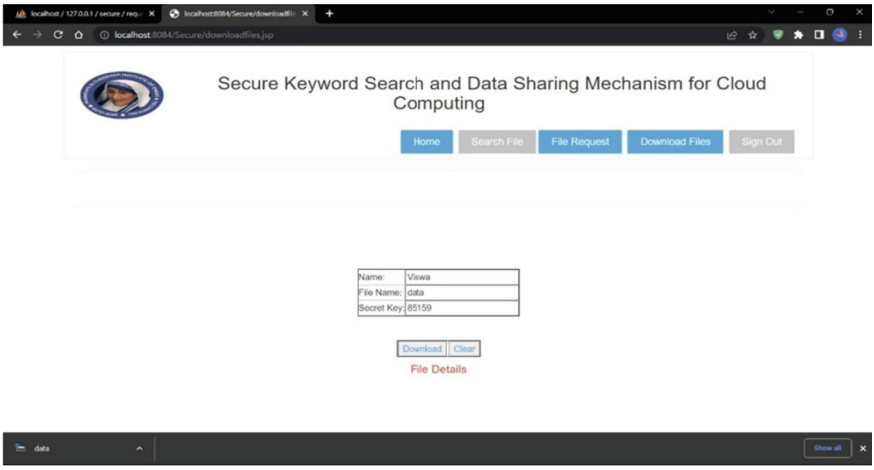


Fig. 7 Download files

endeavor involves offering a secure and effective solution for conducting keyword searches and sharing data in the cloud.

References

1. Bellare M, Boldyreva A, O'Neill AA (2007) Deterministic and efficiently searchable encryption. In: Advances in Cryptology-CRYPTO 2007: 27th Annual International Cryptology

Conference, Santa Barbara, CA, USA, August 19–23. Proceedings 27, pp 535–552. Springer Berlin Heidelberg
2. Chai Q, Gong G (2012) Verifiable symmetric searchable encryption for semi-honest-but-curious cloud servers. In: 2012 IEEE International Conference on Communications (ICC), pp 917–922. IEEE
3. Yi X, Paulet R, Bertino E, Yi X, Paulet R, Bertino E (2014) Homomorphic encryption. Springer International Publishing, pp 27–46
4. Goldreich O (1998) Secure multi-party computation. Manuscript. Preliminary Version 78(110)
5. Sahai A, Waters B (2005) Fuzzy identity-based encryption. In: Advances in Cryptology–EUROCRYPT 2005: 24th Annual International Conference on the Theory and Applications of Cryptographic Techniques, Aarhus, Denmark, May 22–26. Proceedings 24, pp 457–473. Springer Berlin Heidelberg
6. Yan H, Gui W (2021) Efficient identity-based public integrity auditing of shared data in cloud storage with user privacy preserving. Access IEEE 9:45822–45831
7. Phaneendra HD (2014) Identity-based cryptography and comparison with traditional public key encryption: a survey. Int J Comp Sci Inform Tech 5(4):5521–5525
8. Tan SY (2014) Cryptanalysis, provable security, and implementation of fuzzy identity-based cryptography. Doctoral dissertation, UTAR
9. Wang XA, Ma J, Xhafa F, Zhang M, Luo X (2017) Cost-effective secure E-health cloud system using identity-based cryptographic techniques. Futur Gener Comput Syst 67:242–254
10. Lakshmi SM, Mogili U, Eluri S, Rao DR (2023) Online dynamic out patient queue system for automated token generation in hospitals, science, technology and development, 12(7):71–78
11. Zhang K, Liu X, Li Y, Zhang T, Yang S (2020) A secure enhanced key-policy attribute-based temporary keyword search scheme in the cloud. Access IEEE 8:12S7845–127855
12. Liang K, Fang L, Susilo W, Wong DS (2013) A ciphertext-policy attribute-based proxy re-encryption with chosen-ciphertext security. In: 2013 5th International Conference on Intelligent Networking and Collaborative Systems, pp 552–559. IEEE
13. Zhang L, Hu G, Mu Y, Rezaeibagha F (2019) Hidden ciphertext policy attribute-based encryption with fast decryption for personal health record system. IEEE Access 7:33-202–33-213
14. Ge C, Susilo W, Fang L, Wang J, Shi Y (2018) A CCA-secure key-policy attribute-based proxy re-encryption in the adaptive corruption model for Dropbox data sharing system. Designs Codes Cryptograh 86:2587–2603
15. Qian H, Li J, Zhang Y, Han J (2015) Privacy-preserving personal health records using multi-authority attribute-based encryption with revocation. Int J Inf Secur 14:487–497
16. Sun J, Chen D, Zhang N, Xu G, Tang M, Nie X, Cao M (2021) A privacy-aware and traceable fine-grained data delivery system in cloud-assisted healthcare IoT. Internet of Things J IEEE 8(12):10034–10046
17. Shen H, Zhang M, Wang H, Guo F, Susilo W (2021) Efficient and privacy-preserving massive data processing for smart grids. Access IEEE 9:70616–70627
18. Mingwu Zhang Y, Chen JH (2021) SE-PPFM: a searchable encryption scheme supporting privacy-preserving fuzzy multikey word in cloud systems. Syst J IEEE 15(2):2980–2988
19. Geeta IS, Mogili U (2022) Use of several machine learning algorithms for effective prediction of cyberbullying communication in online social networks
20. Mogili U, Mohamed A (2023) Artificial intelligence and machine learning in the fields of education, medical, and smartphones. AIP Conf Proceed 2917(1)

Prediction of Covid-19 Recovery Chances Using Supervised Machine Learning Classification



R. Dhanalakshmi, A. Nivashini, and N. Vijayaraghavan

Abstract Predictive analytics if combined with machine learning approaches have the potential to play a significant role in forecasting the spread of respiratory infections. Machine learning approaches aid in the mining of data to better assess and forecast the presence or absence of covid-19 infection. In this paper, XGBoost Ensemble Classification using a fine-tuned approach is being used. Various machine learning algorithms are being analyzed and XGBoost Ensemble Classification algorithm is used to forecast and predict the covid-19 infected patient recovery chances that is the possible outcome of a covid-19 infected patient along with the prediction probability of recovery. The suggested categorization model is applied to a variety of situations. When compared to other ensemble models like random forest, hybrid ensemble and other individual classifiers such as decision tree, logistic regression, K-nearest neighbor, support vector machine and Naive Bayes, the XGBoost Ensemble Classification model gave the highest accuracy. Predicting the correct class is important. Thus, the proposed system discusses the possibility of automated prediction for covid-19 infected patient recovery chances along with the probability of recovery and the effectiveness of such predictions.

Keywords Machine learning · Data processing · Ensemble method

R. Dhanalakshmi (✉)
Centre for Cyber Physical Systems, School of Computer Science and Engineering, Vellore Institute of Technology, Chennai, India
e-mail: dhanalakshmisai@gmail.com

A. Nivashini
Department of Computer Science and Engineering, MNM Jain Engineering College, Chennai, India

N. Vijayaraghavan
Department of Mathematics, KCG College of Technology, Chennai, India

© The Author(s), under exclusive license to Springer Nature Singapore Pte Ltd. 2025

B. B. V. L. Deepak et al. (eds.), *Recent Advancements in Product Design and Manufacturing Systems*, Lecture Notes in Mechanical Engineering,
https://doi.org/10.1007/978-981-97-6732-8_42

1 Introduction

The coronavirus has spread all over the planet in an exceptionally brief period which turned into a pestilence and fell the wellbeing frameworks of numerous nations. In the course of the most recent couple of months, the infection has affected seriously with a ceaseless expansion in the quantity of affirmed cases. As per WHO, internationally 2.38 M individuals have ceased to exist of 108 M affirmed cases (WHO 2021). India with the second biggest populace on the planet remains in the most five impacted nations on the planet.

Detecting the presence of coronavirus is a difficult task. AI gives magnificent strategies to identify it [1]. Also, (DM) can be utilized to remove significant data from enormous information and perform complex assignments to find stowed away information, particularly for clinical datasets [2, 3]. In general, data pre-processing assumes an indispensable part in improving the general exhibition of AI and DM techniques. Further developing information quality in view of information re-adjusting and highlight determination will improve the learning system and stay away from overfitting issues [4–6]. An imbalanced information issue happens when the quantity of tests for one class is bigger than different classes. This will compel the AI classifier one-sided toward one class more than the other one. In the dataset utilized here in this paper, the quantity of patients who recovered and the quantity of not recovered infected patients are balanced after data pre-processing[7, 8].

2 Machine Learning Used in Predictions Related to Covid-19

Machine learning has been utilizing in numerous applications, particularly for time-series issues. The ARIMA calculation has been utilized broadly for anticipating straight time-series issues [5], and it comprises of an autoregressive articulation (AR), a moving normal (Mama) part, and a differencing term (I). Profound learning calculations have been utilized of late for the errand of time-series determining and spatial time-series gauging [6]. One of the generally utilized calculations is long transient memory (LSTM) [9] which is a repetitive brain organization (RNN) that removes the similitudes between consecutive contributions by utilizing three entryways; neglect door, input door and result entryway to control the connection between the past information sources, this info and the result. Each LSTM cell comprises of those three doors, and typically, the LSTM layer contains a few LSTM cells.

Machine learning improvises to predict the following: (a) the episode of an infection, (b) the analysis of patients in view of their side effects, (c) investigating the seriousness of the infection on unambiguous age gatherings, (d) the seriousness of the infection on patients with other medical problems, (e) tracking down a solution for an infection and medication revelation, (f) examining patients who recuperated

from an infection, (g) concentrating on the appropriateness of the climate for the maintainability of the infection and (h) foreseeing the flare-up. Now, artificial intelligence algorithms aid people in giving essential information on covid-19 received from all of these sources on a day-to-day basis, which is a significant improvement over the previous methods. The data reveals some intriguing trends, such as passenger visiting places that are primarily afflicted by viruses and new sites. Machine intelligence approaches, on the other hand, are used to do predictive analytics in the context of respiratory illness. Machine intelligence approaches are being utilized to build deep learning-based models for providing tailored healthcare to patients in the early phases of the research and development process. A variety of machine learning algorithms have been developed during the current epidemic in an effort to identify patients who are most likely to become infected.

3 Related Works

Machine intelligence technology is making strides in healthcare hygiene. The methods and tools for discovering patterns in data are the focus of ML. Predicting infection risk variables is made easier by the patterns found. ML systems are capable of accurately predicting test results once they have been trained on historical data [6]. In the medical field, classification methods come in use, for example, in the treatment of heart disease. According to the data, Lymphopenia is a prevalent symptom in covid-19 individuals [10]. Social isolation and other preventative measures are necessary in order to treat most patients. As the virus transmits from person to person, maintaining a social distance is essential for protection. The RT-PCR test is performed on nasopharyngeal swabs. The virus's genetic material, RNA, is isolated for further study. Python's methods for data categorization, clustering and so on [11] can be used to make predictions. A precise forecast of travel history is needed to prevent the spread of the virus, and ML approaches must be employed [12]. On the test dataset, the classification algorithms run iterations that automatically enhance their performance. There are no labels, classifications, or categorizations in the test dataset that the models are trained on. Data that hasn't been seen is fed into the model, which is built on previous experiences. The dataset is mined by ML algorithms, which extract interesting patterns [13]. Researchers analyzed the impact of covid-19 with machine learning and gleaned public health insights [14]. Digital signal processing may be used to build supervised ML algorithms for genome research.

The random forest ML ensemble method with climatic data predicted the development of African swine fever-like illnesses [15]. In order to make accurate predictions of influenza epidemics, the researchers relied on comparative analysis rather than time-series methodologies. It is vital to detect fever hotspots and illness breakout forecasts linked to climatic conditions in Taiwan with the use of machine learning algorithms. A Bayesian classifier was employed in a similar investigation to forecast dengue outbreaks, and the results were quite accurate. Data mining techniques were utilized in a study that forecasted the number of cases of dengue fever in New Delhi.

4 Proposed System

The objective of this paper is to predict the covid-19 recovery chances using supervised machine learning classification ensemble methods and give the prediction results with the best and maximum accuracy by comparing and analyzing different supervised machine learning classification algorithms. The proposed system predicts the covid-19 recovery chances of patients and the approach used is supervised machine learning classification ensemble algorithms (ensemble methods combine more than one algorithm of the same or different kind for classifying objects). The dataset is obtained from the openly available dataset which is from Kaggle. The system architecture is depicted in Fig. 1. The dataset contains the pre-condition clinical records of more than 5 lakh patients with 23 attributes or features. Due to large real-time pre-condition dataset, the data pre-processing and data analysis of visualization is the challenging part to capture variable identification like dependent and independent variables, missing and duplicate value treatments, data validation, data cleaning/preparing on the entire given dataset. These data then use the multiple supervised machine learning classification algorithms to predict the best accuracy results of the model.

This study follows a series of measures that address the anticipation of sickness as well as the transmission of contamination. Prior to being pre-processed in the setup, the valid informative index with the crucial boundaries needed for analysis should be selected. This will allow the ML algorithm to handle the dataset with ease. Establishing the degree of preparation and testing data is necessary before running the classifier. Utilizing the experimental technique, this is completed. Then, at that point, every one of the grouping calculations is prepared and afterward tried. The last advance is to look at the changed presentation measurements talked about as in segment IV for all the ML algorithms.

Stage 1 patients are individuals who are undergoing the first medical evaluation and treatment. As part of their examination, patients in stage 2 have previously been

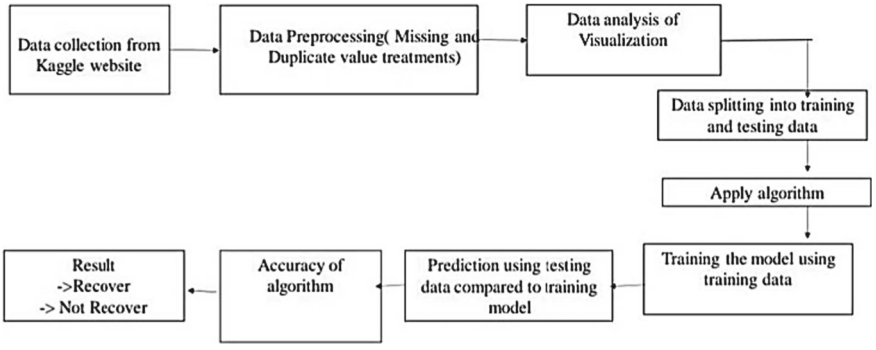


Fig. 1 System architecture

diagnosed with covid-19 and may have had covid-19-related pneumonia. Consequently, pneumonia features and the covid-19 status are added to a vector that includes other variables. If a patient is at stage 3, it means they have been given the option of being admitted into a hospital or being discharged. As a result, the vector's attributes now include the patient's hospitalization status. In addition to being hospitalized, patients in stage 4 are either intubated or admitted to an intensive care unit (ICU). Therefore, the properties of intubation and the ICU are incorporated to the vector. For the sake of accuracy, the system initially utilized a sample size of 5,66,602 observations, which after all the data pre-processing is reduced to a sample size of 20,352 observations with 8447 observations representing all known deceased patients in the database and another 11,905 observations drawn at random from the database of recovered patients. The system employed a 70/30% training/testing split of the final balanced data set.

5 Modules and Description

5.1 Dataset

We used data from www.kaggle.com, a public informative collection, to investigate and anticipate the recovery prospects of patients afflicted with the coronavirus. With 5,66,602 entries, the dataset includes 23 highlights that are pre-conditions for covid-19 patients. These highlights lead Kaggle to the enormous used information base for analysts and clinicians around the world. Thus, in this work, Kaggle informational collection is favored contrasted with other openly accessible informational indexes. It also has other datasets that give a few highlights of the infection in different stages, area-wise obsessive subtleties, the spread of illness and the death rate. These are used in various works to find out about contaminations and illness movement as depicted in Fig. 2 process flow

5.2 Pre-processing

The dataset contains categorical features, based on pre-condition clinical records. The data is pre-processed by doing the missing value treatments, duplicate value treatments and removing columns not needed. The dataset which initially had more than 5 lakh records with 23 features gets reduced to 20,352 records with 19 features after pre-processing. Clinical perceptions and reports are additionally considered for factual assessment of information and give data about sickness orders. Henceforth, barring non-huge and abundance elements and lessening the dimensionality of the subordinates furnished us with more exact execution. Utilizing a name encoder pre-handling technique, the system converted the distinct highlight into numerical

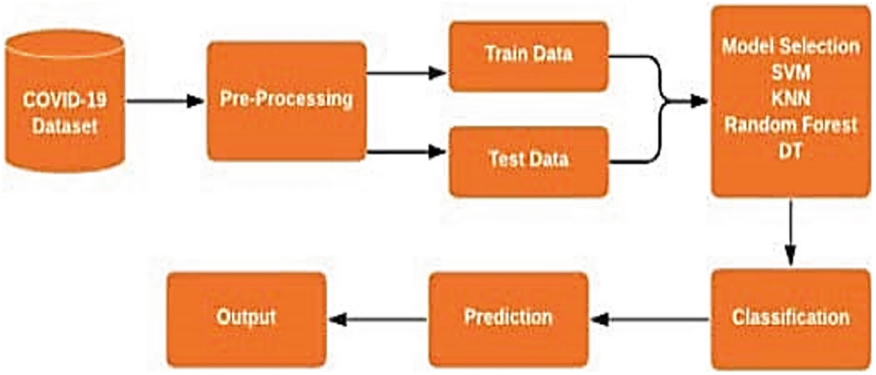


Fig. 2 Process flow

attributes. This authentic dataset is divided into datasets for testing and preparation. The machine is prepared by the use of prepared information.

5.3 Model Selection

Various machine learning algorithms are employed to analyze and predict the odds of recovery for coronavirus patients, as well as their likelihood of recovery based on the pre-conditions provided by the patients. The information conveyance in the present element choice is learned by the use of directed learning models such as DT, KNN and RF. Picking K-closest neighbor method contrasted with the calculations utilized by the prior analysts [2], gives numerous computations and disseminated learning assessments. After the comparison and analysis of all the machine learning algorithms including the ensemble algorithms, the XGBoost Ensemble Classification model gives the highest accuracy and maximum performance. So, the model selected for implementation and deployment using Flask is the XGBoost Ensemble Classification model since it has given the highest accuracy compared to the other machine learning algorithms applied to this dataset.

Few of the analyzed execution models are reviewed below.

5.3.1 Support Vector Machine (SVM)

The current study is able to execute characterization and relapse tasks that provide exact expectation with coronavirus highlights because SVM employs supervised learning models, as shown in Fig. 3. The data foci in support vectors that are closest to the choice surface are also known as hyper-planes. The system can forecast how many inputs will be needed to analyze a plane's maxima and minima by defining the hyper-plane.

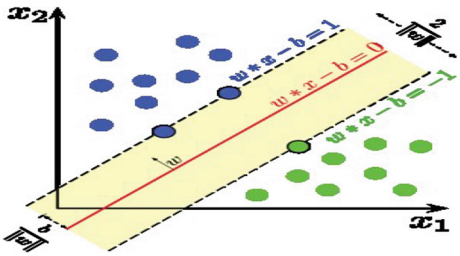


Fig. 3 Maximum-margin hyper-plane

$$\text{sqrt}(P2Q2) \tag{1}$$

5.3.2 KNN Algorithm

While brain networks are acquiring prominence in the PC vision, object location and example acknowledgment field, one region where K-closest neighbor's (KNNs) models are still regularly and effectively being utilized for arrangement undertakings that utilize different subsets of highlights in the PC vision. KNN is additionally called 'an apathetic learning calculation' thus however with most elevated expectation exactness. The cycle stream for KNN calculation is as per the following. Here assume the preparation test as 'm' and the obscure point as 'p.' The examples for preparing are put away in exhibit a [ ].For each preparing test, the Euclidean distance is determined by utilizing $d\,(a[i], p)$. Allow it to be meant as 'K' neighbors. Count the quantity of important informative elements in every classification which are nearer to the new element. Then the new information point is apportioned to the class which has all the nearest neighbors. Category A—covid positive patients, category-B—covid negative patient

5.3.3 Decision Tree

Decision tree (DT) uses supervised learning algorithm to predict coronavirus dataset on three basic criteria of age, area and spread from infected person. Each node is first organized with people who are affected by this virus and then decision tree resembles the sickness criteria and its effect in leaf node from which ensuing choice guidelines are spread to the leaf hub. A decision tree has two sorts of hubs.

Step 1: Each leaf node processes the data needed to predict positive case and help in decision making.

Step 2: Each inner node addresses the leaf node to predict covid positive patients.

5.3.4 Random Forest Classifier

Random forests work with an ensemble tree method where each tree consumes the random vector sampled, where these vectors help in increasing the accuracy in the final prediction. Selecting a suitable class has made to develop the accuracy of the most suitable class. eventual chosen class in the random tree for each node of tree and the best split is calculated based on m training set variable. We can determine the accuracy of ensemble method by selecting the input class in all levels.

6 Performance Evaluation Metrics

The confusion matrix to predict actual and predicted values using four different parameters is shown in Table 1. The confusion matrix provides results for the patients admitted covid patients in the matrix form and this can be predicted by the ML models.

In this paper, the accuracy, efficacy, precision, F1 score and recall values are evaluated using true positive and true negative, true positive, false positive and false negative. Thus, the accuracy is calculated which is a great measure of performance when the used data sets are symmetrical. Different classification machine learning approaches are utilized in the prediction, and the ultimate covid-19 recovery chances prediction is done using the results of these procedures. It has also been demonstrated that feature selection is beneficial in the prediction process. So, the XGBoost Ensemble Classification model has outperformed all other state-of-the-art approaches in terms of accuracy when compared to each other. As a result, XGBoost has demonstrated the best overall performance, followed by logistic regression and hybrid ensemble model (Fig. 4).

The above figures give a crystal-clear view of predicting accuracy in different algorithms of machine learning like decision tree, logistic regression, K-nearest neighbor, SVM, Naive Bayes, random forest, XGBoost and hybrid ensemble model. According to the results of the accuracy test, the XGBoost Ensemble Classification model was the most accurate of all the models developed, with an accuracy of 66.25%. This is in comparison to other models developed using decision tree, logistic regression, K-nearest neighbor, SVM, Naive Bayes, random forest, hybrid ensemble which scored 64.50, 66.02, 62.60, 64.70, 63.70, 62.32 and 65%, respectively, when the accuracy test was performed.

Table 1 Confusion matrix

	Predicted class		
		Class yes	Class no
Actual class	Class yes	True positive	False negative
	Class no	False positive	True negative

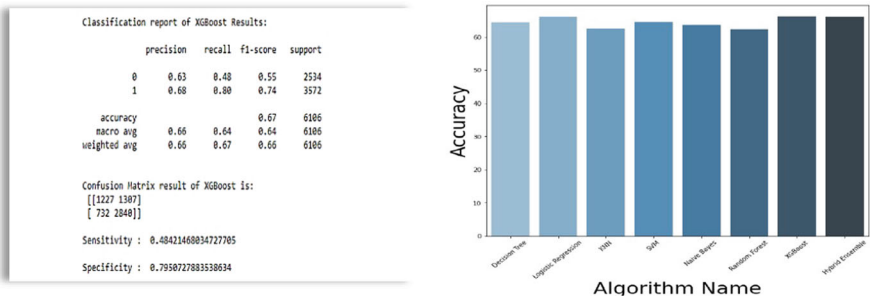


Fig. 4 Results for XGBoost algorithm and comparison

7 Conclusion

The paper has summarized the impact of covid in the patients and predicted covid positive patient's recovery chances. Since this disease has spread to approximately 213 nations across the world, it is important to predict the disease at early stage as possible. Covid-19 is spread by direct contact with an infected person, usually through sneezing or coughing, and there is currently no medically approved treatment to treat it. The system implemented ensemble method, probabilistic method and supervised learning method to predict covid-19 recovery chances along with the prediction probability of recovery.

References

1. Van Doremalen N, Bushmaker T, Morris DH, Holbrook MG, Gamble A, Williamson BN et al (2020) Aerosol and surface stability of SARS-CoV-2 as compared with SARS-CoV-1. N Engl J Med 382(16):1564–1567
2. Wadhwa P, Aishwarya Tripathi A, Singh P, Diwakar M, Kumar N (2020) Predicting the time period of extension of lockdown due to increase in rate of COVID-19 cases in India using machine learning. Mater Today 37:2617–2622. https://doi.org/10.1016/j.matpr.2020.08.509
3. Johnson M (2019) Predictive analysis based efficient routing of smart garbage bins for effective waste management. Int J Recent Technol Eng 8(3):5733–5739
4. Luckner M, Topolski B, Mazurek M (2017) Application of XGBoost algorithm in fingerprinting localisation task. In: Proceedings of the 16th IFIP international conference on computer information systems and industrial management. Springer, Bialystok, pp 661–71. https://doi.org/10.1007/978-3-319-59105-6_57
5. Vanden Driessche P (2017) Reproduction numbers of infectious disease models. Infect Dis Model 2:288–303. https://doi.org/10.1016/j.idm.2017.06.002
6. Iwendi C, Bashir AK, Peshkar A, Sujatha R, Chatterjee JM, Pasupuleti S et al (2020) COVID-19 patient health prediction using boosted random forest algorithm. Front Public Health 8:357. https://doi.org/10.3389/fpubh.2020.00357
7. Joy MR, Bairavel S, Dhanalakshmi R (2021) Implementing QR code-based contact tracing framework. In: Proceedings of the 2021 international conference on system, computation, automation and networking (ICSCAN). IEEE, pp 1–6

8. Sujatha R, Chatterjee JM, Hassanien AE (2020) A machine learning forecasting model for COVID-19 pandemic in India. Stoch Environ Res Risk Assess 34:959–972
9. Bhattacharya S, Maddikunta PKR, Pham QV, Gadekallu TR, Krishnan SSR, Chowdhary CL et al (2021) Deep learning and medical image processing for coronavirus (COVID-19) pandemic: a survey. Sustain Cities Soc 65:102589. https://doi.org/10.1016/j.scs.2020.102589
10. Dhanamjayulu C, Nizhal UN, Maddikunta PK, Gadekallu TR, Iwendi C, Wei C et al (2021) Identification of malnutrition and prediction of BMI from facial images using real-time image processing and machine learning. IET Image Process
11. Srinivasan K, Garg L, Datta D, Alaboudi AA, Jhanjhi NZ, Chang CT et al (2021) Performance comparison of deep CNN models for detecting driver's distraction. Comput Mater Continua 68:4109–4124
12. Wangping J, Ke H, Yang S, Wenzhe C, Shengshu W, Shanshan Y et al (2020) Extended SIR prediction of the epidemics trend of COVID-19 in Italy and compared with Hunan, China. Front Med 7:169
13. Zivkovic M, Bacanin N, Venkatachalam K, Nayyar A, Djordjevic A, Strumberger I et al (2021) COVID-19 cases prediction by using hybrid machine learning and beetle antennae search approach. Sustain Cit Soc 66:102669
14. Dhanalakshmi R, Anuja Mary A, Shrijith D, Vijayaraghavan N (2021) A study on covid-19: impacting Indian education. Mater Today Proc 18:2021. https://doi.org/10.1016/j.matpr.2021.02.786
15. Yang Z, Zeng Z, Wang K, Wong S-S, Liang W, Zanin M et al (2020) Modified SEIR and AI prediction of the epidemics trend of COVID-19 in China under public health interventions. J Thorac Dis 12:165–174

Considerations in Product Design and Development

Reviving Sawantwadi's Colorful Legacy: Exploring Artisan Perspectives on Traditional Wood Crafts

Omkar Sadashiv Rane and Suyash Khaneja

Abstract Sawantwadi is famous for its colorful wooden crafts made especially from Pangira (Indian coral tree) wood. The migrated Chitrari community is making wooden toys, and replicas of fruits, vegetables, and objects as per local and traditional needs. Due to the unavailability of raw materials, man power, and market demand, Sawantwadi crafts are facing issues to survive in the market which is affecting artisans, crafts retailers, and Sawantwadi crafts businesses. Hence, many of the artisans are changing their occupations to survive. Another challenge is that this type of craft needs to compete with PVC toys, wood toys exported from foreign countries which are comparatively cheaper. This study seeks to investigate the craftsmen's perspective and demonstrate how these crafts might be saved. Additionally, this study tests the variables in a qualitative way by conducting 12 personal detailed interviews with craft professionals. This technique enables an enhanced understanding of the craft process, which has not been done previously. The findings demonstrate support for the qualitative research tool providing a deeper understanding of the toy-making process. This study will be the first one to collaborate with the designers and make new applications, which can compete with toy competitors. The ultimate objective is to combine innovation and tradition to improve artists' livelihoods and protect this unique trade. The research not only identifies problems with Sawantwadi crafts but also suggests a way to revive them and preserve their cultural history.

Keywords Crafts · Wooden toys · Design process · Creativity · Product development · Sawantwadi toys

O. S. Rane (✉)
Symbiosis Institute of Design, Symbiosis International (Deemed University), Pune, Maharashtra, India
e-mail: omkar.rane@sid.edu.in

O. S. Rane · S. Khaneja
School of Business, World University of Design, Sonipat, Haryana, India

© The Author(s), under exclusive license to Springer Nature Singapore Pte Ltd. 2025

B. B. V. L. Deepak et al. (eds.), *Recent Advancements in Product Design and Manufacturing Systems*, Lecture Notes in Mechanical Engineering,
https://doi.org/10.1007/978-981-97-6732-8_43

1 Introduction

Crafts are innovative cultural and traditional expressions of rural areas. Craftsmen get inspiration from the natural world, the surrounding environment, and contextual demands to exhibit their creative abilities via their work. Handicrafts evolved with the evolution of man and society, mixing and stirring influences and events. India is a diversified nation with a sophisticated culture, and the metal, wood, textiles, pottery, and other materials used in crafts may help to illustrate our creative history. Both rural and urban residents benefit from the livelihood and informal economy of crafts. There are more than 23 million artisans working on various crafts, and there are reportedly more than 360 craft clusters in India [1]. Various incursions and settlements from outside people and the tides of time have not been able to diminish our diversity; rather, they have strengthened it. The craft forms, visual tales, and purposes they incorporate serve as a reflection of India's diversity and aesthetic. In India, there are 52 major tribes, 6 major religions, 18 major, and more than 1600 minor languages and dialects, 6400 castes and subcastes, and over one billion people. The variety of forms and colors seen in Indian festivals and months tells the story of more than 100 established crafts from various regions of the country. More than half of them come from rural areas that include mountains, valleys, deserts, forests, backwaters, coastlines, hills, and so on [1].

On a daily basis, Indian villages demonstrate creative competencies by making and transforming materials and spaces through the act of creation. Crafts are an effective source of self-development and long-term employment generation for many people living in difficult economic circumstances. With the advent of industrialization and industrial modes of production in India in the mid-twentieth century, handmade products fell out of favor and were largely ignored until the late twentieth century. Hence, crafts have moved from the forefront of a rising economy to a point where creative collaboration and engagement are required [2]. Also, craftsmen tried to transform their crafts in terms of design and manufacturing due to various factors associated with crafts such as industrialization, market conditions, material availability, skilled labor, and so on.

1.1 Sawantwadi Crafts Cluster

A city of artisans, Sawantwadi has a long history. It is well-known for its lacquerware and ganjifa cards [3], two crafts that the Telangana Brahmins introduced in the seventeenth century. Under Sawant Bhosale's authority, the Chitrari community received royal patronage for lacquerware in the eighteenth and nineteenth centuries. This time saw the introduction of numerous craft schools. Originally intended to be a wooden toy, this lacquerware has since become a geographical marker for Sawantwadi. Lt. Col. H.H. Rajesaheb and mother-of-three H.H. Rajmata Satvashila Devi founded Sawantwadi Lacquerwares in 1971. H.H. Rajesaheb discovered a Sawantwadi Cards



Fig. 1 Variety of Sawantwadi toys [5]

label at the Victoria and Albert Museum in London, which led to the founding of the business. After learning more about Sawantwadi's work, H.H. Rajesaheb went to the area to hunt for the artisans who would make the cards. Pundalik Chitari, who was 80 at the time, then guided H.H. Rajesaheb and his wife in the craft. As a result, they established Sawantwadi Lacquerwares to publicize and revitalize the craft of this neighborhood creator. This scenario has changed in the twenty-first century. Only a few craft workshops are producing wooden toys [4]. Hence, study aims to identify problems faced by Sawantwadi wooden toys through investigation of artisan's perception. It will help to identify preserve and revival techniques for Sawantwadi wooden toys (Fig. 1).

Type of products made in Sawantwadi crafts: Wooden vegetables, fruits, bullock carts, and various animals are well-known toys of Sawantwadi. The size of these toys varies from 4 to 8 inches.

2 Literature Review

The Chitari or Chitrakar community, which the Sawantwadi king recognizes, traditionally produces Sawantwadi crafts. Several communities moved to Sawantwadi from Karwada and established themselves there. Owing to its commercial success, this craft was adopted by other towns. Sawantwadi toys include wooden fruits, bullock

carts, and a variety of animals. These toys range in size from 4 to 8 inches [5]. Sawantwadi toys gave artists a reliable source of income. But, as a result of globalization, MNCs, large corporations, and internal and external rivals pose a serious threat to Sawantwadi toys. Focusing on handicrafts and raising awareness of eco-friendly toys are essential for market viability [6]. The Kanekar family has been producing wooden toys for the past four generations. However, the younger generation is leaving the artisan industry. The Sawantwadi craft is only being preserved by five to six families. The market for wooden toys is being squeezed out by plastic toys manufactured specifically for China products. Thus, the government must take proactive measures to ensure the survival of wooden crafts [7].

The crafts study may be divided into various aspects which are associated with the crafts, which explain elements such as society, education, skill-based learning, and market—product design, technology, aesthetics, and expertise [8].

In the global context, product design interventions have been taking place in select craft clusters. In the case of the Soapstone Craft Cluster in the Dhakotha Area of Kendujhar District, Odisha, India, product exploration involved blending Soapstone carved products and Soapstone turned products to create a fresh series of items. An integral part of this process was the active involvement of skilled craftsmen in the product design and development phases [9]. It is worth noting that there are numerous underprivileged and untapped clusters where similar interventions could bring about positive change. To prepare for such endeavors, frameworks have been proposed to expand the crafts market while respecting traditional approaches. Simultaneously, alternative methods for crafting have been identified [10]. Similarly, one of the studies showcased practical, hands-on experiences, employing design research methodologies. These methodologies led to the creation of diverse accessories using materials like paper. Through such practice-oriented approaches, research tends to focus on craft disciplines, including ceramics, jewelry, and textiles. These disciplines often contain valuable knowledge that is seldom articulated but is deeply ingrained in practice and embodied by practitioners [11].

In Etikoppaka crafts, cluster artists In Etikoppaka crafts, cluster artists identified and adapted a few alternatives like alternate softwoods to resolve the material-related issues. But that material was not available locally. Hence, artists have started plantations of adapted softwoods in forest and non-forest areas. This moment will help the Etikoppaka handicrafts industry in the future [12].

The empowerment of craftsmen for that does not come from the growth of their entrepreneurial skills. Additionally, only developing items are the area of design intervention. Consequently, by applying design thinking throughout the entire process and suggesting a framework to create creative craft businesses in India, specifically targeting change-makers, a sustainable approach can be established [13].

The market often underestimates the true value of crafts, because of which numerous artisans moved to cities looking for poorly paid, low-skilled jobs in the field [14]. To boost the income, craft producers need to update their skills and products to meet the changing market demands and enhance their access to the market and supply. Innovation in crafts and collaborative work between craftsman and design are helpful frameworks to achieve this. Also, the creation and execution of suitable

IPR legislation should take precedence in order to preserve the traditional skill base and safeguard the artisans' traditional knowledge resource [10].

For the awareness of collaboration, craft education needs to be introduced in the traditional education system. When craft applications focus on heritage, they can play an important role in educating the next generation of designers about crafts [15]. According to the craft knowledge and familiarity, crafts methods are divided into various categories; craft educators and researchers can explore those methods [16]. Along with those, the entrepreneurship module will help design students to take advantage of commercial opportunities [17].

Design professionals can try to break social inequality between stockholders and craftsmen from various levels of society. It helps to work together for the development of craft methodologies. It will be helpful for the co-design of tools, products, environments, businesses, and social institutions toward democratic societal outcomes. Designers are supposed to contribute to financial, social, and cultural aspects. Design practice needs to facilitate social changes for craftspeople which will create a better outcome of design practice [18]. The qualities of craft-oriented design classified into product level and material level which helps analyze potential collaboration between designers and craft manufacturers. Durability, secondary use, and refurbishment are significant characteristics of the items at the product level. Recycling and material innovation were part of the material level. This collaboration may have a positive impact on craft designs [19].

Designers and craft craftsmen work together on the Yii (The initiative of the National Taiwan Craft Research Institute and the Taiwan Design Center) initiative to develop new goods. In terms of knowledge, history, and manufacturing techniques, crafts and design are distinct fields. The difficulties in collaborative work are a lack of craft knowledge and inadequate communication between the designer and the craftsman [20].

National Productivity Council Developed a research document on the Productivity and Competitiveness of India's Toy Manufacturing Sector [21]. In 2015, the worldwide toy market is expected to be valued approximately US$ 85 billion. The Indian toy sector accounts for around 0.51% of the global toy market [22]. Because of the country's growing middle class and young population, the industry's potential is enormous. This industry must be restructured to capitalize on this enormous opportunity.

According to the National Productivity Council [21], the toy and game business has the potential to expand. One of new article proposes difficulties linked to raw materials and workforce availability in the Indian wooden crafts sector where researchers should work and offer options about developing technologies [7].

Ministry of Minority Affairs (2018, 2015) launched the USTTAD initiative while focusing on minority groups by giving training and support through exhibits. Craftsmen must meet the criteria in order to participate in the plan. All arts and crafts, in my opinion, will not be able to participate in this system [23]. Thus, research is crucial in this area to create a system that will focus collectively on various crafts from various regions of India.

3 Methodology

The data for this qualitative research study was collected in January 2023 to March 2023 through the expert interviews of artisans, craft retailers, and crafts educators. Participants were six craftsmen and retailers of wood toys from Sawantwadi and 6 crafts educators from Pune. One visiting educator who works as a bamboo artist took part in the interviews with educators. Participants were identified through snowball sampling methods [24] (Table 1).

The interviews were conducted in order to better understand the concept of wood crafts, crafts values, traditional methods, emerging technologies and design intervention process. The interview protocol was designed prior to the qualitative data collection. "An interview protocol is more than a list of interview questions; it also extends to the procedural level of interviewing and includes a script of what you will say before the interview, the script for what you will say at the conclusion of the interview, prompts for the interviewer to collect informed consent, and prompts to remind the interviewer the information that she or he is interested in collecting" [25]. Face validation was used to verify interview questioners. Face validation of finalized questionaries was carried out by five researchers [26].

We did not place the data into any preset groupings and used open coding to analyze the participant tales. While it was crucial to us to maintain the "voices" of the participants in the text, we did make a few minor grammatical corrections to a few direct quotations to make sure the message was not lost in translation. When publishing our findings, we used pseudonyms in quotes to protect participant confidentiality [24].

Table 1 In-depth interviews with artisans

Interviewee no	Interviewee profile	Gender	Age (in years)
1	Crafts retailer	F	35
2	Artisan and crafts retailer	M	37
3	Artisan and crafts retailer	M	52
4	Artisan and crafts retailer	M	29
5	Artisan and crafts retailer	M	60
6	Artisan and crafts retailer	M	35
7	Artist and crafts educator	M	49
8	Crafts educator	M	56
9	Crafts educator	M	55
10	Crafts educator	F	48
11	Crafts educator	F	31
12	Crafts educator and bamboo artisan	M	30

4 Findings and Discussions

Participants addressed relevant scenarios of craft development. While conducting interviews, many repeating themes and hints became apparent. The author made an effort to elucidate these ideas using the interview's topics (Table 2).

The Chitrari community has been active with Sawantwadi wooden toys for the past three to four generations. They have been there for the past century's evolution of wooden toys. The availability of materials, production techniques, labor pools, consumer demands, the range of toys, government regulation of emerging applications, and rising technology all play a role in this progression. Themes from the conversation were blended, taking into account the comparable themes discussed during the interviews. Those are listed below.

4.1 Sawantwadi Wooden Craft: Evolution, Market Trends, and Competition

Wooden crafts are evolving due to market trends and competition in an organized market. The demands have changed, as discussed with the artisans of the Sawantwadi market. They're introducing new series of toys and products, based on consumer preferences. Artisans are adjusting their designs based on feedback and suggestions from consumers.

> Over the past 30–40 years, a variety of products have undergone changes. Products of new varieties were introduced. We made an effort to alter the design in accordance with the demands and needs of the client. (Interviewee 1, Craft retailer)

When we talk about how things have changed, what the consumers think matters a lot. Kids choose toys based on their favorite characters, cool features, and colors. This all changes depending on how old they are and if they're a boy or a girl [27]. One interviewer gave an example that makes it clear. Kids today like toys that they see in their daily life, especially the ones that actually work and move, like the things they're used to,

> Consumers (kids) today like toys with some mechanism; they choose tractors, dump trucks, and other objects with motors. Previously, we marked certain toys like bull carts, buses, vehicles, etc. That being the case, we tried to alter existing toys. The number of toys rose. (Interviewee 2, Craft retailer and artisan)

Table 2 Topics discussed in interviews

1	Sawantwadi wooden craft: evolution, market trends, and competition
2	Materials and technology: meeting market needs
3	Artisans: culture, jobs, and identity

These types of needs may vary from local consumer and tourist. The folks from Sawantwadi who make crafts said they focus on what the people here need and also on the tourists who visit. Craft educators talked about this too when they were talking about the different groups of buyers,

> Craft relies on the local population and tourism. Both have different applications. Local artisans get their supplies. Tourism is certainly becoming more significant nowadays because they can charge lower prices. As Tourism expands, it becomes a more profitable segment. (Interviewee 7, Craft Educator)

Promoting craft projects has gained importance, especially in the context of tourism [28]. To effectively reach tourists, it's essential to understand their perspectives. This means introducing a range of products that hold value either through their utility or traditional significance, all the while considering customer feedback. This approach makes sense to ensure a successful connection between crafts and tourism. During the discussion, one craft educator shared their opinion on these,

> People are ready to buy, however the product they were hoping to find was missing. There isn't much demand for artifacts and showpieces; consumers would rather buy some of the useful products which an artisan needs to make or even something more conventional. Therefore, product diversification is required, and surveys of visitor expectations are necessary. (Interviewee 9, Craft Educator)

When we talk about market trends, the role of wooden crafts in organized markets becomes significant. In the global market, Indian wooden toys contribute only 0.51%. Within our country, around 10% of traditional toys are sold through government-sponsored stores, and a significant 60% of toys are imported from various countries like China, Taiwan, Korea, Singapore, the USA, and the UK [22]. This tough competition from imports poses challenges for local toy industries, including Sawantwadi wooden toys (Fig. 2).

To compete with Chinese wooden toys and PVC plastic toys, some artists mentioned that they buy these items, study their structure, and try to create similar replicas. However, the process and materials they use make Sawantwadi wood toys more expensive. For instance, a similar item made in China costs 100 rupees, while a locally made one costs between 250 and 300 rupees. This shows that the accessibility

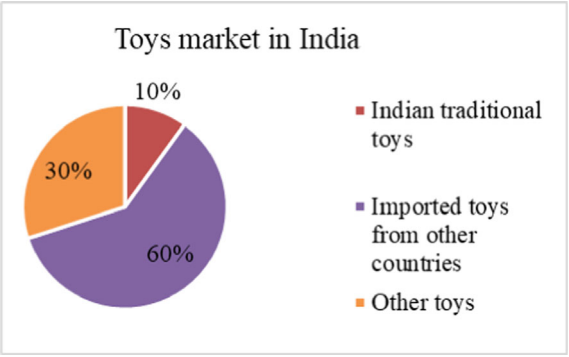


Fig. 2 Toys market in India [22]

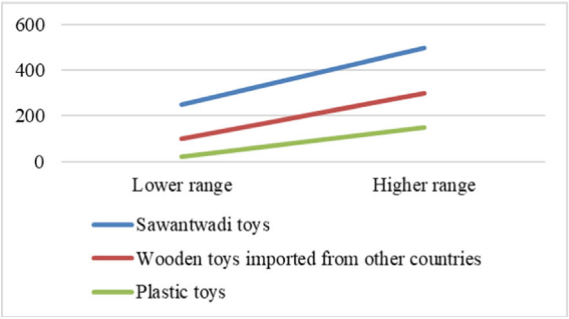


Fig. 3 Tentative representation of toys range in INR (Based on example given by Craftsmen)

of production methods and materials affects the pricing. Example of price range is shown below by taking similar moving toy made in Sawantwadi cluster, plastic and imported from other country (Fig. 3).

While discussing consumer needs, one participant gave an example to explain the situation,

> Products from China have entered the market. They are available very cheaply. If you look at it like this? Chinese. The product has increased. Local is decreasing. But they are less durable…..aaa… I wanted to get a precious sample. So. I have a made in china toy. It costs ₹100. Also playing the same. The one we have made here sells for ₹500 and the smaller one for ₹300.

Thinking about market trends and competition, it's important to look at the toys that are out there and understand how they're made. This helps us see what materials are available and how things are created. This knowledge is really useful for meeting what the market wants.

4.2 Materials and Technology: Meeting Market Needs

During the discussion on craft materials and methods, both craftsmen and educators shared their insights about how things are made. Craftsmen use traditional techniques involving tools like chisels, turning tools, and sculpting tools. The specific tools can vary based on what they're creating. One craft teacher, while elaborating on a particular craft, mentioned,

> Tools were created locally by craftspeople rather than being purchased from a market. They adapt to their trade. (Interviewee 3, Craft retailer and craftsmen)

In the Indian traditional wooden toy-making industry, the main problems include a lack of materials, high material costs, neglect of genetic resources, and traders exploiting gender inequalities. To address these challenges, there's a need for better technological support, enhanced supply chain management, and innovative crafting approaches [29].

When asked about integrating new technology into crafts, artisans and educators gave their insights. Retailers noted that buyers often seek classic items of greater value. Balancing traditional craftsmanship with modern techniques could be advantageous for artisans, considering the time-consuming crafting process. A sculptor and artisan educator shared his viewpoint, stating,

> Handmade things are always handmade, and they have their own values. It was created by an anonymous artisan. The presence of human imperfection in the toys is always allowed since it creates an emotional connection. As a result, there would be some human touch and some mechanical touch. It must be balanced. For example, we can create primary forms using a machine and then add a hand touch with color, finishing, and different types of hand touch while maintaining a balance between the two. (Interviewee 6, Craft Educator)

The statement presented a mixed approach concerning Sawantwadi crafts. To delve deeper into this subject, an artisan specializing in bamboo visited Sawantwadi. This artisan examined both the traditional toys and the present condition of woodcraft in the region. However, upon observation, he found the situation to be quite absurd,

> I visited Sawantwadi last year, the main issue that they are facing is key, the wood is not available. So, the harsh reality what I saw there was all the material was imported from China and they were just reselling it. And there was a factory for namesake. Or they used to just paint it something like that. (Interviewee 12, Crafts Educator and Bamboo artisan)

Looking at Sawantwadi artisans shows how they survive. Their skills match what the market wants, using materials and technology. Artisans rely on their expertise for their jobs and to meet what the market needs.

4.3 Artisans: Culture, Jobs, and Identity

In Sawantwadi less than ten artisans are practicing Wooden toys crafts [30], where they are trying to transform their art to next generation. While discussing skillsets and its transformation of craft artisan and retailer gave his opinion,

> My nephew……(pause)…he is in 7th standard he paints different types of text very well; we say no genetically so children are learning that art from father. My son is also in 2nd grade but they easily make such toys. They are used to it. At the end of the adventure, she meets the divine. (Interviewee 2, Craft Retailer and Artisan)

In the conversation about artisans' skills and their work, a significant point was raised by a craft educator. This point holds great importance as it relates to the credibility, recognition, and identity of craftsmen in the market. Additionally, when exploring different materials and technologies, it's essential to ensure authenticity.

> If we evolve in like techniques and even the materials, we explore but still I feel like. I would love to, See and prefer that the authenticity of the product should remain in that even if develop new things. Even the contemporary designs should remain and as an even as an artisan. Collaborate with any of the designers. The name should always come with them. The credit we should always give to artisans because I have seen they are not getting it right now even though they are collaborating or maybe they are getting a platform through the

> color and many other craft clusters. That should come, actually, probably the name of the artist should come. (Interviewee 11, Craft Educator)

Artisans and retailers have subtly shared their views through craft discussions. Woodcrafts often use local wood, reflecting traditions or local cultures, and their uses vary based on the wood's qualities.

Sawantwadi artisans and instructors acknowledged this. Many customers seek affordable toys, leading to importing wooden toys due to resource and time constraints. This emphasizes the need for creative product design, material studies, and production methods. In the conversation, it emerged that a Sawantwadi workshop tries to blend methods, but labor shortages pose challenges. The owner aimed to train workers but faced financial constraints.

5 Conclusion

The conclusions drawn from these conversations provide a thorough grasp of the complex dynamics present in the field of crafts, particularly in the context of Sawantwadi. The discussions between makers, sellers, and educators emphasize the complex relationship between market trends, competition, and craft evolution. The adaptability of Sawantwadi artisans in a cutthroat industry is highlighted by their ability to launch cutting-edge toy lines and adjust to shifting consumer demands.

Imports and worldwide competition highlight the need for innovative ways to preserve Sawantwadi's crafts' uniqueness. As artisans try to incorporate contemporary methods without sacrificing the authenticity that characterizes their creations, the delicate balance between tradition and technology becomes clear. This combination demonstrates the artists' commitment to maintaining the distinctive uniqueness of their craft.

The discussions also highlight the multilayered relationship between crafts, culture, and identity. Intergenerational learning promotes the cultural value of these crafts and highlights their part in creating regional identities by preserving traditional skills. This intricate web of workmanship, identity, and market dynamics is further complicated by the concern expressed by craft educators about the proper acknowledgment of artists and the significance of giving credit for their works of art.

The insights gained from these interactions offer a priceless window into the difficulties and opportunities faced by craftspeople in a world marked by globalization and quickly changing markets. The adaptability and ingenuity of the Sawantwadi craftsmen are demonstrated by their capacity to adjust while maintaining a commitment to their cultural heritage. These insights will surely aid in the expansion and sustainability of this valued artisan legacy as the market keeps changing.

6 Limitations

The Sawantwadi craft cluster is being studied; comparable clusters exist in India and require design intervention. Also, the conversation is influenced by the perspectives of Sawantwadi artisans and craft educators who teach and perform research in crafts in design institutes. In addition, the study focused on market needs and manufacturing procedures. There will be additional segments to consider for future research.

The study is taking into account the perspectives of craftsmen and crafts educators. Before introducing novel products to the market, it is necessary to consider the perspectives of consumers and policymakers.

7 Contribution of the Study

This research contributes to understanding the ground reality of Sawantwadi wooden toys because interviews were performed offline in the field. The purpose of this paper is to explain why artisans introduced new varieties in order to compete. This research will also contribute to product development possibilities in the context of wood crafts and the developing market.

References

1. Ranjan MP (2007) Hnadmade in India
2. Bhat J (2016) Handicraft sector and its share in Indian economy. Arab J Bus Manag Rev 3:9. https://doi.org/10.4172/2223-5833.S3-009
3. Chavan CY, Chandar S (2022) The relationships between socio-economic, political and cultural profiles of the people and house-forms: Sawantwadi, Maharashtra, India During the British era
4. Preserving Artistic Tradition, Sawantwadi Palace Boutique Art Hotel. Accessed 07 Dec 2023
5. Baral B (2016) D'source digital learning environment for design. www.dsource.in
6. Prabhudesai AK (2021) A theoretical study on wooden toy industry-case study of Sawantwadi, Sindhudurga District, Maharashtra. AMIERJ 10:191–197
7. Jadhav R (2023) Maharashtra's wooden toy hub gasps for survival. https://www.thehindubusinessline.com/news/maharashtras-wooden-toy-hub-gasps-for-survival/article32486762.ece. Accessed 01 Aug 2023
8. Das M, Das AK (2019) Craft education in design
9. Jha SK (2017) Craft study and product design interventions: soapstone craft cluster of Dhakotha Area in Kendujhar District of Odisha, India. Chitrolekha J Art Des 1:103
10. Liebl M, Roy T (2004) Handmade in India: traditional craft skills in a changing world. In: Poor people's knowledge: promoting intellectual property in developing countries, pp 53–74
11. Nimkulrat N (2012) Hands-on intellect: integrating craft practice into design research. Int J Des 6:1–14
12. Rao MV, Balaji M, Joshi SC (2011) Etikoppaka: an Indian village perpetuating the joy of wood through the tradition of toy art. In: International conference and exhibition on art and joy of wood, held at IWST Bangalore, pp 19–22

13. Banerjee A (2022) Mazzarella F (2022) Designing innovative craft enterprises in India: a framework for change makers. She Ji J Des Econ Innov 8:192–216. https://doi.org/10.1016/j.sheji.2022.04.001
14. Kapur H, Mittar S (2014) Design intervention and craft revival. Int J Sci Res 4:1142
15. Kokko S, Räisänen R (2019) Craft education in sustaining and developing craft traditions: reflections from finnish craft teacher education. Techne serien-Forskning i slöjdpedagogik och slöjdvetenskap. 26:27–43
16. Kokko S (2021) Approaches to craft studies at higher education. FormAkademisk forskningstidsskrift for de-sign og designdidaktikk 14:4197. https://doi.org/10.7577/formakademisk.4197
17. White PJ, Kennedy C (2022) Designing a module in entrepreneurship for product design students. Ind Higher Educ 36:217–226. https://doi.org/10.1177/09504222211013742
18. Mamidipudi A (2018) Constructing common knowledge: design practice for social change in craft livelihoods in India. Des Issues 34:37–50. https://doi.org/10.1162/desi_a_00510
19. Haele U (2019) The role of design for craftsmanship in a growth-critical transformation. In: Conference contribution, DHS 2019: the cost of design. Northumbria University, Newcastle-upon-Tyne
20. Tung F-W, Chen I-C (2013) Collaboration of designers and craft artists on innovative design praxis. In: Proceedings of the 5th international congress of international association of societies of design research (IASDR) Tokyo
21. Economic services group national productivity council New Delhi: research study on productivity and competitiveness of toy manufacturing sector in India (2017)
22. Jayan AP (2018) A theoretical paper on research studies about conventional toy industry. Res J Manag 7:6–9
23. USTTAD (2023). http://www.usttad.minorityaffairs.gov.in/. Accessed 08 Aug 2023
24. Hebbani A, Obijiofor L, Bristed H (2010) Intercultural communication challenges confronting female Sudanese former refugees in Australia. Austr Rev Afr Stud 31:37–61
25. Jacob SA, Furgerson SP (2012) Writing interview protocols and conducting interviews: tips for students new to the field of qualitative research. Qualit Rep 17:6
26. Patel N, Desai S (2020) ABC of face validity for questionnaire. Int J Pharm Sci Rev Res 65:164–168
27. Chawla N, Mehta R (2020) Children's influence on parent's purchasing decision in toy industry. Pac Bus Rev Int 13:127–137
28. Bellver DF, Prados-Peña M, García-López AM, Molina-Moreno V (2023) Crafts as a key factor in local development: bibliometric analysis. Heliyon
29. Aggarwal PK, Rao RV, Joshi SC (2013) Wooden toys in India 64:57–60
30. Jain S (2023) An award-winning craftsman and the long legacy of wooden toys on his shoulders. https://www.thebetterindia.com/122140/wooden-toys-sawantwadi-rural-art-maharashtra-crafts-tradition/. Accessed 13 Aug 2023

Unfolding a Hidden Risk of Direct 3D Software Usage for Animation Character Design



Ananda Karmakar and Anirban Chowdhury

Abstract In general, animation character design exercise done by designers using design process, in which they draw character concept first and then they generate the 3D model of the character. However, Gen-Z design students like to develop 3D character concept directly using 3D software as they fell it saves time. However, it is sometime difficult to fruitfully express the detailing of the character concept without detail drawings. This research attempted to compare the average ratings of two animation techniques: conventional hand-drawn animation and 3D computer animation in the context of character design. A total of 20 students skilled in traditional hand-drawn animation and another 20 students trained in 3D computer animation were chosen to make up two groups of students (age range = 18–22 years, male: 60% and female: 40%). The research also explored the distribution of scores among students engaged in hand-drawn character design and 3D computer-based character design. It was observed that conventional hand-drawn animated character (Mean = 7.35) and 3D computer animation character (Mean = 6.20) outcomes significantly different in term of average quality scores evaluated by ten experts. These findings suggest that the expert judges found quality in traditional hand-drawn animation character over 3D computer-generated animation character due to detailing of the design. To get more thorough understandings of the quality and preference features of various animation approaches within the field of animation arts, additional investigation and a wider variety of assessments are advised.

Keywords Animation medium · Character design · Hand-drawn animation · 3D computer animation · Learning outcomes

A. Karmakar
School of Design, Graphic Ear Hill University, Dehradun 248002, India

A. Chowdhury (✉)
Alliance School of Design, Alliance University, Bengaluru, Karnataka 562106, India
e-mail: chowdhuryanirban14@gmail.com

© The Author(s), under exclusive license to Springer Nature Singapore Pte Ltd. 2025

B. B. V. L. Deepak et al. (eds.), *Recent Advancements in Product Design and Manufacturing Systems*, Lecture Notes in Mechanical Engineering,
https://doi.org/10.1007/978-981-97-6732-8_44

1 Introduction

Animation is an assorted and enthralling form of art that has significantly evolved through time. It has adopted a diversity of methodologies and technology, leading to a variety of styles and methods [1]. Animation character design has long been a fundamental component of the creative process, requiring designers to develop characters that resonate with audiences and effectively convey narratives [2]. Traditionally, this process involves the initial creation of character concepts through hand-drawn sketches, which are then translated into three-dimensional (3D) computer-generated models in animation [3]. However, the advents of new technologies and shifts in design preferences, particularly among the Generation Z cohort, have prompted changes in the way character design is approached. Increasingly, design students are bypassing the conventional hand-drawn stage and directly creating 3D character concepts using specialized software, citing time-saving advantages [4]. Nevertheless, a critical challenge emerges: the ability to effectively convey intricate character details without the aid of traditional hand-drawn sketches [5].

The landscape of character design has transformed with the rise of digital tools and software, altering the dynamics of the design process. The traditional workflow involved sketching character concepts on paper before translating them into 3D models, ensuring a comprehensive exploration of character attributes and nuances. However, contemporary design students, driven by the speed and efficiency of technology, are embracing 3D software to conceptualize characters directly. This transition challenges the inherent advantages of the hand-drawn process, as digital tools offer rapid iterations but may compromise the depth of detailing. Striking a balance between efficiency and creative richness is pivotal in this context. Traditional hand-drawn animation and 3D computer animation are two significant methods that have evolved and are still often used in the art of animation [6]. In this method, three-dimensional virtual models are created using computer software and then animated and changed by students [7]. It has been widely employed to produce lifelike characters and striking visual effects in feature films, video games, and advertisements [8]. However, the level of realism and detail offered by 3D computer animation is difficult to match with hand-drawn methods. It provides fine-grained control over intricate motions, camera angles, and visual effects, producing a spectacular and well-finished final output. Depending on the context and intended audience, these animation styles may or may not be seen favorably by viewers [9]. Animation created by hand is sometimes seen to have a more conventional and artistic vibe, which appeals to viewers who value the artistry and beauty of the form [10]. It could make you feel sentimental. On the other side, 3D computer animation has gained popularity among viewers and has become a mainstay in mainstream entertainment [11]. It is widely used in animation movies, video games, and advertising because of its capacity to produce aesthetically pleasing and lifelike environments and students [12]. 3D animation's realism and immersion may enthrall viewers and provide them with a more contemporary and cutting-edge experience [13]. Understanding the advantages and disadvantages of these approaches is crucial as animation continues to gain

popularity across a range of sectors, including entertainment and advertising. The decision between hand-drawn animation and 3D computer animation depends on a variety of elements, including the project's requirements, budget, target audience, and creative vision [14]. Animation artists and filmmakers may produce captivating and aesthetical stunning animations that connect with their target audience by utilizing the distinctive features of each approach [15].

Investigating the perceived quality disparity between conventional hand-drawn animation and 3D computer animation was the goal of this study. Traditional hand-drawn animation, which has its roots in the early days of animation, entails manually generating each frame before assembling them into a sequence [16]. On the other hand, 3D computer animation creates three-dimensional models using sophisticated software and then renders them into animated sequences. Few studies have explicitly compared the perceived quality and preference of the two approaches, despite the fact that previous research has studied the aesthetic and technical features of each [17].

The central problem pertains to the comparative efficacy of two animation techniques: the established approach of hand-drawn character animation and the emergent practice of 3D computer-generated character animation. The dilemma revolves around whether the transition to direct 3D modeling sacrifices the intricate design elements that were traditionally communicated through detailed hand-drawn sketches. This research seeks to address whether design students trained in 3D computer animation can match the quality of character detailing achieved through conventional hand-drawn techniques.

The implications of this research are multifaceted. It delves into the evolving paradigms of character design and contributes to understanding how advancements in technology influence creative workflows. By evaluating the comparative quality of characters created through distinct techniques, the study informs design pedagogy and practice. Furthermore, insights gained from expert evaluations shed light on the nuances that contribute to the perceived quality of animation characters, offering valuable guidance for aspiring character designers.

This research focuses on comparing the outcomes of character design achieved through traditional hand-drawn animation and 3D computer-generated animation, with specific attention to detailing and quality. The study is delimited to design students aged between 18 and 22 years, encompassing both genders. However, the broader animation landscape involves diverse age groups, design preferences, and skill levels. While this study captures essential aspects of the debate between traditional and modern techniques, it acknowledges the need for further exploration encompassing a wider range of animation approaches and diverse participant demographics.

1.1 Literature Review

In reviewing the research literature, Eakta [18] addresses the complexities of bridging traditional hand-drawn animation with 3D computer animation and introduces the concept of using 3D proxies as a potential remedy. The paper highlights that 3D proxies serve as a connection between these two animation techniques, offering a solution to the challenges posed by their integration. These proxies are categorized into three levels: single-points, polygonal shapes, and joint hierarchies, providing a structured approach to facilitating the synergy between hand-drawn and computer-based animation. The scholar discusses the application of subdivision surfaces in 3D computer character animation, with a focus on addressing challenges related to modeling, animating, and rendering complex shapes. While traditional hand-drawn characters are not explicitly mentioned, the review emphasizes the introduction of subdivision surfaces within a production environment to tackle these challenges effectively [19]. Another point of view has been advanced by Jain et al. [20]; their paper explores the creation of 3D animation characters that retain the aesthetic qualities of hand-drawn characters. The authors propose a method to translate hand-drawn sketches into 3D models that capture the original style and essence. The technique involves designing 3D proxies that mimic the lines and shapes found in hand-drawn sketches, allowing for a more intuitive and artistic control over the final 3D character animations. Other investigations have evaluated [21] an approach for generating 3D character animations based on hand-drawn sketches. The authors propose a method to automatically convert 2D sketches into 3D animations, preserving the original style of the sketches. The system utilizes the 2D sketches as a reference to create natural-looking 3D animations, bridging the gap between traditional 2D animation and 3D computer-generated animation [22]. This paper focuses on performance-driven animation techniques that aim to simulate the expressive and artistic qualities of hand-drawn animation in a computer-generated context. The authors discuss methods for capturing and applying artistic variations to 3D animations, allowing for more organic and creative character motions while maintaining computational efficiency [23]. In this paper, the authors introduce a technique to enhance the appearance of hand-drawn characters in 3D scenes using global illumination effects. The approach involves converting hand-drawn textures into bas-relief meshes, allowing for more accurate light interactions and shadows. This method combines the artistic qualities of hand-drawn characters with realistic lighting effects. In another context [24], study presents TexToons, a practical approach to texture mapping for hand-drawn cartoon animations. The authors propose methods for mapping textures onto 3D models that match the style of the original hand-drawn characters. This technique contributes to the seamless integration of hand-drawn aesthetics into 3D animations [25]. This paper examines how Pixar's animations, known for their cutting-edge 3D computer-generated imagery, incorporate and pay homage to the hand-drawn aesthetic. The author explores how this blending of techniques reflects both nostalgia for traditional animation and a commitment to innovation, leading to unique visual storytelling. According to [26], although not directly cited with a publication, it seems

this might be a source discussing the process and methods of integrating 2D artistic styles into 3D animation. The concept of hybrid animation refers to the fusion of 2D and 3D techniques to achieve a specific visual style that draws from both worlds, combining traditional hand-drawn aesthetics with the capabilities of 3D technology.

The present study endeavors to bridge the gap between the conventional and contemporary approaches to animation character design. By analyzing the differences in quality and detailing between hand-drawn and 3D computer-generated characters, it aims to provide insights into the evolving landscape of animation arts, aiding both design education and industry practices.

Hypotheses

- Null hypothesis (H0): There is no significant difference in the average ratings for scores given by animation experts between traditional hand-drawn characters and 3D computer-generated characters designed by animation students.

1.2 Research Method and Computation of Statistical

This research attempted to compare the average ratings of two animation techniques: conventional hand-drawn animation and 3D computer animation. 20 students skilled in traditional hand-drawn animation and another 20 students trained in 3D computer animation were chosen to make up two groups of students. Students are supposed to generate concepts of any human animation character. Each student used their particular method to produce characters. The animations were independently scored on a scale of 1–10 by a group of ten skilled judges who have expertise in animation field (at least 15 years); to check if there was a significant difference in the mean ratings between the two procedures (traditional hand-drawn versus 3D computer-generated animation characters). As the collected data distribution not follow normal distribution assumption, Mann–Whitney *U* test was conducted to compare means between groups (traditional hand-drawn character versus 3D computer-generated character), through SPSS test.

2 Result and Findings

The average ratings of conventional hand-drawn animation (Group 1) and 3D computer animation (Group 2) are being compared in this study. The information is given in terms of sample size ($n1 = 20$ *for Group 1 and* $n2 = 20$ *for Group 2*), mean rating (*M Group 1* $= 7.35$, *SE1* $= 0.17$; *and M Group 2* $= 6.20$, *SE2* $= 0.09$) (Fig. 1). We found a significant mean difference in scores obtained by two different groups of students due to the medium used to design animation characters (traditional hand-drawn character versus 3D computer-generated character) [*Mann–Whitney U value* $= 50.00$, $Z(39) = -4.383$, $p = 0.0001$].

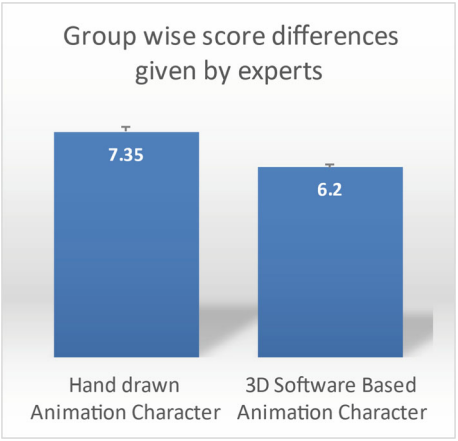


Fig. 1 Mean differences in scores obtained by students involved in character design task

Around 75% of students scored significantly higher than the 70% [X^2 *(1)* $= 5.000$, $p = 0.025$] (Fig. 2). On the contrary, 95% of students scored significantly lower than 70% [X^2 *(1)* $= 16.200$, $p = 0.0001$] (Fig. 3). From chi-square test of association, it was observed that there is a significant association between type of media used by students and character design outcomes [X^2 *(1)* $= 20.417$, $p = 0.0001$]. The odds score for cohort 2 (3D computer-based character design) is 12.667. This means the chance of risk of quality compromised character design is about 13% if students are directly going for character design using 3D computer-based software.

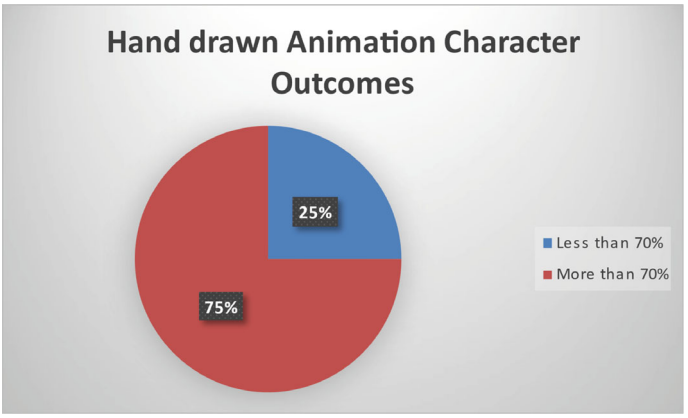


Fig. 2 Frequency distribution of scores students involved in hand-drawn character design

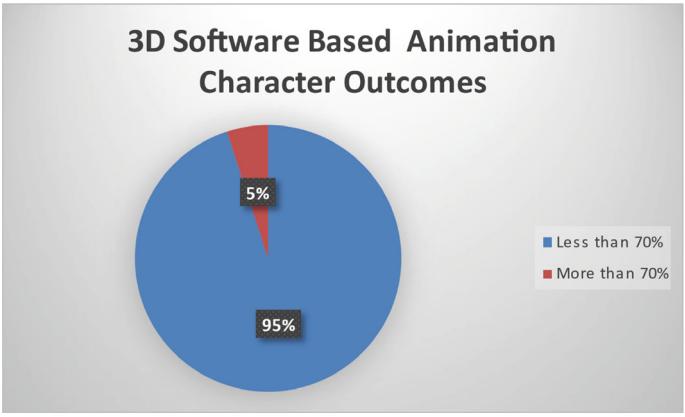


Fig. 3 Frequency distributions scores of the students involved in 3D computer-based character design

3 Discussion

The primary objective of the study was to compare the average ratings of two distinct animation techniques: conventional hand-drawn animation (Group 1) and 3D computer animation (Group 2) in the context of character design. The analysis of the collected data presents insightful results that shed light on the differences between these two approaches. As an initial insight into possible variations in character design quality depending on the animation process utilizing hand-drawn sketches or 3D software which has been reflected by mean ratings, Chen et al. [21] have highlighted the importance of hand-drawn sketches for 3D animation and character design. They stated that easy-to-use method for creating a set of consistent 3D character models is possible to develop from some hand-drawn sketches. Therefore, the hand-drawn sketches of characters are very crucial to design animation characters. It is well-established fact that the edge drawing presents a more pleasing appearance with higher level of detail and is found even to models [27]. Another study has explored that hand-drawn characters allow animators to showcase their unique artistic styles and bring a personal touch to the animation [28]. Also Harrison and Hummell [29] investigated that hand-drawn characters can exhibit fluid movements and intricate details that might be challenging to achieve in computer-generated animation. According to Chamberlain et al. [30], hand-drawn characters can stand out in a world dominated by computer-generated imagery, offering a distinctive visual experience. Hand-drawn characters, with their intricate details and human touch, convey emotions in a relatable, heartfelt manner, forging a timeless connection with audiences. Their expressive range, coupled with nostalgia and cultural diversity, enhances their ability to evoke empathy and resonate across generations, making them truly unforgettable [31]. Hence, hand-drawn characters have more advantages than the directly made 3D character model using software. Moreover, additional tests were

carried out to ascertain the statistical significance of these findings. A chi-square test revealed that around 75% of the students in Group 1 (hand-drawn characters) scored significantly higher than the 70% cutoff. In contrast, 95% of the students in Group 2 (3D computer-generated characters) received results that were significantly below the cutoff of 70%. The idea that there is a significant difference in character design quality between the two groups was further substantiated by these results in this analysis. The statistical tests and frequency distribution analyses underscored the superior quality of traditional hand-drawn animation in terms of character detailing and overall design quality.

Furthermore, the results of the chi-square test of association showed a strong correlation between the students' character design outputs and the media they used. For Group 2 (3D computer-based character design), the computers odds ratio (12.667) refers that students designing characters with 3D computer-based software were 13 times more likely to have risk of poor character design quality than students designing characters with traditional hand-drawn methods. The result shows a considerable correlation between students' character design outputs and the media they employed, suggesting a significant connection between the quality of character designs and the design tool selected. A similar correlation was also found by van Rooij [32] in the context of animation film success due to a specific style of characterization as a possible reason for the overwhelming emotional response. Additionally, students employing conventional methods could profit from hand-drawing's tactile and intuitive qualities, which can promote a closer link between their original thoughts and the finished product. Overall, as shown by the odds ratio, these factors together enhance the likelihood that students utilizing 3D computer-based software would produce inferior designs.

Despite their enhanced capabilities and precision, 3D computer-based design tools frequently have a higher learning curve, which may limit students' ability to express them creatively and produce less visually appealing character designs [33]. Second, the digital media could promote an emphasis on technical tales rather than artistic inventiveness, resulting in designs that lack the distinctive and innovative elements frequently found in hand-drawn characters.

The results of this study indicate a considerable disparity between the two student groups' mean evaluations for cartoon characters. This distinction may be explained by the level of detail that may be achieved using hand-drawn sketches as opposed to the more efficient 3D design method. It makes one wonder how to reconcile complexity and quickness in character design. The observed mean difference supports the theory that the attention to detail in traditional hand-drawn animation may result in higher-quality character designs. The study indicates a new dimension for acquiring character design process that despite the convenience of 3D software, the detailing of character concepts achieved through traditional hand-drawn methods leads to higher-quality outcomes according to expert evaluations. These results shed light on the importance of incorporating detailed drawings in the character design process, even in the age of advanced 3D software, offering valuable insights for animation artists and educators. Future research might use a greater more varied sample and take into account several design evaluation criteria to have a more complete grasp

of character design quality. Additionally, looking at the potential combination of both approaches—fusing efficient 3D rendering with hand-drawn detail—could offer suggestions for streamlining the character design procedure. This result encourages additional research into the complex interactions between design medium, intricacy, and quality.

4 Conclusion

In conclusion, this study substantiates the endorsing of the value of traditional hand-drawn animation in character design over direct 3D software-based character design. This research contributes to the broader discourse on design practices, offering practical insights for design educators and professionals alike. However, while this study sheds light on critical aspects, its limitations, such as a restricted sample size and demographic scope, must be acknowledged. Moving forward, this study opens avenues for further exploration of animation in terms of producing quality animation. Future research could explore into hybrid approaches that leverage the benefits of both traditional and 3D animation techniques, seeking optimal strategies for character design. Additionally, a broader participant pool could provide a more comprehensive understanding of the implications of animation types for successful movie outcomes. Ultimately, the ongoing dialogue sparked by this study has the potential to shape the evolving landscape of animation character design in the years to come. In the end, the paper highlights the value of striking a balance between complexity and efficiency, particularly as the world of animation changes in response to technology developments.

References

1. Dixon S (2015) Digital performance: a history of new media in theater, dance, performance art, and installation. MIT press
2. Hu TY (2010) Frames of anime: culture and image-building. Hong Kong University Press
3. Fossati G (2018) From grain to pixel: the archival life of film in transition. Amsterdam University Press
4. Alexander OR (2009) The digital Emily project: photoreal facial modeling and animation. ACM Siggraph 12:1–15
5. Liu JC (2022) An animation model generation method based on Gaussian mutation genetic algorithm to optimize neural network. Comput Intell Neurosci
6. Pambudi SH (2021) Development of instructional videos for the principles of 3D computer animation. J Phys Confer Ser 1737(1):012022
7. Zhang MZ (2018) Recent developments in game-based virtual reality educational laboratories using the Microsoft Kinect. Int J Emerg Technol Learn 13(1):138–159
8. Meng Q (2022) Intelligent animation creation method based on spatial separation perception algorithm. Comput Intell Neurosci
9. Endler JA (2012) Bowerbirds, art and aesthetics: are bowerbirds artists and do they have an aesthetic sense? Commun Integr Biol 5(3):281–283. https://doi.org/10.4161/cib.19481

10. Garcia MB (2023) Cognitive and affective effects of teachers' annotations and talking heads on asynchronous video lectures in a web development course. Res Pract Technol Enhanced Learn 18:18020
11. Hoon LN (2020) Physically-based animation in performing accuracy bouncing simulation. Int J Adv Comput Sci Appl 11(9):952
12. Kuang R (2021) Design and implementation of 3D film and television scene production algorithm based on the internet of things. Wireless Commun Mobile Comput 32:1–11
13. Aziza DN (2019) Evaluating the effect of YouTube advertising towards young customers' purchase intention. Sci World J. https://doi.org/10.2991/icbmr-18.2019.16
14. Bai ZY (2013) An interval-valued intuitionistic fuzzy TOPSIS method based on an improved score function. Sci World J. https://doi.org/10.1155/2013/879089
15. Li SL (2018) Between light and shadow: analysis of the unique charm of hand-shadow style animation. In: Proceedings of the 2018 international seminar on education research and social science (ISERSS 2018), pp 6–9
16. Zhang D (2015) Research on the application of 3DSMAX in animation. In: International conference on mechatronics, electronic, industrial and control engineering, pp 935–938
17. Tejeda-Ocampo C-CA, Terashima-Marin H (2020) Improving deep interactive evolution with a style-based generator for artistic expression and creative exploration. Entropy 11:e23010011. https://doi.org/10.3390/e23010011
18. Eakta JY (2012) Three-dimensional proxies for hand-drawn characters. ACM Trans Graph 31(1):8. https://doi.org/10.1145/2077341.2077349
19. Rodríguez-Gonzálvez P-M (2021) Design of a didactical activity for the analysis of uncertainties in thermography through the use of robust statistics as teacher-oriented approach. Remote Sens 13(3):402
20. Jain E, Sheikh Y, Mahler M, Hodgins J (2012) Three-dimensional proxies for hand-drawn characters. ACM Trans Graph 31(1):1–16
21. Chen YB, Ono Y, Nishita T (2005) Character animation creation using hand-drawn sketches. Vis Comput 21:551–558
22. Buck IF (2006) Performance-driven hand-drawn animation. In: ACM SIGGRAPH, p 25
23. Sýkora DK-H (2014) Ink-and-ray: bas-relief meshes for adding global illumination effects to hand-drawn characters. ACM Trans Graph 33(2):1–15
24. Sýkora D, Ben-Chen MČ (2011) Textoon: practical texture mapping for hand-drawn cartoon animations. In: Proceedings of the ACM SIGGRAPH/Eurographics symposium on non-photorealistic animation and rendering, pp 75–84
25. Haswell H (2014) To infinity and back again: hand-drawn aesthetic and affection for the past in Pixar's pioneering animation. Alphaville J Film Screen Media 12:1–17
26. Kivistö J (2019) Hybrid animation: the process and methods of implementing 2D style in 3D animation
27. Lake A, Marshall C, Harris M, Blackstein M (2000) Stylized rendering techniques for scalable real-time 3D animation. In: Proceedings of the 1st international symposium on non-photorealistic animation and rendering, pp 13–20
28. Guay M, Ronfard R, Gleicher M, Cani PM (2015) Space-time sketching of character animation. ACM Trans Graph 34(4):1–10
29. Harrison H, Hummell JL (2010) Incorporating animation concepts and principles in STEM education. Technol Eng Teach 69(8):20
30. Chamberlain R, Mullin C, Scheerlinck B, Wagemans J (2018) Putting the art in artificial: aesthetic responses to computer-generated art. Psychol Aesth Creat Arts 12(2):177
31. Catmull E, Wallace A (2014) Creativity Inc. (the expanded edition): overcoming the unseen forces that stand in the way of true inspiration. Random House 8:70
32. van Rooij M (2019) Carefully constructed yet curiously real: how major American animation studios generate empathy through a shared style of character design. Animation 14(3):191–206
33. Wei X, Weng D, Liu YY (2015) Teaching based on augmented reality for a technical creative design course. Comput Educ 81:221–234

Creating a Compatible Design Solution Through Sari Drapes for Visually Challenged Women of India

Shagun Swaroop and Anirban Chowdhury

Abstract Daily, visually impaired women in India encounter hurdles when it comes to clothes. Traditional Indian attire is not only difficult to understand, but it also causes perplexity for the user due to the number of excessive clothing items involved. The aim of this study is to provide a design solution that serves as a substitute for sari. Before creating the design, a survey of fifteen visually impaired women aged 35–60 was conducted. The sari was draped using provided instructions, and the fit of the garment was assessed using wear study. The effectiveness of the two proposed prototypes was evaluated based on feedbacks and observations from sari wearing task. Where applicable, chi-square goodness of fit test was performed on data. It was found that the ready-to-drape sari fit was determined to be 100% satisfactory.

Keywords Apparel design · Drape · Fashion · Sari · Visually challenged women

1 Introduction

Cataract and macular degeneration blinded more women than males in every country and region [1]. People who are "visually impaired" go through irreversible eyesight loss and are called such [2]. Women with vision impairment face a variety of challenges as they go about their daily lives. As a result, the current study was conducted to develop sarees with self-access characteristics and to assess the applicability and comfort of the created drape. A self-structured interview schedule was used to gather information on wearable preferences, which included questions about the garment and garment characteristics. Anthropometric measurements were done on a total of

S. Swaroop
Symbiosis Institute of Design, Symbiosis International (Deemed University), Pune, Maharashtra, India
e-mail: shagun.swaroop@sid.edu.in

A. Chowdhury (✉)
Alliance School of Design, Alliance University, Bengaluru, Karnataka, India
e-mail: chowdhuryanirban14@gmail.com

© The Author(s), under exclusive license to Springer Nature Singapore Pte Ltd. 2025

B. B. V. L. Deepak et al. (eds.), *Recent Advancements in Product Design and Manufacturing Systems*, Lecture Notes in Mechanical Engineering,
https://doi.org/10.1007/978-981-97-6732-8_45

fifteen visually impaired women. The data was combined, and adaptive clothing was created using the mode values of the anthropometric quantifications. Women who are visually impaired are unquestionably among the most vulnerable to social marginalization [3]. As a result, a sari was developed that could be worn as a one-piece garment with pre-stitched pleats. The garment was put to test as a prototype to evaluate how comfortable and functional it was for sight-impaired women. According to the respondents, the sari's adaptive and identification features were exceptionally comfortable, functional, acceptable, and cost-effective. The aim of the paper is to create an alternative to sari (an Indian clothing) for visually challenged women. The objectives of this paper are to examine and comprehend the many issues with sari draping procedures among visually impaired (totally blind) women in India, and, also to design a solution which is an alternative to sari for visually impaired (totally blind) women in India. Finally, to test the design solution which is an alternative to sari.

2 Review of Literature

Readymade one-piece saris with no color-matching techniques were the most popular due to their comfort and ease of assembly from the wardrobe. The following basic points were reviewed while examining the impact of the saree on visually challenged women:

1. There are clothing adaptations for women with vision impairment, which use textures, trims, faces, and closures to define a garment for visually impaired women.
2. The second issue to consider is clothing matching made easier for visually impaired women, where too many components of the same outfit might be confusing for women with impairments.
3. The third issue is the significance of wardrobe choices for visually challenged women. Since fashion is a form of self-expression, their freedom of expression has been limited [4].

2.1 Clothing Modifications for Women with Visually Impaired

The design concept of sensory compensation is a way to reduce the inconveniences faced by visually impaired individuals by utilizing instinct, behavior, and self-reflection of human beings [5]. We also look at some flexible clothing options to help women dress more easily [6].

2.1.1 The Fabric's Surface

Visually impaired women can distinguish the fabric's face due to the seams. As a result, the seam should be positioned to make it simple to tell the front from the back. Similarly, it was found that producing textures with machine embroidery was used as a distinguishing element by women with vision impairment [7].

2.1.2 Color Picking

Since color is necessary for many daily tasks, including social interactions and outfit coordination, its absence has a negative influence on day-to-day life [8]. They emphasized how challenging it is to coordinate clothing colors [9]. To connect with society and the environment, color perception and recognition are crucial [10].

2.1.3 Texture

Visually impaired women develop a much more sensitive touch capacity making elements like color and design more significant. Softer materials are therefore ideal for designing adaptive apparel for women who are sight impaired [11].

2.1.4 Fasteners and Trims

Finally, traditional clothing such as laces, zippers, buttons, and other traditional garments are difficult to utilize for someone with limited visibility. There are alternatives to buttonholes, shoelace loops, and zippers for putting on our garments.

2.2 Clothing Matching for Women Who Are Visually Impaired

Statisticians estimate that 12 million individuals in India are blind, making up one-third of 39 million blind people globally [1]. The majority of visually impaired women get by on the assistance of family members, Braille labels, or other types of stitching patterns to indicate various hues and textures on their clothes [12].

2.3 Clothing Options for Women with Vision Impairment

A challenging assignment for those with visible disabilities is choosing clothing with muddled patterns and colors [13]. The fashion industry has largely overlooked visually impaired women. Most of these visually impaired persons will never see a change in their condition despite numerous advancements in surgery and optometry [14]. Few alterations that have already been made for visually impaired women are trousers with an elastic waistband, Velcro, or zipper as fastening, magnetic buttoned cuffs [15]; and simple-to-match labels. According to the data provided, no research has been done on the most popular and frequently worn Indian traditional attire: the *sari.* Since the traditional drape is difficult to manage with vision difficulties, the study develops a compatible design solution for visually impaired women in India using saree drapes.

2.4 Research Gap

Previous research has been done on everyday Indian traditional clothing like salwar kameez but not on sari. Thus, the research paper helps to understand how different components used in a sari like a blouse and petticoat can confuse visually challenged women. Fashion designers are not helped by specific foundations, models, or concepts when making products for visually challenged consumers [16].

3 Methodology

3.1 Participants

This section describes the research approach used. Data is gathered from both primary and secondary sources. A descriptive study was undertaken in Vimanagar, Pune, Maharashtra, using 15 visually impaired women aged 30–60 years as subjects, chosen by a purposeful sampling technique.

3.2 Interview, Affinity Mapping, and Observational Study

A well-structured opinion survey interview was designed and conducted with visually challenged women who frequently wear sari to understand the present problems for wearing sari and effectiveness of the proposed design intervention (an alternative to sari). All the information shown here was gathered from fifteen visually impaired women in Vimanagar, Pune, Maharashtra, India utilizing the structured interview

Table 1 Questions asked during interviews

Sr. No.	Questions
1	Which is your favorite color and fabric?
2	Are you able to drape your sari independently?
3	How do you differentiate on the face side of the fabric/garment??
4	What is the most difficult aspect of draping a sari?
5	Please state or describe what is your current method of draping your sari

method. As we have used open-ended questions (see Table 1) during the interview, affinity analysis (see Fig. 1) has been done to analyze the responses collected from interviews. In addition, observation studies were also conducted using a phone camera as videography and photography techniques.

Because the visually challenged women were uncomfortable with lengthy talks, the interviews had to be tailored according to their ability to sit for extended periods of time and converse effectively. The interview was a qualitative research technique in which open-ended questions were utilized to interact with respondents and obtain data about draping a sari and the problems that visually impaired women encounter. Because they are more like a usual chat, these interviews typically feature the fewest questions (see Table 1).

3.3 Design Description

The investigation began with a learned search for the appropriate pre-stitched drapes with fabrics and finishes to fulfill the needs of fifteen visually impaired women in Vimanagar, Pune, India; to investigate various drapes techniques on the dress form to meet the needs of women with vision impairments such as comfort and feasibility as an alternative to sari.

The most important thing to remember in this area is to always have sari's center pleats pre-stitched to avoid the challenging part of draping a sari (see Fig. 2). This demonstrates the several draping experiments carried out on the dress form while preserving the sari's original silhouette.

3.4 Study Procedure

A total of fourteen drape styles were experimented on the dress form, out of which one drape style was selected and developed into samples (see Fig. 3). It presents the execution of the prototype sample created for this research. The design included center back placket with magnetic buttons. Pre-stitched pleats were affixed to the front

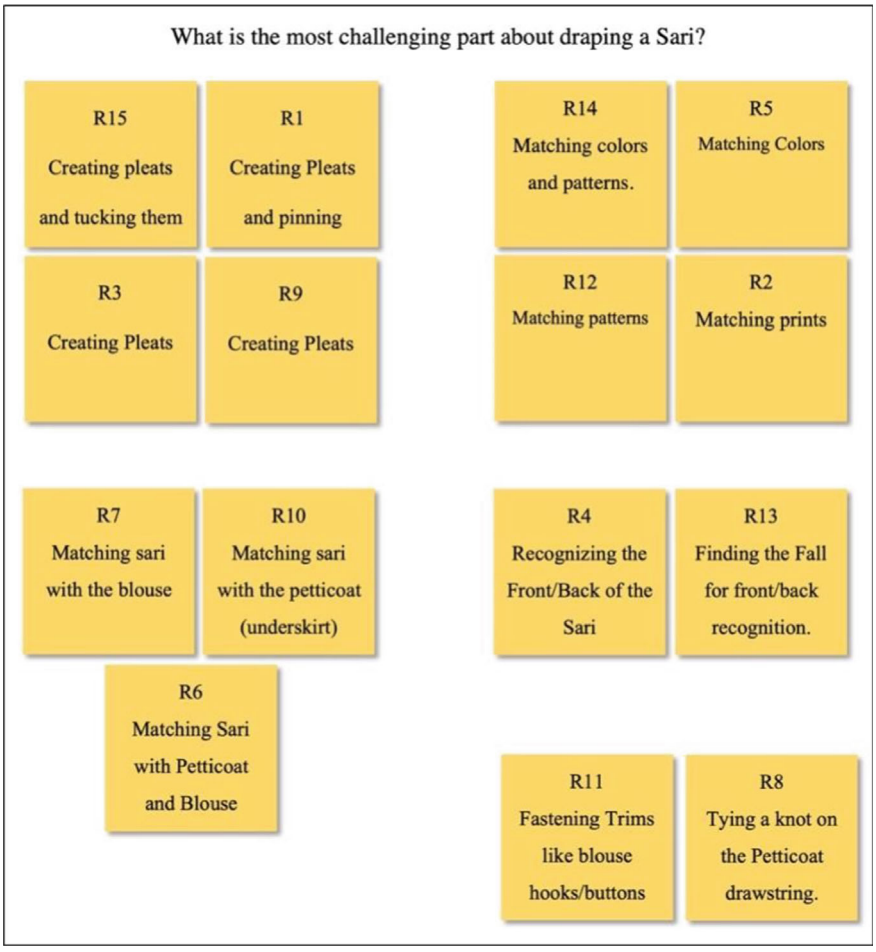


Fig. 1 Sample canvas for affinity mapping to analyze the similarity of responses for asked questions during requirement analysis, "What is the most challenging part about wearing the Sari?"

bodice. Style is quick and easy. As a result, an appropriate drape design solution for visually impaired women in India was developed [15].

3.5 Statistical Tools Used

For this study, descriptive statistics such as frequency of responses, percentage, etc. have been computed. When appropriate, the chi-square goodness of fit test was used on the data. A statistical hypothesis test called the chi-square goodness of fit test is used to assess the likelihood that a variable would originate from a given distribution.



Fig. 2 Drape explorations on the dress form



Fig. 3 Sample-1 prototype testing reactions by first user

Determining how well sample data represents the entire population is a popular use for it.

4 Results and Discussions

4.1 Observations from Affinity Analysis (Current Situations)

All findings from interview were analyzed through affinity analysis method.

1. Majority of participants [26.66%; $X^2(3) = 38.533$; $p = 0.00000002$] stated that they prefer wearing darker colors (black, brown, etc.) and lightweight fabrics (like cotton, muslin, etc.). On the other side, other respondents (20%) said that they prefer easy maintenance colors like black, brown, and gray; and cotton is the most preferred fabric. However, any other textured fabric (such as jacquard, corduroy, etc.) was also picked by 20% of those interviewed participants while 13.66% of participants mentioned that they like to wear sarees in lighter colors.
2. Majority of participants [33.33%; $X^2(3) = 37.267$; $p = 0.00000004$] stated that they are dependent on other family members and friends for using safety pins and hooks. On the other side, other respondents (26.66%) said that they prefer wearing ready-to-wear sarees. Similarly, 20% participants stated that they are still dependent on Family members for pleats. However, 20% of participants also stated that they depend on family members and friends for front and back recognition. To help the visually impaired live freely and interact with others, a psychological support system for clothing self-selection is needed [17].
3. Majority of participants [26.66%; $X^2(3) = 38.533$; $p = 0.00000002$] stated that the fall and the piquot in any given sari help visually impaired women to differentiate the front and the back of any sari. On the other side, 20% of participants also stated that the textures and surfaces on fabrics or garments help visually impaired women to distinguish between the front and back. However, 20% of participants also stated that surface ornamentation is a major distinguishing factor. On the contrary, 13.33% of participants said that the Braille labels in garments help in distinguishing the front and the back side.
4. Majority of participants [26.66%; $X^2(3) = 33.933$; $p = 0.00000005$] stated matching colors and patterns is challenging, whereas 26% stated that creating pleats and tucking the pleats into the petticoat is a major challenge. However, 20% of participants said that matching sari with various components like the blouse and the petticoat (underskirt) is a major issue. Only 13.33% of participants stated that recognizing the front and the back of the sari is challenging. Due to rotation, scale, illumination, and notably significant intra-class pattern changes, automatic garment pattern identification is a difficult research subject [18].
5. Majority of respondents [53.33%; $X^2(3) = 34$; $p = 0.00000002$] stated that they are dependent on family for draping a sari. However, 26.66% of participants can independently drape a sari except creating pleats and pinning the pleats on their shoulders. Also, only 20% of participants are comfortable wearing ready-to-wear sarees. Only 6.66% of participants can independently drape sari without any help or support. Please refer Table 2 for the detailed results.

Table 2 Various challenges faced by blind women for draping sari in current situation

Questions	Response type-1 (%)	Response type-2 (%)	Response type-3 (%)	Others (%)
Q.1	Prefers wearing darker colors and lightweight fabrics such as cotton, muslin, and so on (26.66%)	Colors that are low maintenance, such as black, brown, and gray. Cotton is the most popular fabric (20%)	Any textured fabric is ok; however, there is no color preference (20%)	Lighter colors and fabrics (13.33%)
Q.2	Dependent on others for using safety pins and hooks (33.33%)	Relying on ready-to-wear sarees (26.66%)	Dependent on family members for creating pleats (20%)	Relies on others for front and back recognition (20%)
Q.3	The fall and piquot in the sari help to differentiate the front and the back (26.66%)	Textures and surfaces help to distinguish the front and the back of the fabric (20%)	Surface ornamentation like embroidery acts as a major distinguishing factor (20%)	The Braille label helps in distinguishing (13.33%)
Q.4	Color and pattern matching is difficult for women with low eyesight (26.66%)	Creating pleats and tucking them and later pinning the pleats is a major challenge (26.66%)	Matching sari with the blouse and the petticoat (underskirt) is another challenging issue (20%)	Recognizing the front/back of the sari is challenging for visually impaired women (13.33%)
Q.5	Dependent on family for draping them sarees (53.33%)	Independently drape a sari without creating pleats and pinning the pleats (26.66%)	Comfortable wearing ready-to-wear sarees (20%)	Independently able to drape a Sari (6.66%)

4.2 Findings from Affinity Analysis After Introducing First Prototype

1. Majority of respondents [40%; $X^2(3) = 34.333$; $p = 0.00000017$] stated that stated that they like wearing textured fabrics like Jacquard. On the other side, 26.66% of participants said that they like wearing heavy-weight cotton fabrics. However, 20% of participants stated that they like to wear lightweight cotton fabrics. On the contrary, only 13.33% of participants prefer wearing synthetic materials due to ease of wash and care. Even though these women cannot see, their tactile sense tells them which fabric they like and feel comfortable wearing it every day.
2. Majority of respondents [53.33%; $X^2(3) = 34.267$; $p = 0.00000017$] stated that they are independently able to drape a sari, but center back buttons are an issue since it is uncomfortable to reach the buttons in the back, while 33.33% said

that they are comfortable draping a sari independently in a minute. However, 13.33% of participants stated that they are independently able to drape a sari except fastening the shoulder which is a major issue according to them. On the contrary, 6.66% participants said that they are independent wearing a sari without any safety pins or fasteners.

3. Majority of respondents [33.33%; $X^2(3) = 37.267$; $p = 0.00000018$] stated that the textured Jacquard pattern on the fabrics helps in distinguishing the front of the fabric. On the other side, 26.66% of participants said that the sari pleats stitched at the front help in differentiating the front. However, 13.33% of participants said that the joint of two contrast fabrics helps them in identifying the front. On the contrary, 13.33% of participants also stated that the magnet buttons in the back helps in recognizing the front.
4. Majority of respondents [26.66%; $X^2(3) = 33.933$; $p = 0.00000002$] said that buttons closure is the most challenging part while wearing Prototype-1, whereas 26.66% of participants stated that a closed center front without any opening becomes challenging while wearing Prototype-1. On the other side, 20% said that adjusting the pleats of the sari on the shoulder is a major issue while wearing the Prototype-1. However, 13.33% of participants stated safety pins as a major issue.
5. Majority of respondents [53.33%; $X^2(3) = 34.267$; $p = 0.00000017$] said that buttons closure is the most challenging part while wearing Prototype-1. Instead, visually impaired women prefer a center front opening, whereas 33.33% of participants stated that they found the closed neckline uncomfortable while wearing the dress. On the other side, 13.33% were satisfied with Prototype-1 and said that it saved them from adjusting the pleats of the Sari. However, 6.66% participants said that they were not satisfied with the color of the dress (Table 3 for detailed responses). Compared to their sighted counterparts, people who are visually impaired have different opinions on the relative relevance of selection elements while buying apparel [19]. After, research and interviews, I observed that visually impaired persons have a lot of difficulty with clothing-related tasks such as washing laundry, buying new clothes, and determining what to wear every morning. I also concluded that visually impaired people may take good care of themselves and their clothing if they are given a simple way to identify it [20].

4.3 Results of Observational Study

The first prototype testing was performed on Mrs. X, a 60-year-old woman with arthritis and blindness since birth (shown in Fig. 3). Accessing the magnetic closure buttons located in the center back caused discomfort for the first user. The second user, Mrs. Y, a visually impaired working woman (shown in Fig. 4), tested the drape design (prototype 1) again, feedback from both the trial interviews and observations indicated that it was unpleasant for visually impaired women of different ages.

Table 3 Responses of blind women for draping of proposed dress (prototype I)

Questions	Response type-1 (%)	Response type-2 (%)	Response type-3 (%)	Others (%)
Q.1	Majority of respondents stated that they like the cotton jacquard used for prototype-2 in lighter colors (53.33%)	Prefers the cotton jacquard in warmer tones (26.6%)	Cotton materials in deeper colors that are lightweight (20%)	Darker-colored synthetic materials are preferred (6.66%)
Q.2	Independently able to wear prototype-2 (100%)	Comfortable wearing the dress without any help in a minute (100%)	Satisfied with Prototype-2 without the use of safety pins (100%)	Satisfied with no need of adjusting the pleats (100%)
Q.3	Pleased with the texture of the fabric (100%)	Satisfied with the stitched center pleats (100%)	Comfortable wearing the dress with joints (100%)	Satisfied with the front opening (100%)
Q.4	Comfortable without buttons (100%)	Satisfied with the center front opening in prototype-1 (100%)	Adjusting the pleats on the shoulder is a major issue (100%)	Satisfied with no use of safety pins (100%)
Q.5	Satisfied with wearing the dress as a Sari on regular basis (100%)	Satisfied with the given prototype where there is no need to create the pleats (100%)	Satisfied with ready-to-wear dress that looks like a Sari (100%)	Comfortable without using safety pins (100%)

Furthermore, the suggested solution for the (prototype 1) sari design calls for a minimal number of remedial actions (Fig. 5).



Fig. 4 Sample-2 prototype testing reactions by second user



Fig. 5 Execution and evaluation of newly developed sari drapes for visually challenged women (sample drape design prototype-I)

5 Conclusion

Social acceptance and integration are critical for those with vision impairment. Fashion is a fast-paced industry, and it would be fantastic if the visually impaired could join in this developing trend [21]. The results of this study imply that the visually impaired women had the deficiency since birth. For people everywhere, choosing appropriate clothing for daily use is a necessary ritual. But for those who are blind or visually handicapped, this might be an enormous task [22]. Following the Prototype-I Trial, it was discovered that users encountered difficulties when fastening the magnetic buttons at the center front of the bodice. As a result of the feedbacks received, Prototype-II will be created with all the essential improvements, such as a zip opening to accommodate women with vision impairment and lactating mothers.

There would be no opening in the back, and the design would also include darts. The sari was highly uncomfortable mainly because of its buttons in the back. The study is limited to fifteen visually impaired women in Vimanagar, Pune, India, and the data obtained from this group between February 21 and March 21, 2023.

References

1. Ackland P, Resnikoff S, Bourne R (2017) World blindness and visual impairment: despite many successes, the problem is growing. Commun Eye Health 30(100):71
2. Woodbury WA, McCoy MA, Teutsch SM (2016) Making eye health a population health imperative: vision for tomorrow
3. Raman R, Verma A, Srinivasan S, Bhojwani D (2018) Partial reversal of color vision impairment in type 2 diabetes associated with obstructive sleep apnea. GMS Ophthalmol Cases 8:154
4. Kim J, Choi W, Tsyrenzhapova D, Kang YA, Cho YJ, Shin J, Kim JY (2019) Beyes: a shopping solution for independent clothing experiences of the visually impaired. In: Paper presented at the conference on human factors in computing systems—proceedings. https://doi.org/10.1145/3290607.3312829
5. Ye H, Zeng Y, Xiao H, Yu J, Liu Y, Zhang S, Zhang B (2022) Prevalence and factors associated with visual impairment in middle-aged and older Chinese population. Front Med 9:962729
6. Rowe F, Walker M, Rockliffe J, Pollock A, Noonan C, Howard C, Currie J (2016) Delivery of high quality stroke and vision care: experiences of UK services. Disabil Rehabil 38(8):813–817
7. Pushpanjali GP, Jaimini J (2007) Functional garments for visual impaired adolescents. Textile Trends 50(1):27–29
8. McDaniel TL, Kahol K, Panchanathan S (2007) An interactive wearable assistive device for individuals who are blind for color perception. https://doi.org/10.1007/978-3-540-732792_83
9. Zaharia AC, Dumitrescu OM, Radu M, Rogoz RE (2022) Adherence to therapy in glaucoma treatment—a review. J Person Med 12(4):514
10. Mohammed Z, Kee QT, Fadzil NM, Abd Rahman MH, Din NC, Mariappan V, Shahar S (2023) Association between vision and cognitive function among community-dwelling older adults in Selangor. Malaysia. Int J Ophthalmol 16(1):115
11. Zhao Y, Gong L, Huang Y, Liu C (2016) A review of key techniques of vision-based control for harvesting robot. Comput Electr Agricult 127:311–323
12. Walmiki LN, Vastrad JV (2016) Designed functional salwar-kameez for visually impaired adolescent girls. J Farm Sci 29(5):798–880
13. Sonawane TM, Patil HT (2018) Clothing pattern recognition using features extraction of wavelet coefficient for visually impaired people. In: Paper presented at the proceedings of the 2nd international conference on trends in electronics and informatics, ICOEI. https://doi.org/10.1109/ICOEI.2018.8553846
14. Rose J (2006) Closet buddy: dressing the visually impaired. In: Paper presented at the proceedings of the annual southeast conference, pp 611–615. https://doi.org/10.1145/1185448.1185582
15. Tokens E (2016) Clothes fastenings: 15 different types of fastenings for clothes. https://www.thecreativecurator.com/clothes-fastenings/. Kothari V (2013) Study of apparel trims—zipper. News and insights, research/review paper, textile articles. https://textilevaluechain.in/newsinsights/study-of-apparel-trims-zipper/
16. Pina L, Martins P, Lucas J, Duarte P, Miguel R (2021) Fashion for visually impaired consumers: a case study towards inclusive products. https://doi.org/10.1007/978-3-03055700-3_22
17. Miyake M, Manabe Y, Uranishi Y, Yoshimoto S, Imura M, Kuroda Y, Oshiro O (2016) Support system for clothes selection based on color information for visually impaired persons. Trans Jpn Soc Med Biol Eng 53(5):255–263

18. Yang X, Yuan S, Tian Y (2014) Assistive clothing pattern recognition for visually impaired people. IEEE Trans Hum Mach Syst 44(2):234–243. https://doi.org/10.1109/THMS.2014.2302814
19. Frency NSF, Patrick HCL, May CLF (2000) Selecting and purchasing clothing: the experience of visually impaired people in Hong Kong. J Vis Impair Blind 94(1):34–41. https://doi.org/10.1177/0145482x0009400105
20. Hsu T, Li Z, Lin H, Liou Y, Tsai C (2016) Touch and #tag: improving clothing experiences of people with visual impairment. In: Paper presented at the conference on human factors in computing systems—proceedings, pp 38–43. https://doi.org/10.1145/2851581.2890636
21. Khalid L, Gong W (2022) Vision4All: a deep learning fashion assistance solution for blinds. In: Paper presented at the 2022 IEEE 5th international conference on artificial intelligence and big data, ICAIBD 2022, pp 156–161. https://doi.org/10.1109/ICAIBD55127.2022.9820475
22. Alabduljabbar R (2022) An IoT smart clothing system for the visually impaired using NFC technology. Int J Sens Netw 38(1):46–57

An Experimental Educational Tool for Financial Literacy in Children of 3–10 Years



Debashis Majumder, Ipsita Dasgupta, and Mugdha Tambe

Abstract This innovative study explores the significance of financial literacy for kids between the ages of three and ten, as well as the critical role that educational toys may play in supporting that development. The study emphasizes the value of early financial literacy, its possible long-term benefits, and the efficiency of educational toys in promoting financial knowledge and decision-making among young learners through a thorough literature review and market analysis of educational toys. The researchers hope to shed light on the crucial connection between financial literacy and educational toys through their research and study. Based on the research study, innovative exploration of designing suitable financial toy for young learners is done. Their feasibility and suitability of development for financial awareness in young kids of 3–10 are discussed. The design idea is modeled, and design intricacies are explained.

Keywords Financial literacy · Children toys · Educational tool · Smart toys

1 Introduction

The team of researchers embarked on this study with a focus on unraveling the significance of financial literacy during the critical developmental stage of early childhood of ages 3–10 years. Acknowledging that financial literacy empowers individuals to make informed financial decisions and enhances financial well-being and stability, the researchers aimed to explore the potential long-lasting effects of introducing

D. Majumder (✉)
School of Design, University of Petroleum and Energy Studies (UPES), Bidholi, Via Premnagar, Dehradun, Uttarakhand 248007, India
e-mail: dmajumder@ddn.upes.ac.in

I. Dasgupta
Libra Design Pvt Ltd, Dehradun, India

M. Tambe
UID, Gandhinagar, India

© The Author(s), under exclusive license to Springer Nature Singapore Pte Ltd. 2025

B. B. V. L. Deepak et al. (eds.), *Recent Advancements in Product Design and Manufacturing Systems*, Lecture Notes in Mechanical Engineering,
https://doi.org/10.1007/978-981-97-6732-8_46

financial concepts to young children [1]. By examining the role of educational toys in this context, they sought to provide a fresh perspective on nurturing financial literacy skills among the youngest members of society. The researchers delved into the multifaceted nature of financial literacy, emphasizing that it encompasses essential skills beyond basic money understanding [2]. Concepts like budgeting, saving, and responsible spending choices were recognized as critical aspects of financial literacy for children to comprehend early on. Drawing from existing research, the team observed the positive correlation between early financial education and improved financial decision-making in adulthood, underscoring the significance of instilling financial literacy from a tender age to foster better money management habits and reduce financial pitfalls in later life [3].

2 History

The history of toy design in India is a fascinating journey that spans ancient times to the present day. Archeological evidence reveals the existence of toys made from diverse materials like clay, wood, and metal in various regions of India. Traditional Indian toys often held cultural or religious significance, passing down from generation to generation. Examples of such toys include dolls dressed in traditional Indian clothing, wooden spinning tops, and colorful kites, each representing a glimpse into the rich cultural heritage of the country [4].

As we explored the world of educational toys, we marveled at the impressive designs geared toward facilitating learning and skill development in young children [5]. We recognized that incorporating financial concepts into these toys could provide an interactive and enjoyable avenue for children to learn about money, budgeting, and saving. By utilizing age-appropriate toys, the researchers observed that financial learning could be made more engaging, creating positive associations and memorable experiences for young minds [6]. The team conducted a thorough analysis of the educational toy market, witnessing its remarkable growth in recent years. Manufacturers were observed to be responding to the demand for skill-developing toys, including those designed to promote financial literacy. The researchers meticulously examined key trends, popular products, and the substantial impact of financial literacy-oriented toys on the industry's growth, revealing a compelling market dynamic where educational toys are emerging as essential tools in children's development.

The purpose of smart toys with behavioral challenges is to improve kids' behavioral abilities. For instance, by treating one intelligent toy, the Furby, like a genuine, live creature, kids can practice good behavior [7]. Similar to this, kids may learn basic behaviors like opening and closing the refrigerator using Fisher Price's Learning Kitchen. The focus of smart toys that encourage cognitive tasks, however, is primarily on children's cognitive abilities [8]. Children can, for instance, work on their narrative and reflection skills while playing with a smart toy like Story Mat as shown in Fig. 1.



Fig. 1 Story toys

Self-contained smart toys, on the other hand, can be viewed as a special gadget with built-in digital functions. Instead of needing an external computer, these self-contained smart toys feature playsets, play spaces, or environments with interactive objects and characters or may incorporate digitally merged things or characters within their structure [9]. For example, Sifteo, also known as Shiftable, uses physical blocks with built-in electronic chips. Using Sifteo, kids create various word and image combinations as shown in Fig. 2.

A two-wheeled vehicle called Curly Bot measures, records, and replays its precise motion on any flat surface. Curly Bot falls into the category of self-contained smart

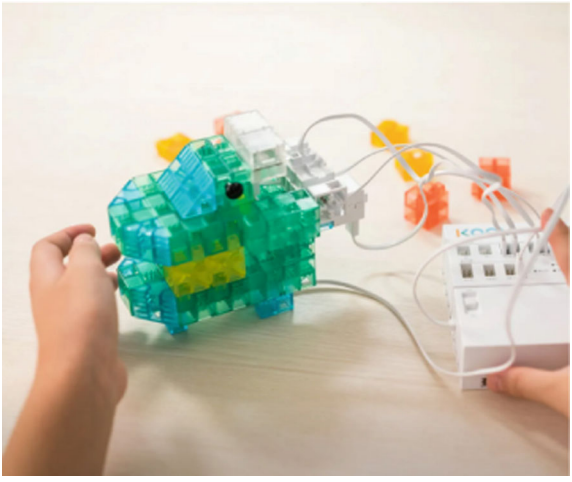


Fig. 2 Electronic toys

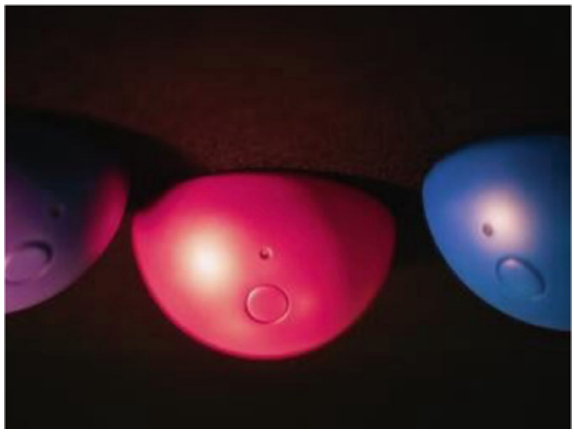


Fig. 3 Curly bot toy

toys that don't require external computers [10]. Additionally, Curly Bot starts cognitive tasks, particularly ones that involve computing and mathematics. A microprocessor drives Curly Bot's two wheels, which may freely spin in addition to moving forward and backward. The smart toy has a memory chip that may be used to record motions as shown in Fig. 3.

Empirical studies on the influence of educational toys captivated the researchers as they unearthed evidence of their positive impact on children's financial literacy [11]. The interactive nature of toys simulating financial transactions, such as play cash registers or coin-counting piggy banks, was found to significantly enhance children's understanding of money and basic arithmetic. Furthermore, the team discovered that board games involving money management provided a platform for teaching children about financial decision-making, risk assessment, and long-term planning skills [12].

Drawing from their extensive research, the researchers crafted a comprehensive guide outlining practical strategies for parents, educators, and caregivers to effectively leverage educational toys in promoting financial literacy among children. They emphasized the importance of seamlessly integrating financial concepts into playtime and offered valuable recommendations for selecting age-appropriate toys that align with specific learning objectives [13].

3 Methodology

Surveys and Interviews: Survey was made using google forms. Most of the questions were asked to parents on how they educate their children about financial literacy. Questions like how do you think a smart toy could support your child's curiosity and interest in learning, other than that questions regarding child grown and learning were also asked. The survey was sent to people through an online medium. The interviews were also conducted to collect information which we were not able to

collect through surveys. The mediums used to collect data were call recordings and live recordings [14]. Questions related to their personal experience while using the toys were used. The researchers conducted interviews with parents, revealing that a substantial 84% of them strongly believe in the benefits of smart toys for their child's development. The study highlighted parents' keen interest in smart toys that specifically aid language and cognitive development in their children. This finding underscores the growing recognition among parents of the educational value these toys can offer [15]. In India, the perception of smart toys for children remains largely positive, with parents acknowledging the educational and developmental benefits these toys can offer.

Several observed points emerged from surveys and interviews:

- A strong need for toys that aid language and cognitive development in children.
- Parents' desire to monitor their child's progress and tailor their experience with smart toys to meet their individual needs.
- An increasing focus on early childhood education and the growing emphasis on Science, Technology, Engineering, and Mathematics (STEM) education in India.
- A willingness among parents to invest in smart toys, provided they prove to be worthwhile and not a waste of money.
- The observation that children are increasingly attracted to screens and mobile phones, prompting parents to seek alternatives to reduce screen time and promote healthier play habits.
- Challenges faced by parents in finding time to take their children to playgrounds due to hectic schedules and the burden of school activities and homework.
- The traditional teaching methods followed in schools, leading parents to seek interactive and effective learning opportunities for their children.
- A concern among parents about their children having less understanding of their mother tongue, indicating a need for language-related educational aids.
- The desire for smart toys that can be used in the long term, providing enduring learning and entertainment experiences.
- A call for universal design in smart toys to ensure they are friendly and accessible to children with disabilities [16].

4 Conceptualization

The Smart Learner is an innovative and interactive smart toy designed to introduce children to the fundamentals of financial literacy through engaging play. This unique toy aims to teach children about basic transactions, saving money, and financial responsibility, all while providing an enjoyable and immersive learning experience. The Smart Learner utilizes cutting-edge technology, including augmented reality, to make the learning process fun, interactive, and effective as shown in Fig. 4.

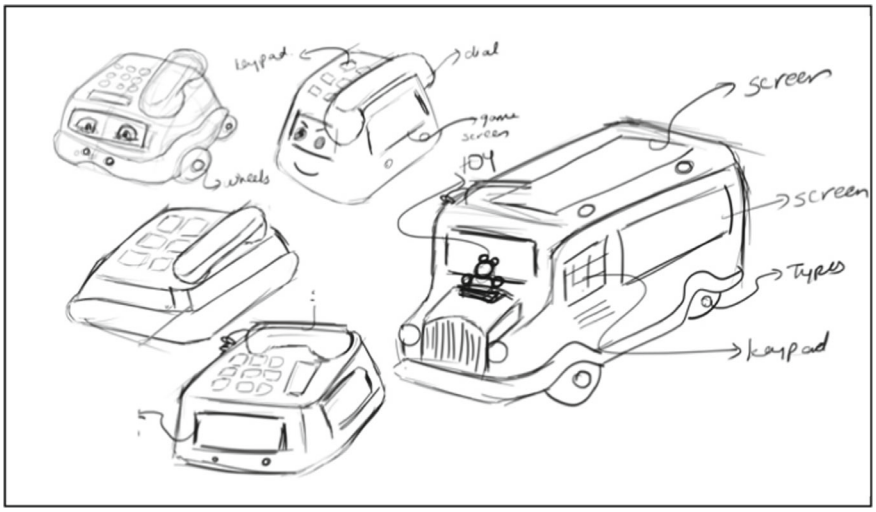


Fig. 4 Ideations

5 Key Features of Smart Learner

Interactive Learning Experience: The Smart Learner provides an interactive learning experience for children aged 5–10 years. By using augmented reality technology, the toy can project 3D models and interactive animations related to financial concepts, making learning exciting and captivating for young minds.

- *Comprehensive Lessons*

The toy covers various aspects of financial literacy, such as understanding the concept of money, differentiating between coins and notes, basic budgeting, and distinguishing between needs and wants. The Smart Learner is designed to lay the foundation for children to develop healthy financial habits early on in life.

- *Real-Life Simulations*

Through interactive play scenarios, children can virtually engage in real-life financial situations, like shopping for groceries, saving money in a piggy bank, or making small transactions at a pretend store. These simulations help children grasp financial concepts in a practical and relatable manner as shown in Fig. 5.

- *Parental Monitoring and Control*

The Smart Learner comes with a mobile app for parents that allows them to monitor their child's progress and control the toy's activities. Parents can access insights on their child's financial learning journey and tailor the content to match the child's learning pace and interests.

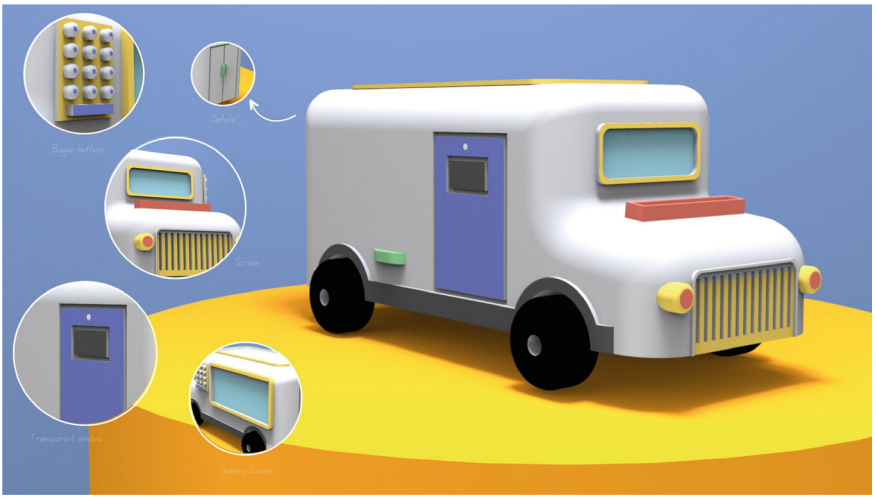


Fig. 5 Concept for children education van

- *Rewards and Challenges*

The toy incorporates a reward system to incentivize children's learning progress. Completing financial challenges and games successfully can earn them virtual rewards, encouraging them to continue exploring and mastering financial concepts.

- *Smart Financial Goal Setting*

As children progress through the learning modules, they can set and track their financial goals. Whether it is saving up for a toy or setting aside money for a future event, Smart Learner instills the value of goal-setting and financial planning from an early age.

- *Playful Design and Engaging Interface*

The Smart Learner features a child-friendly and visually appealing design, ensuring an immersive, and engaging learning experience for children. The interactive interface sparks curiosity and fosters a love for learning about money and finances.

The Smart Learner is a groundbreaking smart toy that combines innovative technology with the crucial need for financial literacy education among children. Through interactive play and augmented reality, it instills valuable financial skills, setting the foundation for responsible money management in adulthood. With parental monitoring and engagement, Smart Learner ensures a holistic and enjoyable learning experience, making financial education an exciting and empowering journey for young learners.

6 Conclusions

In conclusion, the concept of a financial education toy tailored for kids aged 4–12, integrating interactive games, teaching currency types, and simulating day-to-day transactions with a smart piggy bank, represents a forward-thinking approach to nurturing financial literacy from a young age. This innovative educational tool offers several promising benefits:

1. Early Financial Literacy: By introducing kids to the world of money through engaging gameplay, this concept equips them with essential financial skills and knowledge early on, setting a foundation for responsible financial management in adulthood.
2. Hands-On Learning: Interactive play and tasks provide a hands-on learning experience, making complex financial concepts more accessible and enjoyable for children, while also fostering critical thinking and decision-making skills.
3. Technology Integration: The incorporation of a smart piggy bank connects traditional money management with technology, making the learning experience more relevant to the digital age and helping kids become familiar with both physical and digital forms of currency.
4. Rewards-Based Motivation: The rewards system encourages children to make prudent financial choices and cultivate savings habits. This positive reinforcement can contribute to a healthier relationship with money throughout their lives.
5. Parental Involvement: This concept encourages parental involvement in financial education, strengthening family discussions about money and allowing parents to be active participants in their children's financial development.

7 Summary

In summary, the financial education toy effectively addresses current financial challenges by providing a practical solution that instills financial literacy, bridges the gap between physical and digital currencies, involves parents in the process, and sets children on a path toward responsible financial decision-making. By doing so, it helps mitigate future financial problems and promotes a more financially aware and empowered generation.

8 Future Prospect

As for the future, this educational toy concept holds significant potential. With advancements in technology and educational methodologies, we can expect to see:

1. Customization: Tailoring the educational content to the specific needs and interests of individual children, ensuring a more personalized learning experience.

2. Data Analytics: Utilizing data collected from smart piggy banks and gameplay to provide insights into a child's financial behavior and areas where they may need additional support.
3. Expanding Age Ranges: Adapting the concept to cater to older age groups, including teenagers, to provide more advanced financial education as children grow.
4. Integration with School Curriculum: Collaboration with educational institutions to incorporate these tools into formal curricula, making financial education a standard part of a child's education.
5. Global Reach: Expanding the concept to a global audience, adapting it to different currencies and financial systems to teach financial literacy in diverse contexts.

References

1. Kumar V, Saini VK (2020) National strategy for financial education in India. Himal J Soc Sci Hum 15:31–36
2. Hussain I, Sajjad S (2016) Significance of financial literacy and its implications: a discussion. J Bus Strat 10(2):141
3. Nwachukwu C, Chládková H, Žufan P (2017) The relationship between entrepreneurial orientation, entrepreneurial competencies, entrepreneurial leadership, and firm performance: a proposed model
4. Hastings JS, Madrian BC, Skimmyhorn WL (2013) Financial literacy, financial education, and economic outcomes. Annu Rev Econ 5(1):347–373
5. Bureau CFP (2016) Building blocks to help youth achieve financial capability: a new model and recommendations
6. Fernandes D, Lynch JG, Netemeyer RG (2014) Financial literacy, financial education, and downstream financial behaviors. Manag Sci 60(8):1861–1883
7. Caplan MA, Sherraden MS, Bae J (2018) Financial capability as social investment. J Soc Soc Welfare 45:147
8. Lachapelle U, Jean-Germain F (2019) Personal use of the internet and travel: evidence from the Canadian general social survey's 2010 time use module. Travel Behav Soc 14:81–91
9. Lubis RR, Irwanto I, Harahap MY (2019) Increasing learning outcomes and ability critical thinking of students through application problem-based learning strategies. Int J Educ Vocat Stud 1(6):524–527
10. Chowdhury A (2019) Financial socialization for digital natives: a new way to teach children about money
11. Kottman T (2014) Play therapy: basics and beyond. Wiley, Amsterdam
12. Costello AH, Chengappa K, Stokes JO, Tempel AB, McNeil CB (2011) Parent-child interaction therapy for oppositional behavior in children: integration of child-directed play therapy and behavior management training for parents. Integr Play Therapy 12:37–59
13. Axline VM (1969) Dibs: in search of self, vol 6109. Mansion
14. Ray DC, Lee KR, Meany-Walen KK, Carlson SE, Carnes-Holt KL, Ware JN (2013) Use of toys in child-centered play therapy. Int J Play Therapy 22(1):43
15. Norcross JC, Karpiak CP, Santoro SO (2005) Clinical psychologists across the years: the division of clinical psychology from 1960 to 2003. J Clin Psychol 61(12):1467–1483
16. Butterworth G (2014) Principles of developmental psychology: an introduction. Psychology Press

Challenges of Sustainable Urban Planning in Odisha (India): Using the OCRA Method

Kallol Bera and Suchismita Satapathy

Abstract Odisha is well known for its rich historical sites, ancient temple, culture heritage and for its tourism, not only for its sociocultural sites but also Odisha is renowned for its vulnerable climatic changes. Sustainable urban regeneration of Odisha is a well-organized plan to develop the social, cultural, environmental and economic sustainability. But the sustainable regeneration plan will face a number of challenges. In this paper, we have taken a number of questionnaires to set the initial decision matrix. We have used the OCRA method to analyze and rank the most important challenges for urban development. In conclusion, we can say that if the challenges are not been solved, the urban regeneration plan of Odisha may fail. Hence, prioritizing the sustainability issue is crucial for addressing the issues and enhancing the quality of urban life.

Keywords Sustainable urban regeneration plan · Odisha · OCRA method · Urbanization · Ranking · MCDM method

1 Introduction

Sustainable urban regeneration of Odisha is a holistic approach to reinvigorating and developing urban areas with social, cultural, environmental and economic sustainability. Sustainable urban regeneration in Odisha promotes green and environment-friendly infrastructure. It includes the best transport facilities and an organized traffic system. This includes affordable healthcare facilities and education. The regeneration process should include development of road ways and infrastructure. Odisha is well known for its rich heritage and culture, so the regeneration process should also preserve its historical landmarks.

Odisha has witnessed significant urbanization in recent years, which has led to an increase in the population in urban areas. Due to the rapid growth, it creates pressure

K. Bera · S. Satapathy (✉)
School of Mechanical Engineering, KIIT Deemed to Be University, Bhubaneswar, Odisha, India
e-mail: ssatapathyfme@kiit.ac.in

© The Author(s), under exclusive license to Springer Nature Singapore Pte Ltd. 2025

B. B. V. L. Deepak et al. (eds.), *Recent Advancements in Product Design and Manufacturing Systems*, Lecture Notes in Mechanical Engineering,
https://doi.org/10.1007/978-981-97-6732-8_47

on the infrastructure, power source, food and natural resources. With sustainable urban regeneration, growth can be managed easily and efficiently.

The state of Odisha is renowned for its rich historical sites, cultural heritage and ancient temples. The state is also well known for its tourism. To boost tourism as well as to contribute to the economy of Odisha (13% of GDP of Odisha), the sustainable urban regeneration should preserve the cultural heritage of Odisha.

Odisha is on the eastern seaboard of India, hence the state is prone to several natural disasters, which include cyclones and floods. Hence, the regeneration process should be planned in such a way that it can reduce human and economic losses.

A sustainable urban regeneration plan should include creating new job opportunities, investing in small-scale industries, and developing a full-proof plan such that the production rate should fully meet the public demands. As a result of which, the economy of the state will be balance.

Sustainable urban regeneration needs a large amount of energy. To meet the energy need, the plan should include investing in the development and research. The plan should not only develop the energy sources but also focus on making them cost-effective.

Hospital facilities and health care is one of the most important criteria of a sustainable urban regeneration plan. The hospitals should be located strategically in such a way to provide easy access for all residents.

Looking at the vulnerable climate change of Odisha, the sustainable urban regeneration plan should focus on building climate-resilient cities, such that these buildings can adapt to the sudden changes in climate. Even proper water way, dumping of garbage, modification of road ways, tourism spots can change the regenerative process systematically and successfully.

As the criteria are explained, there are some environmental challenges or problems such as, environmental pollution and depletion of resources, which should be addressed. Sustainable urban regeneration can contribute to various economic developments, such as, creating new jobs and developing new small-scale industries.

Sustainable urban regeneration plans focus to prioritize on factors like use of public transport, affordable housing system, green space. The central goal of this plan is to enhance the quality of life.

The main motivation behind writing this paper is to address the crucial challenges like increase in population, change in climate and managing the resources, etc., of sustainable urban planning. Research in this area may lead to find different key challenges along with techniques to solve them. Understanding and analyzing the OCRA method could be a novel approach to contribute in the development of economy, culture and, most importantly, in the development of society as well as environment. This research aims to contribute in the academic literature and expand knowledge about sustainable urban planning along with the OCRA method of ranking. Research in this area will spread awareness and promote the practice of sustainable urban development, which potentially leads to positive environmental as well as social impacts.

The objective of this paper is to find the challenges or obstacles for the development of the existing urban development plan, such that necessary policies can be framed for development of Odisha.

2 Literature Review

A very few number of literates exist in the field of sustainable urban regeneration. URBACT II [1] in their study have found that sustainable urban regeneration is a process or action, in which it points out the socioeconomic, cultural or environmental problems to improve the quality of urban lifestyle and assets.

It was suggested that the sustainable urban regeneration plan of UAE not only focused on the development physical environment, but also emphasized on developing the non-physical environment such as society, economy and culture [2–4].

3 Research Methodology

A standard questionnaire (27 nos) is designed and a survey is conducted to find the challenges of sustainable urban development among the citizens of Odisha and the development authorities of Odisha. Around 200 questions were circulated in east, west, north and south parts of Odisha and only 120 (60%) data was collected. Then statistical analysis and ranking was done to find the most important challenges for urban development.

4 Results and Discussion

After collecting data, factor analysis is conducted and 26 variables/items were selected under 5 dimensions for urban development (i.e., urban environment sectors, sustainability sector, social/cultural sector, transportation sector and economic sector) [5]. They have Cronbach's alpha value more of than 0.5. Those have less value than 0.5 which were discarded as given in Tables 1, 2, and 3 gives the name of the constructs. The operational competitiveness rating application, a collection of competitive alternatives and relative performance, can be determined using the MCDM method known as OCRA. The method incorporates the decision maker preferences regarding the relative weight of the criteria using an intuitive approach [6].

The OCRA method's key benefit is its ability to handle MCDM scenarios in which the relative weights of the criteria depend on the alternatives and different weight distributions are allocated to:

Step 1. Set the initial decision matrix, X:

Table 1 Questionnaire

Questionnaire number	Questionnaire
1	Hospital facilities and health
2	Drainage system
3	Public transport facilities
4	Road ways system
5	Foot path
6	Wide area transportation network
7	Development in the transportation system
8	Taking care of historical and cultural monuments
9	Expansion of medical facilities
10	Local community facilities
11	Housing facilities
12	Policies local community facilities for existing districts
13	Support for low-scale business
14	New job opportunity
15	Policies for low income families
16	Providing of social housing
17	Active use of solar/wind power
18	Energy efficiency related design
19	Waste reduce and management policies
20	Afforestation or greenery
21	Life cycle of the building
22	Disaster management
23	Lightening system
24	Central library facilities
25	Wild animal protection system
26	Renewable energy system
27	Security and safety system

Step 2. Find maximum and minimum.
Step 3. Find the operational matrix.
By using weight.

$$\text{OCRA beneficial} = \text{Weight} * (\text{current matrix} - \text{min matrix}) / \text{min matrix}$$

$$\text{OCRA Non beneficial} = \text{Weight} * (\text{max value} - \text{current value}) / \text{max matrix}$$

Step 4. Find the sum of all beneficial and non-beneficial find the difference between min values.

Table 2 Factor analysis

Factor	Questionnaire number	F1	F2	F3	F4	F5	Cronbach's alpha
Urban environment sector	1	0.567					0.501
	2	0.745					0.523
	5	0.533					0.519
	6	0.624					0.610
	10	0.753					0.623
	11	0.819					0.627
	12	0.533					0.578
	13	0.799					0.555
Sustainability sector	17		−0.647				0.813
	18		−0.641				0.769
	19		−0.811				0.775
	20		−0.884				0.504
	22		−0.759				0.541
	25		−0.539				0.606
	26		−0.657				0.571
	27		−0.729				0.531
Social/cultural sector	8			−0.520			0.529
	9			−0.668			0.503
	16			−0.721			0.512
	20			−0.816			0.592
	21			−0.779			0.588
Transportation sector	3				0.519		0.624
	4				0.622		0.518
	7				0.610		0.509
Economic sector	14					0.823	0.511
	15					0.580	0.505

Table 3 Percentage of variance

Factor	F1	F2	F3	F4	F5
Variance	5.2646	5.1517	4.1317	2.1449	2.0857
% of variance	0.211	0.206	0.165	0.086	0.083

Step 5. Find the rank. All weights are considered 0.33.

Implemented OCRA (MCDM method to rank. Tables 4, 5, and 6 use of OCRA method.

Table 4 Name of items

Items	Name of constructs
1	Hospital facilities and health
2	Drainage system
5	Foot path
6	Wide area transportation network
10	Local community facilities
11	Housing facilities
12	Policies local community facilities for existing districts
13	Support for low-scale business
17	Active use of solar/wind power
18	Energy efficiency related design
19	Waste reduce and management policies
20	Afforestation or greenery
22	Disaster management
25	Wild animal protection system
26	Renewable energy system
27	Security and safety system
8	Restoration of historical and cultural monuments
9	Expansion of medical facilities
16	Providing of social housing
20	Afforestation or greenery
21	Life cycle of the building
3	Public transport facilities
4	Road ways system
7	Development in transportation sector
14	New job opportunity
15	Policies for low income families

The OCRA ranking Table 7 shows that active use of solar/wind power ranked first, hospital facilities and health support ranked 2nd, for low-scale business facility ranked 3rd and public transport facilities ranked 4th. Users should also pay for the facilities that are produced in this way. It should be investigated whether different prices may be applied depending on the type of water used, compensating those who use less of this priceless resource. Finally, this should be supported by campaigns to raise awareness and a reliable feedback system. In this regard, initiatives to promote green buildings and provide incentives for doing so will be essential. Additionally, emphasis should be put on recycling sewage water as well as collecting rainwater. In order to collect rainwater, bio-roofs and green pavements need to be incorporated in addition to rooftop rainwater gathering.

Table 5 Initial decision matrix

Questionnaire number	Municipality	Academia	Industry
1	3.433333333	3.6	3.133333333
2	3.692307692	3.307692308	3.846153846
5	3.1	1.5	2.6
6	3.4	4.4	5.4
10	2.3	3.1	4.3
11	2.15	3.1	4.7
12	2.3	3.3	4.3
13	4.15	2	2
17	4.3	2.4	1.86
18	1.75	2.75	3.75
19	4	3.384615385	3.769230769
20	3.384615385	3.538461538	3.923076923
22	3.461538462	3.615384615	4
25	3.538461538	3.615384615	4.076923077
26	3.615384615	3.615384615	4
27	3.538461538	3.615384615	3.846153846
8	3.461538462	3.538461538	3.692307692
9	3.615384615	3.538461538	3.769230769
16	1.84	2.175	2.005
20	3.31	2	2.75
21	3.769230769	3.615384615	3.615384615
3	3.923076923	3.692307692	3.769230769
4	4	3.615384615	3.846153846
7	4.076923077	3.538461538	3.846153846
14	4	3.384615385	3.769230769
15	3.846153846	3.384615385	3.692307692
Max	4.3	4.4	5.4
Min	1.75	1.5	1.86

5 Future Scope

As the technologies are emerging, the effectiveness of OCRA method of ranking in urban planning will increase. The advancement of artificial intelligence, integrating data analytic and other technology may boost the urban planning. In the future, the concept of smart cities can be implemented, where the basic focus is to digitalize the society. The use of renewable energy like solar energy and wind energy will be a key factor for urban planning. The future generation should not only plan to develop

Table 6 Operational matrix

	Municipality	Academia	Industry	Sum IK	Sum Ok
1	1.218637993	0.317428571	0.462	0.779428571	0.402150538
2	0.835401158	0.366263736	0.397692308	0.763956044	0.275682382
5	1.505376344	0.254571429	0	0.254571429	0.496774194
6	0	0.311142857	0.638	0.949142857	0
10	0.591397849	0.103714286	0.352	0.455714286	0.19516129
11	0.376344086	0.075428571	0.352	0.427428571	0.124193548
12	0.591397849	0.103714286	0.396	0.499714286	0.19516129
13	1.827956989	0.452571429	0.11	0.562571429	0.603225806
17	1.903225806	0.480857143	0.198	0.678857143	0.628064516
18	0.887096774	0	0.275	0.275	0.292741935
19	0.876757651	0.424285714	0.414615385	0.838901099	0.289330025
20	0.794044665	0.308241758	0.448461538	0.756703297	0.262034739
22	0.752688172	0.322747253	0.465384615	0.788131868	0.248387097
25	0.711331679	0.337252747	0.465384615	0.802637362	0.234739454
26	0.752688172	0.351758242	0.465384615	0.817142857	0.248387097
27	0.835401158	0.337252747	0.465384615	0.802637362	0.275682382
8	0.918114144	0.322747253	0.448461538	0.771208791	0.302977668
9	0.876757651	0.351758242	0.448461538	0.80021978	0.289330025
16	1.825268817	0.016971429	0.1485	0.165471429	0.60233871
20	1.424731183	0.294171429	0.11	0.404171429	0.47016129
21	0.959470637	0.380769231	0.465384615	0.846153846	0.31662531
3	0.876757651	0.40978022	0.482307692	0.892087912	0.289330025
4	0.835401158	0.424285714	0.465384615	0.88967033	0.275682382
7	0.835401158	0.438791209	0.448461538	0.887252747	0.275682382
14	0.876757651	0.424285714	0.414615385	0.838901099	0.289330025
15	0.918114144	0.395274725	0.414615385	0.80989011	0.302977668
			Min	0.165471429	0

the energy sources but also focus on making them cost-effective. Proper utilization of open space with prioritize factor can be a boost to urban planning.

6 Conclusion

Social, economic and environmental well being are essential conditions for every city's survival. However, if the approaches and efforts for development are not clear, it will fail. In order to make the sustainable urban regeneration planning successful,

Table 7 Operational competitiveness rating analysis method

	IK	OK	Sum (IK + OK)	Difference	Rank
1	**0.613957142**	**0.402150538**	**1.01610768**	**0.629956989**	**2**
2	0.598484615	0.275682382	0.874166997	0.488016306	16
5	0.0891	0.496774194	0.585874193	0.199723502	22
6	0.783671428	0	0.783671428	0.397520737	19
10	0.290242857	0.19516129	0.485404147	0.099253456	24
11	0.261957142	0.124193548	0.386150691	-1.84332E-10	25
12	0.334242857	0.19516129	0.529404147	0.143253456	23
13	**0.3971**	**0.603225806**	**1.000325806**	**0.614175115**	**3**
17	**0.513385714**	**0.628064516**	**1.14145023**	**0.755299539**	**1**
18	0.109528571	0.292741935	0.402270506	0.016119815	24
19	0.67342967	0.289330025	0.962759695	0.576609004	9
20	0.591231868	0.262034739	0.853266607	0.467115916	18
22	0.622660439	0.248387097	0.871047536	0.484896845	15
25	0.637165933	0.234739454	0.871905388	0.485754697	17
26	0.651671428	0.248387097	0.900058525	0.513907834	14
27	0.637165933	0.275682382	0.912848316	0.526697625	12
8	0.605737362	0.302977668	0.90871503	0.522564339	13
9	0.634748351	0.289330025	0.924078376	0.537927685	11
16	-4.28571E-10	0.60233871	0.602338709	0.216188018	21
20	0.2387	0.47016129	0.70886129	0.322710599	20
21	0.680682417	0.31662531	0.997307727	0.611157036	7
3	**0.726616483**	**0.289330025**	**1.015946508**	**0.629795817**	**4**
4	0.724198901	0.275682382	0.999881283	0.613730592	5
7	0.721781318	0.275682382	0.9974637	0.611313009	6
14	0.67342967	0.289330025	0.962759695	0.576609004	8
15	0.644418681	0.302977668	0.947396348	0.561245657	10
		Min	0.386150691		

we have chosen 27 numbers of standard questionnaire to analyze the challenges. As a result of the study, use of solar/wind power is the top priority, hospital facilities and health support ranked 2nd, low-scale business facilities ranked 3rd and public transport facilities ranked 4th. This means that the use of solar/wind power is suppose to the top priority of the sustainable urban regeneration planning of Odisha.

India is experiencing rapid urbanization, yet the strain on the government has increased due to issues like the large population, resource deficit, scale and condition of planning, stakeholder non-participation, etc. Given the severity of the issues, realistic and people-centered solutions are required. Other than solar/wind power, hospital facilities and health support, low-scale business facilities and public transport

facilities are also the priority. All partiesinvolvedcitizens, policymakers, designers, planners, activists, administrators, politicians, etc., should be aware of their respective roles in ensuring the future of our species.

References

1. URBACT II (2015) Sustainable regeneration in urban areas: URBACT. https://urbact.eu/sites/default/files/04_sustreg-web.pdf
2. Boussaa D (2014) Urban heritage and tourism in the gulf: the case of Dubai in the UAE. J Tour Hosp Manag 2(4):174–181
3. Ricca S (2018) Urban heritage in the Arabian Peninsula, the experiences of Jeddah and Dubai. Built Herit 2:108–122
4. Reynard E, Pica A, Coratza P (2017) Urban geomorphological heritage: an overview. Quest Geogr 36(3):122
5. Jena D, Satapathy S, Das MR (2024) A study on sustainable agri business challenges: as per Indian prospective. In: Sahoo S, Yedla N (eds) Recent advances in mechanical engineering. ICRAMERD 2023. Lecture notes in mechanical engineering. Springer, Singapore. https://doi.org/10.1007/978-981-97-1080-5_62
6. Parkan C, Wu ML (1997) On the equivalence of operational performance measurement and multiple attribute decision making. Int J Prod Res 35(11):2963–88

Design and Development of an IoT-Enabled Ergonomic Material Handling Equipment for Effective Inventory Management



M. Rajesh, Arpitha, Kruthi, Sanskruti, and Trisha Nair

Abstract This technical paper presents the design and development of a state-of-the-art Material Handling Equipment (MHE) system for efficient inventory management in industrial settings. The MHE system is designed using a comprehensive approach, encompassing ergonomic considerations and IoT-based automation. The initial stages of the MHE design involve iterative brainstorming sessions to create a rough sketch, followed by data collection to determine dimensions and ergonomic requirements. Ergonomic standards, including clearances and worker-friendly design, are adhered to throughout the design process. The study also explores into the integration of IoT technology into the MHE system. IoT components, including sensors, microcontrollers, and Wi-Fi modules, are employed to automate various tasks. An IR sensor detects the presence of items on the conveyor belt, initiating its motion. Load cells beneath bins collect weight data, which is transmitted for real-time inventory tracking and the system is driven by an Arduino microcontroller. In conclusion, this paper presents a holistic approach to designing and integrating an IoT-enabled MHE system for industrial inventory management. The resulting system enhances efficiency, accuracy, and ease of use, making it a valuable asset for modern industrial operations.

Keywords Smart material handling equipment · Inventory management · Computer vision · Internet of Things (IoT) · Automation in manufacturing

1 Introduction

In the era of the fourth industrial revolution, marked by rapid technological advancements such as automation, artificial intelligence, and advanced robotics, human labor remains central to many industries, particularly in manual material handling tasks

M. Rajesh (✉) · Arpitha · Kruthi · Sanskruti · T. Nair
Ramaiah Institute of Technology, Bengaluru, India
e-mail: mrajeshiem@msrit.edu

© The Author(s), under exclusive license to Springer Nature Singapore Pte Ltd. 2025

B. B. V. L. Deepak et al. (eds.), *Recent Advancements in Product Design and Manufacturing Systems*, Lecture Notes in Mechanical Engineering,
https://doi.org/10.1007/978-981-97-6732-8_48

[1, 2]. This paper investigates into the work undertaken at a glass partition assembling company specializing in manufacturing glass walls, movable partitions, hall units, and acoustic solutions. The company faced substantial challenges in inventory management, primarily stemming from manual data entry into software systems. This manual process introduced a significant margin for human error, resulting in mishandled secondary inventory, lost parts, and inaccurate inventory records.

To address these critical issues, the decision was made to design and fabricate a smart Material Handling Equipment system tailored for inventory management purposes [3]. The primary objectives of this study were as follows:

- Develop a material handling equipment system that adheres to ergonomic principles, reducing the physical strain on workers.
- Incorporate Internet of Things (IoT) and computer vision techniques to enable the material handling equipment to function as a virtual storekeeper.
- Enhance inventory management processes to reduce errors, improve accuracy, and prevent the mishandling of inventory items.

1.1 Material Handling Equipment and IoT

Material Handling Equipment, commonly abbreviated as MHE, refers to mechanical systems employed for the movement, storage, control, and protection of materials and products throughout various stages, including manufacturing, distribution, consumption, and disposal [3]. IoT enables the seamless connection of web-enabled smart devices, equipped with embedded systems like processors and sensors, which collect, transmit, and act upon data acquired from their surroundings [4]. In this context, these devices facilitate data collection, analysis, and automation.

The study places a significant emphasis on ergonomic design, ensuring that the MHE aligns with the needs of the workers, ultimately boosting efficiency, productivity, and reducing discomfort. Previously, manual inventory counting and data entry led to errors in data management. To overcome this, computer vision techniques were employed. Computer vision is a multidisciplinary field that deals with the automation of tasks typically performed by the human visual system, such as counting inventory items. Computer vision encompasses acquiring, processing, analyzing, and comprehending digital images. It aids in automatically updating the company's inventory by visually counting and recognizing parts through images [5]. By automating these processes using Material Handling Equipment incorporated with sensors, human intervention is minimized, thus reducing errors.

2 Literature

Ergonomic considerations play a pivotal role in material handling operations across various industries, encompassing construction, manufacturing, and services. Several studies have demonstrated the benefits of ergonomic interventions, including reduced worker symptoms and enhanced safety records [6]. Manual material handling, a well-documented risk factor for low back pain, underscores the importance of ergonomic approaches in mitigating workplace health issues [7]. In the realm of agriculture, ergonomic interventions have shown their effectiveness in the cotton industry. These interventions led to the development of a cost-effective smart cotton module tracking system, which monitored the movement of harvested cotton. This innovation not only increased overall efficiency but also reduced damage during handling, highlighting the positive impact of ergonomic solutions [8].

The advent of the Internet of Things (IoT) has ushered in a new era of human–machine interactions, particularly in smart manufacturing environments [9]. IoT, characterized by extensive connectivity among industrial devices via advanced communication technologies, offers unprecedented opportunities for enhancing various facets of internal and external logistics. These opportunities include improvements in efficiency, sustainability, and responsiveness to customer demands [10]. The ability to access real-time information through an integrated network of industrial assets has proven highly advantageous for professionals [3]. The design of material handling equipment is contingent on carefully selected material parameters, as they significantly influence comfort and overall stability [11]. To stay competitive, many companies are implementing lean philosophies, such as world-class manufacturing. This integration of Industry 4.0 technologies and world-class manufacturing principles not only reduces waste and costs but also improves ergonomic and efficiency aspects within the workplace [12]. In light of these findings, it becomes evident that ergonomic considerations are pivotal in optimizing material handling operations. The adoption of smart technologies, such as IoT, presents new opportunities for improving efficiency, safety, and overall workplace performance. By integrating these technologies and ergonomic principles, industries can enhance their competitiveness and reduce the physical strain on workers, ultimately fostering a more productive and sustainable work environment.

3 Design Methodology

The work commenced with preliminary phases of preparatory work, during which the team familiarized themselves with the industry. Several critical issues were identified within the factory, with the most significant ones being:

- Lack of proper organization of inventory, resulting in frequent missing items.
- Inefficient layout planning with no dedicated spaces for finished goods or metal waste, leading to workflow disruptions and workplace injuries.

- Absence of standardized processes, leading to multiple manual errors in material handling and manual assembly.

The company also expressed concerns regarding their productivity, particularly in areas such as lead time for assembly, quality management, and inventory management. After careful consideration, the primary problem area chosen for the study was inventory management. This was further investigated through an analysis of existing literature and direct observation. Although the factory already utilized an MHE for transporting some primary inventory products, shop floor workers were reluctant to use it, often opting to carry inventory by hand. This led to frequent instances of mishandling, resulting in dropped pieces and inaccuracies in inventory data. Mislabeling and improper storage of items further compounded the problem, affecting organization and product quality. Additionally, mishandling contributed to workplace injuries, including cuts from sharp metal and glass edges. Based on observations and the literature review, the work was structured to address the identified problems by leveraging the capabilities of the MHE. The MHE would serve as a central point for secondary inventory products, reducing the need for human intervention in inventory handling and data recording. The fabrication of the Smart MHE encompassed two critical components, namely design component and technical component.

The design component deals with ergonomic design and mechanical analysis were essential for the MHE. The design aimed to facilitate smooth material movement, including loading and unloading, while incorporating technological components in a manner that did not obstruct shop floor workers. Initially, there was consideration of mounting a camera near the handle to capture images, but it was realized that this approach had limitations, such as potential obstruction of the view or angle by the worker's hand and lower accuracy due to the high speed of material loading. Consequently, the design was modified to capture images after the material was loaded into the MHE. Ergonomic design played a crucial role in accommodating users while safeguarding electrical components.

In technical component, the automated system within the MHE relied on Computer Vision (CV) technology to capture images of incoming products placed on the equipment. These images were then segmented into corresponding inventory items using clustering models. The segmented products were subsequently updated in the inventory database. This information could be used to establish an effective database for the company or integrate with their existing inventory management software. The distinct shapes and colors of the products facilitated accurate segmentation. The MHE was also equipped with sensors and a conveyor system to enhance accuracy and prevent miscounts. Hence, the development of a smart MHE promised to address mishandling issues (e.g., dropped items) and reduce human errors associated with inventory management, ultimately boosting worker productivity, reducing assembly downtime, and simplifying lower management tasks.

3.1 Ergonomic Design of MHE

The design and analysis of the Material Handling Equipment (MHE) followed a structured process. Ergonomic considerations played a vital role in this process. The initial stages involved creating rough sketches of the MHE while considering various creative designs and ergonomic factors. This phase was iterative and aimed to conceptualize the MHE's form and functionality. The next step was to collect data on the factory space, specifically measuring the dimensions between racks and pallets to account for the largest and smallest spaces. This data, combined with standard ergonomic clearances, provided rough dimensions for the MHE. Based on the collected data, an initial 3D model of the MHE was created, and mechanical analysis was conducted to validate the model's structural integrity.

Ergonomic principles played a crucial role in designing the MHE. The design aimed to meet workers' needs and reduce fatigue and discomfort. Several ergonomic considerations were taken into account to reduce the need for workers to repeatedly access inventory, and the MHE was designed with adequate storage volume to carry all items at once. The design addressed the issue of items frequently falling on the floor, requiring workers to bend down. Proper dimensions were considered to prevent worker fatigue and mishandling. Based on these criteria, the MHE design was tailored to meet workers' needs with features such as brakes, grippers, wheel motion, height, and other dimensions adhering to standard ergonomic guidelines. Standard ergonomic clearances were determined based on Kodak's Ergonomic Design for People at Work [13]. These clearances included minimum ground clearance, clearance from both sides, handle height from the ground, aisle width, maximum load for a 4-wheel hand cart, minimum aisle width for a 4-wheel hand cart, and maximum distance for a 4-wheel hand cart. The design process underwent multiple iterations, with modifications made at each stage to arrive at the final design.

Eventually, the height of the handle from the ground was set at 1000 mm, length and breadth of the trolley were determined based on the narrowest pathway in the factory workspace (1300 mm). Additional clearance of 245 mm was added on each side to allow for easy turning. A conveyor belt was integrated into the design to enhance image processing. The length of the conveyor belt (386 mm) was determined through trial and error, ensuring optimal item motion. A front box at the end of the conveyor belt provided storage space. Boxes for small items, like screws, were placed at the two corners of the MHE to facilitate item separation and easy access. Adequate access was provided to power sources and circuitry by designing an access avenue along the back wall. Connection of the legs of the MHE was introduced to provide additional strength and storage space.

The dimensions of various components, such as the handle, trolley, conveyor belt, bottom tray, and bins, were determined through careful consideration of ergonomic needs. The final design was created with aluminum as the chosen material due to its lightweight, durability, flexibility, and corrosion resistance. This design aimed to optimize functionality and meet the needs of workers in the factory. The conceptual 3D drawing is presented in Fig. 1.



Fig. 1 3D drawing of MHE

4 Design and Integration of Image Processing

Data collection for image processing within the Material Handling Equipment (MHE) involved the use of a wireless camera positioned atop the MHE's extrusion. This process seamlessly combined two primary stages: Image Capture and Database Update. To initiate image capture, the software tool Sobolsoft was employed. Sobolsoft ensured that the camera captured images at regular intervals, saving them in a designated folder. The initiation of image capture could be triggered either by the IoT system or set to activate automatically when the computer system started up. This approach not only guaranteed timely image capture but also offered control to production and inventory managers.

The subsequent phase entrusted a neural network program with the responsibility of processing the captured images. This program continuously monitored the designated folder for the addition of new images. Upon detecting a new image, the program fed it to the neural network, which classified the item based on the trained dataset. Upon recognition, the program updated the inventory database by decrementing the count associated with the detected class (as the item was removed from inventory). The process concluded by printing a message confirming the successful completion of the database update task. In cases where no changes were observed in the monitored folder, the program waited for one second and then recommenced the monitoring process. The mechanism employed to identify changes within the folder and detect newly added files was based on timestamp tracking and file name comparisons.

5 Design for Integration of Internet of Things

The automation process within the IoT-enabled ergonomic material handling equipment for efficient inventory management was a two-phase operation. Firstly, it involved the IR sensor and conveyor belt, which worked in tandem to detect items on the conveyor belt and automatically activate the motor, eliminating the need for manual intervention, and streamlining the material handling process. The second phase encompassed load cell data processing and inventory updates. Positioned under the bins, the load cells collected weight data for items in the bins. This data was then efficiently processed through an Arduino and swiftly transmitted to a computer. Subsequently, the data was intelligently categorized based on standard weights, facilitating real-time inventory updates. These meticulously integrated technologies collectively empowered industrial settings with efficient and automated material handling and inventory management capabilities.

The essential IoT components employed in the study, including jumper cables, resistors, diodes, an IR sensor, a DC motor, an L293 driver, a piezoelectric load cell, an HX711 driver, an Arduino Pro Mini, a perf board, and an ESP8266 Wi-Fi Module, formed the foundation of the IoT-enabled ergonomic material handling equipment designed to optimize inventory management. The IR sensor detected objects on the conveyor belt, while the DC motor propelled the belt. The L293 driver ensured precise motor control, and the piezoelectric load cell accurately measured applied force. The ESP8266 Wi-Fi Module facilitated seamless data transmission to a computer, resulting in a sophisticated IoT network. The process of motor selection underscoring the significance of choosing the appropriate motor speed to capture high-quality images of items on the conveyor belt. After rigorous experimentation, a 30 rpm DC motor was identified as the most suitable choice for this application, ensuring optimal performance and clear image capture. The automation process unfolded in two distinct phases. The first phase relied on the IR sensor to detect objects on the conveyor belt, triggering the motor via the driver without the need for manual intervention. The second phase focused on gathering weight data from load sensors under the bins and processing it through an Arduino. This process involved key stages such as connection, authentication, communication, and termination, with data publication and organization into topics. Once the data reached a computer, it served to update the inventory.

6 Results

The fabrication of the Smart Material Handling Equipment (MHE) has been successfully completed, resulting in a functional prototype. Figure 2 showcases the final fabricated MHE, highlighting its physical appearance and readiness for operation.

The integration of various components enables the MHE to automate the operation of the conveyor belt and provides valuable data through load cells placed under the



Fig. 2 Fabricated IoT-enabled material handling equipment

bins to measure the weight of screws. While it is important to note that the IR sensor's performance may be slightly slower compared to manual control, this automation eliminates the need for manual activation, enhancing efficiency. This automation, combined with image processing, only requires the computer system to be turned on at the beginning of the workday for inventory updates to commence. The updated inventory data, available in CSV format, can be used directly or as input for the company's existing inventory management system.

The image processing model was trained using 315 pictures, including 105 pictures of three different objects each, to recognize edges and shapes accurately. Once trained, the computer can identify images with a certain percentage of accuracy. This recognition is depicted in Fig. 3, which show edge detection results for a test object.

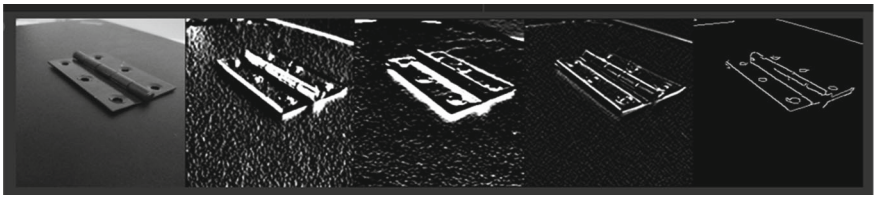


Fig. 3 Edge detection for rectangular hinge

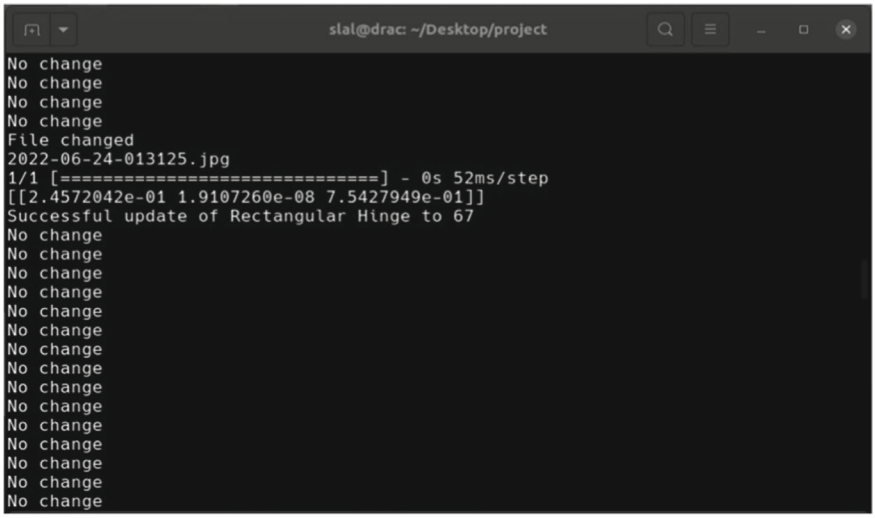


Fig. 4 Final inventory updatation

When an image is captured, the model matches it against the sample images used during training and calculates the probability of it belonging to a particular sample, displaying the name of the sample with the highest probability. If no match is found, it reflects "No change" and concurrently updates the Excel file, maintaining a record of inventory changes as shown in Fig. 4.

7 Conclusion

The objective of designing and developing a Smart Material Handling Equipment (MHE) to address the inventory management challenges faced by the manufacturing industry has been successfully accomplished by creating a specialized trolley for material handling and integrating computer vision and the Internet of Things (IoT) technologies. The MHE has been designed with careful consideration of ergonomic factors, including dimensions, weight, ease of movement, proper grips, and braking mechanisms, to minimize physical strain on workers. The trolley is equipped with a camera that facilitates image detection and utilizes computer vision techniques. To achieve this, a neural network model was developed and trained to compare images and update inventory data. This innovation has significantly reduced the need for manual inventory updating, resulting in fewer errors. The trolley also incorporates technologies such as IR sensors, which detect when items are placed on the conveyor, signaling the motor to begin operation. Additionally, weight sensors positioned beneath bins on the sides of the trolley detect and update the weights of objects, especially items with similar dimensions, such as various types of screws.

This feature assists workers in maintaining an accurate count of items prone to misplacement. The trolley includes a compartment at the end for convenient storage of items needed for a particular order. In summary, the trolley leverages IoT and computer vision technologies to provide a comprehensive solution, encompassing material storage, handling, automation, and error reduction. It significantly reduces the physical exertion required by workers for handling secondary inventory items while also enhancing inventory accuracy. However, the model is to be trained with large datasets to be improve its accuracy.

References

1. Azizi A, Yazdi G, Poorya S, Al-Humairi A (2018) Design and fabrication of intelligent material handling systems in manufacturing with industry 4.0 approaches. Int Robot Automat J 4:121
2. Cronin C, Awasthi A, Conway A, O'Riordan D, Walsh J (2020) Design and development of a material handling system for an autonomous intelligent vehicle for flexible manufacturing. Proced Manuf 51:493–500. https://doi.org/10.1016/j.promfg.2020.10.069
3. Javaid M, Haleem A, Singh R, Rab S, Suman R (2021) Upgrading the manufacturing sector via applications of industrial Internet of Things (IIoT). Sens Int 2:100129. https://doi.org/10.1016/j.sintl.2021.100129
4. Calzavara M, Glock C, Grosse E, Persona A (2016) Sgarbossa F (2016) Analysis of economic and ergonomic performance measures of different rack layouts in an order picking warehouse. Comput Ind Eng 111:1. https://doi.org/10.1016/j.cie.2016.07.001
5. Deng J, Dong W, Socher R, Li LJ, Li K, Fei-Fei L (2009) ImageNet: a large-scale hierarchical image database and usefulness of ImageNet through recognition, classification and clustering. https://doi.org/10.1109/CVPR.2009.5206848
6. Wurzelbacher SJ, Lampl MP, Bertke SJ, Tseng C (2020) The effectiveness of ergonomic interventions in material handling operations. Appl Ergon 87:103139. https://doi.org/10.1016/j.apergo.2020.103139
7. Skals S, Bláfoss R, Andersen L, Andersen M, de Zee M (2020) Manual material handling in the supermarket sector. Part 2: knee, spine and shoulder joint reaction forces. Appl Ergon 92:103345. https://doi.org/10.1016/j.apergo.2020.103345
8. Wang T, Robert V, Ward J, Wanjura J, Barnes E (2022) A smart cotton module tracking and monitoring system for handling logistics and cover damage. Comput Electr Agricult 193:106620. https://doi.org/10.1016/j.compag.2021.106620
9. Lyu M, Li X, Chen C-H (2022) Achieving knowledge-as-a-service in IIoT-driven smart manufacturing: a crowdsourcing-based continuous enrichment method for industrial knowledge graph. Adv Eng Inform 51:101494. https://doi.org/10.1016/j.aei.2021.101494
10. Cimini C, Lagorio A, Romero D, Cavalieri S, Stahre J (2020) Smart logistics and the logistics operator 4.0. IFAC PapersOnLine 53(2):10615–10620
11. Cupar A, Kaljun J, Dolsak B, Harih G (2021) 3D printed deformable product handle material for improved ergonomics. Int J Ind Ergon 82:1–7. https://doi.org/10.1016/j.ergon.2020.103080
12. Ciccarelli M, Papetti A, Cappelletti F, Brunzini A, Germani M (2022) Combining world class manufacturing system and industry 4.0 technologies to design ergonomic manufacturing equipment. Int J Interact Des Manufact 16:832
13. ASM International (2001) Aluminium and aluminium alloys. In: Alloying: understanding the basics J.R. Davis, pp 351–416. https://doi.org/10.1361/autb2001p351

Journeying with Peace of Mind: Reinventing Luggage Safety for Land Explorers



Prasanna Prakash Halbe and Nitin Hadap

Abstract Traveling is a fundamental part of our lives, as we embark on journeys for various reasons such as exploring new cultures, learning, relaxation, and business. The choice of transportation, whether by road, water, or air, depends on the specific journey's context. Regardless of the mode of travel, carrying luggage is always necessary, and we use a range of equipment, including suitcases, handbags, and backpacks. Ensuring the safety and security of our luggage is of utmost importance during our travels. While air travel has received significant attention in terms of safety and security measures, it is equally crucial to address the safety and security of luggage for passengers traveling by buses and trains. This paper highlights the need to provide safety and security solutions for travelers using bus and train transport. To address this issue, researchers conducted surveys through online questionnaires, interviews, and on-site visits. The survey results revealed that bus and train travelers need solutions to enhance the safety and security of their luggage. After identifying the problem and gathering data from various sources, researchers propose a simple, cost-effective, and sustainable design solution based on IoT principles, utilizing the A9G GSM GPRS Board. With this newly designed and affordable device, travelers can continue using their existing luggage-carrying equipment, increasing its durability and contributing to their personal and overall sustainability. This research primarily focuses on budget-friendly solutions for enhancing the safety and security of luggage-carrying equipment. However, it opens the door for exploring more advanced, high-tech solutions in the future.

Keywords IoT · AI · IoT applications · Suitcases · Train/bus travelers' suitcases · Safety security

P. P. Halbe (✉) · N. Hadap
Symbiosis Institute of Design, Symbiosis International (Deemed University), Pune, India
e-mail: prasanna.halbe@sid.edu.in

N. Hadap
e-mail: nitin.hadap@sid.edu.in

© The Author(s), under exclusive license to Springer Nature Singapore Pte Ltd. 2025

B. B. V. L. Deepak et al. (eds.), *Recent Advancements in Product Design and Manufacturing Systems*, Lecture Notes in Mechanical Engineering,
https://doi.org/10.1007/978-981-97-6732-8_49

1 Introduction

The Internet of Things (IoT) has become part of our everyday lives. Consciously or casually, we all utilize Internet of Things, from mobiles to automobiles. This presence of new technology has helped us to make choices and make decisions faster. One area where IoT has a significant impact is the realm of travel, from planning and scheduling to reaching the destination as per itinerary—an important area where IoT can be used is to ensure the safety and security of the passenger's luggage.

In the current market scenario, IoT application is visible in the context of travel in a broader sense as follows.

1. IoT is used for tracking and locating the misplaced luggage [1].
2. By using GPS tracking mechanism and AI algorithms, suitcases are tracked for real-time location [2].
3. Additionally, smart suitcases use machine learning techniques to analyze the history of their travel locations [3].
4. Due to the availability of AI technology, suitcases have become hands-free, and they can follow the user wherever necessary [3].
5. By using biometric authentication along with AI, suitcases get further level of security [4].

India has one of the most extensive railway networks in the world. It serves as a lifeline for the country. As per the statistical summary of Indian Railways [5], 3519 million of the Indian population travels by rail-roads, whereas only 123.2 million passengers use air travel [6]. It means only 3.5% of travelers are using air travel mode.

The train journey facilitates the movement of millions of passengers and their luggage across the country, spanning thousands of kilometers [5]. The train/bus travelers are mostly not from the affluent class and hence get categorized under the bottom of the social pyramid.

Every year, thousands of suitcases are stolen, lost, and left-behind suitcases during the train journey. The number of left-behind suitcases was 25,966 during 2021–22 [5]. This number itself explains the requirement of a device to track and locate the suitcase as well as the owner of the suitcase.

2 Literature Review

The majority of luggage safety and tracking research has primarily focused on the realm of air travel, leaving limited exploration of the safety and security concerns pertaining to train and bus travel. This imbalance in research attention raises a crucial question, particularly in the context of India's lower- and middle-class populations, as introduced by Prahalad through the 'Bottom of the Pyramid' (BoP) concept [7].

Existing studies have offered various innovative solutions to address luggage tracking and security concerns in the domain of air travel. Researchers like Gupta

[8] have investigated real-time luggage tracking through wearable microcontroller devices with wireless communication capabilities, emphasizing their energy efficiency. Similarly, Santosh Krishna B. V. proposed a wristband system communicating with RFID tags embedded in luggage, culminating in an effective airport luggage tracking system [9].

Issues associated with commonly used luggage gadgets, such as power consumption, positioning, and portability, have been examined by Chaturvedi, who suggested the utilization of a microcontroller wireless system integrated with a GSM module placed within luggage for navigation data [10].

Other researchers, including Wong et al. have explored the use of Radio Frequency Identification (RFID) tags in luggage handling systems and delved into the potential of the Internet of Things (IoT) for the development of reusable luggage tags, enhancing luggage tracking accuracy [11].

In addition, studies like Du's work proposed solutions involving short-range wireless Bluetooth technology and advanced positioning algorithms, leading to the creation of an intelligent baggage tracking system that combines phone guidance, automatic tracking, and alarm reporting [12].

Ghazal introduced an intelligent system enabling real-time luggage tracking through mobile applications and smartwatches, relying on Kalman-filtered Wi-Fi fingerprints from active tags [13].

Furthermore, Rouchdi implemented a luggage tracking system that utilized RFID technology, which showcased through the BAGTRAC application. This system emphasized robust authentication and highlighted the positive impacts of RFID on the airline industry [14].

In addressing the significant issue of daily luggage loss at airports worldwide, Ludeiro et al. introduced a novel approach by suggesting the implementation of blockchain technology for efficient luggage tracking [15].

Ajami addressed the concern of abandoned luggage within an intelligent video surveillance system [16].

Khattab offered the Airport Luggage Tracker System (ALTS), which successfully utilized Arduino UNO, RFID technology, and a website application to improve luggage tracking reliability [17].

Wong and Wong presented a sustainable framework involving the use of reusable RFID tags in airport luggage handling systems, providing luggage owners with real-time status updates on their mobile phones [11].

Shobayo's system relied on the GSM communication system to facilitate real-time luggage tracking, enabling owners to access their luggage's location through a smartphone. This approach aimed to reduce the frustration associated with luggage theft or loss during air travel [18].

Jagadheeswaran's innovative intelligent suitcase incorporated facial recognition technology for enhanced security, alerting the owner via email if unauthorized access was attempted [19]. However, this system had its limitations.

Farooq et al. introduced a prototype that utilized an Arduino Uno microcontroller, a load cell, and a GPS module to track luggage in real time and monitor its weight via a mobile phone, addressing both tracking and security concerns [20].

Li's study emphasized the importance of intelligent design principles, ergonomic features, Bluetooth and IoT-based devices, and a GPRS Master Control device integrated into suitcases [21, 22]. This research recognized the growing number of travelers and their evolving needs.

Despite these advances in luggage tracking technology, the existing body of literature predominantly focuses on applications within air travel, often overlooking the unique challenges presented by train and bus travel. This research paper aims to bridge this gap by providing an alternative perspective on technology utilization to enhance luggage safety and security for these modes of travel, contributing to a more comprehensive understanding of this critical issue.

Based on the comprehensive literature review, the following key conclusions can be drawn:

1. The majority of innovative luggage tracking methods explored in the literature are primarily tailored for airport systems and the specific needs of air travelers, creating a notable gap in addressing the distinct requirements of train and bus passengers.
2. These existing tracking systems are often intricate and not easily adaptable for use by train and bus travelers, given the varying constraints and operational differences of these modes of transportation.
3. The technology proposed in the reviewed studies typically demands frequent recharging of tracking units, necessitating their secure placement inside luggage, and often relies on a range of sensors for location monitoring, which may not be practical or cost-effective for all travelers.
4. Among the technology solutions examined, a clear distinction can be made between active systems, which require regular charging of the tracking unit within the luggage, and passive systems, which primarily consist of passive components like RFID tags, offering different trade-offs in terms of cost and convenience.
5. The findings underscore the pressing need for the development of affordable and versatile solutions tailored to meet the diverse requirements of train and bus passengers, addressing the unique challenges posed by these modes of travel and ensuring a practical and accessible approach to luggage safety and security.

3 Methodology

A systematic survey was conducted with population of frequent train/bus travelers from diverse cities in Maharashtra to identify the problem of safety and security of their luggage equipment. The results are interesting and reveal the direction for further work.

The researchers have segregated the flowchart in the journey to go in depth in this direction. The following are the interfaces where the security and safety of the luggage are a concern (Fig. 1).

1. Starting from home to arrive at the railway station,

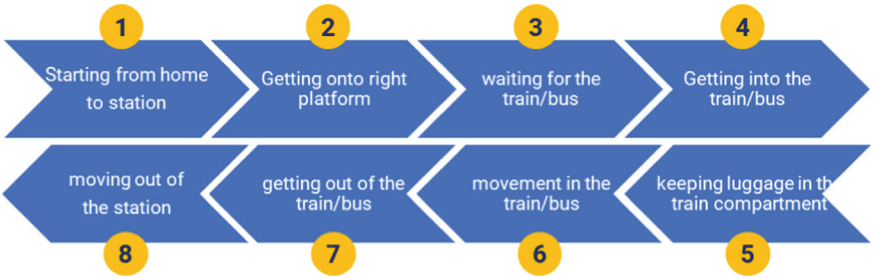


Fig. 1 Flowchart of the luggage movement with the passenger

2. Getting onto the right platform,
3. Waiting for the train,
4. Getting into the train,
5. Keeping the luggage in the train compartment while the journey is on,
6. Movement in the train (while traveling),
7. Getting out of the train when the destination arrives,
8. Move out of the station with the luggage.

4 Research Findings

The survey focused on the challenges faced by travelers during train and bus journeys, with responses from 65 out of 100 respondents, resulting in a population of 65. The surveyed population comprised 84.6% males and 15.4% females.

Figure 2 reveals that private cars (67.2%) are the preferred mode of travel in urban India, followed by train/bus travel (53.1%). Even the economically disadvantaged BoP population demonstrated a preference for bus travel. Travel choices were largely influenced by the journey's distance, with the upper middle class and upper class favoring private cars and air travel (45.3%). This study focuses on addressing the needs of trains/buses and bus travelers.

The survey results show that the primary purpose of travel is visiting friends and family (53.8%), followed by leisure travel (47.7%). Business travel accounted for 38.5% of the responses, whereas 21.5% traveled for other reasons.

Regarding luggage, approximately 69.2% of respondents carried two pieces, 18.5% carried one, and 15.4% carried three, with a small fraction (6.2%) carrying more than three pieces. On average, the respondents carried two pieces of luggage (34.36%).

The respondents' luggage preferences included suitcases (67.7%), backpacks (66.2%), duffel bags (26.2%), and other types (12.3%).

Figure 3 illustrates the factors considered when selecting luggage-carrying equipment. Safety and security (38.5%) were paramount, whereas portability and ease of

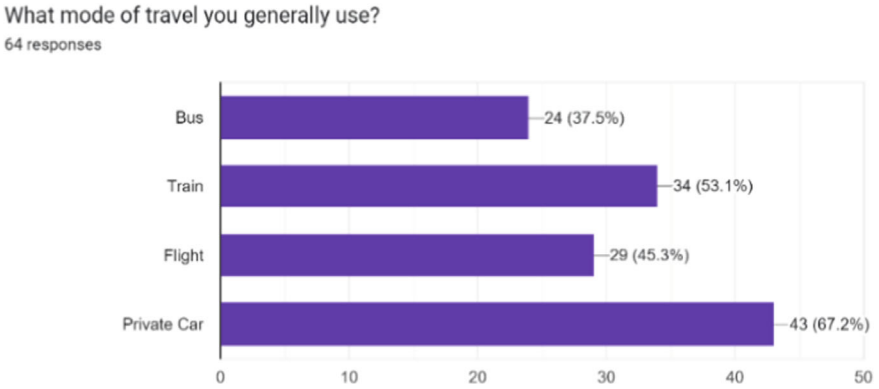


Fig. 2 Distribution of travel mode preferences

use were other crucial factors. A significant portion (27%) carefully evaluated the equipment based on all parameters.

Figure 4 highlights the concerns regarding luggage security during the train/bus journeys. Respondents employed various security measures, such as using padlocks, luggage straps, chains, and cables; keeping valuables in separate pouches; and using small bags as pillows.

Common problems faced by travelers include luggage tampering, theft, misplacement or loss, severe damage, and anxiety over luggage during night journeys, as frequently mentioned by the respondents.

The survey results indicate a need for more luggage storage space within train/bus compartments and stations, with 61.5% of respondents expressing this concern.

A significant proportion (53.8%) of travelers are willing to invest in an affordable and reliable solution for luggage safety and security, suggesting a pressing need for such a device to address these issues.

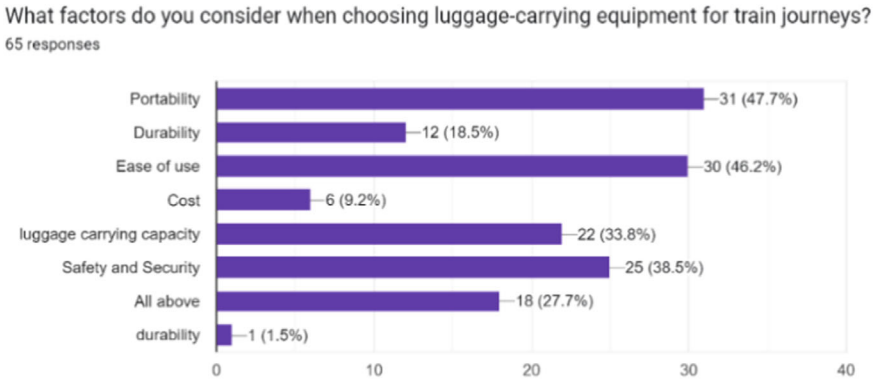


Fig. 3 Factors considered while choosing luggage-carrying equipment for train/bus journey

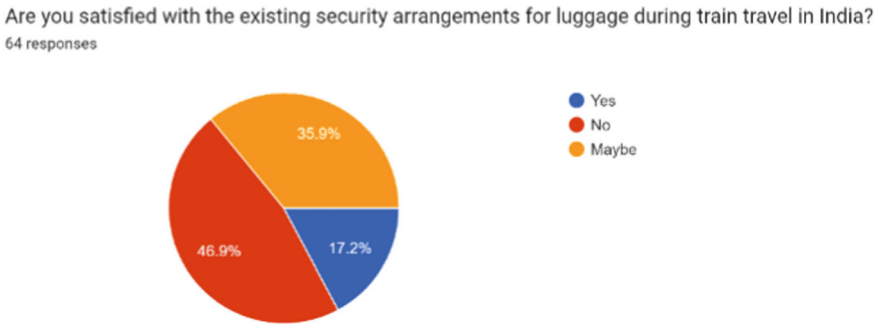


Fig. 4 Level of satisfaction with the existing security arrangements for luggage during train/s/bus travels in India

The survey underscores the importance of raising awareness among travelers regarding technological advancements in luggage safety and security. Such solutions may still be in the early developmental stages but should become readily available in India (Fig. 5).

The concept of 'smart luggage', which offers features such as mobile app connectivity, remote control, tracking, weight monitoring, and device charging, requires more awareness among 76.9% of respondents.

As indicated in Fig. 6, considerable 87.7% of the respondents are open to paying extra for a device that can be integrated into their existing luggage equipment, provided it remains affordable, aligning with the focus on IoT applications for the economically disadvantaged. The indicated price range for these devices was Rs. 200–500 (42.9% of respondents), Rs. 500–1000 (44.4%), and Rs. 1000–2000 (12.7%).

The survey findings affirm the validity of the identified problem and hypothesis, emphasizing the need for innovative technological solutions to enhance luggage

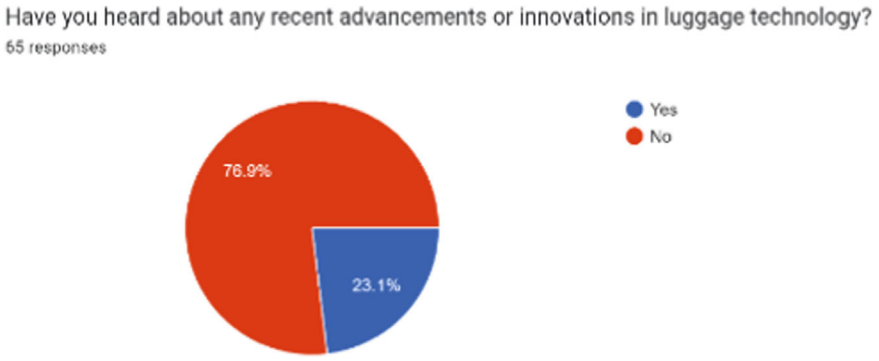


Fig. 5 Awareness about technological innovations in luggage technology

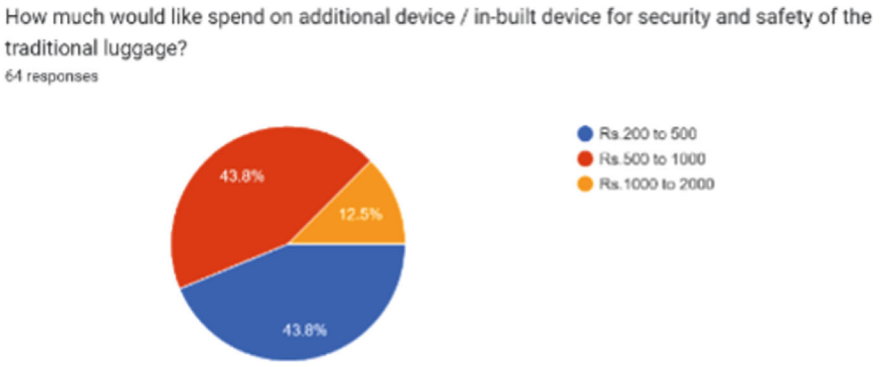


Fig. 6 Readiness to shell out extra money for safety and security of the luggage

safety. The data analysis further indicates that travelers are eager to adopt an affordable solution when it becomes available.

5 Design Solution

This survey clarified the need for an IoT-based solution in this sector. People in almost all age groups use mobile handsets during bus or train/bus travel and belong to the BoP category. Therefore, we propose a tried and tested [23, 24] design solution based on the A9G GSM GPRS Tracker board and accessories.

The A9G GPS Tracker represents an Internet of Things (IoT) solution that incorporates an ATSAMD21G18 microcontroller, a GRRS/GSM + GPS module (A9G), and advanced power management and storage capabilities. The A9G Module is ideally suited for real IoT projects, including applications such as smart homes, outdoor monitoring, long-distance monitoring, and GPS tracking. It can be powered by a 3.7 V Lithium-Ion Battery, as it operates within the voltage range of 3.5–4.2 V, with a typical supply voltage of 4.0 V. The power consumption of this module is very low and varies from 1.03 to 1.14 mA, depending on the specific application. A 2G sim card was used to send and receive messages from the unit [25].

The A9G Board allows to connect GSM and GPS antenna, battery, and a pre-soldered XIAO ESP32C3 board to allow us to charge the battery by using the 'C' type charger. The A9G unit requires programming, which can be performed either through the Arduino Pro Mini or the Arduino Nano [23]. This can also be done through a universal TTL auto-programmer [25].

After programming and inserting a 2G Sim Card inside the A9G Board, we started communicating with the board. We can call the board on the desired mobile phone or send an SMS and the GPS location of the board to the desired mobile phone. We also programmed it in such a way that allows us to send the SMS to determine the GPS location of the unit.

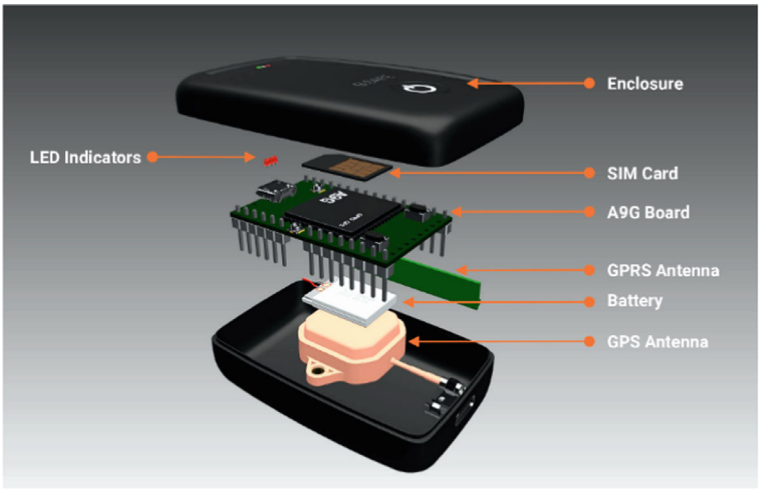


Fig. 7 Assembly of components used in the **B.SAFE** unit

These are the electronics and hardware parts of the unit proposed in the solution. Next, we discuss the design aspect of the unit.

We created a compact enclosure that fits the components (assembly shown in Fig. 7) and allows us to program the unit as well as charge the battery through the 'C' type USB charging port. The case top cover can be opened to insert the SIM Card.

The device depicted in Figs. 8 and 9 measures 55 mm × 95 mm × 25 mm and can be used as needed during travel. It is made from injection-molded polypropylene/ABS and can be made available in attractive colors. The device features an LED that lights up after communication is established between the unit and the customer's mobile phone.

According to Table 1, the indicative cost of the unit is Rs. 1687/-. Consequently, the estimated price that the customer will have to pay is Rs. 1800/-. This is an affordable and sustainable option as it can be used with any suitcase or bag that one carries while traveling.

6 Discussion, Suggestion, and Conclusion

The Internet of Things (IoT) has been integrated into our lives in various ways. IoT is a game in which every product manufacturer or service provider strives to win by utilizing it to their advantage. A literature review revealed numerous applications of the IoT for enhancing the safety and security of luggage, particularly smart suitcases, during air travel. Researchers have proposed using the A9G GSM/GPRS-GPS

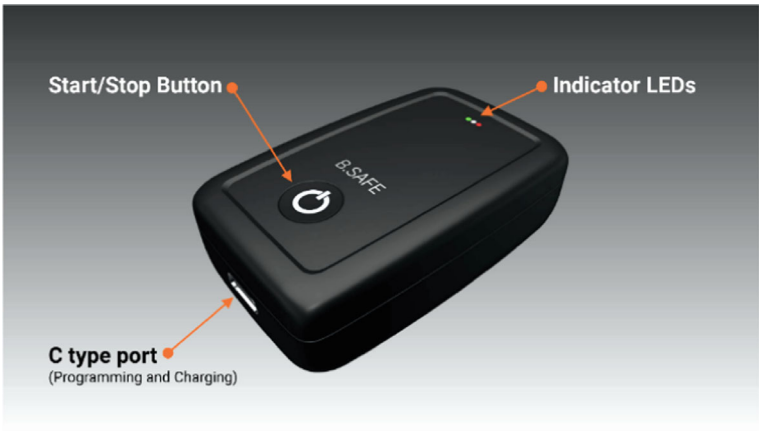


Fig. 8 **B.SAFE** enclosure design with details



Fig. 9 Various views of **B.SAFE** device

Board in a compact, chargeable device called B. SAFE, which can track its location on demand. This innovation also entails the creation of a mobile app that can communicate with SAFE.

Considering the large population of train and bus travelers in India, researchers have aimed to identify the essential requirements of train and bus travelers regarding the safety and security of their luggage. A survey was conducted in the urban areas of Maharashtra, which yielded the following insights.

Table 1 Cost-price figures

No	Component	Quantity	Indicative cost (Rs)
1	Ai Thinker A9G GSM/GPRS + GPS/BDS Development Board × 1	1	759/-
2	2G Sim Card	1	
3	Battery 401,522 3.7v 300mAh	1	145/-
4	Pre-soldered Seeed Studio XIAO ESP32C3	1	415
5	GSM Antenna	1	48/-
6	GPS Antenna	1	220/-
7	Enclosure with branding	1	100/-
Total indicative cost			1687/-
Tentative price (to the customer)			1800/-

1. There is a dire need for enhanced safety and security of luggage in train and bus stations as well as during the journey.
2. Travelers often face issues such as luggage loss, theft, and tampering and require assistance to address these problems.
3. Travelers were willing to pay a premium for the safety and security of their luggage, as indicated in the three price bands.
4. The current study highlights the potential of developing an affordable solution using AI to ensure the safety and security of train and bus travelers' luggage.
5. The Design Solution proposed in this study holds significant potential for the further development and marketing of such devices.

7 Limitations

The limitations of the proposed solution are as follows:

1. The battery capacity is limited, and it can support up to 8–10 h when operating in low-voltage mode. A higher-capacity battery can be used to extend the support time; however, this increases the cost of the unit.
2. The SAFE unit requires a mobile network to achieve effective performance. Mobile networks are widely available in urban areas; however, rural and remote areas may not support them.
3. The unit operates on a 2G mobile network, but support for this facility may not be available to all mobile service providers, and the support for 2G networks is expected to decline. Therefore, a new unit that supports 4G and 5G mobile networks must be designed.

Acknowledgements This paper is part of an ongoing yearlong project awarded by Symbiosis International (Deemed University) under the scheme of Minor Research Project in 2023–24.

Declarations

Conflict of Interest The authors declare that there is no conflict of interest with this research.

References

1. Sivathanu Kumar B, Aravindraj A, Sakthi Priya TA, Nihanth S, Bharati D, Mohankumar N (2023) A machine learning model for predictive maintenance of a stepper motor using digital simulation data. Presented at the. https://doi.org/10.1007/978-981-19-7874-6_5
2. Monti G, Corchia L, De Benedetto E, Tarricone L (2016) Wearable logo-antenna for GPS–GSM-based tracking systems. IET Microw Antennas Propag 10:1332–1338. https://doi.org/10.1049/iet-map.2015.0774
3. Yang CS, Zhang BH, Wei HW, Lee WT (2019) The design of smart suitcase. In: 2019 IEEE international conference on consumer electronics—Taiwan (ICCE-TW). IEEE, pp 1–2 https://doi.org/10.1109/ICCE-TW46550.2019.8991728
4. Kumar A, Manikandan R, Thaventhiran C (2020) Pattern recognition concepts. In: Machine learning and big data. pp 131–152. https://doi.org/10.1002/9781119654834.ch6
5. Ministry of Railways (2022) Govt. of I.: Indian Railways Annual Report & Accounts 2021–22
6. Ministry of Civil Aviation (2022) Govt. of I.: Annual Report | 2022. pp 10–10
7. Prahalad CK (2010) The fortune at the bottom of the pyramid : eradicating poverty through profits. Revised and updated fifth anniversary edition. Upper Saddle River, N.J. : Wharton School Pub., [2010] ©2010
8. Gupta V, Kumar R, Mishra RG, Semwal A, Siwach S (2017) Design and optimization of luggage tracking system on airport. Presented at the (2017). https://doi.org/10.1007/978-981-10-1708-7_97
9. Santhosh Krishna BV, Kamatchi S, Prithisree S, Indira P (2015) An efficient luggage tracking system in airport by RFID tag (Bracelet). Int J Appl Eng Res. 10:8614–8617
10. Chaturvedi R, Darji K, Mahajan A, Varghese M (2018) Real time airport luggage tracking system. In: 2018 international conference on smart city and emerging technology (ICSCET). pp 1–5, IEEE https://doi.org/10.1109/ICSCET.2018.8537255
11. Wong E, Wong W (2016) The development of reusable luggage tag with the internet of things for mobile tracking and environmental sustainability. Sustainability 9:58. https://doi.org/10.3390/su9010058
12. Du MJ (2019) Study for the intelligent luggage tracking system based on near field bluetooth technology. In: 2019 6th international conference on systems and informatics (ICSAI). IEEE, pp 660–664. https://doi.org/10.1109/ICSAI48974.2019.9010429
13. Ghazal M, Ali S, Haneefa F, Sweleh A (2016) Towards smart wearable real-time airport luggage tracking. In 2016 international conference on industrial informatics and computer systems (CIICS). IEEE, pp 1–6, https://doi.org/10.1109/ICCSII.2016.7462422
14. Rouchdi Y, Haibi A, El Yassini K, Boulmalf M, Oufaska K (2018) RFID application to airport luggage tracking as a green logistics approach. In: 2018 IEEE 5th international congress on information science and technology (CiSt), IEEE, pp 642–649 (2018). https://doi.org/10.1109/CIST.2018.8596629.
15. Ludeiro AR (2019) Blockchain Technology for Luggage Tracking. Presented at the https://doi.org/10.1007/978-3-319-99608-0_63
16. Ajami M, Lang B (2016) Using RGB-D sensors for the detection of unattended luggage. Presented at the Sept
17. Khattab O, Almetlaqem A, Almutairi D, Alnaser M, Almutairi M (2021) Prototype of new reliable airport luggage tracker system. Int J Emerg Technol Adv Eng. 11:42–47. https://doi.org/10.46338/ijetae0821_06

18. Shobayo O, Olajube A, Okoyeigbo O, Ogbonna J. (2021) Design and implementation of an IoT based baggage tracking system. Presented at the https://doi.org/10.1007/978-3-030-69143-1_47
19. Jagadheeswaran R, Arjunan R, Balamurugan N, Ramya E (2020) Luggage theft identification and smart lock using face recognition. In: 2020 6th international conference on advanced computing and communication systems (ICACCS), IEEE, pp 302–305. https://doi.org/10.1109/ICACCS48705.2020.9074452.
20. Farooq MH, Zain M, Khalid MB, Zafar S (2021) Easy-weigh-out: design and implementation of internet of things-based smart luggage system. Int J Online Biomed Eng 17:37. https://doi.org/10.3991/ijoe.v17i03.17165
21. Li Y, Li Y, Li B, Lu H, Serikawa S (2016) Anti-lost luggage reminder system using electrically conductive fiber antenna tag. In: 2016 international symposium on computer, consumer and control (IS3C), IEEE, pp 26–29 https://doi.org/10.1109/IS3C.2016.17
22. Li Y (2019) The design research of intelligent suitcase. Presented at the
23. Debashis Das: Build a low power sms based vehicle tracking system with A9G GSM+GPS Module and Arduino, https://circuitdigest.com/microcontroller-projects/a9g-based-gps-tracker-with-arduino, Accessed 02 Nov 2023
24. Howto Electronics: GPS Tracker using A9G GPRS/GPS Module & Arduino, https://how2electronics.com/gps-tracker-using-a9g-gprs-gps-module-arduino/, Accessed 02 Nov 2023
25. TechieSMS: Getting Started with A9G Board | GSM + GPRS + GPS, https://www.youtube.com/watch?v=Yi5dgZBiq7g, Accessed 02 Nov 2023

Design Challenges and Solutions to Create Toys with Reference to Sawantwadi Wooden Toy Manufacturing



Omkar Sadashiv Rane, Sudeep Ray, and Suyash Khaneja

Abstract The earliest physical evidence of toys in India was found from the Indus Valley Civilization. All the found toys are made from natural materials such as clay, bamboo, wood, and sticks. One of the traditional toy-making communities existed in Sawantwadi, Maharashtra. They make toys out of wood and turning/rotary methods are used to manufacture toys, which is manual and human-centric. However, currently, the application of advanced technology and mechanisms has stimulated the toy manufacturing industry. Side by side, there is the availability of industrial materials, which established challenges for traditional toy makers to compete in the present market. There are two significant gaps found in the traditional toy makers: Insufficient supply or availability of products in the market and the mindset of the parents to purchase toys for their children. The research aims to understand the deciding factors of choosing/buying toys and further exploration of the mass manufacturing methods through advanced mechanisms. The respondents for the research are the parents. Important data is collected through mixed methodology using interview and questionnaire methods. Finally, end of the research, a batch of toys will be developed for further observation to evaluate the research hypothesis.

Keywords Toy manufacturing · Toy design · Wooden toys · Traditional toys · Domestic toy production

O. S. Rane (✉) · S. Ray
Symbiosis Institute of Design, Symbiosis International (Deemed University), Pune, Maharashtra, India
e-mail: omkar.rane@sid.edu.in

O. S. Rane · S. Khaneja
School of Business, World University of Design, Sonipat, Haryana, India

© The Author(s), under exclusive license to Springer Nature Singapore Pte Ltd. 2025

B. B. V. L. Deepak et al. (eds.), *Recent Advancements in Product Design and Manufacturing Systems*, Lecture Notes in Mechanical Engineering,
https://doi.org/10.1007/978-981-97-6732-8_50

1 Introduction

India has a great history of indigenous toys made from ancient times when any potential naturally and locally available material was found to be transformed into a toy [1]. The evidence of toys un-earthed from the Indus Valley Civilization was mostly made out of fire baked clay generally known as terracotta. Later, wood became one of the most facilitative materials for creating toys. Since then, India evolved a long way into toy manufacturing business [2]. Traditional wooden toys are mostly hand-crafted. Therefore, mass manufacturing was never a major concern for providing to different classes in society [3].

The availability of industrial materials like plastic, resin, silicon, rubber, and soft fiber has become dominant in the toy industry. The current market contains low-cost, mass-produced plastic toys, rapidly replacing locally made wooden toys [2]. Several other factors influence the toy industry to replace wooden toys. The customers may be inclined to purchase the available items to fulfill their needs. Most parents and kids prefer these toys due to the cost, variety available, colors, lightweight, sound-making, and other factors. Mass-produced toys popularized among the customers [3].

Plastic toys are made in bulk in manufacturing units. However, the negative aspects of industrial materials cause massive negative impacts on the environment [3]. Research found the toxic materials used in the manufacturing of toys, which is extremely harmful for the health of the children [4]. Comparatively, wooden toys are eco-friendly and sustainable since they have a minimum environmental impact and consume significantly less energy while manufactured [3]. Locally produced wooden toys are non-toxic and do not affect kids' health adversely [5].

The deciding factors for buying toys are dependent on the parents. It is also very important to understand the views of the parents, and what makes them purchase a particular toy for their kid/kids. The survey indicates multiple reasons to buy such items according to the age of the kid. These factors are encouraging to look upon the revival of the domestic toy industry as well as for the environment.

1.1 Background of Toys in India

'Play' is the natural form of exploring the world and learning new things. Kids interact with their surroundings through touch, feeling, listening, and seeing everything by themselves because everything is unique and pulls them toward learning more about it. Kids learn about their lives through interaction and discover things they've never known before [6]. Gabriel Guyton states, 'Play is the mechanism by which children learn how they experience their world, practice new skills, and internalize new ideas and is therefore the essential work of children' [7]. Toys function as a 'mediator' between the natural environment and the child's cognition. Every child view the world differently, hence each child's mind contains a distinctive view of the universe.

A child's cognitive and physical growth is related to the environment that the child grows in. Thus, toys used during the formative years of kids play a significant role in supporting kids' growth. It is essential to provide cheerful toys to kids where toys create connections, memories, and stories and a safer space for the child to look back [8].

1.2 Indian Traditional Wooden Toys

India has a rich tradition of colorful handicrafts and indigenous designs. Wooden toys made using locally available materials are one of the handicrafts practiced in various regions of the country. Those toys depict local cultures, countries' history, and emotions through motifs and intricate designs. These toys are linked traditionally with religion, education, art for amusement, and play [2]. Wooden toys have their specialty, like animal figures, fruits, replicas, or idols of deities. Sawantwadi in Maharashtra, Varanasi in Uttar Pradesh, and Channpatna in Karnataka are prominent names in the wooden toy-making industry. Locally available wood is being used while making crafts. Preferred woods are preferably between soft to moderate hard, which is comparatively easy to carve and durable [9]. Artisans use tools like hand lathes, chisels, jigsaws, etc., for wood processing. Many of them perform manufacturing manually, from cutting and chiseling to coloring. Naturally available lac is used to color toys. Then, for polishing, the 'kevada' leaf is used. This whole process is performed manually through locally available materials [10].

1.3 Challenges for Wooden Toys

Wooden toys are in danger because plastic toys are taking over the market. After much effort, artisans are not respected and valued for their hard work. The cost of raw materials is increasing, but the prices that artisans are getting for their products are constant [2]. Considering this, artisans started iterating new design possibilities based on current trends [10]. Even after that, artisans are not able to compete with mass-produced toys imported from foreign countries, specifically from China, at low cost.

The Chinese market also started massively producing similar wooden toys using low-quality materials, making them cheaper. Due to low-quality materials, they are not durable. Even after much innovation, we can differentiate them from wooden toys made locally in Indian crafts clusters like Sawantwadi [11]. Locally produced wooden toys were globally famous for their indigenous concepts, but the scenario is changing because of the rapidly growing toy manufacturing business [12].

1.4 Industrial Toys and Environment

Available toys are mostly made using industrial materials like silicon, synthetic fibers, and plastic. Those toys come with a wide variety and look more attractive and shinier. However, a considerable amount of plastic usage threatens the life of human beings. Plastic is made artificially by using fossil fuels that are non-recyclable or have a low level of recyclability. It comes with a plastic footprint of around 60 kg CO_2 per kg. Dumping, composting, and recycling of plastic creates a large carbon footprint [13]. It contains toxic substances like Nickel (Ni), Cadmium (Cd), Arsenic (As), Lead (Pb), etc., in the form of pigments or stabilizers and microplastics [14]. These substances harm the environment and enter kids' bloodstreams while handling, playing, chewing, or licking the toy [3]. Inhaling plastic is one of the rising concerns [13]. It affects the human nervous and immune system [3].

1.5 Wooden Toys and Environment

Wooden toys are eco-friendly and come from renewable resources. As mentioned earlier, locally made toys are non-toxic and consume less energy in manufacturing than synthetic toys [3]. Wood is contributing to reducing carbon emissions. It is more energy efficient than metal and plastic [15]. Wood leaves hardly minimal residue in the form of sawdust. It can be a source of energy [13]. Artisans from Sawantwadi have tried to make products by using sawdust, which is innovative and more robust than actual wood [11]. Wood is safe, healthy, and inspiring for kids; hence, the Montessori and Waldorf teaching methods strongly favor toy-making using natural lumber [16]. The use of wooden toys in an open-ended and unstructured manner will help kids to imagine and become more creative [17]. Similar studies indicated that touching wood with a palm reduces prefrontal brain activity and increases parasympathetic nerve activity. Consequently, physiological relaxation is induced [18]. At the age of receiving constructive inputs from various resources, wooden toys proved to be very beneficial for their physical and cognitive development. It allows productivity and helps to focus better [19]. When the market is overflowing with flashy plastic toys with lights and sounds, it affects the power of kids' imagination and thinking. Also, it causes indecision in kids. Here, a natural and peaceful environment created by quiet toys helps kids make their play easier and control it [20] (Fig. 1).

1.6 Traditional Toy Manufacturing Methods

The traditional methods of manufacturing are human-centric. Sawantwadi wooden toys are constructed by assembling natural form solid wood logs. Weathered mango wood is lathed into the desired shape of a toy. Each piece goes through multiple



Fig. 1 Practiced wooden toys manufacturing technique (Wood turning) [9]

processes, such as sanding, painting, assembling, and finishing. Every toy is manually painted with natural pigment colors and varnished, making them bright, vibrant, and long-lasting. Generally, women artisans are involved in painting and finishing the product. Painted articles are assembled with the help of delicate joinery to make one piece of toy. It takes a couple of days to make a toy. Except sanding and drilling are all steps of making a single piece of toy, which are done manually [21].

1.7 Objective

This paper aims to understand the views of parent's perspectives and preferences toward toys and materials and the availability of the items in the stores. It also aims to understand how manufacturing could match enough productivity to supply the demand of the current market as well as to carry the essence of hand-crafted products.

2 Methods and Materials

Gathering basic demographic details about the respondents, which provides important context for their responses, with a focus on wooden toys, their availability, and parents' preferences. This section provides structures options for the respondents to choose from allowing for quantitative analysis of their preferences and awareness. The open-ended questions are aimed at capturing detailed and nuanced responses from the respondents regarding the criteria of preferences. Qualitative data helps in understanding perceptions and experiences in-depth. The questionnaire design is structured and intended to receive on-the-spot responses from the respondents. It is essential to ensure that the questions align with the research objectives to gather relevant data.

2.1 Questionnaire Design

The entire questionnaire is designed in a structured manner, including quantitative and qualitative questions to understand the awareness and preferences. The questionnaire contained five personal information and ten multiple-choice questions related to wooden toys, preferences to buy for the children, and three qualitative questions to read the mind of the parents. To gain a better understanding of the topic, data was gathered using questionnaires distributed via Google Surveys. To achieve the goals, the collected data had to be reviewed and interpreted; interpretative, open-ended, and conversational discussion with the participants were required, which meant acquiring an increasing amount of qualitative data.

2.2 Target Respondents

In order to gather basic information about their children and learn more about their awareness of wooden toys, a structured questionnaire consisting of approximately ten multiple-choice questions was given to 37 parents whose children were under six years old. Later, they provided qualitative data via semi-structured telephone interviews. Six wood toy manufacturing companies were contacted via email and social media. Three of them were interviewed over the phone using semi-structured questions. To get insight, five local stores of wooden toys were visited. An in-depth understanding of the craft and input from traditional craftsmen were sought by visiting Sawantwadi. Additionally, five experienced toy manufacturers were interviewed and the local market renowned for its wooden toys was visited (Table 1).

Table 1 Topics discussed

Participants	Topics
Toys manufacturers	1. Market trends and competition in the wooden toy industry
	2. Materials and manufacturing methods for toys
	3. Toy categories and the creative ideas behind their development to date
Parents	1. Awareness about wooden toys
	2. Choices: Colors, brands, materials, and technology
	3. Ways of getting toys
	4. Factors that affect decision-making

2.3 Data Collection

The data collected was analyzed using a variety of qualitative methodologies. The information from the subjects was first made more accessible to understand through the use of discourse analysis. Later, collected data was organized into themes for thematic analysis. The topic data is segregated into two categories. Subsidiary themes were derived from the first category, and content analysis was performed on the second category of data. Similar data from two different sources/stakeholders was analyzed using comparison analysis. The information was entered and coded into an Excel spreadsheet before being manually analyzed.

2.4 Analysis of Collected Data

The received data is manually examined. All qualitative data are organized in an Excel spreadsheet and analyzed using summative statistics. The strategy was chosen to compare the most important keywords in the material and evaluate the context. The observation approach is used to understand the children's likes and preferences.

3 Result

The insights obtained from the questionnaire are presented in the following sections.

According to the survey, 91% of respondents felt that toys are vital and contribute to children's growth. Only a few of them do not believe toys are an essential element of childhood (Fig. 2).

76% of participants have wooden toys at home that they purchased for their children, whereas 24% do not (Fig. 3).

The replies of the children's age groups and their parents to other questions on the questionnaire were evaluated together. It was subsequently observed that children

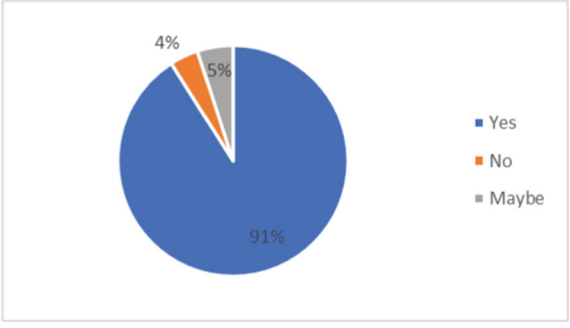


Fig. 2 Participants' opinion on importance of toys

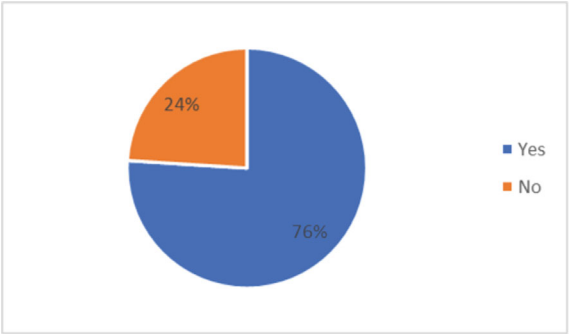


Fig. 3 Participants' answer on wooden toys at home

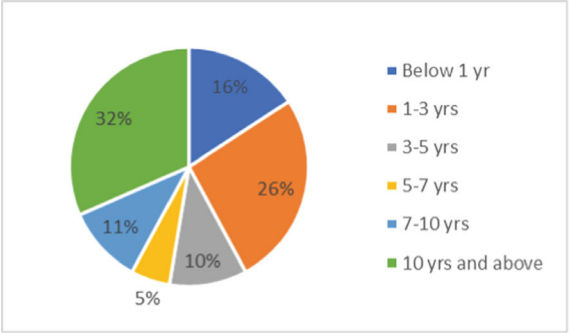


Fig. 4 Participants' answer on children's age group

under the age of ten are more likely to own and interact with wooden toys. There is also a greater range of wooden toys for this age group. It was also discovered that children over the age of ten have a limited selection of wooden toys with which to play, resulting in less interaction with wooden toys (Fig. 4).

It has been noted that when purchasing toys for their kids, the majority of parents don't focus on certain brands. Most of the time, only a few numbers have a list of reliable brands to choose from. It was also discovered that parents prioritize quality above brand. They are more concerned with their children's health and the value of toys than with purchasing certain brands (Fig. 5).

The data demonstrates that parents are steadily migrating to internet shopping for toys, though not entirely. They like to physically inspect and handle the item to confirm its safety and quality for their child. It was also discovered that parents who mostly purchase/explore toys offline only owned a few wooden toys. They are unaware of traditional Indian toys. They also need a better understanding of current toys and play methods. They have yet to open themselves to the present toy world (Fig. 6).

It was noted that the majority of parents were aware with traditional Indian toys. However, they did not view them as playthings for kids to use; rather, they saw them as exhibit pieces. They could identify with them as travel mementos associated with

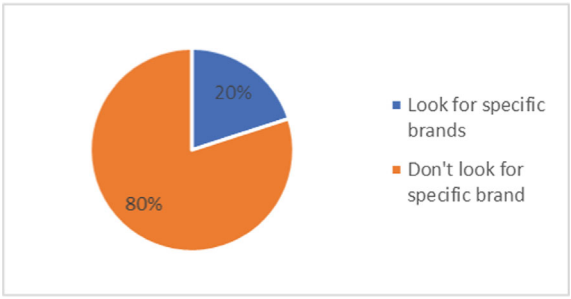


Fig. 5 Participants' opinion on Brand preference

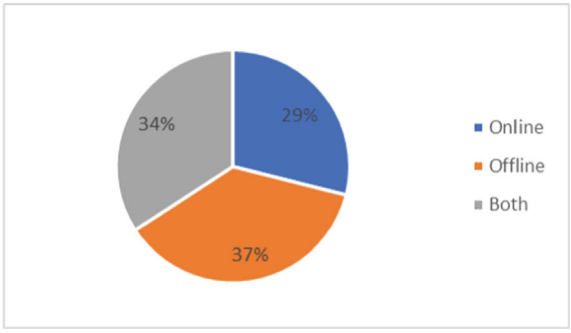


Fig. 6 Participants' mode of preference to buy toys

specific locations. Since they are not commonly available, the majority of them do not own them. Some offline shoppers were unaware of traditional toys (Fig. 7).

When asked which type of play practices they preferred for their child—traditional or modern—equal numbers of parents selected both. Some of them, however, believed that these two approaches ought to be integrated for their children's better development. It is important to remember that they considered and decided on this on their own—they weren't given this option (Fig. 8).

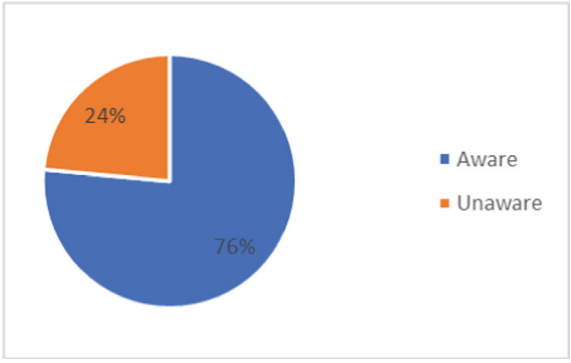


Fig. 7 Participants' awareness about traditional toys

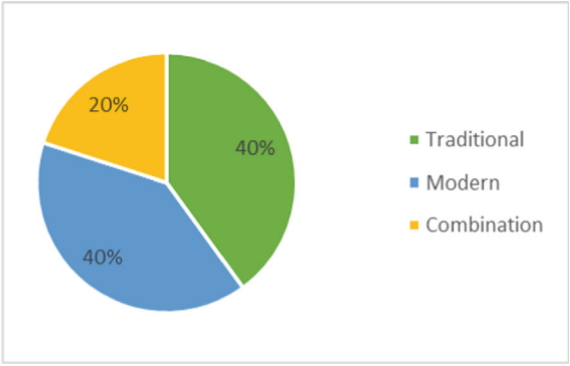


Fig. 8 Participants' preference of toys

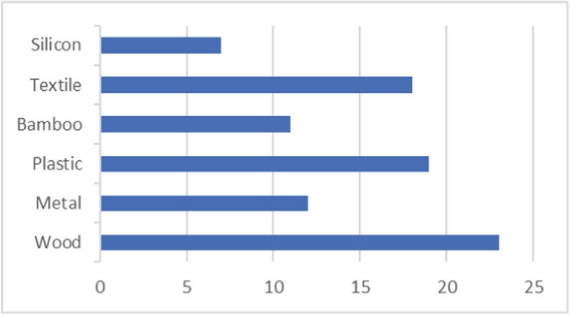


Fig. 9 Participants' material preference on safe toys material

According to the chart's (Fig. 9) results, the majority of parents chose wood as the safest material to use for their children's toys. Wooden toys are safe, according to some, but if edible plastic or fiber is more appealing and lighter than wooden toys, they'll choose it. A few others brought up silicon, but they rejected it themselves because of its drawbacks and expense. When asked why they believe wood is safer than most other materials, they provided a variety of responses. Common features include rounded edges, a lack of small or sharp pieces, the use of natural and non-toxic colors, the eco-friendliness of wood, its suitability for teething babies, and its lack of poisonous ingredients.

4 Discussions

The information gathered through parents' and artisans' interviews and surveys was segregated into the following categories for further discussion.

4.1 Types of Wooden Toys

Parents frequently mentioned puzzles, wooden rattles, shape sorters, cars, and pull-along toys when asked what toys they kept for their children at home. This means most parents only had a limited selection of wooden toys. A subset of the target population that was more educated, qualified, or connected to the online world looked into newer wooden toys.

4.2 Influence of Media

When asked about the media's influence on children and their toy-purchasing decisions, the responses were unanimous. Media is affecting the choices and thinking of the kids. Children connect them with media and become acquainted with characters, environments, and colors. This prompts individuals to purchase familiar items they have seen on screen.

4.3 Parents' Childhood Play Methods

The parents were asked about their childhood games and toys, and we got many common answers that bring nostalgia. Most of the participants used to make their own toys using locally available material that they could find around themselves. Shells, match sticks, stones, bangle pieces, mud, wooden pieces, dry fruit coverings, tree branches, and leaves were used to make indoor and outdoor games and played with them. Since many open spaces and playgrounds were available, they spent more time playing games with peers. A relaxed environment and freedom were the major elements that helped them grow.

4.4 Benefits of Traditional Play Methods

The benefits of the traditional play method have their points because it promotes open and accessible movements to children in open spaces with their peers where they can learn, explore their environment and nature, and boost immunity. Tradition toys require very little investment. Practically, there is zero investment. Traditional toys encourage imagination and creativity through unstructured and open-ended games made by using them. Also, it helps to keep our traditions alive.

4.5 Benefits of Modern Play Methods

Participants who preferred modern toys more said trendy toys are made by doing a lot of research and applying creativity. These toys are more relatable and relevant for a new generation because they use technology and familiar characters, which is helpful to teach children joyfully. Hence, children can learn quickly. It also improves patience and helps in the mental development of kids.

4.6 Challenges of Human-Centric Manufacturing

Human-centric manufacturing of toys is the integrated part of wooden toys, and it can be also described as the essence of hand-made toys, but as far as mass manufacturing as concern, it is difficult to cater the large number of consumers. Therefore, it is inevitable to switch to modern technology for faster production. The method of manufacturing must be emerging from cottage industry to industrial product keeping the human touch in each piece of toys.

4.7 Comparative Analysis

The perspectives and opinions of several stakeholders (parents and wooden toy brands) were compared;

1. View number 1

Parents: Wooden toys are expensive, so we choose plastic toys since they offer a wider range and are inexpensive to buy.

Toy manufacturers: Manpower, labor, raw materials, and skill are the requirements of woodworking. It is a highly intricate process. Plastics are junk since they are made of harmful materials and only provide temporary joy. Wooden toys will last longer. There is a cost to getting value.

2. View number 2

Parents: Plastics are shiny and appealing to children; they enjoy bright colors.

Manufacturers: Plastics, although appealing, are not safe. Wooden toys can be beautiful if they are safely painted and not too flashy. They are natural and peaceful. Plastics that are visually appealing have face value but nothing to learn.

3. View number 3

Parents: Modern toys are more intelligent and advanced in technology, preparing children for the future.

Manufacturers: Noises, whistles, bells, and other electrical elements satisfy the child without requiring them to engage their minds. Battery-powered devices, too

many options, and stimulation confuse and indecisive children while confining them in specific ways that provide little space for thought.

5 Conclusion

The conclusion derived from the conversation provides an overview of customer perceptions about wooden toys. Additionally, manufacturers and artisans discussed their challenges and the state of affairs at the moment.

Wooden toys making industry holds a significant place in India's cultural heritage. The Indian wooden toy industry has experienced remarkable growth, evolving from traditional, locally made toys and traditional games to embracing a diverse range of materials, adhering to international toy standards, and exporting both traditional and modern toys.

However, synthetic, mass-produced toys have gradually overtaken the Indian toy market, leaving traditional wooden toys behind. Traditional wooden toys struggle to maintain their presence, while plastic toys mimic their traditional designs. It is important to note that wooden toys offer numerous health benefits for children and are also environmentally friendly.

Insights from interviews and surveys with parents indicate that,

1. Despite the fact that secondary research indicates that traditional toys are meeting modern standards, the majority of Indian parents either don't prefer or purchase traditional toys for their children.
2. While most parents understand that wood is the safe and eco-friendly material, they often view wooden toys to exhibit, displays as handicrafts rather than toys.
3. Wooden toys must overcome various constraints to reach the Indian parent market.
4. Major variables driving the shift from traditional to modern play methods include globalization, lifestyle changes, synthetic materials, increased awareness, psychological considerations, and restrictions.

Furthermore, the points mentioned provide valuable insights and observations regarding Indian parents' preferences and perceptions of traditional wooden toys.

When comparing the advantages of traditional and modern toys, it becomes clear that both have their unique benefits. Combining the strengths of both can contribute to a child's holistic development while also promoting traditional Indian toys. It is interesting to note that many parents themselves grew up playing with toys made of natural materials, yet they provide plastic toys to their own children because they are more readily available.

References

1. Yadav CS (2020) Incredible "Handmade in India" toys on the brink of extinction. Int J Dis Recov Bus Contin 11:561–571
2. Aggarwal PK, Rao RV, Joshi SC (2013) Wooden toys in India. 64:57–60
3. Rangaswamy J, Kumar T, Bhalla K (2018) A comprehensive life-cycle assessment of locally oriented small-scale toy industries: a study of traditional Channapatna toys as against low-cost PVC (Poly-vinyl chloride) toys made in China. Procedia CIRP 69:487–492. https://doi.org/10.1016/j.procir.2017.12.164
4. Aurisano N, Huang L, Milà i Canals L, Jolliet O, Fantke P (2021) Chemicals of concern in plastic toys. Environ Int 146:106194. https://doi.org/10.1016/j.envint.2020.106194
5. Madar A, Boşcor D, Băltescu C, Neacşu A (2012) Wooden versus plastic toys. In: Proceedings of the international scientific conference eco-trend, pp 254–260
6. Luo S, Wang Y, Xiong N, Shan P, Zhou Y (2018) An interactive smart music toy design for children. In: Distributed, ambient and pervasive interactions: understanding humans, pp 372–390. https://doi.org/10.1007/978-3-319-91125-0_31
7. Guyton G (2011) Using toys to support infant-toddler learning and development
8. Dag NC, Turkkan E, Kacar A, Dag H (2020) Children's only profession: playing with toys. North Clin Istanb 8:414–420. https://doi.org/10.14744/nci.2020.48243
9. Baral B, S DC, G LM (2016) Wooden toys-Sawantwadi
10. Baral B, William A (2015) Channapatna toys of Karnataka
11. Rawat R (2014) Semiotic study of wooden craft of Sawantwadi. http://14.139.111.20:7888/jspui/handle/1/55
12. Khanna S (1987) Indian toys & toy makers: our design heritage. National Institute of Design, Ahmedabad
13. Which is More Ecological: Wood or Plastic? https://okcredit.in/blog/wood-or-plastic-which-is-more-ecological/. Last accessed 31 July 2023
14. Chawla N, Mehta R (2020) Children's influence on parent's purchasing decision in toy industry. Pac Bus Rev Int 13:127–137
15. Ritter MA, Skog K, Bergman RD (2011) Science supporting the economic and environmental benefits of using wood and wood products in green building construction. United States Department of Agriculture, Forest Service, Forest Products Laboratory, Washington, DC, USA
16. Lovevery: The play kit. https://lovevery.com/products/the-block-set. Last accessed 17 July 2023
17. MoonToys: Why Should Children be Given Wooden Toys to Play With? https://moontoys.in/why-should-children-be-given-wooden-toys-to-play-with/. Last accessed 13 Oct 2023
18. Ikei H, Song C, Miyazaki Y (2017) Physiological effects of wood on humans: a review. J Wood Sci 63:1–23. https://doi.org/10.1007/s10086-016-1597-9
19. Cameron A (2015) Nature inspired design. ULTIMO, NSW
20. Chitrani: why wooden toys are better than plastic? https://www.chitrani.com/blog/why-wooden-toys-are-better-than-plastic. Last accessed 31 July 2023
21. Mangaonkar-Vaiude P, Joshi M (2021) Study and revival strategies for traditional art form: case of Sindhudurg. Presented at the (2021). https://doi.org/10.1007/978-981-16-0041-8_67

Leveraging Technology to Enhance Hiker Safety: A Design Intervention

Naureen Khan, Pranita Ranade, and Indresh Kumar Verma

Abstract As urbanization shapes our world, many people adopt outdoor recreational sports and activities to stay active and reconnect with nature. Hiking is an adventure sport rapidly gaining popularity among people from various age groups and backgrounds due to its numerous benefits. Hiking is risky, and a lack of essential knowledge and preparation can lead to a challenging and stressful experience and may even prove fatal. Hikers often encounter hurdles like exhaustion, getting lost on the trail, extreme weather conditions, natural calamities such as landslides or avalanches, and other unforeseen accidents. Modern technological interventions, e.g., GPS, satellite communication, wearables, and immersive media (AR/VR), are creating new means and opportunities for providing training and safety to hikers. The research aims to comprehend the hiker's journey, the challenges faced, and the current scenario of navigation and safety during hiking. The proposed study follows a systematic framework and implementation of the design thinking process. Findings are determined through survey and interview analysis, concept ideation, and usability testing. The study proposes an IoT-based system design for a low-cost wearable integrated with a mobile application with features such as real-time data, location tracking and sharing, checkpoint monitoring, and crowd-sourced information to enhance the safety and well-being of hikers during their expeditions. The system also monitors the hikers' health and sends an SOS signal, contributing to timely search and rescue operations when necessary. The system promotes a safe and seamless hiking experience by providing a secure and enjoyable hiking environment.

Keywords Technology for hiking · Hiking safety · Smart wearable technology · Location tracking · IoT-based system · Design thinking process

N. Khan · P. Ranade (✉) · I. K. Verma
Symbiosis Institute of Design, Symbiosis International (Deemed University), Pune, India
e-mail: pranitaranade@gmail.com

© The Author(s), under exclusive license to Springer Nature Singapore Pte Ltd. 2025

B. B. V. L. Deepak et al. (eds.), *Recent Advancements in Product Design and Manufacturing Systems*, Lecture Notes in Mechanical Engineering,
https://doi.org/10.1007/978-981-97-6732-8_51

1 Introduction

Mountainous regions are hubs of adventure travel, seasonal employment, and permanent living zones. According to a report from the UN's Food and Agriculture Organization (FAO), World Tourism Organization (WTO), and the Mountain Partnership (MP), mountain tourism accounted for approximately 9–16% of global tourist in 2019 amounting to between 195 and 375 million tourists [1]. With the advent of adventure tourism, outdoor activities such as mountain climbing, hiking, rafting, and paragliding have become increasingly popular among people of all ages and backgrounds. There has been a growing trend toward hiking in India in recent years. The country's diverse geography and rich cultural heritage make it an ideal destination for hikers of all levels, from beginner to expert. Moreover, hiking offers unique physical challenges, mental rejuvenation, and a strong connection to nature. As the hiking is gaining the popularity, there is also rise in the accidents and fatalities which is reported by several Indian news agencies in recent times. According to a study conducted by Ascent Descent Adventures, the rate of mountain climbing and hiking accidents in India stood at 43%. Fatalities account for 61% of persons involved in mountain climbing and hiking accidents, with a low rescue rate of only 16% [2]. Thus, despite its fascination, hiking presents various challenges for hikers. These challenges encompass physical and environmental factors, such as altitude sickness, sudden weather changes, and treacherous terrain. Causes of death included falls, avalanches, high-altitude illness, and sudden cardiac events. Factors such as inadequate skills, overestimation, lack of fitness, and pre-existing health issues contributed to different deaths [3]. Additionally, the psychological aspects of hiking, including isolation, mental resilience, and stress-induced decision-making, add complexity to the experience.

The study emphasizes a number of lacunas in the existing system, such as lack of awareness and inadequate preparation, ineffective methods to alert emergency, lack of infrastructure on trails, poor efficiency in locating missing people, and how technology can intervene in order to come up with efficient solutions in the domain of hiking. The paper aims to determine an effective system that can address navigation and safety concerns during hiking. A design thinking methodology is implemented to propose an IoT-based system that will serve as a cost-effective solution for hikers and help authorities locate people quickly and save their lives. The advent of mobile-based applications and present-day technologies can help address some of the mentioned issues.

2 Literature Review

The research phase began with a detailed literature review based on relevant keywords such as adventure sports tourism, hiking experiences, benefits and motivations, case studies in the Indian context, and accident and mortality rates, etc. 37 relevant research

articles to the topic were selected for review. The literature review explores various case studies, effects of environmental impact, trail degradation, natural calamities like landslides and avalanches, and cultural impacts on local communities. The research also highlights technologies such as UAVs, RFID, WSN, GPS, GIS, AI, Big Data, and hiking apps for navigation, route planning, and safety communication. However, there is less research on the effective integration of technology in the Indian context to improve hikers' safety and promote responsible hiking practices. The outcomes of the literature review have been discussed below.

2.1 Motivations and Benefits Associated with Hiking.

Hiking has the potential to stimulate both mental and physical well-being. It offers a multitude of physical, mental, and socio-cultural benefits to individuals and communities. Mountain hiking is an excellent way for both young and elderly people to stay healthy as it involves use of muscles strength for that particular period. Exposure to higher altitudes and mild hypoxic conditions can also have extra health advantages [4]. According to Morita and Shirakawa, "hiking in nature for an hour a day can help decrease fatigue by 65% and increase energy by 20%" [5]. Moreover, hiking fosters enhanced strength, endurance, flexibility, and balance. Spending time in nature has numerous health benefits, such as decreased blood pressure, enhanced immune system functioning, decreased stress levels, muscle tone, weight management, and overall wellness [6]. However, hiking can also lead to exhaustion, physical and mental strain, and the risk of injury. Despite the pain and many inconveniences, countless people still continue their trek. This is because hikers are driven by diverse motivations, including overcoming challenges, personal experiences, self-discovery, love for nature, and social connection**.** Hiking brings a sense of achievement, increases interactions, reduces loneliness, bringing happiness and a sense of togetherness [7].

2.2 Hiking Challenges, Risks, and Accidents in Indian Context

Despite the countless benefits, hiking also encompasses psychological and physical tests that require preparation and adaptability. As per the conducted study, the most notable perceived risks coincided with "public security problems," "traffic accidents," "outdoor medical assistance," "poor communication," and "sudden bad weather." The least prominent perceived risks are "feeling uncomfortable under unfamiliar surroundings," "getting lost during hiking," "terrible team leader organization and management," "physical exhaustion," and "fever, acute disease" [8]. One of the primary physical challenges in hiking is the risk of altitude sickness that causes

symptoms such as nausea, dizziness, and shortness of breath, which may worsen into lethal conditions like high-altitude pulmonary edema (HAPE) or high-altitude cerebral edema (HACE) if not addressed promptly [9, 10]. Furthermore, falls account for almost 50% of all fatal and non-fatal accidents during trekking in the mountains [4]. Slipping, twisting one's ankle, and stumbling are frequent causes of injuries when people fall. About 75% of falls occur during descent [11]. Furthermore, the rigors of long treks can lead to physical exhaustion and increase the risk of injuries. Starvation, dehydration, and maintaining hygiene also emerge. Unpredictable weather is a significant environmental risk in hiking. Hikers may face UV radiation and sudden weather changes, including storms, extreme colds, or blizzards, especially in mountainous regions. Lack of preparation for such conditions can lead to hyperthermia, hypothermia, or frostbite [12]. India is known for some of the most popular hiking destinations, including the Himalayas, Western Ghats, and the Nilgiris. Although these mountain ranges offer diverse hiking trails, India has experienced a significant number of hiking accidents. According to an article published in Times of India (TOI), almost 150 fatalities have been recorded in hiking expeditions in Himalayan states during 2018–2022, and over six people are still missing [13]. Moreover, a substantial number of deaths are left unreported, suggesting a potentially higher count. The Indian states of Himachal Pradesh and Uttarakhand reported the highest death tolls. From 2017 to 2018, altitude sickness was the major cause of death for 43 people in expeditions, while 37 fatalities were recorded from Jan 2019 to Feb 2020 [13]. Post-pandemic (2021 to 2022), the death rate has increased to more than 60. Table 1 gives the deaths in Indian mountaineering and hiking expeditions in the Himalayan region from 2017 to 2022**.** In 2021, the Govt. of Himachal Pradesh temporarily stopped all mountaineering activities in the Kinnaur district due to the *Lamkhaga* Pass tragedy, where ten trekkers died and two were reported missing. Adverse weather conditions took the lives of five trekkers from West Bengal during their *Sunderdhunga* glacier expedition in *Bageshwar* district. Due to avalanche in *Draupadi ka Danda* peak in Uttarkashi district in October 2022 claimed the loss of 27 trainees and instructors of Nehru Mountaineering Institute, two from the group are still missing [13].

Table 1 Deaths in Himalayan expeditions

Year	2017–2018	2019–2020	2021	2022	Total deaths
No. of deaths	43	37	30	36	146

Source TOI [13]

2.3 Use of Technology in Hiking.

Technology has significantly transformed the hiking experience in various ways. GPS, satellite communication devices, and mobile applications have become essential tools for hikers enabling them to effortlessly navigate treks, plan trips, track progress, and discover new trails. UAVs or drones play a crucial role in safety surveillance by aiding search and rescue operations and assessing potential hazards [14]. RFID, WSN, IoT, AI, and AR are other types of technology that are being used in the realm of hiking. Over the years, the wearable technology market has significantly developed, of which wearable trackers are the most common type used to track physical fitness activity. These trackers enable us to understand ourselves, others, and the environment. GPS or RFID can automatically transfer data about users' locations, track weather and environment, and vital signs such as heart rate, calories burned, steps, speed, time, and more [15]. Modern technology can undoubtedly create an easier, safer, and more efficient experience for hikers. A comparative chart highlighting the use of these technologies in hiking is given in Table 2.

3 Methodology

A user-centered design thinking process which includes Empathy-Define-Ideate-Prototype-Test, followed at every stage to develop and propose the final design concept. Primary research was conducted to understand the fundamentals of the target group. The information gathered helped to understand users' needs, challenges, and perspectives on the hiking experience. In the define stage, brainstorming, affinity mapping, mind mapping, 5Whys and 5W + H charts, KWL chart, contextual inquiry models, stakeholder map, and competitor study. Furthermore, user persona, empathy map, storyboarding, and user journey map were created to identify common challenges among the hiking community. User-centered design methods were employed for the ideation and conceptualization phases, and the final concept was proposed. Finally, a task-based method was used to conduct usability testing using the system usability scale.

3.1 Interviews and User Surveys

Primary research included a combination of online surveys and interviews. The online user survey of 35 samples (age group 15–30 yrs with hiking experience ranged from novice to expert levels) curated which helped to understand preferences, needs, challenges, and suggestions for enhancing hikers' trekking experiences. The primary user groups studied were adventure sports enthusiasts and common people who practiced hiking as a hobby or leisurely activity. Survey questions were related to

Table 2 Technologies used in hiking

UAV	RFID	WSN	GPS	GIS	AI	Big Data	Mobile Apps
Capture aerial imagery, scout terrain, locate campsites, monitor weather, search, and rescue operations	Track hikers' location in real-time and ensure all members of a group stay within a safe distance	Real-time environmental monitoring and data collection	Track location, follow pre-loaded routes, and share coordinates	GIS-generated maps display trail difficulty, points of interest, and safety info	Analyze, trail, weather, and hiker's fitness level to suggest routes, identify plants and animals	Study hiker behavior, track weather, and analyze impact of human activities on environment	All-in-one tools that bring together navigation, safety features, and data collection

hikers' training and knowledge, means of communication, hiking equipment and items, accident experiences, navigation, and safety. Both in-person and virtual interviews who have numerous hiking experience were conducted with 5 participants aged 20–30 years. The interview questionnaire consisted of open-ended questions to understand the hiking experience from start to finish. Questions focused mainly on the user's challenges, needs, and technology's role in hiking which provided valuable insights into the overall hiking experience, the integration of technology to enhance hiking navigation and safety, and the user's opinion on contemporary technologies. Participants expressed interest in low-cost wearable devices enabling easy navigation, tracking location, monitoring health, sharing live location, and alerting contacts in case of accidents or emergencies.

3.2 Contextual Inquiry

Contextual inquiry comprehends users' in-depth thought processes and interactions with complex systems. Three different inquiry models were created: flow, cultural, and sequential. The cultural model captures the cultural values and policies of the hikers and their influencing factors. The flow model (shown in Fig. 1) identified different roles involved in the system and the detailed connections (communication and coordination) between them. Lack of knowledge and experience, communication barriers, time and financial constraints, and underestimation of risks were some of the significant break-downs among different influences.

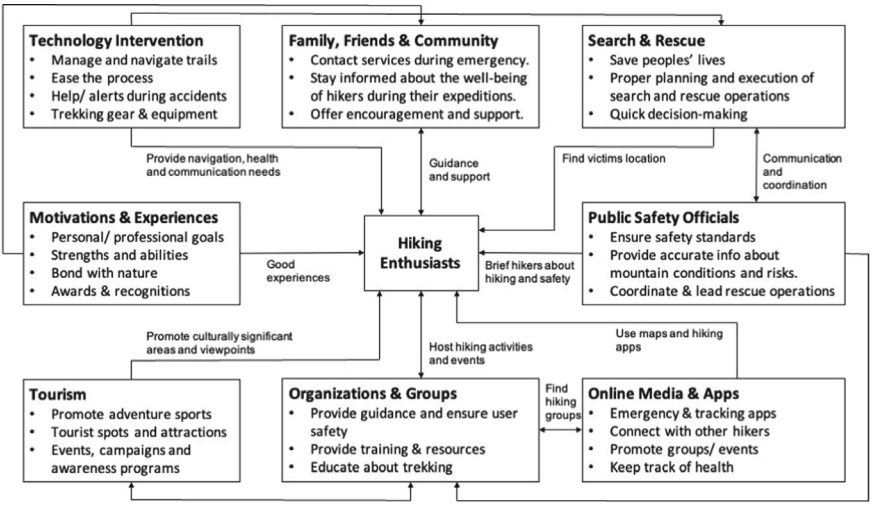


Fig. 1 Flow model of hikers and roles involved in the system

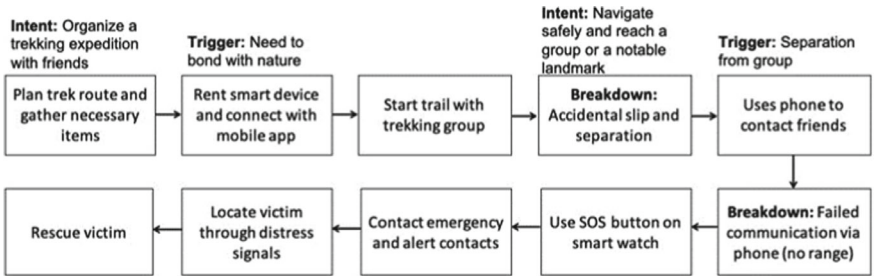


Fig. 2 Sequential model–how to use the smartwatch product

The sequential model (shown in Fig. 2) helps capture the detailed steps performed to accomplish tasks with respect to the user's strategy, goals, intent, trigger, and pain points. Deeper insights were gained into the hikers' actions on using the current technology available and how a better solution can be proposed to enhance their experience. Thus, a widespread intelligent wearable assistive application-based wearable system has been pro-posed as the final design concept.

3.3 Competitor Study

A competitor benchmarking study (shown in Table 3) was conducted to know the direct and indirect competitors currently in the market. Direct competitors include apps/systems such as All Trails, Gaia GPS, Komoot, and Cairn. Indirect competitors include Garmin, Saved by Spot, Samsung watch 5 pro, and Google pixel Watch 2.

4 Insights from Interviews, User Surveys, and Competitor Study

Surveys were sent through online mode, and 35 responses were received. The study found that 69.3% of the respondents had no prior training or knowledge about hiking, and 69.2% had faced accidents during their trek. 89.6% of the respondents tried to contact emergency through phones, but 61.5% had ineffective communication (mainly due to un-reliable network connection). During the interview, participants stated that accurate trail information, clear and detailed trail maps, and interactive way-finding cues were crucial for route planning and avoiding getting lost, especially on less-traveled routes. Several participants also advocated for a platform with real-time trail updates, crowd information, and hazard alerts. Participants expressed interest in low-cost wearable devices enabling easy navigation, tracking location, monitoring health, sharing live location, and alerting contacts in case of accidents or emergencies. The competitor study helped to perceive the advantages, scope, and

Table 3 Benchmarking study of competitors in the market

Features	Competitor's							
	Direct competitor's				Indirect competitor's			
	All trails	Gaia GPS	Komoot	Cairn	Garmin	Spot	Samsung Galaxy Watch5 Pro	Google Pixel Watch 2
Search trails	✔	✔	✔	✔	✗	✗	✗	✗
GPS tracking	✔	✔	✔	✔	✔	✔	✔	✔
Real-time trail updates (traffic, hazards, closures)	✗	✔	✗	✗	✗	✔	✗	✗
Weather information	✔	✔	✗	✗	✗	✗	✗	✗
Trek information (time, distance, altitude)	✔	✔	✔	✔	✗	✔	✔	✔
Elevation data	✔	✔	✔	✔	✗	✗	✔	✔
Physical activity data	✗	✔	✔	✗	✔	✗	✔	✔
Offline maps	✔	✔	✔	✔	✗	✗	✔	✔
Personalization	✔	✔	✔	✔	✔	✔	✔	✔
Hiking navigation and safety knowledge	✗	✔	✗	✗	✗	✗	✗	✗
Smart device integration	✗	✗	✔	✗	✔	✔	✔	✔
Share and track live location	✗	✗	✗	✔	✗	✔	✔	✔
Track group members location	✗	✗	✗	✗	✗	✔	✗	✗
Emergency SOS	✗	✗	✗	✔	✗	✔	✔	✔
Notify safety circle	✗	✗	✗	✔	✗	✔	✔	✔
Satellite messaging	✗	✗	✗	✔	✔	✔	✔	✔
Community feed	✔	✔	✔	✗	✗	✗	✗	✗
Total features	8	11	9	10	5	10	11	11

areas of improvement of current solutions. GPS tracking, trek details, and personalization were primary features found in most of the competitors. Secondary features like search trails, physical activity and elevation data, offline maps, and community feeds were also found. Although features such as real-time updates, weather data, hiking knowledge, share and track live location, tracking group members' location, emergency SOS, notifying emergency contacts, and satellite messaging are of prime importance to hikers, most competitors did not integrate these features. Most applications and products focused on hikers' navigation safety but over-looked hikers' communication during emergency situations.

4.1 Conceptualization and Ideation

Various ideas and features were listed and plotted in the priority matrix, following which different concepts were created based on feasibility, novelty, and priority of features. Further, a mobile application and a smart wearable that worked in sync were pro-posed based on the essential requirements of the target users. To come up with an innovative solution, the SCAMPER method was used. Replacing an LED screen with a monochrome display in a smartwatch has numerous advantages, viz. longer battery life, better performance in direct sunlight, easy readability, affordable, and high durability. **The salient features of the proposed design are**:

- Real-time data on danger-prone zones, crowd information trail traffic, and natural calamities
- Track hiking members' location
- Send live location to safety circle (family or friends at home)
- Checkpoint monitoring—towers at various checkpoints monitor if hikers have crossed it, else notify central database
- Auto sends health and location information upon fall/accident detection.

In the conceptualization and ideation phase, low-fidelity paper prototypes of the mobile application were prepared and based on the feedback collected from the users, ans Hi-fidelity (shown in Fig. 3) visual designs were created in Figma software. The smart wearable would work in sync with the mobile application, providing easy navigation and a quick, efficient way to alert emergency services in case of an inability to use a mobile phone during an accident.

4.2 Smart Wearable Device

Hikers benefit from the multi-faceted features of the smart wearable device. Users can rent/buy the smart wearable before starting their trek. The smart wearable device works by connecting it to the app through the unique identification number on the band. Data between the smart wearable and mobile app is synced. The smart wearable

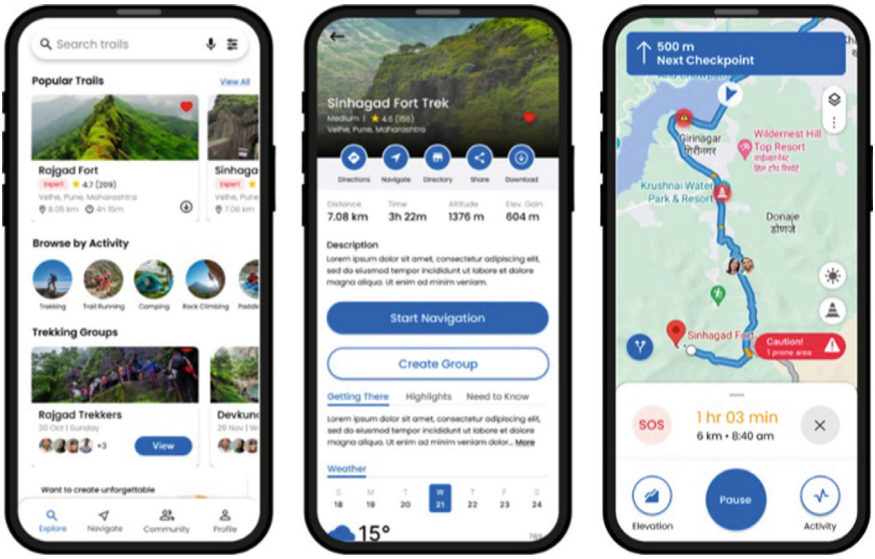


Fig. 3 Hi-fidelity interactive prototype of the proposed mobile app (author made)

displays the trail navigation based on information input by the user through the mobile app. It shows users' and group members' current location and provides visual cues to denote the correct trail route. The wearable also measures trek data, e.g., longitude, latitude, elevation, and health data, e.g., blood pressure, heart rate, steps, and calories burned. In case of any accident, the SOS button can send a distress signal and current location to alert emergency services. Sensors at checkpoints will monitor if the user has passed through to the next checkpoint or not. This will make it easy for search and rescue teams to locate the user quickly. The device also has haptic and sound feedback for user accessibility. The product's functionality and technological implementation are shown in Fig. 4.



Fig. 4 Smart wearable–Functionality, technological implementation of product (author made)

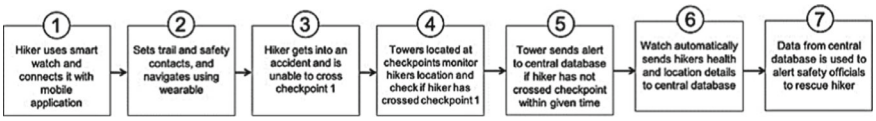


Fig. 5 Flowchart-working of the system

4.3 Working of the System–Implementation Methodology

Different checkpoints on the mountain consist of towers that monitor hikers. These towers check if the hiker has crossed the checkpoint or not. An alert is sent to the central database if the hiker does not cross the checkpoint within the estimated time. The central database sends a message to the hikers' smart watch inquiring if they need help. The smart wearable also automatically sends health, elevation, and location details to the central database. In an emergency, rescuers can extract data from the central database by tracing the last checkpoint passed by the victim and reducing search area, time, and cost. Working of the system is shown in Fig. 5.

4.4 Usability Testing

The system usability scale (SUS) was used to measure the proposed design's usability [20]. It was administered to 10 users to test the proposed design. Users were briefed about the concept, and a prototype was provided to perform the task. The task given were (a) connect smart wearable to the app, (b) search for Pune treks through the search bar and find Sinhagad Fort Trek, (c) create a group and add two friends from contacts and start navigation of the trail, (d) view elevation, activity data and call for emergency SOS." Based on the task, users' reviews, time, and observations were noted down, and the SUS ratings for the proposed solution were tabulated (shown in Table 4).

The SUS method was used for summative testing, and the results showed that 100% task completion and rated the system with a satisfactory rating of 88.75% (> standard 85.5%), suggesting that the system met their expectations effectively. It states that the design is efficient in terms of accessibility, desirability, navigation, and usability to satisfy the goal.

5 Discussion

Curated research methods state upcoming challenges for hikers, mainly during trail navigation and alerting someone in case of an emergency. However, the implementation of an efficient and secure system for mountain accidents is not seen in India.

Table 4 System usability scale ratings for the proposed solution

SUS questions	Ratings, n (%), total $n = 10$				
	Strongly disagree (1)	Disagree (2)	Neutral (3)	Agree (4)	Strongly agree (5)
I think that I would like to use this system frequently	0 (0)	1 (10)	5 (50)	3 (30)	1 (10)
I found the system unnecessarily complex	0 (0)	0 (0)	3 (30)	5 (50)	2 (20)
I thought the system was easy to use	0 (0)	1 (10)	2 (20)	6 (60)	1 (10)
I think that I would need the support of a technical person to be able to use this system	1 (10)	0 (0)	1 (10)	6 (60)	2 (20)
I found the various functions in this system were well integrated	0 (0)	1 (10)	2 (20)	4 (40)	3 (30)
I thought there was too much inconsistency in this system	0 (0)	2 (20)	1 (10)	3 (30)	4 (40)
I would imagine that most people would learn to use this system very quickly	0 (0)	1 (10)	2 (20)	2 (20)	5 (50)
I found the system very cumbersome to use	2 (20)	0 (0)	3 (30)	3 (30)	2 (20)
I felt very confident using the system	0 (0)	2 (20)	5 (50)	2 (20)	1 (10)
I needed to learn a lot of things before I could get going with this system	0 (0)	0 (0)	4 (40)	4 (40)	2 (20)
Average SUS score = 88.75					

Conducted user surveys highlighted a need for a low-cost and effective technological intervention for hiking, which can be used by a range of target groups, i.e., novice to expert-level users. Most hikers are not aware of hiking rules and safety regulations and also do not want to spend considerable money on hiking gear and equipment as they might not use it often. It was observed that most hiking practitioners extensively use mobile phones for navigation and emergency purposes. However, a better product was required to cater to the inability to use mobile phones in mountain areas due to problems such as reduced connectivity in remote areas, physical damage due to terrain to phone, etc. Users showed keen interest in wearable technology as a modern solution to their hiking needs. The competitor analysis focuses on industry trends and already know applications and products. Both direct and indirect competitors provide valuable insights for shaping design concepts with an aim to address existing shortcomings. Smartwatch serves the primary purpose during hiking and provides specialized features through IoT and AI-based algorithms, providing scope for proposing a practical design concept. According to TOI, 17-year old Smit Metha slipped and fell 130 m down into a gorge at Vilaspur Fort near Lonavala on July 2022, and suffered with an injury of two broken ankles. His friends were unable to

find him and he could not contact them as he was not carrying his phone. However, he was wearing his Apple Watch Series 7 (cellular model) smartwatch which had Jio connectivity during the time of the accident. He was able to contact his family and friends, who then contacted the rescue authorities about his whereabouts [1, 15]. Thus, the proposed system would be beneficial for hikers to have an intelligent system that they can rely on to navigate safely, and notify someone in case of accidents, saving time during search and rescue operations [2].

6 Conclusion

This paper proposes an end-to-end concept proposal for hikers to navigate their trail safely, reduce accidents during hiking, and provide a quick emergency search and rescue system. Smart wearable, a habitual part of many peoples' lives, is easy to adapt. With the help of contemporary technologies such as IoT, AI, personalization, and smart assistance, users can get appropriate information about the trail route, know about sudden weather changes and natural calamities, monitor their health and environment, track their location and their group members' location, and alert emergency contacts and services during an accident. The actual implementation of the design concept will be advantageous not only for hikers to navigate quickly and enjoy a safe hiking experience but also to reduce the time and costs spent by search and rescue teams to locate victims during an emergency. It also provides peace of mind for hikers and their families and helps boost tourism and economic activity through safe and accessible hiking. Thus, modern technology can bring a fun, efficient, and safer hiking experience.

References

1. Food and Agriculture Organization of the United Nations (FAO) (2023) Understanding and quantifying mountain tourism. In: World Tourism Organization (UNWTO) (ed.) World Tourism Organization (UNWTO). ISBN 978-92-844-2402-3
2. Lagwal P, Understanding adventure sports accidents India. Available online: https://ascentdescentadventures.com/blog/understanding-adventure-sports-accidents-india/. Accessed on 6 Nov 2023
3. Burtscher M, Niedermeier M, Gatterer H (2021) Editorial on the special issue on "Mountain sports activities: injuries and prevention." Int J Environ Res Public Health 18:1405. https://doi.org/10.3390/ijerph18041405
4. Faulhaber M, Ruedl G, Schneider F, Walter D, Sterr R, Schobersberger W, Schwendinger F, Pocecco E (2020) Characteristics of victims of fall-related accidents during mountain hiking. Int J Environ Res Public Health 17:1115. https://doi.org/10.3390/ijerph17031115
5. D'souza TB, Puttaraju S, Examining the influence of trekking in nature on adaptive response to stress in individuals. Int J Indian Psychol 8:913–923. https://doi.org/10.25215/0801.114
6. Mitten D, Overholt JR, Haynes FI, D'Amore CC, Ady JC (2018) Hiking: a low-cost, accessible intervention to promote health benefits. Am J Lifestyle Med 12:302–310. https://doi.org/10.1177/1559827616658229

7. Mayer K, Lukács A (2021) Motivation and mental well-being of long-distance hikers: a quantitative and qualitative approach. Heliyon 7:e06960. https://doi.org/10.1016/j.heliyon.2021.e06960
8. She S, Tian Y, Lu L, Eimontaite I, Xie T, Sun Y (1986) An exploration of hiking risk perception: dimensions and antecedent factors. Int J Environ Res Public Health 2019:16. https://doi.org/10.3390/ijerph16111986
9. Hackett PH, Roach RC (2001) High-altitude illness. N Engl J Med 345:107–114. https://doi.org/10.1056/NEJM200107123450206
10. Basnyat B, Murdoch DR (2003) High-altitude illness. The Lancet 361:1967–1974. https://doi.org/10.1016/S0140-6736(03)13591-X
11. Faulhaber M, Pocecco E, Niedermeier M, Ruedl G, Walter D, Sterr R, Ebner H, Schobersberger W, Burtscher M (2017) Fall-related accidents among hikers in the Austrian Alps: a 9-year retrospective study. BMJ Open Sport Exerc Med 3:e000304. https://doi.org/10.1136/bmjsem-2017-000304
12. Brocherie F, Girard O, Millet GP (2015) Emerging environmental and weather challenges in outdoor sports. Climate 3:492–521. https://doi.org/10.3390/cli3030492
13. Talwar G (2022) 150 Killed in trekking expeditions in Himalayan states in last 5 years. Times India TOI
14. Dhumale S (2023) Harnessing technology: advancements in trekking equipment for an enhanced experience. Times India TOI
15. Koo SH, Fallon K (2018) Explorations of wearable technology for tracking self and others. Fash Text 5:8. https://doi.org/10.1186/s40691-017-0123-z
16. Sharma A (2022) Apple CEO Tim cook writes to 17-year-old boy from Maharashtra after apple watch “saves” his life. Times India

Textile Defect Classification Using Deep Convolutional Neural Networks (DCNN)



Sri Sashank Potluru, Tarun Karnati, Ramesh Mande, Hruthi sri Gudavalli, and Sai Manikanta Miriyala

Abstract The textile industry has a standing history and offers a diverse range of products, such as clothing, home furnishings, and more. The quality of the product is undeniably impacted by the fabric's quality. The caliber of the merchandise is undeniably impacted by the fabric's quality. Still, several complications can surface during the fabric production process due to factors, like imperfect yarn or mechanical glitches. Neglecting these flaws can incur losses and harm the brand's reputation. At times, researchers have put forth machine learning techniques, like CNN, RCNN, and others to detect defects in fabrics. However, there is still a challenge in achieving time and accurate segmentation and classification of these defects. This research paper introduces an new approach that combines the power of DCNNs with the efficiency of the YOLOv7 detection mechanism to bridge this gap. We propose a network architecture that includes preprocessing feature extraction using ResNet-50 and defect detection using YOLOv7 and then classify the fabric defect into their category using a deep convolutional neural network. This results in classification of fabric defects. Impressively, this network achieves an accuracy of 96.29%. By conducting this study, we hope to raise the bar for fabric defect detection and offer the textile industry a reliable, automated, and extremely precise instrument for ensuring fabric quality.

S. S. Potluru (✉) · R. Mande · H. Gudavalli · S. M. Miriyala
Department of Information Technology, V R Siddhartha Engineering College, Vijayawada, India
e-mail: sashank.potluru22@gmail.com

R. Mande
e-mail: ramesh.welcome@gmail.com

H. Gudavalli
e-mail: hruthigudavalli@gmail.com

S. M. Miriyala
e-mail: Saimanikantamiriyala5756@gmail.com

T. Karnati
Department of Computer science, SRK Institute of Technology, Vijayawada, India
e-mail: tarunk1109@gmail.com

© The Author(s), under exclusive license to Springer Nature Singapore Pte Ltd. 2025

B. B. V. L. Deepak et al. (eds.), *Recent Advancements in Product Design and Manufacturing Systems*, Lecture Notes in Mechanical Engineering,
https://doi.org/10.1007/978-981-97-6732-8_52

Keywords Fabric quality · Fabric defect classification · Deep convolutional neural network · YOLOv7 · ResNet-50

1 Introduction

The textile business encompasses a wide range of goods, from basic clothing to opulent home furnishings, and is intricately woven into the tapestry of human history. The fabric, a component whose quality may increase or decrease the final product's value, is essential to the appeal and usefulness of these items. Although complex in both design and execution, fabric manufacture is not without its difficulties. Neglecting imperfections like stray threads or mechanical abnormalities can escalate from minor manufacturing errors to significant financial burdens, potentially harming brand integrity [1].

The ability to identify and correct fabric flaws has always been crucial in the huge tapestry that is the textile business. In the past, human inspectors were tasked with this important responsibility and would meticulously inspect fabrics to verify their excellence. This conventional approach did not, however, come without difficulties. The procedure required a lot of effort and was prone to human error, including the possibility of mistakes and inconsistencies [2]. The shortcomings of manual inspections became painfully clear when the world entered a time of rapid industrialization and the demand for textiles soared. A more advanced and trustworthy technique to flaw identification was required due to the sheer amount of textiles produced and rising customer expectations. The urgent need in the realm of machine learning prompted exploration into advanced techniques like CNN and RCNN as potential remedies for the challenge of fabric defects shown in Fig. 1. These methodologies promised precision, scalability, and efficiency, despite challenges like real-time detection needs, managing skewed data due to sporadic defects, and the relentless pursuit of high accuracy (citation). The paramount objective persisted in guaranteeing flawless quality for each fabric item, irrespective of its intended purpose. The intricacy of this endeavor is underscored in Fig. 1, emphasizing defect detection as indicative of a brand's dedication to excellence and customer contentment. This study introduces methods for fabric defect categorization, involving grayscale conversion, noise reduction with mean filtering, feature extraction using ResNet-50, and fabric detection via YOLOv7. Fabric defect classification is conducted using deep convolutional neural networks. The key components of this research are:

- Initially, the raw input image is converted to a grayscale image. Then noise is eliminated using a filter during preprocessing.
- For feature extraction, we employ the ResNet-50 method to extract features, like plain, stain, basket, stripes, ikat, paisley, houndstooth from fabric.
- By applying the YOLOv7 technique for detection to enhance classification results and categorizing bamboo species using a deep convolutional neural network.

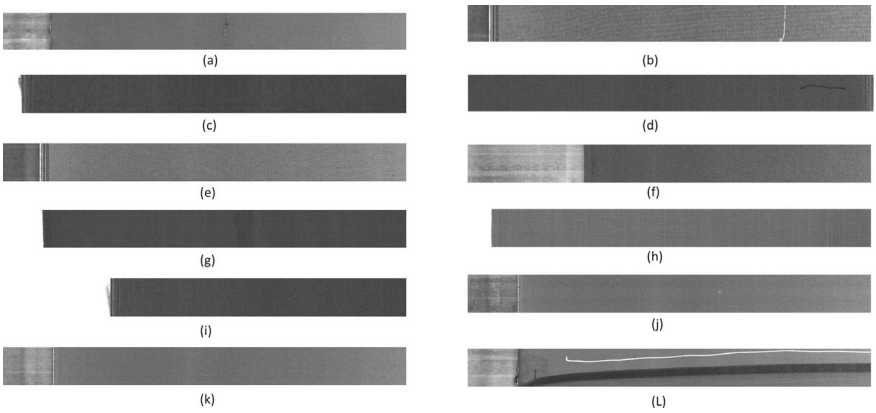


Fig. 1 **a** Broken end, **b** broken yarn, **c** broken pick, **d** weft curling, **e** fuzzy ball, **f** cut selvage, **g** crease, **h** warp ball, **i** knots, **j** contamination, **k** nep, **l** weft crack

This paper's subsequent sections are structured as follows: Sect. 2 delves into research on fabric defect classification. Our proposed methodology and its detailed components are explained in Sect. 3. The experimental approach we employed is described in Sect. 4. Lastly, Sect. 5 discusses our study findings and suggests research directions.

2 Literature Survey

Using convolutional neural networks, the author explored the field of fabric defect detection in this research, concentrating on real-time performance and correcting data imbalances brought on by uncommon defects [1]. Despite the potential of their method, it was still unable to consistently achieve high-speed detection in practical situations. In order to get beyond these restrictions, our study takes advantage of the YOLOv7 detection mechanism's advantages as well as ResNet-50's capability for feature extraction.

Compressive sensing and convolutional neural networks (CS-CNN) have been combined in a unique way to improve fabric defect recognition, which is especially useful for datasets with small sample sizes [2]. The research still had difficulties dealing with many kinds of flaws, though. By combining sophisticated preprocessing methods and a customized DCNN for accurate defect categorization, our suggested methodology provides a more comprehensive and reliable solution. End-to-end fault segmentation made considerable strides once the Mobile-Unet was introduced, successfully correcting sample imbalances [3]. For smooth incorporation into fast fabric manufacturing processes, the model needed more tweaks. By using the YOLOv7 detection technique in our article, we expand on this by assuring accurate

and quick defect identification that is in line with the needs of real-time manufacturing. Traditionally, human inspections—a procedure fraught with inconsistencies and inefficiencies—were used to discover fabric defects. The research highlights the limitations of approaches when it comes to time online detection in today's era [4]. By automating the flaw identification process and using cutting-edge neural network topologies to assure reliable, quick, and accurate inspections, our study gets around these difficulties. This research demonstrated the use of CNN for a variety of computer vision applications, with a particular emphasis on classifying fabric texture defects. The technique seemed promising, but due to the random nature of errors, there were still issues with real-time identification and data imbalances [5]. Our approach offers a thorough remedy, improving real-time performance and providing a balanced fault categorization. It is supported by the YOLOv7 mechanism and ResNet-50. In this study, we introduced FabricNet, a network designed to detect defects in fabrics. It combined the Faster RCNN [6] with the feature pyramid network (FPN), the deformable convolution (DC) network, and the distance IoU loss function. Although this showed improved speed and accuracy of prediction, there were still some issues, notably when addressing various fault kinds. Our study fills up these gaps by providing a more sophisticated mechanism for defect identification and classification, assuring thorough coverage of fabric abnormalities. By incorporating activation layers into convolutional neural networks, this article investigates the identification of fabric defects [7]. Although this method showed improvements in defect detection, it was still hampered by issues with scalability and real-time flaw identification in a variety of fabric types. Our proposed study combines the YOLOv7 detection mechanism with ResNet-50, hoping to build on the advantages of earlier approaches while resolving their drawbacks, enabling thorough and quick flaw identification across a range of textile samples. Fabric defect detection's importance has grown due to challenges in the textile industry [8], such as rising labor costs and the push for automation. The research advocates a two-stage learning-based paradigm for automated flaw identification. It employs the Le-Net-5 model for thorough defect detection and the Inception-V1 model for localized defect prediction. However, there are opportunities for improvement in real-time application and fabric flexibility. Our study aims to address these limitations with a more efficient technique for comprehensive fabric flaw identification.

3 Proposed Methodology

In the textile sector, the quality of a fabric is primarily judged by its appearance and texture. Defects, which can occur during various production stages like weaving or dyeing, significantly affect fabric quality and value. Traditionally, manual defect detection is prone to errors, highlighting a rising demand for automated solutions provided by deep learning. **Preprocessing**: To improve contrast and make it easier to see defects, the raw fabric image is first changed from color to grayscale. **Noise**

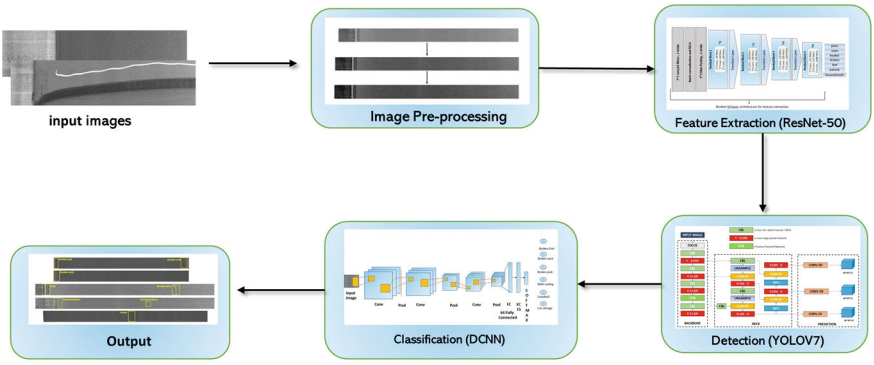


Fig. 2 Proposed methodology architecture

reduction: Any noise present in the image, which might interfere with defect detection, is mitigated using bilateral filter technique. **Feature extraction**: Critical features of the fabric, such as patterns, weaves, and potential defects, are extracted using the ResNet-50 technique. This step is vital as it isolates potential defects for further analysis.

Defect detection and classification: Using YOLOv7, fabric defect areas are identified and classified into various types using DCNN, including broken end, broken yarn, broken pick, weft curling, fuzzy ball, cut selvage, crease, and others. The goal is to create an automated quality control system for the textile industry by detecting fabric flaws, as illustrated in Fig. 2.

3.1 Preprocessing

Preprocessing plays a crucial role in enhancing the quality of raw images for subsequent analysis. Initially, the raw image undergoes transformation into grayscale, simplifying its information while retaining essential elements. The bilateral filter is then applied to maintain the structural integrity of the image and reduce inherent noise. This filter comprises two primary components: the domain filter, which assigns higher weights to adjacent pixels spatially close to each other, and the range filter, which considers variations in pixel intensity. By effectively smoothing the image while preserving edge sharpness, the bilateral filter creates optimal conditions for precise subsequent image analysis. Figure 3 depicts the operation of the preprocessing techniques we provide. Mathematically, the bilateral filter can be represented as: Given a pixel at location i, the bilateral filter output BF(I) at that location is given by:

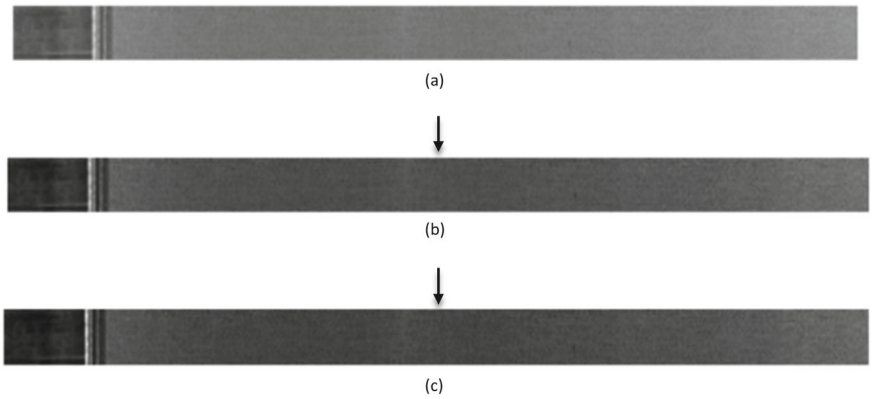


Fig. 3 **a** Original image, **b** greyscale image, **c** denoise image

$$\mathrm{BF}(I)(i) = \frac{1}{Wp} \sum_{j \varepsilon \cap} G\sigma_x(||i - j||) \times G\sigma_y(||I(i) - \mathrm{I}(j)||) \times I(j),$$

Ω is the neighborhood around pixel i.
$G\sigma_x$ is the spatial Gaussian that gives weight depending on spatial distance.
$G\sigma_y$ is the range Gaussian that gives weight depending on intensity difference.
Wp is a normalization term defined as:

$$Wp = \sum_{j \varepsilon \cap} G\sigma_x(||i - j||) \times G\sigma_y(||I(i) - \mathrm{I}(j)||),$$

where σ_x and σ_y are the standard deviations for spatial and range filters.

3.2 Feature Extraction

After initial preprocessing, a specialized method is introduced to extract intrinsic fabric features crucial for defect detection. Using an adapted ResNet-50 architecture, features like plain, stain, basket, stripes, ikat, paisley, and houndstooth are efficiently identified. ResNet-50's unique convolutional and pooling layers make it proficient in feature extraction, aided by residual links to bypass certain layers, addressing the vanishing gradient challenge. This allows effective training in deeper networks. Through this structure, refined fabric images yield a comprehensive feature set, aiding in accurate fabric anomaly detection and categorization. ResNet-50 initiates with channeling the input image through a 7×7 convolutional layer utilizing 64 filters and a stride of 2, aiding in basic visual element identification as shown in Fig. 4. Batch normalization and ReLU activation function stabilize features and introduce nonlinearity. A 3×3 max-pooling layer condenses image dimensions while

retaining crucial features. The architecture comprises four groups of residual blocks, each integrating specific convolutions for dimension reduction, spatial nuances, and dimension amplification. A key feature, the shortcut or skip connection, merges input directly with output post-convolutions, recurring six times within the first block. Transition phases recalibrate channel dimensions using 1×1 and 3×3 convolutions and employ average pooling for spatial down-sampling. Subsequent residual block groups maintain a similar structure, with adjusted filter dimensions and repetition counts for extracting intricate visual patterns. The structure of the ResNet-50 utilized is detailed in Table 1.

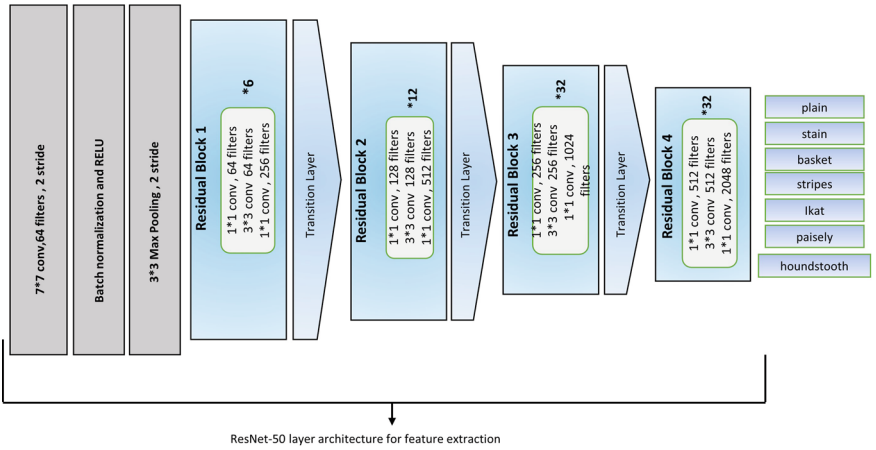


Fig. 4 Illustrates the flowchart of ResNet-50 demonstrating how our methodology was implemented

Table 1 ResNet-50 structure

Layers	ResNet-50
Convolution	7×7 convolution, 64 filters, stride 2
ReLu	Batch normalization and ReLU
Pooling	3×3 max-pooling, stride 2
Residual block 1	{(1×1 con, 64 filters)(3×3 conv, 64 filters)(1×1 conv, 256 filters)} $\times$ 6
Transition layer 1	1×1 conv + 2×2 avg pooling, stride 2
Residual block 2	{(1×1 con, 128 filters)(3x3 conv, 128 filters)(1×1 conv,512 filters)} $\times$ 12
Transition layer	1×1 conv + 2×2 avg pooling, stride 2
Residual block 3	{(1×1 con, 256 filters)(3×3 conv, 256 filters)(1×1 conv, 1024 filters)} $\times$ 32
Transition layer 3	1×1 conv + 2×2 avg pooling, stride 2
Residual block 4	{(1×1 con, 512 filters)(3×3 conv, 512 filters)(1×1 conv, 2048 filters)} $\times$ 32

3.3 Detection

Utilizing the YOLOv7 object recognition algorithm, renowned for its speed and accuracy, is integral to our fabric flaw detection method. Given its real-time detection capabilities crucial for identifying fabric anomalies, we specifically opted for the tiny variant of YOLOv7. The architecture comprises essential components, including the backbone, neck, and prediction, which collaborate to ensure reliable detection. Annotation of the dataset with class labels using VGG annotator facilitated YOLOv7 training.

The focus module in the backbone is used to resize the original image, which has dimensions of 640 × 640 × 3. To increase the model's capacity for learning, a sophisticated layer network called the enhanced efficient layer aggregation network (E-ELAN) is used. The E-ELAN in the tiny version of YOLOv7 consists of 16 layers, each of which is a convolutional layer equipped with 16 filters measuring 3 × 3. The backbones focus framework receives the input image with a resolution of 640 × 640 × 3. Through the slicing technique, it initially transforms into a 320 × 320 × 12 feature map, and subsequently after applying a convolution operation with 32 convolution kernels, it ultimately becomes a feature map. These 16 layers can be categorized as follows:

- 1–4: Transform features into a latent space.
- 5–8: Reconstruct latent space features.
- 9–12: Integrate the reconstructed features with the original ones.
- 13–16: Implement the expand, shuffle, merge cardinality technique.

These layers incorporate advanced techniques such as 'expand, shuffle, and merge' and 'cross-stage partial networks (CSP)' to improve learning capabilities and mitigate overfitting risks. The convolutional block (CBL) focuses on feature extraction, while the feature pyramid network (FPN) creates a hierarchical feature map. Integrating these layers and methods enhances YOLOv7's object recognition abilities, making it suitable for fabric defect detection. This enhancement not only boosts the model's learning capacity but also improves computational efficiency by reducing parameter count. The study aims to optimize the training epoch for YOLOv7, thereby enhancing its effectiveness in classification tasks as shown in Fig. 5.

The use of an advanced object detection system (YOLOv7) aimed at boosting defect detection capabilities in the manufacturing sector. The latest YOLO version launched in January 2023 provides significant enhancements compared to the earlier versions. As shown in Table 2, the YOLOv7 outperformed YOLOv5 and YOLOv3 on mAP at different IoU thresholds. YOLOv7 also shows high accuracy, including small and the tough objects, commonly found in fabric defects datasets at the higher IoU threshold of 0.95. It means YOLOv7 is well advanced in detecting minute quality deviations that normally happen with such little flaws as small and obscured defects. Therefore, the YOLOv7 is undoubtedly a new frontier and step toward efficiency and quality control in the textile defect detection domain.

Table 2 Comparative analysis between YOLO models at varying IoU thresholds

Model	mAP@0.5	mAP@0.75	mAP@0.95
YOLOv7	98.5	98.7	97.9
YOLOv5	96.7	97	95.2
YOLOv3	95.9	94.2	93.5

3.4 Classification

We then offer a dual-track deep neural network (DNN) architecture for classifying the identified defects in the next phase of our methodology for discovering fabric problems. This architecture effectively categorizes twelve types of faults including end, broken yarn, broken pick, weft curling, fuzzy ball, cut selvage, crease, warp ball, knots, contamination, nep, and weft crack. To enhance system efficiency, the model combines a profound convolutional neural architecture with max-pooling in one track and fully connected layers in another. It includes four hidden layers: a densely interconnected layer and three convolutional-pooling layers, with an output layer. Initial input represents RGB values of a 150 × 150 image. After a convolutional-pooling layer generates 32 feature maps, max-pooling over a 2 × 2 region is applied. Subsequent convolutional-pooling layers use a 3 × 3 local receptive field to produce 64 and 128 feature maps. Output layers consist of 15 softmax neurons representing fabric species, with a fourth fully connected layer containing 64 ReLU neurons. ReLU activation functions' use in convolutional-pooling layers is illustrated in Fig. 6. Convolution employs 3 × 3 filters to preserve spatial pixel correlation while extracting image attributes. ReLU is selected as the nonlinear function for its efficiency in facilitating learning progress without significant accuracy compromise compared to tanh/sigmoid neurons, which require computationally intensive calculations. The resulting layer integrates a softmax activation function within a conventional multilayer perceptron, facilitating feature capture from images using max-pooling and convolutional layers for fabric defect classification.

3.5 Algorithm

Algorithm for fabric defect classification
Input: Raw fabric image I
Output: Classified defect type D
Steps:

1. Preprocessing:
   1.1 Load the raw fabric image I.
      I. Raw fabric image
   1.2 Convert I to grayscale G.

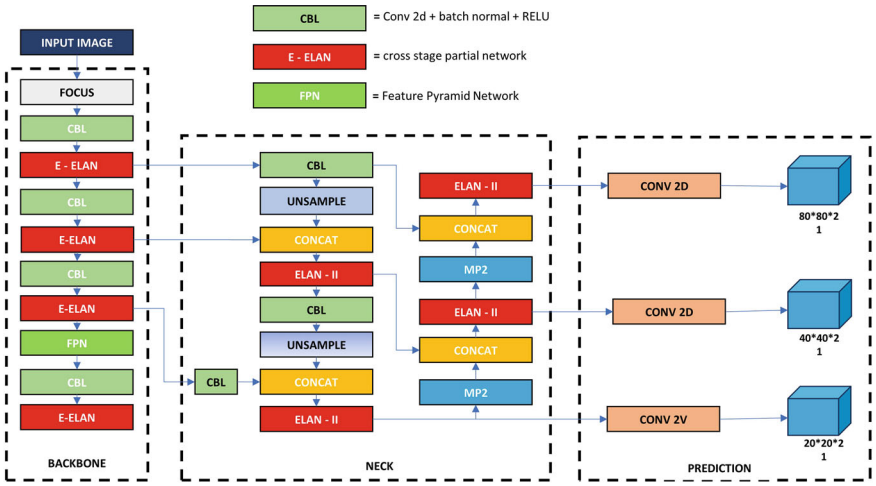


Fig. 5 Tiny-YOLO V7 network structure

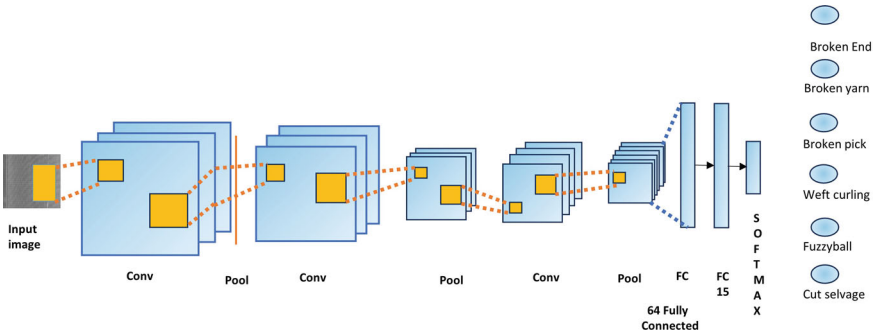


Fig. 6 Proposed deep convolutional neural network structure

$$G(x, y) = 0.299 \times R(x, y) + 0.587 \times G(x, y) + 0.114 \times B(x, y)$$

1.3 Apply Bilateral Filter F to G to remove noise.

$$F(x, y) = \frac{1}{W} \sum_{x'=x-r}^{x+r} \sum_{y'=y-r}^{y+r} G(x', y') * d(x, x') * r(G(x, y), G(x', y'))$$

W is the normalization term, d(x, x') is the spatial closeness between x and x', and r(G(x, y), G(x', y')) is the range similarity.

2. Feature extraction using ResNet-50:

2.1 Feed F into a ResNet-50 architecture

2.2 Extract feature map Φ.

$$\Phi = \text{ResNet} - 50(\text{F})$$

2.3 Normalize for further processing.

3. Defect detection using YOLOV7:

3.1 Use Φ as input to a YOLOv7 model.
3.2 Detect potential defects δ and their locations ?? in the image.

$$(\delta, \lambda) = \text{YOLO}\nu 7(\Phi)$$

3.3 Generate bounding boxes β in detected region

4. Classification using DCNN:

4.1 Extract regions within β from F to create R.
4.2 Feed R into a deep convolutional neural network (DCNN).

$$\text{D} = \text{DCNN}(\text{R})$$

4.3 4.3. Classify the defect types D based on the output layer's activation.

5. Output:

5.1 5.1 Return the classified defect type D and its location ? in the original image.

4 Results and Discussions

By classifying fabric defects through our dataset and methodology, this section initially compares our approach with prevailing 'state of the art.' Subsequent subsections present evaluation results based on experimental data to assess the effectiveness of our methods in fabric defect classification using DCNN.

4.1 Dataset Description

Our dataset is a unique amalgamation of various sources, including publicly available datasets and images culled from the internet and Google Images. This comprehensive collection focuses on capturing an array of fabric defects, specifically: Broken end, broken yarn, broken pick, weft curling, fuzzy ball, cut selvage, crease, warp ball, knots, contamination, nep, and weft crack. The dataset comprises a total of 6432 images, which are evenly distributed across the defect categories, with each category

housing 536 images. For the intent to train and evaluate the model, we divide the dataset into training, testing, and validation subsets. The training set includes 3859 images, the testing set contains 2573 images, and the validation set comprises 717 images. This division ensures a robust and comprehensive appraisal of our profound convolutional neural architectures-based fabric defect classification methodology.

4.2 Quantitative Metrics

This segment elaborates on quantitative assessments conducted to validate the effectiveness of our profound convolutional neural architectures model in identifying and categorizing fabric flaws. Accompanying these assessments is visual representation depicted in Fig. 7, providing supplementary evidence for the model's proficiency. These visual aids can be examined alongside performance indicators such as F1 score, recall, precision, and accuracy. The objective is to provide a comprehensive evaluation affirming the model's suitability for fabric defect detection applications.

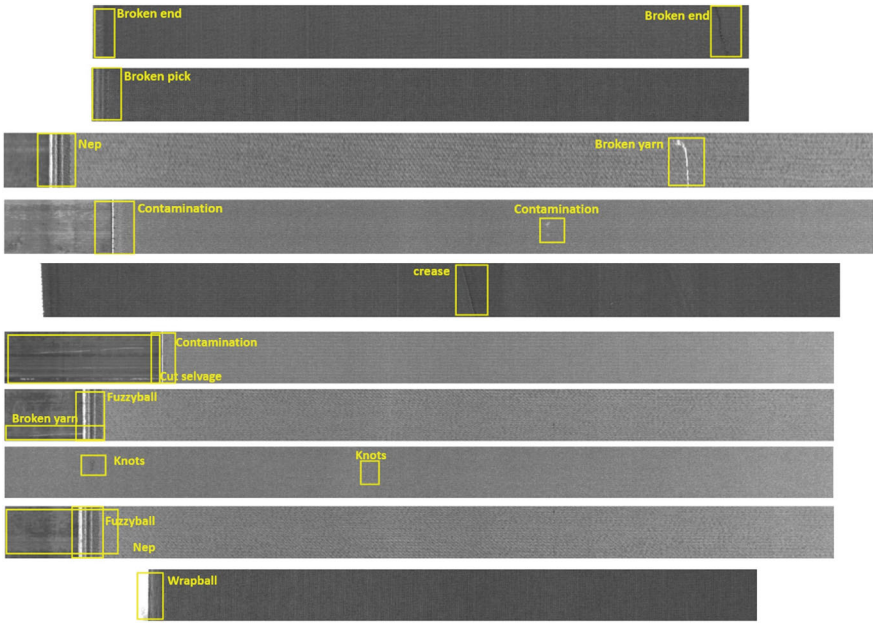


Fig. 7 Results images of fabric defects

4.3 Evaluation Metrics

The efficacy of the suggested fabric defect classification methodology is assessed using four key performance indicators: F1 score (F), precision (P), recall (R), and accuracy (A). These metrics are defined as follows.

4.3.1 Accuracy

Accuracy serves as an indicator of the model's ability to correctly classify fabric defects. It is computed using the formula:

$$\frac{\text{True Positive} + \text{True Negative}}{\text{True Positive} + \text{True Negative} + \text{False Positive} + \text{False Negative}}.$$

4.3.2 Precision

Precision measures how well the model correctly identifies observations among all predicted positives. It is given by:

$$\frac{\text{True Positive}}{\text{True Positive} + \text{False Positive}}.$$

4.3.3 Recall

Also known as positive rate (TPR) or sensitivity recall, this metric evaluates the models ability to accurately identify all instances.

$$\frac{\text{True Positive}}{\text{True Positive} + \text{False Negative}}.$$

4.3.4 F1 Score

The F1 score is a measure that combines precision and recall through the harmonic mean calculation as:

$$2 \times \frac{\text{Precision} \times \text{Recall}}{\text{Precision} + \text{Recall}}.$$

4.4 Performance Evaluation

In a comparative evaluation among established methodologies, our newly proposed deep convolutional neural network (DCNN) demonstrates outstanding performance in fabric defect classification. Table 3 summarizes the performance of CNN, KNN, RCNN, U-Net, and SegNet alongside our DCNN, focusing on key metrics such as recall, accuracy, f-measure, and precision. This assessment is particularly relevant for our dataset containing 13 types of fabric defects, including broken ends, knots, and creases.

The empirical data underscores the superior accuracy of our network model, with Fig. 8 further elaborating on the accuracy comparisons. In addition, Fig. 9 provides a graphical representation of how our model fares in terms of precision, recall, and f-measure against existing models.

Table 3 Percentages of recall (%), precision (%), accuracy (%), and f-measure (%)

Approaches	Accuracy	Recall	Precision	F-measure
CNN	89.71	83.6	89.6	76.5
KNN	90.62	84.7	73.8	83.2
RCNN	94.35	89.5	88.6	90.3
U-NET	92.78	75.2	86.6	80.2
SEGNET	93.63	70.6	91.5	80.5
Proposed model (DCNN)	96.29	90.4	94.5	92.6

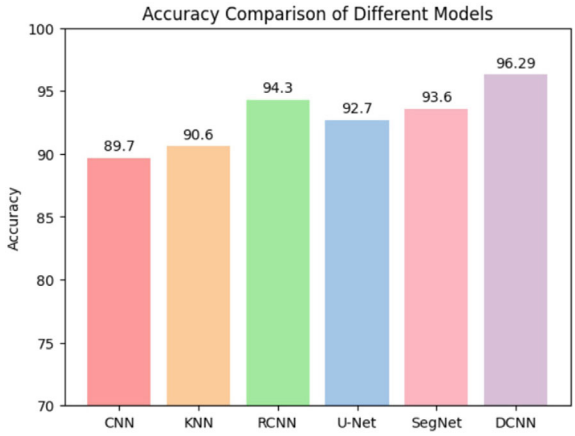


Fig. 8 Evaluation of accuracy using various techniques

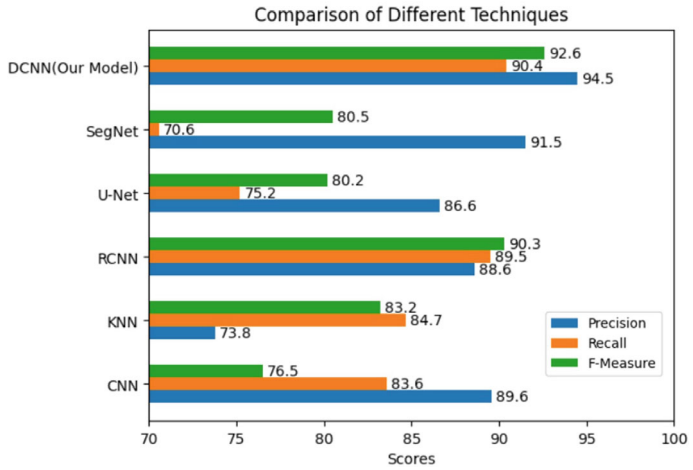


Fig. 9 Metric-based comparative analysis

Table 4 Computational time (in seconds)

Method	Time
DCNN (our model)	0.16
CNN	0.23
KNN	0.19
RCNN	0.18
U-NET	0.17
SEGNET	0.20

4.5 Computation Time

The efficiency of computational time stands as another metric of interest. Our approach strives for computational simplicity, a feature that is evident when compared to other state-of-the-art techniques. Table 4 presents a head-to-head comparison of the computational times for our DCNN model and other existing methods,

4.6 Evaluation of Training Results

The results after 100 epochs displayed an impressive accuracy rate of 96.29%. Figure 10 provides a visual representation of the training and validation accuracy over time.

Although there is minor fluctuation in the validation loss curve, the ultimate convergence of the accuracy curves suggests that additional testing could potentially

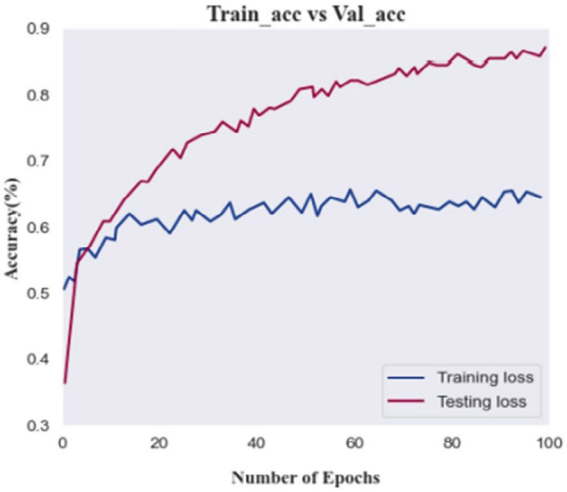


Fig. 10 Training and validation accuracy

improve the results. Nonetheless, the low disparity between the test and training loss and the plateauing of the curve are promising. Figure 11 elucidates the training and validation loss over time. In summary, Figs. 10 and 11 indicate that our DCNN model provides superior estimates of both accuracy and loss, outperforming previous methods in both training and validation phases for fabric defect classification.

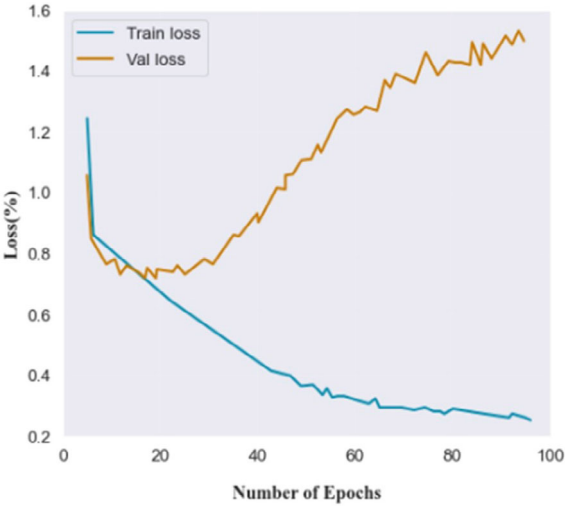


Fig. 11 Training and validation loss

5 Conclusion

Fabric defects present a significant challenge to the textile industry by impacting quality and profitability. This study introduces a framework utilizing deep convolutional neural networks (DCNN) for fabric defect classification. The process includes reducing noise, on both sides converting to grayscale extracting features with ResNet-50 detecting defects using YOLOv5 and classifying with DCNN. Achieving an accuracy rate of 96.29% across 13 types of fabric faults such as broken ends, knots, and wrinkles showcases the effectiveness of our method. This research offers promising prospects for enhancing fabric flaw identification techniques, thereby improving manufacturing quality and reducing waste. The adaptable methodology holds potential for broader applications in various industries, including low-resource environments. This project sets a standard for future research, including the development of low shot learning methods for deep learning in textile quality control.

This study suggests one way to automatically detect fabric flaws that would result in significant advancements in the quality control procedures used in the textile industry.

The proposed methodology can also be applied to other sectors like medical imaging, surveillance, and any other field which depends on pattern classification or defect detection.

References

1. Huang Y, Jing J, Wang Z (2021) Fabric defect segmentation method based on deep learning. IEEE Trans Instrum Meas 70:1–15
2. Wei B, Hao K, Tang X-S, Ding Y (2019) A new method using the convolutional neural network with compressive sensing for fabric defect classification based on small sample sizes. Text Res J 89(17):3539–3555
3. Jing J, Wang Z, Rätsch M, Zhang H (2022) Mobile-Unet: An efficient convolutional neural network for fabric defect detection. Text Res J 92(1–2):30–42
4. Jing J, Zhuo D, Zhang H, Liang Y, Zheng M (2020) Fabric defect detection using the improved YOLOv3 model. J Eng Fibers Fabr 15:1558925020908268
5. Zhao Z, Kang G, Wang P (2020) Fabric defect detection based on cascade faster R-CNN. In: Proceedings of the 4th international conference on computer science and application engineering, pp 1–6
6. Zhou H, Jang B, Chen Y, Troendle D (2020) Exploring faster RCNN for fabric defect detection. In: 2020 Third international conference on artificial intelligence for industries (AI4I). IEEE, pp 52–55
7. Ouyang W, Xu B, Hou J, Yuan X (2019) Fabric defect detection using activation layer embedded convolutional neural network. IEEE Access 7:70130–70140
8. Jun X, Wang J, Zhou J, Meng S, Pan R, Gao W (2021) Fabric defect detection based on a deep convolutional neural network using a two-stage strategy. Text Res J 91(1–2):130–142
9. Mahajan PM, Kolhe SR, Patil PM (2009) A review of automatic fabric defect detection techniques. Adv Comput Res 1(2):18–29
10. Jia L, Chen C, Liang J, Hou Z (2017) Fabric defect inspection based on lattice segmentation and Gabor filtering. Neurocomputing 238:84–102

11. Liu L, Zhang J, Fu X, Liu L, Huang Q (2019) Unsupervised segmentation and elm for fabric defect image classification. Multimedia Tools Appl 78:12421–12449
12. Li C, Li J, Li Y, He L, Fu X, Chen J (2021) Fabric defect detection in textile manufacturing: a survey of the state of the art. Secur Commun Netw, pp 1–13
13. He D, Wen J, Lai Z (2021) Textile fabric defect detection based on improved faster R-CNN. AATCC J Res 8(1_suppl):82–90
14. Li Y, Wang ZW (2021) Research on textile defect detection based on improved cascade R-CNN. In: 2021 International conference on artificial intelligence and electromechanical automation (AIEA). IEEE, pp 43–46
15. Czimmermann T, Ciuti G, Milazzo M, Chiurazzi M, Roccella S, Oddo CM, Dario P (2020) Visual-based defect detection and classification approaches for industrial applications—A survey. Sensors 20(5):1459

Creative Explorations with Bias in Design Thinking Process



Deepshikha and Nisheeth Yadav

Abstract Creativity, cognition, design thinking, emotional intelligence, social intelligence and design methodologies have been well experimented over the decades by researchers across the globe. The objective of this paper is to determine the role and significance of bias in a design thinking process and to establish how it influences the design solution of a design brief. To attain this objective, two experiments were conducted in two premier design institutions located in the North India with students studying at bachelors and masters level programmes. The details have been laid out in the methodology section and the experiment findings have been reported along with a conclusion at the end. The paper concludes inferring that personality and bias have a key role to play in the design solution of the project undertaken; hence, selection or recruitment of designer has to be done meticulously while forming a team leader and a team in an organisation. The paper urges design researchers and leaders to have a convergent and divergent approach as and when needed but choose the design lead carefully as the success or fulfilment or the nature of deliverable solely lies on the biases of this design lead.

Keywords Creativity · Exploration · Bias · Cognition · Design

1 Introduction

Creativity [1–5], cognition [1–3, 6], design thinking [7–10], emotional intelligence [11, 12], social intelligence [13] and design methodologies [14–18] have been well experimented over the decades by researchers across the globe. "Creativity is the act of turning new and imaginative ideas into reality. Creativity is characterised by the ability to perceive the world in new ways, to find hidden patterns, to make

Deepshikha (✉)
Design and Innovation, Jamia Millia Islamia, New Delhi, Delhi, India
e-mail: emaildeepshikhajha@gmail.com

N. Yadav
Lee Kuan Yew School of Public Policy, NUS, Singaapore, Singapore

© The Author(s), under exclusive license to Springer Nature Singapore Pte Ltd. 2025

B. B. V. L. Deepak et al. (eds.), *Recent Advancements in Product Design and Manufacturing Systems*, Lecture Notes in Mechanical Engineering,
https://doi.org/10.1007/978-981-97-6732-8_53

connections between seemingly unrelated phenomena and to generate solutions." "Cognition is a term for the mental processes that take place in the brain, including thinking, attention, language, learning, memory and perception. These processes are not discrete abilities—they are a raft of different, interacting skills which together allow us to function as healthy adults." "Cognitive psychology is a branch of science that investigates how people learn, think and remember. In user experience (UX) design, cognitive psychology is used to understand the mental processes behind a user's behaviours, actions and decisions while they interact with a product or service." "Design thinking is a nonlinear, iterative process that teams use to understand users, challenge assumptions, redefine problems and create innovative solutions to prototype and test. Involving five phases—empathise, define, ideate, prototype and test—it is most useful to tackle problems that are ill-defined or unknown." "Emotional intelligence (EI) is the ability to manage both your own emotions and understand the emotions of people around you. There are five key elements to EI: self-awareness, self-regulation, motivation, empathy and social skills." "Social intelligence is the ability to understand your own and others' actions. Social intelligence is learned and developed from experience with people and learning from success and failures in social settings. It is an important interpersonal skill that helps individuals succeeds in all aspects of their lives." "A design research methodology is an approach and a set of supporting methods and guidelines to be used as a framework for doing design research."

The objective of this paper is to determine the role and significance of bias in any design thinking process and establish how it influences the design solution of any design brief. To attain this objective, two experiments were conducted in two premier design institutions located in the north of India with students studying at bachelors and masters level programmes. The details have been laid out in the methodology section and the experiment findings have been reported along with a conclusion at the end. The paper concludes inferring that personality and bias have a key role to play in the design solution of the project undertaken. Hence, selection or recruitment of designer has to be done meticulously to form a team leader and a team who is handling a project in an organisation.

2 Methodology

Two experiments were conducted. Experiment 1 was an exploratory study conducted at the National Institute of Fashion Technology, Delhi (NIFT, Delhi). Forty-five Semester 1 students of Bachelor in Design Programme took part in the study. 39 students were female while 5 students were male. Age of participants was 17–18 years. The experiment was conducted for 3 h for 10 days with a final presentation to the class on day 11. The students were taught the design thinking process and shown projects of previous batch students for clarity in a 3-h briefing session on day 1. Nine days were given to the students to work upon desired projects following the design thinking process. Students were free to divide themselves in groups or work

as solo. Two groups of three, 14 groups of 2 were formed while eleven students worked on projects individually. On day 2, to begin with, the students had to make a short field visit anywhere inside or outside the college campus to identify problems and then solve the problem using the design thinking approach. Addressing a need or solving a problem was a priority than creating hedonistic experiences via design which may be common in the field of fashion to which the students primarily belonged. The project aimed to tap the creativity and expand student capabilities beyond fashion only. The project could be in any domain within design, namely—graphic, product, system, service, user experience, packaging, or any other. After students found a set of problems to solve, the moderator finalised a potential project for the students to work upon in the remaining eight days. Reviews took place every day to monitor progress, thoughts and process of the students on each day. Forty-five students worked on 27 projects in total. The findings have been reported in the following section—Exploratory Study 1: Exercise and Findings.

Experiment 2 was divided into two parts. The demography comprised Bachelor of Design students from the National Institute of Fashion Technology, Delhi (NIFT, Delhi) and Master of Design students from Jamia Millia Islamia, Delhi (JMI, Delhi). There were 30 students—14 female and 16 male—belonging to age group 20–25 years in the experiment. Part 1 of the experiment was to understand participant ideology by understanding their choice of books they read, movies they liked, personalities they admired or looked up to, solution of societal problems and idea of vacation via three multiple choice objective questions and three descriptive questions. Part 2 was a routine to be designed by the students for a hypothetical case study of a young working female from South of India living and working in the North of India who has to prepare for competitive exams, relax and find ways of leading a better life. Experiment 1 was an open one where students could take up a desired project, while Experiment 2 was more controlled where one problem was provided and all respondents had to participate to address the same problem. Experiment 1 is divergent and Experiment 2 is convergent to assess the impact of bias in a more controlled study. Experiment 2 throws light on how different participants thought in different or similar ways to address the hypothetical case study presented in Part 2 of Experiment 2. Thus, the role of bias gets underlined for analysis in section Exploratory Study 2: Exercise and Findings.

3 Exploratory Study 1: Exercise and Findings

Following were the projects undertaken by students and the observations noted. Forty-five students worked on 27 projects in total. Project 1 is a minimal space design exercise for the hostel warden who resides within the college campus and does not have a well-designed space to work and rest. It was observed that there was no proper ventilation, sleeping area, haphazard storage, poor sitting and working area; hence, the space was redesigned (Fig. 1). Project 2 was a de-addiction app for users heavily dependent on social media (Fig. 2). Project 3 participant went to the nearest

metro station to observe people, environment and problems and jotted a list of them. The participant finalised to design a product to assist elderly and specially abled (physically disabled) to navigate inside the metro station. After several ideations, the participant finalised on a special wheelchair design exercise (Fig. 3). Project 4 comprised two members who observed the problems of local street side vendors outside campus and in the local market nearby—storage, wallet, sun, rain, dust, traffic, waste disposal, security, stray animals, restrooms, etc. They narrowed down to a product design solution to store cash with safety for the vendors on their cart (Fig. 4). The participant of Project 5 went to the nearest bakery shop and identified a set of problems and finally decided to work on cake packaging as many a times cakes get spoilt/damaged while in transit for delivery (Fig. 5). Project 6 was carried out by two female students who wanted to change perception of men and women towards girls and women and designed a social media campaign, graphic design exercise to get vocal about comments and behaviour that commonly offend women and girls (Fig. 6). Project 7 was redesign of online web UI of a store called SSS online store (Fig. 7). A usability audit was carried out and a new UI was created for the online store. Project 8 was another social media campaign, a graphic design exercise based on a series of artworks to raise awareness about obsessive compulsive disorder (OCD) (Fig. 8). Project 9 was in a group of three participants, and they designed a book for sex education for teenagers (Fig. 9). Project 10 was Signage Design for NIFT Delhi campus which is very confusing for a new-comer like the students themselves due to haphazard organisation of the departments (Fig. 10). Project 11 was carried out in groups of two, a product design exercise for waste management of reusable fabric, leather, etc. within campus (Fig. 11). Project 12 was an attempt to solve sparse seating areas at the metro station (Fig. 12). Project 13 was an App UI design exercise for hostel attendance, leave, admissions, paperwork and other administrative works (Fig. 13). Project 14 was a fast food joint space redesign outside NIFT Delhi campus for kitchen and seating area (Fig. 14). Project 15 was a work by two participants to create an emergency Food and Medicine Kit for flood relief activities (Fig. 15). Project 16 was a sustainable packaging exercise for a popular dry snack food (Fig. 16). Project 17 studied the issues faced by roadside tea stall on floor or on carts and provided a design solution for a movable cart (Fig. 17). Project 18 studied the problems faced by fruit and vegetable cart vendors and redesigns the vending cart (Fig. 18). Project 19 was a solo project that aimed to understand the issues faced by roadside imitation jewellery vendors and designs a solution for them (Fig. 19). Project 20 was carried out in a group of two where the participants design a work cocoon, a small workspace for students inside NIFT Delhi campus which is a very compact one (Fig. 20). Project 21 was NIFT Delhi canteen space redesign for more seating and navigation (Fig. 21). Project 22 was understanding the needs and issues faced by a roadside cobbler who repairs shoes and design a solution for storage for him (Fig. 22). Project 23 was a solo project by a female participant to create awareness about polycystic ovary syndrome (PCOS) through digital posters (Fig. 23). Project 24 was exploring creative, usable and efficient tables for student classrooms at NIFT Delhi (Fig. 24). Project 25 was a solo branding project for a lesser-known local shop in the nearby market that provides custom laser cutting

facilities for a wide range of purposes (Fig. 25). Project 26 was a solo project to design wall-hanging home décor using waste tin cans (Fig. 26). Project 27 was a solo project which aimed to design home décor items with coconut shells (Fig. 27).

Analysis of the Exploratory Study 1 Experiment with 45 students—It is important to observe and note how design thinking actually happens inside the minds of young designers being trained at initial stage. How some want to work independently, some in groups of two and some in groups of three. How friendships, likability, bonds, similarity and comfort matter during in the formation of groups for the two-week-long exercise. How development of independent thought happens when working independently and while collaborating in groups of two or three. How



Fig. 1 Hostel warden space redesign

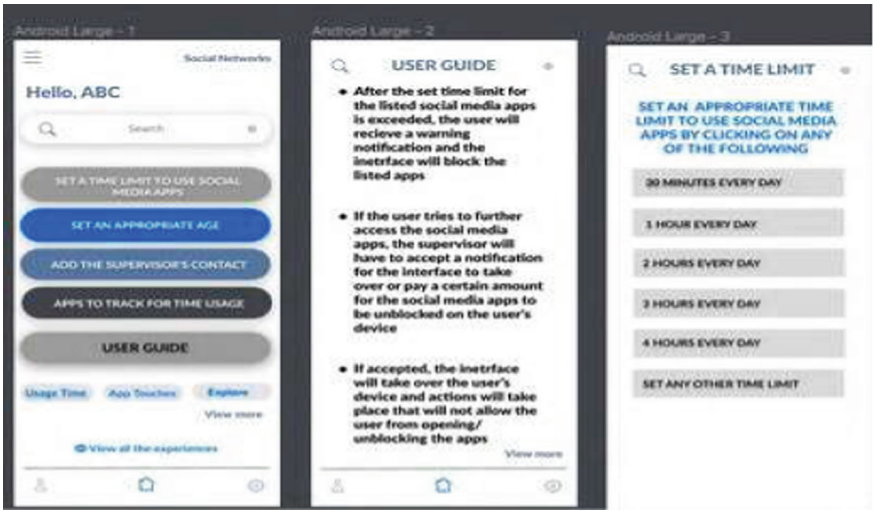


Fig. 2 Social media de-addiction App UI design



Fig. 3 Navigation for the elderly and specially abled at metro station

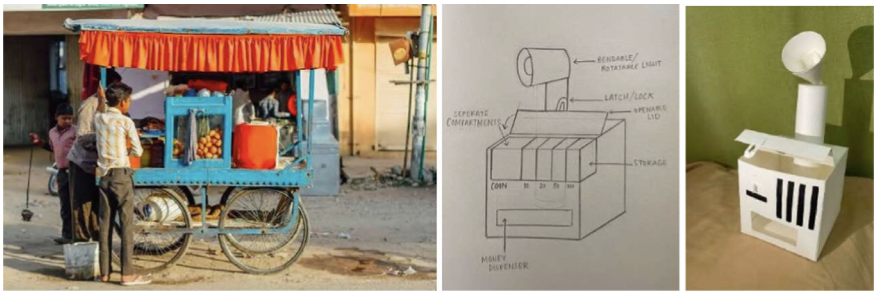


Fig. 4 Safe cash storage for street side vendors

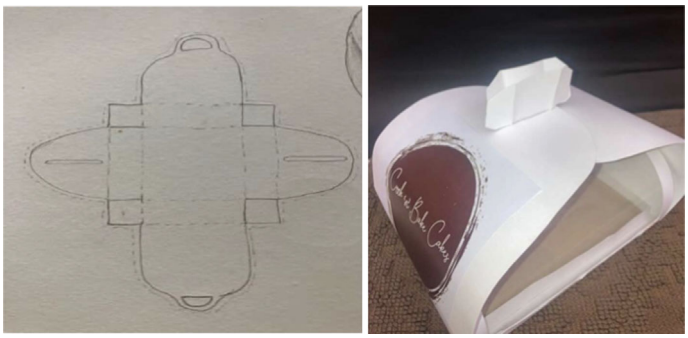


Fig. 5 Cake packaging redesign

individuality is retained or enhanced during the individual and group activities. The role of bias in thinking and design thinking and mindsets and processes and solutions are determined significantly here. The role of environment and creative thoughts in visiting a field or choosing a project whether inside a classroom, nearby markets and stalls and vendors, nearby bakery or shops, what they notice along the roadside, or when they travel by metro while commuting to college. The role of bias in choosing

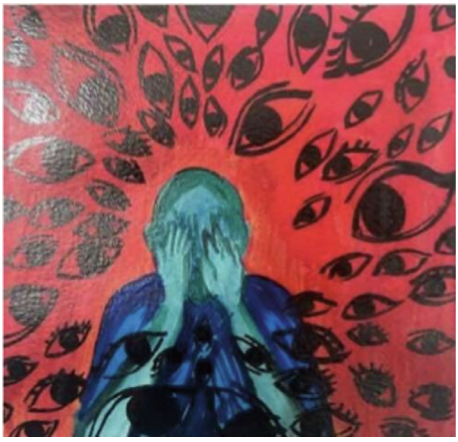


Fig. 6 Artwork for social media campaign for gender issues

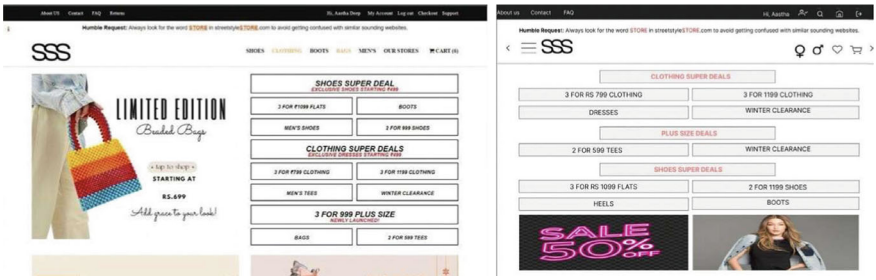


Fig. 7 Present UI and redesigned UI of SSS online store after usability audit

Fig. 8 Artwork for social media campaign for OCD awareness



the subject or the need to be addressed itself is unique in each of the 27 projects discussed—none were similar, they may belong to the domain of graphic or product or service or UI design but each problem being addressed was unique, and in a group of 45, there were no repetitions in the list of problems they identified from their field visit. It leads to the conclusion that every individual works according to their biases

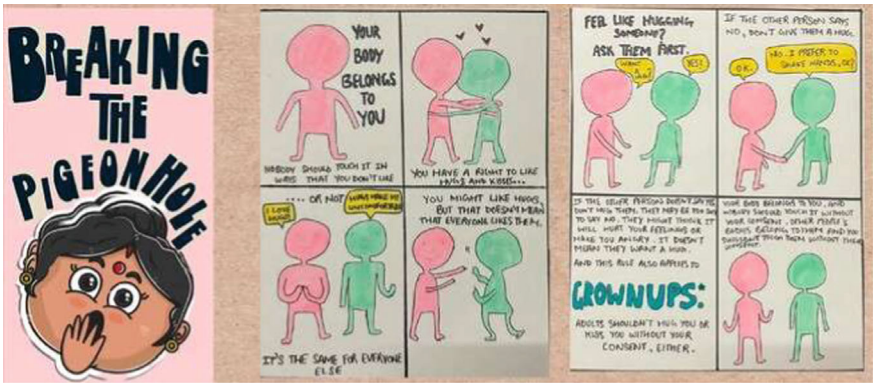


Fig. 9 Book for teenagers for sex education



Fig. 10 Signage Design for NIFT Delhi Campus

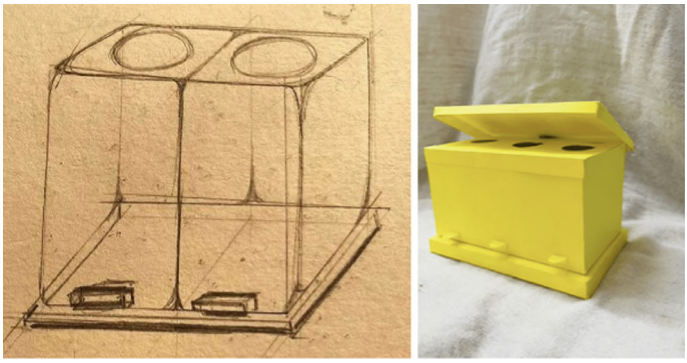


Fig. 11 Waste management for fabric, leather, etc. within NIFT Campus

and chooses, works, determines, carries out processes according to his/her bias and thought processes and the result may vary significantly for a given brief if handled by different people owing to creative, cognitive, cultural, social and environmental biases that exist within our logic and imagination to create a project outcome.

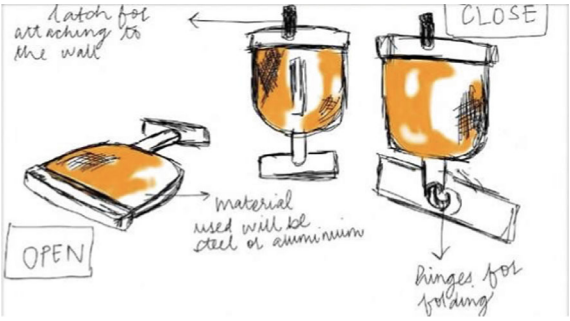


Fig. 12 Seating at metro station

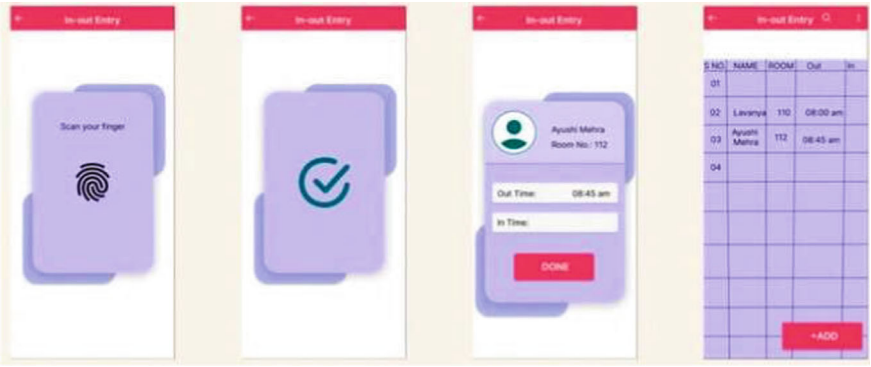


Fig. 13 Hostel management App UI design



Fig. 14 Fast food joint space redesign



Fig. 15 Food and medicine kit for emergency



Fig. 16 Paper packaging for dry snack food

Fig. 17 Roadside tea stall redesign into a movable cart

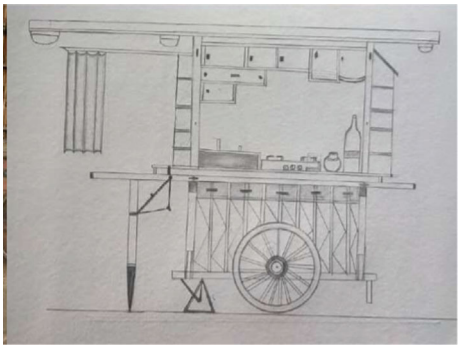




Fig. 18 Vegetable/Fruit cart redesign



Fig. 19 Jewellery vending stand redesign

4 Exploratory Study 2: Exercise and Findings

In this exercise, the authors tried to understand personalities and preferences before embarking on a design thinking project. In Part 1 of the experiment, it was found that they were inspired by a wide range of personalities—Rani Lakshmi Bai, Michelle Obama, Mother Teresa, Prophet Mohammad, Gustav Mahler and Salvador Dali. The choice of iconic figures determines their influence of personalities in their lives or the wish or aspiration to rise up to their level in any way possible. For the choice of books and movies, the participants mentioned the following—"Maja Ma" (talks about female homosexuality), "Phobia" (fear and depression) and "Dear Zindagi" (mental health). Books include polity (The Constitution of India), religion and spirituality (Quran, Gita, The Book of Life, etc.). Analysing the multiple choice and descriptive questions—30% were categorised as religious, 70% were categorised as individualistic, 85% were feminist and 75% were inward looking. In Part 2 of the experiment, they had to design a routine for a young working female from South of

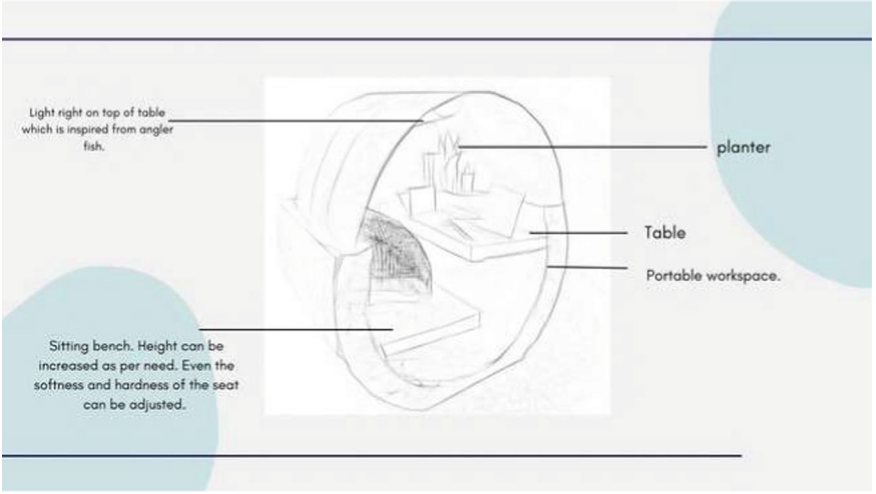


Fig. 20 Personal workspace for NIFT Delhi students

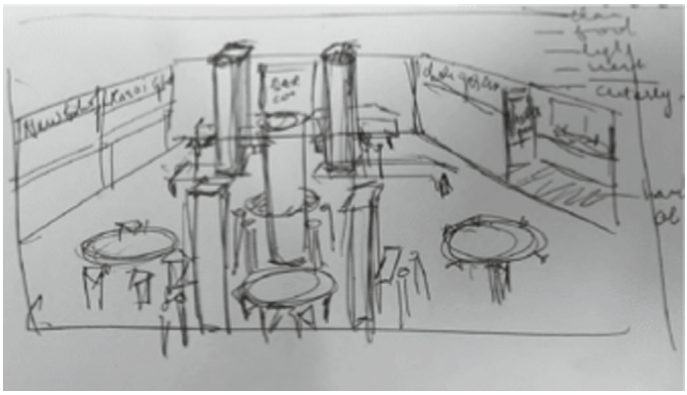


Fig. 21 NIFT Delhi canteen space redesign

India living and working in the North of India who has to prepare for competitive exams, relax and find ways of leading a better life.

Nithya Aiyar works at a private bank in South Extension, New Delhi. She earns 50,000/—per month. She is 28 years old. She completed her M.Com. from Anna University in Chennai. Back home, the family has her parents. Father runs a small convenience store in Erode in Tamil Nadu, and mother is a housewife. She has a sister five years elder to her, who is married and lives in Coimbatore. Nithya moved to Delhi in January 2020. The pandemic hit as she was settling in the new city. In the ensuing months, she worked from her 1-BHK apartment. Luckily for her, the job entailed consulting the clients over phone or web meetings about their investment



Fig. 22 Storage space for cobbler



Fig. 23 PCOS awareness campaign posters

portfolios. Her mother fell ill during the second wave. While her mother came out fine, Nithya had also contributed from her savings for the treatment. While the option of working from any location was available to her during COVID, she decided not work from her parents' place, due to COVID-related travel restrictions and expenses involved in relocating. These days, Nithya is a pale shadow of the happy person she used to be. Since the episode of her mother's illness, the almost complete lack of savings scares her. Since she works most of the time from home, she does not know many colleagues at work intimately, but in one of the web meetings, she overheard

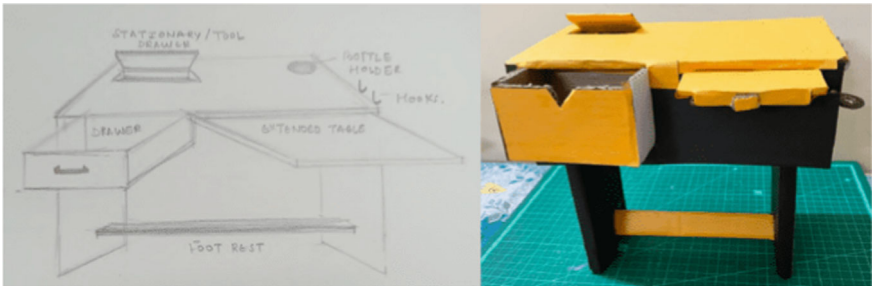


Fig. 24 Table for NIFT Delhi students



Fig. 25 Branding for local laser cutting shop



Fig. 26 Tin can wall hanging

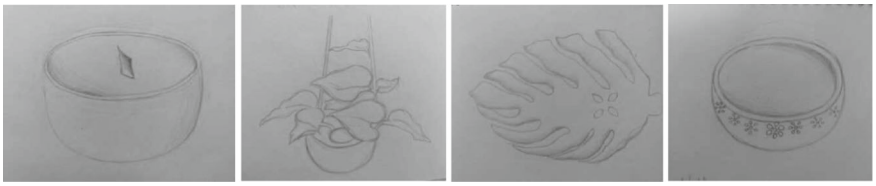


Fig. 27 Home décor products—candle holder, planter, soap dispenser, jewellery box made out of coconut shells

that doing CFA is helpful in promotions at the bank. Doing CFA, however, requires commitment of time and finances. Her sister "suggested" that she should try to save at least 40% of the salary and invest it in mutual funds for future. One silver lining, in her otherwise uneventful life, is the fact that she is able to finish her office work around 4 pm. This gives her ample time to do something new. Exercise: Please design a routine that Nithya should follow for her evenings that, according to you, would be best for her. Try to keep the routine as practical as possible. Please explain in detail how that routine will help her. Feel free to use design thinking framework for designing the routine.

A few responses have been included—She should work as a YouTuber and earn and become a finance expert since she has a background in commerce and banking; she should involve in social activities via online communities and engage on channels such as discord and take some time out for preparation of competitive examinations; she should teach accounts at a private coaching centre which will help her polish her own knowledge beneficial for appearing in upcoming exams; she should work on boosting her moral and emotional confidence as she prepares for her upcoming exams; She should join an online community which is preparing for the same set of exams as her to stay updated about topics and trends; Indulging in activities and working on her hobbies will help her improve her mental state and distract her from stressful life style atleast when she is off to her work; one participant specifically mentioned the breakdown of every hour routine for how to prepare for the upcoming exams; Another participant mentioned how to save her earnings, how to make a social circle and share her life experiences to reduce emotional stress and find a suitable home to live in Delhi since she's from South India, develop hobbies or take up light projects or yoga and gym to stay fit and also prepare for the exams in the evening; If weekends are off for her—she may prepare for exams on weekends and on evenings she could engage in hobbies and relax; After she gets free from work, she can study for 3–4 h comfortably after taking some rest and can study for some time in the morning before leaving for work; She could go to the gym, take some rest, work as a freelancer for foreign clients. Being from M.Com. background, Nithya is eligible enough to do online tuitions for kids/youngsters, or as per her sister suggested, investing in mutual funds, or starting/getting involved in some online business is a smart initiative that she can pursue.

She should buy a planner/journal for scheduling her daily routine. She can pursue an online crash course and take an educational loan for that. She should go out for

some walk or yoga that would keep her sane and fresh because sitting all fays at home can make a person lethargic. She can end the day by listening to calming music before she goes to bed. Nithya has to work hard to meet both the ends. It is very much possible for her to manage her lifestyle for some time so that she could be promoted and help her to save more and plan for future. Her day starts around 6 or 7 where she could give time to herself for preparing for the hectic day. Office hours would be 9 to 5 as usual. After taking a break for 2 h or so, she could start her preparation around 7. This gives her ample time to prepare for the exams. Her day would end around 11 when she could go back to her rest mode. If she is free from 4 to 10 pm (assuming she ideally sleeps 8 h 10 pm–6am) she has 6 h in total. I'm those 6 h she must: 1) increase her knowledge of investment options like mutual funds and independent investments in stocks and govt. grants; for that, she must allocate at least 1 h daily consistently to be able to invest practically. Overtime that would build her knowledge and her savings in the long run. (2.a.) Research on how CFA would be beneficial, how can she get started with the programme and start a habit of saving along with the investment returns. (2.b.) She can find a hobby that she can turn into a little business, this will (2.a.a.) lighten her day as she will be doing something for herself (2.a.b.) earn her some amount that she can again reinvest that would cycle back to her own savings. In the middle of all this, she must finish her 15 min dinner between 8–9 pm. This should engage her about 4.5 h out of the 6 h that she has in the evening. Rest time will be spent on things like self-care, meditation and stretching.

Analysis of Experiment 2 of explorations with understanding participant ideologies and designing a routine for a hypothetical example—It is important to note that in the first experiment, the choice of project and working individually or in groups was given to the participants. Unlike in the second experiment the brief was the same and participants had work individually to assess similarity in responses. It was found in Part 2 of the second experiment that 75% were concerned with Nithya's upcoming examinations and wanted her to relax and yet find time to prepare in for the exams in the evening or in the morning or both. Others however were concerned about her financial health and wanted to give her a boost by hosting her YouTube channel or work as a freelancer and also suggested ways to save her income. A few were very concerned about her emotional, social and physical well-being and wanted her to join the gym, practice yoga, make friends and even change her place of stay since she is new in Delhi and belongs to the south of India. One respondent intended Nithya to devote her time to social activities and hence social well-being via discord and connect with online communities and a few also wanted her to develop hobbies or indulge in them in a way to relax in evenings apart from her regular work time and exam preparations. This again emphasises on the role of BIAS in thinking, thoughts and design thinking. How each respondent has come up with a different way of managing time for hypothetical Nithya and how she should spend her time. It is hence significant to note the role that bias, emerging out of our social, emotional, cultural and environmental circumstances shapes the design solution. It can hence be inferred that the design solution will differ from person to person who is in charge of a project, and hence, the selection of a designer is a crucial step in any design/management/educational/private/NGO or any other organisation. The

bias of the designer will shape the design solutions and future of the organisational objectives.

5 Summary

The paper begins with highlighting the role of creativity, cognition, bias in developing a design solution. The authors carry out two experiments to prove that bias has an important role to play and it emerges from the social, cultural, environmental and emotional circumstances of the designers experiences and upbringings. The paper highlights that if the selection of a designer or design educator is done in a certain manner, the outcome of organisational project objectives will differ from person to person. A more emotional or more social or more cultural or more sustainable or more technological or any other kind of output may be received depending on the project in-charge. Personality and bias will have a key role to play in the design solution of the project undertaken; hence, selection or recruitment of designer has to be done meticulously to form a team leader and a team who is handling a project in an organisation. The paper urges design researchers and leaders to have a convergent and divergent approach as and when needed but choose the design lead carefully as the success or fulfilment or the nature of deliverable solely lies on the bias of this design lead.

References

1. Smith SM, Ward TB, Finke RA (2009) The creative cognition approach. MIT Press, Massachusetts
2. Ward T, Smith S, Finke R (1998) Creative cognition. In: Sternberg R (ed) Handbook of creativity. Cambridge University Press, Cambridge, pp 189–212. https://doi.org/10.1017/CBO9780511807916.012
3. Ward TB, Smith SM, Vaid J (2001) Creative thought: an investigation of conceptual structures and processes. American Psychological Association
4. Deepshikha (2023) Teaching creativity as a fundamental design practice. In: Chakrabarti A, Singh V (eds) Design in the era of industry 4.0, Volume 3. ICORD 2023. Smart innovation, systems and technologies, vol 346. Springer, Singapore, pp 813–824. https://doi.org/10.1007/978-981-99-0428-0_66
5. Deepshikha (2022) Design and creativity in fashion, textiles and accessories domain. In: The proceedings of virtual international conference—tracing seventy-five years of Indian fashion post independence. NIFT Gandhinagar, 20–21 Jan 2022
6. Chan CS (2015) Introduction of design cognition. In: Style and creativity in design. Studies in applied philosophy, epistemology and rational ethics, vol 17. Springer, Cham. https://doi.org/10.1007/978-3-319-14017-9_2
7. Cross N (2011) Design thinking. Bloomsbury, India
8. Lockwood T (2009) Design thinking integrating innovation. Allworth Press, New York
9. Foster MK (2019) Design thinking: a creative approach to problem solving. Sage Manage Teach Rev 6(2). https://doi.org/10.1177/2379298119871468

10. Razzouk R, Shute V (2012) What is design thinking and why is it important? Rev Educ Res 82(3):330–348. https://www.jstor.org/stable/23260048
11. Goleman D (1995) Emotional intelligence. Bloomsbury, India
12. Norman D (2005) Emotional design. Basic Books, NY
13. Goleman D (2006) Social intelligence: the new science of human relationships. Bantam Books, New York
14. Yang X, Zhang M, Zhao Y, Wang Q, Hong J (2022) Relationship between creative thinking and experimental design thinking in science education: Independent or related. Thinking Skills Creat 46:101183. https://doi.org/10.1016/j.tsc.2022.101183
15. Blessing LTM, Chakrabarti A (2009) DRM, a design research methodology, 1st edn. Springer Publishing Company, Incorporated
16. Reich Y (1995) The study of design research methodology. ASME J Mech Des 117(2A):211–214. https://doi.org/10.1115/1.2826124
17. Cross N (1993) Science and design methodology: a review. Res Eng Des 5:63–69. https://doi.org/10.1007/BF02032575
18. Jilcha Sileyew K (2020) Research design and methodology. IntechOpen. https://doi.org/10.5772/intechopen.85731

Textile Crafts of Bharat

Deepshikha and Avinav Krishna

Abstract The origin of Indian textiles dates back to Indus Valley Civilization. The vibrant tradition and culture are deeply embedded in the textile crafts. They are arduously handmade that render a beautiful texture, quality, story and embed memories as traditional artifacts are transferred from one to another generation. Cotton and silk are primarily used for textile crafts apart from jute and wool owing to the climatic conditions. The rich flora and fauna as well as mythological themes are intricately represented by the artisans with skilled handicraft work. The paper presents content curated for various textile crafts in India broadly categorized into the following categories—painted textiles, printed textiles, woven textiles, resist technique and embroidered textiles. The paper summarizes into present status and steps that may be taken for preservation of the textile craft heritage.

Keywords Craft · Tradition · Nature · Heritage · Culture

1 Introduction

The paper presents content curated for various textile crafts in India broadly categorized into the following categories—painted textiles, printed textiles, woven textiles, resist technique and embroidered textiles. Painted textiles include Kalamkari, Pabuji ki phad, Mata ni pachedi, Pichwai and Rogan art. Printed textiles include Sanganeri, Bagh and Bagru, Dabu and Ajrakh. Woven textiles include Maheshwari, Pashmina, Banarasi, Kanjivaram, Tangaliya, Paithani, Kullu Shawls, Kasavu Sarees, Jamdani, and textiles from North East—Mekhla Chador, Phanek and Naga Shawls. Resist-dyed textiles include Bandhani, Patola, Pochampally and Sambalpuri weaving and Batik. Embroidered textiles include Zardozi, Crewelwork, Tilla, Namda, Chikankari,

Deepshikha (✉)
Design and Innovation, Jamia Millia Islamia, Delhi, India
e-mail: deepshikhajha@gmail.com

A. Krishna
International Relations, South Asian University, Delhi, India

© The Author(s), under exclusive license to Springer Nature Singapore Pte Ltd. 2025

B. B. V. L. Deepak et al. (eds.), *Recent Advancements in Product Design and Manufacturing Systems*, Lecture Notes in Mechanical Engineering,
https://doi.org/10.1007/978-981-97-6732-8_54

Kutch Embroidery, Chamba Rumal, Pipli, Kantha, Kasuti and Phulkari. The paper summarizes into present status and steps that may be taken for preservation of the textile craft heritage.

2 Painted Textiles

Painted textiles include Kalamkari, Pabuji ki phad, Mata ni pachedi, Pichwai and Rogan art.

2.1 Kalamkari

The two main centers of practicing Kalamkari art (Fig. 1) are Machilipatnam and Kalahasti in Andhra Pradesh [1, 2]. The origin of the word Kalamkari is supposed to be from Persian language, where 'Kalam' means 'Pen' and 'Kari' refers to craftsmanship. It may be done on paper or textile and involves 17–23 stages from preparation of base fabric to painting and washing of fabric. Textiles with Kalamkari art on it belong to the category of painted textiles of India. The base fabric is first treated with water and cow dung mixture for bleaching the fabric naturally. Then the fabric is washed and dried in the sun and later washed in myrobalam and buffalo milk. Myrobalam seeds from the tree render the fabric an off-white shade and act as mordant to fix dyes to be applied later while the fat from buffalo milk helps in preventing the dye from spreading when applied. The fabric is dried and the outline is made first in black or red and then colors are added from light shade to dark shade that is yellow, green, blue, red and black in sequence. Wax may also be used to resist the fabric from color seeping into regions not required while dipping in a dark color dye, some kalamkari may also follow the wax resist process. The textile may be painted with brush made of squirrel hair or printed with blocks hand-carved from wood. Motifs are design elements that adorn the textile or paper. Motifs in case of Kalamkari include Hindu mythological scenes, flora or fauna. The design may cover the entire surface with intricate details or may be present as buti (isolated medallions or floral patterns) designs in repeat format all over.

2.2 Pabuji Ki Phad

It is a religious scroll painting of Rajasthan depicting a local folk deity—Pabuji (Fig. 3). 'Phad' means 'scroll' [3]. After dusk, a narrator (Bhopas—bard priests belonging to the Nayaka community) moves from village to village with the phad and narrates the story in a musical rendition while playing a violin-like instrument with 18 strings called 'ravanhaatha.' The three parts of the story include the epic

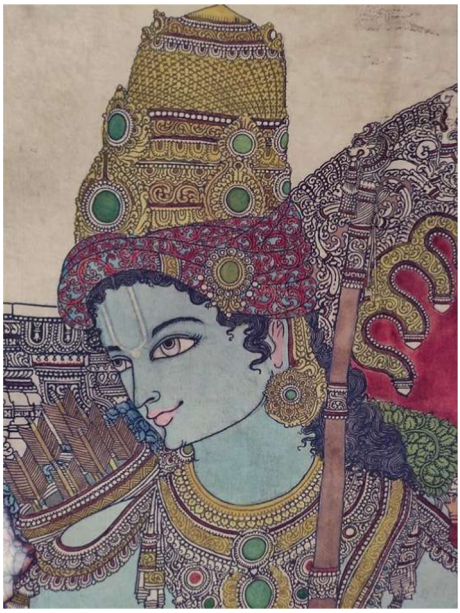


Fig. 1 Kalamkari—mythological figure [7]



Fig. 2 Pichwai [7]



Fig. 3 Pabuji ki phad [7]

story of Pabuji, the fourteenth-century Rathore chief and the incarnation of the Hindu God who is worshiped by the Rabari tribals in certain parts of Rajasthan. The phad is 15 ft by 15 ft in size, a cloth with vivid imagery of the life scenes of Pabuji. The phad depicts the palaces and forts of Pabuji, his companions, his incarnation as Hindu Lord Lakshmana, medieval Rajasthan villages in the backdrop, kings, queens, battlescenes, elephants, peacocks, horses, cows and camels, many armed demons and Pabuji's magnificent Black mare known as Kesar Kalami. These are all depicted in a two-dimensional manner. The narration follows a sequence, it begins with purification rites, tying of the phad on wooden or bamboo posts, the bhopa announcing the beginning of narration by blowing a conch shell, devotes offer money and grains to the deities, the deities depicted on the phad are invoked, the narration of the epic story, collection of monetary donations at the end and a concluding prayer song—arati with a lit up traditional lamp.

2.3 Mata Ni Pachedi

The nomadic Vaghari community of Gujarat was not allowed to enter temples; hence, they created their own painted sacred textile depicting goddess to be worshiped in the center and other themes around the central element of the goddess [4]. The entire piece of rectangular fabric is divided into seven columns to create a narrative format and only black and red color are used for the artwork on a base of beige cotton



Fig. 4 Mata ni Pachedi [7]

material. Chitaras are the artists who create the artwork, Jagorais are the singers who narrate the stories while Bhuva are the priests who perform rituals. Bamboo and dates stick are used as brush to fill colors and blocks are used for printing the borders. The fabric is detsarched by soaking in water for 24 h then soaked in tamarind paste and washed and dried in the sun. Black is prepared by rotting iron in jaggery and fermenting and this is used for outlines and black color fillings to emphasize the drawings. The red color is made by heating water, tamarind and alum (which makes the fabric yellow) and then fabric is boiled in alizarin (which reacts with alum) to bring out the red color. It resembles the Kalamkari folk art form of Andhra Pradesh. Mata ni pachedi (Fig. 4) translates into 'behind the mother Goddess.' The goddess is often depicted on her five animal carriers/vehicles known as 'vahanas'—crocodile, cock, sheep, goat and camel.

2.4 Pichwai

Pichwai (Fig. 2) translates into 'hung at the back' [5]. It is beautiful rendition of Hindu Lord Krishna's imagery in various themes such as Holi, Raas Leela, Janmashtami, Gopashtami, Sharad Poornima, Goverdhan Pooja and various other events, festivals and anecdotes from the life of Lord Krishna. It is hung behind the main deity Krishna as Lord Shrinathji, a 700-year-old version of Lord Krishna in the Nathdwara Temple (1672) of Rajasthan belonging to the Pushtimarg devotional tradition. Originally Pichwai was made on handspun cotton fabric which was starched. The artists would paint the images using handmade brushes and tools and natural colors such as indigo, gold, silver, saffron and other brilliant colors.

2.5 Rogan Art

Rogan art (Fig. 5) is being practiced by two families in Kutch Gujarat, the Khatris of Nirona [6]. It is nearly a 400-year-old art form which nearly died until these two families revived it. Castor oil is boiled for two days to make a thick base to which vegetable pigments and a binding agent are added to create a thick and shiny paint. Artists either block print the fabric with this paint or paint with brush on the textile. The textiles decorated with Rogan art were mostly purchased by women of lower castes to decorate wedding trousseau or bed coverings with beautiful fabrics. Colors are bright and vivid and designs include peacocks, geometric designs, flora and fauna of Rajasthan.

3 Printed Textiles

Block printing [8–10] is popularly done in Rajasthan and Gujarat, and, also in other parts of India—Madhya Pradesh, Andhra Pradesh, Tamil Nadu, Uttar Pradesh and West Bengal. Types of block printing (Fig. 6) include Sanganeri, Bagh and Bagru, Dabu and Ajrakh. Each type of block print has its own elaborate process of preparing the fabric, printing the different colors on designs, washing and drying the fabric. Making the blocks—Block of required size is cut from a seasoned wood

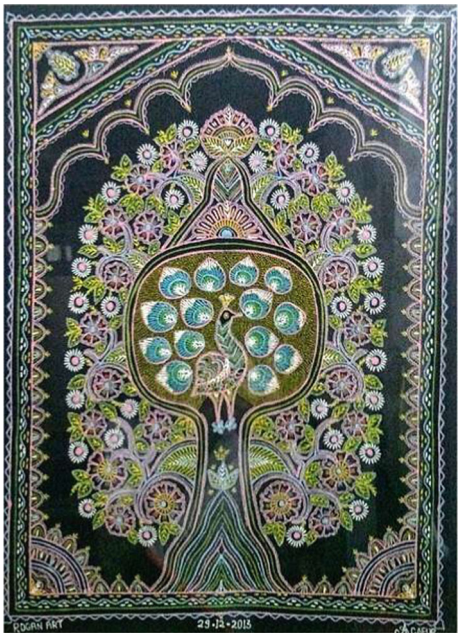


Fig. 5 Rogan art [7]



Fig. 6 Wooden blocks; printing with block; and, printed fabric **(L-R)** [8, 9]

and smoothened to level the plane. The surface is dipped in water; a layer of clay is added and rubbed against stone surface to create a whitish layer. Area is marked and design is transferred through a stencil prepared earlier. A kalam (needle/pen) is used for carving; the size of the needle is decided according to the level of intricacy required. Mustard oil or sometimes water is used to clean the blocks before and after use. Motifs include varied forms of flora and fauna in isolated butis (isolated design elements in straight or alternate repeat patterns), floral patterns, creepers, animal motifs, narratives, etc. Textile material is mostly cotton, sometimes silk. Although initially natural colors were used, synthetic colors of a wide range are being used contemporarily.

There are three techniques of printing—direct, resist and discharge. In direct printing, the base fabric is bleached; the fabric is dyed to a base color if required or left undyed. Printing is done using carved blocks and color mixtures as per the design. The outlines are printed first and the colors are filled light to dark. In resist printing, wax or clay resist is applied on areas to be protected from dye. The fabric is dyed and washed and later designs are printed through blocks where required. Ajrakh and Kalamkari with block prints use this technique. In discharge technique, fabric is first dyed and then areas with designs are treated with chemical to remove the dye applied and re-printed with required designs with blocks. In general, fabric to be printed is washed and bleached according to the design, if needed. Then the fabric is stretched on a long table and held in position with several pins. Colors are mixed with glue and pigment binder and kept separately in trays and evened out for smoothness of application. Block is dipped into the lighter colors and pressed firmly on the fabric with hand. Darker colors follow the lighter colors. Prints are allowed to dry, steamed, washed in water, dried and ironed. Figure 3 represents blocks and block printing.

4 Woven Textiles

Woven textiles include Maheshwari, Pashmina, Banarasi, Kanjivaram, Tangaliya, Paithani, Kullu Shawls, Kasavu Sarees, Jamdani, and textiles from North East—Mekhla Chador, Phanek and Naga Shawls.



Fig. 7 Maheshwari saree

4.1 Maheshwari Sarees

History narrates that the ruler of Indore (a city in Madhya Pradesh, India) designed the Maheshwari sarees [8, 9, 11, 12] to be presented as gifts to the Peshwa Kings. Several weavers were summoned from different parts of the country and established in the small town of Maheshwar, thus naming the craft Maheshwari (Fig. 7). Products include sarees, scarves, salwar kameez fabrics, among others. Saree is a 5.5 m. long fabric draped by women, while salwar kameez is a two-piece tunic-bottom combined with a long rectangular 2–2.5 m. scarf termed as dupatta. Motifs have largely been drawn from architectural elements from the Fort of Maheshwar (Fig. 7) which are primarily inspired from flora, fauna and Mughal-style jaalis (architectural screens). The various elements form different parts of textile (sarees, scarves, etc.). Some common motifs include the brick pattern (linth), woven mat pattern (chatai), flowers (chameli, bel, etc.), elephant, peacocks, etc. Material used is cotton threads of 100 count, silk of 20/22 denier for border and 2/100 for the body of the textile. Textiles may be woven as single ply, two ply or three ply according to the design. The weight of the saree could be as low as 175 gms. Although initially only natural dyes were used, synthetic dyes are common these days. Colors used have local terms, like, light green (angoori), dark green (dhaani), pink (rani), magenta (gul bakshi), purple (jaamla), teal (chintamani), etc.

4.2 Pashmina Weaving

Changpa pastoralists raise Changthangi goats in a difficult environment at an elevation of 4000–5000 m close to eastern Ladakh [13–16]. Every family possesses at least 100 animals, with sheep and goats numbers being equal. Additionally, a household may raise 200–300 games of raw pashmina from a single goat in a year. A



Fig. 8 Pashmina weaving [13–16]

large number of Changpa's are leaving their current cattle and seeking work in other fields. The Changpa households sell raw pashmina to Kashmiri traders for 8000–9000 INR; 20,000 INR may be charged if the pashmina is in great demand or of exceptional quality. When woven into shawls, the cost might reach lakhs for shawls with an entire woven pattern, 30,000 INR for shawls with borders, and 10,000 INR for plain shawls. After being cleansed and combed to remove any tiny fibers from the threads, the wool is hand spun on a charkha. The wool trader separates the warp and weft. At this point, the yarns are transformed into warp-ready bobbins and colored if necessary. When the designs are complete, a writer writes them down in hieroglyphic script, which the weaver reads aloud while weaving. In contrast to Urdu, which is read left to right, Talim is read right to left. A single pashmina shawl can be woven in ten to fifteen days. Some typical motifs seen in pashmina shawls include Badams, Panjdar, Cheet misri, Kev Posh, Gul-e- noor jehan, Gulabkan, Yumberzal Posh, Marder, Gulkar, Ragas Chinar, and Taj (Fig. 8).

4.3 Banarasi Weave

Some of the weaving techniques include Ektaar, Kadhiyal, Kadhwa, Phekwa, Tanchoi and Meenakari [11, 12]. Ektaar or Ektara looks similar to advanced needle point work. A mesh-like fabric that does not crumple readily is created. It is generated by a multi-warp heddle shaft or five-treadle technique on a traditional pitloom. Kadhiyal or Korvai is a weaving technique employing three shuttles to create the upper and lower border of the saree which are interlocked together. Korvai is also common in Kanchipuram. Kadhwa or Kadha hua refers to 'embroidered.' Two artisans work on the saree for 12–14 days minimum; it might take months depending on the complexity of the patterns being generated. One weaver weaves the body of the saree while other embroiders on top such that there are no floats on the back using a wooden spool or tilli. Due to the flexibility of embroidering onto the fabric while being woven multitude of patterns can be generated on the same saree with much freedom and dexterity. Phekwa is the most commonly used technique in Benarasi sarees



Fig. 9 Benarasi saree [19]

where weft is interlaced in the warp from end to end creating textures. It is easier and faster than Kadhwa sarees and more popularly available. Tanchoi sarees use an extra weft buti design technique to create patterns on warp and are one of the most intricate weaving techniques. Meenakari is similar to the enameling handicraft of Uttar Pradesh and Rajasthan. Up to 20 colors of silk or zari can be used as weft to create patterns using Kadhwa or Tanchoi technique. The pattern generated is so complex due to the maximum number of colors involved that even a jacquard loom cannot replicate the handmade design. It is popularly used for weddings and festivals by women for wearing and gifting in North India. Benarasi saree (Fig. 9).

4.4 Kanjivaram Saree

Kanjivaram sarees [11, 12] are woven sarees made in Kanchipuram, Tamil Nadu, for bridal trousseau and festivals and other special occasions (Fig. 10). It received GI tag from the Government of India in 2005. These sarees are made in pure mulberry silk and are known for their wide contrasting borders with temple design, stripes, checks, waves and floral motifs. Temple border refers to triangular motifs all along the sides of the border. The motifs are derived from paintings of Raja Ravi Verma, Temple architecture, Hindu epics of Ramayana and Mahabharata. The sari and the border are woven separately and interlocked later.

4.5 Tangaliya Weaving

Tangaliya [11] is a 700-year-old hand-weaving technique practiced by Dangasia Schedule Caste community in Surendranagar district, Gujarat (Fig. 11). It is very tedious and labor-intensive process. Geometric designs are produced on warp by twisting contrasting threads onto the warp creating dana or dots or bead work.



Fig. 10 Kanjivaram Temple border [20]



Fig. 11 Tangaliya weaving [21]

4.6 Paithani Weaving

Paithani sarees are originated in Paithan, Aurangabad, Maharashtra [11, 12, 17, 18]. The sarees are known for their bright colors and symbolic motifs such as peacocks, parrots, lotus, swan, ashavali (floral vines), coconut and other forms of flora and fauna that bestow the newly married couple with prosperity (Fig. 12). These motifs have been largely derived from the world-famous cave paintings of Ajanta in Maharashtra. The history of weaving can be traced to second century BC, the Satvahana dynasty. Essentially woven in silk, it forms a part of bridal trousseau in Maharashtra. Colors are largely Aboli (pale bittersweet), Firozi (cyan), Gujri (black and white), Kalichandrakala (black), Mirani Morphankhi (cerulean), Motia (pale pink), Neeligunji (blue),



Fig. 12 Paithani Peacock and lotus motif [17]

Pasila Pophali (chrome yellow), Samprus (green–red), Sankirodak (white), Uddani (a fainter black) and Vangi (aubergine purple) combined with zari gold threads.

4.7 Kullu Shawls

Kullu shawls are fine woolen woven shawls generally of plain body but patterns may also be seen [11]. Kullu is a municipality in Himachal Pradesh and was the artifact originated. The wool may be from Yak, sheep or pashmina wool. Colors are often bright but pastels are also seen. Geometric design borders may be present at both ends (Fig. 13). Kullu shawls help the locals in occupation, income and to promote tourism.



Fig. 13 Kullu Shawl on loom and on display [22]



Fig. 14 Kasavu Sarees [23]

4.8 Kasavu Sarees

Kasavu sarees (Fig. 14) essentially belong to Kerala and date back to the Buddhist era [11, 12]. It is an off-white cotton or silk saree with gold border made of intricately woven pattern. While women wear sarees, men wear mundu (cloth tied at waist) and veshtu (cloth used to cover upper body). Dance forms of Kerala—Mohiniyattam, Kaikottikali and Thiruvathirakkali—have performers wearing Kasavu sarees. Women wear a green, gold or red blouse with the saree while men might wear a shirt to pair with the mundu.

4.9 Jamdani Sarees

Jamdani weaving (Fig. 15) originated from Dhaka, Bangladesh, and is widely practiced in West Bengal, India [11, 12]. Since it originated from Dhaka, it is also called Dhakai or Dhakai Jamdani. Designs are largely geometric on a fine cotton muslin fabric. Sarees and salwar kameez are the most popular apparel made out of Dhakai apart from scarves and handkerchiefs. The geometric designs are intricately wound on to the warp on loom using bamboo sticks and spools.



Fig. 15 Jamdani saree [24]

4.9.1 Textiles from North East India—Assamese Silk Weaving, Phanek, Naga Shwals

Sualkuchi is the center for Silk weaving (Fig. 16), located near Guwahati in Assam [11]. 'Sual kuchi' refers to 'silk village.' Beige mua silk is richly decorated with flora, fauna and motifs from the tribes and dynasties of the land. Mekhla chador is a common apparel worn by women unlike sarees in the rest of the country. Mekhla is a rectangular piece of fabric wrapped around like a skirt, a blouse and shawl called chador is wrapped further across the mekhla and the blouse from over the shoulder. Phanek (Fig. 17) is a wrap worn by Manipuri women accompanied by a shawl. They are woven on backstrap looms or loin looms and stitched together to form a longer rectangular piece. Black and red are very important colors for Tangkhul tribe. Tsüngkotepsü and Chakhesang Naga shawl (Fig. 18) belong to the Ao Naga and Chakhesang Naga tribe. Each tribe of northeastern state has its specific motifs with specific significance. For example, Tsüngkotepsü Ao Naga shawl can be worn only by a Naga warrior who successfully has taken the heads of enemy during a war.



Fig. 16 Assamese silk weaving—motifs on mekhla chador—Bodo tribe Arnai Design, Joon biri and King khap pattern of the Ahom dynasty [25]



Fig. 17 Manipuri textile, phanek and shawls [26]



Fig. 18 Ao Naga shawl—Tsüngkotepsü and Chakhesang Naga shawl [27]

5 Resist Technique

Resist-dyed textiles include Bandhani, Patola weaving, Pochampally weaving, Sambalpuri ikat and Batik.

5.1 Patola Weaving

Patola (Fig. 19) is a double ikat woven saree from Patan, Gujarat [11]. The process is kept so secretive that the weavers do not weave even in front of their daughters, as they might carry the knowledge away after marriage when they change households. The warp and. Weft yarn are separately tied and dyed according to the pattern. Then the knots are opened and warp is mound on the loom and weft is wound on the spool for shuttle weaving. Since both warp and weft are tied dyed, it is a double ikat. The Salvi caste is known to practice the craft. The Jain and Hindus prefer to wear



Fig. 19 Patola double Ikat [29]

ikats adorned with elephants, parrots, flowers and dancing figures while the Muslims prefer to wear only geometric and floral designs.

5.2 Pochampally and Sambalpuri Ikat

Ikat is practiced in Gujarat, Odisha and Telangana [11]. Pochampally ikat (Fig. 20) is practiced in Telangana. Ikat heer is locally termed as Paagadu Bandhu and Chitki in different regions. The handkerchiefs made from ikat weaving are called telia rumal. It follows tie-dye of both warp and weft, hence is a double ikat. Silk and cotton both are used. GI status was granted in 2005. Distinct features of pochampally ikat are the hazy pattern due to ikat dyeing and same design on front and back of fabric is seen with same intensity of colors. Sarees, dress materials and bedsheets are also made from ikat technique. Wide variety of vibrant colors is used. Designs are mostly geometrical—squares, triangles and wave-like patterns all over the body. Sambalpuri Ikat (Fig. 20) is also warp and weft-resist dyed before weaving and crafted popularly in Sambalpur, Balangir, Bargarh, Boudh and Sonepur districts of Odisha, India. Motifs are dominated by flora, fauna, geometric and few mythological motifs. Colors are varied and vibrant.

5.3 Bandhani

Bandhani (Fig. 21) is derived from 'bandhana' or 'bandhej' which means 'to tie' [11]. Cotton threads are used to tie intricate knots all over the fabric and dyed part by part allowing the dye to seep and mix to create an ombre effect. More the number



Fig. 20 Pochampally Ikat [30] and Sambalpuri Ikat [31]

and intricacy of knots, expensive the textile becomes. Originally natural dyes were used—madder for red, sunflower for yellow, turmeric for yellow, indigo for blue but now a variety of artificial colors are used. The bandhej fabrics are sold with the cotton thread knots still tied to the fabric to prove that the fabric is not printed. Intricate craftsmanship renders a rippled texture to the fabric. Each community in Rajasthan has a specific pattern. Pattern for male turban bandhej fabric is different from female saree patterns. A Hindu bride wears a red bandhej saree (suhagadi), a mother-to-be wears a yellow bandhej saree (satbhateli) while a widow wears a plain black saree with bandhej only at the borders (jimli). The popular designs have been named Leharia (wave like), Mothra, Ekdali, Shikari, Khombi (white dots on red cloth), Gharchola (wedding scarf or odhni), Patori, Chandrokhani (moon like).

Fig. 21 Bandhani [32]





Fig. 22 Batik, West Bengal [33]

5.4 Batik

It is mostly carried out in West Bengal, Khatris in Gujarat, Cholamandal Artists in Tamil Nadu apart from other craft clusters in the country [28]. It is a 2000-year-old ancient technique of painting design with wax on a stencil-made design, drying, dyeing and scraping off the wax (Fig. 22). The process is repeated as many colors are used in the art form. The dye seeps through cracked wax creating striking visual textures. Batik is widely practiced in Indonesia, Malaysia and Japan and other regions of the world, but each country has specific cultural influences over design and technique. The motifs have religious connotations or are geometric and abstract.

6 Embroidered Textiles

Embroidered textiles include Zardozi, Crewel, Tilla, Namda, Chikankari, Kutch Embroidery, Chamba Rumal, Pipli, Kantha, Kasuti and Phulkari.

6.1 Zardozi Embroidery

It emerged under the patronage of Mughals who brought the technique from Persia [8]. Originally, gold threads were used with precious and semi-precious stones for embellishing the fabric (Fig. 23). In recent times, it is one of the most popular crafts retained on contemporary and traditional styles of apparels and accessories. The karigar (craftsman) sits on the floor with a square adda (frame for embroidering). An Aari (V-shaped needle with hook) is used for the purpose from the top surface,



Fig. 23 Zardozi embroidered fabric [8, 9]

while thread is pulled from the bottom surface and gems are added according to the design from the top surface. Figure 4 represents a zardozi embroidered fabric with floral design.

6.2 Crewel Embroidery

Crewel embroidery (Fig. 24) is an old chain stitch embroidery technique practiced in Kashmir typically on cotton or linen fabric as base [34]. A hook called Aari is used for the chain stitch. Stylized flora and fauna from the rich environment are translated onto the fabric by the artisan. Tree of life, maple and djacobian are the most common designs. The colors are mostly vibrant. The embroidery could be of 1ply or 2 ply woolen yarns which offers a range from low to high while selling the products. The artisan first makes the design on paper and punches holes throughout the lines of the design. Following this, the punched paper is kept on the based fabric and ink is soaked through the pores of the punched paper to translate the design onto the fabric. After this, the artisan embroiders with varied colors, washes and irons the fabric to make it ready for sale. Designs such as pamposh (lotus), sarav (cypress), sosan (iris), dainposh (pomegranate), gulab (rose), other flowers along with rabbits, deer, lion, horses and birds are also commonly seen in crewel embroidery.

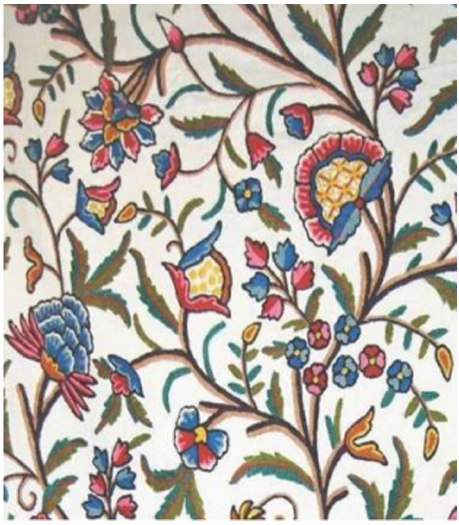


Fig. 24 Crewel embroidery [37, 38]

6.3 Tilla Work

The origin of Tilla dozi (Fig. 25) is believed to have been the Zari village in Persia from where migrated Shah-e-Hamdan with 700 artisans and made their way to Kashmir [34]. The craft grew under the patronage of Mughals who took great interest in art and cultural traditions. Originally, the embroidery was done in real gold and silver threads for bride's apparel and accessories but now artificial threads are used. The design is transferred to fabric just like that of crewel embroidery and the process is termed as 'Trombun.' After embroidering the fabric is washed and ironed.



Fig. 25 Tilla work on traditional Kashmiri women's apparels [39, 40]



Fig. 26 Namda decorated with crewel embroidery [41]

6.4 Namda

Namda (Fig. 26) is made by felting woolen fibers together by applying water and soap under high pressure [35]. Mazenderan, Iran, is supposed to be the birthplace of this craft brought to India by the Mughals under whose patronage Nubi was granted villages to promote this craft. It is often embroidered with crewel embroidery and used commonly as rugs and prayer mats in Kashmir and other parts of the country. They are popular as they complement wooden interiors of Kashmiri domestic architecture. Wooden floorings decorated with namda depict an oriental set-up and keep the interiors warm in harsh weather conditions. Cotton may also be mixed with low-quality wool (sheep fleece) while preparing namdas. The artisans believe that Hakim Lukman was worried about how the wool may be felted and could not find a way. Hence, he started crying in despair. As tears rolled into the wool and bound it together, it was learned that water may bind wool together to create this unique texture of namdas. Hashi is the border that demarcates the central pattern of tessellations of octagons or squares or other geometric patterns as seen in Mughal jalis. Aemberzul is an eight petalled flower that represents daffodil. Gul-i-akhtab is derived from sunflowers. Most of the patterns are either geometric or floral.

6.5 Chikankari

Chikankari (Fig. 27) is practiced in Lucknow, Uttar Pradesh, and is believed to have been brought from Persia under Mughal patronage [36]. Originally, Chikankari was done as white and white but these days variety of background colors are adorned with the craft. The base fabric is chiffon, organza, muslin or silk. Popular stitches include Tepchi, Bakhiya, Hool, Zanzeera, Rahet, Banarsi, Khatau, Phanda, Murri, Jali, Turpai, Darzdari, Pechani, Bijli and many more. GI tag was given to Chikankari



Fig. 27 Intricate Chikankari floral design [42]

in 2008. Bakhia or shadow work is the most popular where the embroidery is done on the back side of the fabric and the shadow is seen on the front side. Mukhaish is a zari technique often accompanying Chikankari as a simple adornment.

6.6 Kutch Embroidery

It originated in nomadic communities of Kutch, Gujarat and dates back to sixteenth–seventeenth centuries [34]. There sixteen different types of embroideries—Aari, Gotauvn, Hekan, Chopad, Katri and Mukko, Jat-Garasia and Jat-Fakirani, Kambira and Khudi-Tebha, Kharek, Neran, Pakko, Rabari and Soof. The base fabric is cotton or woolen silk or mashru. Threads may be cotton or silk. Mirrors, sequins and conch shells are often used to accessorize the embroidery (Fig. 28). Mirrors are used toward of evil eye. The designs are inspired from nature or daily lifestyle—peacock, parrot, camels, elephants, dancing postures, etc.

6.7 Chamba Rumal

It flourished under the patronage of Chamba kingdom in Uttarakhand [34]. One of the earliest Chamba Rumal has been considered to be the one the sister of Guru Nanak Dev, Bebe Nanaki made in sixteenth century. Chamba rumal (Fig. 29) is used as wedding gift or as covering for offerings during religious ceremonies. The themes include Lord Krishna and his life, Geetgovinda and Bhagvat purana, geometric designs and flora and fauna. It is a square or rectangular piece of muslin or khaddar embroidered with silk threads. A fabric border is stitched to the four sides to contain the fine needle work within a frame.



Fig. 28 Kutch embroidery [43]



Fig. 29 Chamba Rumal [44]

6.8 Pipli

Pipli (Fig. 30) is an applique work that's originates from Pipili in Puri district, Odisha [34]. There are two types of applique—one, where a piece of fabric is embroidered on a base fabric and second, the top fabric is cut out in desired shape and edges are embroidered to reveal the base fabric, reverse applique. Colors used are vibrant red, blue, yellow and green with white edges. It is commonly used to depict Lord Jagannatha from Puri, Odisha and used to embellish parasols and canopies during festivals. The designs may also include elephants, peacocks, ducks, parrots, creepers and geometric designs. Several souvenirs—wall hangings, home accessories and apparels—are decorated with Pipli.



Fig. 30 Pipli work, Odisha [45]



Fig. 31 Kantha embroidery [46]

6.9 Kantha

Kantha (Fig. 31) is an embroidery carried out by women in West Bengal, Jharkhand and Odisha [34]. Quilts adorned with Kantha embroidery are called Nakshi Kantha. The motifs are largely raw geometric depictions of nature and daily life. Running stitch embroidery is the prime characteristic of the craft. It is mostly done on off-white muslin fabric but several colored base such as silk or cotton in black, blue, red, orange and other hues are seen contemporarily. Sarees and kurtas for both men and women have becomes a part of fashion statement.

6.9.1 Kasuti

Kasuti (Fig. 32) is a dying folk embroidery of Karnataka [34]. The designs follow a strict grid pattern with four different kinds of stitches on both sides of the fabric rendering the same design on the front and back of the fabric. The knots at the



Fig. 32 Kasuti, Karnataka [47]

beginning and end of embroidery are exclusively hidden so as to not reveal the beginning or end of the embroidery. All representations of flora, fauna, chariots, palanquins, conch shells, geometric designs are essentially in straight lines on a grid pattern. The four stitches are—Gavanthi, Murgi, Negi and Menthi. Gavanthi is a double running stitch, Murgi is a zig-zag stitch, Negi is a running stitch and Menthi is a cross stitch.

6.9.2 Phulkari

Phulkari (Fig. 33) originated in Punjab and is usually a part of the bridal trousseau [34]. Phulkari translates into floral work but includes several geometric designs as well. When phulkari covers the entire fabric with embroidery, it is called as Bagh. Chope is embroidery done along the borders. Leheriya bagh refers to designed as waves, 'satranga' means embroidery with seven colors and 'panchranga' means embroidery with five colors. The base fabric is coarse khaddar upon which silk threads are used to carry out the embroidery.



Fig. 33 Phulkari [48]

7 Summary

India is home to plethora of traditional and centuries old arts and crafts but with industrialization and globalization the arts and crafts have been on a gradual decline. Handicrafts are time taking, painstaking and expensive to make and hence are not able to compete with the cheaper and faster produced machine-made products. Many manufacturers crate knock offs of traditional crafts and sell them readily in cheaper materials. Availability of original crafts is also a concern as not everyone is aware of where and for how much the original craft can be purchased; however, the machine-made goods are readily available through online and offline retail channels. Many artisans have moved to cities as the crafts do not pay them sufficiently to meet the demands of their family. Younger generation does not follow the hierarchical occupation and moves to nearby towns and cities in search of better opportunities and lifestyle.

Designers however have worked extensively in the last three decades in India along with NGOs and the Ministry of Textiles to promote and preserve the traditional crafts. Many designers have launched brands that sell authentic craft products via online and offline channels. Awareness programs and post-covid training have been conducted by NGOs and Government to promote online selling directly from the artisans to the end customers. Many brands such as Gocoop, Itokri, Crafts council of India, Anokhi, Fab India and others have been extensively promoting crafts. Start-ups have also grown popular in the domain and have penetrated through design intervention and retail channels. Many measures may further be suggested to improve the conditions of the artisans in India. Craft education could be made compulsory at school level. Institutes of national importance and ministries may implement uniforms made out of traditional crafts. Increased patronage by regional ministries may be given to regional crafts. Souvenirs and mementoes for major events could be made specifically from the heart of craft villages in India. The Ministry and start-ups may conduct trade fairs, exhibitions and fashion shows to promote Indian handloom and handicrafts extensively in India and abroad.

References

1. Vijaykumar N (2016) From Madhubani to Kalamkari, 10 Indian Folk Art Forms That Have Survived Generations. Retrieved June 2023 from https://www.thebetterindia.com/53993/10-indian-folk-art-forms-survived-paintings/
2. Ramani S (2021) Kalamkari & Traditional Design Heritage of India. Wisdom Tree, Delhi, pp 1–117
3. Wickett E (2010) World Oral Literature Project—Voices of vanishing worlds. University of Cambridge. Museum of Archaeology and Anthropology. Cambridge, UK, pp 1–32
4. Erikson J (1968) Mata ni pachedi—a book on the temple cloth of the mother goddess. National Institute of Design, Ahmedabad, Gujarat, pp 1–25
5. Ambalal A (1987) Krishna As Shrinath Ji. Mapin Publishing Pvt Ltd., Ahmedabad, pp 1–177
6. Sharma S (2020) Rogan art: a coffee table book. NIFT, Gandhinagar, India, pp 1–28. Retrieved June 2023 from https://issuu.com/soumyasharma3021/docs/ctb_final_print

7. Senthilvel R.S (2022) 52 Incredible Indian Folk Art Forms That We Must Protect in Indian Art and Culture. Retrieved June 2023 from https://indianfolkart.org/52-indian-art-and-culture/
8. Deepshikha (2020) Textile crafts: the middle path. In: International AIC 2020 conference: association of color international. Avignon, France
9. Deepshikha (2023) Textile crafts incorporated in this tech-savvy world. AbirPothi. Retrieved June 2023 from: https://abirpothi.com/textilecrafts-incorporated-in-this-tech-savvy-world/
10. Edwards E (2015) Block printed textiles of India: imprints of culture. Niyogi Books, Delhi, pp1–376
11. Singh M, Chishti RK, Jain R (2009) Hand crafted Indian textiles. Lustre Press, Delhi, pp 1–149
12. Chishti RK (2013) Saris: Tradition and Beyond. Roli Books, Delhi, pp 1–276
13. Deepshikha (2023) Handicrafts from Kashmir. AbirPothi. Retrieved June 2023 from: https://abirpothi.com/handicrafts-from-kashmir/
14. Gaatha (2023) Pashmina. Retrieved June 2023 from https://gaatha.com/pashmina-weaving-kashmir/
15. Xinhua (2020) Artisans weave Kani shawl, woven from Pashmina yarn in Indian-controlled Kashmir. Retrieved June 2023 from http://www.xinhuanet.com/english/2020-10/20/c_139454614.htm
16. Mitra P (2019) Weaving the story of the pashmina shawl. Retrieved June 2023 from https://ruralindiaonline.org/en/articles/weaving-the-story-of-the-pashmina-shawl/
17. Khanapurkar M (2020) All About Paithani Sarees And Where To Buy An Authentic One! Retrieved June 2023 from https://www.southindiafashion.com/2020/07/all-about-paithani-sarees-and-where-to-buy-an-authentic-one.html
18. Patil K (2020) Golden Legacy of Paithani. Retrieved June 2023 from http://www.inhcrf.org/blogs/golden-legacy-of-paithani/
19. SPA 2020 Banarasi Sari. Retrieved June 2023 from https://spaindustrialdesign.wordpress.com/2020/12/20/banarasi-sari/
20. Hayagrivas (2023) Kanjivaram. Retrieved June 2023 from https://www.hayagrivassilkhouse.com/
21. Tangaliya Weaving (2023) Retrieved June 2023 from https://www.directcreate.com/craft/tangaliya-weaving
22. Baral B (2023) Kullu Shawls—Himachal Pradesh. Dsource. Retrieved June 2023 from https://dsource.in/resource/kullu-shawls-himachal-pradesh/making-process
23. Pothys (2023) Kasavu Sarees. Retrieved June 2023 from https://www.pothys.com/
24. Kalyani (2019) The Saree Stories: The Art Of Weaving A Jamdani Saree. Retrieved June 2023 from https://www.shethepeople.tv/home-top-video/the-saree-stories-the-art-of-weaving-a-jamdani-saree/
25. Mokashi, Kire (2023) Silk Weaving Tradition of Sualkuchi, Assam. Retrieved June 2023 from https://www.dsource.in/resource/silk-weaving-tradition-sualkuchi-assam/motiffs
26. Shyama VS (n.d.) Visual Ethnography of clothing, Imphal, Manipur—DRS report. IDC School of Deisgn, IIT, Bombay
27. Atcelcius (2020) Naga shawl. Retrieved June 2023 from https://en.wikipedia.org/wiki/Naga_shawl
28. Deshpande S (2003) Batik for the Beginners. Bharatiya Vidya Bhavan, pp 1–32
29. Baral B (2023) Patola Saree Weaving—Patan. Dsource. Retrieved June 2023 from https://www.dsource.in/gallery/patola-saree-weaving-patan-1
30. Baral B (2023) Cotton Sari—Pochampally. Dsource. Retrieved June 2023 from https://www.dsource.in/resource/cotton-sari-pochampally/introduction
31. Rahul (2023) Retrieved June 2023 from https://en.wikipedia.org/wiki/Sambalpuri_sari#/media/File:Sambalpuri_saree_pallu.jpg
32. Sabnani N (2023) Bandhani. Dsource. Retrieved June 2023 from https://www.dsource.in/resource/bandhani/introduction
33. Batik (2019) Batik From West Bengal, India. Retrieved June 2023 from https://direct-create.medium.com/craft-batik-225cce76d905
34. Naik SD (1996) Traditional embroideries of India. South Asia Books, pp 1–157

35. Gaatha. 2023. Namda. Retrieved June 2023 from https://gaatha.org/Craft-of-India/namda-craft-detail-research/
36. Manfredi P (2017) Chikankari: A Lucknawi Tradtion. Niyogi Books, Delhi, pp 1–252
37. Crewel embroidery (2021) Retrieved June 2023 from https://www.bestofkashmir.com/blogs/handicrafts-blog/crewel-embroidery
38. Crewel embroidery (2021) Retrieved June 2023 from https://www.radiochinar.in/crewel-embroidery/
39. Tilla (2019) Retrieved June 2023 from https://www.youtube.com/watch?v=-i8CV1FqxIY&ab_channel=It%27sAllAboutFashionandCrafts
40. Tilla (2019) Retrieved June 2023 from https://www.kashmirbox.com/blogs/craft/the-classical-craft-of-kashmiri-tilla-dozi
41. Qadir G (2020) "Machine can't match handicraft": tilla embroidery continues to denote prestige in Kashmir. Retrieved June 2023 from https://thekashmirwalla.com/machine-cant-match-handicraft-tilla-embroidery-continues-to-denote-prestige-in-kashmir/
42. Gambhir S (2023) Chikankari embroidery. Dsource. Retrieved June 2023 from https://www.dsource.in/resource/chikankari-embroidery-lucknow/products
43. Baral B 2023 Ahir Embroidery—Kutch, Gujarat. Dsoruce. Retrieved June 2023 from https://www.dsource.in/resource/ahir-embroidery-kutch-gujarat/products
44. LACMA textile collection (n.d.) Chamba Rumal. Retrieved June 2023 from https://en.wikipedia.org/wiki/Chamba_Rumal
45. Bannerji B (2012) Traditional applique of Pipli. Retrieved June 2023 from https://www.deccanherald.com/content/222693/traditional-applique-pipli.html
46. Baral, B. 2023. Kantha Embroidery—Kolkata. Dsource. Retrieved June 2023 from https://www.dsource.in/resource/kantha-embroidery-kolkata/products
47. Priya (n.d.) Kasuti. Retrieved June 2023 from https://en.wikipedia.org/wiki/Kasuti#/media/File:Kasuti_embroidery.jpg
48. Gupta S (2023) Phulkari. Dsource. Retrieved June 2023 from https://www.dsource.in/resource/phulkari/products

Cost-Effective and Sustainable Design: A Review of the Variables that Contribute to Exorbitant Rental Rates in PNG



Collettah Kasup and Aezeden Mohamed

Abstract Lae, the second-largest city in Papua New Guinea, has witnessed a significant rise in rental property prices over the last ten years, causing a strain on the finances of many of its citizens. Various factors, such as population growth, a shortage of formal housing, rising construction costs, and limited access to housing finance, have contributed to this sharp increase in rent. The rise in rental costs has made it increasingly difficult for residents of Lae, particularly those from middle and lower-income backgrounds, to find affordable housing. Currently, over thirty percent of households spend more than thirty percent of their income on rent, which is extremely unaffordable housing. Additionally, an increasing number of Lae's population faces the risk of homelessness and displacement due to the inadequate supply of housing available to them. This case study aims to explore the primary reasons behind the significant increase in Lae's rental housing costs over the past decade. It will examine the impact on different communities and socioeconomic groups and highlight the gaps in legislation. The study will provide valuable insights on how the government, developers, landlords, and other stakeholders can work together to improve the affordability of housing in Lae. With a focus on excessive rent, this analysis seeks to establish a data-driven foundation to address this pressing issue, negatively impacting a large portion of Lae's population. By working together, the community can find innovative solutions to this issue that benefit everyone and we hope that this study will serve as a catalyst for positive change.

Keywords Formal rental housing · Housing finance · Rental property · Lae · Landlords · Tenants

C. Kasup
Department of Business Studies, PNG University of Technology, Lae MP411, Papua New Guinea

A. Mohamed (✉)
Department of Mechanical Engineering, PNG University of Technology, Lae MP411, Papua New Guinea
e-mail: aezeden.mohamed@pnguot.ac.pg

© The Author(s), under exclusive license to Springer Nature Singapore Pte Ltd. 2025

B. B. V. L. Deepak et al. (eds.), *Recent Advancements in Product Design and Manufacturing Systems*, Lecture Notes in Mechanical Engineering,
https://doi.org/10.1007/978-981-97-6732-8_55

1 Introduction

The affordability of rental properties around PNG has been increasing rapidly over the past couple of years stressing out low- to middle-class citizens. It can be stated that most properties developed by big companies are targeting first-class citizens in PNG as their income brackets can afford such high rental costs. With the diversity PNG offers, either for tenants or for the landlords, important factors to consider in real estate are your rights and responsibilities, the rental market research, screening process, comprehensive lease agreement, maintaining effective communication with agents, and the maintenance and inspection of the properties [1]. Considering these factors will help either party price and pay for the properties adequately.

According to a report from [2, 3] the research team from NRI, as of 2016, the weekly rental cost has ranged from PGK550 per week—to PGK8000 per week. The factors that influenced how the prices are set are mainly the location, property type, number of bedrooms, how furnished the property is, and most importantly, the economic state of the nation, at the time the pricing was set. Furthermore, a sample economic analysis was carried out by the NRI research team [3], specifically for Port Moresby's formal and informal sectors housing prices. Their finding indicated that accommodation prices in most informal sectors were averaged around PGK 2246, and for the formal sector, it averaged around PGK3147 per calendar month. Addressing the issue, the National Housing Commission partnered with local government and some investors to look into providing affordable housing schemes for people in the Nation's Capital. Similarly, a scholarly article published by Research Gate and written by staff of the Surveying and Land Studies Department of PNG Unitech [4, 5] also provided an analysis of rental markets in Port Moresby and Lae. Collectively, these articles provided a perspective on why properties are priced as they are, influenced by several factors that will be indicated further in this document.

As the second-largest city in PNG, the industrialization of Lae is growing rapidly, resulting in a faster growth in real estate [5], to cater to the vast growing population. With the current investment in the mining and petroleum sector within the province, it is expected rental prices will increase in the foreseeable future which is what is experienced at the moment. The increase in rental property cost due to the increase in cost of living and other additional economic factors has affected the population of Lae. As a result, most working-class people can afford rental properties away from the city limits and that is affecting their work schedules as well.

Given a brief overview and background of what rental is like both in Port Moresby and Lae, as a newly established Property Management Company in Lae, the focus will be only on the properties in Lae City. The industrial hub of this country is experiencing a high rental crisis, and as an intermediary between the tenants and the landlord, it is our job to ensure our clients are satisfied, whether it is putting a property on the market or negotiating a good rental price for tenants ensuring the best interest of both are prioritized.

In recent years, Papua New Guinea's Lae city has faced an affordable rental housing crisis [6]. Lae, the second-largest urban area in the country, is experiencing

population [7] growth due to migration and natural growth. But housing supply has not kept pace, leading to rising rents well above local income levels.

Comprehensive data are lacking, but according to various studies, average rental prices in Lae have soared by an estimated 75% between 2010 and 2020 [4]. This dramatic increase will hardly put rental housing out of reach for many low- and middle-income residents. Currently, over 30% of households in Lae state are believed to have high rents and spend over 30% of their income on housing [8].

The purpose of this case study is to shed light on the main factors driving rental property prices in Lae over the past decade. It will assess the impact on Lae residents and identify the regions and socioeconomic groups most affected by the shortage of affordable rental housing. By analyzing housing policy gaps, this study seeks to identify opportunities for stakeholder intervention through solutions that can improve rent affordability in vulnerable communities in Lae [9]. Addressing this crisis through evidence-based interventions is imperative to provide home security for rapidly growing urban populations.

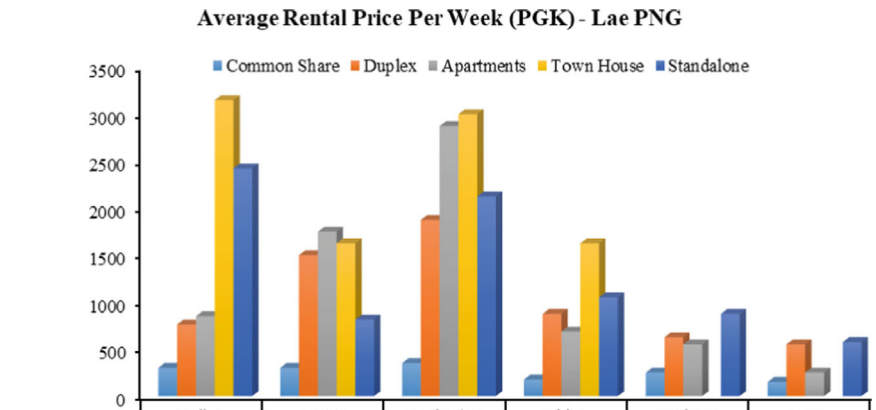
2 Problem Statement

Over the past decade, rental prices for housing in Lae, the second-largest city in Papua New Guinea, have risen sharply, causing increasing unaffordability for many residents. This rapid increase in rents has been driven by factors such as high population growth, lack of formal housing supply, rising costs of construction, and limited access to housing finance.

The rise in rental prices has impacted Lae's residents, especially middle- and low-income groups, struggling to find affordable accommodation. Over 30% of households now spend more than 30% of their income on rent, meeting the definition of severely unaffordable housing. With demand continuing to rise faster than supply, a growing segment of Lae's population is at risk of housing insecurity and displacement.

This case study will analyze the key drivers causing the sharp increase in Lae's rental housing prices over the past decade. It will examine the impacts on different socioeconomic groups and neighborhoods. The study will identify gaps in housing policy and areas for intervention by government, developers, landlords, and other stakeholders to improve housing affordability in Lae. This analysis aims to provide an evidence base to tackle this urgent challenge negatively affecting much of Lae's population through unaffordable rents.

The graph below summarizes the average rental properties types and average cost per week [10, 11] in PGK (Figs. 1, 2 and 3).



	Eriku	Town	Market/Voco Point	China Town	Kamkumung	Igam
Common Share	300	300	350	175	250	150
Duplex	761	1500	1875	875	625	550
Apartments	850	1750	2875	687	550	250
Town House	3150	1625	3000	1625		
Standalone	2423	813	2125	1050	875	575

Fig. 1 Example of current rental prices within Lae City-PNG

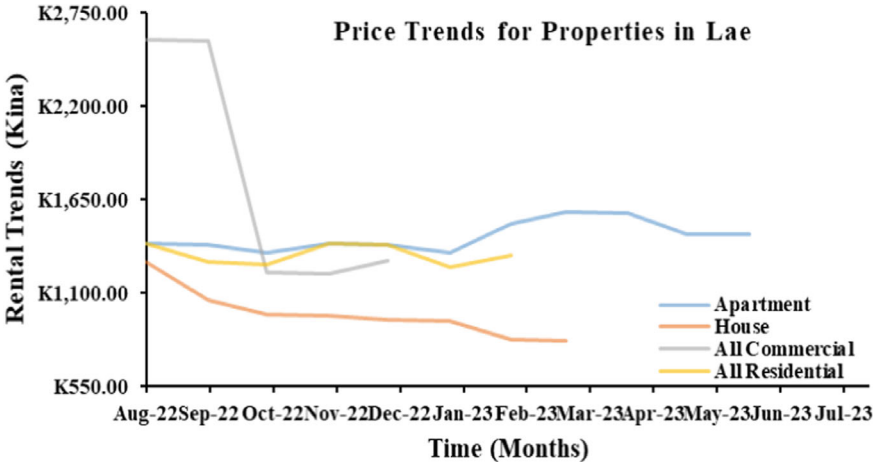


Fig. 2 Past six-month rental trends in Lae PNG [7]

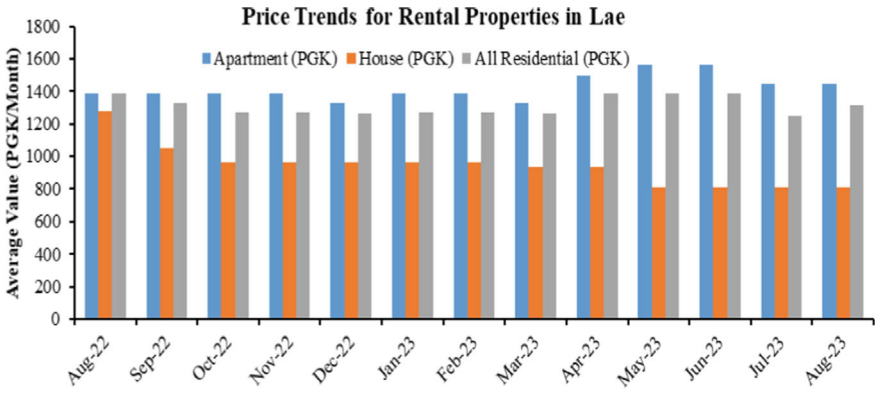


Fig. 3 Past one-year rental trends in Lae PNG [7]

3 Problem Evaluation

3.1 Causes of High Rental Prices

A major driver of the rental price increases in Lae is the rapidly growing housing demand that has outpaced supply. Lae's population growth rate is over 2% annually, largely from high birth rates and migration from rural areas seeking economic opportunities [12]. However, formal housing development has not kept up, with under 3,000 new units built annually compared to demand for 5,000 units [8]. This supply–demand gap leads to more competition and higher rents for available housing.

Another factor is the high costs of construction in PNG which relies heavily on imported materials. A study by PNG's National Research Institute found that transportation and import costs can account for up to 30% of building expenses [13, 13, 15]. Land prices have also increased with growing demand. These costs make new low-cost housing developments financially unviable for most builders without government subsidies. Additionally, lack of access to credit and housing finance limits both developers and renters [13, 14].

Finally, cultural factors and land tenure issues unique to PNG have constrained supply. Much of the land in urban areas is held communally or customarily, causing difficulties in establishing titles and developing housing [8, 15]. Speculative buying of property for investment rather than occupancy also affects the availability and affordability of rentals.

3.2 Impacts of High Rental Prices

The soaring rental costs have created an affordability crisis where over a third of households are classified as rent-burdened, spending more than 30% of their income on housing. Homelessness and growth of informal settlements have accelerated, with reports indicating over 60 illegal settlements now housing nearly 100,000 people lacking adequate services.

The housing crisis also compounds economic and social struggles. Lower-income workers face rising transportation costs to live further from urban jobs, potentially impacting productivity. Overcrowding as families double up raises risks of diseases like tuberculosis. Women and children face heightened vulnerability, with single mothers, especially at risk of homelessness.

Moreover, the housing affordability gap has reinforced spatial inequality and social divisions. Poorer groups are displaced to the urban periphery in informal settlements, while inadequate mixed-income areas reduce social cohesion. Closing these housing-driven divides through progressive policy is key.

3.3 Policy Solution

A framework or flow chart on how the current rental crisis in Lae can be managed (Fig. 4).

To address Lae's rental housing challenges, further research should be conducted to fully analyze supply and demand dynamics in the local market. Studies can quantify the current shortage of affordable units and project future rental housing needs based on population growth forecasts. Econometric modeling can provide data-driven insights.

With this foundation, a comprehensive national housing strategy should focus on increasing affordable rental stock through measures like public–private partnerships to construct quality low-cost units, subsidized land and tax incentives for developers, investing in social rental housing for low-income groups, streamlining land titling and regulations, and improving access to construction finance.

The strategy can be implemented through coordinated efforts across government agencies and the private sector, targeting the highest-need areas first. Impacts should be monitored to identify issues and adopt policies based on regular rental market assessments. The aim is to systematically increase supply while protecting tenants through balanced regulations. Sustained community engagement is essential for effective and just policy delivery.

Regular review and fine-tuning of interventions are critical, as the rental market evolves over time. The overall goal is to quantify and meet Lae's affordable housing needs through responsive, evidence-based policies.

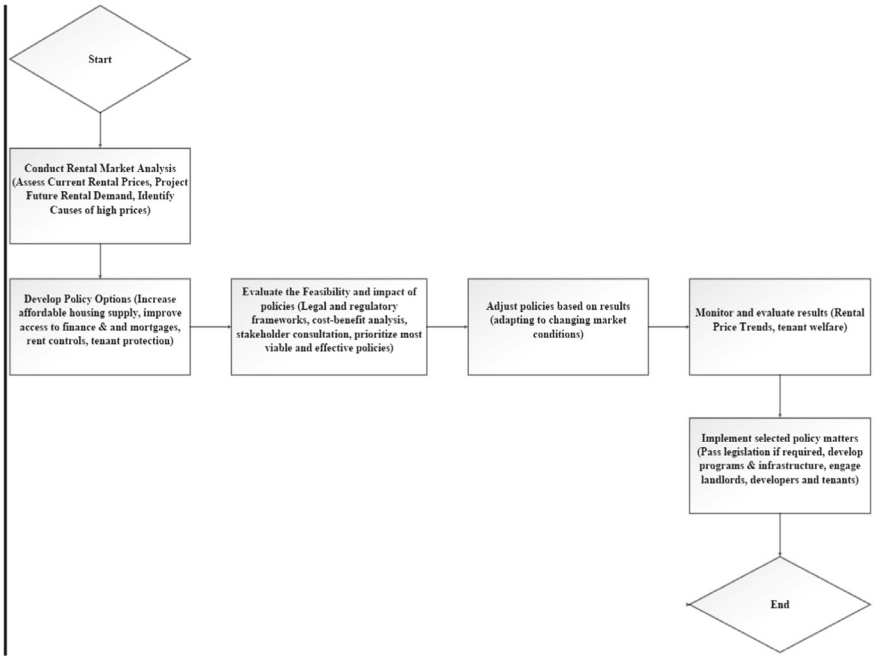


Fig. 4 Frameworks on how the high rental prices in Lae PNG can be managed

4 Conclusion

In conclusion, the city of Lae faces a severe housing affordability crisis driven by surging rental costs that have far outpaced local incomes. The fundamental supply–demand imbalance in Lae's housing market, fueled by rapid population growth and urbanization, is the primary factor driving heightened rental prices. Constraining forces like high construction costs, lack of financing, and land tenure issues have limited the supply response.

The impacts of this crisis are multifaceted, creating economic, social, and spatial inequalities that disproportionately affect lower-income groups. Addressing Lae's affordable housing shortage requires coordinated efforts from all stakeholders including government bodies, the private sector, communities, and civil society.

A comprehensive, evidence-based housing strategy is urgently needed to expand affordable rental availability through integrated policy solutions. These should encompass both increasing housing supply, through public–private partnerships and incentives, as well as tenant protections. Sustained interventions and regular review are critical to effectively tackle the deeply entrenched housing crisis that threatens Lae's social and economic development.

Providing adequate, secure, and affordable housing is essential for an equitable, prosperous city. Lae's policymakers must make substantial investments and reforms

today to create an inclusive housing system enabling affordable rents and dignified living for all its residents now and in the future.

References

1. Insight HRE (2023) Navigating the PNG Rental Market. https://Www.Linkedin.Com/Pulse/Navigating-Png-Rental-Market-Hausples-Com-Pg/. Accessed 1st Friday Sep 2023
2. Ezebilo E E, Nao L, Hamago L, Thomas M (2017) Dynamics of market prices of rental properties in papua new guinea: evidence from port moresby, Port Moresby. National Reasearch Institute PNG
3. Thomas M, Thomas M (2019) Economic analysis of the housing rental market in the formal and informal built areas of Port Moresby PNG, Port Moresby. National Research Institute PNG
4. Motoro Paulus, B. J. H. S., 2019. Analysis of The Rental Market in Informal Settlements Complementing Housing Needs in Cities: The Case of Port Moresby & Lae Cities, Papua New Guinea, Lae, PNG: Research Gate
5. Oxford Business Group (2016) Rental prices fall as supply exceeds demands in PNG. PNG Construction Real Estate
6. https://Oxfordbusinessgroup.Com/Reports/Papua-New-Guinea/2017-Report/Economy/Market-Moderation-Rental-Prices-Have-Fallen-As-Supply-Exceeds-Demand-While-The-Affordable-Segment-Presents-Opportunities-For-Growth. Accessed Friday1st Sep 2023
7. Hausples PNG (2023) Market Trends for Lae. https://www.hausples.com.pg/market-trends/lae/. Accessed 6 Sep 2023
8. Allen RMBAB (2021) Estimating the Population of PNG in 2020. Crawford School of Public Policy, The Australian National University, Canberra
9. Ezebilo E E (2019) Papua new guinea's drive to provide affordable housing, are we ready? Port Moresby. The National Research Institute PNG
10. Ezebilo E E (2021) Government interventions are needed for house rent to be affordable
11. https://pngnri.org/index.php/news-events/research-corner/301-government-interventions-are-needed-for-house-rent-to-be-affordable. Accessed 6 Sep 2023
12. PNG NRI (2023) Government Should Do More to Address House Rent Problem. https://pngnri.org/index.php/news-events/news/414-government-should-do-more-to-address-house-rent-problem. Accessed 6 Sep 2023
13. Professionals (2023) Lae Residential Rent Weekly Updated. https://theprofessionals.com.pg/storage/pdf/lae%20residential%20rent%20properties%20-%20professionals%2001sep2023.pdf. [Accessed 1st Friday Sep 2023]
14. Anderson T (2006) Land Titling Issues on The Economic Value of Customary Land in Png. University of Sydney, Sydney
15. World Bank (2021) Papua New Guinea
16. https://Data.Worldbank.Org/Country/Pg. Accessed 6 Sep 2023
17. Dr. Elizabeth Kopel LI (2020) Prospects and Challenges of The Informal Rental Housing Market in Suburbs. https://Pngnri.Org/Index.Php/News-Events/Research-Corner/185-Prospects-And-Challenges-Of-The-Informal-Rental-Housing-Market-In-Suburbs. Accessed 6 Sep 2023
18. Japan International Corporation Authority (2017) The Project for The Study on Lae-Nadzab Urban Development Plan. Jica, Lae
19. Lae City Authority (2021) A Vibrant City of Growth and Opportunity. Lae City Authority, Lae PNG
20. PNG Haus Ples (2023) Houses for Rent in Lae. https://Www.Hausples.Com.Pg/Rent/Lae/House/?Active_Tab=Popularlocations&Categories=House&Order_By=Relevance&Property_Type=Residential&Q=Location%3a%20morobe%20%3e%20lae&Search_Type=Rent. Accessed 1st Friday Sep 2023

Presence of Gestalt Traits in a Brand Logo and Its Impact in Evoking the Intended Meaning

Ruchi Srivastav and Anirban Chowdhury

Abstract The study delves into applying gestalt theory in visual brand identities, specifically Indian letterform and monogram logos. By categorizing these logos based on high, medium and low gestalt traits, the research aimed to explore how these traits influence consumer perception of the logos' intended meanings. Using a quantitative approach, ten logos were evaluated and through a questionnaire, consumers' interpretations of the logos were collected. The findings highlighted that logos with higher gestalt traits were more communicative and better conveyed their intended meanings compared to those with fewer gestalt traits. This underscores the significance of gestalt principles in designing effective and communicative visual brand identities.

Keywords Brand attributes · Gestalt principles · Logo design · Semiotics and symbolic meaning · Visual perception

1 Introduction

Visual elements in a logo can have positive and negative influences; they are informative, give a direction or arouse emotions, create confusion and at times infuriate [1]. To communicate effectively and meaningfully through visuals, one needs to be aware of the principles of perceptual organization along with the basic foundation in design education [2]. The core of a good design is its simplicity and ability of our mind to perceive it as a whole, so that the meaning is communicated effectively [3]. Gestalt psychology along with experimental aesthetics in the field of graphic design and logo strategy helps to analyze the visual characteristics of logos [4]. The

R. Srivastav (✉)
Symbiosis Institute of Design, Symbiosis International (Deemed University), Pune, India
e-mail: ruchi.srivastav@sid.edu.in

A. Chowdhury
Alliance School of Design and Creative Arts, Alliance University, Bengaluru, India
e-mail: chowdhuryanirban14@gmail.com

© The Author(s), under exclusive license to Springer Nature Singapore Pte Ltd. 2025

B. B. V. L. Deepak et al. (eds.), *Recent Advancements in Product Design and Manufacturing Systems*, Lecture Notes in Mechanical Engineering,
https://doi.org/10.1007/978-981-97-6732-8_56

Gestalt Laws of Visual Perception enable designers to execute their ideas visually and communicate effectively [2]. The brand identity of a brand captures its attributes and characteristics which differentiates it from other brands and adds uniqueness [5]. Great logos are created very thoughtfully with deliberate and conscious design process, nothing is accidental and it is planned and meticulously developed stage by stage and refined till it reaches a final desired meaningful form [6]. Logos can be classified as typographic or pictorial or both [7]. Letterform is a typographic logo where only the first letter of the company's name or the brand name or the individuals' name is represented as a stylized or abstract text-only graphic form [8], while a monogram is a combination of two or more typographic characters to form a logo, usually using the initials of the individual, company or the brand [9]. This research proposes to study the influence of gestalt traits present in the selected Indian letterform and monogram type of logos as visual identities in communicating the intended meaning of the selected brands.

2 Literature Review

2.1 Gestalt Theory of Visual Perception

Gestalt psychology was founded in 1910 by three German psychologists, Max Wertheimer, Kurt Koffka and Wolfgang Köhler [10]. Christian von Ehrenfels, was the first one to introduce the word 'gestalt' which means unified or meaningful whole in human psychology, in his paper titled 'On Gestalt Qualities' [11]. Our mind subconsciously captures the whole picture even before the individual parts enter our consciousness, this happens due to continuous processing in the brain, rather than the combination of each individual component [12]. In 1923, Wertheimer published a paper where used patterns of dots and lines to explain the gestalt principles in a simplistic manner, hence nicknamed 'the dot essay' [13]. These findings led to formulation of the gestalt laws—'Law of Proximity,' 'Law of Similarity,' 'Law of Closure,' 'Law of Good Continuation,' 'Law of Symmetry' and the 'Law of Simplicity' [14]. Gestalt psychology acts like a tool and helps designers in designing and communicating ideas through visual forms [15]. The visual representation of the brand through a logo design helps in connecting with the consumer and in communicating the core message effectively [16].

2.2 Branding and Logo Design

The word 'brand' originated from the Old Norse word 'brandr' that referred to burn, by which the owners of livestock would mark their cattle to identify [17]. 'Father of Advertising', David Ogilvy defined brand as—'the intangible sum of a product's

attributes' [18]. Brand identity expresses what the brand stands for and brings out its attributes and brand personality [19]. A logo symbol is a visual representation of a brand that captures the values and personality of the organization and builds brand recognition [20]. There are no specific numbers of gestalt traits that can be applied in a logo design; however, there is a significant relationship between the use of gestalt traits in a design and its audience responses in having a consensus in deriving the meaning of the logo design [21]. Visual elements of the brand logo like shape and color influence how the brands are perceived by the consumers and create symbolic associations with the brand [22].

2.3 Role of Semiotics in Creating Consensual Meaning of the Logo

The meaning of the logo is well communicated to its consumers if it evokes a similar clear response across people [23]. Semiotics is a research methodology which uses signs to produce meaning out of visual signals; here logo forms the visual sign and acts as communicative tool to connect with the consumer [24]. Consensus meaning of the logo is interpreted by recording the first association that comes to mind by the respondents [25]. Visual interpretation of signs involves drawing inference from the given visual codes, where the viewer uses semiotics to decode the visual signs to decipher a meaning [26, 27]. Designers often create logos which have universal symbolic concepts, for example, the Ferrari logo uses the 'Prancing Horse' where the black horse signifies all the symbolic qualities of the horse [28]. Companies use the logo in order to convey a certain meaning through these visual symbols, like in the case of Apple all products have a symbol of the fruit with a bite removed [29].

2.4 Monogram and Letterform Logo Designs

The term monogram is originally derived from Latin word, 'monogrammon' which means 'intertwined letters.' Adrian Frutiger proposed a simpler definition of monogram where he treated monogram and trademarks as equals and considered both as acronyms [30]. While letterform logo involves a symbol design using only one single letter, mostly the first letter in an abstract or stylized form. Monograms and letterforms have been in use since centuries, great empires, kings, nobles all had their own monograms [31]. Initially, they appeared on coins to identify the city they were issued and for trading. Today, a number of companies across the world use monogram or letterform as their visual identities [9]; Chanel uses the initial 'C' reversed and repeated twice to form an interesting and iconic monogram symbol design [32].

2.5 Meanings of Selected Indian Logos Considered for This Study

Descriptive meaning of selected Indian logos from various online sources regarding their intended meaning as per the designer and the brand officials. These inputs regarding the meaning of individual logos were used in order to format the questionnaire for the survey.

Hero MotoCorp—Designer: Wolff Olins

The new logo comprises three shapes which form the letter 'H' at an angle in 3D depiction. The two rectangular planes represent the vertical sides of letter 'H' and the connecting bar is discreet using the white rectangular shape. The shape represents a 'catapult' and has a deep connection with the Indian cultural roots depicting 'leap toward new horizon' [33].

Axis Bank—Designer: Ogilvy & Mather

The logo design is a letterform 'A' which stands for Axis Bank; it is constructed using two geometric strokes in solid burgundy color like the previous UTI logo to link its heritage. The first stroke depicts growth and the second stroke signifies a solid support system and conveys a sense of authority and credibility [34].

Asian Paints—Designer: WPP's Singapore-Based Design Agency, Fitch

Indian consumers are very conventional and opt for lighter pastel colors when decorating their homes; this thought was carried forward while designing the new logo for Asian Paints. The vibrancy of the logo was to make people more confident and open toward bold colors. The new logo is like a ribbon flowing which creates the lowercase alphabets 'a' and 'p,' which signifies flow, dynamism and possibilities the company offers [35].

Bajaj—Designer: Elephant Design

The new brand identity reflects the change in consumer age group, their aspirations and ideology of the brand. The 'flying B' symbol has been designed on the lines of the old hexagonal logo and depicts smooth ride, flying speed and excitement [36]. Essence of the brand lies in the five brand values—learning, innovation, perfection, speed and transparency. The emblem appears like two bold ticks which appear like horizontally overlapped letter 'V' [37].

Reliance—Designer: Mudra Communications

The core logo of Reliance has not been changed since its inception, although few transitions have been made to it. The logo has a golden flame over the letter 'I' of the word Reliance. The symbol is in gold as it symbolizes eternal flame in Hindu philosophy [38].

Airtel—Designer: The Brand Union, London

The latest logo of the company is a stylized 'a,' which the company officials refer as the Airtel wave and the symbol conveys the idea of 'no boundaries' [39].

Tanishq—Designer: Michael Foley, Titan Design Studio

The name Tanishq was coined by marrying the words 'tan' meaning body and 'nishk' meaning necklace of gold coins; it stands for superior craftsmanship, exclusive designs and product quality [40]. The symbol 'T' and the luxurious, silky and shiny curvaceous letterforms of the word Tanishq depict wealth along with feminine elegance [41].

Kotak Mahindra Bank—Designer: Ray and Keshavan, Bangalore

The symbol of 'Ka' is uniquely Indian and the curve forms the universal 'infinity' sign, reflecting the global Indian personality. The needs of a man are unlimited and the infinity symbol in form of Devanagari alphabet 'Ka' symbolizes the infinite ways to meet those needs [42].

Videocon—Designer: Interbrand, Singapore

The symbol is the representation of fluid lava that changes shape; it reflects the brand idea—'experience change' [43]. The green fluid-like drops appear like an abstract and stylized 'V.' The new logo symbolizes innovation and aims at establishing an emotional connection with the consumers. The color selected is symbolic to the company's ecology drive [44].

Punjab National Bank—Designer: R.K. Joshi

The design of the logo captures the form of Gurmukhi letter 'P' and the orange color brings out the Indian ethos and traditional essence. The letterform 'P' in Gurmukhi encloses a circle which complements the identity of PNB as a nationalized bank [45].

3 Aim and Objective of Research

Aim of the study is to observe the number of gestalt traits present in the selected monogram and letterform logos and to determine if it aids in effectively communicating the intended meaning. The consumers are unaware about the gestalt laws of visual perception and are they able to decipher the intended meaning of these logos as conceived by the designer or the brand officials? These thoughts helped in framing the following hypothesis—$\mathbf{H_a}$: **Logo with greater gestalt traits helps in better understanding of the intended meaning**.

4 Methodology

4.1 Study Design

The research was conducted in two phases, where in the first phase, the selected letterform and monogram brand logos were segregated as high, medium and low gestalt logos, based on the number of gestalt laws present in each of the logos as suggested by the target group for this study—design students, educators and professionals ($N = 49$, Age range = 18–56 years, $F = 40\%$, $M = 60\%$). A brief write-up was given to refresh and recall the gestalt principles before taking the survey. Informed consent form was taken from the participants prior to their participation in the study. The designers were asked to identify the number of gestalt traits present in ten monograms and letterforms of Indian logos. Based on their rating, these logos were segregated as high, medium and low gestalt. High gestalt logo means 5–6 gestalt traits are present, medium gestalt logo means 3–4 gestalt traits present and low gestalt logo means 1–2 gestalt traits present in the logo. All the ratings (see Table 1) were taken to validate the gestalt traits present in each logo, using a questionnaire as mentioned in Table 2. In the second phase, the selected logos were shared with consumers as well as with design professionals to see whether the meaning of the logo was successfully communicated as per the intention of the designer and brand officials. For the consumers with no design background, the questionnaire was different and the section with only the intended meaning of the logo was shared ($N = 95$, age range = 18–56 years, female = 40%, male = 60%).

5 Results and Analysis

5.1 Determination of Gestalt Traits for Selected Logos

We had selected ten Indian brand identities in letterform and monogram format for this study. With the help of rating given by design professionals, we segregated the logos into three categories—high, medium and low. Videocon was validated as a low gestalt logo exhibiting two gestalt traits (law of closure and law of continuity) by 39 (79.5%) responses. Airtel also had two gestalt traits (law of closure and law of continuity) which were validated by 36 (73.4%) respondents. The logos of Hero motor and Axis Bank were categorized as medium gestalt logo as it displays 3–4 gestalt traits. Hero Motor has three gestalt traits (law of similarity, law of proximity and law of closure) which are validated by 34 (69.3%) respondents, while Axis Bank logo displays four gestalt traits (law of similarity, law of proximity, law of closure and law of figure-ground), which are validated as per Table 1 by 45 (91.8%) respondents. The logos of Tanishq and Kotak Mahindra Bank were rated as high with five gestalt each (law of similarity, law of proximity, law of closure, law of symmetry and law

Table 1 Expert validation responses for gestalt traits present in each logo

Name of the company	Gestalt traits present						
	Similarity	Proximity	Closure	Continuity	Symmetry	Figure-ground	No. of experts validated (%)
Videocon (L)	**–**	**–**	**Y**	**Y**	**–**	**–**	**39 (79.5)**
Asian Paints (M)	Y	Y	–	Y	Y	–	47 (95.9)
Axis Bank (M)	**Y**	**Y**	**Y**	**–**	**–**	**Y**	**45 (91.8)**
Bajaj (M)	Y	Y	Y	–	Y	–	40 (81.6)
Hero (M)	**Y**	**Y**	**Y**	**–**	**–**	**–**	**34 (69.3)**
Kotak Mahindra Bank (H)	**Y**	**Y**	**Y**	**Y**	**Y**	**–**	**48 (97.9)**
Reliance (M)	Y	Y	Y	**–**	**–**	Y	44 (89.7)
Airtel (L)	**–**	**–**	**Y**	**Y**	**–**	**–**	**36 (73.4)**
Tanishq (H)	**Y**	**Y**	**Y**	**Y**	**Y**	**–**	**49 (100)**
Punjab National Bank (L)	Y	Y	–	–	–	–	39 (79.5)

of figure-ground) and were validated by 49 (100%) and 48 (97.9%) respondents respectively. In Table 1, it is evident that most of the selected logos fell in the category of medium gestalt logo, therefore we selected two high (Tanishq and Kotak Mahindra Bank), two medium (Hero Motor and Axis Bank) and two low (Videocon and Airtel) gestalt logos for our analysis.

5.2 Effect of Level of Gestalt Traits on Correct Understanding of Meaning

In the case of the Airtel logo, a significant number of respondents (40%) failed in understanding the correct intended meaning of the logo and a significant number of respondents (60%) gave incorrect responses [$X_2(1) = 3.8$; p 0.05] due to low gestalt traits (refer Table 3). For the Videocon logo, a significant number of respondents (80%) failed to recognize the correct intended meaning of the logo and only 20% of the respondents could understand the correct meaning of the Videocon logo [X_2 (1) $= 34.200$; $p = 0.0001$]. So, we notice that the logos which have low gestalt traits like

Table 2 Questionnaire used for collecting data

S. No.	Name of the brand	Question with options
Section I. Design professionals		
1	All brands	Law of Similarity, Law of Proximity, Law of Closure, Law of Continuity, Law of Symmetry and Law of Figure-Ground
Section II. Design professionals and consumers		
1	Airtel	1. Flowing symbol that shows seamless strong network 2. Stylized letter 'a' signifies the Airtel wave to convey endless boundaries 3. Circular network for better connectivity
2	Videocon	1. Flowing smooth curvy brush creating 'V' 2. Fluid lava flow represents 'experience change.' 3. Young, fresh and ecofriendly
3	Hero Motor	1. Sharpness, speed and action 2. Angular 'H' in a catapult shape depicting leap toward new horizon 3. Dynamic and powerful
4	Axis Bank	1. Authority and rich heritage in banking sector 2. Two strokes forming letter 'A,' longer stroke for growth and shorter for support 3. Three triangles for solidity and security of the bank
5	Tanishq	1. Curvaceous letter 'T' denotes elegance, luxury and wealth 2. Dot on 'i' symbolizes 'bindi' worn by women 3. Represents Indian ornamental designs
6	Kotak Mahindra Bank	1. Flowing 'S' denotes flow of wealth and open economy 2. Devanagri letter 'K' denoting infinite ways to meet infinite human needs 3. Circle represents reliability and stability of the bank

Airtel and Videocon had a significant number of incorrect responses (60% and 80% respectively) and failed to understand the correct meaning of the logo as intended by the designer or the brand officials.

No significant differences were found between the number of correct and incorrect responses in understanding the meaning of Hero Motor logo [X_2 (1) = 0.011; p = 0.918] due to medium gestalt traits. In Hero Motor, we got neutral results as almost an equal number of respondents gave correct (50.5%) and incorrect (49.4%) responses. While a significant number of respondents (68.4%) have correctly recognized the intended meaning of Axis Bank logo [X_2 (1) = 12.895; p = 0.0001] due to medium gestalt traits. Therefore, in the case of the Axis Bank logo, a significant number of respondents (68.4%) succeeded in understanding the correct meaning of the logo.

Significant number of respondents (68.4%) correctly recognized the intended meaning of the Tanishq logo as well [X_2 (1) = 12.895; p = 0.0001]. Similarly, in Kotak Mahindra Bank logo also, we see that a significant number of respondents (64.2%) have correctly recognized the intended meaning of the logo [X_2 (1) = 7.674; p = 0.006]. Hence, in the case of the logos with high gestalt traits like Tanishq and Kotak Mahindra Bank, we observed that there were a significant number of correct

Table 3 Results of Chi-square goodness of fit test

Logo name (gestalt trait)	Total number of respondents	% of correct response (*n*)	% of incorrect response (*n*)	Chi-square (d*f*)	*p*-value
Airtel (low)	95	40.0 (38)	60.0 (57)	3.8 (1)	0.05
Videocon (low)	95	20.0 (19)	80.0 (76)	34.200 (1)	0.0001
Hero Motor (medium)	95	50.5 (48)	49.4 (47)	0.011 (1)	0.918
Axis Bank (Medium)	95	68.4 (65)	31.5 (30)	12.895 (1)	0.0001
Tanishq (high)	95	68.4 (65)	31.5 (30)	12.895 (1)	0.0001
Kotak Mahindra Bank (high)	95	64.2 (61)	35.7 (34)	7.674 (1)	0.006

responses (68.4% and 64.2%, respectively), and the meaning of the logo was correctly understood by the respondents.

5.3 Effect of Gender and Participant Type

Airtel

While studying the correlation between the gender and type of response, we observe no significant association between the responses in understanding the meaning of Airtel Logo (correct/incorrect) and gender type (female vs. male) [Please refer Table 4 and Fig. 1 (A)]. Similarly, no significant association was seen between the responses in understanding of the meaning of the Airtel logo (correct/incorrect) and the participant type (designer vs. consumers). When referring to Fig. 1 (B), it was observed that both respondents, the designers and the consumers, were unable to correctly understand the meaning of the logo.

Videocon

While studying the correlation between the gender and type of response, we observe no significant association between the responses in understanding the meaning of Videocon (correct/incorrect) and gender type (female vs. male) [Please refer Table 4 and Fig. 2(A)]. While there is a significant association seen between the responses in understanding of the meaning of the Videocon logo (correct/incorrect) and the participant type (designer vs. consumers) [$X_2(1) = 4.647; p = 0.031$]. When referring to Fig. 2(B), it was observed that both the designers as well as consumers were unable to correctly understand the meaning of the logo.

Table 4 Results of Chi-square test of association (effect of gender and participant type)

Term of relationship	Odd score	95% confidence interval		Chi-square (d*f*)	*p*-value
		Lower bound	Upper bound		
Correct understanding of Logo x Gender					
Airtel (low)	1.502	0.642	3.516	0.885 (1)	0.347
Axis (medium)	0.815	0.334	1.987	0.203 (1)	0.652
Hero (medium)	1.036	0.456	2.354	0.007 (1)	0.933
Tanishq (high)	1.000	0.414	2.418	0.000 (1)	1.00
Videocon (low)	3.036	0.922	9.999	3.553 (1)	0.059
Kotak Mahindra Bank (High)	1.576	0.672	3.696	1.099 (1)	0.294
Correct understanding of Logo x Participant Type					
Airtel (low)	0.782	0.343	1.781	0.344 (1)	0.557
Videocon (low)	0.305	0.100	0.931	4.647 (1)	**0.031**
Hero (medium)	2.693	1.175	6.176	5.590 (1)	**0.018**
Axis (medium)	1.108	0.466	2.636	0.054 (1)	0.816
Tanishq (high)	0.411	0.169	1.003	3.904 (1)	**0.048**
Kotak Mahindra Bank (high)	0.520	0.222	1.218	2.294 (1)	0.130

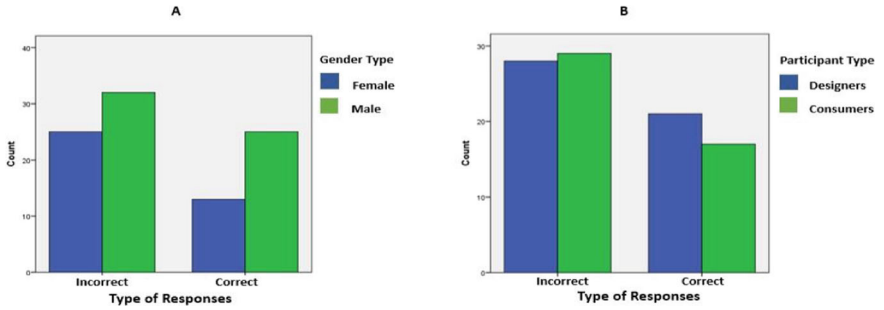


Fig. 1 **a** Gender-wise responses given by participants for Airtel logo; **b** participant type-wise responses given by participants for Airtel logo

Hero Motor

To study the correlation between the gender and type of response, we see no significant association between the responses in understanding the meaning of Hero Motor Logo (correct/incorrect) and gender type (female vs. male) [Please refer Table 4 and Fig. 3 (A)]. Whereas, there is a significant association seen between the responses

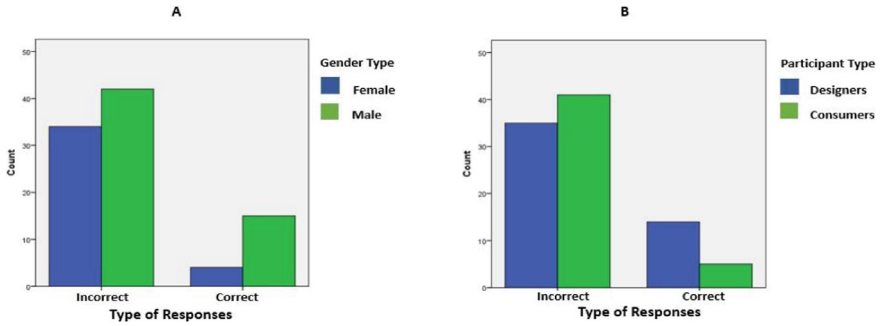


Fig. 2 **a** Gender-wise responses given by participants for Videocon logo; **b** Participant type-wise responses given by participants for Videocon logo

in understanding of the meaning of the Hero Motor logo (correct/incorrect) and the participant type (designer vs. consumers) [$X_2(1) = 5.590; p = 0.018$]. When referring to Fig. 3 (B), it was observed that the designers were unable to correctly understand the meaning of the logo and the consumers successfully understood the intended meaning.

Axis Bank

While studying the correlation between the gender and type of response, we observe no significant association between the responses in understanding the meaning of Axis Bank logo (correct/incorrect) and gender type (female vs. male) [Please refer Table 4 and Fig. 4 (A)]. Similarly, no significant association was seen between the responses in understanding of the meaning of the Axis Bank logo (correct/incorrect) and the participant type (designer vs. consumers). When referring to Fig. 4 (B), it was observed that both respondents, the designers as well as the consumers, were able to correctly understand the meaning of the logo.

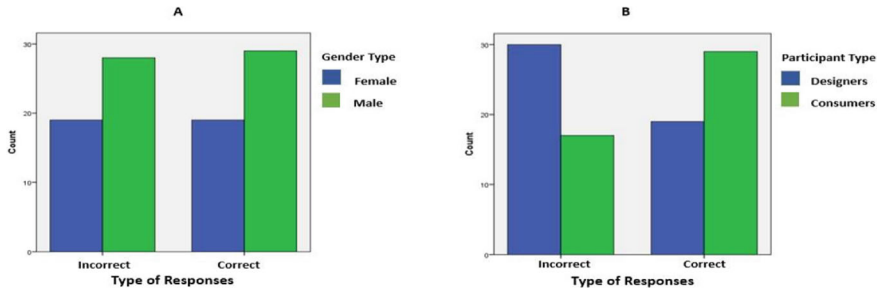


Fig. 3 **a** Gender-wise responses given by participants for Hero motor logo; **b** Participant type-wise responses given by participants for Hero Motor logo

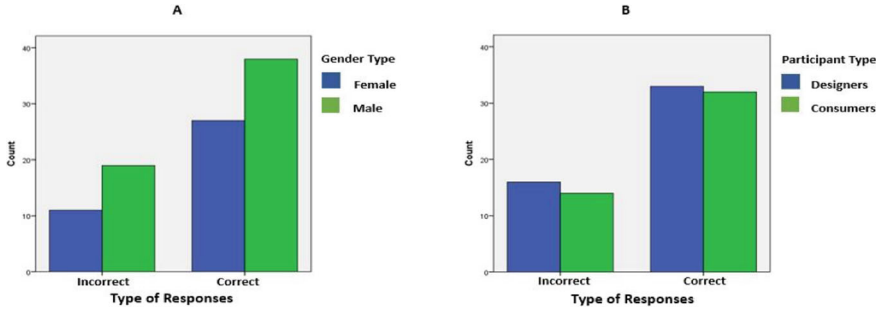


Fig. 4 **a** Gender-wise responses given by participants for Axis Bank logo; **b** Participant type-wise responses given by participants for Axis Bank logo

Tanishq

To study the correlation between the gender and type of response, we see no significant association between the responses in understanding the meaning of Tanishq Logo (correct/incorrect) and gender type (female vs. male) [Please refer Table 4 and Fig. 5 (A)], whereas there is a significant association seen between the responses in understanding of the meaning of the Tanishq logo (correct/incorrect) and the participant type (designer vs. consumers) [$X_2(1) = 3.904$; $p = 0.048$]. When referring to Fig. 5 (B), it was observed that the number of correct responses given by designers in understanding the meaning of the logo was significantly higher than the consumers.

Kotak Mahindra Bank

While studying the correlation between the gender and type of response, we observe a significant association between the responses in understanding the meaning of Kotak Mahindra Bank logo (correct/incorrect) and gender type (female vs. male) [Please refer Table 4 and Fig. 6 (A)], whereas no significant association is seen between the responses in understanding of the meaning of the Kotak Mahindra Bank logo (correct/incorrect) and the participant type (designer vs. consumers). When

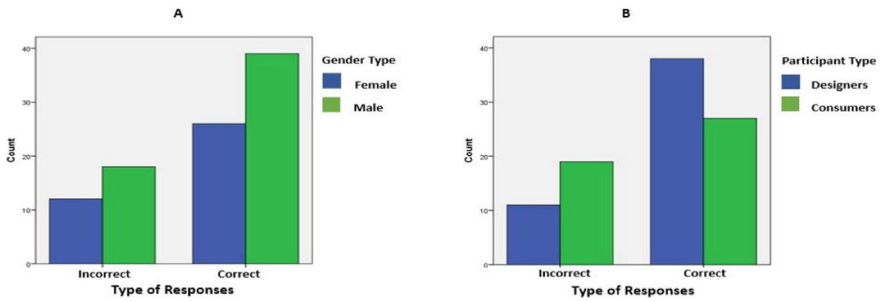


Fig. 5 **a** Gender-wise responses given by participants for Tanishq logo; **b** participant type-wise responses given by participants for Tanishq logo

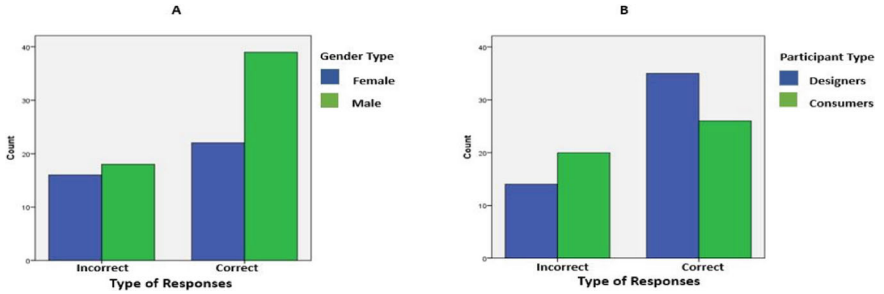


Fig. 6 **a** Gender-wise responses given by participants for Kotak Mahindra Bank logo; **b** participant type-wise responses given by participants for Kotak Mahindra Bank logo

referring to Fig. 6(B), it was observed that the number of correct responses given by designers in understanding the meaning of the logo was significantly higher than the consumers.

6 Discussion

In the context of the undertaken research problem, it is seen that development of brand identity is essential for building strong and trusted brands. The results of this study help us to effectively incorporate visual symbols in a logo design in order to impart the correct meaning of the logo. A positive brand image encourages consumers to purchase the product and logo along with advertisements play an important role in creating brand image [46]. The effectiveness of the brand identity is through various factors—understanding the intended meaning of the visual logo, its association with the brand values and finally leading to its brand recall. Another important aspect of the study was to see how the number of gestalt traits present in the logo design impacted in understanding the correct meaning of the logo.

The brand logos which had fewer gestalt traits, like Videocon and Airtel (low gestalt), showed poor response when it came to understanding their correct meaning, while logos like Kotak Mahindra Bank and Tanishq (high gestalt) had positive response toward understanding their meaning. The four core assets of brand equity are: perceived quality, brand loyalty, brand awareness and brand associations [19]. Hence, better understanding of the meaning of the logo enhances the brand association and brand awareness.

7 Limitations

In the limitations of the study paves way for further research, firstly the present research only focused on letterform and monograms types of logos to study the gestalt traits in each of them. The logos with natural and abstract forms can be further explored. The comparison between typographic and form-based logos can contribute to a richer study in terms of effectively communicating the brand attributes along with meaning of the logos.

8 Conclusion

Designing a brand identity is a serious and costly affair and this research demonstrates that the logos with high gestalt traits were visually more effective in communicating the correct meaning and connecting with the consumers. The application of the gestalt principles helps in creating interesting visual identities by incorporating visual clues in the logo to reinforce the meaning of the logo. The findings add evidence in support to the notion that better understanding of the meaning of the logo enhances the brand association and brand awareness. Finally, this study helps the designers and brand managers to consciously consider and apply the gestalt principles while designing an effective brand identity which would foster brand association and help build successful brands in the competitive market.

Conflict of Interest The discussion based on the logos of the brands have been taken purely from academic research point of view and therefore the author doesn't have any conflict of interest regarding the use of these brand names and logos for this study.

References

1. Heskett J (2005) Design: a very short introduction, vol 136. Oxford University Press, p 55
2. Ware C (2019) Information visualization: perseption of design. Morgan Kaufmann
3. Grinsven V, Das E (2016) Logo design in marketing communications: brand logo complexity moderates exposure effects on brand recognition and brand attitude. J Mark Commun 22(3):256–270
4. Henderson PW, Cote JA (1998) Guidelines for selecting or modifying logos. J Mark 14–30
5. Keller K, Webster F (2004) A roadmap for branding industrial markets
6. Airey D (2009) Logo design love: a guide to creating iconic brand identities. New Riders publication
7. Guru DS, Vinay Kumar N (2016) Symbolic representation and classification of logos. In: Proceedings of international conference on computer vision and image processing, vol 1, pp 555–569
8. Dabner D, Stewart S, Vickress A (2017) Graphic design school: the principles and practice of graphic design. Wiley
9. Mauris M (1878) About monograms. Art J 36–42

10. Behrens RR (1998) Art, design and gestalt theory. Leonardo 31(4):299–303
11. Smith B (1988) Gestlat theory: an essay in philosophy
12. Gallagher S (2006) How the body shapes the mind. Carendon Press
13. Wertheimer M (1923) A brief introduction to gestalt, identifying key theories and principles. Psychol Forsch 4(1):301–350
14. Koffka K (2013) Principles of gestalt psychology, vol 44. Routledge
15. Sinico M (2021) Scientific phenomenology in Design pedagogy: legacy of Walter Gropius and Gestalt Psychology. Int J Art Des Educ 40(1):99–107
16. Wheeler A (2017) Designing brand identity: an essential guide for the whole brabnding team. Wiley
17. Keller KL, Oh TT, Neslin SA, Reibstein DJ, Lehmann DR (2020) The past, present and future of brand research. Mark Lett 151–162
18. Park HY, Chang SR (2022) When and how brands affect importance of product attributes in consumer decision process. Eur J Mark
19. Aaker D (2014) Aaker on branding: 20 principles that drive success. Morgan James Publishing
20. Matusova JG (2021) Logo as the gteatest symbol of brand. Eur J Media Art Photogr 9(2):126–133
21. Henderson PW, Cote JA, Leong SM (2003) Schmitt building strong brands in Asia: selecting the visual components of image to maximize brand strength. Int J Reserach Mark 20(4):297–313
22. Fajardo T, Zhang J, Tsiros M (2016) The contingent nature of the symbolic associations of visual design elements: the case of brand logo frames. J Consum Reserach 43(4):549–566
23. Durgee J, Stuart R (1987) Advertising symbols and brand names that best represnt key product meanings. J Consum Mark 15–24
24. Kelly M (2017) Analysing the complex relationship between logo and brand. Place Brand Public Dipl 13:18–33
25. Henderson PW, Cote JA (1998) Guidelines for selecting or modifying logos. J Mark 62(2):14–30
26. U. Eco (1979) A theory of semiotics, vol 217
27. Moriarty S (2002) The symbiotics of semiotics and visual communication. J Vis Lliteracy 22(1):19–28
28. Danesi M (2007) Why it sells: decoding the meanings of brand names, logos, ads, and other marketing and advertising ploys. Rowman & Littlefield Publishers, p 90
29. Heilbrunn B (1997) Representation and Legitamacy. Approaches Semiot 175–190
30. Frutiger A (1989) Signs and symbols. Their Des Mean
31. Garipzanov IH (2006) Metamorphoses of the early medieval signum of a ruler in the Carolingian world. Early Mediev Eur 14(4):419–464
32. Hardy G (2011) Smashing logo design: the art of creating visual identities, vol 24. Wiley
33. Logos-World.net (30 March 2023) [Online]. Available: https://logos-world.net/hero-logo/
34. Business Standard (14 06 2013) [Online]. Available: https://www.business-standard.com/article/finance/uti-bank-is-axis-now-107073101066_1.html. Accessed 7 Nov 2023
35. New logo: Asian Paints (3 October 2012) [Online]. Available: http://brandingsource.blogspot.com/2012/10/new-logo-asian-paints.html
36. elephantdesign.com (9th June 2023) [Online]. Available: https://elephantdesign.com/bajaj
37. Bajaj Logo (4 Feb 2023) [Online]. Available: https://1000logos.net/bajaj-logo/
38. Naidu KB, Pinto VSHistory of Reliance Logo (18 March 2014) [Online]. Available: https://www.pressreader.com/india/business-standard/20140318/page/1
39. Airtel Logo (6th June 2023) [Online]. Available: https://1000logos.net/airtel-logo/.
40. Inside Tanishq (2023) [Online]. Available: https://www.tanishq.co.in/inside-tanishq?lang=en_IN. Accessed 7 Nov 2023
41. Zero Creativity (27 May 2016) [Online]. Available: https://zerocreativity0.wordpress.com/2016/05/27/tanishq-logo/
42. Zero Creativity (13 May 2016) [Online]. Available: https://zerocreativity0.wordpress.com/tag/kotak-mahindra-logo/

43. Nanki N, Poovaiah R (7 Nov 2023) [Online]. Available: https://dsource.in/sites/default/files/resource/logos-india/downloads/file/162_logos_india_new.pdf
44. logos-world.net (14 April 2023) [Online]. Available: https://logos-world.net/videocon-logo/#:~:text=The%20Videocon%20logo%20shows%20the,base%20of%20the%20oil%20subsoil
45. Poovaiah R, Nath N (5 July 2023) "Classic Logos of India" [Online]. Available: https://www.dsource.in/gallery/classic-logos-india
46. Mubarok M (2018) The effect of brand image and consumer attituides on the desicion to purchase batik Jetis sidoarjo mediated by intent to buy. Journal of Economics, Business and Accountancy Ventura 21(1):105–116

Skill Development and Assessment Through Game-Based Learning: A Review



Venkateswara Rao Tadiboyina, B. B. V. L. Deepak, and Dhananjay Singh Bisht

Abstract Learner abilities can be enhanced in game-based learning (GBL) environments. Natural user interface (NUI)-based games can help to improve the academic and physical capabilities of children. Educational games being a subset of *serious games* could therefore be very well deployed for the players to learn various skills. A gamification approach to learning is enabled by carefully picked game design elements, meaningful ways of engagement with a focus on nurturing cognitive, motor, and academic skills. A conceptual framework is proposed in this paper for design research based on GBL environments with a discussion on different methods for assessment of learner abilities. This work promotes the idea that a focus on different skills for learner ability enhancement during GBL activities is a recommended practice for the current school-level educational system.

Keywords Game-based learning (GBL) · Cognitive skills · Motor skills · Academic skills

1 Introduction

An important focus of any educational programme is to enhance the capabilities of students/trainees. In the field of education, gamification is a fast-emerging practice [1]. Gamification is being widely adopted in teaching and learning environments and appeals to the users by often enhancing their engagement, motivation, and social influence [2]. The research on gameful learning attracts significant attention from industry and academia as it seems to offer novel opportunities for the benefactors to enhance knowledge and foster skills [3]. There lies an enormous opportunity for gamification to improve the user knowledge relying on action research [4]. Game-based learning (GBL) and gamification use meaningful game elements to develop usable learning

V. R. Tadiboyina · B. B. V. L. Deepak (✉) · D. S. Bisht
Department of Industrial Design, National Institute of Technology, Rourkela, Odisha 769008, India
e-mail: bbv@nitrkl.ac.in

© The Author(s), under exclusive license to Springer Nature Singapore Pte Ltd. 2025

B. B. V. L. Deepak et al. (eds.), *Recent Advancements in Product Design and Manufacturing Systems*, Lecture Notes in Mechanical Engineering,
https://doi.org/10.1007/978-981-97-6732-8_57

environments and attain learning goals [5]. GBL is a complex phenomenon involving more than one perspective to think about learning. For example, there are important ideas such as motivation and its conceptual foundations like affection and socio-cultural cognition which be examined for design interventions specific to an intent [6].

2 Game Design Elements

In the context of non-gaming, gamification can be introduced using different design elements in a digital game application to motivate user behaviour. Game elements are the fundamental components of gamification. A commonly agreed-upon classification of game elements is generally considered to have not been identified [7]. This is probably because different games consider different approaches for learning. Some of the essential game design elements which are commonly referenced are—(i) game mechanics, (ii) interactive storytelling, (iii) visual aesthetics, (iv) musical score, (v) incentive system, and (vi) learning content and skills for the learning objectives [6].

2.1 Game Mechanics

For successful gameplay, game mechanics is one of the essential elements which describes the activity or a set of activities performed by the player in different parts of the game. The primary objective of these activities is either learning or assessment and a focus on both in many cases. Mechanics guide the player actions by framing rules of the game as well as by determining the different responses to actions performed by the player [8]. Game mechanics would determine how effectively the game can be played. Sources have defined game mechanics differently, for, e.g. as *"systems of interactions between the player and the game"* and *"the rules and procedures that guide the player and the game response to the player's moves or actions"*. Game mechanics exists in games depending on different operational theories which determine the outcomes of the game [9].

2.2 Interactive Storytelling

Interactive storytelling is a form of digital game-based entertainment or *edutainment* where the storyline is not predetermined. For this, a designer engineers the characters, cuts scenes, introduces settings, frames in-game actions, situations, and even proposes dialogues which would determine the their interactions with the game world [10]. A concern for interactive storytelling might also involve determining the contents for learning, the tasks for characters, rules of play, and the events. Depending

of the intent of gaming, interactive storyline could be informed to different extents by methods and concepts in the fields of cognitive science, psychology, user interface design, linguistics, sociology, computer science, and emergent intelligence [11].

2.3 Visual Design

For making a positive impact on players, visual elements in a game should preferably be aesthetically pleasing by considering focusing on parameters such as pattern, visual weight, balance, scale, movement, shapes, and colour [12]. The usability and functionality of games could be enhanced by deliberate use of visual aesthetics. Concerns for visual design might also include design of feedbacks and visual cues which have both aesthetic and cognitive functions. Superior visual aesthetics offer an attractiveness bias and can make a player more tolerant of usability issues [13].

2.4 Musical Score

Background sounds in a game are often used to bring attention of the players to key moments, actions, or events in the game. Typically, these would elicit positive or negative emotions, signal the presence of opportunities or dangers, or acknowledge the triumph or failure in a specific task. Even the scores might be displayed by a human voice and/or contextually relevant sounds. Background musical scores may play across the length of a game. Musical scores are also strategically synchronized with haptic information from game controllers [14].

2.5 Incentive System

The incentive system is a key design element in games; many games engineer reinforcements in the gameplay to motivate the players in acquiring knowledge and performing well or *"meritoriously"* at each stage of the game. Incentives may be introduced by designing motivational elements such as points and scores, badges, stars, trophies, and other rewards [15]. Players might be motivated intrinsically as well as extrinsically. Incentive systems can significantly influence learning and game performance. Incentive systems could be systematically and specifically explored by conducting ethnographic research. The appeal of intrinsic motivation could be understood by examining self-determination theory [16].

2.6 Content of Learning and Skills Enhancement

During GBL, the learner could acquire knowledge in different ways for which the game designers need to incorporate design elements creatively [17]. Learning goals could be achieved by designing appropriate contents for genres such as casual games, real-time strategy games, role-playing games, puzzle games, etc. A set of four heuristics for deciding upon the contents of such games are—(1) development of skills for the twenty-first century (giving an opportunity to enhance highly convoluted socio-emotional skills corresponding to collaborative, creativity, team work, and issue sorting communication, etc).; (2) teach new skills and knowledge (games are created by introducing new skills and knowledge for learners to develop skills further that are inclusive through of the gameplay); (3) reinforcing and practising existing skills and knowledge (educational game provides chance to practice inbuilt cognitive skills and knowledge in order to automate them); (4) future learning preparation (in any type of game irrespective of learning objective, the learners gain a lot of experience that can be used for problem solving that could be an aid in future learning activities) [18].

3 Enhancement of Learning Skills

Learning processes and GBL systems could achieve learning specific goals of children by focusing on development of (i) cognitive skills; (ii) motor skills, and; (iii) academic skills.

3.1 Cognitive Skills

Communication and language play a vital role in the cognitive growth of a child. Reading and writing skills are crucial for the development of language and knowledge acquisition. Language learning in children typically begins with an acquiring of vocabulary for common objects aided by aspects of fundamental literacy and numeracy of surrounding environments which may involve (but is not limited to) number sense, knowledge colours and shapes [19]. The process of learning is heavily influenced by observations of the surrounding environment and common objects encountered in daily life. Cognitive skills comprise capabilities like observation, identification, matching, classification, pattern identification, sequential thinking, creative thinking, problem solving, etc. [20]. In children, the development of cognitive skills can be enhanced by GBL including activities based on visual and verbal representation as well as through the integration of these activities [21]. Researchers and designers have contributed variously in thematic representations and design of

game mechanics to engage the learner with a focus on cognitive skill development [22] (Table 1).

Table 1 Some of the cognitive skills addressed in scientific literature

Code	Skill	Ref	Game/ activities	Research method used
C1	Attention development	[9, 19, 23]	• Serious game training • ATHYNOS game • Escola do Cerebro • Zoo and house game • Bump Bash, Target Kick	• Quasi-experiments • Wilcoxon rank sum test (two-tailed test): scores, task on time • Analysis of variance (ANOVA): no. of errors • Quantitative analysis: game scores • Movement ABC-test
C2	Short-term/ working memory	[20, 21, 24, 25]	• Kinems gaming platform • Escola do Ce´rebro, • Monkey Tales	• Both qualitative and quantitative analysis: no. of errors and survey questions •Paired sample t-test: task on time • Analysis of variance (ANOVA): game scores • Qualitative analysis: survey questions
C3	Recognition	[26, 27]	• Fun to learn • Matching games	• Quasi-experiments • Both qualitative and quantitative analysis: game scores, no. of errors, survey questions
C4	Decision making	[26, 28]	• Fun to learn • “KiNEEt” virtual activities	• Quasi-experiment • Both qualitative and quantitative analysis: task on time, game scores, survey questions • Usability test of virtual interface
C5	Problem-solving	[29, 30]	• ATHYNOS game • Escola do Cerebro	• Analyses of variance (ANOVA): task on time, no. of errors • Qualitative data: game scores
C6	Visual processing	[31, 32]	• Auxiliary training system • “Kinems” gaming platform	• Vineland adaptive behaviour scale •Function assessment: task on time •Learning analytics: no. of errors, game scores

3.2 Motor Skills

At the school level, concerns for motor skills involve fundamental capabilities related to specific movements of the body parts (muscles and bones) in order to complete specific physical tasks. Here, the brain, nervous system, and the musculoskeletal system have to all work together [29]. Typically, the goal is to optimize certain observable physical abilities measured on the basis of parameters such as precision and success rates, or energy efficiency during task performance. Biological system coordination along with physical balance and agility are important considerations related to motor skills. Repeated practising of motor skills leads to greatly improved physical performance which could also be termed as motor learning [33]. They are two major groups of motor skills namely gross motor skills and fine motor skills.

Gross motor skills involve the use of body parts with larger muscles and bones for performing activities such as balancing, walking, throwing, catching, crawling, jumping, etc. For children, the development of these skills gradually occurs during regular school-level activities [34]. Fine motor skills involve the use of smaller muscle or bones such as those in human hands, fingers, wrists, toes, etc. for performing dexterous activities. These activities are typically precise in nature such as holding and handling objects, buttoning clothes, dialing the phone, hand–eye coordination, touch performance on touch devices, etc. [27] (Table 2).

3.3 Academic Skills

Academic skills like reading written text and performing mathematical operations are fundamental for successful schooling and are powerful predictors for future academic achievement [39]. Children are made to continuously learn and refine their academic skills through training and practice in order to build a strong foundation for academic and social success in future [20]. New developments and emerging pedagogical trends stress on the need to design curricula which are indigenous, developmentally appropriate, activity- and play-based, and holistic [40]. At the school level, activity and play-based games are known to be effective media for content learning and physical development of students [33]. Gaming environment offers an interactive platform, where self-initiated play or those which are clearly goal-based and directed can help in grooming academic skills and imparting knowledge in children [41] (Table 3).

Table 2 Some of the motor skills addressed in scientific literature

Code	Skill	Ref	Game/activities	Research method used
M1	Hand–eye coordination	[23, 28, 29, 33, 35]	• ATHYNOS • "KiNEEt" virtual activities • Bangos • Froggy Bobby • Catching game	• Both qualitative and quantitative: no. of errors, game scores, survey questions • Teacher assessment: reaction time • Quasi-experiments • Analyses of covariance (ANCOVA): game scores, no. of errors
M2	Psychomotor ability and its Speed	[24, 31, 36]	• "Kinems" gaming platform • Exergames: Xavix boxing, Gamercize	• Both qualitative and quantitative: time on task, survey questions • Analyses of variance (ANOVA): no. of errors • Analyses of multiple variances (MANOVA): task on time, no. of errors • Teachers' self-reports • Qualitative analysis: survey questions
M3	Gross motor skill	[34, 37]	• Rackets game • Froggy Bobby	• Paired sample t-test: task on time, game score • Interview-based assessment
M4	Fine motor skill	[27, 38]	• Matching games • Baseball, soccer	• Both quantitative and qualitative analysis: game scores, task on time, survey questions • Analyses of variance (ANOVA): task on time, no. of errors

Table 3 Some of the academic skills addressed in scientific literature

Code	Skill	Ref	Game/activities	Research method used
A1	English skill	[7, 26, 28, 42, 43]	• Suffiz, Sea Formuli, Marvy Learns • Vocabulary game/ sentence game Erasmus • Fun to learn • KiNEEt • English learning system • Kinect motion-sensing interactive system (KMIS)	• Analysis of variance (ANOVA): game scores • Quasi-experiments • Mann–Whitney U test: time on task • Analysis of covariance (ANCOVA): time on task • Both quantitative and qualitative analysis: survey questions, no. of errors
A2	Reading	[44]	• Interactive digital game	• Analysis of variance (ANOVA): time on task, game scores
A3	Arithmetic	[25, 29, 31, 45, 46]	• Suffiz, Sea Formuli, Marvy Learns • Virtual intervention platform • "ATHYNOS" game • "Kinems" gaming platform • Monkey tales	• Multivariate analysis of variance (MANOVA): game scores • Wilcoxon rank sum test (two-tailed test): task on time • Analysis of variance (ANOVA): no. of errors, game scores • Questionnaire data: survey questions
A4	Learning performance	[24, 33]	• "Kinems" gaming platform • Gesture interactive learning	• Quasi-experiments • Analysis of covariance (ANCOVA): time on task, game scores • Quantitative analysis: survey questions

4 Conclusion

This paper presents a systematic discussion on the idea of game-based learning (GBL) and some of the important considerations to be made for developing and evaluating GBL systems. The work begins with a clear focus on exploring and understanding the scope of implementing digital GBL offering interactive, embodied, and kinesthetic learning experiences. The idea is to explore opportunities for skill-aware learning in children in playful settings. Different elements of game design were examined to

some detail in order to make clear the scope for specific design interventions. Also, the idea of distinct (but overlapping) skills which have been addressed by researchers in the past has been discussed in this paper. Finally, different parameters and methods to design/engineer and evaluate three categories of skills, namely cognitive, motor, and academic, respectively, have been examined.

Based on the systematic discussion of the possibilities in design and evaluation of GBL systems offered in this paper, there exist enormous opportunities for researchers to develop and evaluate learning-based games focusing on improving different skills of children/students. Future research could also establish and demonstrate the nature of association between different cognitive, motor, and academic skills in specific contexts. This will strengthen our understanding of different situations of embodied learning in the field of education.

References

1. Al-Shamayleh AS, Ahmad R, Abushariah MAM, Alam KA, Jomhari N (2018) A systematic literature review on vision based gesture recognition techniques. Multimed Tools Appl 77(21):28121–28184. https://doi.org/10.1007/s11042-018-5971-z
2. de la Peña D, Lizcano D, Martínez-Álvarez I (2021) Learning through play: gamification model in university-level distance learning. Entertain Comput 39. https://doi.org/10.1016/j.entcom.2021.100430
3. Seaborn K, Fels DI (2015) Gamification in theory and action: a survey. Int J Hum Comput Stud 74:14–31. https://doi.org/10.1016/j.ijhcs.2014.09.006
4. Hamari J, Shernoff DJ, Rowe E, Coller B, Asbell-Clarke J, Edwards T (2016) Challenging games help students learn: an empirical study on engagement, flow and immersion in game-based learning. Comput Human Behav 54:170–179. https://doi.org/10.1016/j.chb.2015.07.045
5. Chen YL, Hsu CC (2020) Self-regulated mobile game-based English learning in a virtual reality environment. Comput Educ 154:103910. https://doi.org/10.1016/j.compedu.2020.103910
6. Plass JL, Homer BD, Kinzer CK (2015) Foundations of game-based learning. Educ Psychol 50(4):258–283. https://doi.org/10.1080/00461520.2015.1122533
7. Lee-Cultura S, Sharma K, Aloizou V, Retalis S, Giannakos M (2020) Children's interaction with motion-based touchless games: kinecting effectiveness and efficiency. Extended Abstracts of the 2020 Annual Symposium on Computer-Human Interaction in Play, pp 140–145. https://doi.org/10.1145/3383668.3419937
8. Lee E, Liu X, Zhang X (2012) Xdigit: an arithmetic kinect game to enhance math learning experiences. Retrieved Febr 14:2013
9. Liu W, Tan L, Huang D, Chen N, Liu F (2021) When preschoolers use tablets: the effect of educational serious games on children's attention development. Int J Hum Comput Interact 37(3):234–248. https://doi.org/10.1080/10447318.2020.1818999
10. Yilmaz RM (2016) Educational magic toys developed with augmented reality technology for early childhood education. Comput Human Behav 54. https://doi.org/10.1016/j.chb.2015.07.040
11. Xu M et al (2019) Personalized training through Kinect-based games for physical education. J Vis Commun Image Represent 62:394–401. https://doi.org/10.1016/j.jvcir.2019.05.007
12. Gunawan TS, Bahari B, Kartiwi M (2017) Development of educational game for primary school mathematics using microsoft kinect. Indones J Electr Eng Comput Sci 6(2):457–463. https://doi.org/10.11591/ijeecs.v6.i2.pp457-463

13. Gao Z, Li SH, Zhu YJ, Wang C, Zhang H (2017) Collaborative sparse representation leaning model for RGBD action recognition. J Vis Commun Image Represent 48:442–452. https://doi.org/10.1016/j.jvcir.2017.03.014
14. Altanis G, Boloudakis M, Retalis S, Nikou N (2014) Children with motor impairments play a kinect learning game: first findings from a pilot case in an authentic classroom environment. Interact Des Archit 19(1):91–104
15. Pavlovic VI et al (2019) Touch gesture performed by children under 3 years old when drawing and coloring on a tablet. Multimed Tools Appl 11(2):1–13. https://doi.org/10.1007/s10462-012-9356-9
16. Aguilar SJ, Holman C, Fishman BJ (2018) Game-inspired design: empirical evidence in support of gameful learning environments. Games Cult 13(1):44–70. https://doi.org/10.1177/1555412015600305
17. Meluso A, Zheng M, Spires HA, Lester J (2012) Enhancing 5th graders' science content knowledge and self-efficacy through game-based learning Comput Educ 59(2):497–504. https://doi.org/10.1016/j.compedu.2011.12.019
18. Garnar AW (2017) Educational technology
19. Hung IC, Chen NS (2018) Embodied interactive video lectures for improving learning comprehension and retention. Comput Educ 117:116– 131. https://doi.org/10.1016/j.compedu.2017.10.005
20. Kosmas P, Ioannou A, Zaphiris P (2019) Implementing embodied learning in the classroom: effects on children's memory and language skills. EMI Educ Media Int 56(1):59–74. https://doi.org/10.1080/09523987.2018.1547948
21. Tsai CH, Huang JY (2018) Augmented reality display based on user behaviour. Comput. Stand Interfaces 55. https://doi.org/10.1016/j.csi.2017.08.003
22. Duijzer C, Van den Heuvel-Panhuizen M, Veldhuis M, Doorman M, Leseman P (2019) Embodied learning environments for graphing motion: a systematic literature review. Educ Psychol Rev 597–629. https://doi.org/10.1007/s10648-019-09471-7
23. Tang TY, Falzarano M, Morreale PA (2018) Assessment of the utility of gesture- based applications for the engagement of Chinese children with autism. Univers Access Inf Soc 17(2):275–290. https://doi.org/10.1007/s10209-017-0562-8
24. Kosmas P, Ioannou A, Retalis S (2018) Moving bodies to moving minds: a study of the use of motion-based games in special education. TechTrends 62(6):594–601. https://doi.org/10.1007/s11528-018-0294-5
25. Núñez Castellar E, All A, De Marez L, Van Looy J (2015) Cognitive abilities, digital games and arithmetic performance enhancement: a study comparing the effects of a math game and paper exercises. Comput Educ 85:123–133. https://doi.org/10.1016/j.compedu.2014.12.021.
26. Lai NK, Ang TF, Por LY, Liew CS (2018) Learning through intuitive interface: a case study on preschool learning. Comput Educ 126:443–458. https://doi.org/10.1016/j.compedu.2018.08.015
27. Cai S, Zhu G, Wu YT, Liu E, Hu X (2018) A case study of gesture-based games in enhancing the fine motor skills and recognition of children with autism. Interact Learn Environ 26(8):1039–1052. https://doi.org/10.1080/10494820.2018.1437048
28. Ojeda-Castelo JJ, Piedra-Fernandez JA, Iribarne L, Bernal-Bravo C (2018) KiNEEt: application for learning and rehabilitation in special educational needs. Multimed Tools Appl 77(18):24013–24039. https://doi.org/10.1007/s11042-018-5678-1
29. Avila-Pesantez D, Delgadillo R, Rivera LA (2019) Proposal of a conceptual model for serious games design: a case study in children with learning disabilities. IEEE Access 7:161017–161033. https://doi.org/10.1109/ACCESS.2019.2951380
30. Ramos DK, Melo HM (2019) Can digital games in school improve attention? A study of Brazilian elementary school students. J Comput Educ 6(1):5–19. https://doi.org/10.1007/s40692-018-0111-3
31. Kosmas P, Ioannou A, Retalis S (2017) Using embodied learning technology to advance motor performance of children with special educational needs and motor impairments. Lecture notes in computer science (Including subseries lecture notes in artificial intelligence lecture notes in

bioinformatics), vol 10474. LNCS, pp 111–124. https://doi.org/10.1007/978-3-319-66610-5_9
32. Wuang Y et al (2018) Department of healthcare administration and medical informatics. Kaohsiung. https://doi.org/10.1016/j.compedu.2018.05.008.This
33. Hsiao HS, Chen JC (2016) Using a gesture interactive game-based learning approach to improve preschool children's learning performance and motor skills. Comput Educ 95:151–162. https://doi.org/10.1016/j.compedu.2016.01.005
34. Vukićević S, Đorđević M, Glumbić N, Bogdanović Z, Đurić Jovičić M (2019) A demonstration project for the utility of kinect-based educational games to benefit motor skills of children with ASD. Perceptual and Motor Skills 126(6):1117– 1144. https://doi.org/10.1177/0031512519867521
35. Caro K, Tentori M, Martinez-Garcia AI, Alvelais M (2017) Using the FroggyBobby exergame to support eye-body coordination development of children with severe autism. Int J Hum Comput Stud 105(March):12–27. https://doi.org/10.1016/j.ijhcs.2017.03.005
36. Sun H (2013) Impact of exergames on physical activity and motivation in elementary school students: a follow-up study. J Sport Heal Sci 2(3):138–145. https://doi.org/10.1016/j.jshs.2013.02.003
37. Caro K, Tentori M, Martinez-Garcia AI, Zavala-Ibarra I (2017) FroggyBobby: an exergame to support children with motor problems practicing motor coordination exercises during therapeutic interventions. Comput Human Behav 71:479–498. https://doi.org/10.1016/j.chb.2015.05.055
38. Vernadakis N, Papastergiou M, Zetou E, Antoniou P (2015) The impact of an exergame-based intervention on children's fundamental motor skills. Comput Educ 83:90–102. https://doi.org/10.1016/j.compedu.2015.01.001
39. Liang JM, Su WC, Chen YL, Wu SL, Chen JJ (2019) Smart interactive education system based on wearable devices. Sensors (Switzerland) 19(15). https://doi.org/10.3390/s19153260
40. Holmes J, Gathercole SE (2014) Taking working memory training from the laboratory into schools. Educ Psychol 34(4):440–450. https://doi.org/10.1080/01443410.2013.797338
41. Kourakli M, Altanis I, Retalis S, Boloudakis M, Zbainos D, Antonopoulou K (2017) Towards the improvement of the cognitive, motoric and academic skills of students with special educational needs using Kinect learning games. Int J Child-Computer Interact 11:28–39. https://doi.org/10.1016/j.ijcci.2016.10.009
42. Wang F, Hwang WY, Li YH, Chen PT, Manabe K (2019) Collaborative kinesthetic EFL learning with collaborative total physical response. Comput Assist Lang Learn 32(7):745–783. https://doi.org/10.1080/09588221.2018.1540432
43. Pan WF (2017) The effects of using the kinect motion-sensing interactive system to enhance English learning for elementary students. Educ Technol Soc 20(2):188–200
44. Homer BD et al (2014) Moved to learn: the effects of interactivity in a Kinect-based literacy game for beginning readers. Comput Educ 74:37–49. https://doi.org/10.1016/j.compedu.2014.01.007
45. Lee-Cultura S, Sharma K, Papavlasopoulou S, Retalis S, Giannakos M. (2020) Using sensing technologies to explain children's self-representation in motion-based educational games. In: Proceedings of Interaction Design Children Conference IDC, pp 541–555. https://doi.org/10.1145/3392063.3394419
46. Peralbo-Uzquiano M, Fernández-Abella R, Durán-Bouza M, Brenlla-Blanco JC, Cotos-Yáñez JM (2020) Evaluation of the effects of a virtual intervention programme on cognitive flexibility, inhibitory control and basic math skills in childhood education. Comput Educ 159. https://doi.org/10.1016/j.compedu.2020.104006